

**Distribution, Diversity, and Activity of Bacteria from the
Central Indian Ocean Basin**

Thesis submitted for the degree of

Doctor of Philosophy

in

Marine Sciences

to the

Goa University

by

Anindita Das, M.Sc.

under guidance of

Dr. P.A. Loka Bharathi

National Institute of Oceanography

(Council of Scientific and Industrial Research)

Dona Paula, Goa-403004, India

February, 2011

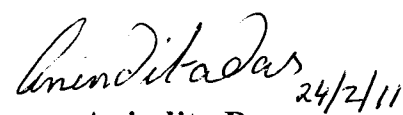
579.3

Dis / Dis

797

Statement

As required under the University ordinance 0.19.8(iv), I state that the present thesis entitled “***Distribution, Diversity, and Activity of Bacteria from the Central Indian Ocean Basin***” is my original contribution and the same has not been submitted on any previous occasion. To the best of my knowledge the present study is the first comprehensive work of its kind from the area mentioned. The literature related to the problem investigated has been cited. Due acknowledgements have been made wherever facilities and suggestions have been availed of.


Anindita Das 24/2/11

Certificate

This is to certify that the thesis entitled “*Distribution, Diversity, and Activity of Bacteria from the Central Indian Ocean Basin*”, submitted by Ms. Anindita Das for the award of the degree of Doctor of Philosophy in Marine Sciences is based on the original studies carried out by her under my supervision. The thesis or any part thereof has not been previously submitted for any other degree or diploma in any universities or institutes.

Place: NIO, Dona Paula

Dated: 24 February, 2011


Dr. P.A. Loka Bharathi

Biological Oceanography,

National Institute of Oceanography,

Dona Paula, Goa-403 004.

All the corrections suggested by both referees have been incorporated.


22/2/11

- P.A. Loka Bharathi
21.11.2011

"Science moves, but slowly, slowly, creeping on from point to point".

-Alfred Lord Tennyson

Dedication

*Dedicated to the three decades of perseverance of
all Senior and Contemporary Colleagues of
Polymetallic Nodules Programme, Govt. of India
and all the Associates*

"Art is I: Science is we".

- *Claude Bernard.*

Acknowledgement

I convey my hearty thanks to the *Council of Scientific and Industrial Research (CSIR)* for this opportunity of working as Junior and Senior Research Fellow (2004-09) at its constituent laboratory, the *National Institute of Oceanography*, Dona Paula, Goa, India.

I am also thankful to our *Director, Dr. Satish R. Shetye* who took keen interest in encouraging all students for quality research, amidst his hectic schedule. His constructive criticisms kept us on our toes to try and give our best to our theses. He taught and sowed the interest in mathematical modelling. Later, unstinted support from his team members prompted me to try my hand at numerical simulations.

My Guide, *Dr. Loka Bharathi P.A.*, mentored me towards the subject "Chemosynthesis" and "RuBisCO". I would like to recall here that I had decided against studying Botany, as a high school student, because I could never understand why half of "*Photo*-synthesis" was called the "Dark Reactions". Dr. Loka, a teacher per excellence initiated a stubborn student afresh to the Planet's chosen carbon fixation enzyme.

My Field Mentor, *Dr. Bejugam Nagender Nath*, introduced me to the geo-chemically important problems to be answered in the Central Indian Ocean Basin. A true man of Science, Dr. Nath did not hesitate then to show even his unpublished work to encourage me towards the subjects “Hydrothermal alteration” and “Early-Diagenesis” and their relation to Bacteria.

Also it is pertinent to mention here that our Project Leader *Dr. Rahul Sharma* rendered continuous support to my work under all circumstances.

My sincere thanks to *Drs. Shyam Prasad, Biswajit Chakraborty, V. Banakar, A.L. Paropkari, V. Ramaswamy, P. Das* and *R. Agnihotri, A. Mazumdar* and *Sri S. Jaishankar* for all the help rendered during different phases of the thesis.

I am indebted to *Dr. C. Prakash Babu* for all the time and effort he spared for helping me with Elemental Carbon analysis. *Mr. V. Kedekar* spent patient and dedicated hours at the SEM and *Mr. Subramanyam* and *Mr. Balsubramaniam (RC-Kochi)* helped me with scintillation counters.

I acknowledge the support of the professors and personnel of the *Departments of Marine Science and Marine Biotechnology, Goa University* for their scientific and technical advisory support.

I would like to specially remember all my *Professors and Teachers* of *Cochin University of Science and Technology (CUSAT)* to whom I owe my initiation to Marine Sciences.

I am obliged to the *Libraries of NIO, Goa, Indian Institute of Science, Bangalore and Indian Institute of Chemical Biology, Kolkata*. I specially acknowledge the *Administration, Accounts, HRM, ITG, Workshop, Civil, Electrical and Security* sections of NIO for their constant help.

My colleague and friend *Ms. Christabelle E. G. Fernandes* deserves a very special appreciation for all the learning and training that we shared during our work. I initiated ^{14}C uptake experiments with *Dr. Judith* and on-board microbiology work with *Ms. Sonali S. Naik*. I would remember *Dr. Shanta Achuthankutty* for all the moments of joy, sorrow, discussions and the affectionate fights and arguments.

I convey my gratitude to all my fellow lab-mates and friends especially *K. P. Krishnan* (now in NCAOR, Vasco, Goa), *Haridevi C.K., Baby Divya Daniel, Anne Feby Felix, Sree S. Kumar, Sheryl Fernandes, Sujith P.P., Samita Helekar, Sushanta Biche, Babu Sashikant Mourya, Tresa Remya, Sunita Pandey...*

I had that scope for working with some very bright and hard working dissertation students from different corners of the country, here at NIO. I recall the work of *Neelam Sharma, Asmita Sonawane, Shankar Narayan., Theyambattil, Anuradha Seshu, Melissa Periera and Sashikala.*

Here again the words actually fail to express my gratitude to ***Dr. Mohandass C. and family*** and ***Dr. Prakash Mehra and family*** for a life-saving favour.

This study was possible by the constant support and blessing of ***Babuji*** and ***Ma***. They shared all my moments of sorrow and joy ignoring their age and ailments.

My prayers and thanksgiving to my ***Gurudev Sri Sri Thakur Anukul Chandra*** for all the strength, courage and peace bestowed on me during all times of miseries and consolation and in this regard everything is dedicated and placed to the lotus-feet of Him.


Anindita Das

NIO, Goa, February, 2011

Contents

1.0	Chapter I Introduction	1
1.1	Distribution of Bacteria	2
1.2	Diversity of Bacteria	2
1.3	Activity of Bacteria	3
1.4	Deep-sea environments and bacteria	4
1.5	Deep-sea environment of Central Indian Ocean Basin (CIOB)	6
1.5.1	<i>Central Indian Ocean Basin- Geology, Geophysics, Geochemistry</i>	6
1.5.2	<i>Central Indian Ocean Basin- Thermohaline Circulation, Chemistry and Biology</i>	8
1.5.3	<i>Central Indian Ocean Basin- Microbiology and Biochemistry</i>	8
1.6	Aim of the study	10
1.7	Objectives of the study	10
1.8	Importance of the present study	10
2.0	Chapter II Review of literature	12
2.1	Abundance and Distribution	13
2.2	Diversity	15
2.3	Activity	24
2.4	Response to various geochemical settings	28
2.4.1	<i>Diagenesis and bacteria</i>	28
2.4.2	<i>Hydrothermal alterations and bacteria</i>	31
2.4.3	<i>Chemosynthesis and bacteria</i>	36
2.5	Minerals, metals, energy currency and bacteria	37
2.5.1	<i>Phosphates, Pyrophosphates, Silicates, metal oxides and bacteria</i>	37
2.5.2	<i>ATP and bacterial biogeochemistry</i>	42
2.5.3	<i>Use of ATP in understanding biogeochemical processes</i>	45
2.6	Quantification of biogeochemical processes	46
2.6.1	<i>Diagenetic interactions</i>	46

2.6.2	<i>Fluid interactions</i>	47
2.7	Geological, setting of the Central Indian Ocean Basin	48
2.7.1	<i>Geological features of northern siliceous oozes</i>	49
2.7.2	<i>Geological features of southern pelagic red clay</i>	50
2.8	Geomicrobiology of the Central Indian Basin	50
2.8.1	<i>Northern siliceous ooze</i>	50
2.8.2	<i>Southern pelagic red clay</i>	51
3.0	Chapter III Material and Method	53
3.1	Environmental Parameters	54
3.1.1	<i>Temperature</i>	54
3.1.2	<i>Depth and pressure</i>	54
3.2	Sampling area and frequency	54
3.3	Classification of stations	56
3.4	On-Board processing	56
3.5	Geochemical parameters	57
3.5.1	<i>Rock colour</i>	57
3.5.2	<i>Porewater parameters</i>	58
3.5.2.1	<i>pH and Eh</i>	58
3.5.2.2	<i>Dissolved oxygen</i>	59
3.5.2.3	<i>Salinity</i>	59
3.5.2.4	<i>Ammonium</i>	60
3.5.2.5	<i>Sulphide</i>	60
3.5.2.6	<i>Fe</i>	60
3.5.2.7	<i>Mn</i>	61
3.5.3	<i>Elemental Carbon and Nitrogen -Total Organic Carbon (TOC), Total inorganic carbon (TIC) and C/N ratio</i>	61
3.6	Biochemistry	61
3.6.1	<i>Labile organic matter (LOM)</i>	61
3.6.1.1	<i>Proteins</i>	61
3.6.1.2	<i>Carbohydrates</i>	62
3.6.1.3	<i>Lipids</i>	62
3.6.1.4	<i>LOM</i>	62
3.6.2	<i>Adenosine Triphosphate (ATP)</i>	62
3.7	Microbiology	63

3.7.1	<i>Bacterial counts</i>	63
3.7.1.1	<i>Total counts of bacteria</i>	63
3.7.1.2	<i>Frequency of dividing cells (FDC)</i>	63
3.7.1.3	<i>Autofluorescent F₄₂₀ cells</i>	64
3.7.1.4	<i>Direct Viable Counts (DVC)</i>	64
3.7.2	<i>Image Analysis</i>	65
3.7.3	<i>Culturable bacteria</i>	65
3.7.3.1	<i>Heterotrophs</i>	65
3.7.3.2	<i>Potential autotrophs</i>	66
3.7.3.3	<i>Fe and Mn oxidizers</i>	66
3.7.3.4	<i>Phosphate and silicate solubilizers</i>	67
3.7.3.4	<i>Formaldehyde utilizers</i>	67
3.8	Activity	67
3.8.1	<i>Hydrolytic Enzymes of bacterial isolates</i>	67
3.8.2	<i>BIOLOG and ECOLOG carbon substrate utilization pattern analysis</i>	68
3.8.3	<i>Formaldehyde utilization rates by cultures</i>	68
3.8.4	<i>Microbial carbon fixation</i>	68
3.8.5	<i>Ribulose bis-phosphate carboxylase/oxygenase (RuBisCO)</i> <i>enzyme activity in cultures and sediments</i>	69
3.8.6	<i>Estimation of phosphate solubilizing activity in sediments</i>	71
3.9	Diversity	72
3.9.1.	<i>Biochemical methods</i>	72
3.9.2.	<i>Microbial diversity using molecular techniques</i>	72
3.9.2.1	<i>16S rDNA</i>	72
3.9.2.2	<i>Pyrosequencing using 454 technology</i>	73
3.10	Data analysis and statistical significance	79
3.11	Simulation	79
3.11.1	<i>Quantification of the influence of non-steady state diagenetic condition on microbial community by numerical simulation</i>	79
3.11.2	<i>Quantification of hydrothermal alterations on pore-water and microbial community by numerical simulation</i>	81
4.0	Chapter IV Results	84
4.1	Environmental Parameters	85
4.1.1	<i>Temperature</i>	85

4.1.2	<i>Depth and pressure</i>	85
4.2	Geochemical parameters	85
4.2.1	<i>Rock Colour</i>	85
4.2.2	<i>Pore water geochemistry</i>	87
4.2.2.1	<i>pH and Eh</i>	87
4.2.2.2	<i>Dissolved oxygen</i>	87
4.2.2.3	<i>Salinity</i>	88
4.2.2.4	<i>Ammonium</i>	88
4.2.2.5	<i>Sulphide</i>	88
4.2.2.6	<i>Fe</i>	89
4.2.2.7	<i>Mn</i>	89
4.3.	Elemental carbon, nitrogen, C/N ratio	92
4.4	Distribution of bacteria in the Central Indian Ocean Basin	93
4.4.1	<i>Labile organic matter (LOM)</i>	98
4.4.2	<i>Adenosine triphosphate (ATP)</i>	103
4.4.3	<i>Total counts and frequency of dividing cells</i>	106
4.4.4	<i>Direct viable counts (DVC a and DVC an)</i>	117
4.4.5	<i>Culturable counts</i>	118
4.5	Diversity of Bacteria in Central Indian Ocean Basin	141
4.5.1	<i>Biochemical characterization of isolates</i>	141
4.5.2	<i>16S rRNA characterisation for CIOB Isolates</i>	147
4.5.2.1	<i>Phylogenetic affiliation of culture CIOB 25A</i> <i>-an Aerobic Thiobacillus denitrificans like-organism</i>	147
4.5.2.2	<i>Phylogenetic affinity of culture CIOB BIN2</i> <i>- a deep-sea heterotroph</i>	147
4.5.2.3	<i>Phylogenetic affinity of culture CIOB BIN 3</i> <i>- a deep-sea heterotroph</i>	149
4.5.2.4	<i>Phylogenetic affinity of Culture CIOB BIN 4</i> <i>- a deep-sea heterotroph</i>	151
4.5.3	<i>Community analysis from whole sediment</i>	151
4.6.	Activity of Bacteria in Central Indian Basin	154
4.6.1	<i>Hydrolytic enzyme activity</i>	154
4.6.2	<i>Carbon substrate utilization</i>	155
4.6.3	<i>Carbon fixation</i>	160
4.6.4	<i>RuBisCO enzyme activity</i>	169
4.6.5	<i>Phosphatase activity</i>	172

4.7	Elemental Carbon, Biochemistry and Microbiology of Nodule and associated sediments	178
4.7.1	<i>Total organic carbon (TOC), TIC and C/N ratio</i>	178
4.7.2	<i>Labile organic matter (LOM)</i>	178
4.7.3	<i>Adenosine Triphosphate (ATP)</i>	179
4.7.4	<i>Bacterial counts</i>	179
4.7.5	<i>Microbial uptake of carbon in sediments and nodules</i>	181
4.7.6	<i>Carbon substrate utilization by nodules and sediments</i>	181
4.8	Interrelations	186
4.8.1	<i>The Siliceous oozes –Cores 26, 25, 20</i>	186
4.8.2	<i>The Siliceous-Pelagic transition-Cores 34, 35</i>	189
4.8.3	<i>The pelagic red clays- Cores 08, 36, 38</i>	192
4.8.4	<i>The calcareous ooze</i>	193
4.8.5	<i>Interrelationships between microbial and biochemical parameters in nodules</i>	197
4.9	Simulations	201
4.9.1	<i>Quantification of the influence of non-steady state diagenetic condition on microbial community by numerical simulation</i>	201
4.9.2	<i>Quantification of hydrothermal alterations on pore water and microbial community by numerical simulation</i>	202
5.0	Chapter V Discussion	204
5.1	Characteristics of the deep-sea	205
5.2	Environmental setting of the CIOB	206
5.2.1	<i>Depth, temperature and pressure</i>	206
5.2.2	<i>Rock Colour</i>	207
5.2.3	<i>Pore water Geochemistry</i>	208
5.3	Elemental Carbon, Nitrogen, C/N ratio	209
5.4	Distribution - Biochemical and microbiological parameters	211
5.4.1	<i>Labile organic matter (LOM) and Adenosine triphosphate (ATP)</i>	211
5.4.2	<i>Abundance and distribution of bacteria in CIOB</i>	212
5.4.3	<i>Total counts and frequency of dividing cells</i>	212
5.4.4	<i>Direct viable counts (DVC a and DVC an)</i>	213

5.4.5	<i>Culturable counts and endeavour to improve culturability</i>	213
5.4.6	<i>Aerobic culturability</i>	213
5.4.7	<i>Heterotrophs (ZMA medium)</i>	214
5.4.8	<i>Nitrifiers</i>	215
5.4.9	<i>Aerobic sulphur oxidizers (Aerobic TDLO)</i>	215
5.4.10	<i>Corewise distribution of heterotrophs, NI, NII and aerobic TDLO</i>	216
5.4.11	<i>Fe and Mn oxidizers</i>	217
5.4.12	<i>Phosphate and silicate solubilizers</i>	219
5.4.13	<i>Anaerobic culturability</i>	221
5.5	Spatial distribution	221
5.5.1	<i>Bacterial response to contrasting geochemistry</i>	221
5.5.1.1	<i>Northern core TVBC 26</i>	223
5.5.1.2	<i>Southern core TVBC 08</i>	226
5.6	Temporal Distribution	232
5.6.1	<i>Inter-annual variations conceal seasonal variations in microbial and biochemical parameters in Central Indian Basin</i>	232
5.7	Bacterial activity in relation to cell morphology sediment- biochemistry geotechnical properties and sediment texture	238
5.8	Bacterial role on geological time scale: Early diagenesis and bacteria	240
5.9	Activity of bacteria in sediments	241
5.9.1	<i>Heterotrophic activity</i>	241
5.9.1.1	<i>Hydrolytic enzyme activity</i>	241
5.9.1.2	<i>Carbon substrate utilization</i>	242
5.9.1.3	<i>Alkaline Phosphatase activity</i>	242
5.9.2	<i>Autotrophic activity</i>	245
5.9.2.1	<i>Formaldehyde tolerance</i>	245
5.9.2.2	<i>Extent of autotrophy and chemosynthetic hotspots in CIOB</i>	251
5.9.2.3	<i>RuBisCO enzyme activity in isolates and whole sediments</i>	252
5.10	Diversity of Bacteria in Central Indian Ocean Basin	254
5.10.1	<i>Biochemical identification</i>	254
5.10.2	<i>16S rDNA phylogenetic affinities of CIOB cultures</i>	255
5.10.3	<i>Diversity of bacteria by 454 pyrosequencing technique</i>	257
5.11	Parameter-wise cluster pattern of microbial and biochemical parameters	259

5.12.	Interactions between bacteria and environmental parameters	262
5.13	Core-wise principal component analysis (PCA) of distribution patterns	265
5.14	Numerical Simulations	267
5.14.1	<i>Quantification of the influence of non-steady state diagenetic condition on microbial community by numerical simulation</i>	267
5.14.2	<i>Quantification of hydrothermal alterations on pore-water and microbial community by numerical simulation</i>	268
5.15	Bacterial participation affects quantity and quality of nodules	270
5.16	Conclusion and Future scope	273
6.0	Chapter VI Summary, Conclusion and Future scope	275
	References	282
	Appendices	323
Appendix	<i>I – List of Tables</i>	324
Appendix	<i>II – List of Figures</i>	327
Appendix	<i>III – Photographs</i>	331
Appendix	<i>IV – List of abbreviations</i>	333
Appendix	<i>V- List of media used for culturable bacteria</i>	335
Appendix	<i>VI- List of important chemicals and buffers</i>	340
Appendix	<i>VII- Molecular probes</i>	355
Appendix	<i>VIII- Standard curves</i>	357
Appendix	<i>IX- MATLAB code</i>	360
Appendix	<i>X- List of publications</i>	362

Copies of published papers related to Thesis

“Everything should be made as simple as possible but not simpler”

-Albert Einstein

Chapter I

Introduction

1.1 Distribution of Bacteria

Understanding the distribution of bacteria is important because they are the main link between non-living and higher living resources. This is especially significant in deep-sea systems. The deep sub-seafloor biosphere comprises about 65% of the global prokaryotic biomass (Parkes *et al.*, 1994; Whitman *et al.*, 1998). There are hotspots of bacterial distribution in regions like vents and seeps and low distribution spots like abyssal plains and deep sub-surface. The seafloor environment is a dynamic geosphere that provides a varied range of living conditions that are host to diverse microbial communities (Jørgensen & Boetius, 2007).

Microorganisms although ubiquitous in deep-sea sediments decline in abundance with increasing depth (Parkes *et al.*, 1994, 2000) due to the influence of preferential paths in transport through the sediment profile (Abu-Ashour *et al.*, 1994), limited input of fresh organic carbon at the surface and/or use of recalcitrant old buried organic matter by deep bacteria (Parkes *et al.*, 2000; Wellsbury *et al.*, 2002; Zhang *et al.*, 1998), and low hydraulic conductivity or diffusion for the transport of required chemicals (Fredrickson *et al.*, 1991; Phelps *et al.*, 1994).

1.2 Diversity of Bacteria

The diversity of a system decides the degree of stability. The deep sub-seafloor biosphere supports a diverse population of Bacteria and Archaea both in terms of phylogeny and function. The diversity of prokaryotes is low in ephemeral systems like the hydrothermal vents and high in the more stable systems like the abyssal basins.

The insights about the extent of diversity that may be gained by considering patterns that occur, or are likely to occur, in the relative abundance of prokaryotic taxa are studied. The relationship between structure and function in a community can only be understood, predicted and engineered through an understanding of the source of diversity from which the community is drawn (Curtis and Sloan, 2004).

Recent molecular analyses show that microbial communities of deep marine sediments harbour members of distinct, uncultured bacterial and archaeal lineages, in addition to Gram-positive bacteria and Proteobacteria that are detected by cultivation surveys (Teske, 2006). Several of these subsurface lineages show cosmopolitan occurrence patterns; they can be found in cold marine sediments and also in hydrothermal habitats, suggesting a continuous deep subsurface and hydrothermal biosphere with shared microbiota. The physiologies and activities of these uncultured subsurface lineages remain to be explored by innovative combinations of genomic and biogeochemical approaches (Teske, 2006).

1.3 Activity of Bacteria

The phylogenetic diversity is closely linked to metabolic and functional diversity. The metabolic diversity is greater in case of deep-sea as these systems have diverse substrates as compared to the coastal systems (Harder and Dijkhuizen, 1982, Goltekar *et al.*, 2006). Consequently, the activity of bacteria is highly diversified and varied. So understanding the metabolic activity would be relevant.

Microbes govern the biogeochemical cycles and may function heterotrophically or autotrophically. Heterotrophy might be the most important mode of metabolism in

detrital depositional settings. Chemoautotrophy prevails when heterotrophy is limited by the increasing recalcitrance and decrease in quantity of organic matter (Fry *et al* 2008).

The present thesis entitled “*Distribution, Diversity, and Activity of Bacteria from the Central Indian Ocean Basin*” (CIOB), aims to study the above aspects of sediment bacteriology in the context of geochemical and sedimentological background of this ocean basin. The study deals with bacteria and their interaction with deep-sea sediments and nodules. The interactions cover three austral seasons with samples collected from area enclosed within 10°-16°S and 73°30'-77°30'E. Chemosynthetic potential has been measured in these sediments to understand the chemoautotrophic contribution to carbon fixation. Though several enzymes have been shown to participate in chemosynthetic activity the present study is restricted to the enzyme RuBisCO. The activity of this enzyme is detected for the first time in this part of the ocean basin. Other activities examined include those that feed chemosynthetic processes like nitrification and metal oxidation. Phosphate and silicate solubilization give insights into the community's contribution to the release of these essential nutrients into the surrounding environments.

1.4 Deep-sea environments and bacteria

Microorganisms comprise a large fraction of total benthic biomass and dominate the turnover of organic matter. Microorganisms are the primary agents in the diagenesis of organic matter in the deep sea (Deming and Baross, 1993). Bacteria play a major role in the decomposition of organic matter arriving at the deep-sea floor, and hence there is a need to determine accurate rates of bacterial production associated with sediment particles.

Much of the inherited organic matter is decomposed as a result of oxygen diffusion into the sediment and bacterial activity. Both oxidized and reduced forms of nitrogen are produced in the active oxidation zone. Geochemical processes taking place in the oxidation zone and in the subsequent modification of paleo-oxidation zones almost certainly have a significant impact on the reflux of elements back into the ocean environment.

The bacteria in the deep-sea are generally psychrophilic and barophilic in nature. However, thermophilic and mesophilic bacteria are present in the hydrothermal vents and fluids. ZoBell and Johnson (1949) started work on the effect of hydrostatic pressure on microbial activities. The term “barophilic” was first used, defined as optimal growth at a pressure higher than 0.1 MPa or a requirement for increased pressure for growth. Recently, the term “piezophilic” was proposed to replace “barophilic” as the prefixes “baro” and “piezo” , derived from Greek, mean “weight “and “pressure”, respectively (Yayanos, 1995). Thus, the word piezophilic may be more suitable than barophilic to indicate bacteria that grow better at high pressure than at atmospheric pressure.

Interdisciplinary approaches clarify the question to what extent microorganisms leave their imprint on geochemical processes in the deep, hydrothermally active sediment, cold marine subsurface sediments and in crustal continental rocks. Combinations of culture-dependent, nucleic acid based, and organic biomarker approaches, together with microbial rate measurements, allows functional and phylogenetic identification of bacteria, archaea, and eukaryotes throughout the microbially inhabited sediment column. Methodologically, Ocean Drilling Project (ODP)

legs demonstrate the power of multidisciplinary study of deep subsurface ecosystems (D'Hondt et al., 2003).

The above polyphasic or interdisciplinary strategies have been successful in oligotrophic abyssal environments like the west Pacific warm pool (Wang *et al.*, 2004) and east Pacific nodule rich province (Xu *et al.*, 2005) and other similar environments (Kato *et al.*, 1999; D'Hondt *et al.*, 2002; Glud *et al.*, 1996, Fenchel, 2002).

1.5 Deep-sea environment of Central Indian Ocean Basin (CIOB)

1.5.1 Central Indian Ocean Basin- Geology, Geophysics, Geochemistry

The Polymetallic nodules Project has given Indian scientists at National Institute of Oceanography and many other laboratories an opportunity to perform elaborate research in the CIOB. The Indian Ocean Nodule field has been studied for various aspects of geology, geophysics, geochemistry, physical, chemical and biological oceanographic processes. Some of these aspects are introduced below:

The CIOB has an area of 5.7×10^6 km². The average water depth is about 5400 m (Ghosh and Mukhopadhyay, 1999a, b). The CIOB has been studied for nodule abundance (Sharma and Nath, 2000; Sudhakar 1989), nodule distribution and nature (Ghosh and Mukhopadhyay, 1999; Jauhari and Pattan 1999, Banerjee and Mukhopadhyay, 1991) early diagenetic features like nitrification (Nath and Mudholkar, 1989) and erosional features (Banakar et al, 1991). The basin is divided into five geological sub-environments namely, terrigenous mud, siliceous ooze with and without nodules, pelagic red clays and calcareous ooze (Nath *et al.*, 1989; Rao and Nath, 1988; Mudholkar et al., 1993). The oxygen and nutrient-rich Antarctic Bottom Water Current

entering the CIOB from 5°S (Gupta and Jauhari, 1994) maintains oxic condition with near neutral pH in the basin. CIOB is bordered by the 90°E Ridge in the East, the Central Indian Ridge (CIR) in the West and the Southeast Indian Ridge (SEIR) in the South. The region is marked by fracture zones namely the Vishnu fracture or La Boussole (FZ along 73° E) and the Indrani Fracture or L'Astrolabe (FZ along 79°E) and 76.5°E FZ (Mukhopadhyay *et al.*, 2002; Iyer *et al.*, 2007) and trace of the Rodriguez Triple Junction roughly between 76°and 78°E (Dyment, 1993; Kamesh Raju and Ramprasad, 1989). Seamounts hosting Normal-Mid Ocean Ridge basalts are located along eight chains and represent propagative fractures (Das *et al.*, 2005, 2007). The southern pelagic volcanic realm bears signatures of hydrothermal alterations of recent origin due to tectonic reactivation of fracture zones (Mascarenhas-Pereira *et al.*, 2006, Iyer *et al.*, 2007 and Nath *et al.*, 2008).

Internationally, geophysical and geochemical studies on the northern and northeastern parts of CIOB are more common. The lithosphere beneath those parts of Central Indian Basin is characterized by high heat flow, widespread deformation of sediment and acoustic basement, and unusually high seismicity. The high heat flow suggests that temperatures in the lithosphere may be higher than expected for its age. Despite the heat flow anomaly, the lack of an average bathymetric anomaly and the observation of seismicity to a depth of 40 km indicate that lithospheric temperatures in the Central Indian Basin are not significantly different from those expected for its age (Stein and Weissel, 1990). Later studies showed that the heat flow in the actively deforming Central Indian Basin is on average 30 mW/m² higher than the theoretical

55mW/m² heat flow expected from plate cooling of a Cretaceous oceanic lithosphere (Delescluse and Chamot-Rooke 2008).

1.5.2 Central Indian Ocean Basin- Thermohaline circulation, Chemistry and Biology

Thermohaline circulation has been studied during austral summer and winter periods. A saddle overflow at the Ninety East Ridge links the deep water of CIOB (Ramesh Babu *et al.*, 2001). Chemical characteristics were studied during austral summer. Subsurface salinity maximum at 125-200m coincided with oxygen minimum and weak maxima in nutrients (De Souza *et al.*, 2001). Deep oxygen minimum at 250-700m coincided with nutrient minima and relatively higher pH (De Souza *et al.*, 2001). Water of minimum salinity corresponding to the Antarctic Intermediate Water (AAIW) was detected at 800-1200m (De Souza *et al.*, 2001). Distribution of dissolved organic matter (DOM) in the water masses suggested the refractory nature of DOM (Sardessai and De Sousa, 2001).

Faunal diversity of macro- and meiofauna has been documented (Ingole *et al.*, 2005). Distribution of macrofauna in the basin has been correlated to labile organic matter and sedimentary properties (Pavithran, 2008). Damare *et al.*, 2006 studied the distribution and activity of deep-sea fungi.

1.5.3 Central Indian Ocean Basin- Microbiology and Biochemistry

Bacteriology of ferromanganese nodules in the Central Indian Basin showed a variety of heterotrophic bacteria capable of mobilizing and immobilizing manganese (Chandramohan *et al.*, 1987). Biochemical and microbial studies in the sediments of

Central Indian Basin have predominantly discussed the role and response of bacterial community to artificially simulated disturbance (Nair *et al.*, 2000, Raghukumar *et al.*, 2001) and long term response to the same (Raghukumar *et al.*, 2006). Artificial disturbance appeared to revive dormant bacteria and enhance bacterial culturability (Loka Bharathi and Nair, 2005). More specific studies on deep-sea cultures and their role in nitrification have also been reported (Ram *et al.* 2001). With clay and silt dominating sediment textures, sediment grain size and associated bacterial properties were suggested as indicators of biogeochemical processes useful for mineral exploration and harnessing in marine environments (Khadge, 2002; Valsangkar, 2004; Sharma, 2005). Early diagenetic processes and extensive nitrification in this region influence the origin, type and quality of manganese nodules (Nath and Mudholkar, 1989) and sediment biogeochemistry as a whole. The microbial community might co-express both chemolithotrophy and organotrophy. This would enable efficient recycling of the limited photosynthetically derived organic matter (Stevens, 1997; Ehrlich, 1998). Cultured bacterial representatives showing both phases of nitrification have been isolated from this region (Ram *et al.*, 2001).

Early phases of diagenesis are controlled by several biotic and abiotic factors, an important component being bacteria. Multiple phases of nitrification and oxic respiration are observed corroborating to previous results (Ram *et al.*, 2001, Nath and Mudholkar, 1989). Sub-oxic mottles have been discussed in literature as aspects of paleoproductivity, preservation, and present bacterial activity. Simulated disturbance in the sea floor brought about an increase in culturable abundance, taxonomic and functional diversity of deep-sea sediments of the CIOB (Loka Bharathi and Nair, 2005). Despite all these efforts the

geomicrobiology and biogeochemistry of the Central Indian Basin remains understudied. Some parts of the basin especially the southern pelagic red clay sector was unexplored.

1.6 Aim of the study

The present study aims to understand the diversity, activity, and function of bacteria in the Central Indian Basin. It would also endeavour to improve their culturability. Besides profiling for various enzymatic activities, attempts would be specifically made to delineate the spread of RuBisCO activity and its function, as it is hypothesised that this function is widespread in oligotrophic environment.

1.7 Objectives of the study

- To understand the quantitative and qualitative distribution of bacteria along latitudinal gradient.
- To improve culturability of deep-sea bacteria by different combinations of media.
- To understand the interaction of bacteria with environmental parameters.
- To elucidate their contribution to activities like autotrophic growth, nitrifying activity/denitrifying activity, metal oxidizing and reducing potential, phosphate solubilization and silicate solubilization. These activities would be measured holistically in sediments or individually with cultures.

1.8 Importance of the present study

- The knowledge on bacterial distribution and activity could be used for better management of deep-sea ecosystems for marine mining of resources.

- Understanding deep-sea bacterial diversity and harnessing marine microbes for biotechnological applications could be some of the important outcome of the present work.
- Robust numerical simulations explaining thermodynamics of the biogeochemical reactions in CIOB would be possible with the availability of data on heat flux and fluid flow.
- The present work would also trigger interesting research on the deep-biosphere in CIOB and could stimulate the pursuit of chemosynthesis for sequestering CO₂ in the deep sea floor.

“The chemistry of the universe seems to be leading to life.

The universe seems to be in the business of creating life.”

-Cyril Ponnampereuma

Chapter II

Review of Literature

2.1 Abundance and Distribution

Microorganisms although ubiquitous in deep-sea sediments decline in abundance with increasing depth (Parkes *et al.*, 1994, 2000) due to the influence of preferential paths in transport through the sediment profile (Abu-Ashour *et al.*, 1994), limited input of fresh organic carbon at the surface, recalcitrance old buried organic matter (Parkes *et al.*, 2000; Wellsbury *et al.*, 2002; Zhang *et al.*, 1998), and low hydraulic conductivity or diffusion for the transport of required chemicals (Fredrickson *et al.*, 1991; Phelps *et al.*, 1994). Geometrical constraints and mechanical interactions restrict bacterial movement and activity (Fredrickson *et al.*, 1997), limit nutrient transport (Wellsbury *et al.*, 2002), diminish space availability (Zhang *et al.*, 1998), slow the rate of division (Boivin-Jahns *et al.*, 1996), and lead to reduced biodiversity and spatial isolation of lineal descendants of bacteria entombed by geologic deposition (Boivin-Jahns *et al.*, 1996; Kieft *et al.*, 1998; Treves *et al.*, 2003; Zhou *et al.*, 2002, 2004). Mechanical consolidation of deep sediment sequences and interaction between bacteria and sediments predict the fate of bacteria as: “active and motile,” “trapped inside pores,” and “dead or dormant.” (Rebata-Landa and Santamarina, 2006).

The subsurface biosphere on Earth appears to be far more expansive and physiologically and phylogenetically complex than previously thought. Molecular and biogeochemical data, as well as characteristics from new isolates, suggest that ecosystems below deep-sea hydrothermal vents are inhabited primarily by thermophilic archaea and bacteria. The void spaces and conduits in basalt at mid-ocean ridges, and, even more so, at sediment covered hydrothermal vent sites represent promising hunting grounds for novel chemosynthetic archaea and bacteria. In the deep continental

subsurface, microbial studies have primarily targeted aquifers in basaltic and granitic rock, with an almost exclusive emphasis on H₂-driven chemolithoautotrophy. For example, in the subsurface water from Lidy Hot Springs, Idaho (USA), H₂-consuming methanogenic archaea represent the most populous organisms, comprising >95% of all cells. Besides H₂, other potential sources of chemical energy (reducing power) are considered, including abiotically synthesized organic matter and reduced sulfur compounds. In addition, the well-established sequences of redox couples in microbial metabolism are investigated at elevated temperatures using a thermodynamic approach. Although many modes of metabolism may be employed by subsurface biota, sulfate reduction appears to be one of the more ubiquitous strategies. Recent studies of sulfate-reducing archaea and bacteria in marine and continental systems have been reviewed (Amend and Teske, 2005).

Recent molecular analyses show that microbial communities of deep marine sediments harbor members of distinct, uncultured bacterial and archaeal lineages, in addition to Gram-positive bacteria and Proteobacteria that are detected by cultivation surveys. Several of these subsurface lineages show cosmopolitan occurrence patterns; they can be found in cold marine sediments and also in hydrothermal habitats, suggesting a continuous deep subsurface and hydrothermal biosphere with shared microbiota. The physiological activities of these uncultured subsurface lineages remain to be explored by innovative combinations of genomic and biogeochemical approaches (Teske, 2006).

Studies of deeply buried, sedimentary microbial communities and associated biogeochemical processes during Ocean Drilling Program Leg 201 showed elevated prokaryotic cell numbers in sediment layers where methane is consumed anaerobically at

the expense of sulphate. Here, it is shown that extractable archaeal rRNA, selecting only for active community members in these ecosystems, is dominated by sequences of uncultivated Archaea affiliated with the Marine Benthic Group B and the Miscellaneous Crenarchaeotal Group, whereas known methanotrophic Archaea are not detectable (Biddle *et al.*, 2006). Carbon flow reconstructions based on stable isotopic compositions of whole archaeal cells, intact archaeal membrane lipids, and other sedimentary carbon pools indicate that these Archaea assimilate sedimentary organic compounds other than methane even though methanotrophy accounts for a major fraction of carbon cycled in these ecosystems. Maintenance energies of these subsurface communities appear to be orders of magnitude lower than minimum values known from laboratory observations, and ecosystem-level carbon budgets suggest that community turnover times are on the order of 100–2,000 years (Biddle *et al.*, 2006).

2.2 Diversity

Global reservoirs of diversity are an important driving force behind patterns in localised diversity. Thus, where the reservoir community is very large and relatively even, chance alone will prevent physically identical communities from having the same, or sometimes even stable, communities. By contrast, communities that tend to be similar (even when not physically identical) and stable are observed where the source diversity is low. Thus the relationship between structure and function in a community can only be understood, predicted and engineered through an understanding of the source of diversity from which the community is drawn. Patterns in global microbial diversity have been known to affect community composition, stability and functionality at a local level. To

understand microbial systems at a local level something of the metacommunity from which it is drawn would have to be understood. Moreover, one would have to correctly understand the relationship between random factors and deterministic factors. It has been pointed out that microbiologists have typically ignored the former and that it would be fruitful to rectify this situation and to develop a deeper appreciation of the role of chance in microbial ecology (Curtis and Sloan, 2004).

a. The Non-culturable diversity

The term “the great plate count anomaly” was coined by Staley and Konopka in 1985 to describe the difference in orders of magnitude between the numbers of cells from natural environments that form colonies on agar media and the numbers countable by microscopic examination (Jannasch, and Jones, 1959). Marine ecosystems are a well-studied example of this phenomenon: only 0.01 to 0.1% of oceanic marine bacterial cells produce colonies by standard plating techniques (Kogure *et al.*, 1979). There are numerous explanations for this anomaly. Species that would otherwise be “culturable” may fail to grow because their growth state in nature, such as dormancy, prevents adjustment to conditions found in the medium used for the plate counts (Deming and Baross, 2000). Many of the microbial species that dominate in natural settings are not adapted for growth in media containing high concentrations of complex organic carbon. Many microorganisms may need oligotrophic or other fastidious conditions to be successfully cultured. Button and colleagues pioneered an approach that has been successful in isolating novel oligotrophic, heterotrophic cells from marine ecosystems (Button *et al.*, 1993). This method uses unamended environmental water as the medium and is often referred to as “extinction culturing” to distinguish it from dilution culturing,

which also uses natural water, but involves complex microbial communities (Ammerman, *et al.*, 1984, Carlson and Ducklow, 1996, Li and Dickie, 1985). High-throughput culturing (HTC) methods would enable a large number of extinction cultures to be identified so that the efficacy of this approach could be assessed with a larger sampling of isolates. The results indicate that these newly developed HTC techniques yield isolates of many novel microbial strains, including members of previously uncultured groups that are believed to be abundant in coastal seawater (Connon and Giovannoni, 2002).

Recent advances in the estimation of prokaryotic diversity have brought insight into the question: what is the extent of prokaryotic diversity? The evolution of marine microbes over billions of years predicts that the composition of microbial communities should be much greater than the published estimates of a few thousand distinct kinds of microbes per liter of seawater. Recently, however pyrosequencing has emerged as a new sequencing methodology. This technique is a widely applicable, alternative technology for the detailed characterization of nucleic acids. Pyrosequencing has the potential advantages of accuracy, flexibility, parallel processing, and can be easily automated. Furthermore, the technique dispenses with the need for labelled primers, labelled nucleotides, and gel-electrophoresis (Ronaghi, 2001). By adopting a massively parallel tag sequencing strategy, it has been shown that bacterial communities of deep water masses of the North Atlantic and diffuse flow hydrothermal vents are one to two orders of magnitude more complex than previously reported for any microbial environment. A relatively small number of different populations dominate all samples, but thousands of low-abundance populations account for most of the observed phylogenetic diversity. This “rare biosphere” is very ancient and may represent a nearly inexhaustible source of

genomic innovation. Members of the rare biosphere are highly divergent from each other and, at different times in earth's history, may have had a profound impact on shaping planetary processes. By necessity, microbial oceanographers have focused their efforts on dominant components of microbial communities that mediate biogeochemical processes. What they have not tackled are very low-abundance members of microbial populations. The extreme phylogenetic diversity of the rare biosphere suggests these minor populations have persisted over geological time scales and that they may episodically reshape planetary processes (Sogin *et al.*, 2006).

Evolutionary relationships of cultivated barophilic bacteria showed psychrophilic and barophilic isolates were affiliated with one of five genera of the gamma subdivision of the class *Proteobacteria* (γ -*Proteobacteria*): *Shewanella*, *Photobacterium*, *Colwellia*, *Moritella*, and a new group containing strain CNPT3. The data indicate that the barophilic phenotype has evolved independently in different γ -*Proteobacteria* genera (Delong *et al.*, 1997).

The prokaryotic phylogenetic diversity was determined for a sample associated with an in situ growth chamber deployed for 5 days on a Mid-Atlantic Ridge hydrothermal vent. No Archaea were detected in the sample. Eighty-seven clones containing bacterial 16S rDNA inserts were selected. Based on restriction fragment length polymorphism analysis, 47 clones were unique, however, based on comparative sequence analysis some of these were very similar, and thus only 22 clones were selected for full sequence and phylogenetic analysis. The phylotypes were dominated by ϵ -*Proteobacteria* (66%). The remainder formed a novel lineage within the *Proteobacteria* (33%). One clone formed a distinct deeply branching lineage, and was a distant relative

of the Aquificales. This report further expands the growing evidence that ϵ -Proteobacteria are important members in biogeochemical cycling at deep-sea hydrothermal ecosystems, participating as epibionts and free living bacteria (Corre *et al.*, 2001).

Though microbes are known to play varied roles, including the large role in metal cycling in many environments, their in nodule province of even Pacific is scantily studied. The Pacific nodule province covers about 4.5 million km² in the eastern tropical Pacific with abundance of polymetallic nodules. Phylogenetic studies based on 16S rRNA gene sequence analysis, together with bacterial cultivation were used to study the microbial populations in the Pacific nodule province deep-sea sediment. Bacterial 16S rRNA gene sequence analysis demonstrated that Proteobacteria division mainly of γ -Proteobacteria dominated the microbial community of the nodule province A core. Among the γ -Proteobacteria, *Shewanella* species which were known as Fe and Mn-reducing bacteria were found prevalent. Besides Proteobacteria, green nonsulfur bacteria, the candidate subdivision OP3, *Cytophaga-Flexibacter-Bacteroides* bacteria and novel unidentified strains were also detected. Archaeal 16S rDNA sequence analysis data and results from hybridization with crenarchaeotal marine group I specific probe revealed that all archaea detected at the station belong to Crenarchaeota nonthermophilic marine group I. Among bacteria assigned to the gamma Proteobacteria which were isolated, none of them showed capability of manganese oxidation (Xu *et al.*, 2005).

b. Culturable diversity

Bacteria living in the deep-sea display several unusual features that allow them to thrive in their extreme environment. The first pure culture of a piezophilic isolate, strain CNPT-3, was reported in 1979 (Yayanos *et al.*, 1979). This spirillum-like bacterium had

a rapid doubling rate at 50 MPa, but no colonies were formed at atmospheric pressure even after incubation for several weeks. Numerous piezophilic and piezotolerant bacteria have since been isolated and characterized by the DEEPSTAR group at JAMSTEC, from deep-sea sediments at depths ranging from 2,500 m-11,000 m (Kato *et al.*, 1995a; 1996a; 1996b; 1998).

Many deep-sea piezophilic bacteria have been shown to belong to the γ -Proteobacteria through comparison of 5S and 16S rDNA sequences. As a result of a taxonomic study based on 5S rDNA sequences, Deming reported that the obligate piezophilic bacterium *Colwellia hadaliensis* belongs to the Proteobacteria γ -subgroup (Deming *et al.*, 1988). DeLong *et al.* (1997) have also documented the existence of piezophilic and psychrophilic deep-sea bacteria that belong to this subgroup, as indicated by 16S rDNA sequences.

Actinomycetes have also been cultivated using a variety of media and selective isolation techniques from 275 marine samples collected around the island of Guam. In total, 6,425 actinomycete colonies were observed and 983 (15%) of these, representing the range of morphological diversity observed from each sample, were obtained in pure culture. The majority of the strains isolated (58%) required seawater for growth indicating a high degree of marine adaptation. The dominant actinomycete recovered (568 strains) belonged to the seawater-requiring marine taxon '*Salinospora*', a new genus within the family Micromonosporaceae. A formal description of this taxon includes a revision of the generic epithet to *Salinispora* gen. nov. Members of two major new clades related to *Streptomyces* spp., tentatively called MAR2 and MAR3, were cultivated and appear to represent new genera within the Streptomycetaceae. In total, five new marine

phylotypes, including two within the Thermomonosporaceae that appear to represent new taxa, were obtained in culture. These results support the existence of taxonomically diverse populations of phylogenetically distinct actinomycetes residing in the marine environment. These bacteria can be readily cultured using low nutrient media and represent an unexplored resource for pharmaceutical drug discovery (Jensen *et al.*, 2005).

Two bacterial strains BBH5 and BBH87T were isolated from a deep-sea sediment sample collected from the Chagos Trench of the Indian Ocean (11°06' S, 72°31' E). Both the strains, based on their 16S rRNA gene sequence similarity (99.9 %), DNA-DNA relatedness (93 %) and a number of similar phenotypic characteristics have been identified as strains of the same species. The phylogenetically nearest species of BBH5 and BBH7T based on 16S rRNA gene sequence similarity (97.9 – 98.4 %) were identified as *Brevibacterium iodinum*, *Brevibacterium epidermidis*, *Brevibacterium linens* and *Brevibacterium permense*. However, BBH5 and BBH7T differ from the above four nearest phylogenetic relatives by a number of phenotypic characteristics and the DNA-DNA similarity between the two isolates and the above was 35 – 42 %. Therefore, it was proposed to classify BBH5 and BBH7T as belonging to a new species of *Brevibacterium* for which the name *Brevibacterium oceani* sp. nov. was proposed with BBH7T (=LMG23457T = IAM15353T) as the type strain (Bhadra *et al.* 2008).

Filter-feeder macroinvertebrates were found to be key players in the control of biodiversity of culturable bacteria in a case of study with *Sabella spallanzanii* (Polychaeta: Sabellidae). The comparison was made between the bacterial diversity in transplanted polychaetes and the surrounding seawater. Some bacterial genera showed higher average abundances in polychaetes than in seawater (i.e. *Lucibacterium* and

Photobacterium). *Aeromonas* represented a conspicuous component of the bacterial community both in *S. spallanzanii* and seawater. The presence of *Cytophaga* and *Pseudomonas* was also relevant in the examined seawater samples. The selective concentrations of some bacterial genera inside *S. spallanzanii* either by grazing on bacteria or their capability as bacterial reservoirs, provides evidence for the role of macrobenthic invertebrates as key determinants for microbial diversity (Licciano *et al.*, 2007).

During the past several years, understanding of the ecological importance of culturable and uncultured lineages of marine picoplankton has been repeatedly challenged. Some genera of marine bacteria that are frequently isolated by classic ZoBell techniques are apparently rare in the picoplankton of coastal North Sea surface waters, as determined by direct counts after specific fluorescence *in situ* hybridization (FISH) (Eilers *et al.*, 2000a, b). Representatives of such readily culturable bacterial lineages with conspicuously low *in situ* population densities in the German Bight are *Alteromonas*, *Colwellia*, *Pseudoalteromonas*, and *Vibrio* (Eilers *et al.*, 2000b). Since members of these genera typically form larger cells than so-called “oligotrophic” marine isolates (Button *et al.*, 1998, Rappe *et al.*, 2002), they hypothesized that these opportunistically growing γ -proteobacteria might be a preferred target of selective predation. Beardsley *et al.*, 2003 showed that selective grazing mortality on these groups accounted for low culturability.

Microbial diversity studies based on the cloning and sequencing of DNA from nature support the conclusion that only a fraction of the microbial diversity is currently represented in culture collections. Out of over 40 known prokaryotic phyla, only half have cultured representatives. In an effort to culture the uncultured phylotypes from

oligotrophic marine ecosystems, high-throughput culturing procedures that utilize the concept of extinction culturing have been standardised to isolate cultures in small volumes of low-nutrient media. In these experiments, marine bacteria were isolated and cultivated at *in situ* substrate concentrations—typically 3 orders of magnitude less than common laboratory media. Microtiter plates and a newly developed procedure for making cell arrays were employed to raise the throughput rate and lower detection sensitivity, permitting cell enumeration from 200- μ l aliquots of cultures with densities as low as 10^3 cells/ml. Approximately 2,500 extinction cultures from 11 separate samplings of marine bacterioplankton were screened over the course of 3 years. Up to 14% of the cells collected from coastal seawater were cultured by this method, which was 14- to 1,400-fold higher than the numbers obtained by traditional microbiological culturing techniques. Among the microorganisms cultured were four unique cell lineages that belong to previously uncultured or undescribed marine *Proteobacteria* clades known from environmental gene cloning studies. These cultures are related to the clades SAR11 (α subclass), OM43 (β subclass), SAR92 (γ subclass), and OM60/OM241 (γ subclass). This method proved successful for the cultivation of previously uncultured marine bacterioplankton that have consistently been found in marine clone libraries (Connon *et al.*, 2002) .

The intestinal flora of seven deep-sea fish retrieved at depths of from 3,200 to 5,900m were examined for population sizes and growth responses to pressure. Large populations of culturable bacteria, ranging from 1.1×10^6 to 3.6×10^8 cells per ml of contents, were detected when samples were incubated at conditions characteristic of those of the deep sea. Culturable cell counts at *in situ* pressures were greater than those at

atmospheric pressure in all samples. Most of the strains isolated by the spread-plating method at atmospheric pressure later proved barophilic. Barophilic bacteria were the predominant inhabitants of the abyssal fish intestines (Yano *et al.*, 1995).

2.3 Activity

Microorganisms comprise a large fraction of total benthic biomass and dominate the turnover of organic matter. Microbial organisms are the primary agents in the diagenesis of organic matter in the deep sea (Deming and Baross, 1993a, and references therein). Bacteria play a major role in the decomposition of organic matter arriving at the deep-sea floor, and hence there is a need to determine accurate rates of bacterial production associated with sediment particles. However, sediment-based procedures are not well defined and sampling deep-sea sediments is technically difficult, time consuming, and expensive, often only producing relatively small amounts of undisturbed sediment for analysis. Waters >2,000 m cover 60% of the Earth's surface; thus bacterial production in deep-sea sediments must contribute an important fraction of oceanic and global bacterial production (Dixon and Turley, 2001).

In natural and man-made environments microorganisms often grow in the presence of a diversity of functionally similar substrates. The pattern of utilization of these mixed substrates is generally dependent upon their concentration. When substrates are present in high (non-growth-limiting) concentrations, sequential utilization and diauxic growth is often observed and the substrate that supports the highest growth rate is utilized preferentially from the mixture. When the substrate concentrations are growth

limiting, simultaneous utilization of the various compounds present in the mixture appears to be the general response (Harder and Dijkhuizen, 1982).

Chemical analyses of the pore waters from hundreds of deep ocean sediment cores have over decades provided evidence for ongoing processes that require biological catalysis by prokaryotes. This sub-seafloor activity of microorganisms may influence the surface earth by changing the chemistry of the ocean and by triggering the emission of methane, with consequences for the marine carbon cycle and even the global climate. Despite the fact that only about 1% of the total marine primary production of organic carbon is available for deep-sea microorganisms, sub-seafloor sediments harbour over half of all prokaryotic cells on Earth. This estimation has been calculated from numerous microscopic cell counts in sediment cores of the Ocean Drilling Program. Because these counts cannot differentiate between dead and alive cells, the population size of living microorganisms is unknown. Here, using ribosomal RNA as a target for the technique known as catalysed reporter deposition-fluorescence *in situ* hybridization (CARD-FISH), authors provide a direct quantification of live cells as defined by the presence of ribosomes. They have shown that a large fraction of the sub-seafloor prokaryotes is alive, even in very old (16 million yr) and deep (>400 m) sediments. All detectable living cells belong to the Bacteria and have turnover times of 0.25–22 yr, comparable to surface sediments (Schippers *et al.*, 2004).

In order to observe the effect of hydrostatic pressure on the deep-sea bacterial population, growth experiments were conducted with water samples collected from depths of 0, 2000, 4000 and 6000 m at two locations in the northwest Pacific Ocean. When the water samples were incubated under different pressures at 2°C, good growth

was observed at pressure levels of the depths where the samples were collected. These results suggest that the bacterial population at each depth of the deep-sea is well adapted to the environmental conditions, as has been suggested by Yayanos (1986) with pure culture isolates from the deep-sea (Sakiyama and Ohwada, 1998).

Fluxes of particulate matter to depth and dynamics of dissolved organic matter in the water column are influenced by microbial processes associated with organic aggregates like marine snow. These microscale processes include the encounter between bacteria and aggregates, which has been previously modelled and tested with well-fed and actively growing bacteria. The effects of starvation on initial bacterial colonization of aggregates have been investigated by measuring colonization and detachment of 6 isolates in different physiological states (fed vs. starved) using model aggregates. Because aggregate encounter depends on motility, the motility behaviours of fed and starved bacteria of 3 selected strains were also compared using image analysis. All 6 fed isolates colonized faster and achieved significantly higher steady-state abundances on model aggregates than those that were starved. However, there was no difference in detachment rates between fed and starved bacteria. The 3 selected strains had significantly lower average swimming speeds when starved. Diffusivities calculated from motilities of 2 starved isolates were more than 6 times lower than those of their fed counterparts. Starvation significantly affected bacterial behaviour and bacteria–aggregate interactions, which might have lead to differences in particulate and dissolved organic matter fluxes and cycling under different productivity regimes (Yam and Tang, 2007).

Diffusive flux of dissolved organic carbon (DOC) from deep-sea sediments, a poorly constrained component of the global marine carbon cycle, but might play an

important role for DOC concentrations in the oceans. Pore-water DOC concentrations were usually one order of magnitude greater than in bottom waters, with maximum DOC contents between 509 and 1526 mmol L⁻¹ in the uppermost sediment interval (0–0.5 cm). DOC values generally decrease towards ~3 cm core depth with slightly increasing concentrations in deeper layers under sub-oxic to anoxic conditions. In deep-sea sediments, about 21–25% of the sedimenting POC flux is decomposed to DOC and subsequently released from the sediments. Incoming POC fluxes and diffusive DOC effluxes are strongly positively correlated in open-ocean regions. (Lahajnar *et al.*, 2005).

Influence of fauna and food supply vis-à-vis bioturbation was studied in the Arabian Sea Biological mixing of sediments (bioturbation) and could modify the physical, chemical and biological properties of sediments. Therefore, bioturbation affects early diagenesis and the evolution of the sedimentary record in surface sediments. Two principal modes of bioturbation could be differentiated. Particles may be mixed in a way resulting in diffusive-looking tracer profiles (diffusive mixing) or by non-local mixing i.e., transport of particles between non-adjacent sediment layers (Turnewitsch *et al.*, 2000 and references therein).

Isotopic analyses of *Candidatus "Brocadia anammoxidans,"* a chemolithoautotrophic bacterium that anaerobically oxidizes ammonium (anammox), show that it strongly fractionates against ¹³C; i.e., lipids are depleted by up to 47‰ versus CO₂. Similar results were obtained for the anammox bacterium *Candidatus "Scalindua sorokinii,"* which thrives in the anoxic water column of the Black Sea, suggesting that different anammox bacteria use identical carbon fixation pathways, which may be either the Calvin cycle or the acetyl coenzyme-A pathway. The study of the stable carbon

isotopic compositions of lipids and the biomass of anaerobic ammonium oxidizing bacteria shows that they possess a carbon fixation pathway which strongly fractionates against ^{13}C . The results are consistent with either the use of the Calvin cycle or perhaps more likely, based on the large ^{13}C depletions, the acetyl-CoA pathway (Schouten *et al.*, 2004). These activities measured in bacteria are in response to different geochemical settings.

2.4 Response to various geochemical settings

2.4.1 *Diagenesis and bacteria*

Diagenesis is the “sum of all processes that change a sediment or sedimentary rock subsequent to its deposition from water, but excluding metamorphism and weathering” (Berner, 1980).

Diagenetic reactions in marine sediments have long been recognised by detailed examination of chemical gradients in pore solutions. Many of the observed variations with depth in the sediments have been attributed to the effects of early oxidation of organic matter in the near-surface sediment column (Lynn and Bonatti, 1965; Presley *et al.*, 1967; Bischoff and Ku, 1970; Li *et al.*, 1969; Li and Gregory, 1974; Bender *et al.*, 1977; Froelich *et al.*, 1979; Emerson *et al.*, 1980; Sayles, 1981; Goloway and Bender, 1982; Jahnke *et al.*, 1982; Sawlan and Murray, 1983; Burdige and Gieskes, 1983).

The TOC concentrations and the organic C/N ratios fluctuate with depth and do not consistently increase or decrease. Mean values of 7.7 ± 1.4 indicates that the organic matter originates predominantly from marine sources (Premuzic *et al.*, 1982; Emerson and Hedges 1988; Jasper and Gagosian 1990; Meyers 1994; Prahl *et al.*, 1994). In

general, marine organic matter is considered more susceptible to *in situ* oxidation in marine sediments than is the more refractory organic matter derived from land plants (Lallier-Vergès *et al.*, 1993). Degradation of organic matter in organic-carbon poor sediments tends to lower C/N ratios as nitrogenous compounds break down to produce ammonia, which is retained by clay minerals, and the CO₂ released originate from the thermal breakdown of organic matter in deeper sediments and upward migration to shallower levels (Claypool and Kvenvolden 1983).

Emphasis was placed on manganese remobilization in near-surface sediments due to these diagenetic effects (Michard, 1971; Bender, 1971; Calvert and Price, 1972). Attempts have been made to refine models which link microbial decomposition of organic matter with the formation of authigenic metal precipitates (Suess, 1979; Pedersen and Price, 1982). The scope of a few such studies also included several trace metals (Hartmann, 1979; Sawlan and Murray, 1983). Lyle (1983) pointed out that the brown-green color transition can probably be used to mark the ferric-ferrous iron boundary in sediments. Based in part on earlier work by Muller and Suess (1979) which concluded that the organic matter content in buried sediments reflects the paleo-productivity of the oceans, Lyle (1983) also concluded that studies of the variation in thickness of the brown (oxidized) sediments could be used to define regional differences in primary productivity.

Much of the deposited organic matter is decomposed as a result of oxygen diffusion into the sediment and bacterial activity. Both oxidized and reduced forms of nitrogen are produced in the active oxidation zone. Geochemical processes taking place in the oxidation zone and in the subsequent modification of paleo-oxidation zones almost certainly have a significant impact on the reflux of elements back into the ocean

environment. Refinement of geochemical models of diagenesis and oceanic cycling has been suggested by Buckley and Cranston, 1988. The authors cautioned against possibility of these features being misinterpreted as reflecting periodic changes in oceanic productivity, rather than diagenetic features. Also, the color transitions were cautioned against erroneous interpretations as being due to fluctuations in oceanic redox conditions caused by changes in bottom water oxygen content (Buckley and Cranston, 1988).

The west Pacific deep-sea sediment surface is slightly oxic, the occurrence of oxic methylotrophs have been detected in the sediment surface layer (Wang *et al.*, 2004). Open ocean deep-sea sediments of this region are generally organic poor, low methane, low oxygen, dark and cold (1–2°C) environments (Kato, 1999; D'Hondt *et al.*, 2002). However, the properties of sediment core are very complex. The sediment structure is seldom uniform, it contains complex and different microenvironments even in the same sediment layer (Glud *et al.*, 1996, Fenchel *et al.*, 2002). Presence of anaerobic microbial community taking part in the C-1 metabolism in the oxygen limited deep-sea sediment cores was therefore highlighted (Wang *et al.*, 2005).

Early phases of diagenesis are controlled by several abiotic and biotic factors an important component being bacteria. Multiple phases of nitrification and oxic respiration are observed corroborating to previous results (Ram *et al.*, 2001, Nath and Mudholkar, 1989). Sub-oxic mottles have been discussed in literature as aspects of paleoproductivity, preservation, and present bacterial activity.

Deep-sea sediments that are primarily formed through the continual deposition of particles from the productive ocean surface cover approximately 70% of the earth's surface. The organic matter settled on the sea floor is re-mineralized by the benthic

microbial communities that colonize the sediments. The activities of ocean sediment microorganisms play important roles in the global cycling of carbon and nutrients (Vetriani *et al.* 1999; D'Hondt *et al.*, 2002).

In broad terms, the progression of terminal electron acceptors begins with O₂ near the surface, followed, by increasing depth, with NO³⁻, NO²⁻, Mn(IV), Fe(III), SO₄²⁻, and finally CO₂. This thermodynamically predicted progression, determined from values of the standard Gibbs free energies of reaction ($\Delta G'^{\circ}$), is typically paralleled by a microbial metabolic succession (Stumm and Morgan, 1996). In oxic systems, aerobic respiration tends to dominate, followed, with increasing depth and decreasing oxygen concentration, by denitrification, dissimilatory Mn- and Fe reduction, sulfate-reduction, and lastly autotrophic methanogenesis; fermentation and acetoclastic methanogenesis also occur at very low redox potentials. It is worth noting that the predicted succession of reactions is:

a) based on thermodynamic properties under standard state conditions and not conditions that exist in the natural environment;

b) calculated only at 25°C and 1 bar and not at in situ temperatures and pressures. The *in-situ* energy-yields from a reaction depend on temperature, pressure, and chemical composition, and are therefore site- or sample-specific (Amend and Teske, 2005); however,

c) sometimes kinetic considerations over-ride thermodynamics.

2.4.2 *Hydrothermal alterations and bacteria*

Hydrothermal vents on or near mid-ocean ridges are excellent candidates for biologically active hot spots in the Earth's crust, since they provide chemical energy

sources that can be utilized by microorganisms (Karl, 1995). The deep hydrothermal subsurface includes the extensive zone where seawater is entrained into porous, freshly formed ocean crust and undergoes hydrothermal alteration. The steep thermal gradients there favour the presence of thermophilic microorganisms. At present, the temperature-limit for growth of the two most hyperthermophilic microorganisms in pure culture stands at 113 and 121°C; even higher temperatures may be tolerated during short-term survival (Blöchl *et al.*, 1997; Kashefi and Lovley, 2003). Interpreting these microbially permissible temperature maxima in the context of standard geothermal gradients in the Earth's crust suggests that the habitable zone in the subsurface may be several kilometers deep (Colwell, 2001). The extent of the habitable subsurface zone at hydrothermally active mid-ocean ridges is unknown, but must be limited by the depth of the magmatic heat source. At the fast-spreading East Pacific Rise (EPR), for example, the depth of the magmatic heat source is circa 1.6–2.4 km below the sea floor, but at the slow-spreading Mid-Atlantic Ridge (MAR), the geothermal heat source is located at 3–3.5 km below the rift valley floor (Alt, 1995). Independent of temperature constraints, low-permeability dikes that overlie the magmatic heat source probably limit the microbially accessible subsurface environment to the upper few hundred meters of permeable volcanic basalts and metal-sulfide deposits (Alt, 1995).

Deep marine hydrothermal vents as windows to the subsurface biosphere have gathered much attention in our quest to explore and understand the limits of life on Earth (e.g., Deming and Baross, 1993b). However, the deep continental biosphere has not gone unnoticed. Numerous studies have targeted flood basalts, granites, sedimentary deposits, and mine shafts to find signs of past or present microbial life (e.g., Fredrickson and

Onstott, 2001; Gold, 1992; Gold, 1999; Kotelnikova and Pedersen, 1998; Pedersen, 1997; Pedersen, 2000a,b; Pedersen, 2001; Stevens, 1997; Stevens and McKinley, 1995; Whitman et al., 1998). A recurring fundamental theme in these studies is the source of metabolic energy. Generally, the focus is on endogenous supplies of electron donors and acceptors, sources that are completely decoupled from surface processes. In other words, the deep subsurface biosphere considered in this and many other studies is obligately photosynthesis-independent. However, there are doubts about microbial process being truly decoupled from photosynthesis. For example, are photosynthesis-independent sulfate-reducing prokaryotes (SRPs) is still doubtful. The rise in seawater sulfate concentrations from $<200 \mu\text{M}$ prior to 2.3 Ga to approximately present day levels by 1.8 Ga (Habicht *et al.*, 2002; Lyons *et al.*, 2004) is attributed to the preceding rise in molecular oxygen, which in turn is attributed to the emergence of cyanobacteria at or before ~ 2.7 Ga (Brocks *et al.*, 1999; Summons *et al.*, 1999). It is also difficult to readily differentiate a microbial community feeding on abiotically synthesized organic matter (terrestrial or extraterrestrial) from one that metabolizes photosynthetically derived reduced carbon compounds. To minimize the ambiguity, previous studies have categorically dismissed chemoorgano-heterotrophy as a surface-independent lifestyle and hence considered only chemolithoautotrophy. More specifically still, molecular hydrogen (H_2) is generally the sole electron donor considered in these investigations. H_2 -based microbial communities in the continental subsurface, reminds of the possible relevance to extraterrestrial ecosystems, potential electron donors other than H_2 and organic matter, and propose the possibility of novel (undiscovered) redox strategies.

It has been argued that if the base of the food chain in the deep subsurface is occupied by heterotrophs, the ecosystem must be linked to photosynthesis at the surface (Stevens, 1997). However, this theory ignores the possibility that under certain geochemical and geophysical conditions, organic compounds may be synthesized abiotically. Heterotrophic organisms that feed on such compounds would be photosynthesis-independent primary producers of biomass. Controversial theories regarding the abiotic origin of petroleum notwithstanding (Gold and Soter, 1982), it has been shown repeatedly that the synthesis of methane, carboxylic acids, amino acids, and other simple organic compounds from CO₂ (or CO) and H₂ can be thermodynamically favourable under reducing conditions, which may obtain in a variety of near-surface and deep subsurface environments (Shock, 1990; Shock and Schulte, 1998). In fact, Fischer-Tropsch-type reaction pathways are commonly invoked (Holm and Charlou, 2001; McCollom *et al.*, 1999). Since organic synthesis of this type is not biologically mediated, the H₂ used as the electron donor does not represent the energy source at the base of the hypothesized food chain. Nevertheless, H₂ is essential to the emergence, propagation, and persistence of that food chain.

Sediment-covered hydrothermal vent sites represent unique natural laboratories where diverse chemical and microbial processes occur. In contrast to their un-sedimented counterparts, where hydrothermal end member fluids with variable admixtures of seawater emerge directly into the water column, fluids in sediment-covered vents rise through the accumulated sediment layers and undergo complex chemical transformations in tandem with the hydrothermally affected sediments (Von Damm, 1995). These extensive, up to several hundred meter thick hydrothermal sediments may be home to a

large diversity of anaerobic and thermophilic microbial life. Further, in these sediments, organic and inorganic electron donors are abundant, as are carbonate, sulfate, and other terminal electron acceptors (TEAs). Sedimented vents have been and continue to be an inexhaustible source for novel microorganisms (Karl, 1995).

The plume of particulate DNA (0.7–1 µg/l) was extended from a black smoker vent (c.a. 1340 m depth) to the west-southwest directions in the Izena bottom-water region. High concentrations of particulate materials (70–110 µg C/l; 300–570 µg S/l) were also detected in the bottom-waters. Microscopic observation showed that the bottom-waters were rich in alcian blue-stainable large amorphous particles which contained coccoid and rod-shaped microbial cells mostly smaller than 1 µm. These microbial matrix compounds appeared to contribute to low P-DNA/ P-C ratio (0.011 ± 0.008 ; $n = 27$) in the vent environment. Sulfur was detected in various kinds of particles in the waters, while the content varied with calcium.

Microbial population in the p-DNA plume water was in the order of 10^5 cells/ml and the most (>99.9%) were non-culturable. The composition of culturable heterotrophs differed between the bottom-waters and surface sediments surrounding the vent; contributions of low temperature (4°C)-culturable bacteria and manganese-oxidizing bacteria to the total heterotrophs were higher in the sediments than in the waters. In contrast, percentages of orange-pigmented heterotrophs and microorganisms capable of growing in thiosulfate- and ammonia-based media to the total heterotrophs were higher in the waters than in the sediments. These results suggest that the culturable bacterial community in the bottom-waters was nutritionally versatile. Izena hydrothermal activities seemed to have a great influence in concentrations and compositions of particulate

materials and in biomass and compositions of microbial community in the vicinity of this aphotic deep-sea environment (Maruyama *et al.*, 1993).

2.4.3 *Chemosynthesis and bacteria*

Chemosynthetic bacteria are primary producers in deep-sea environments that use chemical energy to produce biomass. Chemolithoautotrophic bacteria oxidize reduced inorganic compounds to obtain both energy and reducing power for fixing inorganic carbon. Access to both oxygenated seawater and reduced compounds is important for chemosynthetic communities. The term *chemosynthesis* is generally used to describe chemoautolithotrophic processes at hydrothermal vents and seeps (Jannasch, 1989). However, it is being increasingly appreciated that this activity is more widespread than commonly thought, as synthesis of organic carbon by primary producers is one of the essential functions in any ecosystem. Autotrophic bacterial processes (other than those of cyanobacteria) have been shown to be significant in many habitats (e.g. Casamayor, *et al.*, 2001 and references therein). In the case of primary production, dark incorporation is either subtracted from carbon incorporation in light bottles or ignored (Casamayor *et al.*, 2008 and references therein). The importance of dark carbon fixation has been shown for oxic–anoxic interfaces, anoxic waters in lakes (Culver and Brunskill 1969; Jørgensen *et al.*, 1979; García-Cantizano *et al.*, 2005 and references therein) and seas (Tuttle and Jannasch 1977; Juniper and Brinkhurst 1986; Jørgensen *et al.*, 1991). The perpetually dark, deep abyssal basins with scanty amounts of organic detritus would therefore be constrained to fix carbon to various extents depending upon the accessibility of reduced inorganic substrates.

Reduced compounds may become available in an environment either via the degradation of organic matter or from magmatic/geothermal sources. Ambient oxygen, nitrate and sulphate in seawater might be consumed to varying extents depending on the amount of organic matter available for early or late diagenesis (Schulz and Zabel, 2000). These processes have long been associated with the degradation of organic matter settling from surface waters. Although well-known to co-occur with nitrification-denitrification, metal oxidation and even oxic respiration, the process of fixation of carbon dioxide is disproportionately biased towards the iron, sulphur and methane cycles.

Chemosynthetic endosymbioses occur ubiquitously at oxic–anoxic interfaces in marine environments. In these mutualisms, bacteria living directly within the cell of a eukaryotic host oxidize reduced chemicals (sulfur or methane), fueling their own energetic and biosynthetic needs, in addition to those of their host. In habitats such as deep-sea hydrothermal vents, chemosynthetic symbioses dominate the biomass, contributing substantially to primary production. Although these symbionts have yet to be cultured, physiological, biochemical and molecular approaches have provided insights into symbiont genetics and metabolism, as well as into symbiont–host interactions, adaptations and ecology. Studies of endosymbiont biology are reviewed, with emphasis on a conceptual model of thioautotrophic metabolism and studies linking symbiont physiology with the geochemical environment. (Stewart *et al.*, 2005).

2.5 Minerals, metals, energy currency and bacteria

2.5.1 Phosphates, Pyrophosphates, Silicates, metal oxides and bacteria

A compilation of dissolved phosphate and solid-phase P data from the oceanic crust to evaluate the effects of hydrothermal processes on the oceanic budget of P was examined by Wheat *et al.*, 1990. Concentrations of phosphate in fluids that emanate from ridge-axis hydrothermal systems are less than that in bottom seawater. The extent of removal in these fluids is at least 30% and in some hydrothermal systems dissolved phosphate is removed completely from the circulating fluid. Evidence for the removal of phosphate in each of six ridge-flank hydrothermal systems is based on systematic variations in porewater profiles of phosphate and speeds of pore-water flow. The extent of removal is >80% in these ridge-flank systems. These removal processes are recorded in the basaltic crust as an increase in P concentration that coincides with an increase in extent of alteration and content of ferric iron. Phosphate also is removed in hydrothermal plumes by co-precipitation with Fe-oxyhydroxide particles, which eventually deposits on the seafloor. Each of these hydrothermal processes results in a flux of P into the oceanic crust. Bottom seawater flow through ridge-axis hydrothermal systems removes at most 0.4% of the pre-industrial dissolved riverine flux of P, while ridge flanks remove at least 5%, but less than 50% of the dissolved riverine flux, consistent with P data from Deep Sea Drilling Project (DSDP) Sites 417 and 418. Removal of phosphate by co-precipitation with Fe-rich particles in hydrothermal plumes along ridge axes accounts for 18-33% of the dissolved riverine flux. Thus, hydrothermal systems remove about 50% of the pre-industrial dissolved riverine flux of phosphate (Wheat *et al.*, 1990). Interface-

linked and organic diagenesis linked phosphorus precipitation were studied in relation to phosphorite formation (Froelich *et al.*, 1998)

Enhanced biological phosphate removal (EBPR) is an established activated sludge process although many of the fundamental metabolic mechanisms are still poorly understood. Therefore, the stoichiometry and enzymatic reactions of the anaerobic phase of this process were studied in a laboratory reactor with acetate as organic substrate. Enzyme assays showed that acetate activation is performed by acetyl-CoA synthetase. Results of ^{13}C -NMR measurements after feeding ^{13}C -labeled acetate indicated that glycogen is degraded via the Entner-Doudorof pathway. Energy is supplied by glycolysis, hydrolysis of polyphosphate and probably also by hydrolysis of pyrophosphate and the efflux of MgHPO_4 . The ratio of phosphate released to acetate taken up is variable and apparently dependent on the contents of polyphosphate and glycogen. A biochemical model is proposed explaining the experimental results in terms of carbon, redox, and energy balances. Anaerobic operation of an incomplete tricarboxylic acid cycle (TCA) is proposed to explain the generation of extra reducing equivalents (Hesselmann *et al.*, 2000). Although this study is not from the deep-sea system, the implied scientific points are valid towards understanding the processes.

In order to understand co-diagenesis of Fe and P in hydrothermal plume fallout sediments from $\sim 19^\circ\text{S}$ on the southern East Pacific Rise, 3 distal sediment cores from 340–1130 km from the ridge crest, collected during DSDP Leg 92, were analysed for solid phase Fe and P associations using sequential chemical extraction techniques. The sediments at all sites are enriched in hydrothermal Fe-oxyhydroxides, but during diagenesis a large proportion of the primary ferrihydrite precipitates were transformed to

the more stable mineral form of goethite and to a lesser extent to clay minerals, resulting in the release of scavenged P to solution. However, a significant proportion of this P is retained within the sediment, by incorporation into secondary goethite, by precipitation as authigenic apatite, and by re-adsorption to Fe-oxyhydroxides (Poulton and Canfield, 2006).

Sulfate-reducing bacteria belonging to the genus *Desulfotomaculum* utilized inorganic pyrophosphate as a source of energy for growth in the presence of fixed carbon (acetate and yeast extract) and sulfate. Pyrophosphate does not support the growth of *Desulfovibrio* under the same growth conditions. Over a limited range of concentrations, growth is proportional to pyrophosphate, and extracts of bacteria grown on pyrophosphate medium have enzymatic activities similar to extracts prepared from bacteria grown on medium containing lactate plus sulfate. The variety of cell types observed in crude anaerobic pyrophosphate-enrichment cultures from a marine environment suggests that this unique type of energy metabolism is not restricted to the sulfate-reducing bacteria of the genus *Desulfotomaculum* (Liu *et al.*, 1982).

Growth and metabolic activities of *Bacillus cereus* were found to cause the extraction of iron atoms from the octahedral position in mica in the kaolin sample (49%) and in the quartz sands sample (17%) after 3 months of bioleaching, while aluminium removal was only 5%. Mica destruction was detected in kaolin and quartz sands samples by X-ray diffraction analysis and also by i.r. adsorption spectroscopy in quartz sands samples. The structural changes obtained were confirmed by scanning electron microscopy (SEM) analysis. The SEM pictures show a different morphology in the boundary region of mica grains before and after bioleaching. Bacterial destruction effects were feeble in the interlayer sites and were specially directed to split planes, which are occupied by a number of bacterial cells. The biological destruction of mica with

the more stable mineral form of goethite and to a lesser extent to clay minerals, resulting in the release of scavenged P to solution. However, a significant proportion of this P is retained within the sediment, by incorporation into secondary goethite, by precipitation as authigenic apatite, and by re-adsorption to Fe-oxyhydroxides (Poulton and Canfield, 2006).

Sulfate-reducing bacteria belonging to the genus *Desulfotomaculum* utilized inorganic pyrophosphate as a source of energy for growth in the presence of fixed carbon (acetate and yeast extract) and sulfate. Pyrophosphate does not support the growth of *Desulfovibrio* under the same growth conditions. Over a limited range of concentrations, growth is proportional to pyrophosphate, and extracts of bacteria grown on pyrophosphate medium have enzymatic activities similar to extracts prepared from bacteria grown on medium containing lactate plus sulfate. The variety of cell types observed in crude anaerobic pyrophosphate-enrichment cultures from a marine environment suggests that this unique type of energy metabolism is not restricted to the sulfate-reducing bacteria of the genus *Desulfotomaculum* (Liu *et al.*, 1982).

Growth and metabolic activities of *Bacillus cereus* were found to cause the extraction of iron atoms from the octahedral position in mica in the kaolin sample (49%) and in the quartz sands sample (17%) after 3 months of bioleaching, while aluminium removal was only 5%. Mica destruction was detected in kaolin and quartz sands samples by X-ray diffraction analysis and also by i.r. adsorption spectroscopy in quartz sands samples. The structural changes obtained were confirmed by scanning electron microscopy (SEM) analysis. The SEM pictures show a different morphology in the boundary region of mica grains before and after bioleaching. Bacterial destruction effects were feeble in the interlayer sites and were specially directed to split planes, which are occupied by a number of bacterial cells. The biological destruction of mica with

phengite composition after iron removal led to development of illite, which was detected by energy-dispersion microanalysis (EDS). Illite development caused also the enrichment of the kaolin sample by fine-grained fraction (Styriakova *et al.*, 2003).

Barren slides with only a few bacteria that apparently dissolved debris of siliceous tests of diatoms were reported by Smetacek (1999). The bacteria were apparently responsible for the barrenness of the slide, and had thrived because the sample had escaped its shot of preservative. Mysteriously, the silica shells of the diatoms had also vanished, although they were beautifully preserved in the treated samples. The observation contradicted the view that diatom shells are of no nutritional value and that their dissolution is controlled by physico-chemical and not biological factors (Smetacek, 1999).

This research focused on whether bacteria living in aerobic environments where Fe is often a limiting nutrient could access Fe associated with the clay mineral kaolinite. Kaolinite is one of the most abundant clays at the Earth's surface, and it often contains trace quantities of Fe as surface precipitates, accessory minerals, and structural substitutions. It was hypothesized that aerobic bacteria may enhance kaolinite dissolution as a means of obtaining associated Fe. To test this hypothesis, Maurice *et al.*, 2001 conducted microbial growth experiments in the presence of an aerobic *Pseudomonas mendocina* bacterium that is incapable of using Fe as a terminal electron acceptor for oxidative phosphorylation and that requires only μM concentrations of Fe, for metabolism. The presence of kaolinite allowed the bacteria to grow above levels of non kaolinite containing controls, in Fe-limited conditions. We further demonstrated that the bacteria significantly enhanced Al- and Si-release from the kaolinite. These results indicate that clays that contain even trace quantities of Fe need to be considered as

additional sources of Fe in aerobic environments and suggest that microbial processes may exert important, but until now largely overlooked influences on the dissolution rates of clays (Maurice *et al.*, 2001)

Mn(II)-oxidizing microbes have an integral role in the biogeochemical cycling of manganese, iron, nitrogen, carbon, sulfur, and several nutrients and trace metals. There is great interest in mechanistically understanding these cycles and defining the importance of Mn(II)-oxidizing bacteria in modern and ancient geochemical environments. Linking Mn(II) oxidation to cellular function, although still enigmatic, continues to drive efforts to characterize manganese biomineralization or formation of manganese minerals by the help of microbes. Recently, complexed-Mn(III) has been shown to be a transient intermediate in Mn(II) oxidation to Mn(IV), suggesting that the reaction might involve a unique multicopper oxidase system capable of a two-electron oxidation of the substrate. In biogenic and abiotic synthesis experiments, the application of synchrotron based X-ray scattering and spectroscopic techniques has significantly increased our understanding of the oxidation state and relatively amorphous structure (i.e. δ -MnO₂-like) of biogenic oxides, providing a new blueprint for the structural signature of biogenic Mn oxides (Tebo *et al.*, 2005). For all these mineralization process energy is required and ATP could be indicative of live biomass involved directly or indirectly.

2.5.2 *ATP and bacterial biogeochemistry*

Adenosine triphosphate (ATP) has long been used as a measure of microbial biomass in sediments and soils (Lee *et al.*, 1971; Anderson and Davies, 1973; Ausmus, 1973; Oades and Jenkinson, 1979; Ross *et al.*, 1980; Sparling, 1981; Fairbanks *et al.*,

1984; Joergensen *et al.*, 1989; Arnebrant and SchnuÈrer, 1990; Lin and Brookes, 1996). For ATP to be a reliable tool for microbial biomass quantification in sediment, a fairly constant biomass C-ATP ratio in different sediments and under different conditions is required. Martens (2001) reported that Jenkinson and Oades (1979) method for measuring adenosine 5' triphosphate (ATP) in soil leads to serious underestimations. Martens (2001) recommended the DMSO method as a suitable technique to estimate ATP in soils. The recovery of added ATP standards was almost 100% and was independent of the soil under investigation. These findings contradicted after comparing the Jenkinson and Oades extraction technique, which corrects for incomplete extraction of ATP by reference to a 'spike' of added ATP, with a sequential extraction procedure as used by Martens (Contin *et al.*, 2001, Contin *et al.*, 2001). Measurements of the ATP contents of four soils by the two procedures showed no significant differences, in contrast to Martens' findings (Contin *et al* 2002). Jenkinson (1988) laid down strict criteria for the inclusion of biomass and ATP analyses in his original correlation. These were:

1. The soils had received a conditioning incubation of at least several days at 25°C before analysis.
2. The soil moisture contents were below 60% water holding capacity.
3. The soil pH was not below 4.8.
4. All biomass C measurements were done by Fumigation-Incubation (Jenkinson and Powlson, 1976).
5. All ATP measurements were done following extraction with strongly acidic reagents.

Adenosine 5'-triphosphate (ATP) occurs in all living cells but exocellular ATP has a half-life of less than 1 h (Conklin and MacGregor, 1972). Adenosine 5-triphosphate

therefore provides a useful indicator of life in soil or a measure of microbial biomass (Jenkinson and Ladd, 1981). ATP can be measured readily and accurately by the luciferin luciferase system. ATP in dead cells is rapidly decomposed (Holm-Hansen and Booth, 1966) as is extracellular ATP in soil (Conklin and Macgregor, 1972). The main difficulties in using ATP as a quantitative measure of soil biomass are in extracting it efficiently from soil and in relating the amount of ATP in a soil to the amount of biomass in that soil. The most widely used extractants for ATP in soil and sediment are :

1. Cold 0.3 M H₂SO₄ (Lee et al., 1971; Greaves *et al.*, 1973; Karl and La Rock, 1975).
2. Butanol-octanol (Conklin and Macgregor, 1972; Anderson and Davies, 1973).
3. Boiling Tris buffer (Lee *et al.*, 1971; Conklin and Macgregor, 1972; Ausmus, 1973; Karl and La Rock, 1975; Kaczmarek *et al.*, 1976).

In oceanographic studies the boiling Tris-buffer extraction has been widely used as extractant for ATP (HOTS-ALOHA, Karl and La Rock, 1975, Raghukumar *et al.*, 2001).

The biomass C-ATP ratios by the various methods were different: 120 (Oades and Jenkinson, 1979), 171 (Tate and Jenkinson, 1982), 300-450 (Martens, 2001). During the growth the microbial cultures, the biomass C:ATP ratio can vary from 1000: 1 to 40: 1 (Paul and Clark, 1989). Based on a summary of research done using laboratory cultures Parkinson and Paul (1982) recommended a ratio of 250:1. However, the biomass C:ATP ratio of sediment micro-organisms would be expected to be higher than 250: 1. The microbial population in soils is dormant (inactive) most of the time. Thus the biomass C: ATP ratio in soil is probably high relative to that in laboratory cultures.

2.5.3 Use of ATP in understanding biogeochemical processes

ATP is a very important parameter to detect life in any environment and is crucial in understanding biogeochemical processes. Some such studies are highlighted below.

The structure of a benthic community at 4626 m depth on the Nova Scotian continental rise (Western Atlantic) showed conspicuously higher abundances of polychaetes, bivalves and isopods are compared to those reported from comparable depths. Bacterial numbers and ATP concentrations are also high. These anomalous abundances were suspected to result from enhanced food availability caused by the strong near-bottom currents that flow through the area (Thistle *et al.*, 1985).

In a later study at Nova Scotia the presence of low current speeds a depositional sedimentation regime, and additions of labile POM, were shown to be the likely key variables in significantly increasing ($p < 0.05$) the ATP content. ATP concentrations and standing stocks of microorganisms and meio- and macrofauna were compared with the Deep site and the Mid site during times of strong flow conditions ($\geq 15\text{-}25 \text{ cm s}^{-1}$). Standing stocks were higher than in typical deep-sea regions, mean sizes of individuals were larger, adult organisms were present, with greater diversity of feeding strategies and life habits than encountered in most deep-sea habitats. During times of intermediate flow conditions ($5\text{-}15 \text{ cm s}^{-1}$) at the Mid site, microbial production and activities were enhanced relative to low flow conditions, total numbers of epifauna decreased, abundance of infaunal burrowers and tube builders increased, and a higher proportion of smaller individuals were found (Aller, 1997).

Higher C/N ratios were observed during the higher current flow indicating the removal of the more labile and N-rich organic matter during periods of erosion and exposure of more refractory organic matter from below the sediment surface (Yingst and Aller, 1982).

Raghukumar *et al.*, 2001 report similar decline in LOM, ATP and lipase activity, indicating importance of quality food for the deep-sea benthos immediately after the simulated “benthic disturbance” in the Central Indian Basin (CIB). This was accompanied by a decrease in meiofauna, macrofauna and bacterial numbers. Bacterial carbon (derived from total counts of bacteria) contributed nearly 47% of ATP-C, and the remaining 53% could be from meiofauna, macrofauna and other living biomass in the pre-disturbance sediments. Bacterial carbon contribution was reduced to 3.3% in the postdisturbance samples. Bacterial densities as determined by TC showed direct correlation to ATP-C in the post-disturbance samples indicating that most of the living biomass was contributed by bacteria.

At unique ecological spots like Loihi seamount, though bacterial populations flourished (particulate ATP concentrations up to 100X above ambient bottom seawater), macrobenthic communities were notably absent (Karl *et al.*, 1988). Very high concentration of Fe in oxide form did not permit intracellular symbioses in this region (Edwards *et al.*, 2004). In order to understand biogeochemical processes better, several authors modelled different oxidation fronts.

2.6 Quantification of biogeochemical processes

2.6.1 Diagenetic interactions

A series of models were proposed to describe the development of oxidation fronts in various deep sea sediment types. These models included cases for the development of nonsteady-state diagenetic processes in which downward diffusing oxidants, such as oxygen and nitrate, result in the depletion of initially deposited organic carbon and the formation of metal enrichment zones in the upper part of the sediment column (Thomson *et al.*, 1984a, b; Colley *et al.*, 1984; Colley and Thomson, 1985; Wilson *et al.*, 1985, 1986; Jarvis and Higgs, 1987).

2.6.2 Fluid interactions

Mass and energy were conservative in nature and ore forming systems within the upper crust of the earth were no exception. Thus, the mass conservation law is valid for a closed system, and an open system. In the latter case, exchange between the system and its surroundings was considered. Based on the mass conservation law, a number of different roles of geofluid flow in ore forming systems were realized. Due to the concurrence of these roles, interactions between fluid flow, heat transfer, mass transport and chemical reactions were considered in a comprehensive manner (Zhao *et al.*, 2009).

To explore concealed giant ore deposits under the cover of the earth's surface, it was necessary to develop scientific and predictive methods, by which the controlling physical and chemical processes associated with ore body formation at depth could be evaluated. It was in this direction, that the framework of computational geoscience was developed in recent years. Computational geoscience combines mathematical, physical,

and chemical approaches through computer algorithms to solve geoscience problems. (Zhao *et al.*, 2008a).

The major physical and chemical processes, which were commonly considered in the computational simulation of ore forming systems, were material deformation, geofluid flow, heat transfer, mass transport and chemical reaction processes (Garven and Freeze 1984, Yeh and Tripathi 1991, Steefel and Lasaga 1994, Zhao *et al.*, 2009). Microbial component in these models are still in nascent stages and require further development.

2.7 Geological, setting of the Central Indian Ocean Basin

The Indian Ocean Nodule Field (IONF) in the Central Indian Ocean Basin (CIOB) was examined for environmental variability in terms of live microbial biomass and bacterial abundance. Roughly bordered by the 10°S to 16°30'S and 72°E to 80°E, the area hosts the world's second largest and second high-grade manganese nodule deposits after the equatorial nodule belt in the North Pacific Ocean (Mukhopadhyay *et al.*, 2002). Hence, an in-depth understanding of the microbial interactions with the sediment chemistry and biochemistry would be extremely important for harnessing these resources with minimal effect on the ecosystem. Results of previous mining experiments impress upon the need of strong baseline variability data of the world-ocean beds (Morgan, 2005, Weidicke, 2005).

The Central Indian Ocean Basin (CIOB) with an area of $5.7 \times 10^6 \text{ km}^2$ (Ghosh and Mukhopadhyay, 1999) has five sediment types namely, terrigenous mud, siliceous ooze with and without nodules, pelagic red clays and calcareous ooze (Fig. 1A; Nath *et al.*,

1989; Rao and Nath, 1988). The basin is bordered by the Indian Ocean Ridge system and marked by prominent fracture zones (FZ) and seamounts hosting normal-Mid Ocean Ridge Basalts (Fig. 1B; Kamesh Raju and Ramprasad, 1989; Mukhopadhyay *et al.*, 2002; Das *et al.*, 2007).

The oxygen and nutrient-rich Antarctic Bottom Water Current (AABW) entering the CIOB from 5°S (Gupta and Jauhari, 1994) maintained oxic conditions during the past *ca* 1100kyr (Pattan *et al.*, 2005). Terrigenous influx decreases from north to south (Rao and Nath, 1988; Nath *et al.*, 1989). Higher surface productivity and therefore higher detrital rain from overlying surface waters (Matondkar *et al.*, 2005), make the organic matter supply to the siliceous ooze higher than the red clays (Gupta and Jauhari, 1994). Other factors influencing distribution of organic carbon are sedimentation rates, bottom water oxygenation, water depth, topography, bioturbation, recalcitrance and age (Lyle *et al.*, 1983; Nath *et al.*, 1997; Lochte *et al.*, 1999).

The biogeochemical set up of the Central Indian Ocean is a complicated and diverse one (Banakar *et al.*, 1991, Mukhopadhyay *et al.*, 2000). Not only is the basin remarkable as a major nodule deposit among the world oceans but it is also geophysically active, with chains of seamounts, trails of fracture zones, wide differences in sediment types, characters and depths (Nath *et al.* 1989, 1992). The existing knowledge on the geophysical, and geochemical properties of this basin throws light not only on the geological evolution of the CIOB but also emphasizes upon the need to look at the basin as a biome of many sub-environments with a profuse spatio-temporal variability of habitats and inhabitants.

2.7.1 Geological features of northern siliceous ooze

The sea-floor spreading rate at this location is fast at 90mm kyr⁻¹ (Mukhopadhyay *et al.*, 2002). Temperature and dissolved oxygen of bottom water is 0.9 to 1.03°C and 4.2 to 4.3ml l⁻¹ respectively (Warren *et al.*, 1982; Nath *et al.*, 1992). Surface C/N ratios of this TOC- rich core ranges from 3 to 6 (Gupta and Jauhari, 1994; Pattan *et al.*, 2005). Illite is the dominant clay type with a SiO₂/Al₂O₃ ratio of 6.7 and biogenic silica varies from 10 to 35 %. Early diagenetic processes are attributed to the formation of rough nodules when the Mn/Fe ratio > 1, with higher Mn, Cu, Ni and todorokite mineralogy (Rao and Nath, 1988; Nath *et al.*, 1989).

2.7.2 Geological features of southern pelagic red clay

The sea-floor spreading rate is slow at 26mm kyr⁻¹ (Mukhopadhyay *et al.*, 2002). Temperature and dissolved oxygen of bottom waters are >1.03°C and 4.1 to 4.2ml l⁻¹ respectively (Warren *et al.*, 1982; Nath *et al.*, 1992). Surface C/N ratio of this TOC-poor core ranges from 3 to 6 (Gupta and Jauhari, 1994). The abundant clay type is montmorillonite with a SiO₂/Al₂O₃ ratio 4.5 and biogenic silica amounting to 5 to 10 %. The Mn/Fe is < 1 suggesting hydrogenetic metal precipitation (Rao and Nath, 1988; Nath *et al.*, 1989). The nature of its glass shards (Mascarenhas-Periera *et al.*, 2006), native aluminium content (Iyer *et al.*, 2007) and signatures of degassing (Nath *et al.*, 2008) suggest hydrothermal alteration of recent origin in some locations. Late Tertiary sediments are probably exposed in this area due to explosive volcanism Mascarenhas-Periera *et al.* (2006).

2.8 Geomicrobiology of the Central Indian Basin

2.8.1 Northern siliceous ooze

The northern siliceous setting is rich in total organic carbon (TOC) with *ca* 0.3% concentration. Early diagenetic processes and extensive nitrification in this region influence the origin, type and quality of manganese nodules (Nath and Mudholkar, 1989) and sediment biogeochemistry as a whole. The microbial community might co-express both chemolithotrophy and organotrophy. This would enable efficient recycling of the limited photosynthetically derived organic matter (Stevens, 1997; Ehrlich, 1998). Cultured bacterial representatives showing both phases of nitrification have been isolated from this region (Ram *et al.*, 2001). Microbial processes like manganese oxidation (Ehrlich, 1998 and references therein) and manganese cycling in tan-green mottled zones (Meister *et al.*, 2009) possibly co-occur (Wang *et al.*, 2008) along with the coupling of nitrification-denitrification (Luther III *et al.*, 1997). Similarly, microbial sulphide oxidation and iron reduction could co-occur. Here the mixotrophic combination of chemolithotrophy and organotrophy might be due to simultaneous dependence on the organic matter delivery and possible rock alteration features. The setting might be analogous to the hydrocarbon deposits except for the scale and extent (Canfield, 1991, Ma *et al.*, 2006, Campbell, 2006).

2.8.2 Southern pelagic red clay

The southern pelagic red clay setting is TOC-poor with a concentration of < 0.1%. It bears the signature of recent hydrothermal alteration due to tectonic reactivation of fracture zones (Mascarenhas-Pereira *et al.*, 2006; Iyer *et al.*, 2007; Nath *et al.*, 2008).

Microbiologically, the southern part of the CIOB is also largely unexplored. It is therefore hypothesized that chemolithotrophy, though widespread, would be more pronounced in the oligotrophic southern CIOB than in the detritally dominated northern region. Proximity to tectonic features such as the Trace of Rodrigues Triple Junction (Kamesh Raju and Ramprasad, 1989) may indicate sulphide oxidation with iron reduction (Bach and Edwards, 2003). Thiotrophic nitrate reduction may also be an important contributing process especially in diffuse flow regimes (Childress *et al.*, 1991) with temperatures varying between 2 to 25°C (Chevaldonne *et al.*, 1991). The chemoautotrophy might be totally independent of organic matter rain and this system could be analogous to settings like the Loihi Seamount (Edwards *et al.*, 2004).

“It is the man not the method that solves the problem”.

- *H. Maschke*

Chapter III

Materials and Methods

3.1 Environmental Parameters

3.1.1 Temperature

Temperature of sediment cores from the Central Indian Ocean Basin were measured on-board as soon as sample was retrieved using a thermometer. *In situ* temperature from the sea-bed was not available.

3.1.2 Depth and pressure

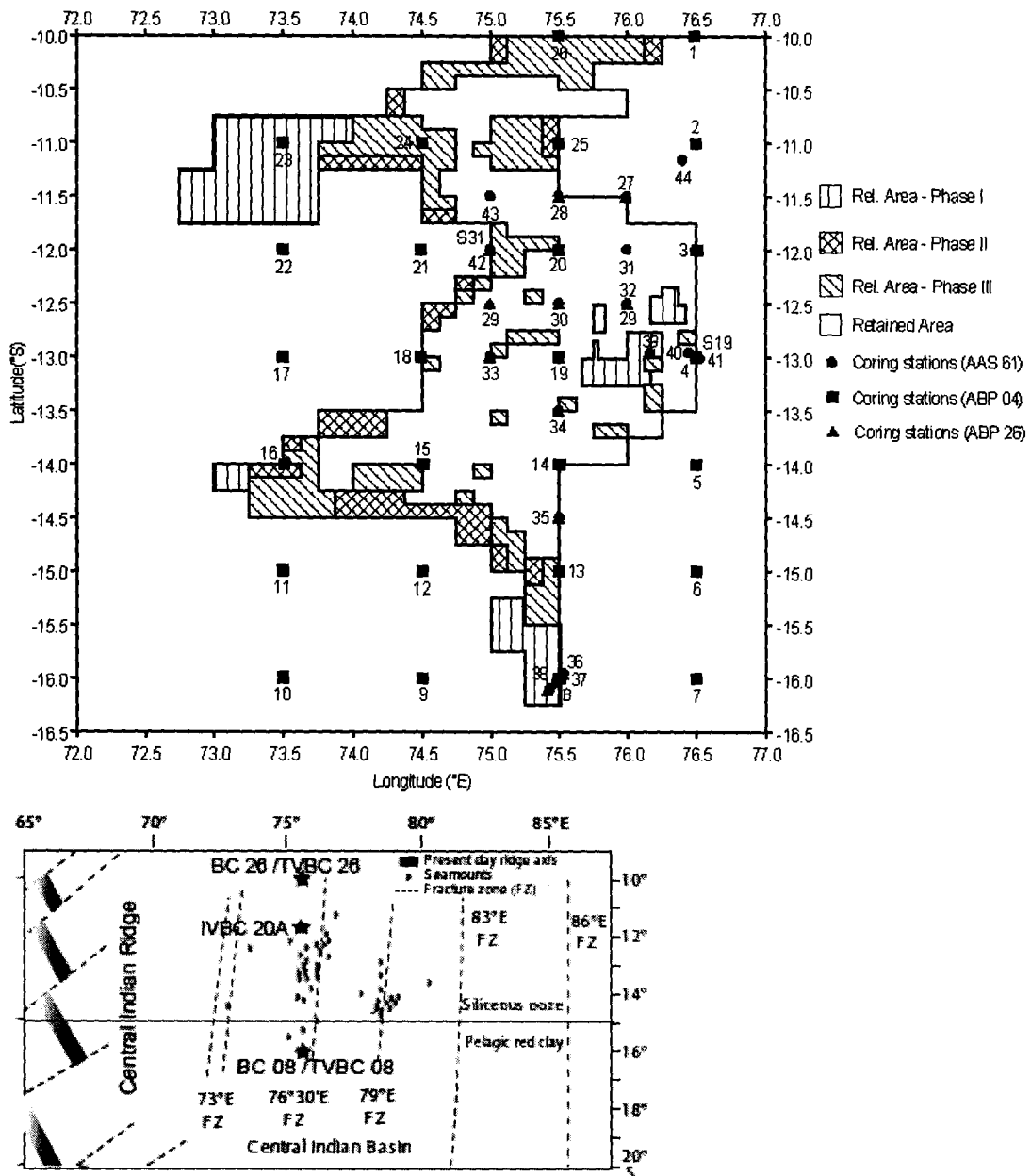
Depth of the sample was acquired from the cruise reports (Courtesy: PMN-EIA, NIO-Goa, India). Data was collected on-board from hydrosweep / parasound measurements. Depth of most sample were >5000 m to <6000 m below sea surface. Difference between given and touch- position was usually within 10-100 m, thus providing reliability in sampling repeats between different stations and seasons. *In situ* pressure measurements were unavailable. Pressure was calculated as 1 atmosphere increase per 10 m decent in depth.

3.2 Sampling area and frequency

Sediment cores were collected on board R.V. *Akademic Boris Petrov* (ABP) cruise nos. 4, 26 and 38 as a part of “Environmental studies for nodule mining in Central Indian Basin (PMN-EIA)” programme. ABP-04 was undertaken during the austral winter of March-May, 2005, ABP-26 during austral summer of December 2006-January 2007 and ABP-38 during austral spring of September-October 2009 as a part of Environmental Variability Data Collection (EVDC). The cruises were named EVDC II, III and IV respectively. Some data from EVDC I was used for comparison (Fig. 3.1).

Additionally nodule and their associated samples were frozen and brought back from ABP-17 (PMN Survey, May, 2006).

Fig. 3.1. Sampling area and topographic features with locations (Courtesy: PMN EIA, NIO, Goa; Mascarenhas-Pereira *et al.*, 2007)



3.3 Classification of stations

Sampling during the EVDC-II was carried out as follows:

- i. Temporal variability: Ten stations of EVDC-I were re-sampled during EVDC-II. These were Temporal variability box-core (TVBC) 03,04,08,13,14,18,19,20,25,26.
- ii. Spatial variability: Along north-south profile at: 75.5° E the stations 26,25,28, 20,30,19,34,14,35,13,8 were sampled.
- iii. High resolution sampling at the first generation mine site (FGM): Sampling in the First Generation Minesite was done at half degree intervals in the stations BC-27, 28, 29,30,31,32, and 33 in addition to TVBC-03, 04, 18, 19, 20.
- iv. Special geological features: The sampling in the sea-mount area were carried out at sea-mount top (BC-37), plateau near TVBC 08 (BC-36), and valley sample (BC-38) in addition to TVBC-08.

The same stations were sampled during EVDC III and were named Seasonal variability box-core (SVBC) and during EVDC IV as Intermediate variability box-core (IVBC).

3.4 On-Board processing

The samples were collected with the help of United States Naval Electronics Laboratory (USNEL) –type box core of 50 cm x 50 cm x 50 cm dimension. Sub-cores were collected using acrylic cores of 6.3 cm inner diameter (Appendix III). The sediment cores were sectioned at 2 cm intervals up to 10 cm and at 5 cm interval thereafter. Samples from each section were collected in sterile plastic bags for further processing. Microbial samples were processed at 4°C and 1 atm pressure onboard immediately after

sediment collection. Samples for biochemical studies were collected and analysed in three sets. The first was oven-dried at 30°C, the second was frozen at -20 °C and the third was lyophilized. Nodules and their associated sediments were collected with the help of van Veen grab and aseptically, packed in sterile plastic bags and frozen at 0°C. These were then brought to shore laboratory and analyzed within 20 days of retrieval.

Two nodules and their associated sediments were analyzed for the present study. Sample 147 was a surface nodule with the typical hamburger shape and sample 142 was a buried nodule. The nodules were sectioned aseptically from surface to interior through the visible coloured growth bands. Surface nodule 147 (SN 147) was sectioned into five parts from surface to interior based on colour differentiation namely, SN1 to SN5. Buried nodule 142 (BN 142) was sectioned into four parts from surface to interior namely, BN1 to BN4. Associated sediment of nodule SN 147 was named S147 and that of nodule BN 142 as S142 (Fig. 3.2).

3.5 Geochemical parameters

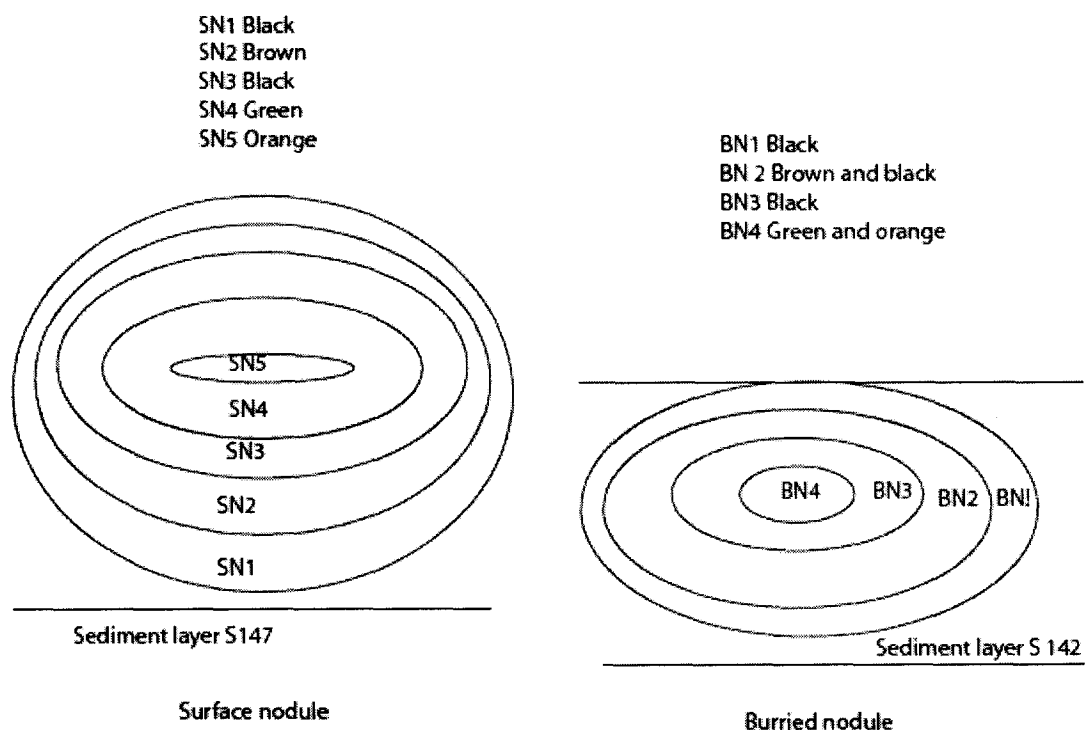
3.5.1 Rock colour

Rock colour was analyzed on-board in accordance to *Rock color chart* of the Geological Society of America, Boulder, Colorado (Courtesy: Cruise report of ABP-04, NIO, Goa, India). Colour codes used for the rock colour map in this work are as follows:

0=5Y5/2 1=5Y5/4 2=5Y5/6 3=5YR2/2 4=5YR3/4 5=5YR4/4
6=5YR7/2 7=10YR4/2 8=10YR5/4 9=10YR6/6 10=10YR7/4

Using the above codes, rock colour map was generated using Surfer 8 software.

Fig. 3.2 Schematic internal layers of surface nodule SN147 and buried nodule BN142



3.5.2 Porewater parameters

The following pore-water parameters were estimated for two representative cores IVBC 20A and IVBC 18C. Station IVBC 20A was relatively nodule-rich area with nodule abundance of 1-2 kg m⁻² at the depth of ~5225m and IVBC-18C was nodule poor with < 1kg m⁻² at the depth of ~5100m (Courtesy: PMN data; NIO, Goa).

3.5.2.1. pH and Eh

The pH and Eh were measured using a Labindia Phan µp controlled pH analyser probe directly from sediment as soon as the core was retrieved. The pH meter was

calibrated using standard buffers of pH 4, 7, 9.2 (Himedia) respectively. Relative Eh was also measured. Eh was calibrated using standard reference solutions (Appendix VI). Reference solution A was 192 mV and reference solution B was 258 mV. Approximately 60-66 mV difference is acceptable between the two solutions where mV of solution B is greater than solution A.

3.5.2.2. *Dissolved Oxygen (DO)*

The DO was measured in sediment porewater by Winkler's titrimetric (Carpenter 1965) method and spectrophotometric method Pai *et al.*, 1993. Measured amount of fresh wet sediment immediately after retrieval was introduced into deoxygenated cold seawater using a cut syringe. The blank value was measured and corrected. Care was taken not to introduce bubbles. Winkler's A and B solutions (Appendix VI) were added and the closed bottles kept in dark for 1 hour (Carpenter, 1965). Acid digestion gave a yellow colour whose intensity was directly proportional to the intensity of dissolved oxygen (Appendix VI). The spectrophotometric measurement was done at 450 nm and oxygen was expressed as $\mu\text{M l}^{-1}$ of pore-water.

3.5.2.3. *Salinity*

Salinity was measured in pore-waters extracted from the sediment. Measurement was done using a hand-held refractometer (ATGO 2442-W01 S/MILL-E) calibrated to zero with distilled water. About a gram of fresh wet sediment was centrifuged at 5000 rpm for 10 min at 4°C. The pore-water extracted was used for measuring salinity.

3.5.2.4. *Ammonium*

Ammonium was measured using indo-phenol blue method (Koroleff, 1969) as described in Grasshoff *et al.*, (1983). Measured amount of fresh wet sediment immediately after retrieval was introduced into deoxygenated cold seawater whose blank value for ammonium was measured and corrected. Sample was treated with phenol, trisodium citrate and trione (Appendix VI) gently vortexed and microwaved for 60 seconds. Sample was then centrifuged at 5000 rpm for 5 minutes at 4°C and the supernatant was measured spectrophotometrically at 630 nm. Ammonium concentration was expressed as $\mu\text{M l}^{-1}$ of pore-water.

3.5.2.5. *Sulphide*

Sulphide was measured according to Pachmayr, (1960). Measured amount of fresh wet sediment was introduced quickly into zinc acetate fixative immediately after retrieval. Proportionate amounts of dimethyl-para-phenylenediamine sulphate and ferric ammonium sulphate were added (Appendix VI). Sample was gently vortexed and centrifuged at 5000 rpm for 5 minutes at 4°C and the supernatant was measured spectrophotometrically at 670 nm. Sulphide content was expressed as $\mu\text{M l}^{-1}$ of pore-water.

3.5.2.6. *Fe*

Pore-water was extracted by centrifuging measured amount of sediment at 5000 rpm for 5 minutes. Total iron was measured by sampled direct current (Aldrich and van der Berg, 1998; Appendix VI). Iron was expressed as mg l^{-1} of pore-water.

3.5.2.7. *Mn*

From the above extracted pore-water total Mn was measured by differential pulse polarographic method (Colombini and Fuocco, 1983, Appendix VI). Total manganese was expressed as mg l⁻¹ of pore-water.

3.5.3 *Elemental Carbon and Nitrogen -Total Organic Carbon (TOC), total inorganic carbon (TIC) and C/N ratio*

Total carbon and nitrogen was measured by NCS 2500 Elemental Analyser (Patient *et al.*, 1990) using L-Cistina (Therma Quest Italia SpA) as standard. Total carbon was counter-checked with UIC CM 5014 coulometer and found similar in range. Total inorganic carbon was analyzed by UIC CM 5014 coulometer using CaCO₃ (Merck, Germany) as the standard. Total organic carbon was determined by subtracting total inorganic carbon from total carbon. The C/N was calculated as the ratio between total organic carbon and total nitrogen.

3.6 Biochemistry

3.6.1 *Labile organic matter (LOM)*

3.6.1.1 *Proteins*

Total proteins of sediments were estimated by Lowry's Folin Ciocalteu method using bovine serum albumin as standard (Lowry *et al.*, 1951). Protein was extracted by digesting 0.5 g of sediment with 2 ml of 1N NaOH in a water bath at 100°C for 5 min. The slurry was centrifuged and the clear supernatant was used for estimation using Folin-phenol reagent (Appendix VIII for standards curves).

3.6.1.2 *Carbohydrates*

Total carbohydrates of sediments were estimated by phenol-sulfuric acid method using glucose as standard (Kochert, 1978). Carbohydrates were extracted by digesting 0.5 g of sediment with 3 ml of trichloroacetic acid in water bath at 90°C for 3 hrs. The slurry was centrifuged and the supernatant was used for estimation of total carbohydrates.

3.6.1.3 *Lipids*

Total lipids of sediments were estimated by Bligh and Dyer method using stearic acid as standard (Bligh and Dyer, 1959). Lipids were extracted from dried sediment samples by direct elution with chloroform and methanol (5:10). This was followed by oxidation with 0.15% acid dichromate and spectrophotometry using stearic acid as the standard (Parsons et al., 1984).

3.6.1.4 *LOM*

The sum of total proteins, carbohydrates and lipids was expressed as LOM. The nature and origin of the organic matter was estimated by the protein /carbohydrate ratio (Cauwet, 1978; Fichez, 1991; Danovaro et al., 1993; Raghukumar *et al.*, 2001). To convert the components of LOM to their respective carbon values, protein, carbohydrate and lipids were multiplied by 0.45, 0.5, 0.7 respectively. The sum of these converted values is the labile organic carbon (LOC).

3.6.2 *Adenosine Triphosphate (ATP)*

Adenosine Triphosphate (ATP) content was estimated to determine the total biomass of living organisms in deep-sea sediments by luciferin-luciferase reaction (Holm-Hansen and Booth, 1966), using adenosine triphosphate disodium salt as standard

(Sigma Chemicals, USA). Photons produced were counted on a Perkin Elmer, Wallac 1409 DSA, and Liquid Scintillation Counter as counts per minute and converted to ATP equivalents (Delistraty and Hershner, 1983).

3.7 Microbiology

3.7.1 Bacterial counts

3.7.1.1 Total counts of bacteria

Total counts of bacteria were estimated according to Hobbie *et al.*, 1977. About 1 g of sediment was diluted with 9 ml of sterile seawater; 3 ml of this slurry was fixed with buffered formalin at a final concentration of 2% and stored at 4°C until analysis. At the on-shore laboratory the aliquot was sonicated at 15 hertz for 15 seconds. The supernatant (1 ml) was stained with 75 µl of 0.01% acridine orange (3 mins, in dark) and filtered on 0.22 µm black polycarbonate filter paper (Millipore, USA). This procedure minimized masking by sedimentary particles. About 10-15 microscopic fields per sample were counted on Nikon 80i epifluorescence microscope. The counts were normalized to cells per gram dry sediment.

3.7.1.2 Frequency of dividing cells (FDC)

The FDC was enumerated among the total counts (Naganuma *et al.*, 1989) and represented as the natural viable population. In the filtered and stained samples of total bacterial counts, dividing cells of bacteria were counted as elaborated above. Bacteria showing an invagination, but not a clear intervening zone between cells were considered as one dividing cell (Hagstrom *et al.*, 1979).

3.7.1.3 *Autofluorescent F₄₂₀ cells*

Cells containing fluorescent pigment F₄₂₀ exhibit autofluorescence when exposed to UV light. These are the potential methylotrophic methanogens (Leigh, *et al.*, 1985) which are known to be both O₂ and H₂S tolerant (Sieburth *et al* 1993). From the sediment slurry made for counting total counts, 1 ml of supernatant was filtered on 0.22 µm black polycarbonate filter paper (Millipore, USA). About 10-15 microscopic fields were counted per sample under UV excitation using Nikon 80i epifluorescence microscope.

3.7.1.4 *Direct Viable Counts (DVC)*

Direct Viable Counts (DVC) of bacteria was determined according to Kogure *et al.*, (1984). Aerobic viable counts (DVC-a) and anaerobic viable counts (DVC-an) were enumerated separately. Three ml of this slurry was amended with 0.001% final concentration of yeast extract and 0.0016% final concentration of an antibiotic cocktail of piromedic, pipemedic and nalidixic acid solution and incubated at 4°C for 30 hours. The addition of the yeast extract in low concentration permits growth of cell and replication of nucleic acid but the antibiotic cocktail prevents cell division. The cocktail composition and incubation time were suitably modified from Joux and Lebaron, (1997). At the end of the incubation the aliquots were fixed with 2% buffered formalin and stored at 4°C until analysis. The elongated and enlarged dividing cells were counted using similar procedure as total counts (Kogure *et al.*, 1984). For determining viability under anaerobic conditions, in addition to yeast extract and antibiotic cocktail, 12µl of Na₂S .9H₂O was added as reductant at a final concentration of 0.125 % before incubation

(Loka Bharathi *et al.*, 1999). Representative stations one each for siliceous ooze, siliceous-pelagic transition, pelagic red clay and calcareous ooze were counted.

3.7.2 Image Analysis

Images of epifluorescent slides for bacterial counts and size of the bacterial cells were obtained using the Nikon image analyzer pro plus v6. The scanning electron micrographs (SEM) of the cells were also taken to observe the size and morphology (JSM-5800LV-SEM, JEOL). Prior coating of the sample on filter paper (0.22 μm) was done using gold sputter coater (SPI Module).

3.7.3 Culturable bacteria

3.7.3.1 Heterotrophs

Colony forming units on varying concentrations of ZoBell Marine Agar (ZMA) were assessed using of 20% ZoBell Marine broth in 1.5% agar. Previous studies have shown that dilute Zobell Marine Agar (20% ZoBell Marine Broth, Himedia, Mumbai, amended with 1.5% agar) yield maximum CFU in CIB sediments (Raghukumar *et al.*, 2001a, b, Nair *et al.*, 2000, Loka Bharathi and Nair, 2005). The plates were incubated at 2-5°C. Heterotrophic colonies appeared within 4-10 days. For a few selected samples four different concentrations of ZoBell Marine broth namely, 100%, 50%, 25% and 12.5% were used to study the response of heterotrophic population to changing nutrient concentration. Retrievable heterotrophic population was assessed on ZMA plates, normalized per gram dry sediment and expressed as colony forming units (CFU) per gram dry sediment.

3.7.3.2 *Potential autotrophs*

Nitrifying bacteria were enumerated on modified Winogradsky's media for ammonia oxidizers and nitrite oxidizers by substituting the medium with ammonium sulphate at 2 mM (final concentration) or sodium nitrite at 0.5 mM (final concentration) as energy source (Ram *et al.*, 2001). Medium for aerobic thiosulphate oxidizing bacteria was similar to that of TDLO as described below except for the addition of KNO₃ in case of inorganic nitrate reducers medium. Inoculation for all oxidizers was done by standard plating techniques. See Appendix V for media compositions.

Nitrate reducers were enumerated on inorganic nitrate reducers medium which is a modification Leiske's medium (Loka Bharathi, 1989; Loka Bharathi & Chandramohan, 1990; Loka Bharathi *et al.*, 2004). The bacteria cultured on this medium reduce nitrate at the expense of inorganic substrates. For simplicity this group is termed as denitrifiers hereafter as these are known to be functionally similar to *Thiobacillus denitrificans*. A second group of nitrate reducing bacteria that reduce nitrate at the expense organic matter were also cultured. For simplicity this group is termed as Nitrate Reducing Bacteria (NRB). Reducers were inoculated in agar-shake tubes as described in Loka Bharathi, (1989). See Appendix V for media compositions.

3.7.3.3 *Fe and Mn oxidizers*

Fe-oxidizers were cultivated on iron oxidizers medium (Himedia, Mumbai, India). In order to maintain a mild acidic to near neutral condition (Rodina, 1972), the salinity was adjusted to 35 ppt while the pH was adjusted to 6.8± 0.2. Mn-oxidizers were cultivated on modified Beijerinck's medium (Rodina, 1972, Havert, 1992). In order to

maintain a near neutral condition, the salinity was adjusted to 35 ppt and pH was adjusted to 7.8 ± 0.2 (See Appendix V for media compositions).

3.7.3.4 *Phosphate and silicate solubilizers*

Phosphate solubilizers were enumerated on Pikovskaya Agar (Himedia) according to Rodina (1972). Silicate solubilizers were enumerated according to Rodina, 1972 on bentonite clay amended plates (See Appendix V for media compositions).

3.7.3.5 *Formaldehyde utilizers*

Formaldehyde utilizers were grown on mineral medium amended with 0.1% buffered formaldehyde. Mineral medium for methanol utilizers was modified by using 0.1% formaldehyde instead of methanol for enumeration of culturable formaldehyde utilizers (Green, 1991).

3.8 Activity

3.8.1 *Hydrolytic Enzymes of bacterial isolates*

Isolates were examined for enzymes that degrade polymers and solubilise phosphate. These tests were carried out on agar media containing starch, gelatin, tween 80 (polyoxyethylene sorbitan mono-oleate) at 1% concentration, p-nitrophenyl phosphatase at 0.02% concentration and DNase at 5% concentration. Petri plates containing media were spot inoculated with test isolates and the presence of extracellular hydrolytic enzymes was detected after 4-days incubation at 5°C, 1 atm (Loka Bharathi

and Nair, 2005; Raghukumar *et al.*, 2001). Media composition for testing the above extracellular hydrolytic enzyme is presented in Appendix V.

3.8.2 *BIOLOG and ECOLOG carbon substrate utilization pattern analysis*

Carbon substrate utilization pattern of bacterial cultures, sediment and nodule dilutions using BIOLOG and ECOLOG plates were analysed as per manufacturer's instruction. Pinkish purple colour development indicated positive substrate utilization.

3.8.3 *Formaldehyde utilization rates by cultures*

Selected cultures were grown at 5°C on sea water amended with varying concentrations of buffered formaldehyde from 0.2-1.0%. Formaldehyde was estimated spectrophotometrically using Schiff's reaction (Bahl and Bahl, 1995). Although schiff's reagent is non-specific for most aldehydes, it could be utilized successfully in the culture experiments as no other aldehyde was used. Alternatively, use of acetylacetone in the presence of ammonium salts produces a yellow coloured end-product 3, 5-diacetyl-1,4-dihydrolutidine measured at 412 nm in presence of formaldehyde (Nash, 1953). The utilization rates were normalized per cell and expressed as $\text{ng cell}^{-1} \text{hr}^{-1}$.

3.8.4 *Microbial carbon fixation*

Autotrophic uptake of $\text{NaH}^{14}\text{CO}_3$ by sediments and cultures

Autotrophic potential in sediments was measured using $\text{NaH}^{14}\text{CO}_3$ uptake [$5\mu\text{Ci/ml}$ activity, Board of Radiation and Isotope Technology (BRIT), Navi Mumbai, India] adopting methods described earlier (Nelson *et al.*, 1989; Tuttle and Jannasch,

1977). Briefly, about 1 g of sediment was suspended in 9 ml sterile seawater and this sediment slurry was incubated with 0.08 $\mu\text{Ci ml}^{-1}$ final concentration of $\text{NaH}^{14}\text{CO}_3$ at 4°C for 24 h in the dark. Unincorporated labelled carbon was carefully washed with sterile seawater. The filtered slurry was acidified for removal of unbound ^{14}C and trace inorganic carbon. The filter with the trapped sediment was further dried at 35°C and then suspended in scintillation vial containing cocktail. The sample was counted after 12-24 hrs in a Liquid Scintillation counter (Model Perkin Elmer, Wallac 1409 DSA). Suitable controls for unlabelled and heat killed sediments, wash water and labelled carbon were included. The incorporation of carbon was read as disintegrations per minute (integrated for 5 minutes) and was expressed as $\text{nmol C g}^{-1} \text{ day}^{-1}$. In case of cultures, 10 ml suspension was injected with 0.08 $\mu\text{Ci ml}^{-1}$ final concentration of $\text{NaH}^{14}\text{CO}_3$ at 4°C. At the end of incubation the suspension was filtered through 0.22 μm filter paper and treated similarly as mentioned above.

3.8.5 Ribulose bis-phosphate carboxylase/oxygenase (RuBisCO) enzyme activity in cultures and sediments

Ribulose-1, 5-diphosphate carboxylase (EC 4.1.1.39) was assayed in crude cell-free extracts by a radioisotope method (Romanova *et al.*, 1971, Chakrabarti *et al.* 2003) and modified suitably for estimation in cultures and sediments.

a. Preparation of cell-free extract

RuBisCO enzyme activity was measured in three representative cores namely SVBC 26, a siliceous ooze core, SVBC 36, a pelagic red clay core and SVBC 37, a calcareous core. The calcareous sediments comprising mainly of foraminiferal tests were

further fractionated into carbonate and clay fractions by gravimetric separation. About 2 g of sediment containing at least 5×10^6 cells g^{-1} was taken in an Oakridge tube and 18 ml of homogenization buffer was added (Appendix VI). The samples were sonicated thrice at 40 hertz for 30 seconds. Care was taken such that foaming did not occur. The supernatant was decanted and centrifuged for 4 mins at 14,000 rpm. The clear supernatant was collected in labelled serum bottle, sealed with rubber stopper and placed in ice. Protein estimation of the crude enzyme was done according to Lowry *et al.*, 1951.

b. Enzyme assay

Reaction mixture of 0.1 ml final volume was used for RuBP (Ribulose bisphosphate) dependent incorporation of $NaH^{14}CO_3$ into acid stable product.

c. Reaction

About 0.1 ml each of stock solution A, B, C (Appendix VI) was pipetted into four 15 ml glass centrifuge tubes. Water (0.3 ml) was added. Total volume was made to 0.8 ml and the contents were placed in an incubator at 4°C. About 0.1 ml of boiled extract was added to the control. To each of the other 3 tubes, 0.1 ml cold cell free extract was added. The contents were pre-incubated for 10 minutes.

d. Initiation and termination

At the start of the reaction, 0.1 ml RuBP was added in all four tubes. To the control tube, 0.1 ml of water was added. Samples were incubated for 10 minutes at 4°C and the reaction was terminated using 1 ml of 24% w/v of tricarboxylic acid to each tube.

e. *Analysis*

The tubes were dried and 1 ml of warm water was added. Centrifugation was done at 5000g for 10 minutes. 0.1ml aliquot of each supernatant was pipetted into scintillation vial. Cocktail was added and left overnight in the dark before counting. Carboxylase activity was calculated according to the following formula :

Specific activity of Carboxylase in $\mu\text{mol}/\text{min}/\text{mg}$ protein

$$= \{[^{14}\text{C}(\text{dpm})]/[(\text{dpm } ^{14}\text{C}/ \mu\text{mol CO}_2) \times \text{time (min)} \times \text{mg protein}]\}$$

3.8.6 *Estimation of phosphate solubilizing activity in sediments*

Extracellular enzyme activity can be detected by using fluorogenic substrate analogues such as Methylumbelliferyl phosphate (MUF-P) (Chrôt, 1990). Alkaline Phosphatase activity was determined by a common fluorometric method (Hoppe 1983, 1993) using a fluorogenic substrate, 4-Methylumbelliferyl Phosphate (MUF-P) (Sigma chemical). The alkaline phosphatase hydrolyses the fluorogenic substrate MUF-P and yields a highly fluorescent product (Methylumbelliferon: MUF) and a phosphate group in equimolar concentrations. The MUF produced was detected as increase in fluorescence with a FLUOstar Omega, BMG Labtech. A standard curve with MUF (Sigma Co.) was used to quantify the amount of MUF produced by APA, so the phosphate liberated in the reaction could be estimated. To 0.5 g of the frozen sediment 0.1ml of $1\mu\text{M}$ MUF-P substrate was added along with 9.9ml of the Tris-HCl buffer (pH 8.3). The reaction tubes were incubated for 45 minutes at 4°C in the dark. The assay was performed in triplicates. Aliquots of $350\mu\text{l}$ of filtrate were loaded into 96 well-automated microtiter plate fluorometer (FLUOstar Omega, BMG Labtech) with excitation and emission filters of

355 and 460 nm, respectively. The controls of each sample were measured and deducted from the values obtained from the fluorescence. Standard calibration curves were run with Methylumbelliferon to get the calibration factor as the slope of regression line. The activity was expressed as the quantity of MUF liberated per gram of sediment per hour.

3.9 Diversity

3.9.1. Biochemical methods

Representative colonies were isolated, checked for purity and identified up to generic levels using phenotypic traits as described by Oliver (1982), and elaborated in the Bergey's Manual of Determinative Bacteriology, (13th Ed.).

3.9.2. Microbial diversity using molecular techniques:

3.9.2.1 16S rDNA

a. Extraction and amplification

DNA was extracted from isolates by the method described by Maniatis *et al.* (1982). The primers used for 16S ribotyping analysis were as per MicroSeq 500 kit (*Applied Biosystems, USA*). Amplification of DNA was carried out on a thermocycler (GeneAmp PCR, *Applied Biosystems, USA*). The mixture was incubated through initial denaturation at 94°C for 2min, followed by 30 cycles at 94°C for 30sec, 54°C for 1min and 72°C for 1min. A final extension period consisted of 1min at 72°C. The entire 500bp long sequence generated was used for further analysis. The amplified DNA fragment was purified using the PCR purification kit (*Vivantis, Malaysia*). The purified PCR product was sequenced using the BDT v3.1 cycle sequencing PCR kit (*Applied Biosystems, USA*)

on a 3130 Genetic Analyzer (*Applied Biosystems Inc, USA*) at the geneOmbio Technologies sequencing facility.

b. Sequence analysis

All of the sequences used for comparison were retrieved from the NCBI BLASTn database. Sequences were aligned and edited by using the CLUSTAL W program. Evolutionary trees were constructed by distance, and maximum-likelihood methods by using programs contained in the phylogeny inference package (PHYLIP, version 3.69). For each alignment, 100 bootstrapped replicate re-sampling data sets were generated by using the SEQBOOT program with random sequence addition and global rearrangement. Evolutionary distances were constructed with the program DNADIST by using the option Jukes-Cantor model for nucleotide substitution. The resulting evolutionary distance matrices were used to reconstruct phylogenetic trees by the neighbor-joining method by using NEIGHBOR and MEGA 4 (Felsenstein, 1993)

3.9.2.2 Pyrosequencing using 454 technology

a. Extraction of total DNA for pyrosequencing using PowerSoil™ DNA Isolation Kit (MoBio)

Sediment sample representing a chemosynthetic interface at depth 2-4 cms bsf belonging to TVBC 08 was selected for bacterial diversity using the 454 pyrosequencing method. Approximately 5 gm of sediment sample was lyophilized and genomic DNA was extracted using the Mo Bio power soil DNA isolation kit (CA, USA). This kit

minimized the interference of humic substances. The genomic DNA was extracted as follows:

Approximately 0.25 g of lyophilized sediment was weighed in clean pre-weighed 2 ml eppendorf tubes and added to PowerBead tubes containing glass beads provided in the kit. The tubes were gently vortexed to mix and 60 μ l of Solution C1 containing sodium dodecyl sulfate (SDS). The PowerBead tubes were inverted several times to mix. Further, tubes were vortexed at a maximum speed for 10 min on a horizontal vortexer. This step was used to disperse sediment particles while dissolving humic acids such that nucleic acid was prevented from degradation.

The tubes were centrifuged at 13,000 g for 1 min at 4°C. The supernatant was transferred to a clean 2 ml collection tube and 250 μ l of solution C2 was added. The tubes were vortexed for 5 seconds and incubated at 4 °C for 5 min. Solution C2 contained a reagent to precipitate non-DNA organic and inorganic material including humic substances, cell debris and proteins.

The tubes were centrifuged at 4°C for 1 min at 13,000 g and avoiding the pellet, up to 600 μ l of supernatant was removed and added to a clean 2 ml collection tube. To this supernatant, 200 μ l of solution C3 was added and vortexed briefly. The tubes were incubated at 4 °C for 5 min. The solution precipitated additional non-DNA organic and inorganic material including humic acid, cell debris and proteins. The tubes were centrifuged at 4°C for 1 min at 13,000 g. Avoiding the pellet, 750 μ l of supernatant was transferred to a clean 2 ml collection tube.

To this supernatant, 1200 μ l of solution C4 was added and the tubes were vortexed for 5 seconds. Solution C4 is a high concentration salt solution. Since DNA

binds tightly to silica at high salt concentrations, this adjusted the DNA solution's salt concentration such that the DNA is bound to the spin filters. However, the non-DNA organic and inorganic material which could be present at low levels was prevented from doing so.

Approximately 675 μl was loaded onto a spin filter and centrifuged at 13,000 g for 1 min at 4 $^{\circ}\text{C}$. The flow through was discarded and an additional 675 μl of supernatant was added to the Spin Filter and centrifuged at 13,000 g for 1 min at 4 $^{\circ}\text{C}$. To the spin filters, 500 μl of solution C5 was added and centrifuged at room temperature for 1 min at 13,000 g . Solution C5 is an ethanol based wash solution and is used to further clean the DNA that is bound to the silica filter membrane in the spin filter. This wash solution removes residual salt, humic acid, and other contaminants while allowing the DNA to stay bound to the silica membrane.

The flow through was discarded. The tubes were centrifuged again at 4 $^{\circ}\text{C}$ for 1 min at 13,000 g . The spin filters was carefully placed in a clean 2 ml collection tube avoiding splashing of any solution C5 on to the spin filter. A 100 μl of solution C6 was added to the centre of the white filter membrane. As Solution C6 (elution buffer) passed through the silica membrane, DNA that was bound due to the presence of high salt was selectively released by solution C6 (10 mM Tris) which lacked salt.

The tubes were centrifuged at 4 $^{\circ}\text{C}$ for 30 s at 13,000 g and the spin filter was discarded. DNA samples were checked for purity [$\text{OD}_{260}/\text{OD}_{280} \sim 1.8$]. Purity and quantification of the extracted DNA was carried out using Nanodrop ND-1000 spectrophotometer (Nanodrop Technologies, Wilmington DE). The final volume of eluted DNA (100 μL) was concentrated by adding 4 μL of 5M NaCl and inverting 3-5

times to mix. Next, 200 μ L of 100 % cold ethanol was added and the tubes were inverted 3-5 times to mix. Samples were centrifuged at 10,000g for 5 min at room temperature. All liquid was carefully decanted. Residual ethanol was removed by drying the precipitate overnight in a dessicator.

b. Amplification of the V6 region of the 16S rRNA gene using high-throughput pyrosequencing

Precipitated DNA was re-suspended in sterile water. The hypervariable region of 16S rRNA gene (BV6-rRNA tags) region was amplified and subjected to high-throughput using the 454 technology as described by Sogin *et al.*, (2006) and Huber *et al.*, (2007).

Pyrosequencing is a DNA sequencing technique that is based on the detection of released pyrophosphate (PPi) during DNA synthesis. In a cascade of enzymatic reactions, visible light is generated that is proportional to the number of incorporated nucleotides. The cascade starts with a nucleic acid polymerization reaction in which inorganic PPi is released as a result of nucleotide incorporation by polymerase. The released PPi is subsequently converted to ATP by ATP sulfurylase, which provides the energy to luciferase to oxidize luciferin and generate light. Because the added nucleotide is known, the sequence of the template can be determined. The nucleic acid molecule can be either RNA or DNA. However, because DNA polymerases show higher catalytic activity than RNA polymerases for limited nucleotide extension, efforts have been focused on the use of a primed DNA template for pyrosequencing (Ronaghi, 2001).

The following sequence adaptors and primers were used
(<http://vampr.mbl.edu/resources>).

Roche amplicon sequencing adaptors:

A-adaptor 5'-GCCTCCCTCGCGCCATCAG-3'

B-adaptor 5'-GCCTTGCCAGCCCGCTCAG-3'

For bacterial V6 sequencing a mixture of the following
5 forward and 4 reverse primers were used.

Forward Primers (967F)

CNACGCGAAGAACCTTANC

CAACGCGAAAAACCTTACC

CAACGCGCAGAACCTTACC

ATACGCGARGAACCTTACC

CTAACCGANGAACCTYACC

Reverse Primers (1046R)

CGACAGCCATGCANACCT

CGACAACCATGCANACCT

CGACGGCCATGCANACCT

CGACGACCATGCANACCT

Thus, to amplify the V6 hypervariable region of the bacterial 16S rRNA (*Escherichia coli* positions 967-1046) (Sogin *et al.*, 2006) and sequence it in the forward direction (relative to the 5'-3' orientation of the gene) using the Roche A primer, the forward primer consisted of the A-adaptor, 5-base key and sequence designed to bind to the 967F region of the SSU.

5'-GCCTCCCTCGCGCCATCAGgatctCNACGCGAAGAACCTTANC-3'

The reverse primer would consist of the B-adaptor and a sequence designed to bind to 1046R:

5'-GCCTCCCTCGCGCCATCAG CGACAGCCATGCANACCT -3'

c. Sequence analyses

Trimming and removal of low-quality reads was done as described by Sogin *et al.*, (2006), Huber *et al.*, (2007) and <http://vamps.mbl.edu/resources>. The likely low-quality sequences were identified based on previous assessment of pyrosequencing error rates (Huse *et al.*, 2007) and was removed. In addition, the sequences were aligned using the NAST tool provided on the GreenGenes web site <http://greengenes.lbl.gov>, and only sequences >40 base pairs were retained. Significant matches were defined as having at least 75% identity with a known sequence. Finally, those sequences that occurred only once among the dataset were removed.

The 454 tags served as query to identify its closest match in a reference database (V6RefDB) containing ~40,000 unique V6 sequences (Sogin *et al.*, 2006). Taxonomic counts from the VAMPS database (vamps.mbl.edu) were then downloaded and imported on to a MS office excel worksheet. Sequence characteristics such as average length and tag aggregates were estimated using the R program (Kirchman *et al.*, 2010).

3.10 Data analysis and statistical significance

In case of epifluorescence counts, 10-15 microscopic fields cumulating to not less than 500 cells were considered for deriving standard deviations. All parameters were analyzed in triplicates and normalized per gram sediment dry weight unless mentioned otherwise. Parameters were plotted as averaged profiles with error bars representing range of individual samples using GRAPHER 4 or Microsoft Excel. Two dimensional and three dimensional figures for showing basin-scale variations were plotted using SURFER 8. Single or two-factor analysis of variance (ANOVA) without replication was used for confirming significance in variations. Correlation parameters were analyzed for Spearman's Rank correlation using *Statistica* version 6. Multivariations were analysed using PRIMER v6 package (Plymouth Routines in Multivariate Ecological Research) to the fourth root transformed data to determine which variable contributes most to the distribution in an ordination diagram (Clarke and Warwick, 2001).

3.11 Simulation

3.11.1 Quantification of the influence of non-steady state diagenetic condition on microbial community by numerical simulation

A non-steady state diagenetic model was constructed to explain the formation of the tan green mottled zone showing chemoautotrophy in core TVBC 26 (Courtesy I. Suresh, NIO, Goa). Transient diffusion model (Meister *et al.*, 2007) including a sink term, was used to simulate NO_3^- porewater profiles (Courtesy B.N.Nath and M.B.L. Mascarenhas-Pereira, NIO, Goa) as shown in equation 5:

$$\partial c / \partial t = \kappa (\partial^2 c / \partial x^2) + s(x) \quad (5)$$

where, $c(x,t)$ is the concentration of NO_3^- (μM), t is time (yr), and x is the depth below sea floor (cm bsf).

$$\kappa = \varphi \tau^{-2} D_s \text{ and } \tau^2 = \varphi F \quad (6)$$

where, D_s is the diffusion coefficient for NO_3^- ($\text{m}^2 \text{s}^{-1}$), φ is the porosity (dimensionless) and F is the formation factor (dimensionless). Nitrite oxidation rate $s(x)$ and the nitrate reduction rate $s'(x)$ is:

$$s(x) = 0 \mu\text{mol m}^{-3} \text{ yr}^{-1}, \text{ if } t < 10,000\text{yr};$$

$$s(x) = 1000 \mu\text{mol m}^{-3} \text{ yr}^{-1}, \text{ if } 10,000\text{yr} < t < 11,200\text{yr and } 3 < x < 7\text{cm bsf}$$

$$s'(x) = -1000 \mu\text{mol m}^{-3} \text{ yr}^{-1}, \text{ if } 10,000\text{yr} < t < 11,200\text{yr and } 5 < x < 9\text{cm bsf}$$

Thus, $s(x)$ represents nitrification and is substituted by $s'(x)$ in case of denitrification.

The following initial conditions and boundary conditions were used:

$$c = 26.13 \mu\text{M} \quad \text{for } x > 0$$

$$c = 8.87 \mu\text{M} \quad \text{for } x = 0$$

$$c(0, t) = 8.87 \mu\text{M}$$

$$c(L, t) = 26.13 \mu\text{M}$$

where, L is the length of the model domain.

Explicit finite difference method was used to solve equation 5. A time step of 10 years and a grid size of 1 cm were chosen. Tortuosity factor was calculated from porosity and formation factor (Schulz & Zabel, 2000). A diffusion coefficient for NO_3^- of $9.03\text{E-}10\text{m}^2 \text{ s}^{-1}$, at 0°C was considered (Schulz & Zabel, 2000). Both $s(x)$ and $s'(x) =$

0 for the first 10,000 years of the computation, which is the time required for an organic matter pulse to reach the present tan-green mottled zone at 13 to 25 cm bsf without being diagenetically altered. After setting these conditions, nitrite oxidation and nitrate reduction are switched on separately in the depth interval $3 < x < 7$ cm bsf and $5 < x < 9$ cm bsf respectively to simulate the effect of strong nitrite oxidation followed by nitrate reduction in an organic carbon-rich sediment layer. A nitrite oxidation rate of $1000 \mu\text{M m}^{-3} \text{ yr}^{-1}$ was assumed in a horizon from 3 to 7 cm bsf (Ward *et al.*, 1989). In the horizon from 5 to 9 cm bsf a maximum nitrate reduction rate of $-1000 \mu\text{M m}^{-3} \text{ yr}^{-1}$ was assumed.

3.11.2 Quantification of hydrothermal alterations on pore-water and microbial community by numerical simulation

A modified transient diffusion model (Meister *et al.*, 2007) including a source term was considered to explain the influence of hydrothermal activity on the porewater profile. This model in turn was used to explain the enhanced chemoautotrophic microbial activity at the Pleistocene-Tertiary stratigraphic transition zone of core TVBC 08. Porewater NO_3^- profiles were simulated as shown in equation 7:

$$\partial c / \partial t = \kappa' (\partial^2 c / \partial x^2) + sr(x) \quad (7)$$

where, $c(x,t)$ is the concentration of NO_3^- (μM), t is time (yr), and x is the depth below sea floor (cm bsf).

$$\kappa' = \varphi \tau^{-2} D_s \text{ and } \tau^2 = \varphi F' \quad (8)$$

where, D_s is the diffusion coefficient for NO_3^- ($\text{m}^2 \text{ s}^{-1}$), φ is the porosity (dimensionless) and F is the formation factor (dimensionless). Nitrite oxidation rate $sr(x)$ and the nitrate reduction rate $sr'(x)$ is:

$$sr(x) = 0 \mu\text{mol m}^{-3} \text{ yr}^{-1}, \text{ if } t < 1000 \text{ yr};$$

$$sr(x) = 1000 \mu\text{mol m}^{-3} \text{ yr}^{-1}, \text{ if } 1000 \text{ yr} < t < 1170 \text{ yr and } 3 < x < 7 \text{ cm bsf}$$

$$sr'(x) = -1000 \mu\text{mol m}^{-3} \text{ yr}^{-1}, \text{ if } 1000 \text{ yr} < t < 1170 \text{ yr and } 5 < x < 9 \text{ cm bsf}$$

Thus, $sr(x)$ represents nitrification and is substituted by $sr'(x)$ in the case of denitrification.

The following initial conditions and boundary conditions were used:

$$c = 9.71 \mu\text{M} \quad \text{for } x > 0$$

$$c = 4.85 \mu\text{M} \quad \text{for } x = 0$$

$$c(0, t) = 4.85 \mu\text{M}$$

$$c(L, t) = 9.71 \mu\text{M}$$

where, L is the length of the model domain.

Explicit finite difference method was used to solve equation 7. A time step of 1 year and a grid size of 1 cm were chosen. Tortuosity factor was calculated from porosity and formation factor (Schulz & Zabel, 2000). A diffusion coefficient for NO_3^- of $9.03\text{E-}10\text{m}^2 \text{ s}^{-1}$, at 0°C was considered (Schulz & Zabel, 2000). Both $sr(x)$ and $sr'(x) = 0$ for the first 1000 years of the computation, when up-welling of hydrothermally derived NO_3^- occurs as a focused jet to the present Pleistocene-Tertiary stratigraphic transition zone at 3 to 12 cm bsf without being dispersed laterally. After setting these conditions, nitrite oxidation and nitrate reduction are switched on separately in the depth interval $3 < x < 7\text{cm}$ and $5 < x < 9 \text{ cm bsf}$ respectively. The effect of strong nitrite oxidation followed by nitrate reduction in the stratigraphic transition zone is simulated due to lateral dispersion and phase separation of solutes carried upward by the hydrothermal fluid and resultant

microbial activity. A nitrite oxidation rate of $1000 \mu\text{M m}^{-3} \text{yr}^{-1}$ was assumed in a horizon from 3 to 7cm bsf (Ward *et al.*, 1989). In the horizon from 5 to 9 cm bsf a maximum nitrate reduction rate of $-1000 \mu\text{M m}^{-3} \text{yr}^{-1}$ was assumed. The model source code in MATLAB 7.0.4 used for this work is presented in Appendix IX. For details of the simulation refer Das *et al.*, 2010.

*“There is no phenomenon in a living system that is not molecular,
but there is none that is only molecular either.”*

-Paul Weiss

Chapter IV

Results

4.1 Environmental Parameters

4.1.1 Temperature

Temperature of sediment cores ranged between 6°-10°C when brought on board. *In situ* temperature in the Central Indian Basin was found to be ~1°C (Warren et al., 1982).

4.1.2 Depth and pressure

Depth of most sample were >5000m to <6000m below sea surface. Difference between given and touch- position was usually within 10-100m, thus providing reliability in sampling repeats between different stations and seasons (Fig. 4.1). All stations except station 37, a sea-mount summit are located ~1000m below the Calcite Compensation Depth. Apart from the sea-mount at the fracture zone at 16°S and 75.5°E, the central part of the basin from 12°-13°S was the deepest part of the CIOB. *In situ* pressure was >500 to < 600 atmospheres assuming 1atm raise every 10m descent.

4.2 Geochemical parameters

4.2.1 Rock Colour

The northern sediments between 10°-12°S is dominated by sediment hues 10YR4/2 (dark yellowish brown), 10YR5/4 (moderate yellowish brown) and to a lesser extent by 5Y5/2 (light olive grey). Central sediment from 12°-14°S dominated by five hues 5Y5/2, 5YR3/4 (moderate brown), 10YR4/2, 10YR5/4 and 10YR6/6 (dark yellowish orange). The southern pelagic clay between 14°-16°S is dominated by the hue 5YR3/4 (Fig. 4.2). The rock colour map clearly shows the diagenetic haloes of mottle

formations. These colour changes coincide with hotspots of microbial distribution and activity.



Fig. 4.1 Seabed topography derived from water depth data at sampled stations. Plot indicates good replication of station positions. Variation noted at 76.5°E and 12°S are due to rough sea-state and ship-drift.

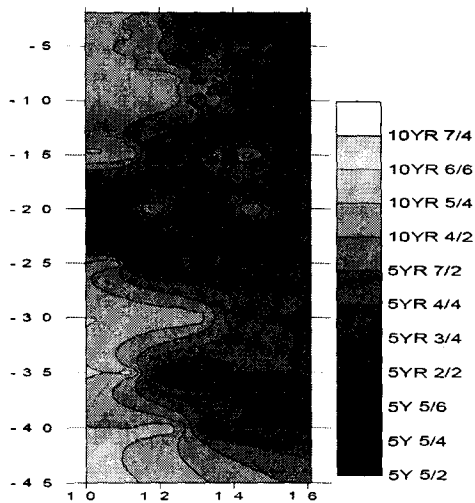


Fig. 4.2 Down-core variation of rock colour along North-South transect along 75°30'.

4.2.2 *Pore water geochemistry*

The relatively nodule-rich core IVBC 20A and nodule-poor core IVBC 18C showed distinct differences in their pore water parameters. Station IVBC 20A at 12°S, 75.5°E harbours 1-2 kg nodules m⁻². Station IVBC 18C at 13°S, 74.5°E harbours <1 kg nodules m⁻².

4.2.2.1. *pH and Eh*

The pH and Eh were measured on-board immediately after core retrieval. The pH of pore waters varied from 5-9. Eh varied from +150 mV to -370 mV. Down-core variation in pH and Eh variations are plotted in Fig. 4.2. The pH averaged at 6.33 ± 0.56 and Eh averaged at 25.32 ± 49.87 mV at temperature 17.7 ± 3.16 °C for core IVBC 20A. For IVBC 18C the pH averaged at 6.59 ± 1.22 and Eh averaged at 40.06 ± 142.60 mV (Fig 4.3). The variation in Eh was responsible for 16.48% variation in pH in case of IVBC 20A, and 48% in case of IVBC 18A (Fig. 4.4).

A time-series experiment was done using representative samples from core IVBC 20A to show the relative variation of pH and Eh with temperature (Fig. 4.5). The top 8-10 cm bsf did not show appreciable difference with time and temperature. At the lower depths of 16-18 and 20-22 cm bsf the Eh decreased and pH increased with increase of temperature.

4.2.2.2 *Dissolved Oxygen*

The oxygen concentrations in nodule-rich core IVBC 20A varied from 180 to 370 $\mu\text{M l}^{-1}$ with peaks at 10 and 20 cm bsf indicating consumption of oxygen at the

reactive layers above 10 cm and mottles above 20 cm (Fig. 4.6). The oxygen concentration in nodule poor core IVBC 18C ranged from non detectable to $123 \mu\text{M l}^{-1}$.

4.2.2.3 *Salinity*

Salinity was checked in representative samples and was found to vary from 35 to 39 ppt at 15°C .

4.2.2.4 *Ammonium*

Ammonium concentrations in porewater of core IVBC 20A varied from non detectable to $0.14 \mu\text{M l}^{-1}$ with peaks generally corresponding to oxygen depletion (Fig. 4.6). Core IVBC 18C showed a higher range of porewater ammonium varying from 0.2 - $0.91 \mu\text{M l}^{-1}$ in its pore-water.

4.2.2.5 *Sulphide*

Sulphide concentrations in core IVBC 20A varied from 0.03 to $0.18 \mu\text{M l}^{-1}$ with maximum concentration at 7 cm bsf (Fig. 4.6). Core IVBC 18 showed a sulphide concentration ranging from non detectable level (ndl) to $0.22 \mu\text{M l}^{-1}$.

4.2.2.6. *Total Fe*

Fe concentrations in core IVBC 20A varied from 0.39 to 0.79 mg l^{-1} with highest peak at 17 cm bsf (Fig. 4.6).

4.2.2.7. *Total Mn*

Mn concentrations in core IVBC 20A varied from 0.14 to 9.95mg l⁻¹ with peaks above 7 and 19 cm bsf (Fig. 4.6).

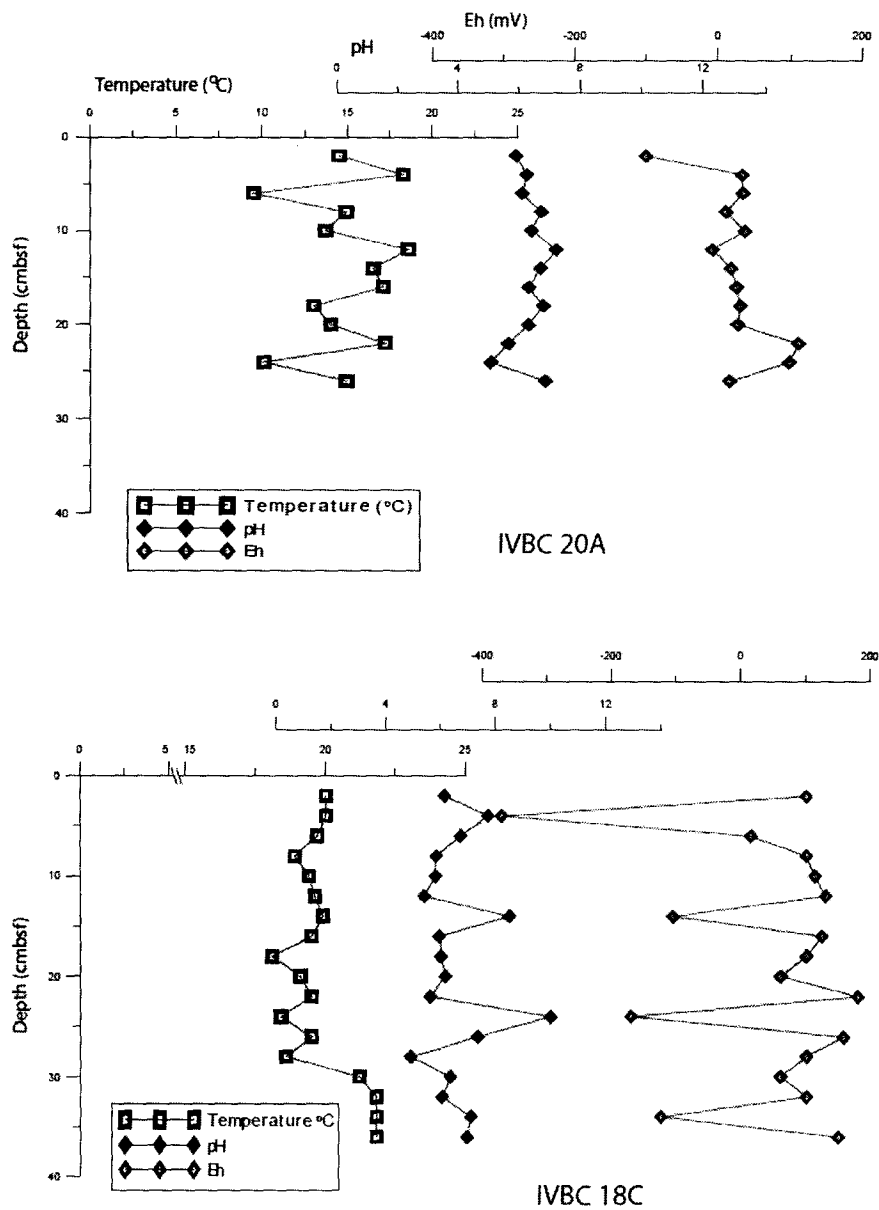
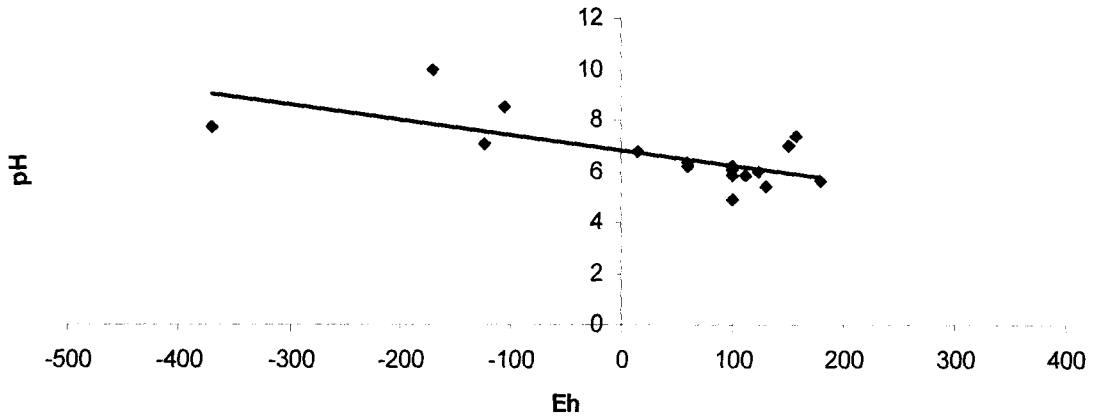


Fig. 4.3 Down core variation of temperature, pH and Eh checked on-board.

A. pH-Eh correlation for IVBC 18A

$$y = -0.0059x + 6.824$$
$$R^2 = 0.4676$$



B. pH-Eh correlation for IVBC 20A

$$y = -0.0046x + 6.4417$$
$$R^2 = 0.1648$$

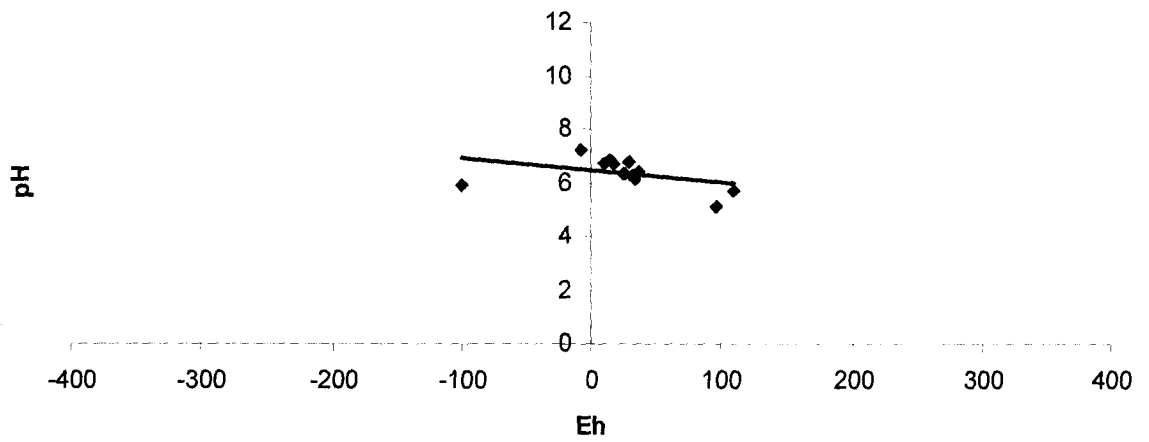


Fig. 4.4. pH-Eh correlation in stations IVBC 20A and IVBC 18C.

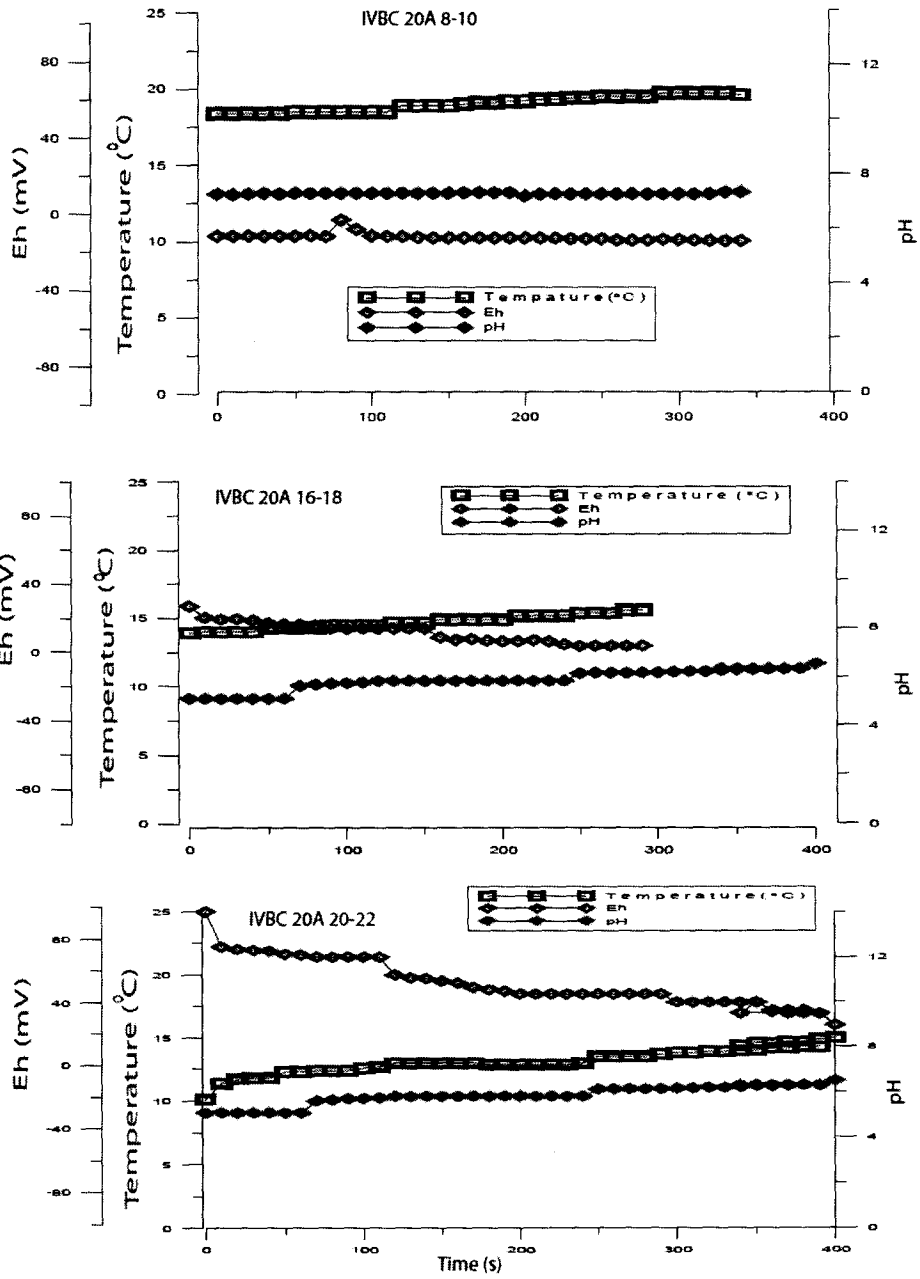


Fig.4.5

Change of pH and Eh of sample on-board with increasing temperature and time.

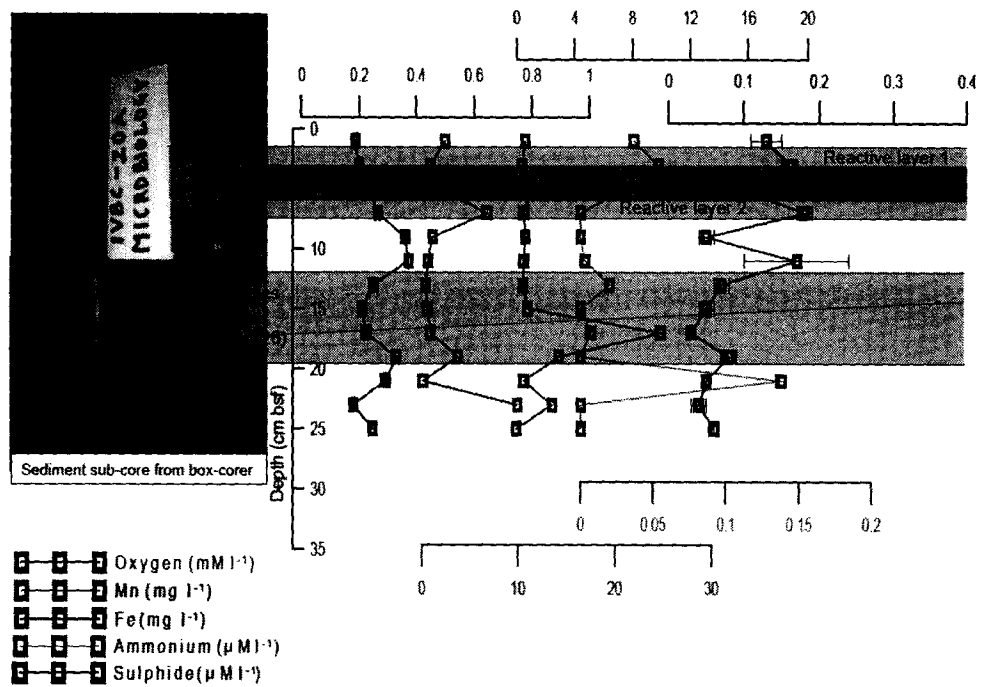


Fig. 4.6 Pore-water oxygen, manganese, iron, ammonium and sulphide in core IVBC 20A.

4.3 Elemental carbon, nitrogen, C/N ratio

TOC varied from 0.03 to 1.3% in the northern siliceous oozes. In the pelagic red clays TOC ranged from 0.01 to 1%. Latitudinally, TOC decreased from northern to southern part of the basin. The central part of the Basin (in and around station 19) recorded some of the highest values of TOC, lowest total nitrogen and consequently the highest C/N ratios (Fig. 4.7 A and B). TOC in the calcareous oozes varied from 0.17 to 0.35%.

C/N ratio varied from 2-24 in the northern siliceous ooze, 1-32 in the pelagic red clays and 0.2-22 in the central part of the basin. In the calcareous oozes the C/N ratio varied from 19-145.

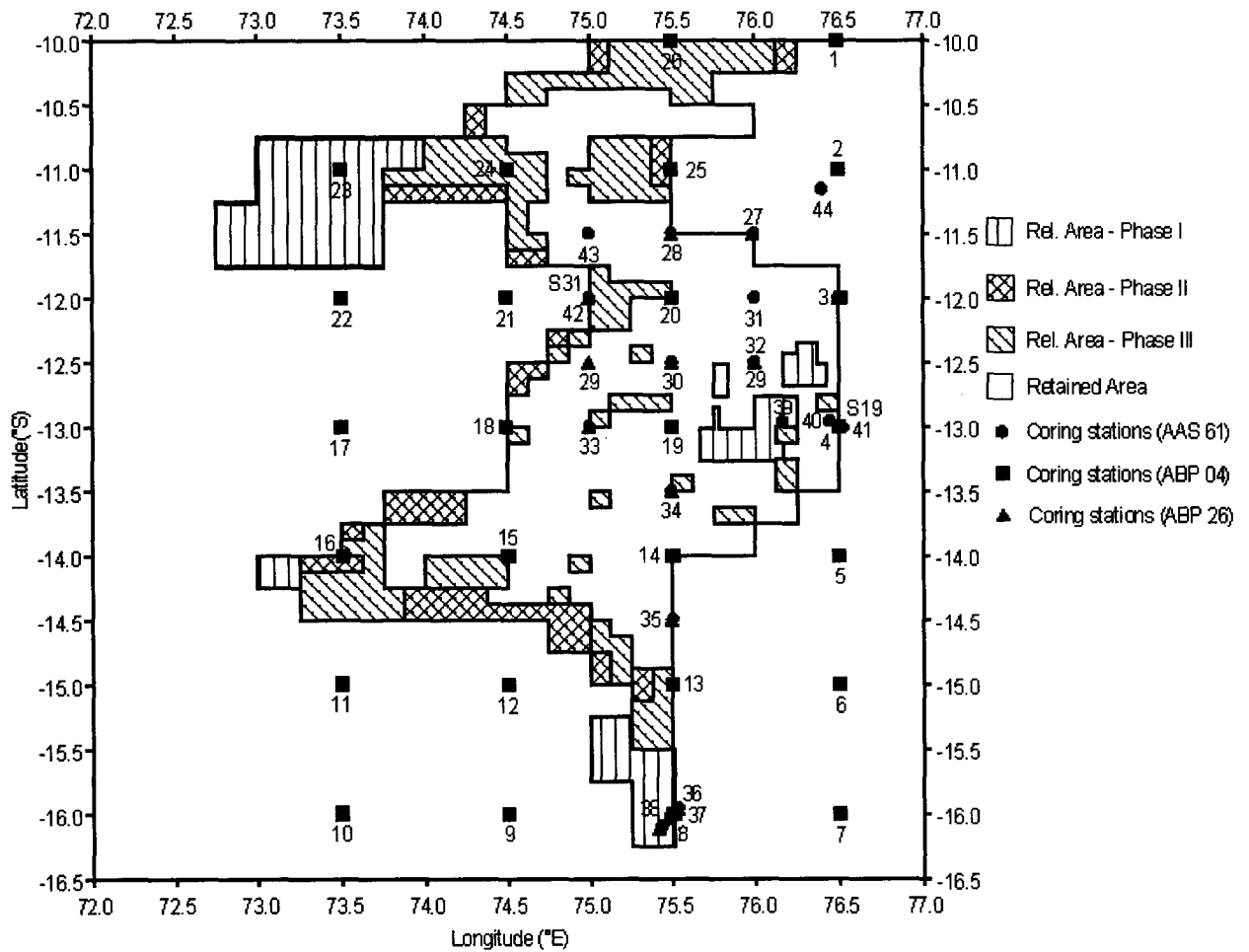
Total inorganic carbon (TIC) varied from non-detectable to 700 ppm in the basin. Again, the central part of the basin showed some of the highest values. Above the calcite compensation depth (CCD) the calcareous oozes showed values as high as 6-10%. Calcareous ooze station 37 is not included in the clusters because it is a single core of its type, while all others are below CCD.

Down-core variation was checked along North-South profile of 75°30' (Fig. 4.8). The highest values of TOC and C/N were conspicuous in the down-core profiles between 12-14°S. Cluster analysis for TOC (Fig. 4.7A) showed that station 19 was separated from the rest of the cores at a dissimilarity cut off of nearly 90%. At 40% dissimilarity, two major clusters appeared separating cores 13 and 38 from the rest of the cores. Cluster analysis for C/N ratio (Fig. 4.7B) showed that stations 19 and 36 were separated from the rest of the cores at nearly 85% dissimilarity cut off. At 40% dissimilarity, two major clusters appeared separating cores 20 and 13 from the rest of the cores.

4.4 Distribution of bacteria in the Central Indian Ocean Basin

Understanding the distribution of bacteria is important because they are the main link between non-living and higher living resources. This is specially significant in deep-sea systems. The deep sub-seafloor biosphere comprises about 65% of the global prokaryotic biomass (Parkes *et al.*, 1994; Whitman *et al.*, 1998). There are hotspots of bacterial distribution in regions like vents and seeps and low distribution spots like abyssal plains and deep sub-surface. The seafloor environment is a dynamic geosphere

that provides a diverse range of living conditions that are host to varied microbial communities (Jørgensen & Boetius, 2007).



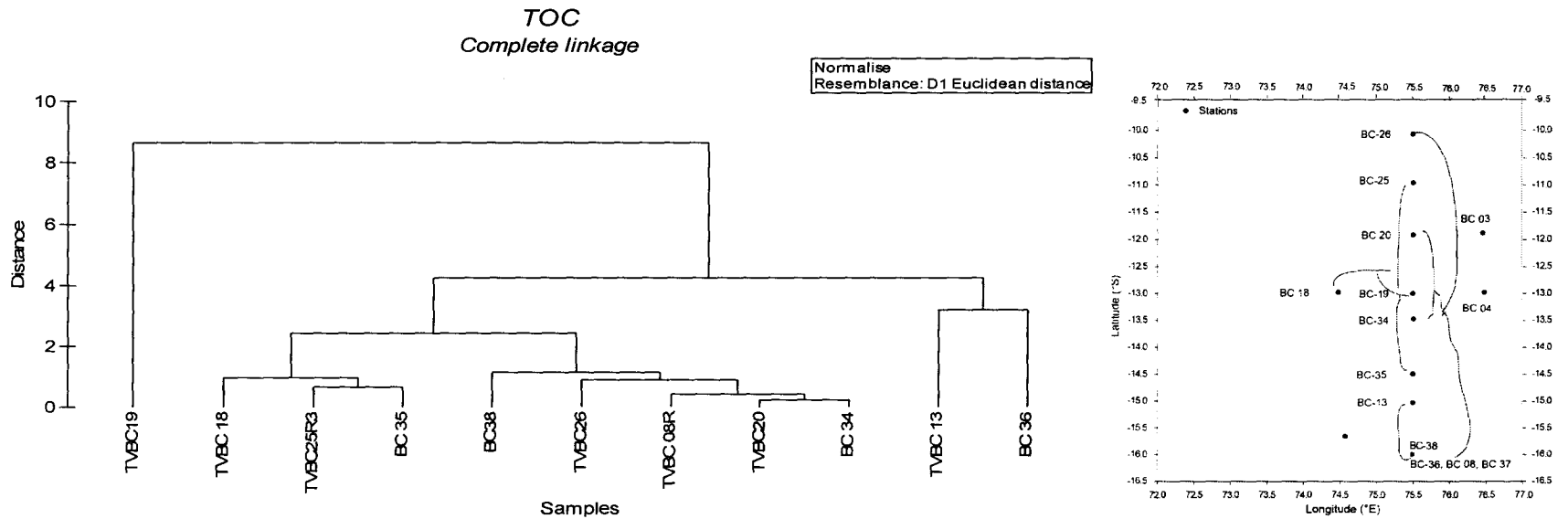


Fig. 4.7A Cluster analysis of CIOB stations based on TOC content. Inset shows station locations in the basin. Cluster shows stations under influence of trace of Rodrigues triple junction on Indian Plate (RTJ-IO) grouping together. Organic depocentres in valleys like 38 in the south cluster with organic rich northern sediments.

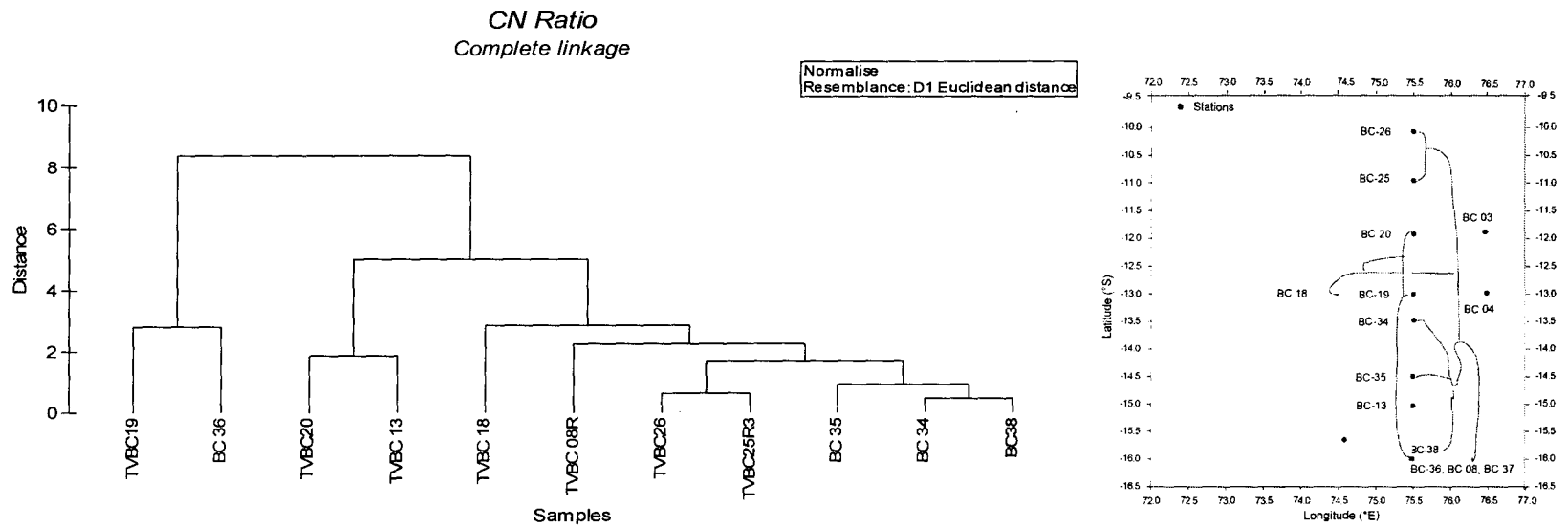


Fig. 4.7B Cluster analysis of CIOB stations based on C/N ratios. Like TOC stations under the influence of RTJ-IO.

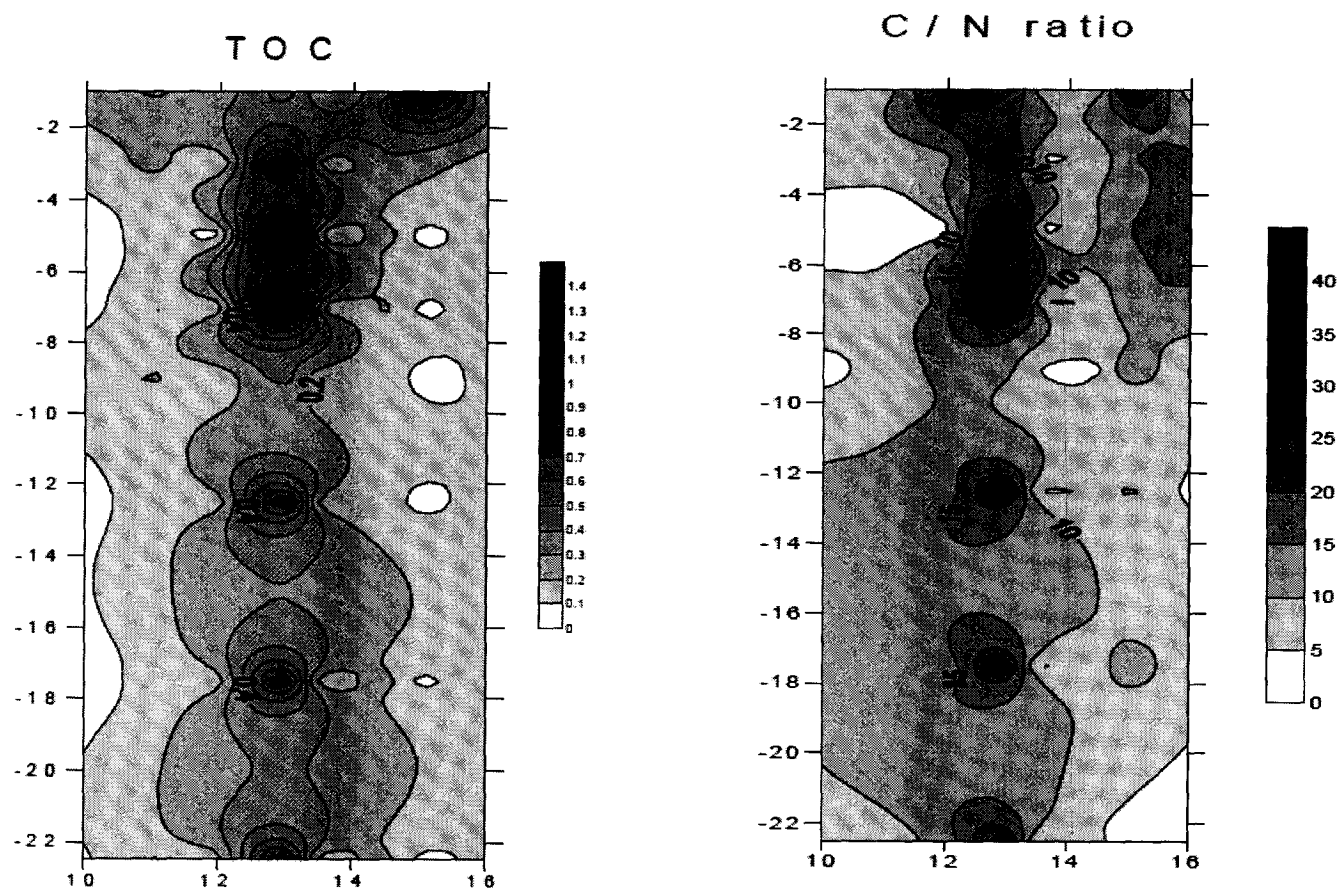


Fig. 4.8 Down-core variation of TOC and C/N ratio along North-South transect along $75^{\circ}30'$.

4.4.1 Labile organic matter (LOM)

a. Latitudinal variation

LOM varied from 0.4 to 1.00 mg·g⁻¹ dry sediment in the north, 0.3 to 0.6 mg g⁻¹ in the centre and 0.2 to 0.6 mg g⁻¹ in the south. Cluster analysis of LOM contents (Fig. 4.10) separated northern stations 26 and 25 from the rest of the cores at 70% dissimilarity. At 40% dissimilarity stations 20, 19 and 18 were separated from rest of the stations analysed in the basin.

b. Down-core variation

Down-core variations showed decrease in LOM contents for the northern and southern stations, while in the central stations these parameters remained uniform down the core. The latitudinal differences are more prominent than the down-core variations (Fig. 4.11).

c. Seasonal variation

The LOM varied from 0-2 mg g⁻¹ sediment and there is no distinguishable difference between the two samplings. In general, seasonal variation of LOM among the austral winter and austral summer was not statistically significant. The only marked variation was seen in case of station 38 (Fig. 4.9). Proteins ranged from ndl-1.5 mg g⁻¹ sediment, carbohydrates from nd-1 mg g⁻¹ sediment and lipids varied from ndl-1 mg g⁻¹ sediment.

i. Seasonal variability in LOM along North-South Profile (75°30'E)

Though the range of LOM values was same between EVDC II and III, 0.5-1.5 mg g⁻¹ the pattern of distribution was different between the two sampling seasons. Most cores showed their highest protein, carbohydrate and lipids values within the top 10 cm of sediment profile. There is a variation in profile between samples from north and south of 14°S. While the northern stations show a gradual down-core decline of proteins and carbohydrates, the southern cores show a drastic fall below 5-10 cm.

ii. Seasonal variability in LOM for the proposed First Generation Mine site:

The First Generation Mine site also shows maximum LOM usually in the top 10 cm of sediment. Occasional mid-depth maxima are noted both during EVDC II and III. There was no major seasonal variation in LOM except a narrower range during EVDC-III. The value of LOM ranged from 0.17-0.71 mg g⁻¹ during EVDC-II and 0.37-0.66 mg g⁻¹ during EVDC III.

iii. Seasonal variability in LOM at sea-mount area

In general the lipids are the predominant form of LOM in the Seamount. There is a general decrease in LOM during EVDC III. There is a drastic fall in LOM values of BC-38 from 2.41 to 0.34 mg g⁻¹. Also, the down-core variations were reduced to negligible, suggesting mixing or bio-turbation during EVDC III.

iv. *Variability in the LOM during EVDC I, II and III.*

Average LOM during EVDC I, II and III varied from $< 0.5-1.5 \text{ mg g}^{-1}$ with occasional mid-depth maxima of about 2 mg g^{-1} . Stations BC-25, BC-20, BC-03 and BC-14 showed minimum variation. Stations BC-26 in the north, BC-04 and BC-08 showed prominent variation from EVDC I and II.

d. *Comparison of proteins, carbohydrates and lipids, labile organic matter between relatively nodule rich and nodule-poor region*

i. *Core IVBC 20A (relatively nodule rich)*

Proteins ranged from 0.02 to 0.06 mg g^{-1} dry sediment and measured lowest among the 4 samplings from EVDC I-IV. Carbohydrates ranged from 0.005 to 0.024 mg g^{-1} dry sediment. Lipids ranged from 0.003 to 0.3 mg g^{-1} dry sediment. Lipids generally measured the lowest among the 4 samplings. LOM ranged from 0.04 to 0.35 mg g^{-1} dry sediment. LOM also measured lowest among the 4 samplings (Fig. 4.12).

ii. *Core IVBC 18C (relatively nodule poor)*

Proteins ranged from 0.03 to 0.09 mg g^{-1} dry sediment. Protein measured lowest among the 3 sampling i.e., EVDC II, III, IV during EVDC IV. Carbohydrates ranged from 0.011 to 0.029 mg g^{-1} dry sediment. Carbohydrates also measured lowest among the three samplings, during EVDC IV. Lipids ranged from 0.338 to 0.418 mg g^{-1} dry sediment. Lipids measured highest among the three samplings. LOM ranged from 0.39 to 0.52 mg g^{-1} dry sediment (Fig. 4.12).

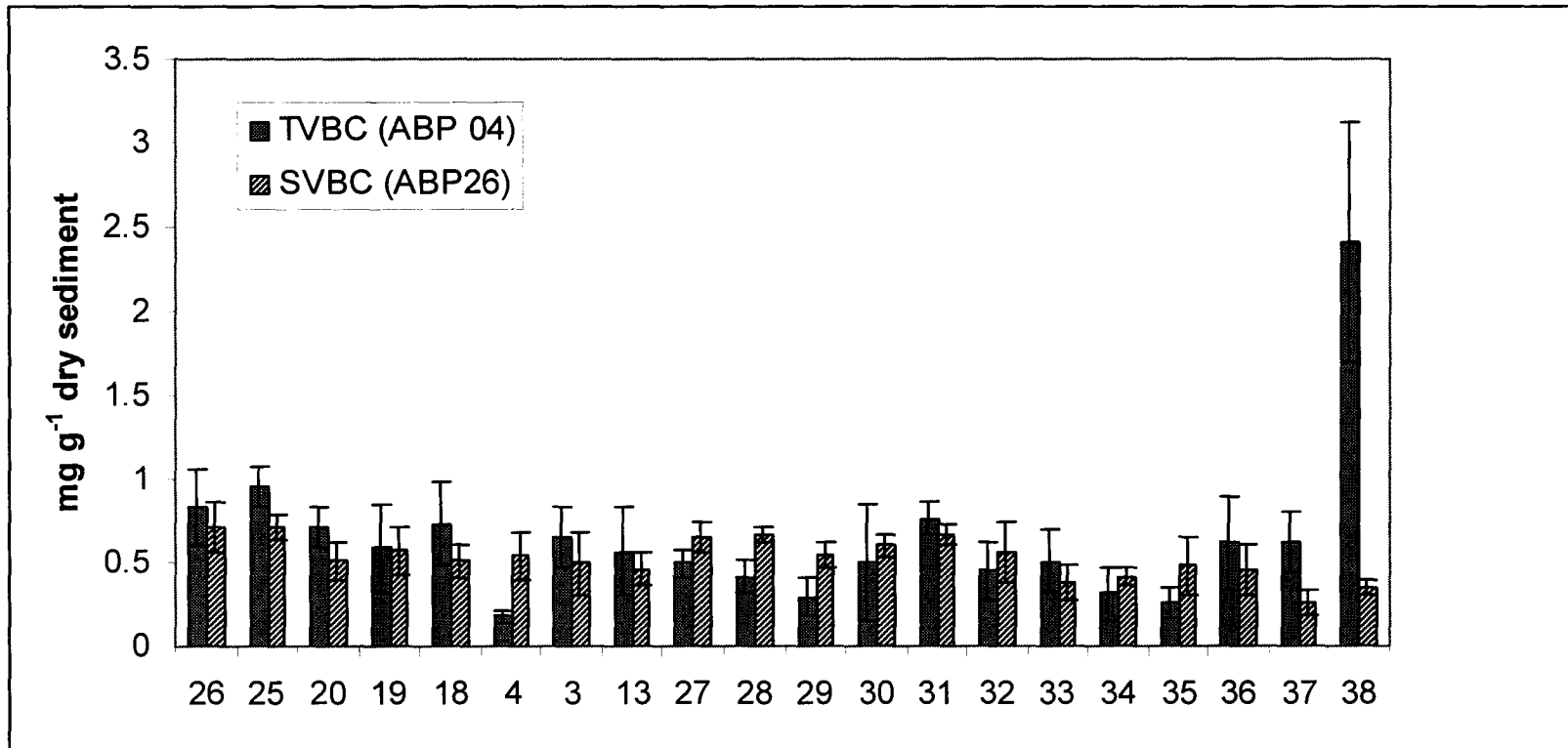


Fig. 4.9 Seasonal variation in LOM (mg g⁻¹ dry sediment) in sediment cores Central Indian Ocean Basin. Numbers on x-axis denote core numbers.

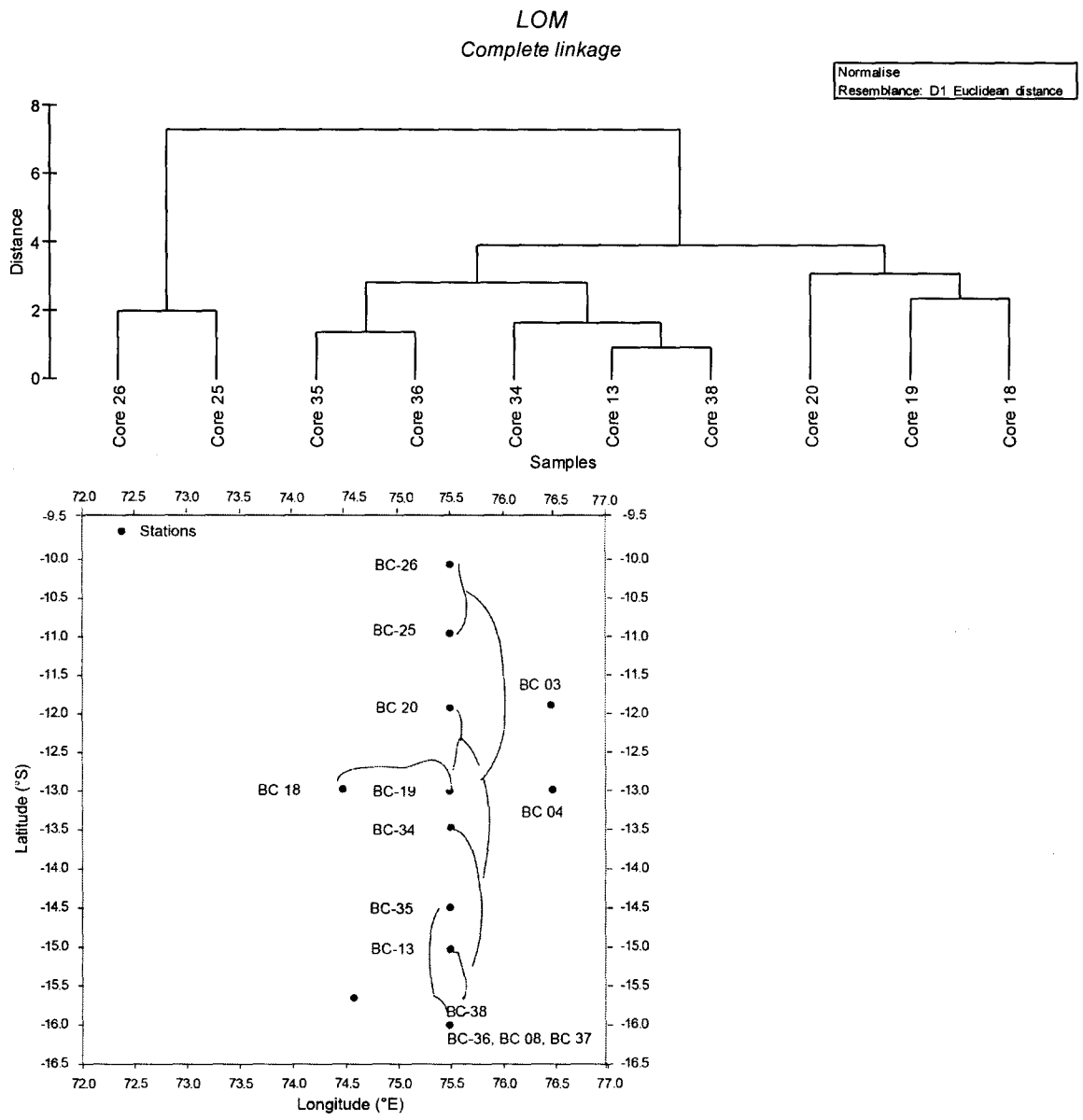


Fig. 4.10 Cluster analysis of CIOB stations based on LOM content. Inset shows station locations

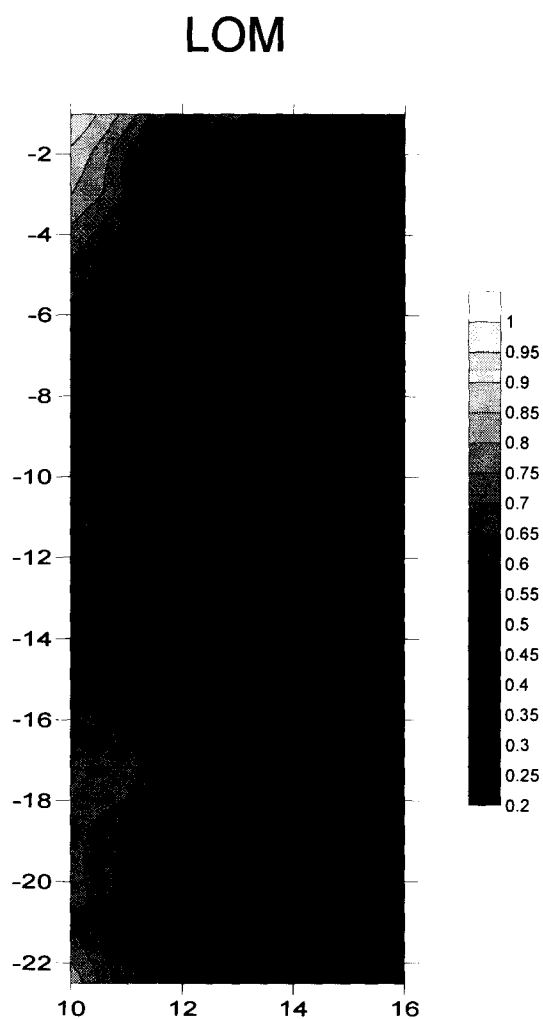


Fig. 4.11 Down-core variation of LOM along North-South transect along 75°30'.

4.4.2 *Adenosine triphosphate (ATP)*

ATP varied from 10 to 10^4 $\eta\text{g g}^{-1}$ dry sediment. Total bacterial carbon remained well within 2% of the total ATP carbon as stated in Karl, (1980).

a. *Spatial-temporal variability in ATP along North-South profile (75°30' E)*

ATP varies by three orders spatially. It ranges from 10-100 $\eta\text{g g}^{-1}$ dry sediment at 10°S up to 500-1000 $\eta\text{g g}^{-1}$ dry sediment at 16°S.

b. Half degree Environmental Database of ATP for First generation mine site

The ATP values show a high pocket on the east and a low on the west of the first generation mine site.

c. ATP at seamount area stations

ATP ranges from 10^3 - 10^4 $\eta\text{g g}^{-1}$ at the top of the seamount (BC- 37), 10^2 - 10^3 at the plateau (BC-36) and TVBC-08 (flank) and from 10^1 - 10^4 in the valley (BC-38).

d. Latitudinal variation

Cluster analysis separated core 36 from the rest of the cores at 80% dissimilarity cut off. At 50% two more clusters separated out dividing stations 20, 34 and 08 from the rest of the cores (Fig. 4.14).

e. Down-core variation

ATP showed elevated levels in pockets and did not show any distinct latitudinal or down-core variation (Fig. 4.16). Down-core variation was also more negligible during EVDC III as compared to EVDC II in most stations.

f. Seasonal variation

ATP showed distinct seasonal variation between austral winter and austral summer. Austral summer exhibited higher ATP content than austral winter. However, the difference was not statistically significant. The variations ranged from 0 to 2 orders of difference between the two seasons. Maximum variation was shown by station 13 (Fig. 4.15).

ATP varied from 10^2 to 10^4 $\eta\text{g.g}^{-1}$ dry sediment during EVDC-III. During EVDC-II ATP ranged from 10 to 10^4 $\eta\text{g g}^{-1}$.

i. Seasonal variability in ATP along North-South Profile (75 °30'E)

ATP did not change drastically between the two seasons. However, the range narrowed down from 10^3 - 10^4 during EVDC II to 10^2 - 10^4 ng g^{-1} during EVDC III. Significant seasonal variation with 1-2 order increase has been noted in a few stations like SVBC-26, 13 and 19 during EVDC III. However, other stations along the north south profile of $75^\circ 30'E$ longitude remained fairly unaltered in ATP concentrations between the two seasons.

ii. Seasonal variability for the First generation mine site

The ATP of the first generation mine site mostly remained unaltered except SVBC 29 and 31 showing a one order decline. SVBC-33, 19 and 04 showed 5-10 times increase during EVDC III or austral summer (Fig. 4.15).

iii. Seasonal variability in ATP at sea-mount area stations

ATP ranged from 10^3 - 10^4 ng g^{-1} at the seamount. While ATP has doubled in SVBC – 37 (seamount top) and SVBC-36 (flank-plateau), it reduced to nearly one fourth the concentration in the valley of SVBC-38. Down-core variations are minimal during EVDC-III.

g. Variability in the ATP during EVDC I, II and III.

ATP levels during EVDC-III are higher than EVDC-II but did not reach the values of EVDC I. ATP varied from 10^4 - 10^5 ng g^{-1} during EVDC-I, 10^3 - 10^4 ng g^{-1} during EVDC II and 10^2 - 10^4 ng g^{-1} during EVDC-III.

h. Comparison of ATP content between relatively nodule rich and nodule poor region

ATP measured lowest among 4 samplings during EVDC IV in core IVBC 20A. In IVBC 18C, the range remained unchanged through 3 consecutive samplings. ATP ranged from 230.81 to 423.79 ng g^{-1} dry sediment in core IVBC 20A. In core IVBC 18C it ranged from 105.66 to 340.46 ng g^{-1} dry sediment (Fig. 4.13).

4.4.3 Total counts and frequency of dividing cells

The total counts (TC) of bacteria in the CIOB vary by 3 orders from 10^6 to more than 10^9 cells g^{-1} dry sediment. The down-core variation is mixed with mid depth maxima or minima. The images of TC are presented in Appendix III.

a. Spatial variability in TC along North-South Profile (75 °30' E)

Spatially, TC varied over 3 orders from 10^6 - 10^9 , with the highest at the extreme north and south. There is an increase in order of TC towards extreme north and south (10° S and 16° S), and a decrease towards the middle 13° S and 14° S. There was no such change at 11° S and 12° S.

b. Half degree environmental database of TC for First generation mine site

The total population of bacteria remained at 10^7 to 10^8 cells g^{-1} dry sediment in the First Generation Mine site.

c. TC at sea-mount area stations

The total count of bacteria ranges over three orders in the sea-mount stations. TC is 10^8 - 10^9 cells g^{-1} dry sediment, at the station on top of seamount (BC- 37), 10^6 - 10^7 cells g^{-1} at the plateau (BC-36), 10^9 cells g^{-1} at the flank (TVBC-08R) and 10^6 - 10^7 cells g^{-1} in the valley (BC-38).

d. Latitudinal variation

Total counts varied from 10^6 to 10^9 cells g^{-1} dry sediment. Frequency of dividing cells (FDC) varied from 10^4 to 10^8 cells g^{-1} dry sediment. Cluster analysis of total counts separated station 26 and 8 from the rest of the basin at 80% dissimilarity cut-off. A second split at 50% separated station 20 from the rest of the samples. In case of FDC, station 26 and 8 were separated from the rest of the cores at 70% dissimilarity (Figs 4.17 and 4.18).

e. Down-core variation

The central and southern parts of the basin showed some of the lowest total counts. A large patch of low viability was seen in the central and southern part (Fig. 4.18).

f. Seasonal variation

Seasonal variations were exhibited by total counts of bacteria. The variation ranged from 0 to 3 orders (Fig. 4.19).

i. Seasonal variability in TC along North-South Profile (75°30'E)

During EVDC-II the maxima were distributed both in the north and south with minima in the BC-35 at 14.5°S. There was a general increase in TC during EVDC-III along the North-South profile as compared to EVDC-II. During EVDC-II TC varied over 3 orders from 10^6 - 10^9 , with the highest at the extreme north and south. During EVDC-III, it varied over 2 orders from 10^7 - 10^9 , with the highest at the extreme north.

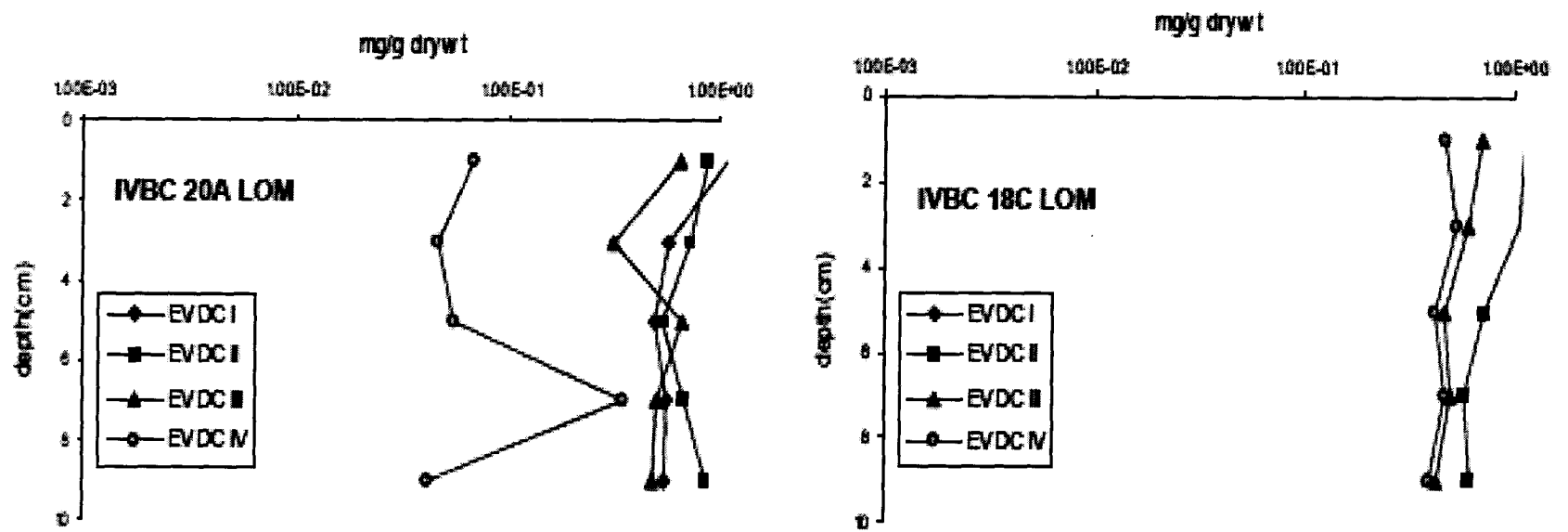


Fig. 4.12 Down-core profiles of LOM of relatively nodule rich and nodule poor cores.

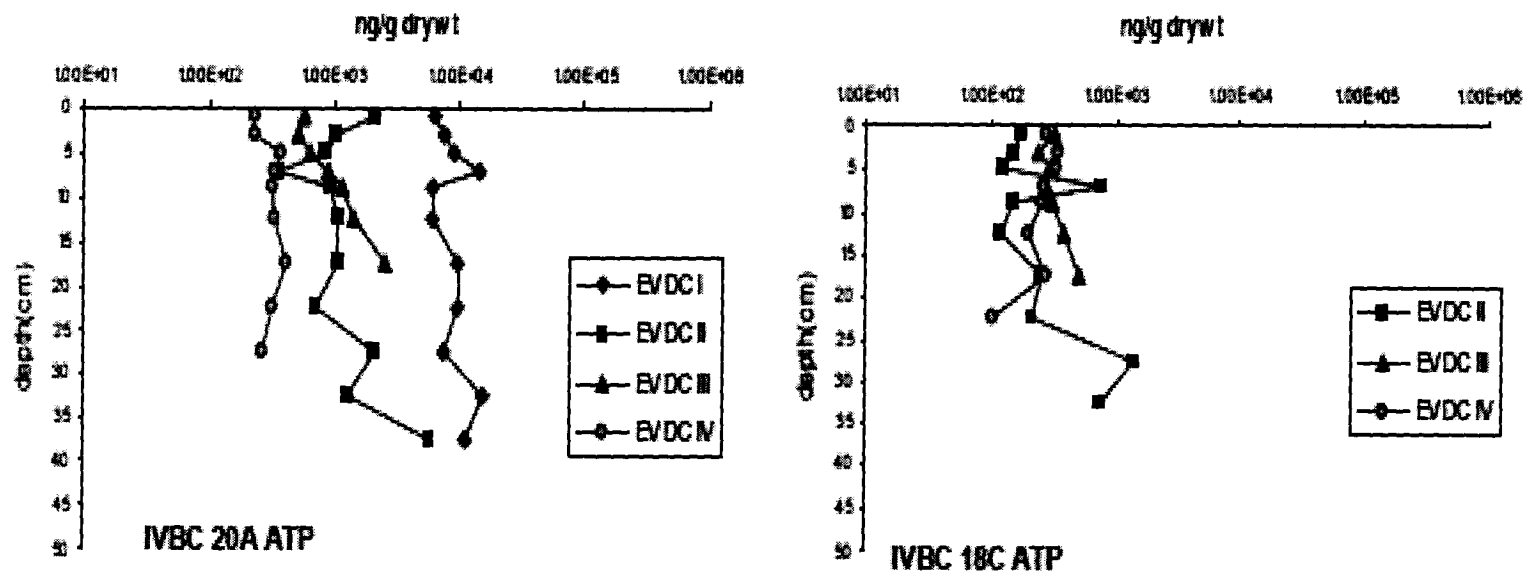


Fig. 4.13 Down-core profiles of ATP in relatively nodule rich and nodule poor cores

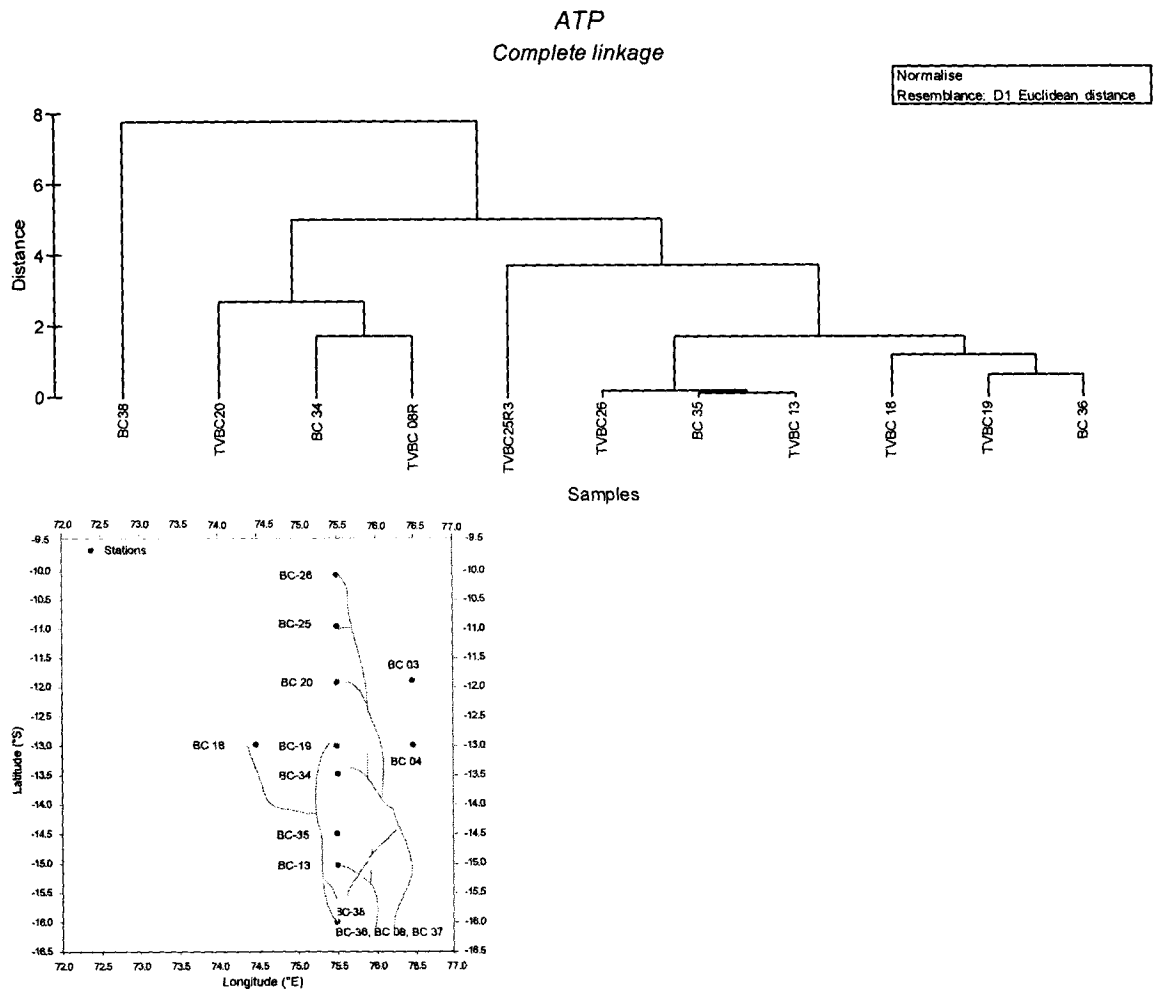


Fig. 4.14 Cluster analysis of CIOB stations based on ATP content. Inset shows station locations.

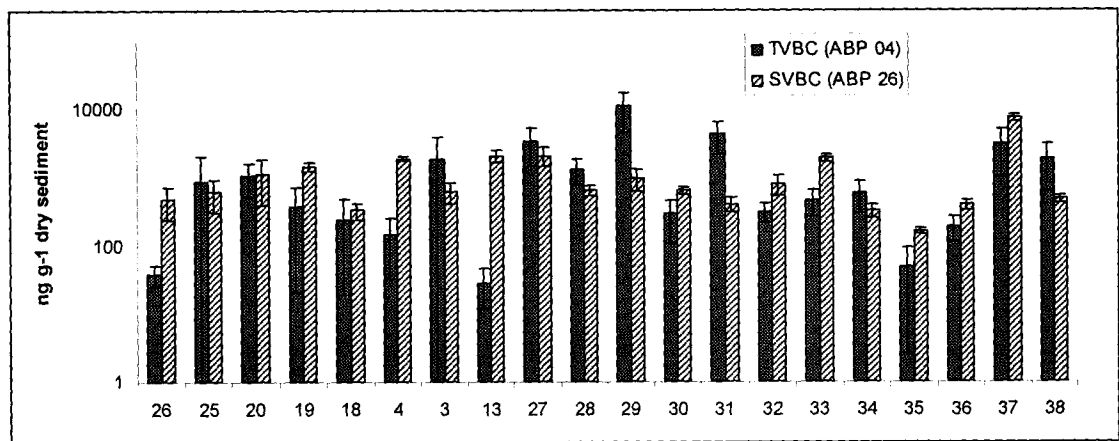


Fig. 4.15 Seasonal Variation in ATP at CIOB stations

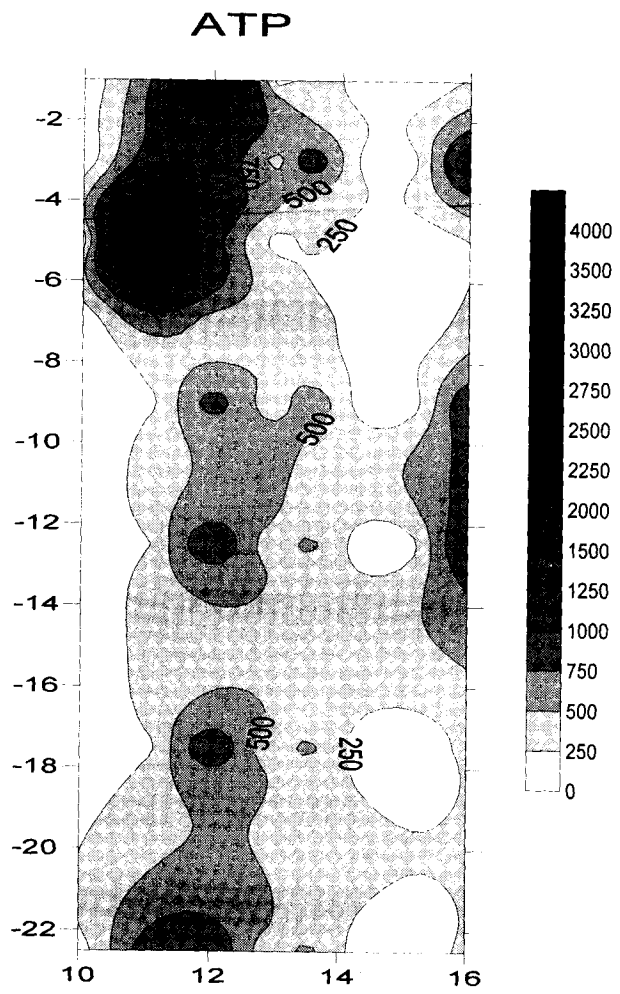


Fig. 4.16 Down-core variation of ATP along North-South transect along 75°30'

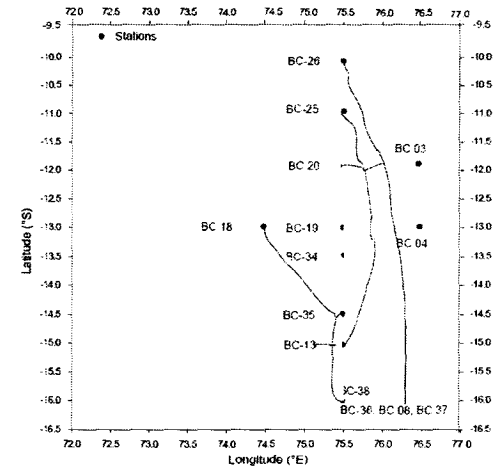
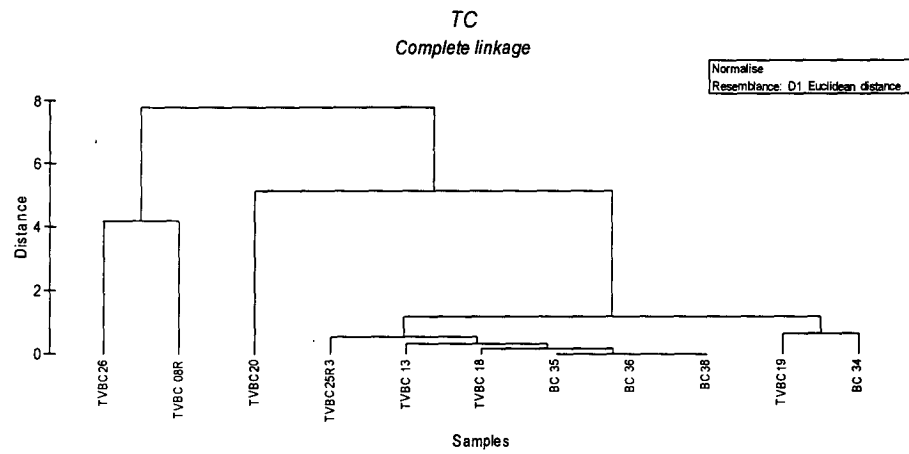


Fig. 4.17A Cluster analysis of CIOB stations based on total counts of bacteria. Similar TC counts in geographically distant cores may be due to similar porosity.

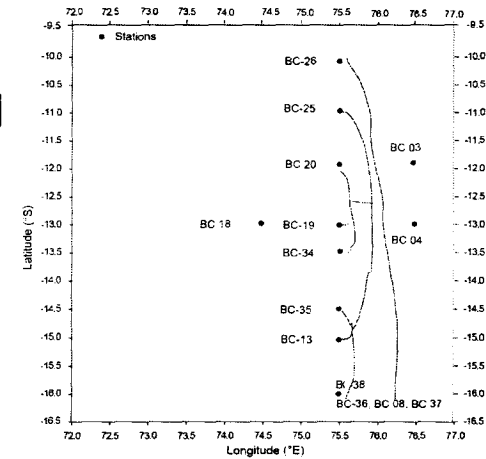
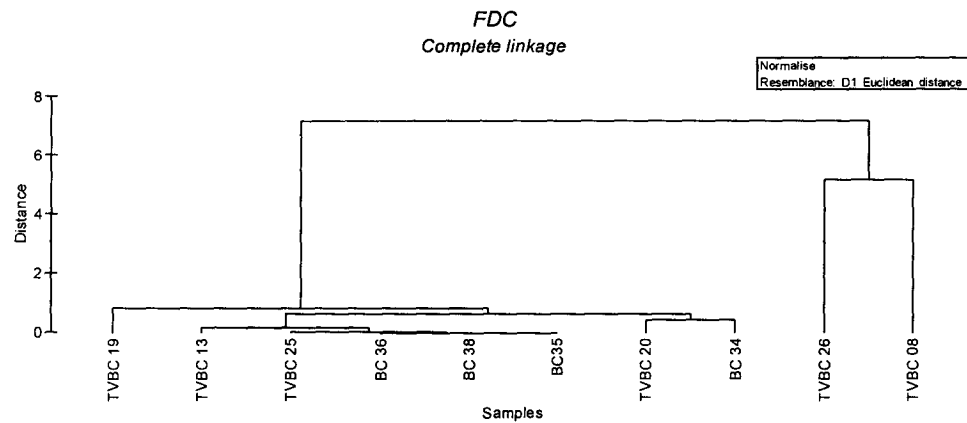


Fig. 4.17B Cluster analysis of CIOB stations based on frequency of dividing cells (FDC). Similar TC counts in geographically distant cores may be due to similar porosity. Similarity in geochemical properties may also be responsible for FDC distribution patterns.

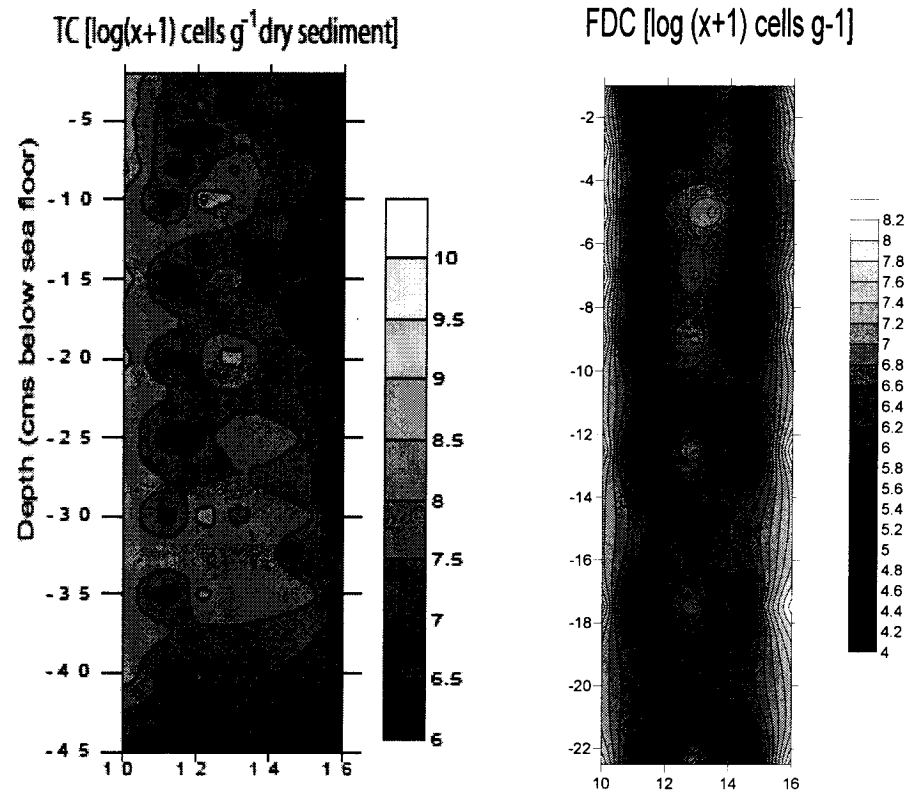


Fig. 4.18 Down-core variation of TC and FDC along N-S transect along 75°30' showing concentric pattern emanating from the centre of the basin at 13°S.

ii. *Seasonal variability in TC for the proposed First generation mine site (FGM)*

There was no variation between the sampling at EVDC-II and EVDC-III. There was very little variation within the FGM area extending from 11.5°S to 13°S. The total population of bacteria remains at 10^7 to 10^9 cells g^{-1} dry sediment in the first generation mine-site during EVDC-III.

iii. *Seasonal variability in TC at sea-mount area stations*

There is a decreasing gradation in TC from the top of the seamount to the deep-valley during EVDC-III. The TC ranged over two orders in the seamount stations. TC was 10^9 cells g^{-1} dry sediment, at the station on top of seamount (BC- 37), 10^8 - 10^9 cells g^{-1} at the plateau (BC-36), and 10^7 - 10^8 cells g^{-1} in the valley (BC-38). There is an increase in TC at BC-37 by two orders during EVDC-III as compared to EVDC-II. The other two stations did not show any significant seasonal variation.

g. *Variability in total counts during EVDC I, II and III.*

Though there was an increase in TC by one order from EVDC-II to EVDC-III, the values of EVDC-III were similar to those of EVDC-I. Overall the total count of bacteria in CIOB remained within 10^7 - 10^9 cells g^{-1} .

h. *TC in relatively nodule rich and nodule poor sites*

i. *Core IVBC 20A (relatively nodule rich)*

Total counts (TC) declined from $1.43 \times 10^8 \pm 1.61 \times 10^8$ cells g^{-1} dry sediment during EVDC I to $5.43 \times 10^6 \pm 3.21 \times 10^6$ cells g^{-1} dry sediment during EVDC IV. TC recorded lowest among the 4 sampling season in IVBC 20A (Fig. 4.20).

ii. Core IVBC 18C (relatively nodule poor)

TC varied from $1.11 \times 10^8 \pm 1.27 \times 10^8$ cells g^{-1} dry sediment during EVDC II to $4.98 \times 10^7 \pm 1.16 \times 10^8$ cfu g^{-1} dry sediment during EVDC IV.

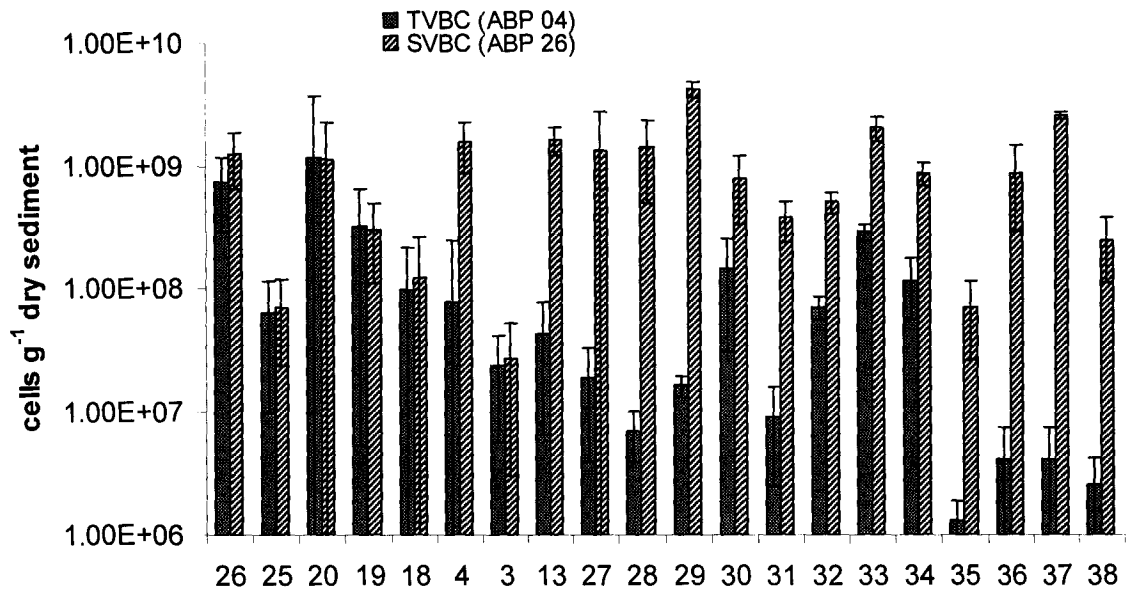


Fig.. 4.19. Seasonal variation in total bacterial counts showing general increase especially towards south.

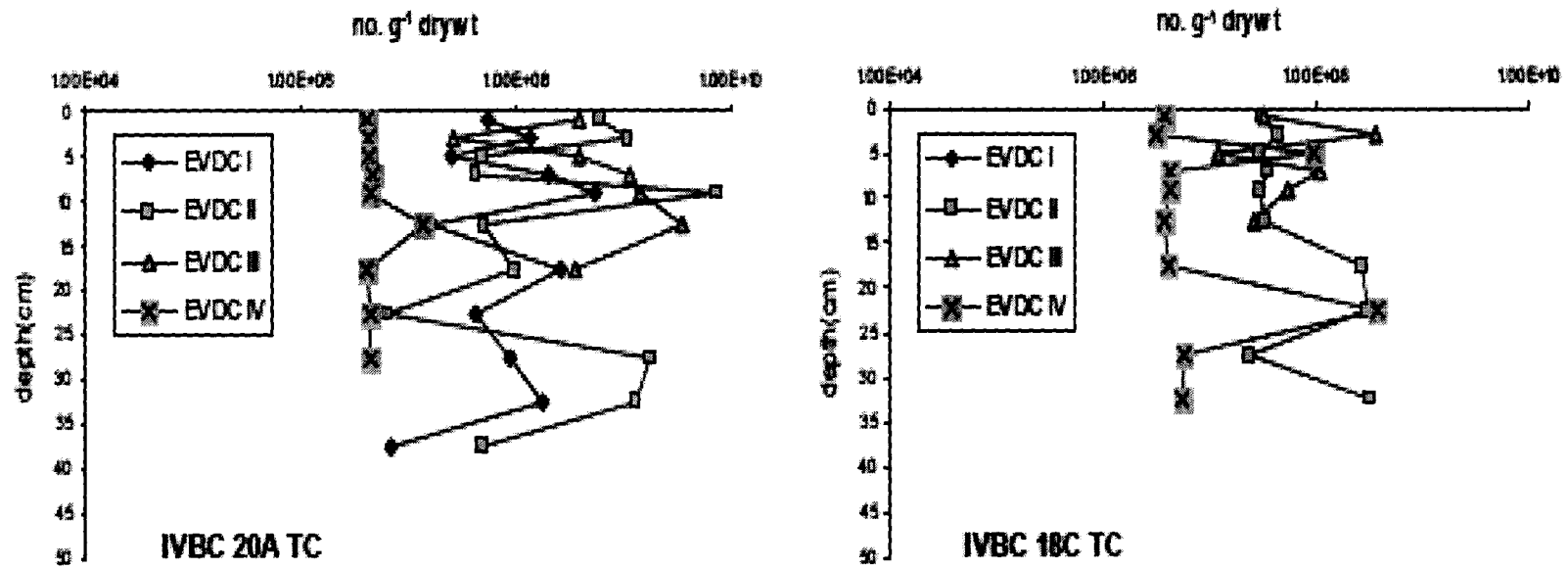


Fig. 4.20 Total counts of relatively nodule-rich and nodule-poor cores. Down-core seasonal profile of TC showing marginally higher abundance at nodule rich than nodule poor cores.

4.4.4 Direct viable counts (DVC a and DVC an)

Direct viable counts under aerobic condition (DVC-a) and under anaerobic condition (DVC-an) varied from 10^4 to 10^8 cells g^{-1} dry sediment. With the exception of calcareous oozes, the DVC-a was higher than DVC an.

There was almost an order difference between DVC-a and DVC-an in these cores. In calcareous core 37, the DVC-an was marginally higher than DVC-a (Fig. 4.21).

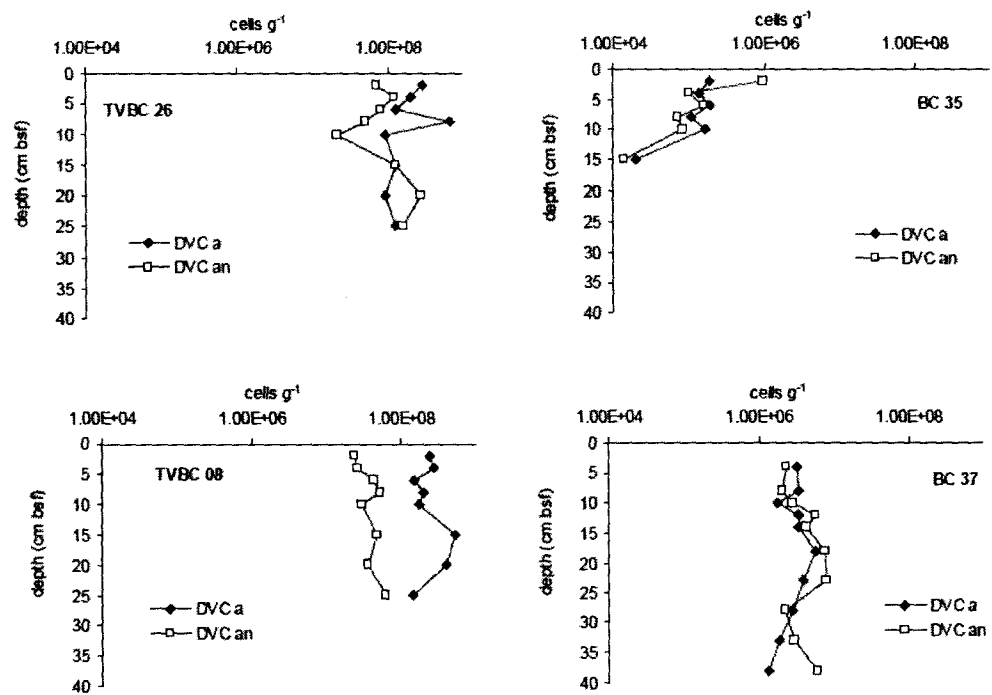


Fig. 4.21 Direct viable counts- DVC-a (aerobes) and DVC-an (anaerobes)

4.4.5. *Culturable counts*

The retrievability in the CIOB area ranges from $10^4 > 10^6$ cfu g⁻¹ dry sediment. In general, the heterotrophs decrease from north to south while the nitrifiers increase.

a. *Temporal Variation in bacterial retrievability*

Increase in retrievability by an order is marked during second observation at EVDC II especially in the southern cores.

b. *Spatial variability in bacterial retrievability along North-South profile (75°30' E)*

Retrievability in general increases from 10^3 - 10^4 cfu g⁻¹ at 10°S and from 10^5 - 10^6 cfu g⁻¹ at 12°30'S; it remains almost invariant up to 14°S. At 14°30'S there is a drastic fall by almost two orders in both heterotrophs and the nitrifiers.

c. *Half degree Environmental Database of bacterial retrievability (including First generation mine site)*

Bacterial retrievability ranges from 10^3 to 10^4 cfu g⁻¹ dry sediment.

d. *Bacterial retrievability at seamount*

Retrievability is generally low with higher nitrifiers than heterotrophs in BC-36 and 37. Almost equal amounts of heterotrophs and nitrifiers were retrieved from BC-38. Station TVBC-08 show highest retrievability of 10^4 - 10^5 cfu g⁻¹ dry sediment in ZMA, NI and NII media.

The retrievability in the CIOB area ranged from 10^2 to 10^5 cfu g⁻¹ dry sediment. In general, the heterotrophs decreased from north to south while the nitrifiers increased during EVDC-II. Also, during EVDC-III the nitrifiers continued to increase

southwards. Though heterotrophs were less variant in the north, they increased by nearly 2 orders in the south.

e. Seasonal variability in bacterial retrievability along North-South Profile (75°30'E)

Retrievability in general increased from 10^2 - 10^3 cfu g⁻¹ in the north and 10^4 - 10^5 cfu g⁻¹ in the south for both heterotrophs and the nitrifiers during EVDC-III. The heterotrophs remained same in the north during EVDC-III as compared to EVDC-II. In the south, the heterotrophs increased by two-three orders and the nitrifiers by one order during EVDC-III.

i. Seasonal variability in bacterial retrievability for the proposed First generation mine site

Bacterial retrievability ranged from non-detectable levels or ndl to 10^5 cfu g⁻¹ dry sediment during EVDC-III. The first generation mine site showed a wider range in retrievability during the austral summer (EVDC-III) as compared to EVDC-II where retrievability was 10^3 - 10^4 cfu g⁻¹.

ii. Seasonal variability in bacterial retrievability at sea-mount

Retrievability of both nitrifiers and heterotrophs increased in the seamount. The nitrifiers increased by 1-2 orders, while the heterotrophs have increased by nearly 3 orders. While EVDC-II showed dominance of nitrifiers in the seamount, EVDC-III shows almost equal populations.

f. Variability in retrievability during EVDC I, II and III.

Bacterial retrievability shows a very wide range in CIOB from ndl- 10^6 cfu g⁻¹. On an average EVDC-I and -III showed very high retrievability especially in the south.

EVDC-II showed lower range. However, the South has persistent high nitrifier population with a gradual increase of heterotrophs from EVDC-I to EVDC-III.

g. Comparison of retrievable counts between nodule-rich and nodule poor regions.

i. Core IVBC 20A

The heterotrophs showed an arithmetic increase from non-detectable during EVDC I to $666 \text{ cfu} \times 10^2 \text{ g}^{-1}$ dry sediment during EVDC IV. The ammonium oxidizers (NI) increased from 13 in EVDC I to 812 in EVCD III and then dropped again to $16 \text{ cfu} \times 10^2 \text{ g}^{-1}$ dry sediment. The nitrite oxidizers (NII) increased from 0 in EVDC I to $1.13 \times 10^5 \text{ cfu g}^{-1}$ dry sediment in EVDC III and then declined to $2 \text{ cfu} \times 10^2 \text{ g}^{-1}$ dry sediment in EVDC IV.

ii. Core IVBC 18C

The heterotrophs showed an order decline from 43 in EVDC II to $3 \times 10^2 \text{ cfu g}^{-1}$ dry sediment in EVDC III followed by a two order increase to $1.29 \times 10^4 \text{ cfu g}^{-1}$ dry sediment during EVDC IV. The ammonium oxidizers (NI) decreased from $163 \text{ cfu} \times 10^2 \text{ g}^{-1}$ dry sediment in EVDC II to non-detectable in EVDC IV. The nitrite oxidizers (NII) decreased from 59 during EVDC II to $4 \text{ cfu} \times 10^2 \text{ g}^{-1}$ dry sediment during EVDC IV (Fig. 4.22).

h. Down-core distribution of aerobic bacteria

i. Heterotrophs on ZMA, nitrifiers and aerobic TDLO

Representative cores were studied for bacterial culturability. Stations 26, 25 and 20 represented the siliceous oozes. Stations 34 and 35 represented the siliceous-pelagic transition. Station 36 represented the pelagic red clays and 37 that of calcareous ooze. The culturability on all media varied from non-detectable to $>10^5 \text{ cfu g}^{-1}$ dry sediment.

Cores were clustered medium-wise to find out their similarity in distribution pattern. Heterotrophs on ZMA, NI and NII showed some similarity in clustering pattern with core 26 and 25 clustering together. Overlaps of niches in geographically and geochemically distance cores were observed in many cases e.g., Heterotrophs of Core 35 and 37 clustering together (Fig. 4.23).

Core 26 (10°S, 75.5°E; siliceous ooze) showed multiple maxima and minima from 0-40 cm bsf for heterotrophs on ZMA. The cfu ranged from 0 to $>10^3$ cfu g⁻¹. For ammonium oxidizers (NI) it ranged from ndl to $>10^2$ cfu g⁻¹ with mid depth maximum from 15-30cm bsf. In case of nitrite oxidizers (NII) cfu ranged from ndl to $>10^2$ cfu g⁻¹ with mid depth maxima at 5cm bsf and 15 cm bsf. Among the aerobic *Thiobacillus denitrificans* like organism (aerobic TDLO), the colony counts varied from 0 to $>10^5$ cfu g⁻¹ with mid depth maxima at 7 cm bsf and 30 cm bsf (Fig.4.24A).

Core 25 (11°S, 75.5°E; siliceous ooze) showed two maxima and one minimum from 0-25 cm bsf for heterotrophs on ZMA. The cfu ranged from 0 to $>10^2$ cfu g⁻¹. For ammonium oxidizers (NI) it ranged from 0 to $>10^2$ cfu g⁻¹ with mid depth maxima at 5 cm bsf and 25 cm bsf. In case of nitrite oxidizers (NII) cfu ranged from 0 to $>10^2$ cfu g⁻¹ with mid depth maximum at 15 cm bsf and 25 cm bsf. Among the aerobic *Thiobacillus denitrificans* like organism (aerobic TDLO) the colony counts was $>10^5$ cfu g⁻¹ with mid depth maxima at 5 cm bsf and 20 cm bsf (Fig. 4.24A).

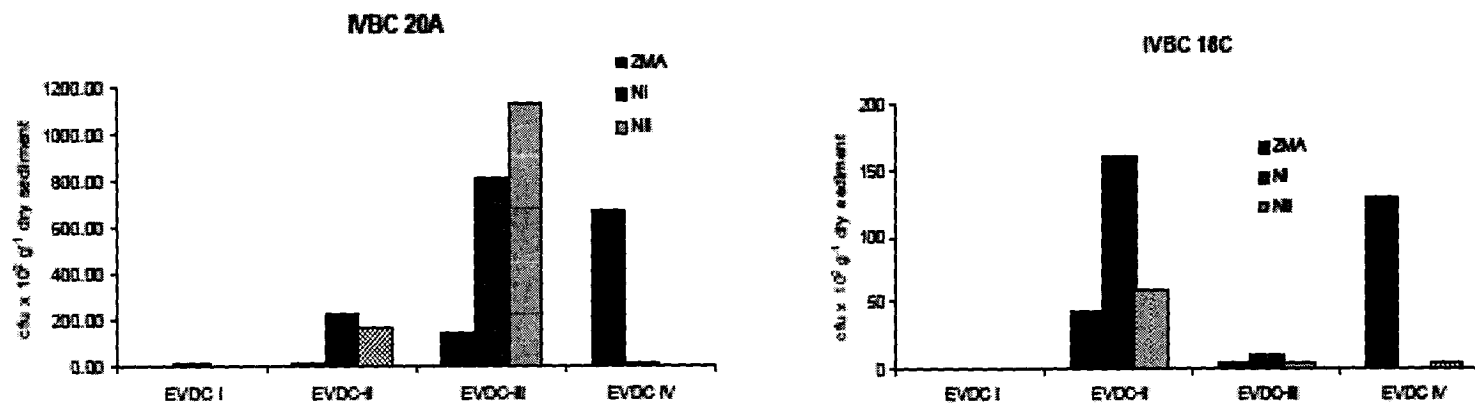
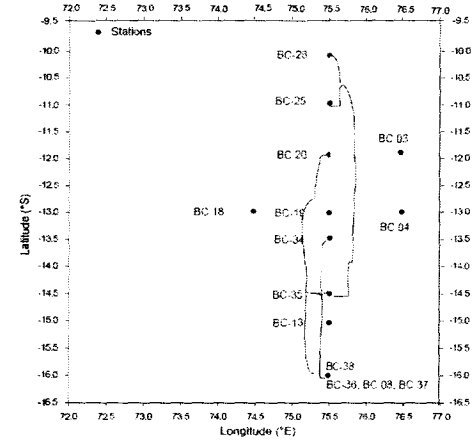
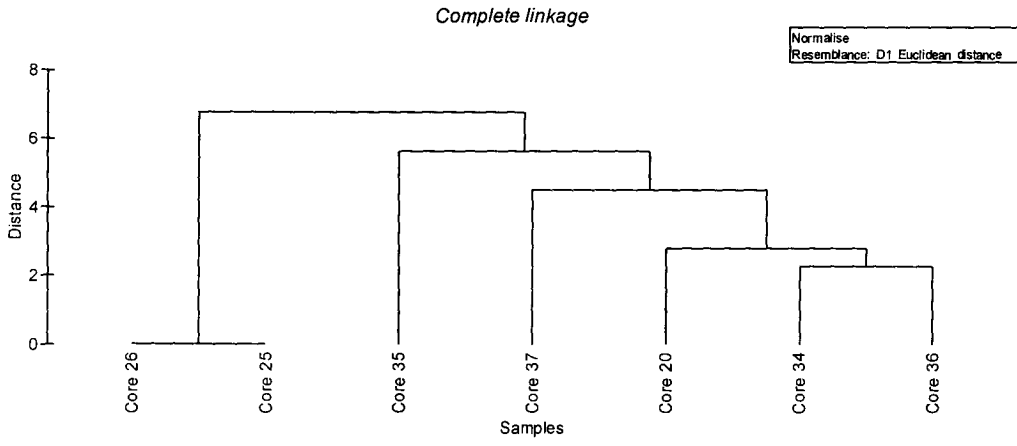
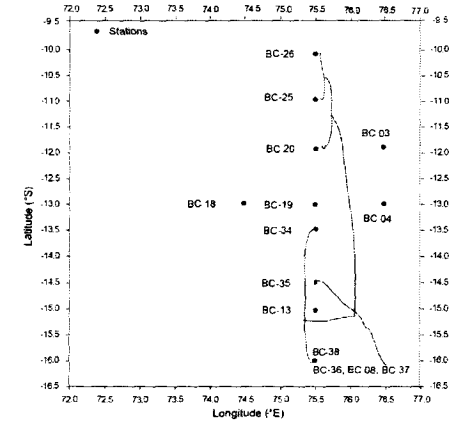
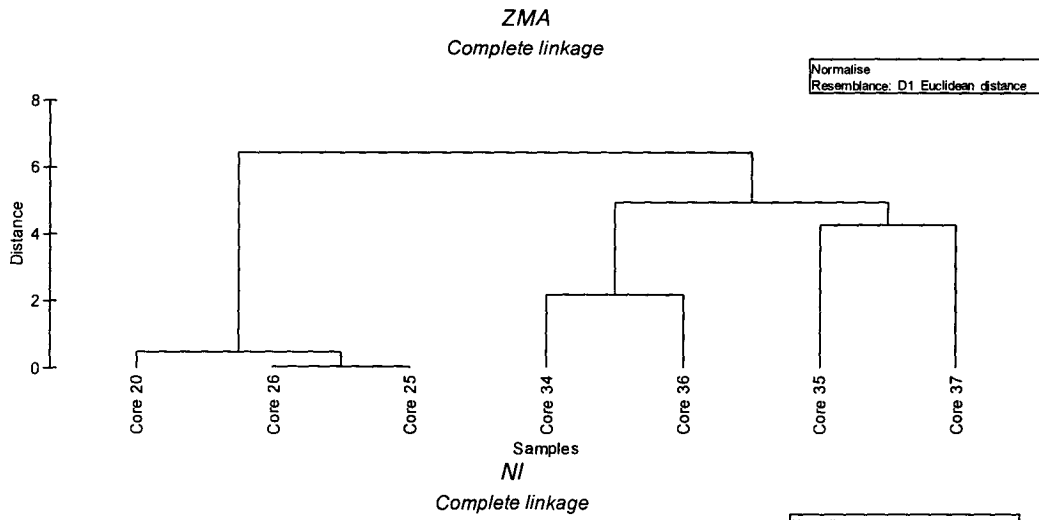


Fig. 4.22 Retrievable count from cores IVBC 20A and IVBC 18C. Note that the scale of IVBC 18C is different.



Contd...

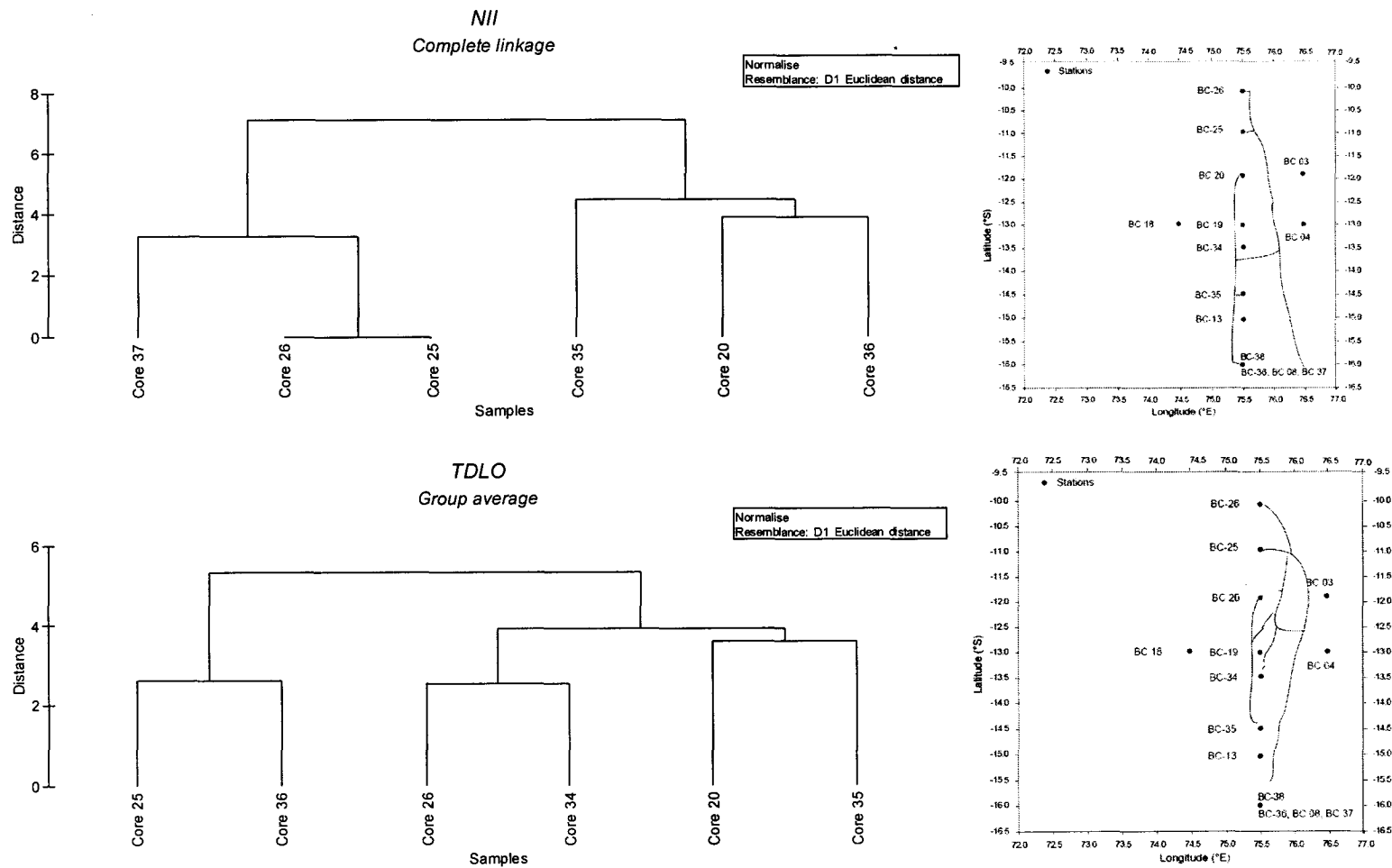


Fig. 4.23 Cluster analyses of CIOB stations based on ZMA, NI, NII and aerobic TDLO. The north-south clustering is featured only by the heterotrophs.

Core 20 (12°S, 75.5°E; siliceous ooze) did not show prominent maxima or minima like cores 26 and 25. The profile almost superimposes on the NI profile. Both heterotrophs and NI varied from 10^4 - 10^5 cfu g⁻¹. NII varied from 10^1 to 10^5 cfu g⁻¹ with minimum at 30 cm bsf. Aerobic TDLO varied from 10^5 - 10^6 cfu g⁻¹ with no prominent minimum (Fig. 4.24B).

Core 35 (14.5°S, 75.5°E; siliceous-pelagic transition) also showed shallow maxima and minima in cfu counts like core 20. Heterotrophs on ZMA and NI ranged from 10^4 - 10^5 cfu g⁻¹. NII varied from 10^1 - 10^5 cfu g⁻¹. NII showed a steep minimum at 35 cm bsf. Aerobic TDLO varied between $> 10^5$ - $<10^6$ cfu g⁻¹ (Fig. 4.24B).

Core 36 (16°S, 75.5°E; pelagic red clay) showed shallow maxima and minima for all the culturable bacterial profiles. All the four groups of culturable bacteria ranged between 10^5 - 10^6 cfu g⁻¹ (Fig. 4.24C).

Core 37 (16°S, 75.5°E; calcareous ooze) was unique in having similar profiles for ZMA, NI and NII indicating a mixed niche. A very steep minimum occurred between 20-25 cm bsf. Culturability ranged from 10^0 - 10^6 cfu g⁻¹ (Fig. 4.24C).

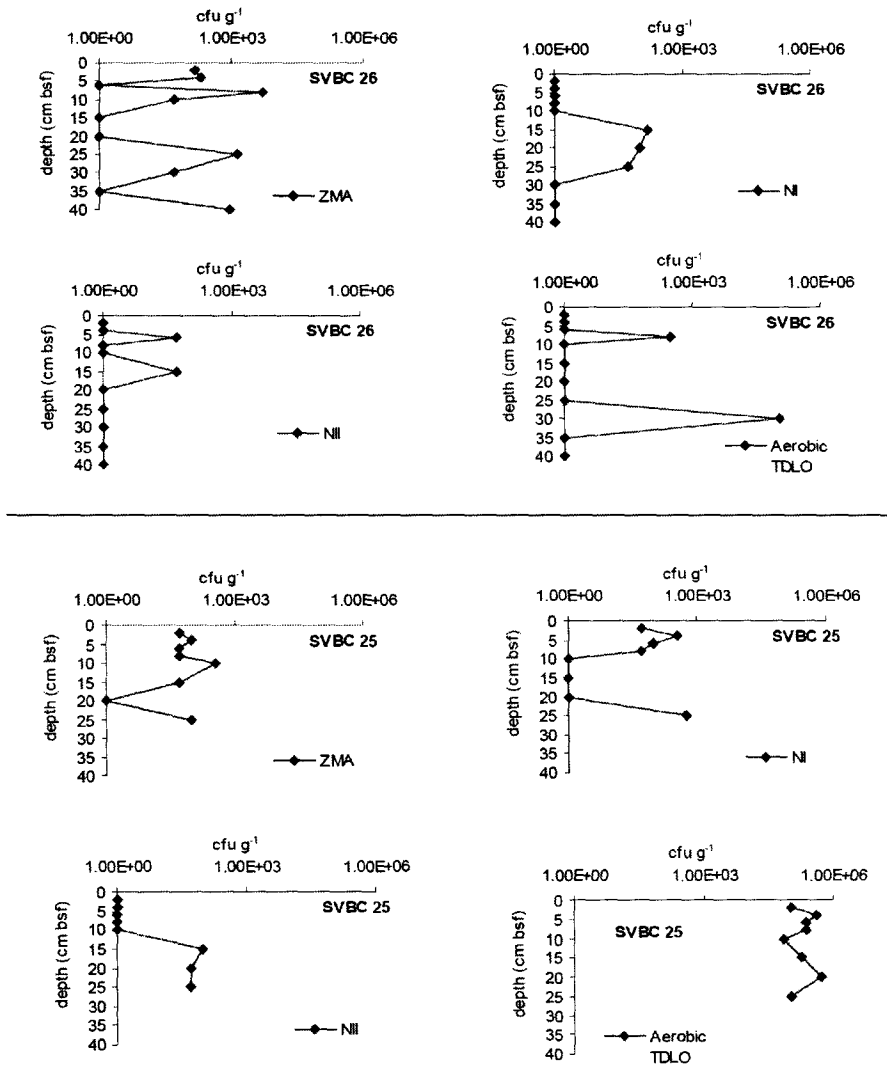


Fig. 4.24A. Heterotrophs (ZMA), ammonium oxidizers (NI), nitrite oxidizers (NII) and aerobic sulphur oxidizers (Aerobic TDLO) in cores SVBC 26 and SVBC 25.

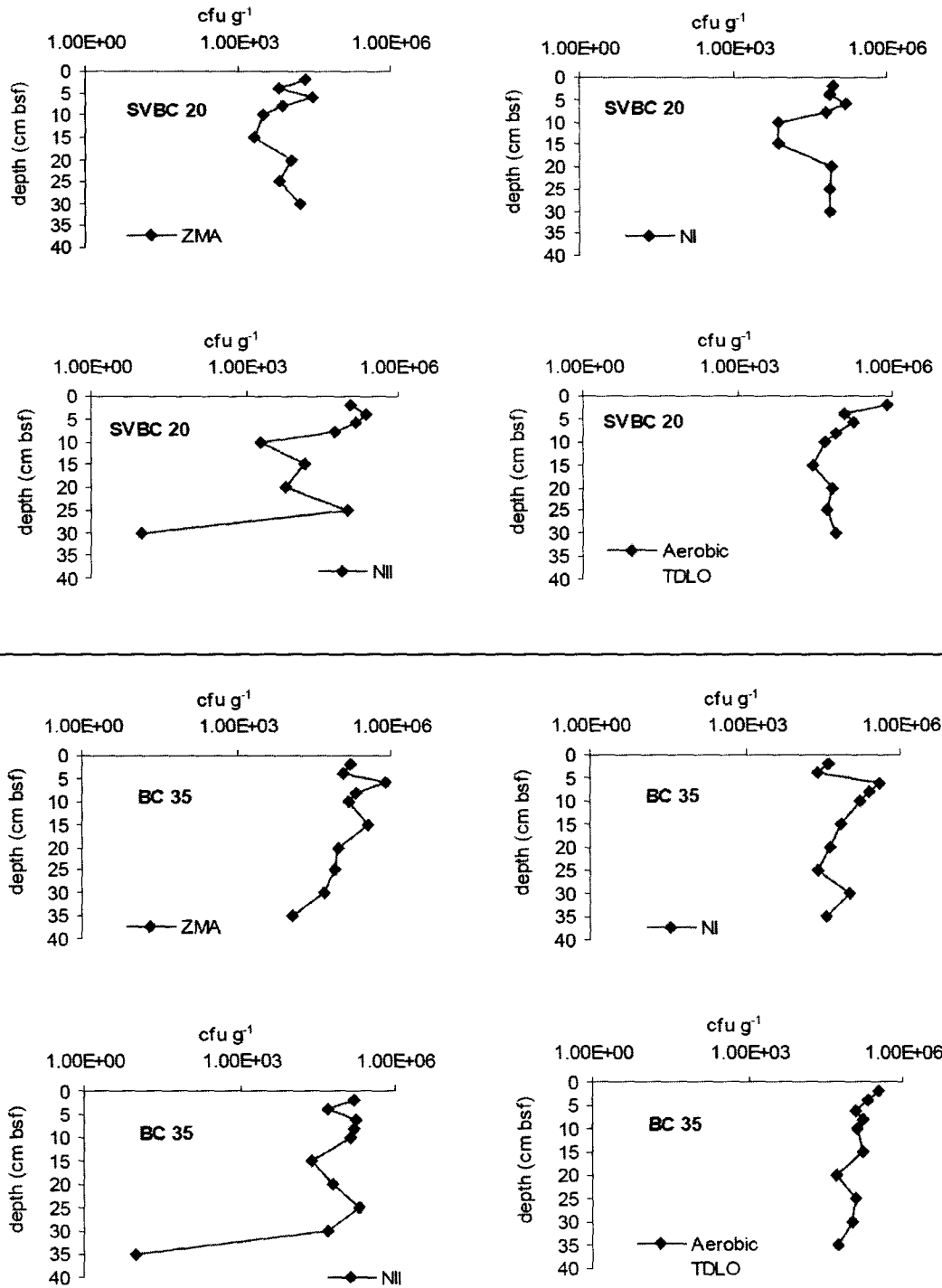


Fig. 4.24 B. Heterotrophs (ZMA), ammonium oxidizers (NI), nitrite oxidizers (NII) and aerobic sulphur oxidizers (Aerobic TDLO) in cores SVBC 20 and SVBC 35.

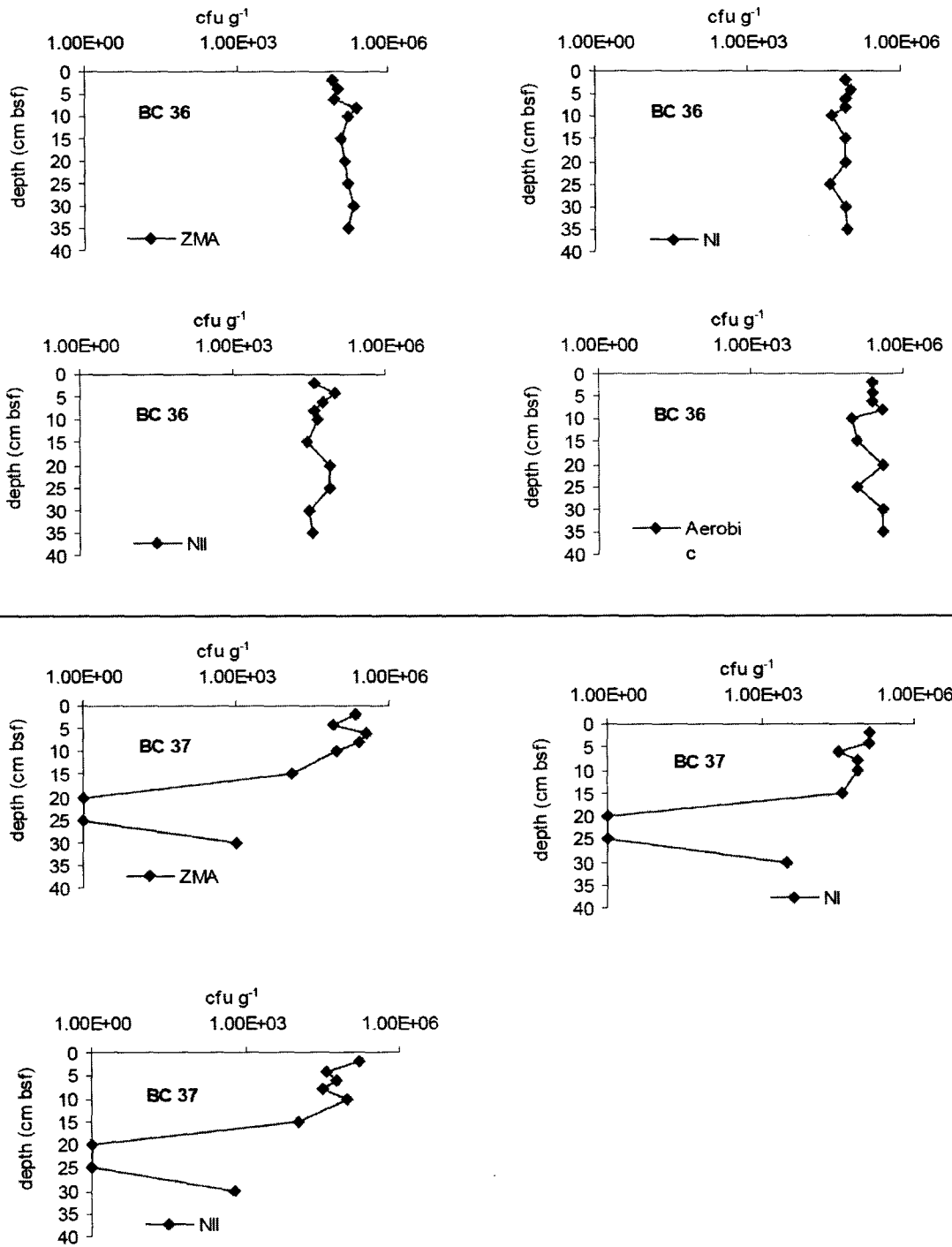


Fig. 4.24 C. Heterotrophs (ZMA), ammonium oxidizers (NI), nitrite oxidizers (NII) and aerobic sulphur oxidizers (Aerobic TDLO) in cores SVBC 36 and SVBC 37.

ii. *Fe- and Mn- oxidizing bacteria*

The Fe and Mn- oxidizing bacteria were also ubiquitous with numbers varying from 10^2 to 10^4 cfu g^{-1} dry sediment. The highest numbers of these groups were found in the pelagic red clay cores 08 and 36. The lowest numbers were recorded at pelagic red clay core 38. In most of the cores analysed, the numbers of Fe-oxidizers overlap with those of Mn-oxidizers. However, in the pelagic core 36 and calcareous ooze 37 the Fe-oxidizers were nearly an order higher than the Mn-oxidizers. The Fe- and Mn-oxidizers are generally homogenous down the cores with no steep maxima and minima like those of ZMA, NI, and NII (Fig. 4.25 and 4.26). Fe and Mn are known to be co-active. This to a great extent is noted in the clusters with cores 37, 26, 25 and 38 clustering together in both the Fe- and Mn- oxidizers (Fig 4.25).

iii. *Phosphate and silicate solubilizers*

The phosphate solubilizers varied from nd to 10^3 cfu g^{-1} dry sediment. The silicate solubilizers varied from nd to 10^4 cfu g^{-1} dry sediment (Fig 4.28). The lowest numbers of phosphate and silicate solubilizers were recorded at siliceous-pelagic transition core 35 while the highest numbers were recorded at stations 26 and 25. Down-core variation showed a variety of patterns, some of which are given below: In the northern siliceous cores 26 and 25 both phosphate and silicate solubilizers are homogeneously distributed with their profile overlapping with each other. The siliceous-pelagic transition cores 34 and 35 showed steep mid-depth maxima and minima (Fig. 4.27 and 4.28). The distribution of phosphate and silicate solubilizers clustered in a rather mixed pattern with no distinct north-south distinction.

Although pelagic cores 36 and 08 are located very near to each other, the distribution of phosphate and silicate solubilizing bacteria are very different. In core 36 the culturability varied over a wide range from ndl to $>10^3$ cfu g^{-1} . In core 08, the down-core variation is homogenous with culturability varying around 10^3 cfu g^{-1} . Core 38 a pelagic core in a valley near core 08 showed parallel distribution patterns around 10^3 cfu g^{-1} for phosphate and silicate solubilizers. In calcareous ooze core 37, the phosphate solubilizers showed a sharp minimum at 20-25 cm bsf and is possibly related to sediment compaction. Silicate solubilizers were homogenous down-core with 10^3 cfu g^{-1} (Fig. 4.27 and 4.28).

Contd...

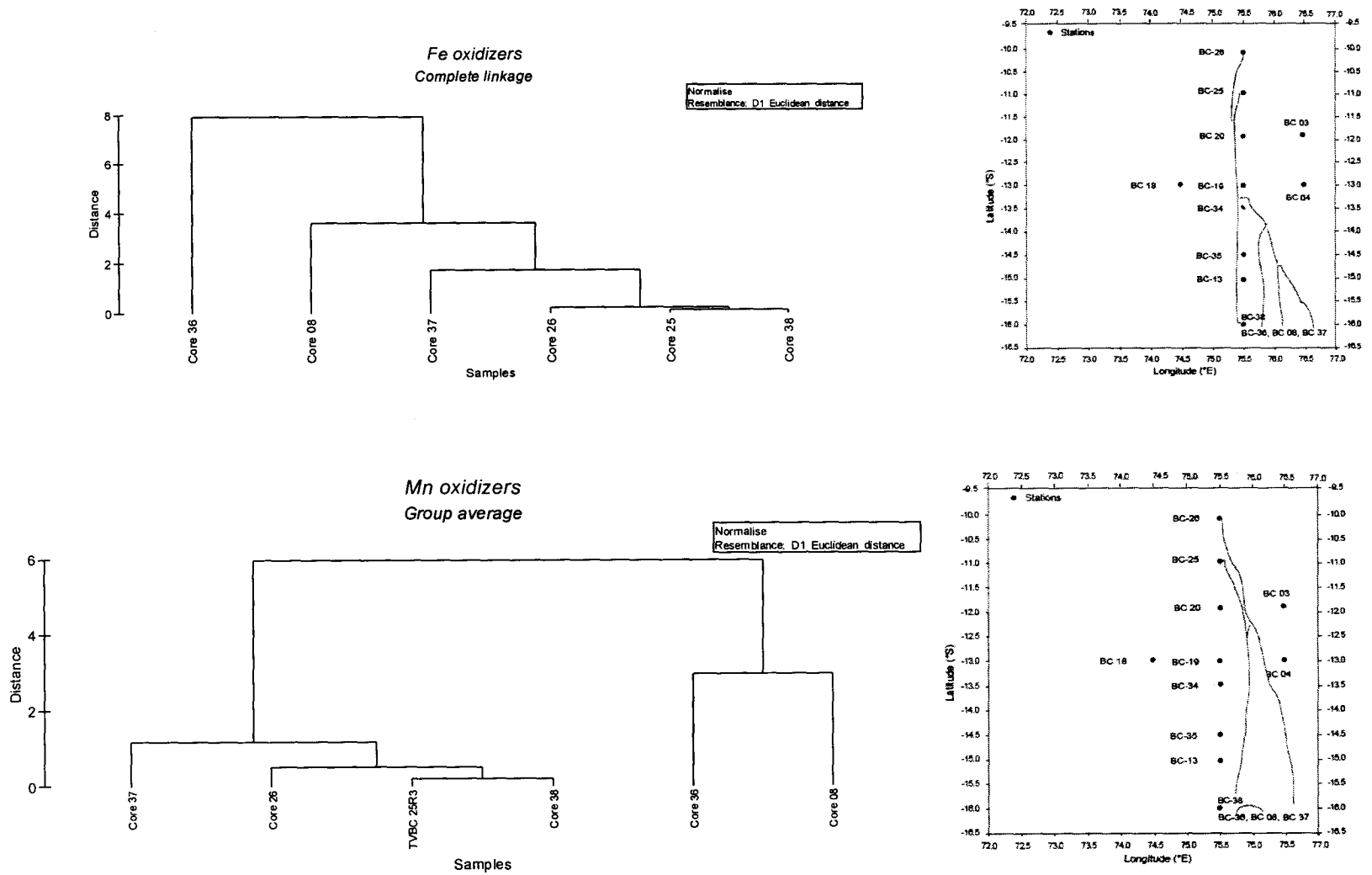


Fig. 4.25 . Cluster of CIOB stations based on distribution of Fe and Mn oxidizing bacteria. Inset shows station locations.

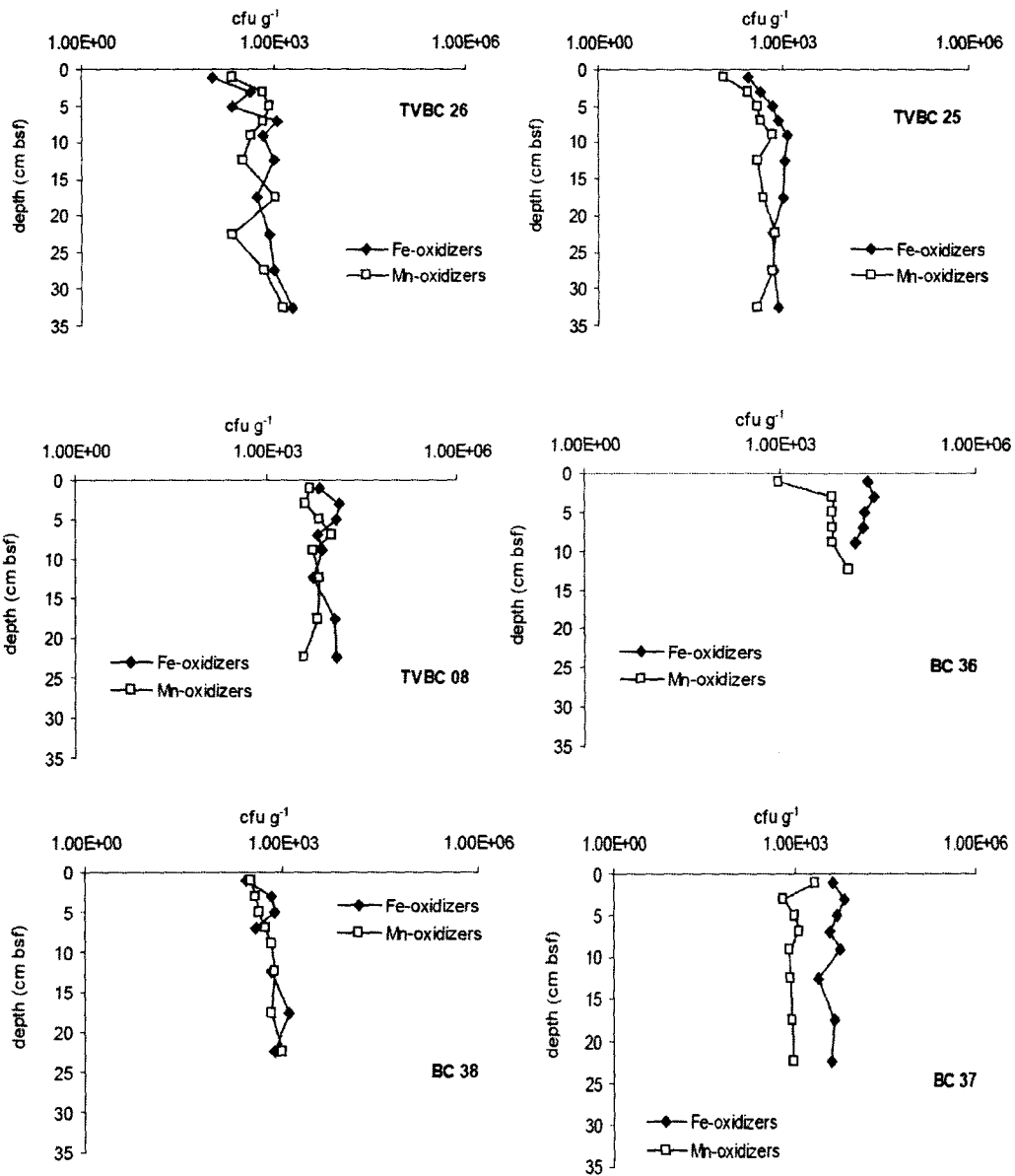


Fig. 4.26 Fe- and Mn- oxidizer profiles for representative stations in CIOB

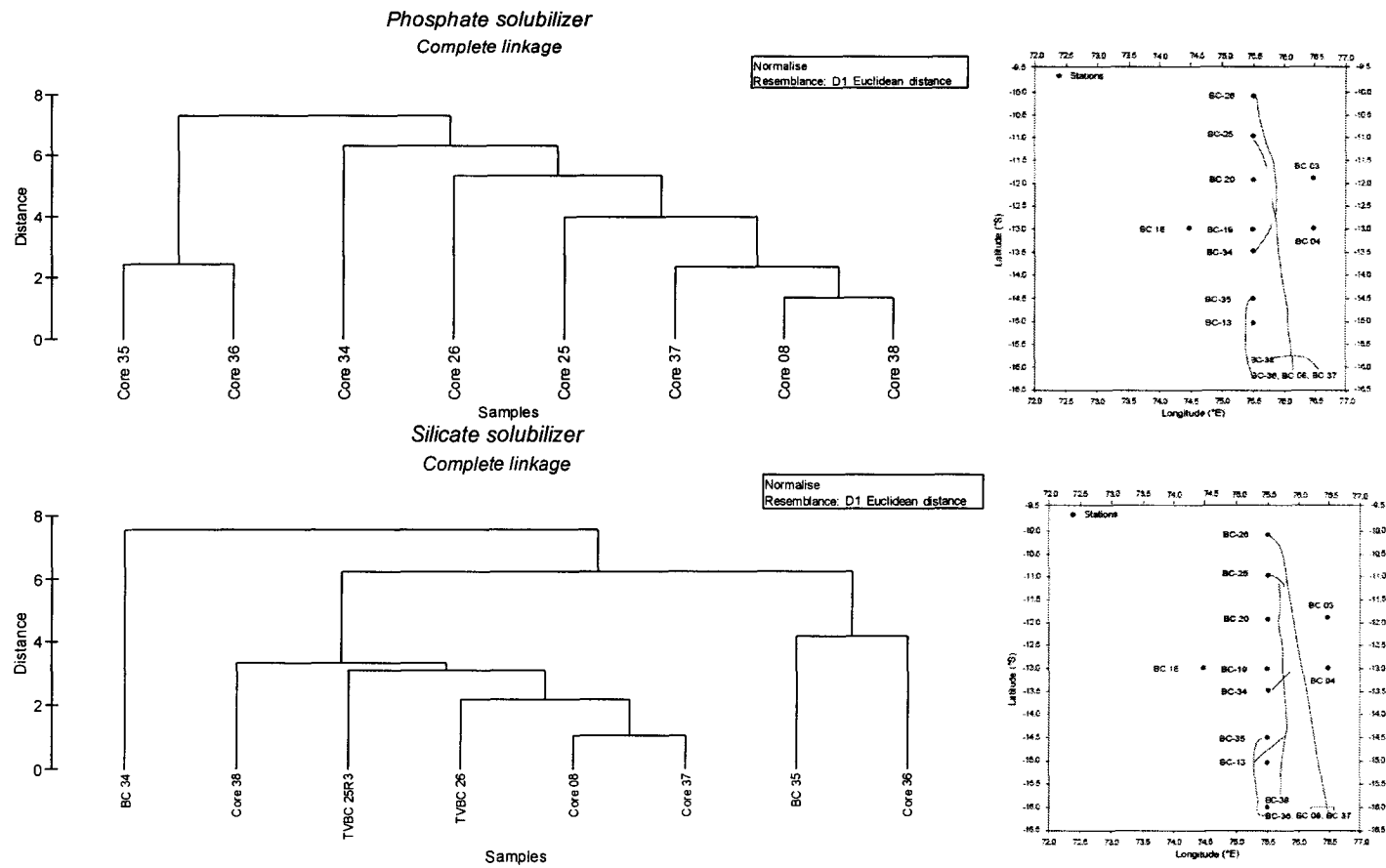


Fig. 4.27 Cluster of CIOB stations based on distribution of phosphate solubilizers and silicate solubilizers. Inset shows station locations.

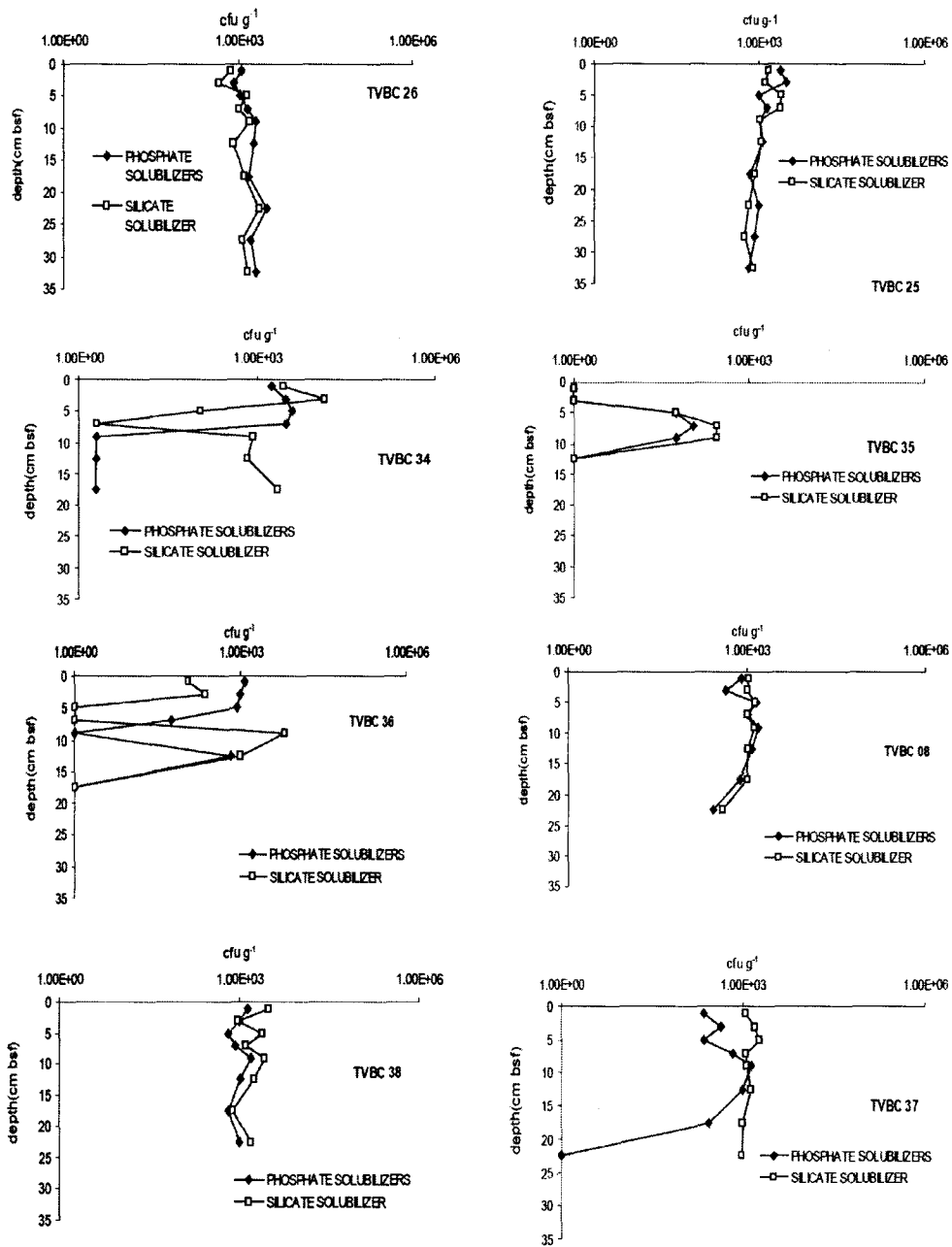


Fig. 4.28 . Phosphate and silicate solubilizer profiles for representative stations in CIOB

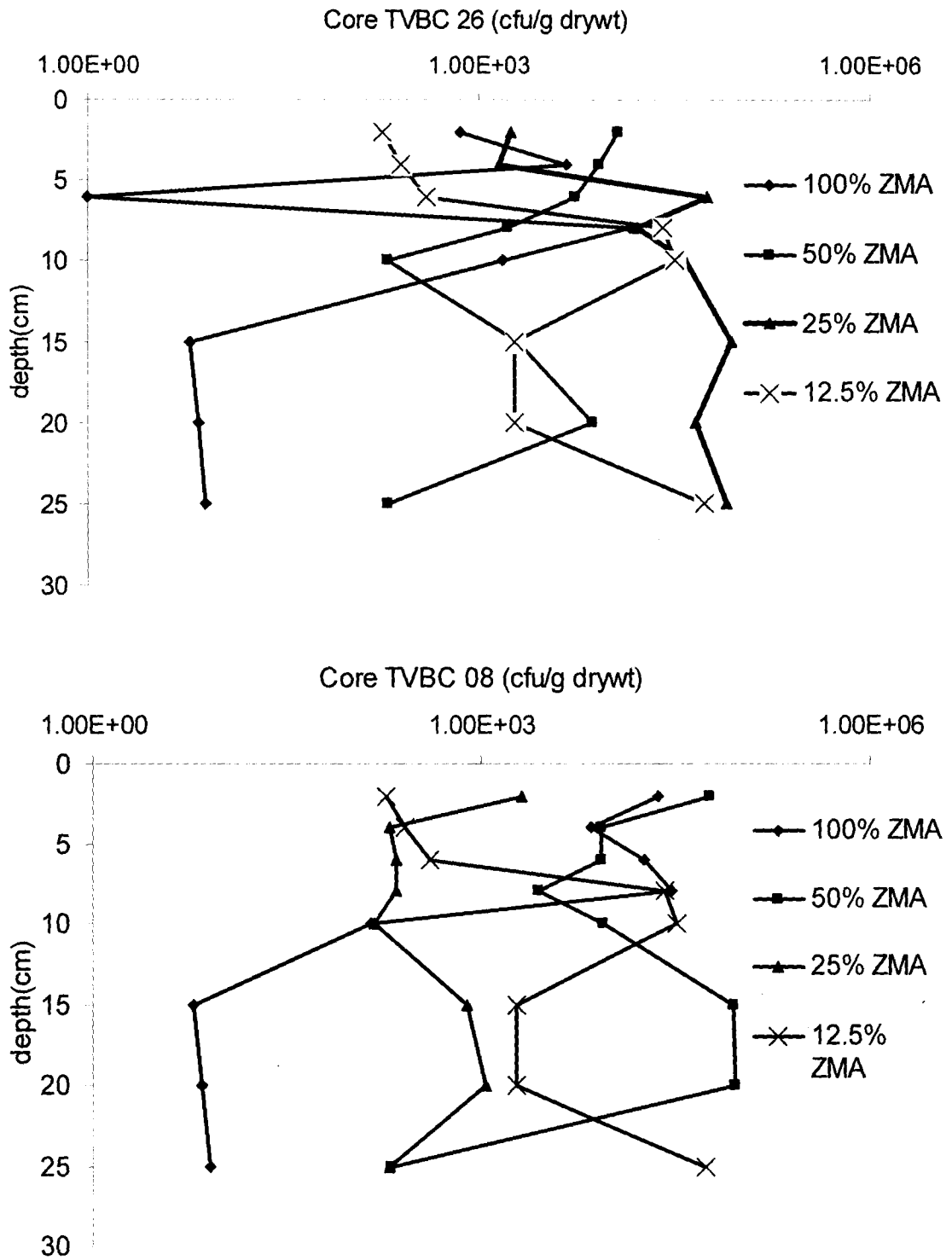


Fig. 4.29 Culturability of bacteria on varying strengths of Zobell Marine Agar

i. *Improvement of culturability with change in medium concentration*

Heterotrophs enumerated on different strengths of ZMA ranged from non-detectable to 2.95×10^4 cfu g⁻¹ at 100% concentration of ZMA. At 50% concentration the culturability improved by two orders and varied from 2.00×10^2 to 9.19×10^4 cfu g⁻¹. The maximum culturability was obtained on 25% ZMA concentration in case of station 26 in the north and varied from 1.47×10^2 to 8.85×10^4 cfu g⁻¹. At 12.5% concentration the culturability varied from 1.82×10^2 to 6.63×10^4 cfu g⁻¹. In the case of station 08, 25% concentration yielded the minimum culturability. Here the other concentrations did not vary significantly (Fig. 4.29).

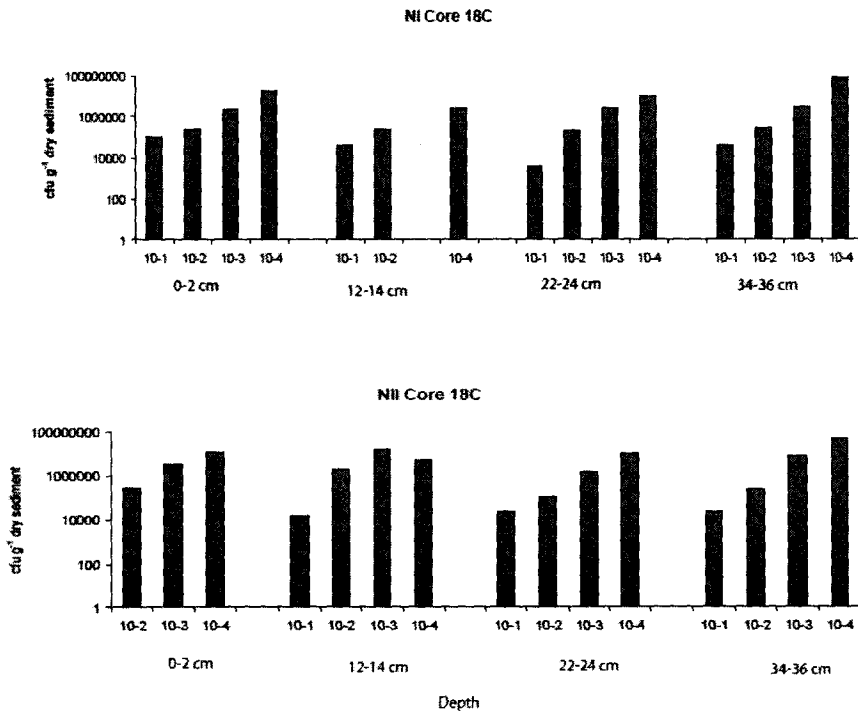


Fig.4.30A Increase in culturable counts in core 18C by serial dilution of sediment slurry

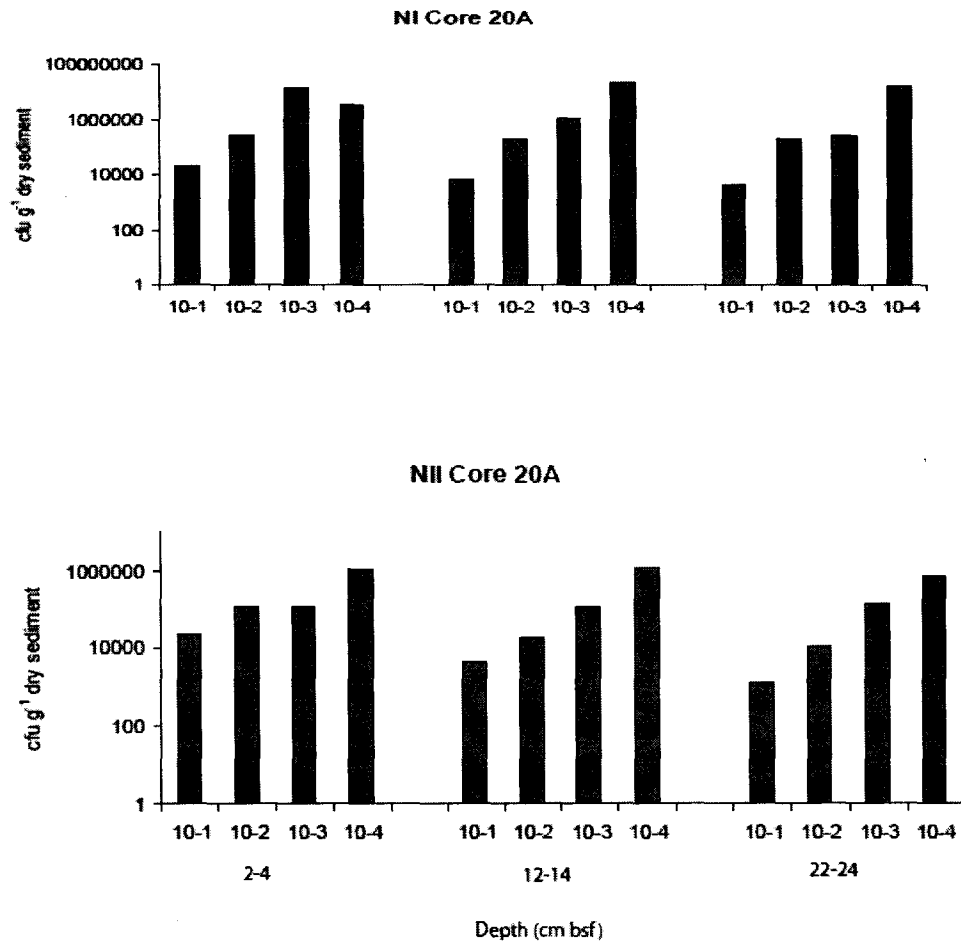


Fig. 4.30B Increase in culturable counts in core 20A by serial dilution of sediment slurry

j. Improvement of culturability

Culturability improved by one to three orders when the sediment slurry was diluted from 10^1 to 10^4 . This feature was noted for nitrifiers I and nitrifiers II for cores 18 and 20. This increase was noted at all depths analysed in the two cores (Fig. 4.30 A and B).

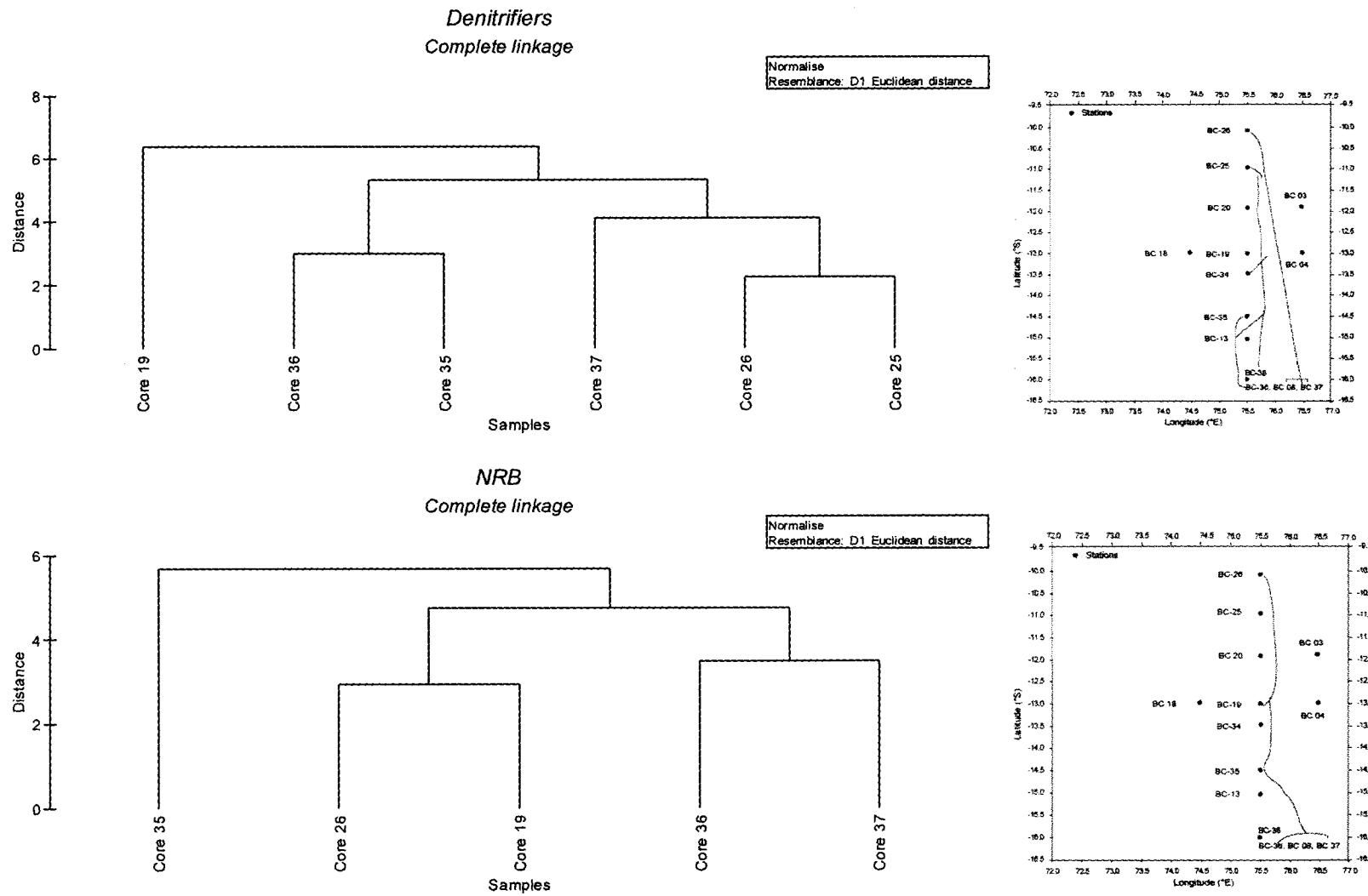


Fig. 4.31 Cluster analysis of CIOB stations based on distribution of denitrifiers and nitrate reducing bacteria

k. Down-core distribution of anaerobic bacteria

Anaerobic culturability was checked for representative cores. Stations 26 and 25 represented the siliceous ooze. Station 19 and 35 represented the siliceous-pelagic transition. Station 36 represented the pelagic red clays and 37 the calcareous ooze. Cluster analysis separated core 19 from rest of the cores at 65% in case of the denitrifiers. A second split at 50% divided stations 36 and 35 from the siliceous and calcareous ooze. In the case of nitrate reducing bacteria or NRB station 35 was separated from the rest of the cores at 55%. Core 26 clustered with 19 at 30% while core 36 clustered with 37 at 35%. Anaerobic counts in CIOB varied from non-detectable to $>10^3$ cfu g⁻¹ dry sediment (Fig. 4.31).

Denitrifiers and nitrate reducers showed partial niche separation with their peaks partially overlapping with each other in core 26. In core 25 the denitrifiers show a non-steady transient behaviour in their distribution patterns up to 25 cm bsf after which they decline to non detectable limits. Core 19 showed high numbers of denitrifiers varying from $<10^2$ to 10^4 cfu g⁻¹. Nitrate reducers varied from non-detectable to 10^4 cfu g⁻¹. Very steep minima and maxima were noted for both denitrifiers and nitrate reducers. In core 35, the denitrifiers ranged from non-detectable to $>10^3$ cfu g⁻¹. The nitrate reducers varied from non-detectable to $>10^4$ cfu g⁻¹. In pelagic clays 36, the denitrifiers varied from $<10^2$ to 10^3 cfu g⁻¹. The profile had a single prominent mid-depth minimum at 10 cm bsf. The nitrate reducers in this core ranged from non-detectable levels to 10^3 cfu g⁻¹, with three prominent mid-depth maxima. In calcareous core 37, denitrifiers ranged from non-detectable to 10^4 cfu g⁻¹. Nitrate reducers varied from non-detectable to $>10^3$

cfu g⁻¹. Distinct niche separation is noted in this core between denitrifiers and nitrate reducers (Fig. 4.32).

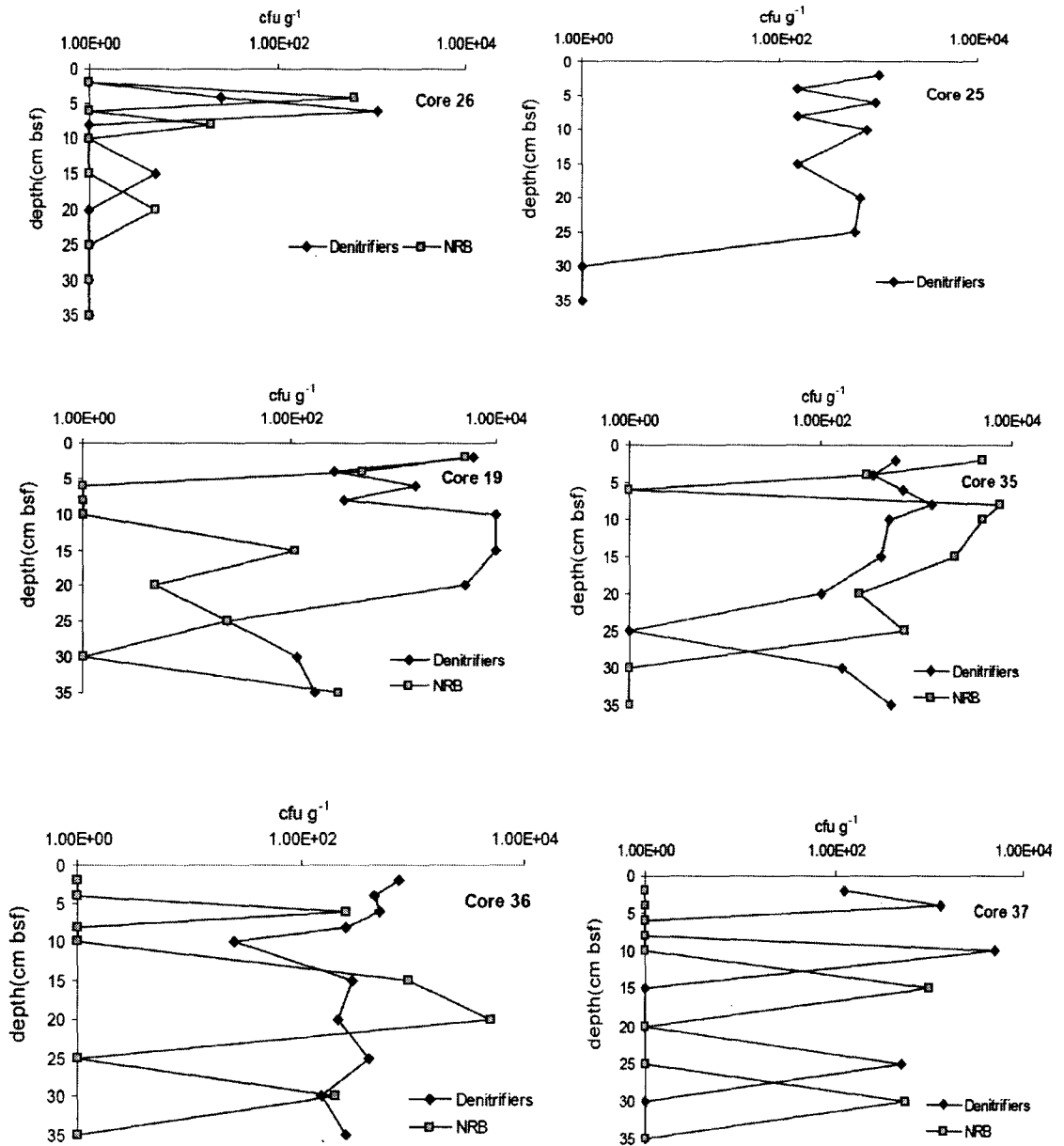


Fig. 4.32 Denitrifier and Nitrate reducing bacterial profiles for representative stations in CIOB.

l. Formaldehyde tolerant bacteria

As the deep sea sediments are oligotrophic it would be pertinent to examine chemotrophic tendencies by checking for C1 compound utilization. Besides, it was also surprising to see that formalin preserved samples showed active motile bacteria under epifluorescent microscopy. In the course of routine investigations for total bacterial counts in Central Indian Ocean Basin (CIOB) sediments, it was surprising to find that 12/22 cores (48/140 samples) showed the presence of formaldehyde tolerant bacteria ranging from nearly 0.65-47.22% of TC (Fig. 4.33). It was interesting to note that their abundance was generally restricted to changing interfaces of rock colour in the deeper parts of cores. Core TVBC 20 with only 0.65% formaldehyde utilizing bacteria was the lowest while TVBC 25 was highest in abundance with 47.22% (Table 4.1).

4.5 Diversity of Bacteria in Central Indian Ocean Basin

The diversity of a system decides the degree of stability. The deep sub-seafloor biosphere supports a diverse population of bacteria and archaea both in terms of phylogeny and function. The diversity of prokaryotes is low in ephemeral systems like the hydrothermal vents and high in the more stable systems like abyssal basins.

4.5.1 Biochemical characterization of isolates

A total of 361 isolates from representative cores were characterised biochemically according to Oliver, 1982. The siliceous-pelagic transition harboured the largest number of culturable bacterial genera. Cores 34 and 35 in this region showed 5 and 7 genera respectively. The calcareous ooze of core 37 harboured 6 genera. A

prominent absence of *Cytophaga* was noted in the siliceous oozes. The identified genera are tabulated in Table 4.2.

Contd....

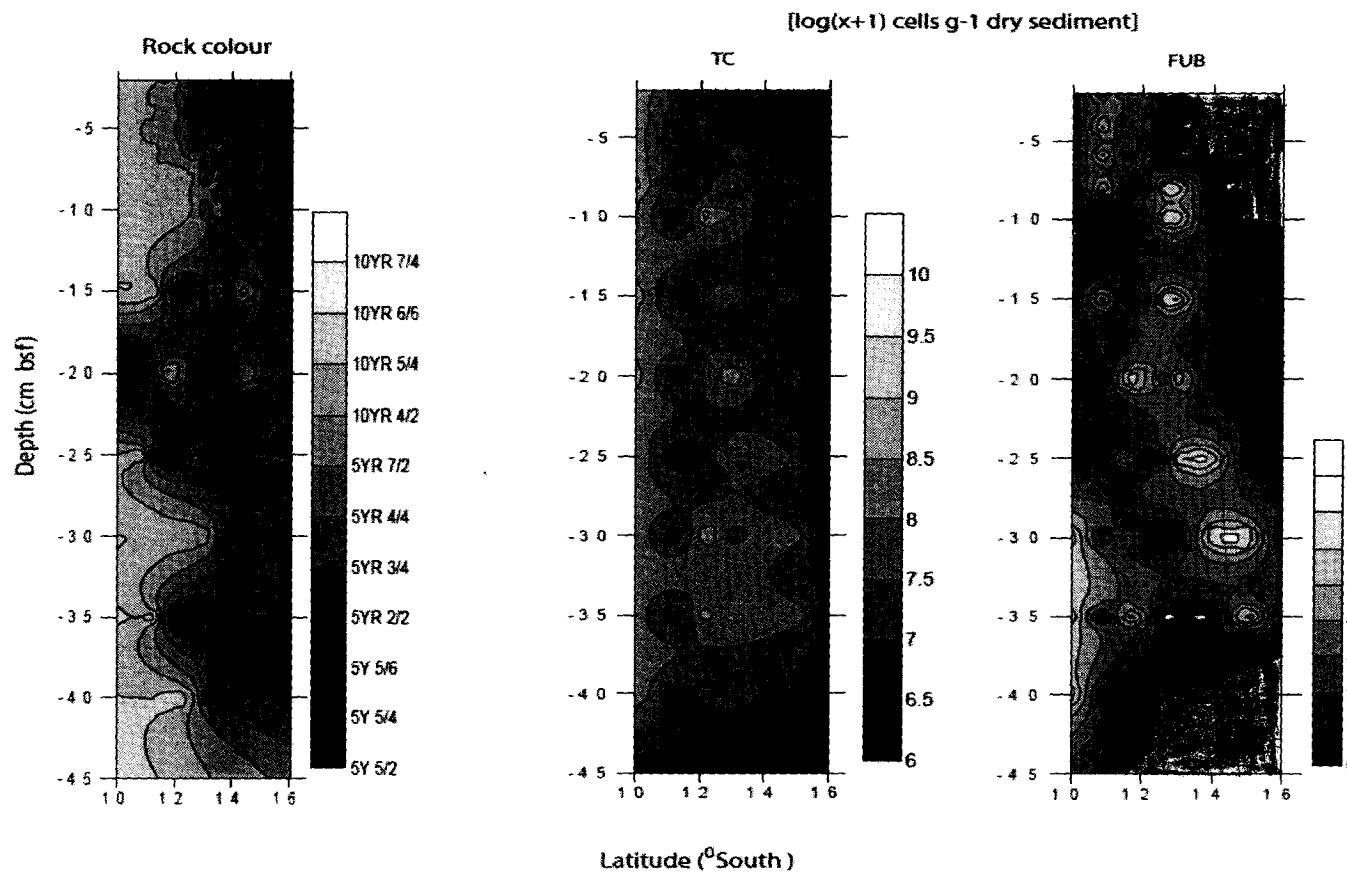


Fig. 4.33 Distribution of formaldehyde utilizing bacteria (FUB) occur at interfaces of changing rock colour.

Table 4.1 . Percentage of averaged formaldehyde utilizing bacteria (FUB) in averaged total bacterial counts at different cores in CIOB.

Core no.	Total bacterial count ($10^8 \times \text{cell g}^{-1}$)	Formaldehyde utilizing bacteria (FUB) ($10^7 \times \text{cell g}^{-1}$)	Percentage
TVBC 25	0.840 ± 0.575	3.97 ± 3.74	47.22
TVBC 26	4.23 ± 1.36	1.87 ± 0.376	4.41
TVBC 20	6.38 ± 5.81	$0.416 \pm 0.400E$	0.65
TVBC 03	0.278	0.982E	35.39
BC 29	0.424	0.550	12.97
BC 30	2.09 ± 0.453	0.946 ± 0.333	4.52
BC 32	0.963 ± 0.464	0.142 ± 0.107	1.47
TVBC 19	4.54 ± 3.18	1.27 ± 0.407	2.80
TVBC 04	0.256	0.720	28.13
TVBC 33	2.99 ± 0.402	1.77 ± 0.227	5.91
TVBC 14	2.37	1.77	7.47
TVBC 13	2.66 ± 0.180	2.55 ± 0.520	9.60

Table 4.2 Generic diversity by biochemical characterisation of bacteria from representative stations in CIOB.

Core no.	Sediment type		No. of isolates	No. of genera	Names of genera
26	Siliceous ooze		45	3	<i>Flavobacterium</i> <i>Alcaligenes</i> <i>Pseudomonas I</i>
25	Siliceous ooze		100	4	<i>Pseudomonas</i> <i>Pseudomonas/Alteromonas</i> <i>Xanthomonas</i> <i>Aeromonas</i>
34	Siliceous-Pelagic clay transition	red	52	5	<i>Psuedomonas/Alteromonas I</i> <i>Psuedomonas/AlteromonasII</i> <i>Xanthomonas</i> <i>Pseudomonas II</i> <i>Pseudomonas IV</i>
35	Siliceous-Pelagic clay transition	red	76	7	<i>Pseudomonas I</i> <i>Pseudomonas II</i> <i>Pseudomonas III</i> <i>Pseudomonas IV</i> <i>Alcaligenes</i> <i>Vibrio</i> <i>Flavobacterium</i>
8	Pelagic red clay		12	3	<i>Cytophaga</i> <i>Alcaligenes</i> <i>Flavobacterium</i>
36	Pelagic red clay		33	5	<i>Xanthomonas</i> <i>Pseudomonas/Alteromonas I</i> <i>Pseudomonas/Alteromonas II</i> <i>Pseudomonas/Alteromonas IV</i> <i>Pseudomonas IV</i>
38	Pelagic red clay		8	2	<i>Cytophaga</i>

37	Calcareous ooze	40	6	<i>Alcaligenes</i>
				<i>Vibrio-Aeromonas</i>
				<i>Pseudomonas I</i>
				<i>Pseudomonas II</i>
				<i>Acinetobacter</i>
				<i>Moraxella</i>
				<i>Flavobacterium</i>

Contd....

4.5.2 16S rRNA characterisation for CIOB Isolates

4.5.2.1 Phylogenetic affiliation of culture CIOB 25A -an Aerobic *Thiobacillus denitrificans* like-organism

Partial Sequence of CIOB 25A

```
TGGGGGTCGGGTTACTATAATGCTGTGCGAGTGGTACAGAGAGTAGCTTTGC
TACTTTTGCTGACGAGCGGCTGACGGGTGAGTAATTCTTGGGAATATGCCT
TATGGTGGGGGACAACAGTTGGAAACGACTGCTAATACCGCATGATGTCTA
CGGACCAAAGTGGGGGGACCTTCGGGCCTCACGCCATAAGATTAGCCCAA
GTGGGATTAGCTAGTTGGTGAGGTAATGGCTCACCAAGGCGACGATCCCTA
GCTGGTTTGAGAGGATGATCAGCCACACTGGGACTGAGACACGGCCCAGA
CTCTACGGGAGGAGCAGTGGGGATATTGCACAATGGGCGCAAGCTTGAT
GCAGCCATGCCGCGTTGTAAAAAAGGCCTTGGGGTTGTAAAGCATTTTCA
GTAAGGGGGAAAGTTTAAAGTGTATTAGCATTTAGTTTTGGCGTACTTAAA
GAAGAAGCCCGGCAACCTCCTCCCAGCGCCGCGGTAATACGGAGGTGCGA
GGTTAATCGGATTTATGGGCTAAAGCGTCCCGGCGTTTGTAAAGCGAGTGTA
AACCCCGGGCTAACCTGGAATCCTTTCGACTGGAACTAATTGTGAAGAGG
GGAAAAATTCAGGTTAGCGTGAAAGCTTAGAATCGAAGGAACCGATGGGA
AGGAGCACCGGGTCACATGACCTATGTACGAAGCTGGGAGCAACAGTTGA
TCCGGTTGCACAA
```

BLAST analysis showed that Culture CIOB 25A was 91% similar to *Pseudoalteromonas* sp. The phylogenetic affiliation of the culture is shown in Fig. 4.34A The numbers denote the bootstrap values. It is suggested that *Pseudoalteromonas* sp. CIOB 25A is a novel species.

4.5.5.2 . Phylogenetic affinity of culture CIOB BIN2- a deep-sea heterotroph

Partial Sequence of CIOB BIN2

> CIOBBIN2

```
TAGGGGGGGGTCCTACCATGCAATCTGAGCGGTTTTCTGGAGCTTGCTTCTT
GATTCAGCGGCGGACGGGTGAGTAACACGTGGTCAACCTGCCTGTAAGACT
GGGATAACTTCGGGAAACCGGAGCTAATACCGGATAATCCTTTCGCTCTCA
TGTGCTAAAGCTGAAAGATGGTTTCCGCTGTCACTTACAGATGGGCCCCGCG
GCCATTAGCTAGTTGGTGAGGTAACGGCTCACCAAGGCAACGATGCGTA
GCCGACCTGAGAGGGTGATCGGCCCACTGGGACTGAGACACGGCCCATA
CTCTACGGGAGGCAGCAGTAGGGAATCTTCCGCAATGGACGAAAGTCTTG
ACGGAGCAACGCCCCCGTGAACGATGAAGGTTTTCCGGATCGTAAAGCTTC
TGTTGTTAGGGAAGAACAAGTACCGGAGTAACTGCCGGGACCTTGACGGT
ACCTTAACCAGAAAGCCACGGCTAATTACCGTGCCACCGGCCGCGGATAT
TACGTAGGTGGCAAGCGTTGTCCGGAATTATTGGGCGTAAAGCGCGCGCAG
GCCGTCCTTTAGTCTGATGTGAAGCCCCGGCTCAACCGTGAAGGTCATTGG
```

AAACTGTGGACTTTGAGTGCAGAAGAGGAGAGTGCAATTCCACGTTAGCGT
 GAAATGCGTAGAGATGTGAGTATCAACAGTGGCGAAGTGA CTCTGGCC
 GTA ACTGACGCTTGAGCGCGAATGCGTGGGCGCGAATCGGAGTAGACTGC
 CTGTTATTCAGCGCTAACGATTAGTGTCTTGAGCGTA

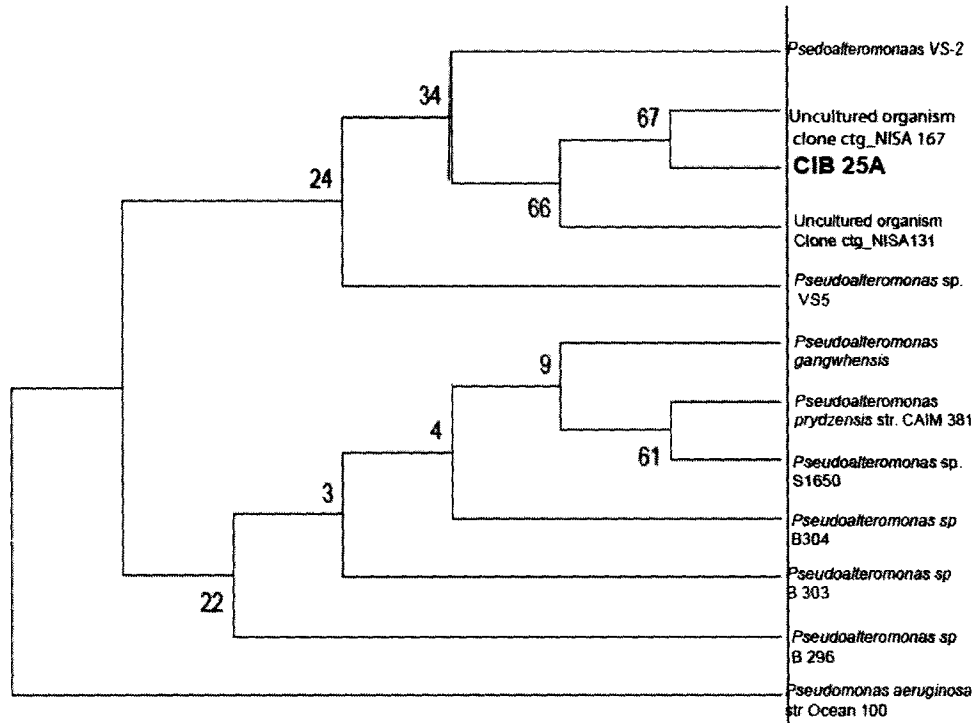


Fig. 4.34 A Phylogenetic affiliation of culture CIOB 25A

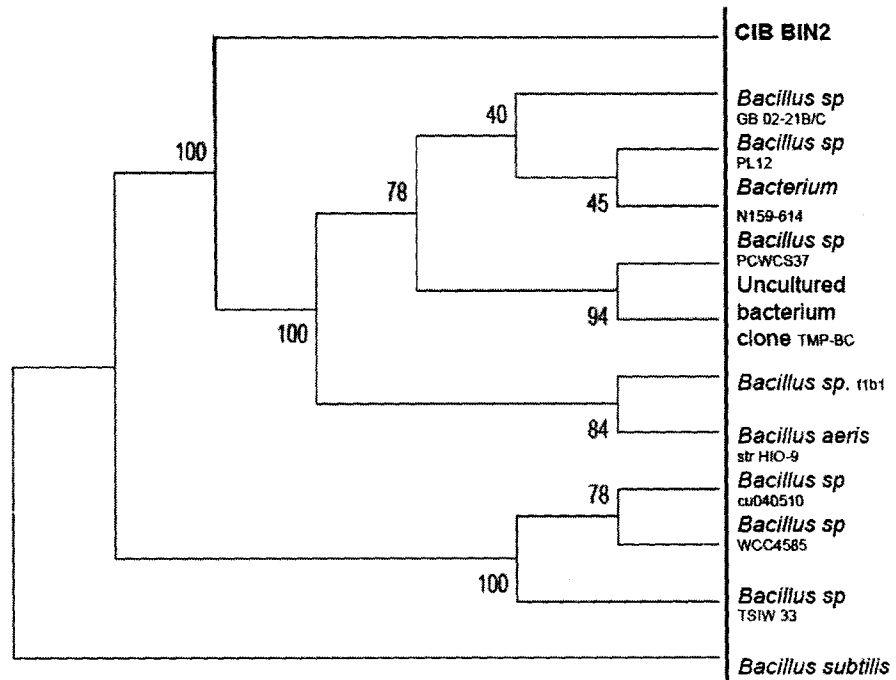


Fig. 4.34B Phylogenetic affiliation of culture CIOB BIN2

Culture CIOB BIN2 showed 92% similarity to *Bacillus* sp. Fig. 4.34B shows the phylogenetic affinity of the culture. This deep-sea heterotroph, with a common ancestry to several *Bacillus* sp. and uncultured bacteria is suggested to be a novel species. The deep-sea heterotroph CIOB BIN3 shows phylogenetic affinity to several *Pseudomonas* sp. and uncultured bacterial clones (Fig. 4.34C). As this strain shared 97% similarity with those clones, the isolate is suggested to be a novel strain.

4.5.2.3 Phylogenetic affinity of culture CIOB BIN 3- a deep-sea heterotroph

Partial Sequence of CIOB BIN 3

>CIOBBIN3

```
TGGAAAGAAAGGCTTTGCTTTCTCCTTGAGAGCGGCGGGACGGGTGAGTAATG
CCTAGGAATCTGCCTGGTAGTGGGGGATAACGTTTCGGAAACGGACGCTAATAC
CGCATACGTCTACGGGAGAAAGCAGGGGACCTTCGGGCCTTGCGCTATCAGA
TGAGCCTAGGTCGGATTAGCTAGTTGGTGAGGTAATGGCTCACCAAGGCGACG
ATCCGTAAC TGGTCTGAGAGGATGATCAGTCACACTGGA ACTGAGACACGGTC
CAGACTCCTACGGGAGGCAGCAGTGGGGAATATTGGACAATGGGCGAAAGCC
TGATCCAGCCATGCCGCGTGTGTGAAGAAGGCTTCGGATTGTA AAGCACTTTA
AGTTGGGAGGAAGGTTGTAGATTAATACTCTGCAATTTTGACGTTACCGACAG
ATAAGCACCGCTAACTCTGTGCCAGCAGCCGCGGTAATACAGAAGGGTGCAAG
CGTTAATCGGAATTACTGGGCGTAAGCGCGCGTAGGTGGTTTGTTAAGTTGGA
TGTGAAATCCCCGGGCTCAACCTGGGAACTGCATTCAA AACTGACTGACTAGA
GTATGGTAGAGGGTGGTGGAAATTCCTGTGTAGCGGTGAAATGCGTAGTTTGG
AAGGAACCCAGTGGCGAAGGCGACCACCTGGGCTAATACTGACCTGAGGGGC
AAAGTTGGGGAGCAACAGGATAAGATACCCGGGGGGCCCCCGCGG
```

Partial sequence of CIOB BIN 4

>CIOBBIN4

```
TCGGATGCAATTCCAAGGTTGAGCCCTGGGCTTTCACATCCGACTTAACACACC
GCCTACGCGCGCTTTACGCCAGTAATTCGGATTAACGCTCGCACCTTTCGTAT
TACCGCGGCTGCTGGCACGAAATTAGCCGGTGCTTCTTCTGTAGGTAACGTCA
AGTACTCCAGGGTATTAACCCAAAGCCTTCCTCCCTACTGAAAGTGCTTTACAA
CCCGAAGGCCTTCTTCACACACGCGGCATGGCTGGATCAGGCTTGCGCCATT
GTCCAAGATTCCCCACTGCTGCCTCCCGTAGGAGTCCGGGGCCGTGTCTCAGTCC
CGGTGTGACTGGCCATCCTCTCAGACCAGTTACGGATCGTTCGCCTTGGTGGGCC
ATTACCCACCAACAAGCTAATCCGACGCGGGCTCATCCATCAGCGCAAGGTC
CGAAGATCCCCTGCTTTCCCCCGTAGGGATTATGCGGTATTAGCTCGAGTTTCC
CCGAGTTATCCCCACTAATGGGCAGATTCCCACGTGTTACTACCCGTCCGCC
```

GCTCGACGCCTGGGAGCAAGCTCCCATCGTTTCCGCTCGACTTGCATGTGTTAG
 GCCTGCCGCCAGCGTTCAATCTGAGCCAGGATCAAACCT

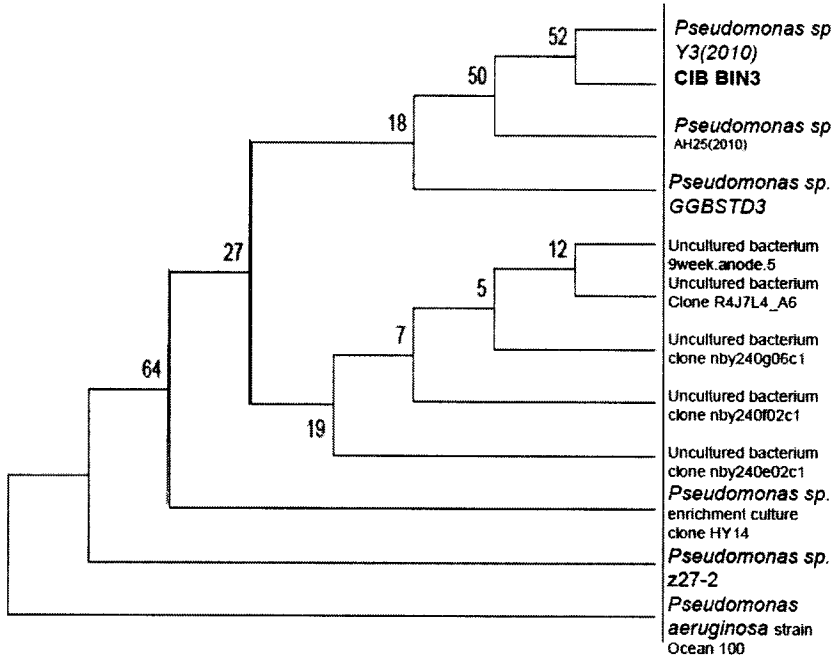


Fig. 4.34C Phylogenetic affinity of isolate CIOB BIN3

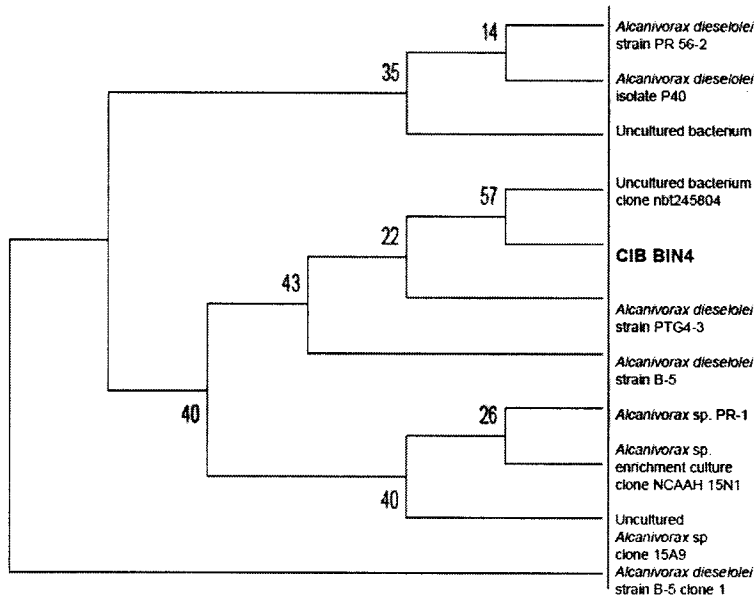


Fig. 4.34D Phylogenetic affinity of isolate CIOB BIN4

4.5.2.4 Phylogenetic affinity of Culture CIOB BIN 4- a deep-sea heterotroph

The deep-sea heterotroph CIOB BIN4 showed phylogenetic affinity to *Alcanivorax dieselolei* and several uncultured bacterial clones (Fig. 4.34D). It shared 99% similarity with these clones, and suggests that hydrocarbon degrading bacteria could be present in the deep-sea.

4.5.3 Community analysis from whole sediment

The deep –sea pelagic clay from CIOB with volcanic signatures was analysed for its bacterial community by 454 Pyrosequencing technique targeting the Bv6 region of 16SrRNA. The Aerobic Anoxygenic Phototrophic (AAP) Genus *Erythrobacter* dominated a rather simple microbial ecosystem. Total number of sequence reads at species level was 15,223. Number of phyla present was 14. The first 4 dominant phyla were Proteobacteria at 97.86 %, Actinobacteria at 0.75 %, unassigned phylum at 0.45 %, and Firmicutes at 0.28 %. In the present study, rarefaction analysis (Fig. 4.35) showed that a large part of the rare biosphere in TVBC 08 still remains untapped although the dominant genus was *Erythrobacter*.

The most dominant phylum Proteobacteria was dominated by the α - Proteobacter at 93.64 %. This was followed by β -Proteobacter at 1.51 %, γ -Proteobacter at 2.53 %, δ - Proteobacter at 0.11 %, and unknown Proteobacter at 0.06 %. Family Erythrobacteraceae belonging to α - Proteobacter dominated the system at 92.12 %. Genus *Erythrobacter* sp. (84.29 %) and one more unknown genus (7.82%) is most abundant. Among the other phyla OP11, OP3 and one unassigned phylum were detected. The phylum Thermomicrobia was also encountered (0.026%). The important groups were the

Firmicutes, Gemmatimonadetes, Nitrospira, Planctomycetes, Bacteroidetes, Chloroflexi, Deferribacteres.

Table 4.3 presents similarity-based OTUs and species richness estimates of the CIOB sample. Indices reveal polarization of the bacterial community as implied by the dominance of *Erythrobacteriaceae* suggesting the prevalence of a simple community.

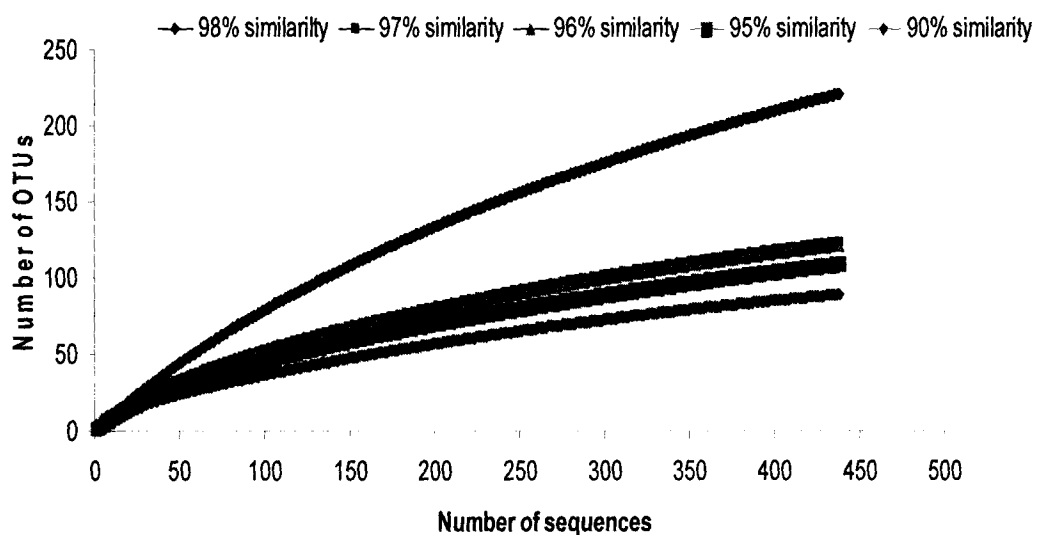


Fig. 4.35 Rarefaction analysis of bacterial diversity at station TVBC-08

Table 4.3 Similarity-based OTUs and species richness estimates

Index	Unique	2%	3%	4%	5%	7%	8%	9%	10%
OTU*	439	221	123	121	109	98	97	90	89
ACE**	0	428	220	218	218	205	194	166	162
Chao1	96580	381	193	189	178	156	148	133	132
Jack	878	429	196	190	179	155	150	138	136
Simpson's	0	0.006	0.03	0.032	0.037	0.49	0.048	0.062	0.062
Shannon's	6.089	5.07	4.08	4.05	3.89	3.61	3.6	3.52	3.517

*Operational taxonomic unit

**Abundance-based coverage estimator

4.6. Activity of Bacteria in Central Indian Basin

Microbes govern biogeochemical cycles and may function heterotrophically or autotrophically. Heterotrophy might be the most important mode of metabolism in detrital depositional settings. Chemoautotrophy prevails when heterotrophy is limited by the increasing recalcitrance and decrease in quantity of organic matter (Fry *et al.* 2008).

The phylogenetic diversity is closely linked to metabolic and functional diversity. The metabolic diversity is greater in case of deep-sea as these systems have diverse substrates as compared to the coastal systems (Harder and Dijkhuizen, 1982, Goltekar *et al.*, 2006). Consequently, the activity of bacteria is highly diversified and varied. So understanding the metabolic activity would be relevant.

4.6.1 Hydrolytic enzyme activity

Hydrolytic enzyme activity was tested in 366 isolates from 8 selected representative cores. The isolates in siliceous oozes from core 26 and 25 showed highest utilization of DNase and lipase. This behaviour is strange as more recalcitrant substrates were utilized in spite of the cores being LOM rich. Isolates of core 34 at the siliceous-pelagic transition were more versatile and showed high activity of lipase, protease and phosphatase. Similarly core 35 was also versatile in showing DNase and phosphatase activity. The more oligotrophic pelagic red clay cores 8, 36 and 38 were also versatile with lipase, protease and DNase activity. The calcareous ooze 37 showed maximum utilization of lipase (Table 4.4). The results of the enzyme activity have been tabulated below:

Table 4.4 Hydrolytic enzyme activity in bacterial isolates (n=366).

<i>Core no.</i>	<i>Amylase%</i>	<i>Lipase%</i>	<i>Protease%</i>	<i>DNase%</i>	<i>Phosphatase%</i>
26	1.13	13.33	20	35.56	0
25	16.9	75.42	15.9	17.12	14.64
34	33.5	63.6	56.06	25.86	50.59
35	94.7	15.79	0	68.42	31.57
8	41.16	66.66	33.33	50	0
36	27.05	28.75	27.05	57.78	82
38	0	50	62.5	87.5	0
37	55	80	37.5	3.0	0

4.6.2 Carbon substrate utilization

Five selected sediments were tested for carbon substrate utilization on BIOLOG ECO plates. Some of the sediments responded sparsely to this test. However, the selected cores showed a wide diversity in the substrates they utilised. Lipids, amino acids and carbohydrates were utilized by the siliceous oozes. Among the siliceous oozes, core 20 used a maximum of 13 substrates (Table 4.5). Five deep-sea cultures (E4-E8, Table 4.6) were studied for carbon substrate utilization on BIOLOG GN plates. *E.coli*, a typical heterotroph used only 13 substrates while deep-sea ammonium oxidizer, E4 utilized 84 substrates out of 96. A wide array of substrates was utilized by these deep-sea cultures. The details of the cultures used for various activity studies have been shown in Table 4.7. The results are tabulated as follows:

Table 4.5 Carbon substrate utilization by sediments

<i>Core no.</i>	<i>Sediment type</i>	<i>Carbon sustrate utilized</i>
26	Siliceous ooze	Tween 40 Tween 80 D-Xylose L-Arginine L-Asperigine L-serine Putrescine
25	Siliceous ooze	D-Xylose
20	Siliceous ooze	Pyruvic acid Tween 40 Tween 80 α -Cyclodextrin Glycogen D-Cellobiose α -D- Lactose D-L- α -glycerol phosphate D-Malic acid L-serine L-threonine Glycyl L-glutamic acid Phenyl ethyl amine
37	Calcareous ooze	D-Xylose
38	Pelagic red clay	D-Xylose Tween 40

Table 4.6 Carbon substrate utilization by cultures

	C1	C3	E1	E2	E3	E4	E5	E6	E7	E8
α - Cyclodextrin		+	+	+	+	+				
Dextrin		+	+	+	+	+				
Glycogen		+	+	+	+	+				
Tween 40		+	+	+	+	+				
Tween 80		+	+	+	+	+		+	+	
N-Acetyl D-Galactosamine		+	+	+	+	+		+		
N-Acetyl D-Glucosamine		+	+	+	+		+	+		+
Adonitol		+	+	+	+	+	+	+		
L-Arabinose		+	+	+	+	+		+		
D-Arabitol	+	+	+	+	+	+	+	+		+
D- Cellobiose		+	+	+	+	+	+	+		+

i-Erythritol		+	+	+	+	+			+
D-Fructose		+	+	+	+	+			+
L-Fucose		+	+	+	+	+			
D- Galactose		+	+	+	+	+			+
Gentiobiose		+	+	+	+	+	+		+
α -D-Glucose		+	+	+	+	+			+
m- Inositol		+	+	+	+	+	+		
α -D-Lactose		+	+	+	+	+	+	+	+
Lactulose		+	+	+	+	+	+	+	+
Maltose		+	+	+	+	+	+	+	+
D-Mannitol	+	+	+	+	+	+	+	+	+
D-Mannose	+	+	+	+	+	+	+	+	
D-Melibiose		+	+	+	+	+			+
β -Methyl-D-Glucoside		+	+	+	+	+			+
D-Psicose		+	+	+	+	+			
D-Raffinose		+	+	+	+	+			+
L-Rhamnose		+	+	+	+	+	+		+
D-Sorbitol		+	+	+	+	+			+
Sucrose		+	+	+	+	+	+	+	+
D-Trehalose		+	+	+	+	+	+	+	+
Turanose		+	+	+	+	+	+		
Xylitol		+	+	+	+	+	+	+	
Pyruvic acid methyl ester		+	+	+	+		+		
Succinic acid mono-methyl ester									
Acetic acid		+	+	+	+	+	+		+
Cis-Aconitic acid		+	+	+	+	+	+	+	+
Citric acid		+	+	+	+	+	+		+
Formic acid		+	+	+	+				+
D-Galactonic acid lactone		+	+	+	+	+			
D-Galacturonic acid		+	+	+	+	+	+	+	+
D-Gluconic acid		+	+	+	+	+	+	+	+
D-Glucosaminic acid		+	+	+	+	+	+		
D-Glucuronic acid		+	+	+	+	+	+	+	
α - Hydroxybutric acid		+	+	+	+	+	+		
β -Hydroxybutric acid		+		+	+	+	+		+
γ -Hydroxybutric acid	+	+		+	+	+	+		
p-hydroxy phenyl acetic acid			+						
Itaconic acid		+	+	+	+	+	+	+	+
α -ketobutyric acid		+	+	+	+				
α -ketoglutaric acid		+	+	+	+	+			
α -ketovaleric acid			+		+		+		
D,L- Lactic acid		+	+	+	+	+			+
Malonic acid		+	+	+	+	+	+	+	
Propionic acid				+	+	+			
Quinic acid		+	+	+	+	+	+	+	
D-Saccharic acid		+	+	+	+	+	+		
Sebaccic acid							+		
Succinic acid	+	+		+	+	+	+		
Bromosuccinic acid		+	+	+	+	+			
Succinamic acid		+	+	+	+	+		+	

Glucuronamide	+	+	+	+	+				
L-Alaninamide	+	+	+	+	+		+		
D-Alanine	+	+	+	+	+				
L-Alanine	+	+	+	+	+		+		+
L- Alanyl glycine	+	+	+	+	+		+	+	
L-Asparigine	+	+	+	+	+	+	+		+
L-Aspartic acid	+	+	+	+	+	+	+	+	
L-Glutamic acid	+	+	+	+	+	+	+		+
Glycyl-L-aspartic acid	+	+		+	+	+	+		
Glycyl-L-glutamic acid	+	+	+	+	+	+		+	
L-Histidine	+	+	+	+	+				
Hydroxyl L-Proline	+	+	+	+	+				
L-Leucine	+	+	+	+	+			+	
L-Ornithine	+	+	+	+	+		+	+	
L-Phenylalanine	+	+	+	+	+			+	
L- Proline	+	+	+	+	+		+	+	+
L- Pyroglutamic acid	+	+	+	+	+		+		
D-Serine	+	+	+	+	+	+	+	+	
L-Serine	+	+	+	+	+	+	+		+
L-Threonine	+	+	+	+	+	+	+		
D,L- Carnitine	+	+	+	+	+	+	+		
γ-aminobutyric acid	+	+	+	+	+	+			
Urocanic acid		+	+	+	+				
Inosine		+	+	+	+			+	
Uridine		+	+	+	+				
Thymidine		+	+	+	+				
Phenylethyl amine		+	+	+	+				
Putracine		+	+	+	+		+		
2-Aminoethanol		+	+	+	+		+		
2,3-Butanediol		+	+	+	+	+	+		
Glycerol		+	+	+	+	+	+	+	+
D,L-α Glycerol phosphate	+	+		+	+	+	+		
α-D glucose-1 phosphate	+	+		+	+	+	+		
D glucose-6-phosphate	+	+		+	+	+	+		

Table 4.7 Details of bacterial isolates used for detecting chemosynthetic potential and carbon substrate utilization.

C= *E.Coli*
 E1-E3 = Mixotrophic experimental isolates worked upon earlier;
 E4-E8 = Experimental isolates from CIOB

Sl. No.	Culture	Nature	Culture source
C	<i>E.coli</i>	<i>Typical heterotroph</i>	<i>NIO microbiology laboratory collection</i>
E1	<i>Halomonas</i> sp 12G	Ammonium oxidizer	CIOB EIA*** @
E2	<i>Halomonas</i> sp CR35	Metal oxidizer	Carlsberg Ridge ***#
E3	<i>Halomonas</i> sp CR48	Metal oxidizer	Carlsberg Ridge***#
E4	2NC6a	Ammonium oxidizer	CIOB *
E5	2NNC3a	Nitrite oxidizer	CIOB *
E6	2NTC5a	TDLO 1^	CIOB *
E7	CIOB25A	TDLO 2^	CIOB *
E8	2TTC4a	Formaldehyde utilizer	CIOB *
E9	2ZC12A	Deep-sea heterotroph	CIOB *

* Central Indian Basin EVDC-2 Core 25, 0-2 bsf

*** Earlier studies

@ Ram *et al.*, 2001

Fernandes *et al.*, 2005

^ *Thiobacillus denitrificans* like organisms, also called aerobic sulphur oxidizers

4.6.3 Carbon fixation

a. *Whole sediments*

Preliminary analyses were conducted with one of the cores (13) at $4\pm 2^\circ\text{C}$, 1 atm and $4\pm 2^\circ\text{C}$, 500 atm. As there was no difference in the results obtained with both the sets incubated for 24 hrs, experiments were conducted at $4\pm 2^\circ\text{C}$, 1 atm. Microbial carbon fixation measured from $15.30 \pm 15.91 \text{ nmol g}^{-1} \text{ day}^{-1}$ in BC 34 to $5399.53 \pm 4771.85 \text{ nmol g}^{-1} \text{ day}^{-1}$ in BC 37 during austral winter sampling (Fig. 4.36A). Two major clusters separating BC 38 from the rest of the stations were observed at 40% distance. The clusters separate the most autotrophic cores core 08 and 38 from the rest of the basin. A second cluster relating cores 19, 25R3, 20 and 13 separates the next lower chemosynthetic hotspots from the relatively heterotrophic cores (Fig. 4.36B).

b. *Latitudinal and longitudinal variation*

Latitudinal variation along the north-south transect of 75.5°E fixation measured from $15.30 \pm 15.91 \text{ nmol g}^{-1} \text{ day}^{-1}$ in BC 34 to $696.39 \pm 592.21 \text{ nmol g}^{-1} \text{ day}^{-1}$ in TVBC 08. The longitudinal variation along 13°S showed highest fixation at the central TVBC 19 at $105.93 \text{ nmol g}^{-1} \text{ day}^{-1}$ (Fig. 4.36C and 4.36D).

c. *Down-core variation*

Down-core variations show the prominent mid-depth maxima in most cores. The highest mid-depth maxima values are those of TVBC 08 at 16°S up to $1596.5 \text{ nmol g}^{-1} \text{ day}^{-1}$ (Fig. 4.36 E).

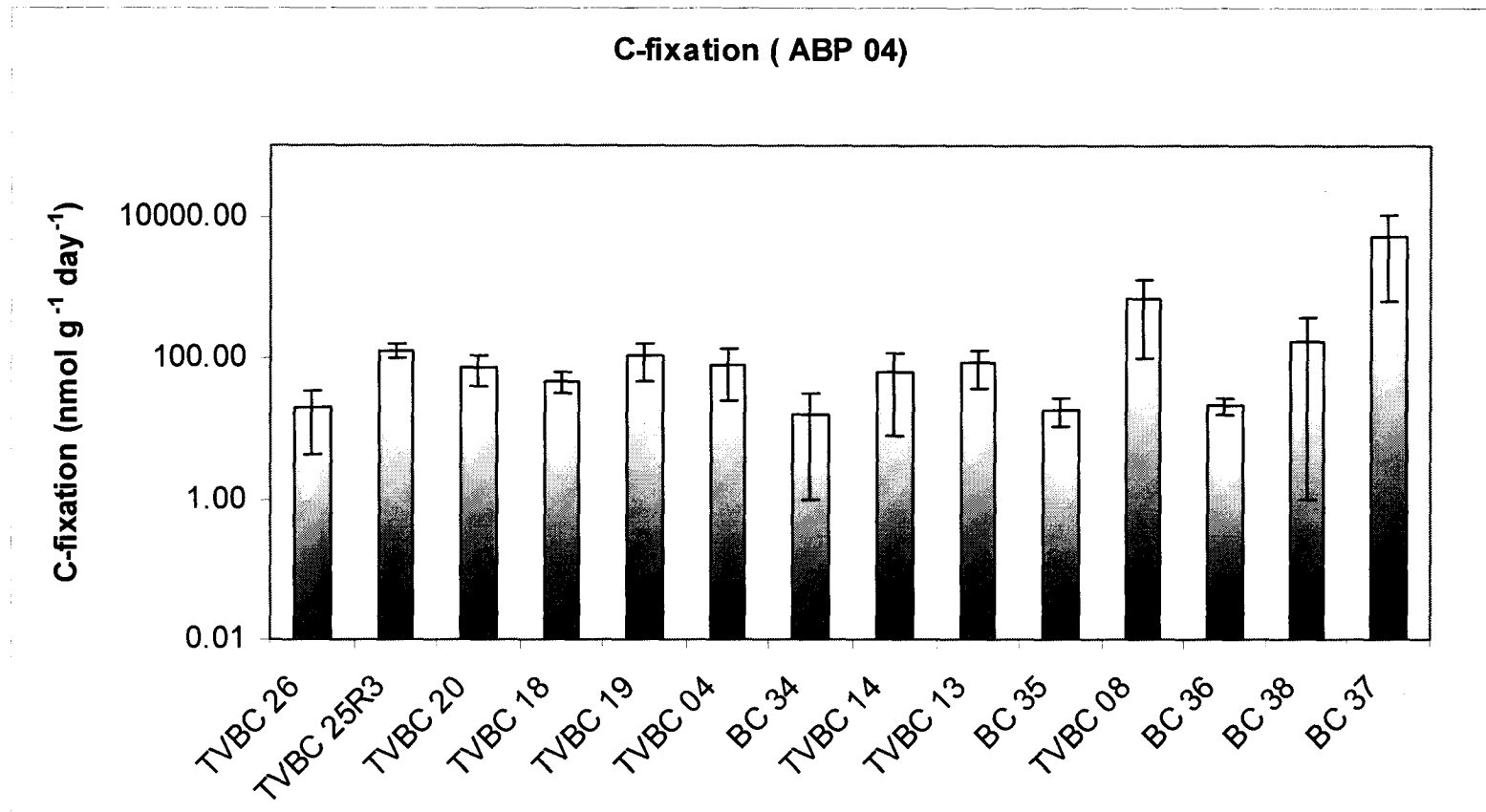


Fig. 4. 36A Carbon fixation by CIOB sediments during austral winter sampling (ABP-04)

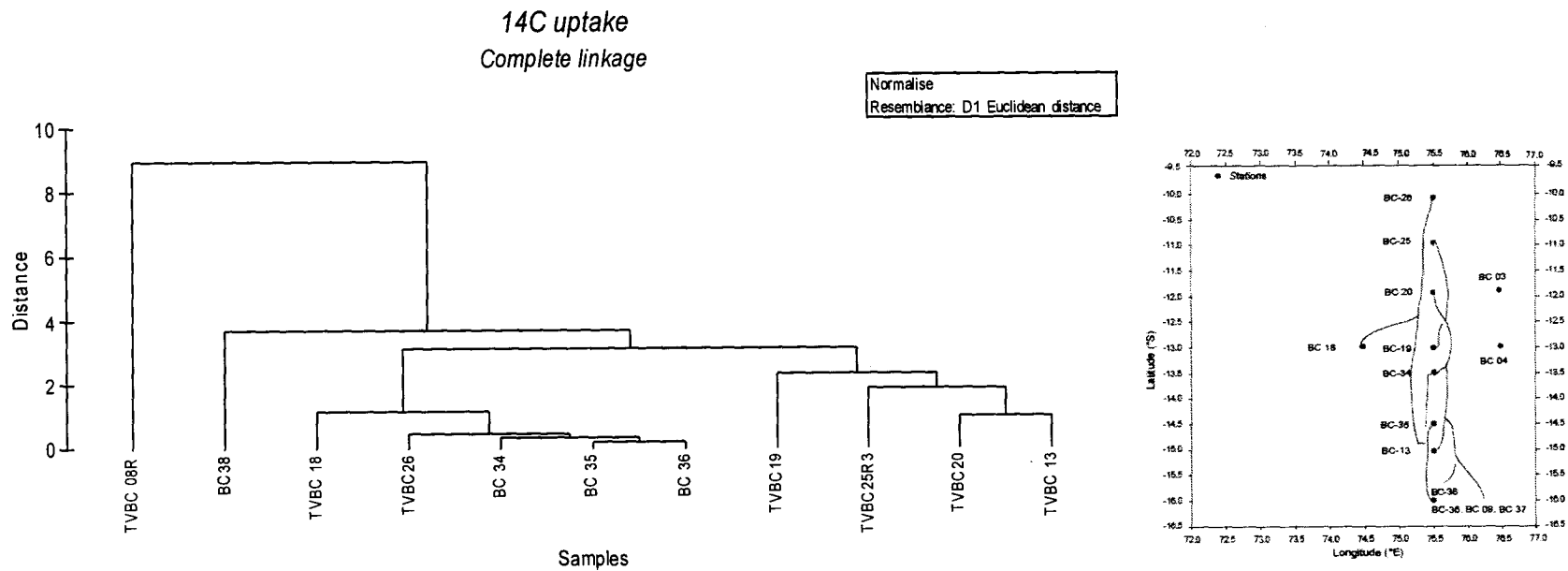


Fig. 4.36 .B Cluster analysis of CIOB stations based on microbial carbon uptake during austral winter sampling (ABP-04).

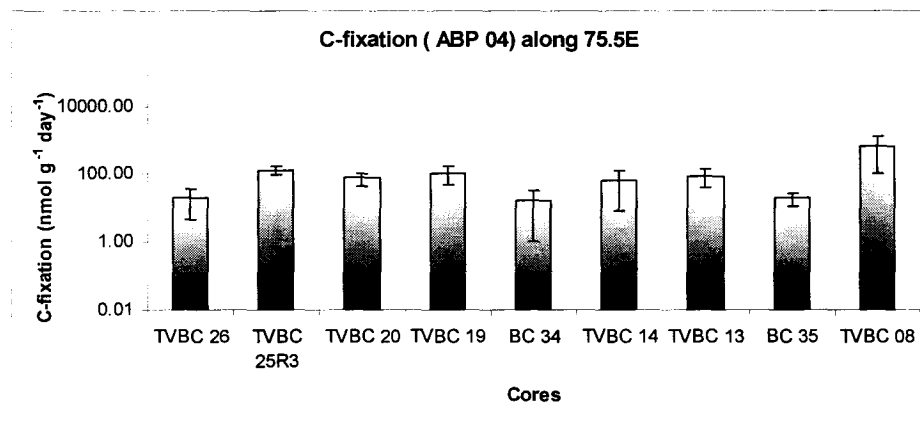


Fig. 4.36.C Microbial carbon fixation along cores of 75.5°E during austral winter sampling (ABP-04).

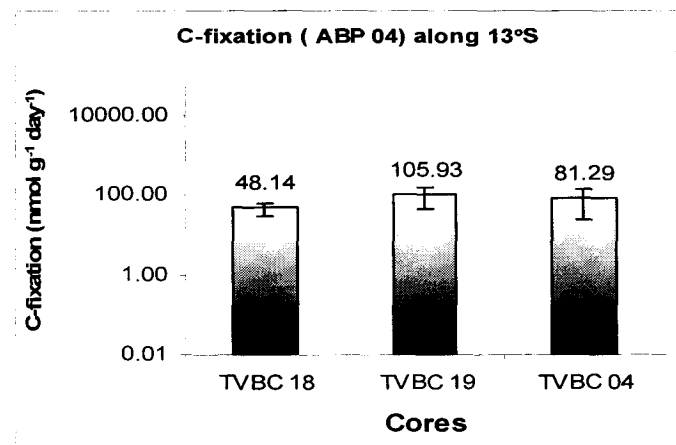


Fig. 4.36.D Microbial carbon fixation along cores of 13°S during austral winter sampling (ABP-04).

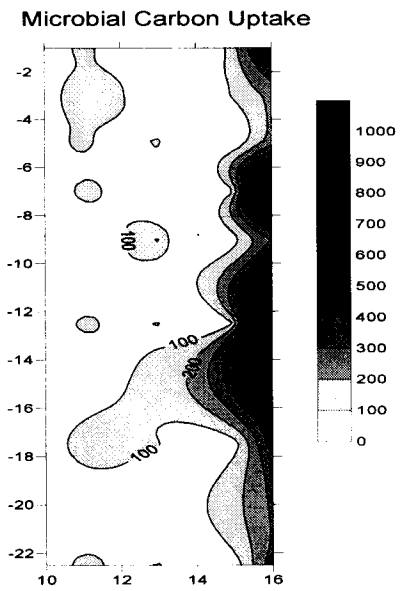


Fig. 4.36 .E Down-core variation of microbial carbon uptake ($\text{nmol g}^{-1} \text{day}^{-1}$) showing mid-depth hot-spots along 75.5°E during austral winter sampling (ABP-04).

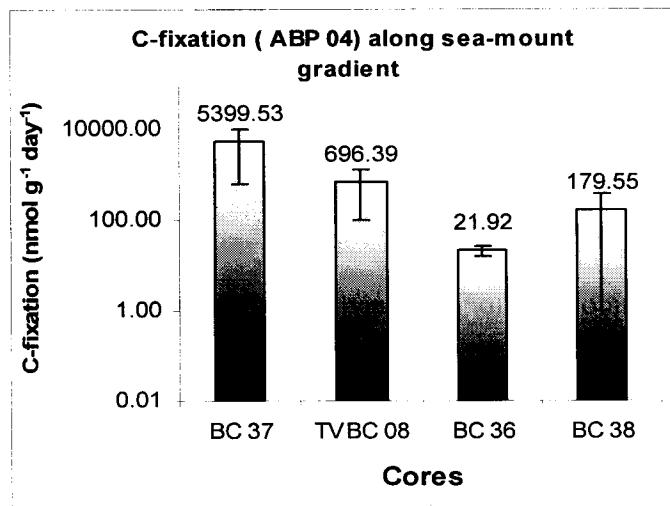


Fig. 4.36 .F Microbial carbon uptake along the slope of seamount with volcanic alterations at 16°S

d. Variation along sea-mount slope

Along the slope of the seamount at 16°S, highest carbon fixation was at the seamount summit. The calcareous ooze of the summit fixed 5399.53 ± 4771.85 nmol $\text{g}^{-1} \text{day}^{-1}$. The lowest of 21.92 ± 5.57 nmol $\text{g}^{-1} \text{day}^{-1}$ was recorded at the pelagic red clay of BC 36 at the plateau of the seamount (Fig. 4.36F).

e. Seasonal variation

A marked seasonal variation is observed between austral winter (ABP-04) and austral summer (ABP-26) samplings. A 75-99% increase in carbon fixation was observed in the carbon fixation during austral summer in cores 13, 04, 35 and 36 while 19% and 147% decrease was observed for cores 38 and 37 respectively (Fig. 4.36G).

f. Variation in fractions of calcareous core 37

Gravimetrically fractioned calcareous core fixed $4,627.65 \pm 2,087.05$ nmol $\text{g}^{-1} \text{day}^{-1}$ in its clay fraction. The carbonate fraction fixed $3,143.35 \pm 1,538.60$ nmol $\text{g}^{-1} \text{day}^{-1}$ of carbon. The whole sediments fixed $2,184.68 \pm 790.46$ nmol $\text{g}^{-1} \text{day}^{-1}$. It appears that the calcareous ooze masked the uptake by its clay component when measurements were made with intact whole sediments (Fig. 4.36H).

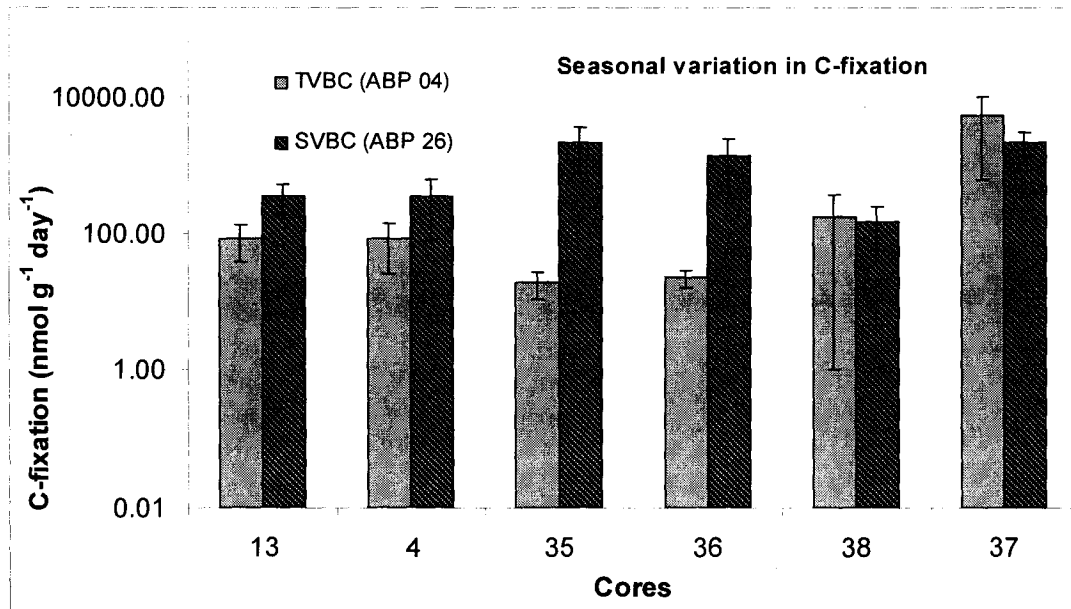


Fig. 4.36 .G Seasonal variation in microbial carbon uptake during TVBC and SVBC samplings.

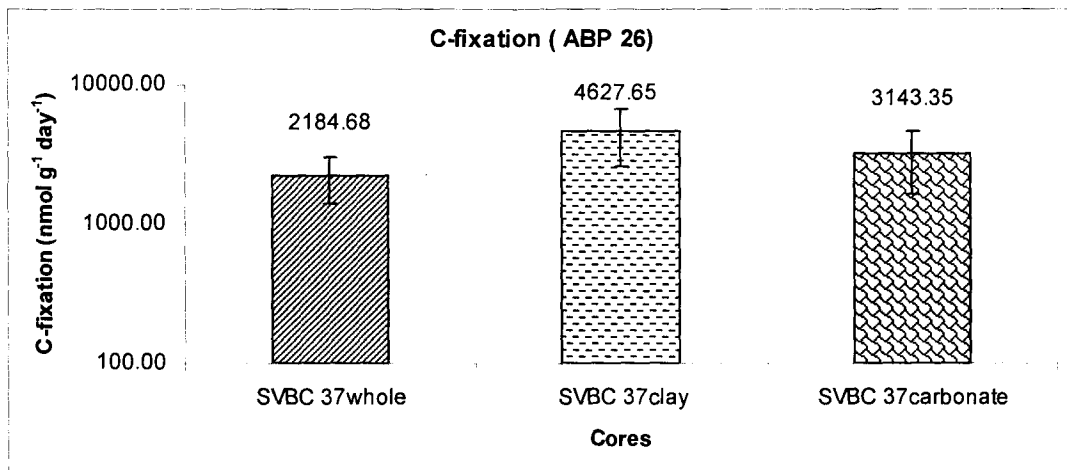


Fig. 4.36 .H Variation in microbial carbon uptake in different fractions of calcareous core 37

g. *Isolates*

i. *Carbon fixation in presence of reduced nitrogen species*

TDLO culture CIOB 25A was used to study carbon fixation in the presence of ammonium and nitrite under aerobic and microaerophilic conditions at $5^{\circ}\pm 2^{\circ}\text{C}$. 2mM final concentration of ammonium sulphate and 0.5mM of nitrite was used for this experiment as was done previously by Ram *et al.*, 2001. Under aerobic condition the carbon fixation increased from $3.60\text{E-}05$ at 0 hr to $5.17\text{E-}05$ nmol C cell⁻¹ after 192 hrs in presence of ammonium. The rate increased from $4.06\text{E-}05$ to $5.62\text{E-}05$ nmol C cell⁻¹ in presence of nitrite during the same time. The fixation rate measured was $8.18\text{E-}08$ nmol C cell⁻¹ hr⁻¹ in presence of ammonium and $8.10\text{E-}08$ nmol C cell⁻¹ hr⁻¹ with nitrite. The results indicate that fixation of carbon can occur in the presence of all the nitrogen sources supplied.

Under microaerophilic condition, the carbon fixation rate increased from $3.96\text{E-}05$ to $1.52\text{E-}04$ nmol C cell⁻¹ in presence of ammonium. The rate increased from $4.42\text{E-}05$ to $1.11\text{E-}04$ nmol C cell⁻¹ in presence of nitrite during the same time. The fixation rate measured was $5.85\text{E-}07$ nmol C cell⁻¹ hr⁻¹ in presence of ammonium and $3.48\text{E-}07$ nmol C cell⁻¹ hr⁻¹ with nitrite (Fig. 4.37).

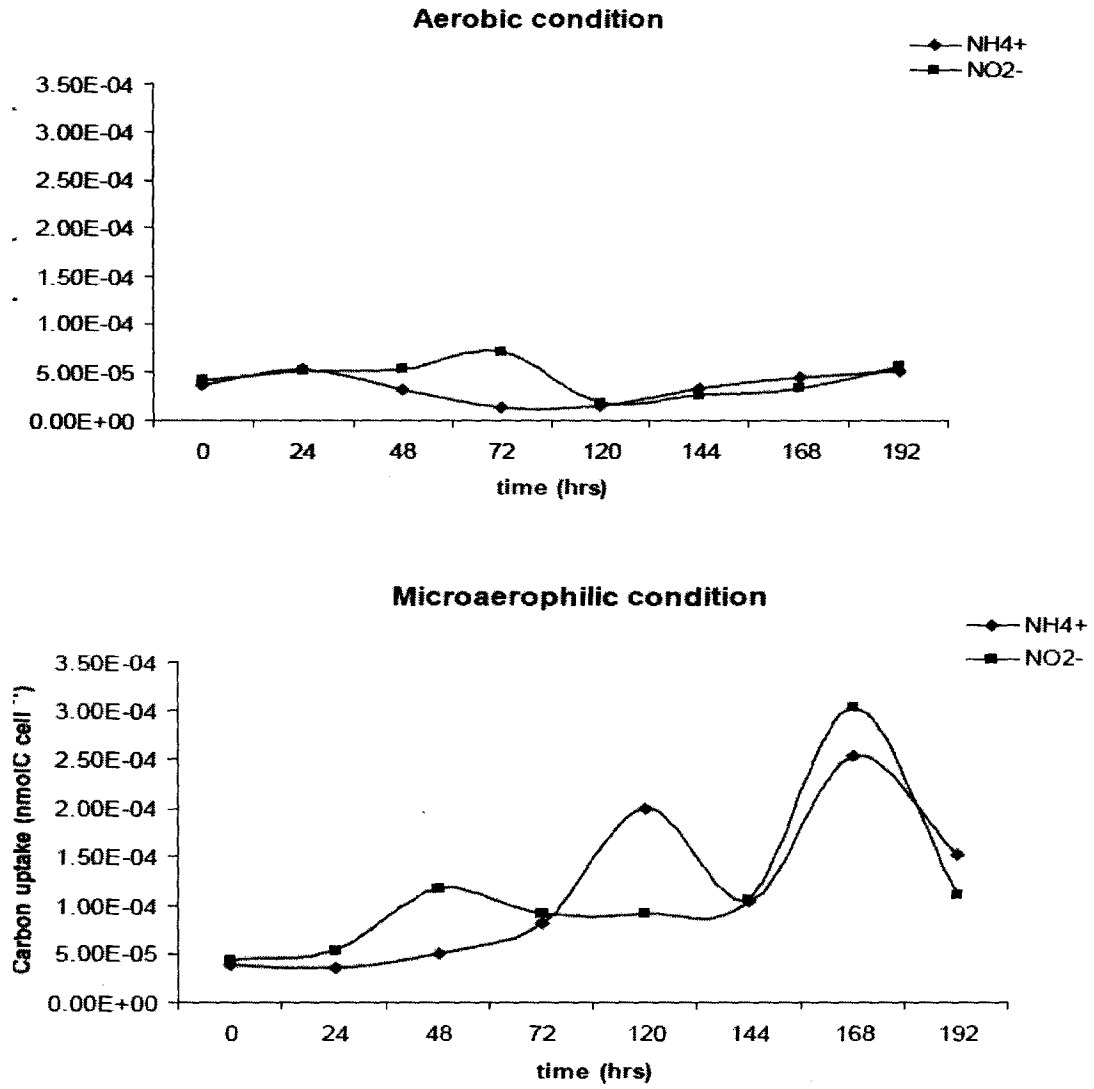


Fig. 4.37 Carbon fixation in presence of reduced nitrogen species

A. Aerobic condition B. Microaerophilic condition

ii. *Carbon fixation and C-1 compound utilization in cultures*

Experiments with some of the deep sea isolates confirm their ability to use C-1 compounds like HCHO albeit at different concentrations. Some of these could fix $\text{NaH}^{14}\text{CO}_3$, while still others could express RuBisCO better than other isolates. More importantly, these rates were better at $5\pm 2^\circ\text{C}$ than at $25\pm 2^\circ\text{C}$. Among the deep-sea cultures, the highest autotrophic carbon fixation of $8.47 \text{ fmol cell}^{-1}\text{hr}^{-1}$ was exhibited by culture E7. Highest RuBisCO activity was shown by culture E5 at $693 \text{ nmol CO}_2 \text{ fixed min}^{-1}\text{mg}^{-1} \text{ protein}$. Highest HCHO utilization was shown by culture E9 at $44.3 \text{E fmol cell}^{-1}\text{hr}^{-1}$ (Table 4.8).

4.6.4 RuBisCO enzyme activity

a. *Whole sediments*

RuBisCO enzyme activity varied from 8.60 to $26.82 \text{ nmol min}^{-1}\text{mg protein}^{-1}$ in siliceous ooze core SVBC 26 with activity progressively decreasing down the core. The activity varied from 6.83 to $37.77 \text{ nmol min}^{-1}\text{mg protein}^{-1}$ in pelagic red clay SVBC 36 with activity progressively increasing down the core. The highest value was observed at 22.5 cm bsf . In the calcareous ooze core SVBC 37, the activity ranged from 16.08 to $10,588.94 \text{ nmol min}^{-1}\text{mg protein}^{-1}$ with activity progressively increasing down the core. After fractionating into clay and carbonates the activity yielded surprising results. In clay, the activity ranged from 0.033 to $131.37 \text{ } \mu\text{mol min}^{-1}\text{mg protein}^{-1}$ with values increasing down the core (Fig. 4.38 A and B).

Table 4.8 Carbon fixation, RuBisCO activity and HCHO utilization at 5°C on 288 hrs of incubation. Concentration of formaldehyde used for the experiment is 2000 ppm.

Isolates	Autotrophic uptake of ^{14}C ($\text{fmol cell}^{-1}\text{hr}^{-1}$)	RuBisCO ($\text{nmol CO}_2 \text{ fixed min}^{-1} \text{mg}^{-1} \text{ protein}$)	HCHO utilization ($\text{fmol cell}^{-1} \text{hr}^{-1}$)
C	5.32E-06	1.74E+03	7.80E-01
E1	7.83E-01	3.13E+02	3.47E+01
E2	not detectable	2.452E+03	3.50E+01
E3	2.82E+00	not detectable	1.06E+02
E4	5.55E+00	not detectable	2.67E+00
E5	3.17E+00	6.93E+02	2.07E+01
E6	5.11E-01	4.91E+01	3.70E+01
E7	8.47E+00	1.60E+02	3.40E+01
E8	4.79E+00	1.71E+02	3.47E+01
E9	2.91E+00	4.67E+02	4.43E+01

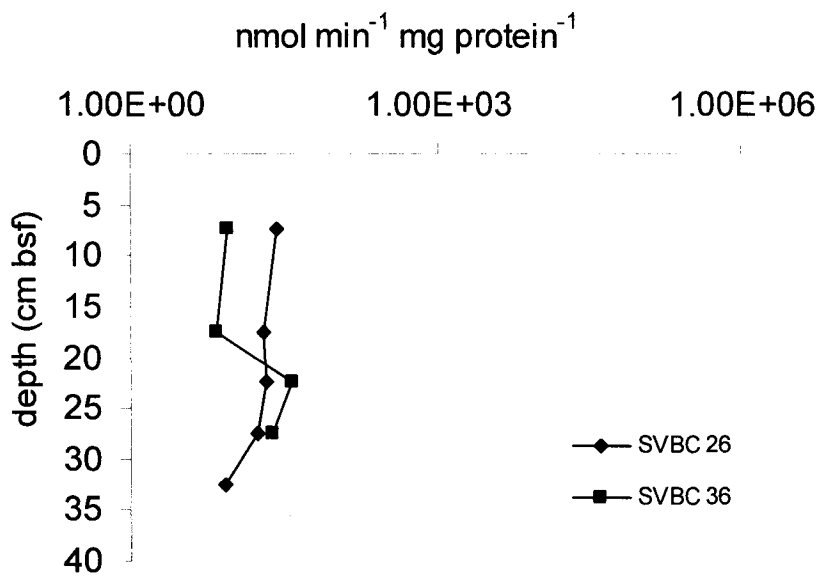


Fig. 4.38A. RuBisCO activity in siliceous core SVBC 26 and pelagic red clay SVBC 36.

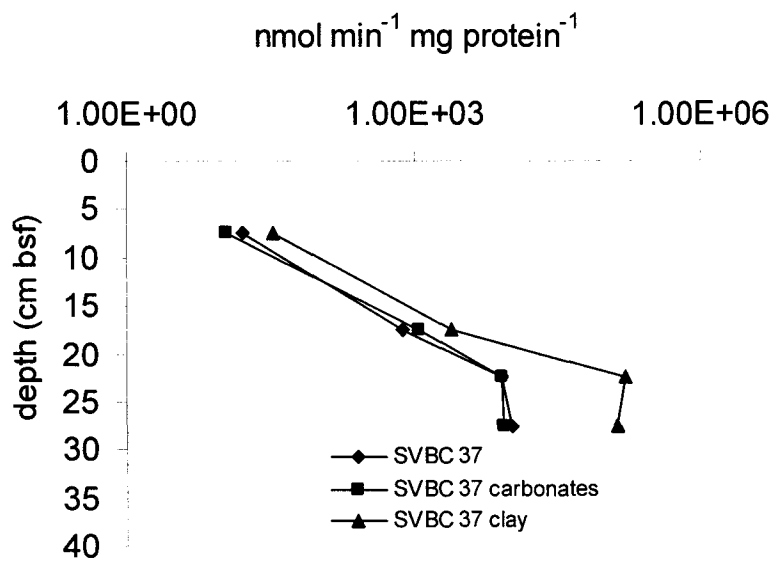


Fig. 4.38B. RuBisCO activity in whole and fractions of calcareous ooze SVBC 37

b. *Isolates*

RuBisCO enzyme activity in cultured isolates varied from not detectable levels to 68.1 nmol min⁻¹mg protein⁻¹ at 25°C and from not detectable to 693 nmol min⁻¹mg protein⁻¹ at 5°C (Fig. 4.39).

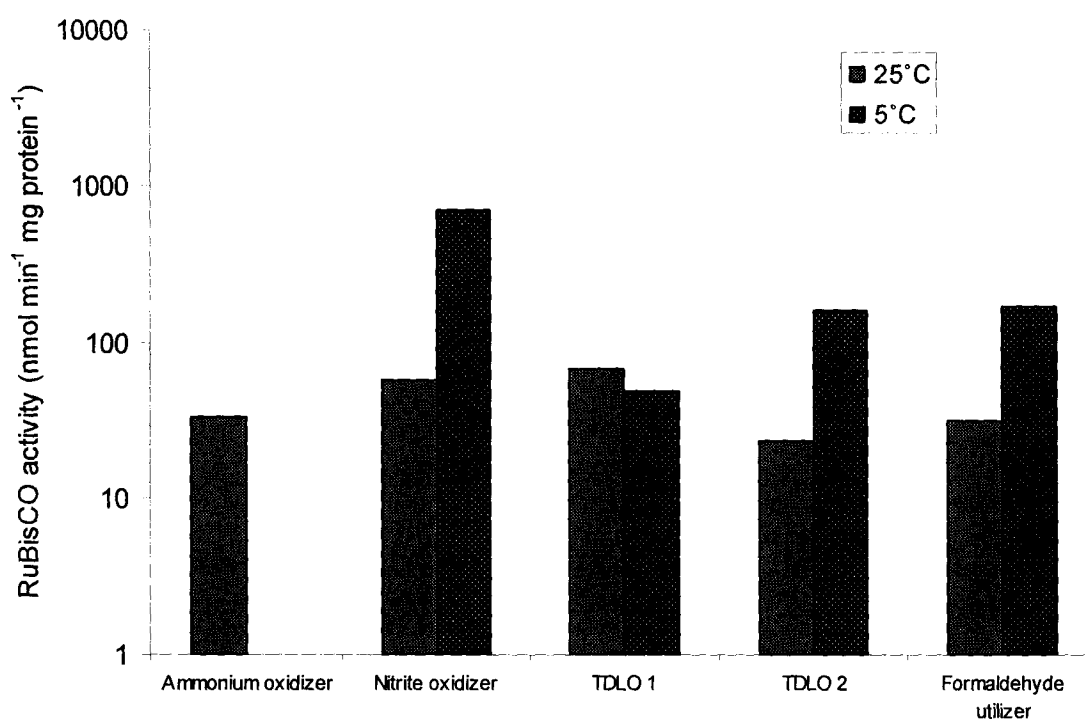


Fig. 4.39 RuBisCO activity in cultures at 25°C and 5°C.

4.6.5 *Phosphatase activity*

The CIOB was divided into northern and southern cluster based on the pore-water phosphate concentrations (Fig. 4.40). Phosphatase activity was checked in relation to pore water phosphate. Enzyme activity was observed in all the 20 cores (Fig. 4.41A). The average phosphatase activity in the northern cluster was $0.23 \pm 0.19 \mu\text{mol g}^{-1} \text{h}^{-1}$ and in the

southern it was $0.21 \pm 0.28 \mu\text{mol g}^{-1} \text{h}^{-1}$. Standard deviations in the down-core values were high (Fig. 4.41A). Depth averaged spatial distribution of alkaline phosphatase activity showed two peaks at 11°S and 14.5°S along 75.5°E (Fig.. 4.42).

Pore water phosphate ranged from $0.9\text{-}4\mu\text{M}$ and $0.2\text{-}1.4\mu\text{mol}$ in the north and south respectively. Likewise, ALP was higher and ranged from $0.3\text{-}700 \text{ nmol g}^{-1} \text{h}^{-1}$ in the north, and $0.2\text{-}400 \text{ nmol g}^{-1} \text{h}^{-1}$ in the south. Pore water phosphate and ALP activity were positively related with an r-value 0.44 ($n=43$) in the north and an r-value of 0.41 ($n=46$) in south at $p<0.01$. Both phosphate and phosphatase relate negatively with total count of bacteria (TC).

Response of hyperbaric condition on alkaline phosphatase activity was different for two different sediments of core 20A and 18C. In core 20A there was no significant difference on the activity under 4°C , 500 bars In the case of core 18C however, the activity declined by 2 orders after 7 and 15 days of incubation under the above conditions (Fig. 4.41B).

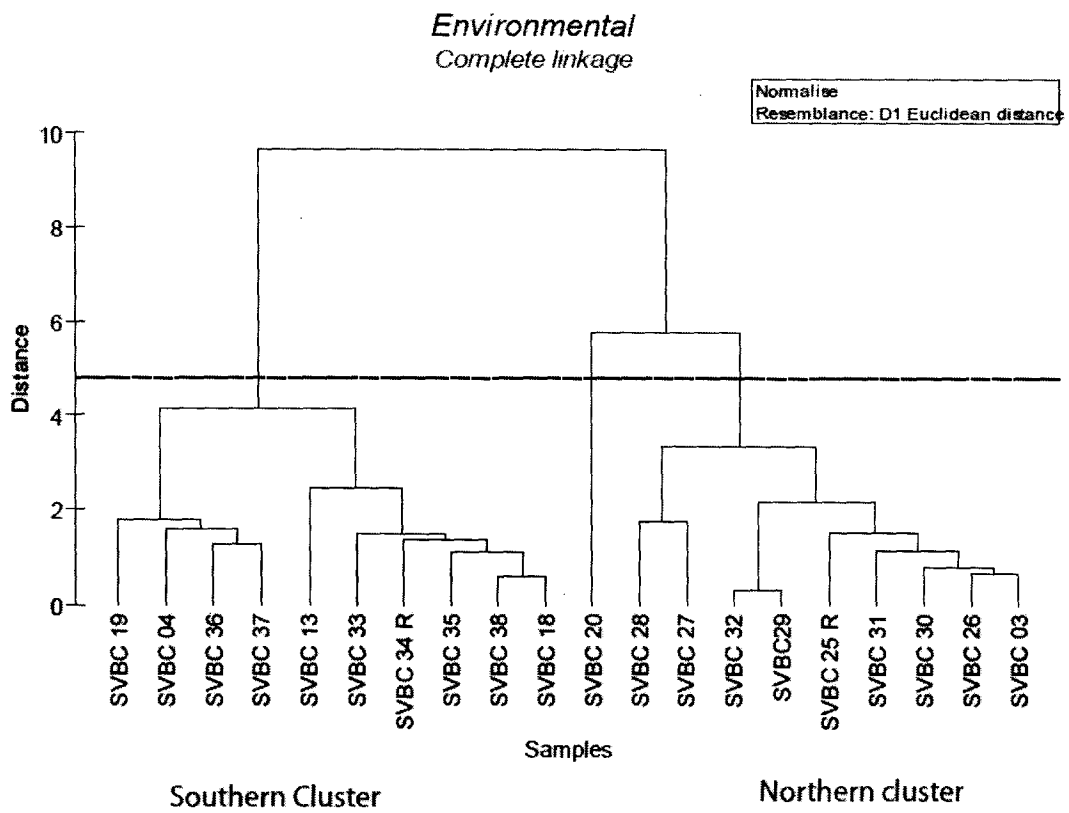


Fig. 4.40 Cluster analysis of CIOB stations based on pore-water phosphate.

(Data courtesy to Dr. B.N.Nath and M.B.L. Mascarenhas Pereira , NIO, Goa)

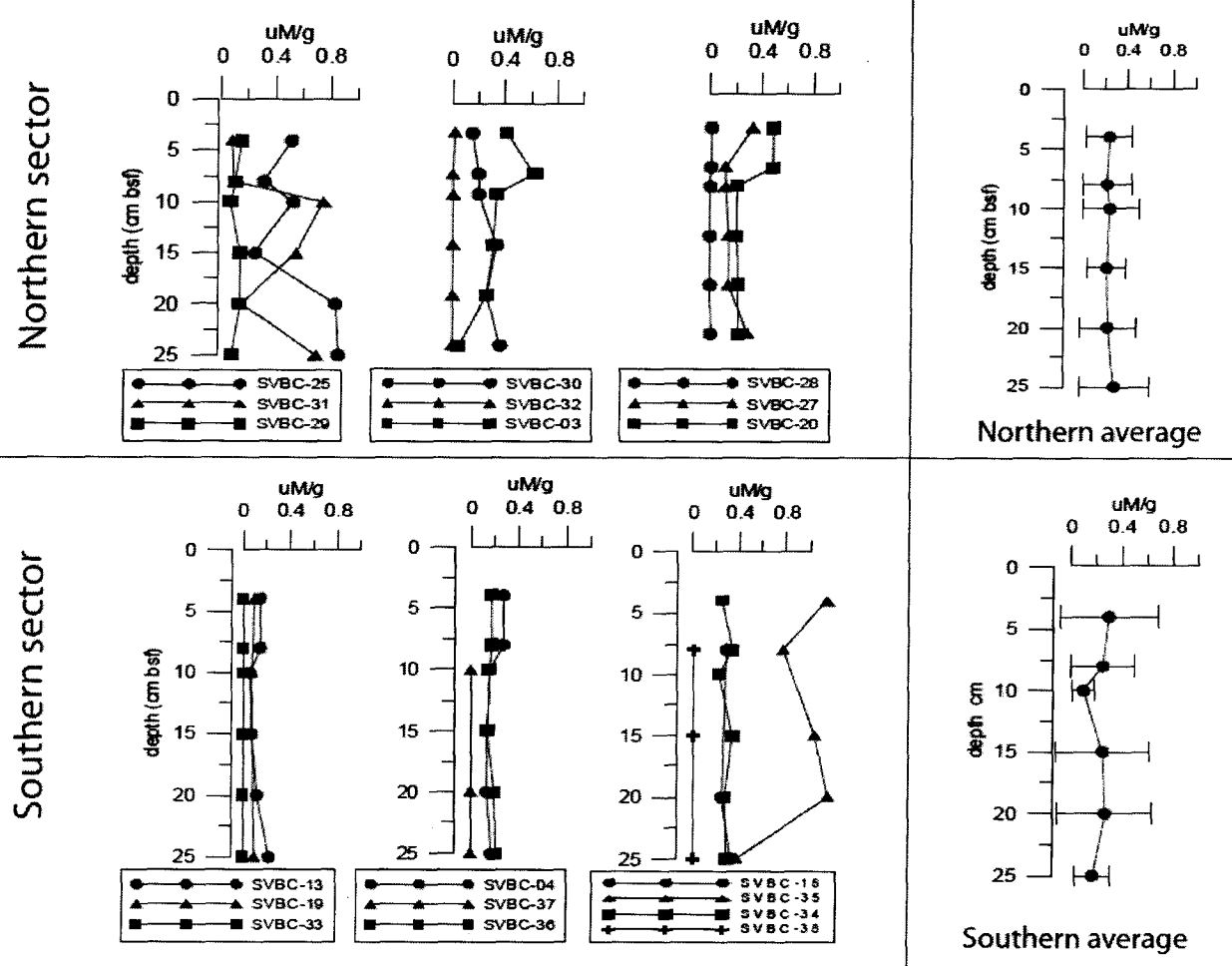


Fig. 4.41A Alkaline phosphatase activity in CIOB sediments.

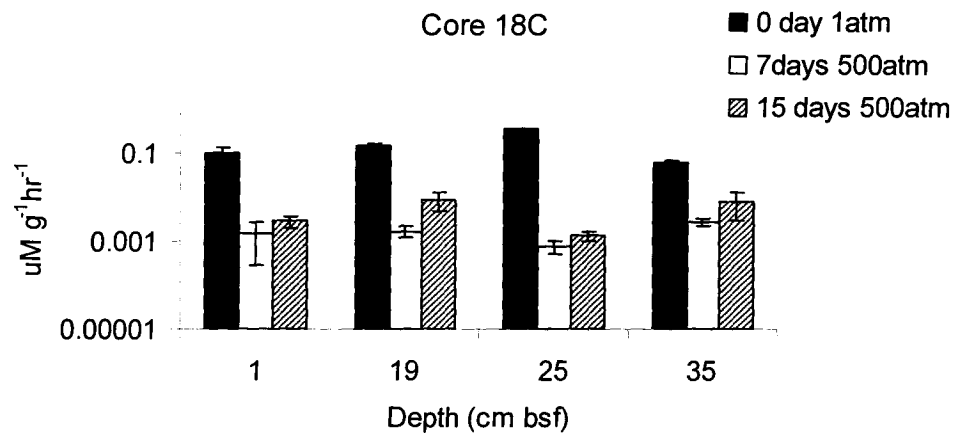
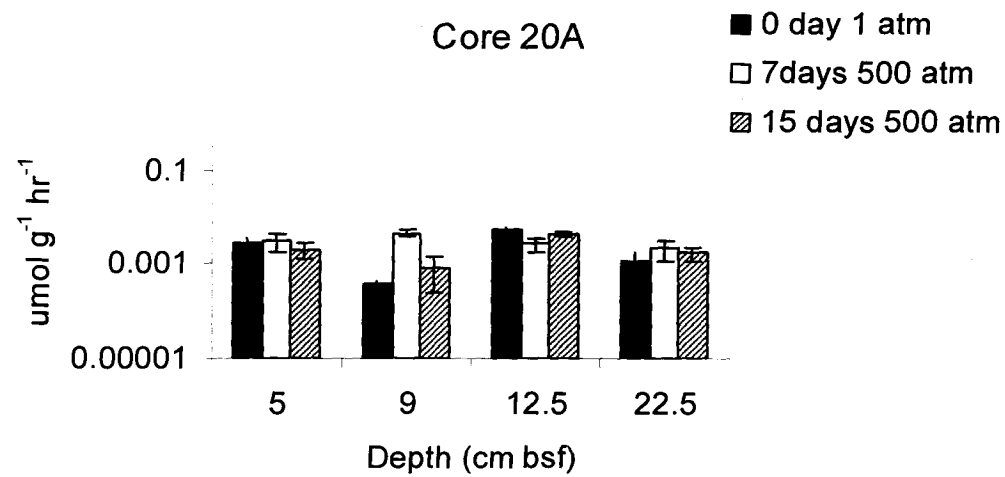


Fig. 4.41B Alkaline phosphatase activity in CIOB sediments under 1atm and 500atm pressure.

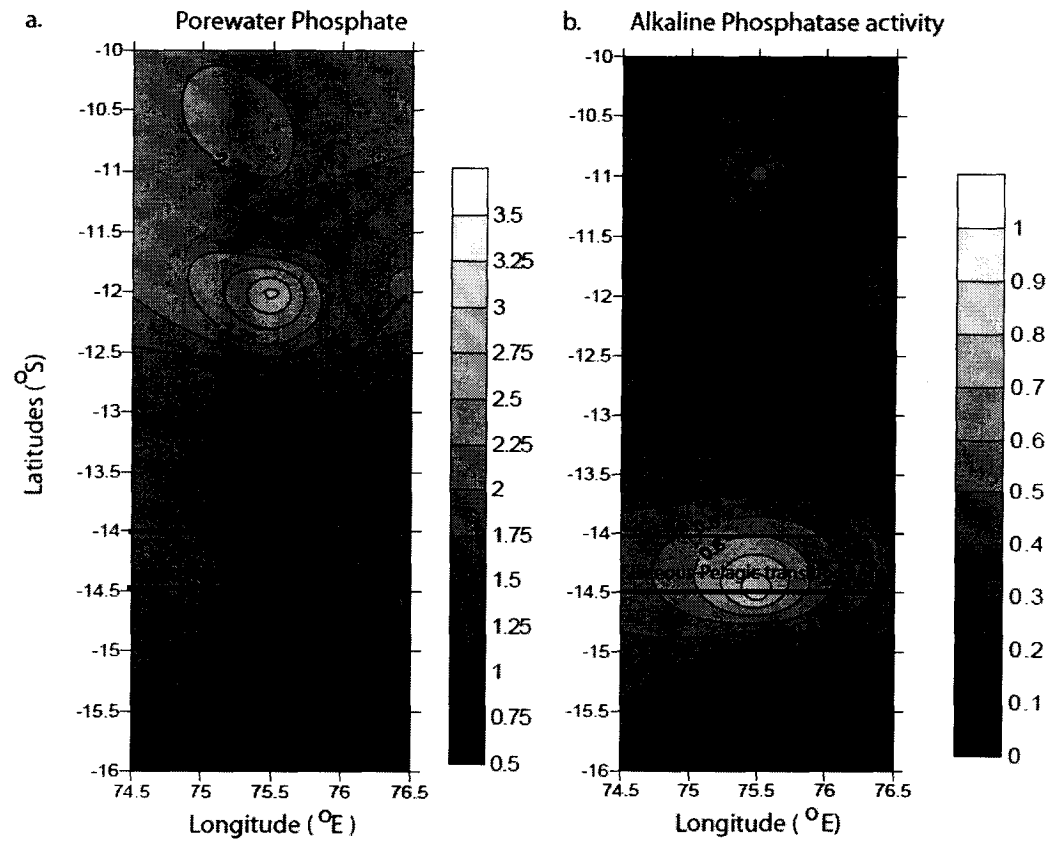


Fig. 4.42 Spatial distribution of a. pore water phosphate and b. alkaline phosphatase activity.

4.7 Elemental Carbon, Biochemistry and Microbiology of Nodule and associated sediments

4.7.1 Total organic carbon (TOC), TIC and C/N ratio

TOC ranged from 0.07-0.41% in the nodule and associated sediments. In both surface and buried nodules, maximum TOC was detected at the nodule surface with an order decline towards the interior. The TOC of the associated sediments of both surface and buried nodules were 0.1% lower than the nodule surface. TIC was non detectable. Nitrogen depletion up to non-detectable levels was noted at the nodule surface and associated sediments of both surface and buried nodules. There was large variation in C/N ratios ranging from non-detectable to infinite values. Depletion in nitrogen was noted in the SN4 layer of surface nodule (SN 147) (Fig. 4.43).

4.7.2 Labile organic matter (LOM)

Proteins varied from 0.01-0.40 mg g⁻¹ dry weight in the surface nodule (SN 147) and its associated sediment with proteins declining from nodule surface to interior. The associated sediment of SN 147 was 0.13 mg g⁻¹ lower than nodule surface. Carbohydrates measured 0.05-0.20 mg g⁻¹ and declined from surface to interior of nodule with highest value at the nodule surface. Lipids formed the major component of LOM in the surface nodule with values ranging 0.35-0.79 mg g⁻¹ (Fig. 4.43).

Proteins varied from ndl -0.15 mg g⁻¹ dry weight in the buried nodule (BN 142) and its associated sediment with proteins declining from nodule surface to the core. Carbohydrates measured 0.03-0.17 mg g⁻¹ and declined from surface to interior of nodule with highest value at the nodule surface. Lipids again formed the major component of

LOM in the buried nodule with values ranging 0.35-0.38 mg g⁻¹ (Fig. 4.43). This feature of the LOM of nodule is strikingly different from the associated sediments and generally the entire nodule bearing sediments of CIOB, where lipids form the smallest fraction of LOM.

4.7.3 Adenosine Triphosphate (ATP)

ATP varied from 900 to 9000 ng g⁻¹ dry weight in the surface nodule (SN 147) and its associated sediment with lowest at the associated sediments and highest in the layer SN3. In the buried nodule BN 142, ATP varied from 250-8500 ng g⁻¹ dry weight with lowest at the topmost BN1 and highest in BN3 (Fig. 4.43).

4.7.4 Bacterial counts

a. Total counts of bacteria

Total bacterial cells in both the nodule and associated sediment system varied from 10⁶-10⁸ cells g⁻¹ with total absence of coccoidal cells. The cells picking up green monomer of acridine orange dominated the total counts of the buried nodule BN 142 while green and orange cells were almost equally abundant in the total bacteria of surface nodule (SN 147) (Fig. 4.44).

b. *Frequency of dividing cells (FDC)*

FDC varied from 10^5 - 10^8 cells g^{-1} in surface nodule SN 147, while in buried nodule BN 142 it varied from 10^6 - 10^7 cells g^{-1} (Fig.4.44).

c. *Autofluorescent F_{420} cells*

Autofluorescent F_{420} cells ranging from 10^5 - 10^6 cells g^{-1} were recorded in all layers of the surface nodule SN 147. In buried nodule BN 142, they were detected up to 10^6 cells g^{-1} only in the two innermost layers BN3 and BN4. Autofluorescent F_{420} cells were notably absent in the associated sediments of both the nodule types (Fig. 4.44)

d. *Direct Viable Counts (DVC)*

In the surface nodule SN 147, direct viable counts under aerobic conditions ranged from 10^5 - 10^7 cells g^{-1} with lowest counts at the layer SN2 and highest at SN1. The direct viable counts under anaerobic conditions ranged from 10^5 - 10^8 cells g^{-1} with lowest counts again at the layer SN2 and highest at SN1. The anaerobic counts were marginally higher than the aerobic, in the surface nodule (Fig. 4.44).

In the buried nodule BN 142 direct viable counts under aerobic conditions ranged from 10^4 - 10^7 cells g^{-1} with lowest counts at the layer BN1 and highest at BN4. The direct viable counts under anaerobic conditions ranged from 10^4 - 10^7 cells g^{-1} with lowest counts again at the layer BN1 and highest at BN3 and BN4. The anaerobic counts were almost equal the aerobic in the buried nodule (Fig. 4.44).

4.7.5 Microbial uptake of carbon in sediments and nodules

Microbial uptake of carbon varied from 92-393 nmol C g⁻¹ day⁻¹ in surface nodule SN147. Uptake by associated sediment S147 was 21 nmol C g⁻¹ day⁻¹. Highest uptake was observed in SN4. In the buried nodule BN142, microbial uptake of carbon varied from 50-450 nmol C g⁻¹ day⁻¹ with 69 nmol C g⁻¹ day⁻¹ in its associated sediment S142. Highest carbon uptake was observed in BN2 (Fig. 4.45).

4.7.6 Carbon substrate utilization by nodules and sediments

Section from nodule utilized fewer substrates than the associated sediments. While microbial population on nodules utilized carboxylic acid, lipids and amino acids, sediments utilized carboxylic acids, carbohydrates, lipids and amino acids (Table 4.9). The pink colour on the wells measured against controls indicating utilization appeared 35 days after inoculation and incubation at 4°C.

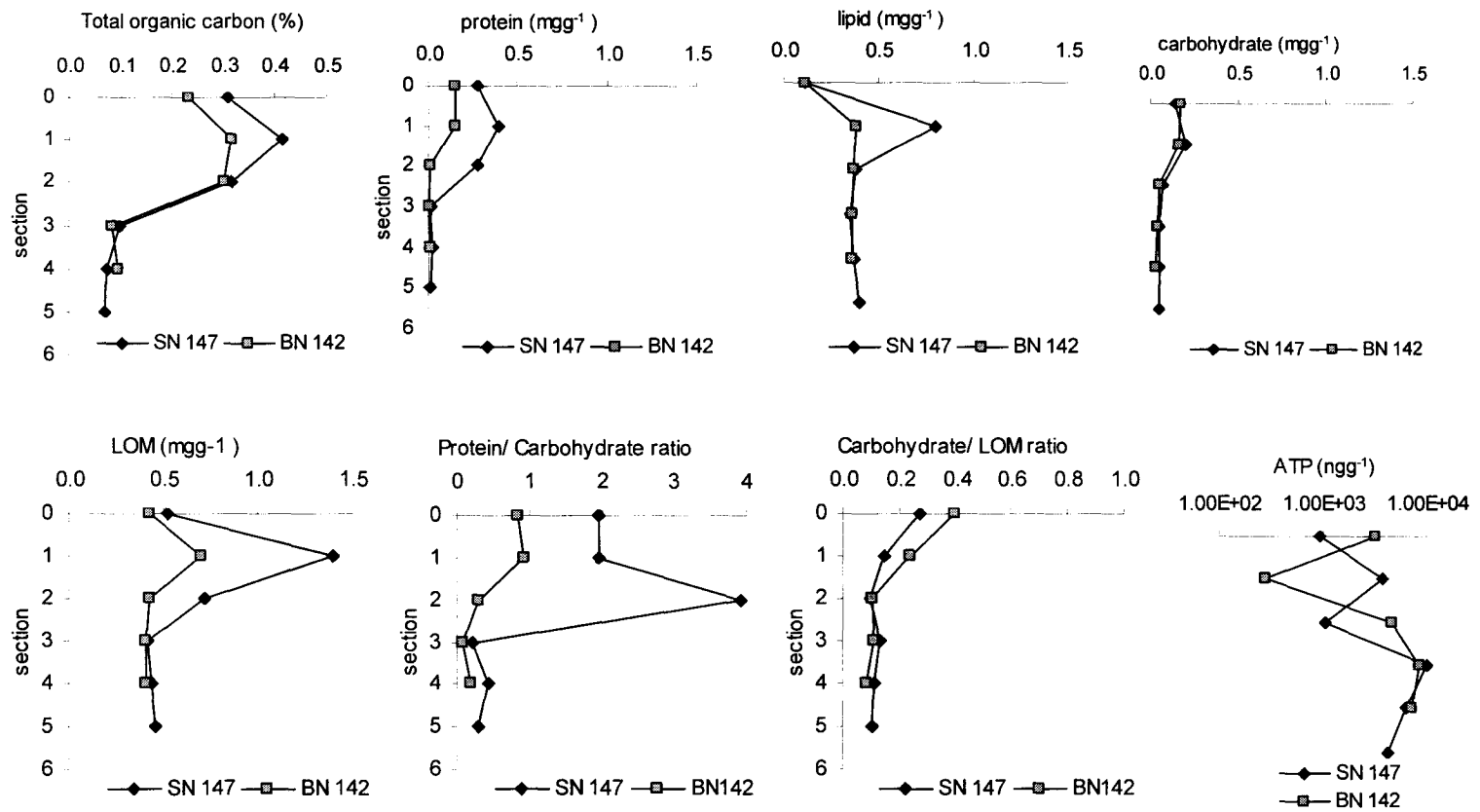


Fig. 4.43 TOC, biochemical and ATP contents in nodules and associated sediments

Fig. 4.44 Bacterial counts in nodules and associated sediments

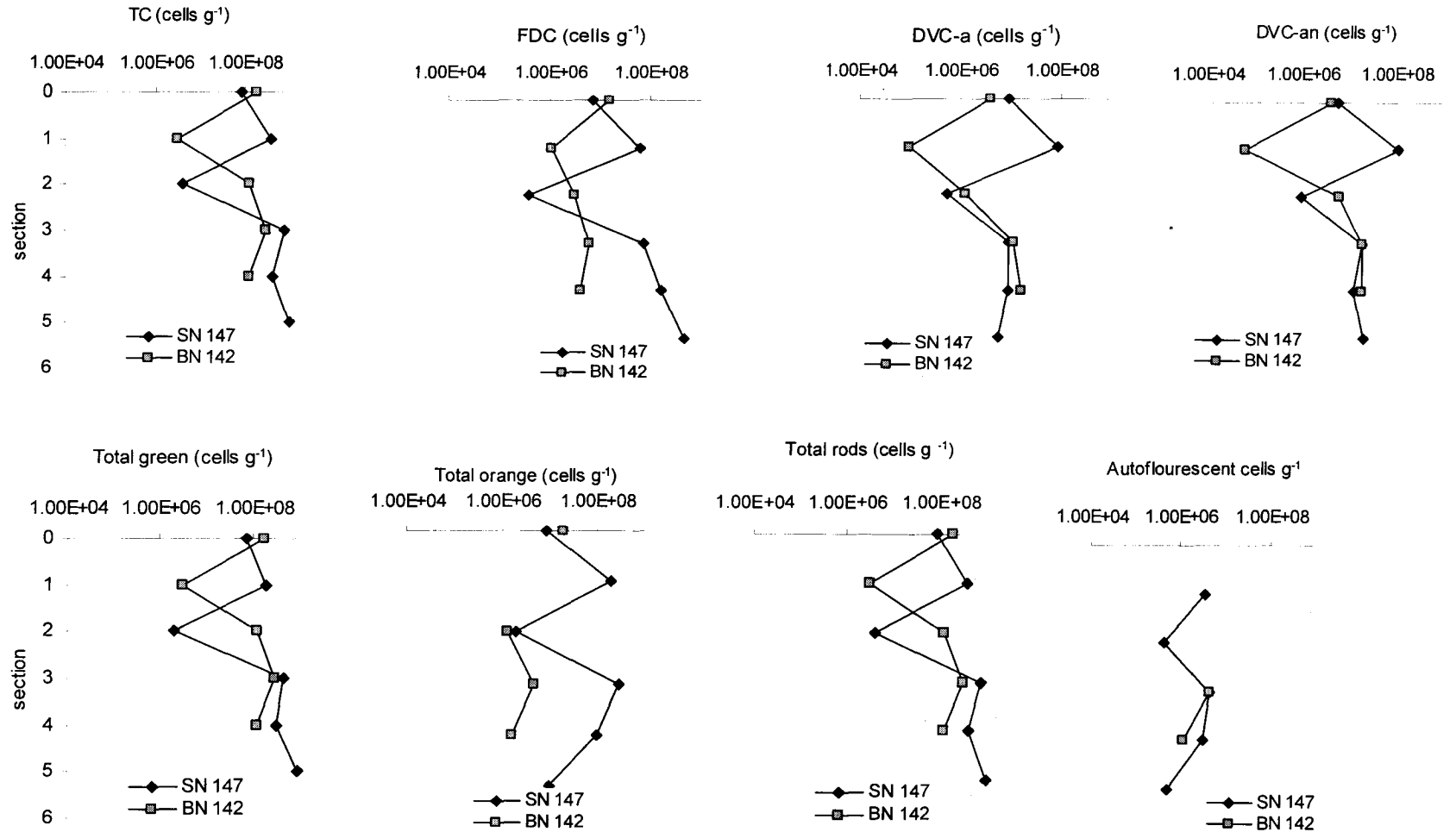
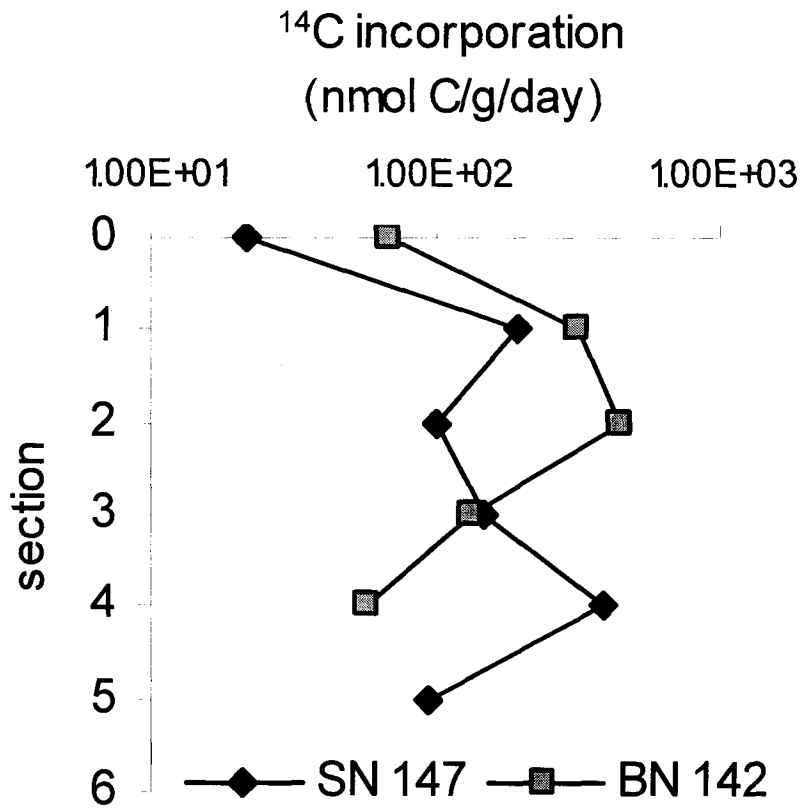


Fig.4.45 Microbial uptake of carbon in nodules and associated sediments



The nodules and their associated sediments were analysed for carbon-substrate utilization on ECO-plates. The utilization was observed after 35 days of incubation at 4°C . The nodules used lesser number of substrates than their associated sediments. The results are tabulated below:

Table 4.9. Carbon substrate utilization by nodules and associated sediments

<i>Sample type</i>	<i>Sample name</i>	<i>Substrates utilized</i>
Surface nodule		
SN 147	SN1	<i>γ hydroxybutric acid,</i> <i>L-serine</i>
	SN3	--
	SN4	--
	SN5	<i>Tween 80</i>
Associated sediment		
S1	S1	<i>Tween 40</i> <i>D-cellobiose</i> <i>D-Galacturonic acid</i> <i>D-Malic acid</i> <i>L-Arginine</i> <i>L-Phenylalanine</i> <i>L-Asperigine</i> <i>L-Serine</i> <i>L-Threonine</i>
Buried nodule		
BN 142	BN1	<i>D-Malic acid</i>
	BN2	
	BN3	<i>Tween 80</i> <i>D-Mannitol</i>
Associated sediment		
S2	S2	<i>Tween 80</i> <i>γ hydroxybutric acid</i> <i>D-Malic acid</i> <i>L-Threonine</i>

4.8 Interrelations

4.8.1 *The Siliceous oozes – Cores 26, 25, 20*

a. *Core 26*

Variation in TC accounted for 62% variation of aerobic TDLO at $p > 0.01$. ATP varied negatively with nitrite oxidizers (NII) and the denitrifiers at $p > 0.05$. The NII and denitrifiers varied positively with each other at $p > 0.05$. LOM varied negatively with Fe-oxidizers and ZMA negatively with NII at $p > 0.05$. Phosphate solubilizers related positively to silicate solubilizers at $p > 0.01$, which in turn related negatively to nitrate reducing bacteria (NRB) at $p > 0.05$.

In the principal component analysis (PCA), the first two components cumulated 53.7% of the variance (Fig. 4.46A). About 91.4% of the variation was explained by the 5 principal components (PC1 to PC5). Coefficients in the linear combinations showed TC, ^{14}C uptake, heterotrophs, aerobic TDLO and Fe-oxidizers as the prime contributors bringing in 27% variance in PC1. Along the second component ATP, phosphate solubilizers and silicate were the key contributors of variance contributing to the next 25% of variance. The highest variance was scored at depth of 8 cms bsf along the first component and at depths 4 and 6 cms bsf along the second component.

b. *Core 25*

TC varied positively with ATP, LOM and phosphate solubilizers up to 57, 44 and 53% at $p > 0.05$ respectively. TC varied negatively with Fe and Mn oxidizers up to 68 and 92% at $p > 0.01$ and $p > 0.001$ respectively. ATP varied positively with ^{14}C uptake at $p > 0.05$ and silicate solubilizers at $p > 0.001$. ATP varied negatively with NII up to 43%. LOM varied negatively with both Fe and Mn oxidizers at $p > 0.05$. Heterotrophs related negatively to aerobic TDLO and NII negatively to silicate

solubilizers at $p > 0.05$. Fe-oxidizers related positively to Mn-oxidizers up to 66%. Both of these groups related negatively to phosphate solubilizers at 58 and 51% respectively.

The first two components cumulated 54.4% of the variance. 91.2% of the variation was covered by the 5 components (Fig. 4.46A). Coefficients in the linear combinations showed TC, Mn oxidizers, ^{14}C uptake, LOM and Fe-oxidizers contributed to variation along the first component. ^{14}C , heterotrophs, nitrite oxidizers, aerobic TDLO and denitrifiers contributed to variation along the second component with a cut off value above 0.3. The highest variation was scored at depths 2,4,10 and 25 cms bsf along the first component and at depth 20 cms bsf for the second component.

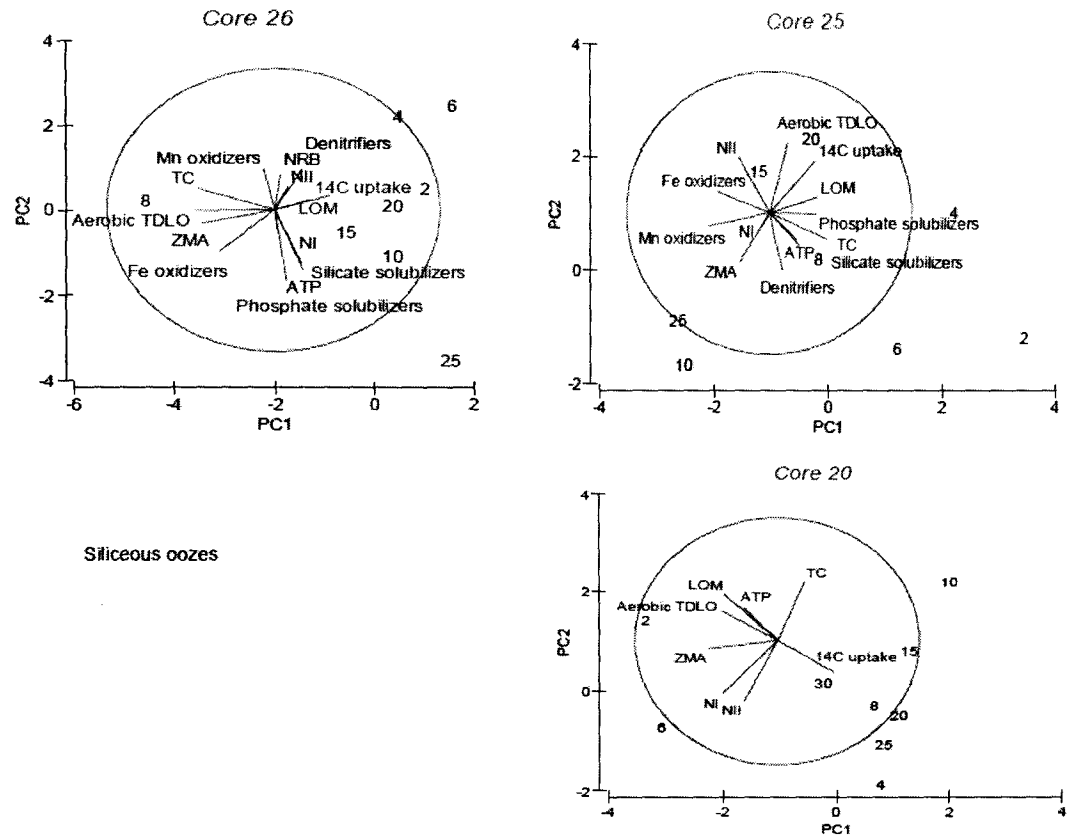
c. Core 20

Variation in LOM affected ^{14}C uptake negatively up to 79% at $p > 0.01$. Heterotrophs related positively to ammonium oxidizers (NI) and aerobic TDLO and were responsible for the variation representing 81 and 65%. There was a 51% overlap between NI and NII ($p > 0.05$).

The first two components accounted for 66.6% of the cumulative variance. 95.9% of the variation was covered by the 5 components (Fig. 4.46A). Coefficients in the linear combinations showed ^{14}C uptake, LOM, heterotrophs, ammonium oxidizers and aerobic TDLO as prime contributors to the variation with a cut off value above 0.3. Along the second principal component TC, LOM and the two nitrifier groups were the important contributors. The variations scored highest at depths 2 and 6 cms bsf along the first component and 4 and 10 cms bsf for the second component.

The difference in relationship patterns is obvious from the two-dimensional PCA diagrams indicating that the cause of variations and heterogeneity is different for

different cores of the northern siliceous oozes (Fig 4.46A and C). The carbon fixation in core 26 is closely related to nitrifiers while that of core 25 to aerobic TDLO. Further examination of the cores depthwise, show that, in the north, ^{14}C uptake is highest at the depths harbouring the diagenetic reactive layers and the tan-green mottled zone at the expense of nitrifiers I and II (Fig 3 Das *et al.*, 2010).



Eigenvectors Core 26

(Coefficients in the linear combinations of variables making up PC's)

Variable	PC1	PC2	PC3	PC4	PC5
TC	-0.461	0.150	0.068	-0.131	0.000
ATP	0.172	-0.429	0.271	-0.105	0.066
^{14}C uptake	0.333	0.099	0.009	-0.434	0.371
LOM	0.220	0.071	0.468	-0.020	-0.204
ZMA	-0.438	-0.097	0.126	-0.294	-0.054
NI	0.019	-0.172	-0.397	0.373	0.282
NII	0.082	0.164	-0.523	0.007	-0.217
Aerobic TDLO	-0.474	-0.005	0.072	-0.236	-0.074
Fe oxidizers	-0.334	-0.297	-0.192	0.027	0.285
Mn oxidizers	-0.065	0.293	-0.145	-0.253	0.527
Phosphate solubilizers	0.072	-0.505	-0.084	-0.119	0.070
Silicate solubilizers	0.161	-0.378	-0.107	-0.442	0.036
Denitrifiers	0.165	0.284	-0.264	-0.454	-0.222
NRB	0.036	0.246	0.324	0.148	0.517

Eigenvectors Core 25

(Coefficients in the linear combinations of variables making up PC's)

Variable	PC1	PC2	PC3	PC4	PC5
TC	0.402	-0.188	-0.154	-0.188	0.013
ATP	0.208	-0.233	0.424	0.187	0.292
¹⁴ C uptake	0.323	0.370	0.203	-0.047	-0.234
LOM	0.334	0.108	-0.306	-0.363	0.116
ZMA	-0.211	-0.348	-0.076	-0.135	-0.562
NI	-0.057	-0.103	-0.408	0.574	0.246
NII	-0.216	0.393	-0.141	-0.135	0.326
Aerobic TDLO	0.127	0.493	0.145	0.083	0.069
Fe	-0.363	0.150	0.266	-0.273	-0.216
Mn	-0.427	-0.094	-0.033	0.113	0.110
Phosphate solubilizers	0.332	-0.007	-0.293	0.246	-0.407
Silicate solubilizers	0.189	-0.188	0.539	0.245	-0.006
Denitrifiers	0.088	-0.408	0.001	-0.464	0.366

Eigenvectors core 20

(Coefficients in the linear combinations of variables making up PC's)

Variable	PC1	PC2	PC3	PC4	PC5
TC	0.191	0.482	0.145	0.748	0.290
ATP	-0.239	0.269	0.697	-0.264	0.315
¹⁴ C uptake	0.403	-0.256	0.270	-0.293	0.321
LOM	-0.379	0.379	-0.406	-0.103	-0.027
ZMA	-0.483	-0.062	-0.072	0.043	0.490
NI	-0.393	-0.429	-0.137	0.115	0.373
NII	-0.237	-0.489	0.359	0.490	-0.349
Aerobic TDLO	-0.395	0.243	0.321	-0.140	-0.460

Fig. 4.46 A. PCA plots and eigenvectors for microbial and biochemical parameters for siliceous oozes

4.8.2 The Siliceous-Pelagic transition-Cores 34, 35

a. Core 34

TC varied positively with ¹⁴C uptake and heterotrophs at $r=0.79$ and 0.81 respectively at $p>0.05$. ATP varied negatively to aerobic TDLO at $p>0.05$. LOM varied negatively to heterotrophs at $p>0.01$.

The first two components cumulated 75.6% of the variance. Cumulative variance up to 100% was explained by the 4 components. TC, ATP, ¹⁴C uptake, ammonium oxidizer and phosphate solubilizer were the prime contributors to variance along the first component. Along the second component ATP, LOM,

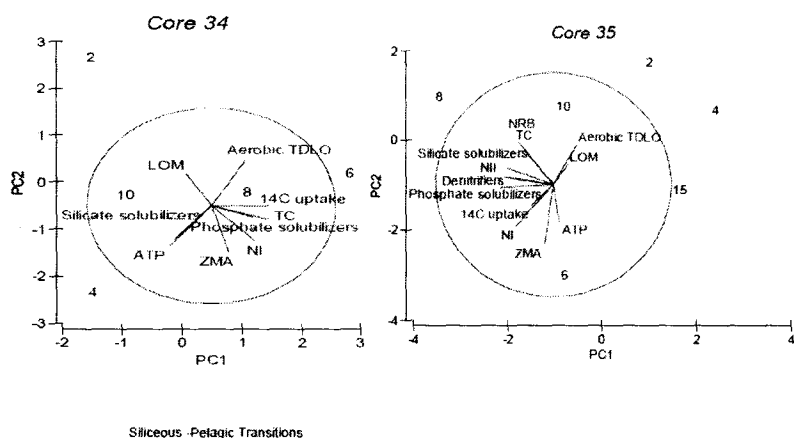
heterotrophs, ammonium oxidizers, aerobic TDLO and silicate solubilizers were the main contributors of variance. The highest variance was scored at depth of 6 cms bsf along the first component and at depths 2 and 4cms bsf along the second component (Fig. 4.46B).

b. Core 35

The variation of TC was influenced by the variation in NII positively up to 76%. NI varied positively with phosphate and silicate solubilizers up to 83 and 70% respectively. Phosphate and silicate solubilizers correlated with each other up to 96%. Heterotrophs varied negatively to NRB and aerobic TDLO to phosphate solubilizers at $p > 0.05$.

The first two components cumulated 63.7% of the variance. Cumulative variance up to 100% was explained by the 5 components (Fig. 4.46B). Ammonium oxidizers, nitrite oxidizers, phosphate solubilizers, silicate solubilizers and denitrifiers primarily contributed to variation along the first component. Along the second component TC, ATP, heterotrophs, ammonium oxidizers, aerobic TDLO and nitrate reducers were the main contributors. The highest variance was scored at depths of 4 and 8 cms bsf along the first component and at depth 6 cms bsf along the second component .

Among the two transition cores 34 appears to be a simpler system and more autotrophic than 35.



Eigenvectors Core 34

(Coefficients in the linear combinations of variables making up PC's)

Variable	PC1	PC2	PC3	PC4
TC	0.466	-0.144	-0.089	0.482
ATP	-0.340	-0.416	0.008	0.234
14C uptake	0.469	-0.004	0.164	0.526
LOM	-0.206	0.337	0.515	0.311
ZMA	0.140	-0.475	-0.353	-0.148
NI	0.344	-0.356	0.284	-0.257
Aerobic TDLO	0.271	0.461	-0.076	-0.299
Phosphate solubilizers	0.328	-0.117	0.540	-0.402
Silicate solubilizers	-0.29	-0.338	0.445	0.020

Eigenvectors Core 35

(Coefficients in the linear combinations of variables making up PC's)

Variable	PC1	PC2	PC3	PC4	PC5
TC	-0.245	0.305	-0.400	0.064	-0.097
ATP	0.051	-0.339	-0.463	-0.122	0.286
14C uptake	-0.192	-0.189	0.167	-0.736	-0.156
LOM	0.126	0.175	-0.495	0.060	-0.589
ZMA	-0.075	-0.538	-0.170	-0.062	0.107
NI	-0.323	-0.378	-0.144	0.156	-0.020
NII	-0.333	0.044	-0.384	0.121	0.384
Aerobic TDLO	0.197	0.351	-0.311	-0.365	0.246
Phosphate solubilizers	-0.457	-0.029	0.045	0.096	-0.223
Silicate solubilizers	-0.390	0.146	0.207	0.318	0.081
Denitrifiers	-0.421	0.067	-0.062	-0.313	-0.320
NRB	-0.296	0.377	0.102	-0.225	0.399

Fig. 4.46 B. PCA plots and Eigen vectors for microbial and biochemical parameters for siliceous-pelagic transition.

4.8.3 The pelagic red clays- Cores 08, 36, 38

a. Core 08

TC varied positively with ^{14}C uptake and Mn oxidizers at $r=0.64$ and 0.62 at $p>0.05$ respectively. ^{14}C uptake and Fe-oxidizers varied negatively with each other at $r= -0.80$ at $p>0.01$. This result is intriguing as it would be expected that a positive relation would exist between the ^{14}C uptake and Fe-oxidizers. ATP varied positively with aerobic TDLO, heterotrophs varied negatively with NII and NI negatively with phosphate solubilizers all at $p>0.05$. Phosphate and silicate solubilizers varied positively among each other up to 74%.

Principal component analysis showed that the first two components explained 53.9% of the cumulative variance. 92.6% of the variation was covered by the 5 components. Coefficients in the linear combinations showed TC, ^{14}C uptake, Fe-oxidizers, Mn-oxidizers and phosphate solubilizers as the most important contributors to variation along the first principal component with a cut off value above 0.3. ^{14}C uptake, LOM, heterotrophs and aerobic TDLO were the important contributors along the second principal component. The variations scored highest at depth of 4cms bsf for first component and at 2cms bsf for the second component (Fig. 4.46C).

b. Core 36

TC varied positively to heterotrophs and negatively to NRB at $p>0.05$. Mn oxidizers varied positively to ^{14}C uptake and negatively to LOM at $p>0.05$. NI varied positively to aerobic TDLO and Fe oxidizers at $p>0.05$. Denitrifiers varied positively with Fe oxidizers and phosphate solubilizers at $p>0.01$.

The first two components cumulated to 56.6% of the variance. Cumulative variance up to 89.7% was explained by the 5 components. LOM, heterotrophs, Fe

oxidizers and phosphate solubilizers were the prime contributors to variance along the first component. TC, ATP, ^{14}C uptake, heterotrophs, aerobic TDLO and phosphate solubilizers contributed to variance along the second component. Depths 2, 4, 10 cms bsf contributed to maximum variance along the first component and depth 15 cms bsf to that of second component (Fig. 4.46C).

c. Core 38

Mn oxidizers varied negatively with ATP and LOM at $p>0.05$ and $p>0.01$ respectively. None of the others correlations were statistically significant.

The first two components cumulated to 68.3% of the variance. Core 38 is the simplest among the three pelagic cores. Cumulative variance up to 94.8% was explained by the 5 components (Fig. 4.46C). TC, ATP, LOM, Fe-oxidizers, Mn-oxidizers and silicate solubilizers contributed to the variation along first component with a factor loading cut off above 0.3. ATP, phosphate solubilizers and silicate solubilizers caused the variation along second component. Depth 2 cm bsf scored for maximum variance along first component. Depth 10 cm bsf scored for maximum variance along the second component.

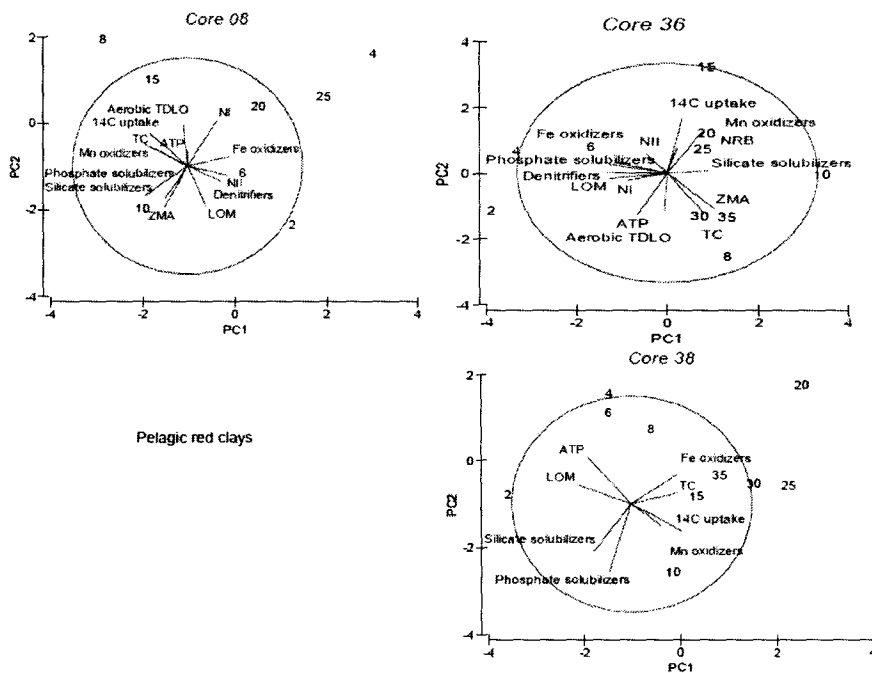
4.8.4 The calcareous ooze

a. Core 37

About 47% of the variation in ATP was responsible for negative variation in LOM at $p>0.05$. About 55% of the variation in ^{14}C uptake at $p>0.01$ was due to Fe oxidizers. LOM varied positively with heterotrophs, NI and NII at $p>0.01$, 0.05 and 0.01 respectively. The heterotrophs correlated with NI and NII at $p>0.001$. Heterotrophs also related positively to phosphate and silicate solubilizers at $p>0.05$.

NI and NII related among each other at $p>0.001$. NI related to phosphate and silicate solubilizers positively at $p>0.05$. NII was also responsible for the variation in phosphate solubilizers at $p>0.05$.

The first two components cumulated to 54.4% of the variance. Cumulative variance up to 91.1% was explained by the 5 components. LOM, heterotrophs, ammonium oxidizers and nitrite oxidizers contributed to the linear variation along the first component. ^{14}C uptake, Fe oxidizers, Mn oxidizers and denitrifiers contributed to variation along the second component. Maximum variation was scored at 2cms bsf along first component. Depths 2, 4, 10cms bsf scored for maximum variation along the second component (Fig. 4.46D).



Eigenvectors core 36

(Coefficients in the linear combinations of variables making up PC's)

Variable	PC1	PC2	PC3	PC4	PC5
TC	0.235	-0.357	-0.083	-0.119	0.228
ATP	-0.193	-0.384	-0.170	-0.176	0.304
14C uptake	0.102	0.502	-0.017	-0.375	0.109
LOM	-0.387	-0.050	-0.187	0.094	0.024
ZMA	0.309	-0.322	0.176	-0.107	0.156
NI	-0.271	-0.065	0.352	-0.378	0.017
NII	-0.141	0.179	0.094	0.475	0.702
Aerobic TDLO	-0.018	-0.355	0.517	-0.069	-0.046
Fe	-0.353	0.099	0.210	-0.153	0.409
Mn	0.229	0.370	0.124	-0.392	0.163
Phosphate solubilizers	-0.382	0.076	-0.182	-0.257	-0.092
Silicate solubilizers	0.273	0.020	-0.424	0.065	0.149
Denitrifiers	-0.396	0.003	-0.106	0.105	-0.255
NRB	0.065	0.229	0.463	0.403	-0.184

Eigenvectors Core 38

(Coefficients in the linear combinations of variables making up PC's)

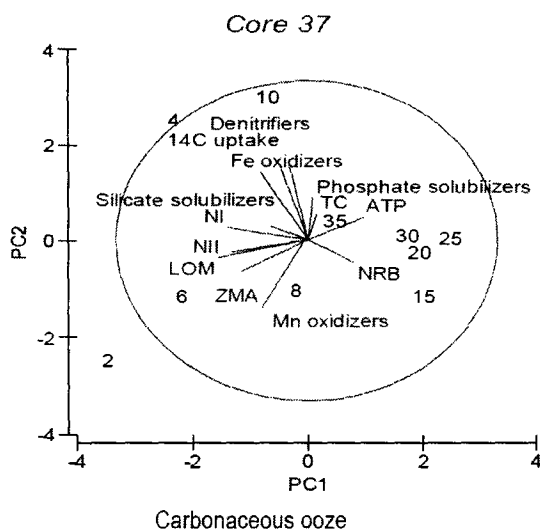
Variable	PC1	PC2	PC3	PC4	PC5
TC	0.386	0.101	-0.012	0.869	0.099
ATP	-0.365	0.436	0.251	0.072	-0.110
14C uptake	0.247	-0.202	0.761	0.017	0.139
LOM	-0.450	0.175	0.280	-0.001	0.137
Fe	0.381	0.269	0.449	-0.227	-0.357
Mn	0.423	-0.251	-0.171	-0.320	-0.194
Phosphate solubilizers	-0.183	-0.631	0.202	0.010	0.406
Silicate solubilizers	-0.310	-0.442	0.090	0.291	-0.781

Eigenvectors 08

(Coefficients in the linear combinations of variables making up PC's)

Variable	PC1	PC2	PC3	PC4	PC5
TC	-0.322	0.181	-0.333	-0.102	-0.014
ATP	-0.004	0.147	0.536	-0.199	-0.004
14C uptake	-0.325	0.300	-0.162	-0.322	0.182
LOM	0.157	-0.366	0.090	-0.481	0.345
ZMA	-0.197	-0.383	0.375	0.098	0.213
NI	0.254	0.423	0.279	-0.187	-0.054
NII	0.356	-0.089	-0.202	-0.269	-0.379
Aerobic TDLO	-0.039	0.386	0.372	-0.270	-0.115
Fe	0.370	0.088	0.023	0.333	-0.381
Mn	-0.372	0.204	-0.178	-0.112	-0.237
Phosphate solubilizers	-0.369	-0.277	0.082	-0.056	-0.359
Silicate solubilizers	-0.198	-0.304	0.197	-0.236	-0.559
Denitrifiers	0.290	-0.143	-0.302	-0.493	-0.013

Fig. 4.46 C. PCA plots and eigen vectors for microbial and biochemical parameters for pelagic red clay.



Eigenvectors core 37

(Coefficients in the linear combinations of variables making up PC's)

Variable	PC1	PC2	PC3	PC4	PC5
TC	0.045	0.164	0.487	-0.084	0.477
ATP	0.291	0.140	0.427	0.138	0.044
14C uptake	-0.145	0.469	-0.180	0.224	-0.261
LOM	-0.467	-0.108	-0.004	-0.002	0.024
ZMA	-0.349	-0.197	0.043	0.049	0.552
NI	-0.420	0.078	-0.014	-0.170	-0.194
NII	-0.400	-0.076	0.205	-0.246	-0.157
Fe	-0.249	0.426	0.011	0.306	-0.058
Mn	-0.224	-0.427	0.253	-0.083	-0.279
Phosphate solubilizers	0.025	0.268	-0.053	-0.665	0.179
Silicate solubilizers	-0.193	0.086	-0.483	0.126	0.460
Denitrifiers	-0.095	0.456	0.152	-0.350	-0.082
NRB	0.238	-0.140	-0.424	-0.388	-0.054

Fig. 4.46D. PCA plots and eigen vectors for microbial and biochemical parameters for calcareous ooze.

The carbon fixation in pelagic core 08 could be at the expense of aerobic TDLO and Mn-oxidizers, while in core 36 it could be at the expense of Mn-oxidizers. In core 38 located in a deep valley, the variable carbon fixation is associated with both Fe and Mn oxidizers. Interestingly, the PCA suggests that the calcareous core 37 at the summit of a seamount could fix carbon at the expense of nitrifiers and Fe-oxidizers. This is plausible as the seamount summit could receive relatively more amount of organic rain than the deeper valley. In core 08, the highest ¹⁴C uptake is

suggested to be associated with Mn oxidizers and aerobic TDLO and is noted at a deeper geochemical boundary that harbours unexpectedly high numbers of heterotrophs and aerobic TDLO. Similar associations are observed in core 36. In calcareous ooze 37 most of the ^{14}C uptake seen in the top 10 cms bsf is apparently at the expense of Fe-oxidizers.

4.8.5 Interrelationships between microbial and biochemical parameters in nodules

Interrelationships between microbial and biochemical parameters in the surface nodule SN 147 showed significant positive relations among microbial parameters at $p > 0.05$, 0.01 and 0.001. Significant positive relations were noted among the TOC and other biochemical parameters. However, there appeared no significant relation between microbial and biochemical parameters (Fig. 4.47A).

Interrelationships between microbial and biochemical parameters in the buried nodule BN 142 showed very complex and significant positive and negative relationships (mostly $p > 0.001$). One of the most striking set of relationships was that of the autofluorescent F_{420} cells. These cells correlated positively with the aerobic viable counts and negatively to carbon uptake, lipids and TOC. The carbon uptake, lipid and TOC positively correlate with each other. ATP correlates positively to all bacterial fractions, negatively to biochemical content and insignificant relation to microbial carbon uptake (Fig. 4.47B).

a. Analysis of variance of microbial and biochemical characteristics between surface nodule SN 147 and buried nodule BN 142

One way analysis of variance of microbial and biochemical characteristics between surface nodule SN147 and buried nodule BN 142 did not show significant variation or between the two sediments S1 and S2.

The variation between the surface nodule SN 147 and its associated sediment S1 are insignificant but that between the buried nodule BN 142 and its associated sediment S2 is highly significant at $p \gg 0.001$. The variation between the outermost and the inner most layers of both the nodule types are marginally below the F_{crit} value of variance at $p > 0.05$.

b. Interrelationships between microbial and biochemical parameters in nodules and associated sediment system

The inclusion of the measurements from the respective associated sediments S1 and S2 to those of the nodules SN147 and BN142 did not change the overall patterns of the interrelationships. However, the complexity of the mesh of interrelations became less and readable due to the reduction in the number of significant relations (Figs. 4.47A and 4.47 B).

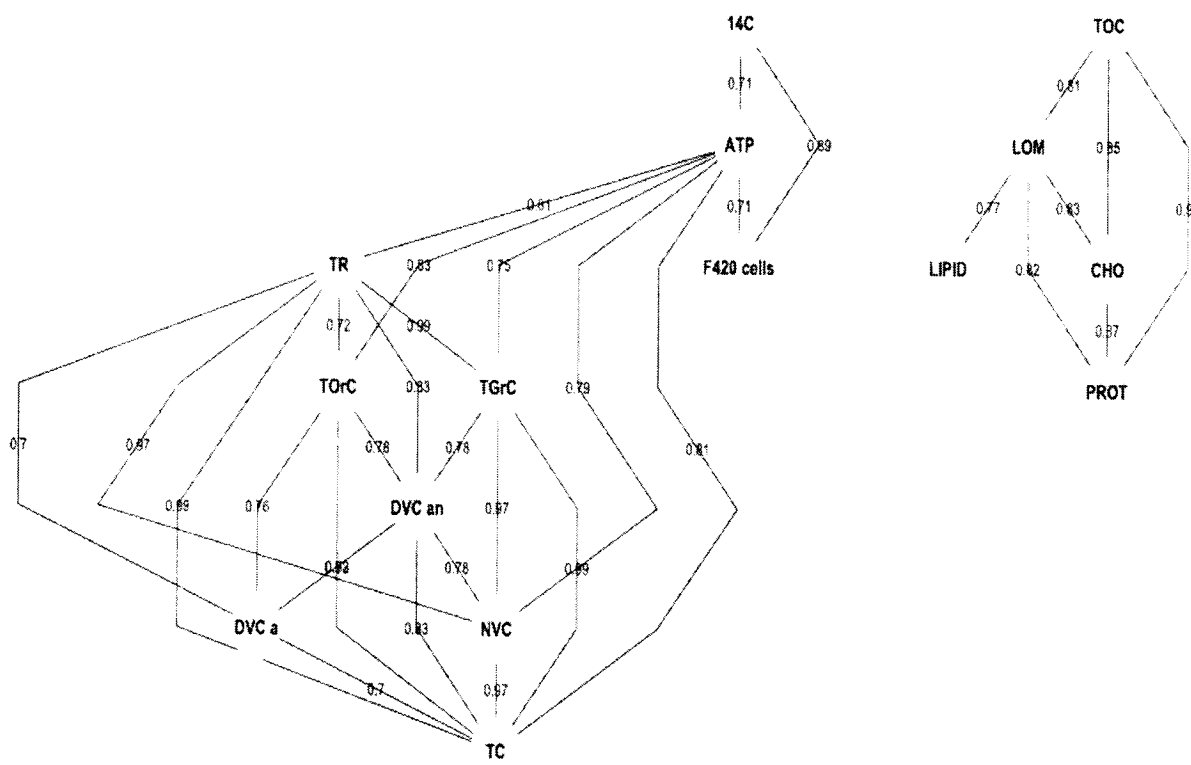


Fig. 4.47A. Interrelation between microbial and biochemical parameters in the surface nodule SN 147 interrelations

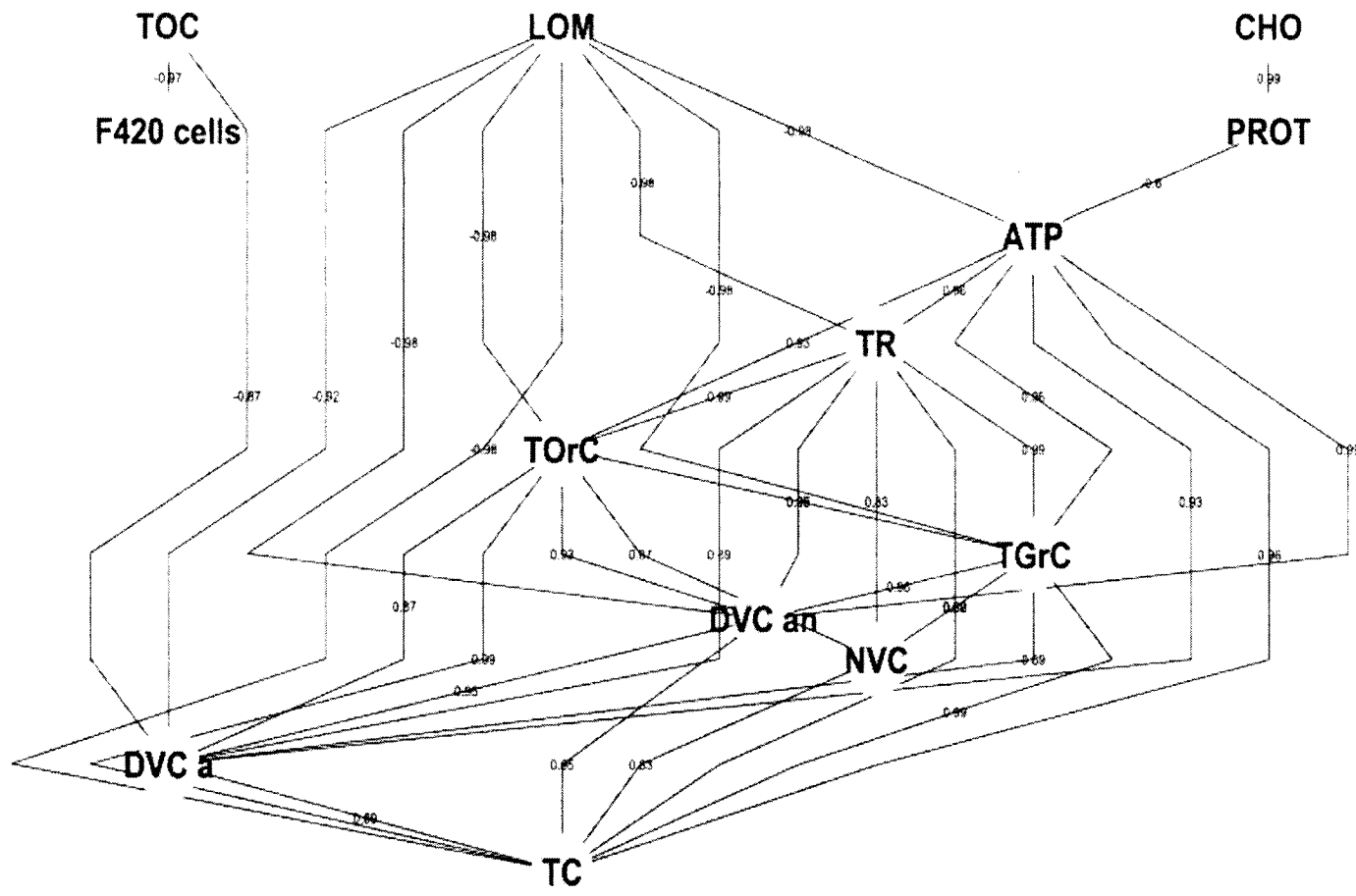


Fig. 4.47B. Interrelation between microbial and biochemical parameters in the buried nodule BN 142 interrelations

4.9 Simulations

Simulations were run to understand the top-down organic sink in the northern diagenetic set up and bottom-up source in the hydrothermal set up.

4.9.1 Quantification of the influence of non-steady state diagenetic condition on microbial community by numerical simulation

The NO_3^- concentration profile measured by shipboard analysis was simulated using a transient diffusion numeric model (Fig. 4.48A). At the sea floor interface, the observed NO_3^- concentration of $8.87\mu\text{M}$ was used as a starting condition. It is also assumed that NO_3^- in sediment pore water is 0. The model calculated the concentration as a function of time and depth. Considering the residence time of NO_3^- and the sedimentation rate of an organic matter pulse, a 10,000 years time scale is required for NO_3^- to reach 17.5cm bsf. Assuming a surface layer with a nitrite oxidation rate of $1000\mu\text{M m}^{-3}\text{ yr}^{-1}$ in the section 3 to 7 cm bsf, the model also shows that the reactant, NO_2^- , will be consumed within a time period of 1000 years in this zone. Conversely, at 5 to 9cm bsf the reactant NO_3^- would be reduced at a reduction rate of $-1000\mu\text{M m}^{-3}\text{ yr}^{-1}$. The reactant NO_3^- will be consumed within 1000 years. The profile returns to its original shape within another 1000 years soon after the consumption of NO_2^- in the upper 3 to 7cm layer and the simultaneous reduction of NO_3^- in the lower 5 to 9 cm ceases. In both halves of the reaction couple a steady nitrification profile is finally achieved and they reproduce the pore water NO_3^- profile measured in the core TVBC 26 (Fig. 4.48A), showing net nitrification.

4.9.2 Quantification of hydrothermal alterations on pore water and microbial community by numerical simulation

The NO_3^- concentration profile measured by shipboard analysis was simulated using a transient diffusion numeric model (Fig. 4.48B). At 12.5 cm bsf i.e., below the stratigraphic transition, the observed NO_3^- concentration of 4.85 μM was used as a starting condition. It was also assumed that NO_3^- in sediment pore water is 0. The model calculated the concentration as a function of time and height of core using the core bottom as height zero. The precise time and duration of the hydrovolcanic explosion is unknown. However, the alteration features indicate a 200 year time span between the explosion and the present time (Nath *et al.*, 2008). Thus, an assumption of a 1000 year focused jet-flow was made to simulate the model. For the first 1000 years of explosive volcanism, NO_3^- had diffused upwards as a focused jet after which it started dispersing laterally. Assuming a surface layer with a nitrite oxidation rate of $1000\mu\text{M m}^{-3} \text{ yr}^{-1}$ at 9 to 5 cm bsf, the model also shows that the reactant, NO_2^- , will be dispersed and consumed by microbes within a time period of 100 to 200 years in this zone. Conversely, at 7 to 3 cm bsf, the reactant, NO_3^- will be dispersed and consumed within 100 to 200 years with a nitrate reduction rate of $-1000\mu\text{M m}^{-3} \text{ yr}^{-1}$. The profile returns to its original shape within another 100 to 200 years soon after the utilization of NO_2^- in the lower 9 to 5cm layer and the simultaneous reduction of NO_3^- in the upper 7 to 3cm ceases. Due to the continuous abiotic supply of NO_2^- and NO_3^- , in both halves of the reaction, a non-steady nitrification-denitrification coupled profile is sustained and they reproduce the pore water NO_3^- profile measured in the core TVBC 08 (Fig. 4.48B).

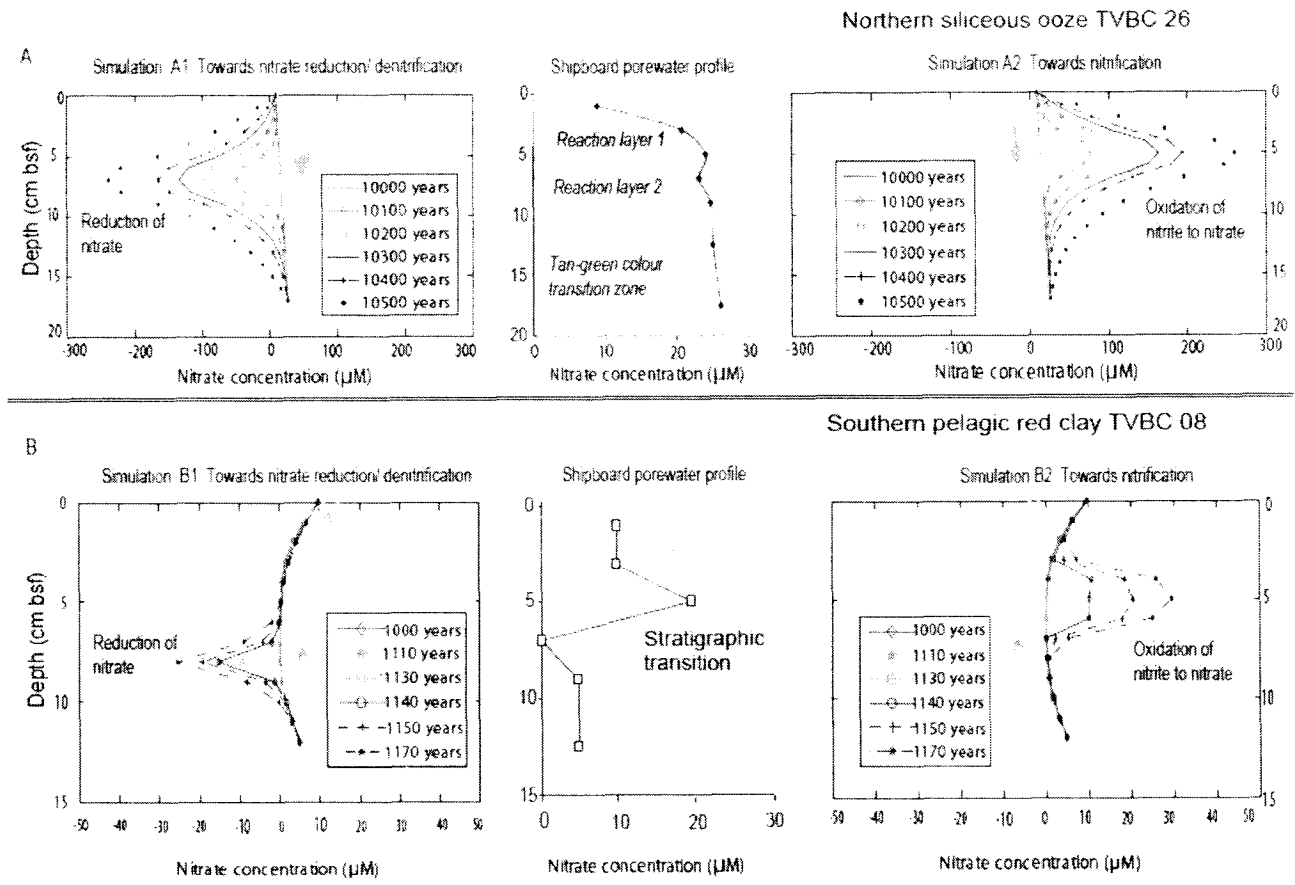


Fig. 4.48 A. Quantification of the influence of non-steady state diagenetic condition on microbial community by numerical simulation.

B. Quantification of hydrothermal alterations on pore water and microbial community by numerical simulation.

"All that glitters may not be gold, but at least it contains free electrons!"

- *J. D. Bernal.*

Chapter V

Discussions

5.1 Characteristics of the deep-sea

The deep-sea benthic ecosystems, can be classified into three groups based on their composition and bacterial response. They are 1) detrital, which is dependent from the organic rain from above (including the nodule provinces of the deep-ocean basins), 2) non-detrital and chemosynthetic as in the hydrothermal vent areas and 3) both detrital and non-detrital as in passive margins and cold seeps (Sibuet, 2005). Most of these often-inaccessible realms are still vastly unknown in terms of baseline knowledge (Morgan, 2005).

Metabolic activities of free-living bacteria in deep-sea sediments have been shown to be at least 50 times lower than microorganisms in shallow waters or on sediments at shallow depths. Environmental factors contributing to this slow rate of bacterial metabolism seem to be the low temperature ($<5^{\circ}\text{C}$), and elevated pressure (500 bars) (Jannasch *et al.*, 1971, Jannasch and Wirsen, 1973), with a greater proportion of metabolic activity devoted to cellular maintenance (Schwartz and Colwell, 1975). On the contrary, there are reports that the deep-sea forms are as active as their counterparts in the shallow regions (Lochte *et al.*, 1999). While those environments that are predominantly detrital are influenced by seasonal variations, the chemosynthetic ones are indifferent to it (Jon Copley, 2005).

The deep-sea environments are no longer monotonously homogenous but show large-scale spatio-temporal variations. The great variety in topographic forms and sediment pattern differences are likely to show up in the benthic community as well.

The broad environmental baseline data in the Central Indian Basin is sparse. However, the program on Polymetallic Nodules Environmental Impact Assessment

provided the opportunity to analyze spatial, inter-annual and seasonal variability in the region.

5.2 Environmental setting of the CIOB

5.2.1 *Depth, temperature and pressure*

The CIOB is one of the deepest parts of the Indian Ocean where sediments have been recovered from 5000m and below (Fig. 4.1). The only *in situ* temperature measured in the vicinity of the basin was by Warren *et al.*, 1982. However, with evidences of widespread volcanic activity, there are possibilities of higher temperature than the observed *in situ* temperature of $\sim 2^{\circ}\text{C}$. Pressure would be 500 bars at these depths. However, the flow of hydrothermally derived fluids through the sediment column indicates that this flow could counteract the hydrostatic pressure with changes in phase chemistry. As a result of this the microbes may be residing at a lower pressure and higher temperature in these sediment pockets. This could explain the large number of mesophiles culturable from these sediments. Heat flux is also not measured in the CIOB except for some parts in the neighbouring Warton Basin. Possibility of varied type of microbial habitats in response to different temperature ranges thus still remains unexplored. As all stations except station 37 are located $\sim 1000\text{m}$ below the Calcite compensation depth (CCD), they are mostly carbonate free. Almost the entire content of elemental carbon is comprised of organic carbon.

5.2.2 Rock Colour

The northern sediments between 10°-12°S are dominated by sediment hues 10YR4/2, 10YR5/4 and to a lesser extent by 5Y5/2. Central sediment from 12°-14°S dominated by five hues 5Y5/2, 5YR3/4, 10YR4/2, 10YR5/4 and 10YR6/6. The southern pelagic clay between 14°-16°S is dominated by the hue 5YR3/4 (Fig. 2).

These colour transition layers are analogous to oxic-anoxic transitions of interfaces prevalent in current systems. These regions could be dominated by both electron donors and acceptors, thus facilitating the existence and proliferation of extremely tolerant mixotrophic bacteria. It is probable that these organisms are metabolically plastic.

Rock colour variations and mottle formations (Fig. 2) are associated to redox boundaries. These layers, often referred to as 'sub-oxic' mottles, had been correlated with dissolved NO_3^- , Mn and Fe (Lyle, 1983; Konig *et al.*, 1997). These mottles otherwise called the tan-green mottled zones are found generally below reactive layers which in turn are prominent below the sediment-water interface. Formations of these mottles in the Pacific Ocean sediments were attributed to high palaeoproductivity, differential sedimentation rates and fluctuations in oceanic redox conditions caused by changes in bottom water oxygen content (Lyle, 1983). Formation of metal enrichment zones in the upper part of the deep-sea sediment column (Colley *et al.*, 1984; Colley & Thomas, 1985) with the active involvement of microbes (Froelich *et al.*, 1979) are also believed to be the cause of these formations. Non-steady state diagenetic processes due to downward diffusing oxidants, such as O_2 and NO_3^- , result in the depletion of initially deposited organic carbon. Both oxidized and reduced forms of nitrogen are produced in

the active oxidation zones (Buckley & Cranston, 1988). More recently, the temporal shift of geochemical interfaces from shallower temporary reactive to deeper layers result in mottle formation in predominantly detrital settings (Meister *et al.*, 2007, 2009). From the present study it can be presumed that rock colour may be closely associated to bacterial activity over geological time-scales.

5.2.3 *Pore water Geochemistry*

Selected cores were used to study pore-water parameters like pH, Eh, oxygen, ammonium, and sulphide. In order to check the change in pH and Eh of sediment with increase in temperature, two cores IVBC 18C and IVBC 20A were examined. Chemically pH and Eh relate to each other by the Nerst equation. But in natural systems, the bacterial actions upset the Eh-pH linear relationships (Figs. 4.3, 4.4). In the present results, pH increased with the rise in temperature to indicate more alkaline conditions in the given time frame, which is intriguing (Fig 4.5). It is observed that the relation between pH and Eh is 30% better in the nodule-poor IVBC 18C than the nodule-rich 20A as temperature changes from 10-20°C (Fig 4.5) after bringing the sample on-board. This possibly shows that microbial activity is greater in the nodule-rich core. It is plausible that at much lower temperatures *in situ* at the sea-floor the pH is more acidic and Eh tilting to the more oxic side. High salinity pockets are noted where salinity rises till 39ppt. These parameters thus need further critical investigation.

Pore-water studies showed distinct differences in concentrations and profile types between nodule poor and nodule rich areas. Pore waters relatively richer in sulphide and

poorer in ammonium appear to support better quality and quantity of polymetallic nodules (Fig. 4.6).

Pore-water oxygen concentrations (Figs. 4.6) are within ranges previously reported for the deep-sea (Jahnke & Jahnke, 2004). Warren & Johnson (2002) reported around 4 to 4.5 ml l⁻¹ (175 to 197 μM) in waters of the northern CIOB at ca 4600 m below surface, along 90°E longitude. The convex profile of NO₃⁻ (Fig. 3A: Das *et al.*, 2010a) is indicative of predominantly oxic conditions with net nitrification (Soetaert *et al.*, 1996). A distinct early diagenetic reactive layer is seen at 3 to 9 cm bsf in station TVBC 26. The PO₄³⁻ concentrations are depleted at the diagenetic reactive layer (Schulz, 2000) and within the tan-green mottled zone and are possibly related to the nitrification-denitrification coupled zones where nitrification is more prominent. The SiO₃²⁻ concentration shows a typical downward increasing trend in TVBC 26 (Das *et al.*, 2010a; Fig 3a) indicating a diffusive flux from the sediment water interface (Nath & Mudholkar, 1989). The distribution of pore-water is closely coupled to microbial distribution and activity.

5.3 Elemental Carbon, Nitrogen, C/N ratio

In general total organic carbon decreased from the northern siliceous ooze to southern pelagic red clays. The values are in consistent range to those reported earlier (Gupta and Jauhari, 1994). Some stations like station 19 in the central part of the basin show high TOC irrespective of being relatively far from the effects of terrigenous influx. They are also high in C/N ratios (Fig. 4.8). Higher C/N ratios in sub-oxic depths of sediments with TOC < 1% has been associated with bacterial oxidation of metals

(Farrimond *et al.*, 1989) and reworking of residual organic matter. The bubbling feature of the graph indicates that high TOC and C/N ratios occurred intermittently with time and might have relations to differential amount of organic matter rain or hydrovolcanic alterations during different time periods. The central deepest parts from 12-13°S showed accumulation of carbon. This region also showed depletion of nitrogen, leaving back the most recalcitrant carbon of the basin. The deep-sea bed, acting as the ultimate sink for organic material derived from the upper ocean's primary production, is now assumed to play a key role in biogeochemical cycling of organic matter on a global scale (Jahnke, 1996). The relevance of deep-sea ecosystems in global biogeochemical cycles has been only recently investigated (Rowe and Pariente, 1992). The concept of a vast "biological desert", depending, on allochthonous organic matter inputs, mainly phytodetritus, for its energetic requirements, (Pfannkuche, 1993; Lampitt and Antia, 1997; Fabiano *et al.*, 2001) is steadily changing (Danovaro *et al.*, 2003). Recent investigations carried out at bathyal depths suggested new opinions of trenches being depocenters of organic matter (Jahnke and Jahnke, 2000) and hot-spots of bacteria-mediated organic matter recycling (Jahnke *et al.*, 1990; Boetius *et al.*, 1996). It is therefore pertinent to analyse labile organic matter as not only an index of natural and artificial disturbance (Nair *et al.*, 2000; Raghukumar *et al.*, 2001a, b; Raghukumar *et al.*, 2006) but also to provide baseline of natural environmental variability on large basin scales determining biogeographic change.

The factors governing the organic carbon variation are surface water productivity, bottom water oxygen content, degradation, sedimentation rate and bioturbation (Fenney

et al., 1998). TOC and C/N ratio are some of the key factors governing microbial distribution and in turn are affected by microbial activity (Figs 4.7A, 4.7B and 4.8).

5.4 Distribution - Biochemical and microbiological parameters

5.4.1 Labile organic matter (LOM) and Adenosine triphosphate (ATP)

The northern CIOB is fresher in its LOM values due to higher terrigenous input (Figs. 4.9 to 4.12). It is also plausible that LOM is produced by the bacteria through chemosynthesis. In general, LOM in the northern part of the basin is dominated by protein, central by carbohydrates and south by lipids.

ATP showed pockets of high values without any distinct latitudinal trend. ATP peaked at the redox boundaries or colour transitions. In general, the southern pelagic red clays had higher values for ATP (Figs. 4.13 to 4.16). Pelagic clays with volcanic alteration might possibly be rich in pyrophosphate as these are prominent components in plumes. Besides, they can be important intermediates towards synthesis of nucleic acids. The present range in ATP values in the study area are similar to the range reported from Guaymas Basin (Karl, 1995).

The present results suggest that the three sectors of the CIOB have distinct microbial distribution, energy content and carbon fixing activity. The northern sector is a high bacterial count, low ATP, low carbon-fixing area. The central sector is a low bacterial count, high ATP, low carbon-fixing area. The southern sector is a high bacterial number, high ATP, high carbon-fixing area. In essence, the most recalcitrant central sector with lowest TOC is marked by lowest bacterial counts, and lowest carbon fixation rate. The strikingly high ATP in this organically depleted sector deviating from the

Redfield ratio is still not clearly understood, though it is speculated that high pyrophosphate content could have a role.

5.4.2 *Abundance and distribution of bacteria in CIOB*

The deep sub-seafloor biosphere supports a diverse population of prokaryotes belonging to the Bacteria and Archaea (Parkes *et al.*, 1994, 2000, 2005). Most of the taxonomic groups identified by molecular methods contain mainly uncultured phylotypes. Despite this, several cultured strains have been isolated from this habitat, but they probably do not represent the majority of the population. Evidence is starting to suggest that some of the activities measured, such as sulphate reduction and methanogenesis, reflected in geochemical profiles, are carried out by a small subset of the community detected by molecular methods (Fry *et al.*, 2008). It is further possible that heterotrophy may not be totally ruled out as a mode of metabolism in subsurface sediments and heterotrophic microorganisms could dominate the uncultured prokaryotic population. Although, heterotrophy is limited by the increasing recalcitrance of organic matter with depth, thermal activation of buried organic matter improves heterotrophy by providing additional substrates at depth (Fry *et al.*, 2008). In addition, a high proportion of the cells detected by AODC were also shown to be viable (Inagaki *et al.*, 2006).

5.4.3 *Total counts and frequency of dividing cells*

Total counts of bacteria varied from 10^6 to 10^9 cells g^{-1} dry sediment. Although geographically separated and geologically contrasting, some stations like 26 and 8 clustered together for total count and frequency of dividing cells. Low FDC occurs at the

central and southern parts (Figs. 4.17 A and B). The TOC-rich core 26 may be under the influence of grazing macro- and meiobenthos. This may be an important factor in keeping the total numbers similar to the TOC-poor 08. In general total counts are consistent with the values reported earlier (D'Hondt *et al.*, 2002, 2004).

5.4.4 Direct viable counts (DVC a and DVC an)

Direct viable counts were examined for the first time in this part of the abyssal sediments. Relative trends of aerobic and anaerobic viability are different for different sediment type. Much literature on this topic is not available for discussion and thus leaves a large area unexplored for further studies (Fig. 4.21).

5.4.5 Culturable counts and endeavour to improve culturability

Although, it was argued that the culturable fraction could wield greater influence on the environment, such inferences remained controversial for two decades, as only 0.001 to 0.01% of the total bacterial count is amenable to cultivation techniques (Van Es & Meyer Reil, 1982). Culturable bacteria are now known to be consistent over large areas of the ocean floor (D'Hondt *et al.*, 2002, 2004)

5.4.6 Aerobic culturability

Bacteria have been divided into two major groups namely autotrophs and heterotrophs. The autotrophs encompass those bacteria that use carbon dioxide as the principle source of carbon. These prokaryotes depend on light and/or the oxidation of inorganic compounds for the generation of metabolic energy. Their energy metabolism

can be divided as photolithotrophic or chemolithotrophic. In the abyssal depths of CIOB chemolithotrophy is expected to flourish out of compulsion. However the organisms growing at the expense of organic energy sources are known as facultative autotrophs. These prokaryotes grow better when small amounts of organic compounds are present in otherwise inorganic medium and are known as mixotrophs. The heterotrophic bacteria obtain their carbon from organic nutrients. Here, the carbon source in most cases is also the energy source. Some bacteria like the *Pseudomonads* are versatile and are known to utilize over hundred different carbon compounds as the sole source of carbon and energy. In contrast to the versatile bacteria, there are more fastidious ones that grow on relatively smaller number of organic compounds like the obligate methylotrophs that grow on methane, methanol and dimethyl ethers etc. (Gottschal *et al.*, 1991). To the extent that C and energy limitations are the rule of natural habitats, mixotrophic organisms may have a selective advantage over the obligate heterotrophs or obligate autotrophs (Leefeldt and Matin, 1980).

5.4.7 Heterotrophs (ZMA medium)

Heterotrophs were enumerated on one fifth strength of Zobell Marine Agar (ZMA). The bacteria in CIOB are known to grow best at this concentration (Nair *et al.* 2000, Loka Bharathi and Nair 2005). Experiments conducted to find out the optimum medium concentration for maximum CFU yield reassured this previous finding. Heterotrophs are ubiquitous in the CIOB and often found in higher numbers in the organically depleted southern region (Figs 4.24 A, B and C). These heterotrophs might have higher adaptability, versatility and resilience as these bacteria are associated with

relatively oligotrophic sediments (Harder & Dijkhuizen, 1982; Goltekar *et al.*, 2006) Similar unexplained high heterotrophic populations have been reported in some earlier findings in vent sites with low organic carbon (Karl, 1995).

5.4.8 Nitrifiers

The nitrifiers comprise of two groups namely ammonium oxidizers (NI) and nitrite oxidizers (NII). The nitrifiers are chemoautotrophic bacteria that thrive in these oligotrophic environments. Although measurably low in ammonium, it is possible that the nitrifiers utilize the ammonium as soon as it is formed. Ammonium must be formed either biogenically from accumulated faecal pellets of benthic animals or abiogenically from hydrothermal sources. The nitrifiers show mid depth maxima in case of many sediment cores. These are most probably associated to the redox boundaries indicated by colour changes. In the southern pelagic red clays the high numbers of nitrifiers are due to the severe organic depletion (Figs 4.24 A, B and C).

5.4.9 Aerobic sulphur oxidizers (Aerobic TDLO)

Another group of chemoautotrophic bacteria are the aerobic sulphur oxidizers. These bacteria may be obligate or facultative chemolithotrophs and facultative anaerobes. They are known to oxidize sulphur or sulphide using oxygen or nitrate as the terminal electron acceptors (Nelson and Fisher, 1995, Loka Bharathi 1989). Thus processes like thiotrophic nitrate reduction may be widespread. In the northern part of the CIOB biogenic sulphide may be present, while in the southern CIOB most abiogenic sulphide from diffuse hydrothermal processes may be prevalent. Either ways sulphide is present in

these sediments albeit at low concentration or they have a dynamic turnover (Figs 4.24 A, B and C).

5.4.10 Corewise distribution of heterotrophs, NI, NII and aerobic TDLO

The cores 26, 25 and 20 are all siliceous oozes in the north, but are very different from each other in their distribution patterns. In core 26, the profiles show a clear existence of non-steady nitrification-denitrification couple with spatial separation of niches for the nitrifiers and denitrifiers. The peaks of the heterotrophs coincided with the crests of nitrifiers indicating niche separation among heterotrophs and autotrophs (Figs 4.24 A, B and C).

In core 25, the profiles again show a clear existence of non-steady nitrification-denitrification couple with spatial separation of niches for the nitrifiers and denitrifiers. The peaks of the heterotrophs were however not clearly separated from the nitrifiers indicating greater mixotrophy than core 26.

In both cores 20 and 35, the similar distribution pattern of heterotrophs on ZMA and NI suggest the probable existence of heterotrophic ammonium oxidizers (Figs 4.24 A, B and C). The cores also share similar NII and aerobic TDLO profiles indicating a couple between nitrite oxidation and nitrate reduction. These two mark the northern and southern boundaries respectively of the nodule rich area of CIOB. The heterotrophic ammonia oxidation and nitrification-denitrification couple between nitrite oxidation and nitrate reduction appear to be important processes in the nodule rich province.

Heterotrophs on ZMA shared similar profile with NII, and NI shared with aerobic FDLO in core 36. Therefore, heterotrophic nitrite oxidation might be prominent processes in the pelagic red clay core.

In core 37 sediment compaction at 20-25 cm bsf probably is an important factor governing culturability as in this layer, the number of culturable bacteria were low. Consequently, niche separation apparently does not occur in this core.

Culturable bacteria are now known to be important over large areas of the ocean-floor (D'Hondt *et al.*, 2002, 2004). This consistency makes them important indicators of ocean biogeochemical processes. However, enough basin-scale data on this same issue is still unavailable and needs to be addressed in the forthcoming studies.

5.4.11 Fe and Mn oxidizers

Ubiquity of Fe and Mn oxidizers is expected as the CIOB encompass the polymetallic nodule fields. The homogenous distribution of both Fe and Mn oxidizers indicate that the reduced ions are available at more or less uniform concentrations down the core. Fe oxidizers are marginally more than Mn-oxidizers (Figs. 4.25 and 4.26).

Iron and manganese oxides are important electron acceptors in the diagenetic sequence of sediments. Iron and manganese oxidizers are widespread in diagenetic as well as hydrothermally altered environments. Deep-sea bacteria participate in the redox coupling of Fe and Mn along with oxygen, sulphur, nitrogen and carbon (Van Cappellen and Wang, 1996). The net rate of organic carbon oxidation could be broken down into the contributions from aerobic respiration, denitrification, dissimilatory Mn (IV) reduction, dissimilatory Fe (III) reduction, sulphate reduction and methanogenesis. The isolation and

physiological characterization of novel, psychrophilic, iron-oxidizing bacteria (FeOB) from low-temperature weathering habitats in the vicinity of the Juan de Fuca deep-sea hydrothermal area has been reported (Edwards *et al.*, 2003). The FeOB were cultured from the surfaces of weathered rock and metalliferous sediments. They are capable of growth on a variety of natural and synthetic solid rock and mineral substrates, such as pyrite (FeS_2), basalt glass (10 wt% FeO), and siderite (FeCO_3), as their sole energy source, as well as numerous aqueous Fe substrates. Growth temperature characteristics correspond to the *in situ* environmental conditions of sample origin; the FeOB grow optimally at 3 to 10°C and at generation times ranging from 57 to 74 h. They are obligate chemolithoautotrophs and grow optimally under microaerobic conditions in the presence of an oxygen gradient or anaerobically in the presence of nitrate (Edwards *et al.*, 2003).

Microbial Fe-oxidizing bacteria are a critical factor in the kinetics of mineral dissolution at the seafloor. They accelerate dissolution of minerals by 6–8 times over abiotic rates. Minerals could be released by bacterial action and reduced Fe thus released could be further oxidized by iron-oxidizing bacteria (Edwards *et al.* 2004). These reactions would catalyse further mineralization in open systems or recycling in closed systems. Microbial Fe-oxidation is widespread in the deep-sea.

Mn(II)-oxidizing microbes have an integral role in the biogeochemical cycling of manganese, iron, nitrogen, carbon, sulfur, and several nutrients and trace metals. There is great interest in mechanistically understanding these cycles and defining the importance of Mn(II)-oxidizing bacteria in modern and ancient geochemical environments. Linking Mn(II) oxidation to cellular function, although still enigmatic, continues to drive efforts to characterize manganese biomineralization i.e. formation and deposition of oxides.

Recently, complexed-Mn(III) has been shown to be a transient intermediate in Mn(II) oxidation to Mn(IV), suggesting that the reaction might involve a unique multicopper oxidase system capable of a two-electron oxidation of the substrate. In biogenic and abiotic synthesis experiments, the application of synchrotron-based X-ray scattering and spectroscopic techniques has significantly increased the understanding of the oxidation state and relatively amorphous structure (i.e. δ -MnO₂-like) of biogenic oxides, providing a new blueprint for the structural signature of biogenic Mn-oxides (Tebo *et al* 2005). Mn(II)-oxidizing bacteria have been identified in a growing number of divergent phylogenetic lineages in the bacterial domain, such as Firmicutes, Proteobacteria and Actinobacteria (Tebo *et al* 2005).

5.4.12 Phosphate and silicate solubilizers

Like Fe- and Mn-oxidizers, phosphate and silicate solubilisers appear to exist and function in tandem (Figs 4.27 and 4.28). Phosphate metabolism could move hand in hand with silicate metabolism. Enhanced biological phosphate removal (EBPR) is a fundamental metabolic mechanism which is still poorly understood (Mino *et al.*, 1998). Phosphorus (P) is a key element that often limits bacterial growth in various freshwater and marine habitats (Farjalla *et al.*, 2002). Inorganic phosphate (Pi), or orthophosphate (PO₄³⁻), can serve as a direct source of P for essentially all physiological groups of microorganisms in both natural environments and laboratory media. Measurements of soluble phosphate in different aquatic environments, however, suggest that concentrations of bioavailable Pi are very low. Recent studies have revealed that Pi represents only a small fraction of soluble reactive P in natural waters and that even in

eutrophic systems, its concentration may be as low as 27 pM (Baldwin 1998). This is not surprising, since in a variety of aquatic systems, soils, and sediments, Pi bioavailability can be controlled by adsorption to metal oxides (Bjerrum and Canfield, 2002) and through chemical reactions with hydrous oxides, amorphous and crystalline complexes of Fe, Al, and Ca, and organic matter (Baldwin 1998). In particular, the reaction of Pi with Fe(III) oxides such as goethite can result in the precipitation of tenticite [$\text{Fe}_6(\text{PO}_4)_4(\text{OH})_6 \cdot 7\text{H}_2\text{O}$] or griphite [$\text{Fe}_3\text{Mn}_2(\text{PO}_4)_2 \cdot 5(\text{OH})_2$] depending on the solution and surface conditions. The latter findings entail important physiological implications for dissimilatory metal-reducing bacteria residing in zones with high concentrations of Fe (III) and Mn (III, IV) oxides, where the levels of bioavailable Pi may significantly limit growth. In that respect, utilization of other bioavailable forms of P may be the key to the ecological success of these bacteria. Alternative sources of P in freshwater and marine environments are organic phosphorus compounds that include phospholipids, phosphoproteins, and nucleic acids. It has been demonstrated that dissolved extracellular DNA constitutes a significant portion of the organic P pool, where DNA concentrations can range from 0.65 to 280 nM P. The main sources of dissolved nucleic acids in aquatic environments include phage-induced cell lysis and excretion by zooplankton feeding on bacteria. Earlier studies showed that the addition of DNA to natural water samples resulted in its degradation and incorporation into cells and sometimes in an increase in bacterial cell numbers (Pinchuk *et al* 2008 and references therein).

5.4.13 Anaerobic culturability

The alternate distribution of denitrifiers and nitrate reducers shows that distinct groups perform different phases of denitrification. Metabolites of one group are substrates to the other (Figs. 4.31 and 4.32).

Although predominately oxic, the presence of sub-oxic pockets allows the proliferation of anaerobic bacteria. Both oxidative and reductive cycle occur in tandem, however one of them is dominant in these systems. For example nitrification-denitrification couple exists in these sediments however nitrification dominates while denitrification happens in pockets, to complete the cycle. Multiple mid depth maxima and minima noted in all the cores indicated a non-steady transient behaviour of the anaerobic bacteria.

5.5 Spatial distribution

5.5.1 Bacterial response to contrasting geochemistry

In order to investigate whether geochemical, physiographic and lithological differences in two end-member sedimentary settings could evoke varied microbe-sediment interactions, two 25 cm long sediment cores from contrasting regions in the Central Indian Basin have been examined. Site TVBC 26 in the northern siliceous realm (10°S, 75.5°E) is organic-C rich with $0.3 \pm 0.09\%$ total organic carbon. Site TVBC 08 in the southern pelagic red clay realm (16°S, 75.5°E), located on the flank of a seamount in a mid-plate volcanic area with hydrothermal alterations of recent origin, is organic-C poor ($0.1 \pm 0.07\%$). Significantly higher bacterial viability under anaerobic conditions, generally lower microbial carbon uptake and higher numbers of aerobic sulphur oxidizers

at the mottled zones characterize core TVBC 26. In the carbon-poor environment of core TVBC 08, a doubling of the ^{14}C uptake, a 250 times increase in the number of autotrophic nitrifiers, a fourfold lowering in the number of aerobic sulphur oxidizers and an order higher of denitrifiers exist when compared to core TVBC 26. This suggests the prevalence of a potentially autotrophic microbial community in core TVBC 08 in response to hydrothermal activity. Microbial activity at the northern TVBC 26 is predominantly heterotrophic with enhanced chemosynthetic activity restricted to tan-green mottled zones. The southern TVBC 08 is autotrophic with increased heterotrophic activity in the deepest layers. Notably, the bacterial activity is generally dependent on the surface productivity in TVBC 26, the carbon-rich core, and mostly independent in TVBC 08, the carbon-poor, hydrothermally influenced core. The northern sediment is more organic sink-controlled and the southern more hydrothermal source-controlled. Hydrothermal activity and associated rock alteration processes may be more relevant than organic matter delivery in these deep-sea sediments. Thus, this study highlights the relative importance of hydrothermal activity versus organic delivery in evoking different microbial response in the CIOB sediments.

Prokaryotic processes are now known to be operating on geological timescales and culturable prokaryotes are reported to be stimulated at interfaces (Parkes *et al.*, 2005). This work reiterates the prevalence of such enhanced bacterial culturability in the CIOB that was earlier shown in the Eastern Equatorial Pacific (Parkes *et al.*, 2005; Meister *et al.*, 2007; Wang *et al.*, 2008). This study also demonstrates the occurrence of chemoautotrophic activity coinciding with geochemical and stratigraphic transition zones in both diagenetic and hydrothermally altered sedimentary settings.

5.5.1.1 Northern core TVBC 26

a. *Influence of organic carbon on microbial carbon uptake*

The comparison of a modern microbial autotrophic uptake profile with the palaeoproductivity profile shows a similar trend suggesting heterotrophy dependent on surface-based production. The microbial degradation and recycling of organic matter is evident in reactive layers 1 and 2 representing two halves of any redox cycle in metabolic zones (Fig. 2; Das *et al.*, 2010a, see Schultz, 2000 for detailed definitions). Interestingly, the occurrence of these processes is evident at the tan green colour transition zone (Konig *et al.*, 1997) and appears to have operated at *ca* 10,000 year time span on the Late Pleistocene-Holocene scale (age derived from ^{230}Th decay). Surprisingly, the biostratigraphic change at 180 ka BP also coincides with the tan-green mottled zone; however, its relationship with elemental carbon and nitrogen, if any, is not clear. Although, a clear dependence on surface derived organic matter is shown by the heterotrophic microbes of TVBC 26, the enhanced chemoautotrophic features at the reactive layers and tan-green transition show that this process is also operational.

b. *Bacterial response to pore-water geochemistry in tan green-mottled zone*

Non-steady state diagenetic processes due to downward diffusing oxidants, such as O_2 and NO_3^- , result in the depletion of initially deposited organic carbon. Both oxidized and reduced forms of nitrogen are produced in the active oxidation zones (Buckley & Cranston, 1988). More recently, the temporal shift of geochemical interfaces

from shallower temporary reactive to deeper layers result in mottle formation in predominantly detrital settings (Meister *et al.*, 2007, 2009).

Tan-green transitions in the sediment columns from the northern CIOB were reported to influence pore-water and sedimentary organic carbon profiles. Extensive nitrification coupled with oxic respiration and the possible involvement of bacteria was previously suggested (Nath and Mudholkar, 1989). However, the relevant direct microbial evidence is now presented in this study. Microbiologically, the zone is characterized by an increasing trend of ^{14}C uptake and higher values for the C/N-ratio, ATP, DVC-an and denitrifiers (Figs. 2, 5, 6 and 7A; Das *et al.*, 2010a). Higher C/N ratios in sub-oxic depths of sediments with TOC < 1% has been associated with bacterial oxidation of metals (Farrimond *et al.*, 1989) and reworking of residual organic matter.

Earlier studies on bacteria from these tan-green mottles at 20 to 25cm bsf highlighted their capability of showing different phases of nitrification (Ram *et al.*, 2001). Nitrate reduction coupled to oxidation of organic matter, followed by fixing of CO_2 is suggestive of recycling and conservation of available organic matter. The depleted NO_2^- concentration (Fig. 3A; Das *et al.*, 2010a) and its negative correlation to NO_3^- indicate coupled bacterial nitrification-denitrification process if explained traditionally. However, formation of dinitrogen and loss of nitrogen under the influence of reactive Mn (Luther III *et al.*, 1997) can be attributed to elevated C/N ratios at these depths. Bacterial chemo-denitrification is known to exist in oxygen containing sediments (Luther III *et al.*, 1997). Non-steady Mn diagenesis resulting in the enrichment of Mn below these sub-oxic or tan-green transition depths has been suggested earlier in these sediments (Pattan & Jauhari, 2001).

Organic carbon in the reactive layers (Fig. 2; Das *et al.*, 2010a) stimulates oxygen consumption by active microaerophilic or facultative anaerobic bacteria (eg. nitrifiers, nitrate reducers, aerobic sulphur oxidizers and heterotrophs) during oxic respiration. This oxic process is followed by nitrate reduction within the total 6cm thick overlapping reactive layers 1 and 2. Also, in these layers, manganese reduction possibly synchronizes with sulphide oxidation. Consequently, the resultant upward diffusion of dissolved metals could feed the nodule accretion process at the sediment water interface (See IVBC 20A pore-water profiles in Fig. 3B; Das *et al.*, 2010a).

The presence of iron-bacteria and manganese-bacteria in higher numbers, along with the thiotrophs, suggests the possible occurrence of sulphide-oxidation along with iron and manganese oxido-reduction in this diagenetic setting, especially at the mottled zone. These associations are common in hydrothermally altered sediments or diffuse flow systems (Bach & Edwards, 2003). While bacterially mediated Mn^{2+} oxidation by O_2 or NO_3^- may be restricted near oxic zones, processes like thiotrophic nitrate reduction in deep-sea settings are gaining importance. These processes over time lead to the conversion of tan green mottled zones dominated by facultative heterotrophs, manganese-oxidizers and aerobic sulphur oxidizers (Fig. 6A; Das *et al.*, 2010a). These bacteria conserve the organic matter chemolithotrophically by recycling (Stevens, 1997) and re-fixing CO_2 formed during breakdown of organic matter.

The occurrence of sulphide in some of these oligotrophic sediments highlights the greater importance of hydrothermal influence and requires renewed investigations. Although, the co-existence of sulphide and oxygen in “sub-oxic” or “oxic-anoxic” transitions are well known (Glazer *et al.*, 2006), the trends suggest that an inverse

distribution of oxygen versus sulphide in pore-waters may not always be true. Co-existence of detectable amounts of sulphide, ammonium and oxygen (Fig. 3B; Das *et al.*, 2010a) and the presence of manganese oxidizers and thiotrophic bacteria indicates possibility of co-occurrence (Wang *et al.*, 2008) or overlap of multiple metabolic zones (Canfield & Thamdrup, 2009). The present results reiterate the importance of sulphide and a possibly underestimated hydrothermal influence in the formation process of ferromanganese nodules (cf. Glassby, 2006).

Alternatively, rock alteration and volcanic degassing could be a significant process in station TVBC 26 due to its proximity to the Trace of Rodrigues Triple Junction. Under such conditions, autotrophy at the mottled zones could be associated with fluid percolation through these sediment strata (Sizaret *et al.*, 2009). Even then, station TVBC 26 would not be an independent chemoautotrophic system as a major fraction of the organic flux is derived from the highly productive South Equatorial Boundary Current-driven surface waters. Core TVBC 26 would be analogous to hydrocarbon rich layers mutually influenced by organic matter rain and hydrothermal fluid flow. However, the scale and extent of the processes could be highly reduced.

5.5.1.2 Southern core TVBC 08

a. *Influence of organic carbon on microbial carbon uptake*

The microbial autotrophic uptake profile of core TVBC 08 shows no relationship to the palaeoproductivity profile suggesting greater chemoautotrophy and independence from surface based production (Fig. 8; Das *et al.*, 2010a). The depletion of organic content and the additional influence of hydrothermally derived pore-fluids appear to have

triggered a greater microbial carbon uptake. A net autotrophic bacterial community with higher nitrifiers and nutritionally flexible heterotrophs inhabit the southern TOC-poor sediments of TVBC 08. These observations are further supported by a positive correlation ($p > 0.05$) between ^{14}C uptake and total bacterial counts. The greater number of FDC at the TOC-depleted lower depths could suggest the utilization inorganic substrates in hydrothermally altered fluids promoting greater autotrophic activity.

b. Influence of hydrothermal alterations on pore-water and bacterial activity

Mid-plate volcanic and hydrothermally altered area, TVBC 08 (Nath *et al.*, 2008, Iyer *et al.*, 2007, Mascarenhas-Pereira *et al.*, 2006) hosts a predominantly chemoautotrophic microbial population. The possibility of nitrogen species emanating out of the circulating hydrothermal fluids (Gieskes *et al.*, 2002) and advecting upwards before spreading laterally at 4 to 8cm bsf (Fig. 3A Das *et al.*, 2010a) due to diffusive transport at the stratigraphic interface (Gieskes *et al.*, 2002) is explored in the present work.

Fluid phase separation during hydrothermal alterations is known to produce higher and lower phases of solutes. While the higher phases rapidly migrate by advection towards the surface, presumably along cracks and faults, the lower ones get transported laterally along more porous zones in the sediments. Here they may get utilized by bacteria. A recent study by Nath *et al.* (2008) interpreted the influence of neutral chloride type hydrothermal fluids to be predominant in these altered sediments. Intense hydrothermal alteration features were reflected in 1) the depleted sedimentary organic carbon also observed in the present study, (see Fig. 2), 2) dissolution features of

radiolarian skeletons, 3) the presence of altered minerals such as smectite and zeolites, and 4) distinctly different magnetic properties in the altered sediments. An excess of ^{210}Pb over its parent was recorded in the lower semi-indurated sediments. Bioturbation and slumping of older sediments from the shallower portions of the seamount were ruled out for the $^{210}\text{Pb}_{\text{exc}}$ since the sediments lacked benthic biota, organic matter and detectable carbonate content (Nath *et al.*, 2008).

The pore-water PO_4^{3-} in TVBC 08 is lower than TVBC 26 perhaps because bulk phosphate is higher. However, the presence of a PO_4^{3-} concentration $> 1\mu\text{M}$ in organically depleted environments with distinct enrichment in Fe in an oxidized state, compared to the pelagic clays occurring in the CIOB (Nath *et al.*, 2008) indicates possible hydrothermal origin and co-precipitation with the metal oxides (Yamagata *et al.*, 1991; Karl, 1995). The SiO_3^{2-} concentrations show little variation and a lower diffusional gradient in TVBC 08.

ATP values (Fig. 5; Das *et al.*, 2010a) are similar to the range reported from Guaymas Basin (Table 1; Das *et al.*, 2010a). Although extensively reported from waters and bacterial mats of vent fields, reports on ^{14}C incorporation rates of whole sediments are still scanty. It is noted that ^{14}C incorporation rates (Fig. 7; Das *et al.*, 2010a) of CIOB sediments when normalized to bacterial numbers are similar to some water samples of Juan de Fuca and white smokers of the 21°N East Pacific Rise (Table 2; Das *et al.*, 2010a).

The contribution of LOM and faunal number to higher measurements of ATP at TVBC 08 is minimal. Negligible numbers of macrofauna and meiofauna (Ingole *et al.*, 2005) suggest that there could be little contribution by these organisms. Moreover, ATP

does not relate to any of the other parameters measured suggesting that the higher ATP in the south could be due to more hydrothermally produced analogues rather than being organically derived (Yamagata *et al.*, 1991; Liu *et al.*, 1982). The high ATP in TVBC 08 (Fig. 5, Table 1; Das *et al.*, 2010a) could therefore be due to the inclusion of large amounts of pyrophosphate or polyphosphates formed during rapid cooling in hydrothermal systems (Yamagata *et al.*, 1991). The presence of Fe in an oxidized state (Nath *et al.*, 2008) and the anomalous bulk phosphate (Nath *et al.*, 2005) suggests scavenging of hydrothermal phosphorus by iron, leading to the formation of pyrophosphate and its subsequent utilization as an alternate pathway for channelling geothermal-based energy in the biosphere (Liu *et al.*, 1982).

The hydrothermal origin of ammonium or other reduced nitrogenous species from deeper layers is indicated by the pore-water profiles of NO_2^- and NO_3^- . Higher total nitrogen values and a C/N ratio <1 at 20 to 25cm bsf both indicate excess of nitrogen. The high C/N ratio and depletion of NO_2^- and NO_3^- is probably caused by the preferential loss of N during metamorphic volatilization (Bebout & Fogel, 1992) at the upper stratigraphic transition between Pleistocene (10 kyr BP – 1.8Myr BP) and Tertiary sediments (1.8 Myr BP – 65Myr BP; Fig. 2 Das *et al.*, 2010a). Where there is minimal contribution of organic matter, this excess can only be derived from hydrothermal fluids. Similar findings have been reported from Suiyo Seamount at Izu-Bonin backarc system (Takano *et al.*, 2004) and the shallow vent systems of Vulcano Islands (Gugliandolo & Maugeri, 1998). Rapid conversion of dissolved NO_3^- and NO_2^- to NH_4^+ rather than to N_2 , particularly in the presence of Fe and Ni as seen in ODP Leg 201 pore-water data (Smirnov *et al.*, 2008), could explain the abrupt fluctuations of nitrogen. Different

transport routes for higher and lower phases of hydrothermally altered fluids while cooling can produce distinct changes both in bacterial number and activity. These alterations occur (Figs. 5, 6 and 7; Das *et al.*, 2010a) at sediment layers with varying porosity and pH (Figs. 2 and 3; Das *et al.*, 2010a; Gieskes *et al.*, 2002).

The high peak of the C/N ratio with low TOC (Fig. 2; Das *et al.*, 2010a) and LOM in the upper 2 to 4 cm bsf (Fig. 4; Das *et al.*, 2010a) corresponds to the highest ATP, ammonia oxidizers and aerobic sulphur oxidizers (Figs. 5 and 6; Das *et al.*, 2010a). This layer is sandwiched between carbon uptake maxima (Fig. 7; Das *et al.*, 2010a) suggesting chemolithotrophic utilization of inorganic substrates made available during phase separation of solutes.

Venting activities can produce ammonia where nitrifying bacteria can thrive (Karl, 1995). The higher number of autotrophic nitrifiers and the significant correlation between ammonium oxidizers and aerobic sulphur oxidizers suggests a more hydrothermal origin for the ammonium feeding the nitrite oxidizers (Karl, 1995; Wirsen *et al.*, 1986). The presence of large numbers of thiotrophs, iron-oxidizers and manganese-oxidizers indicate that hydrothermal alterations or diffuse flow might influence the sulphide-oxidation and iron metabolism in this core (Bach & Edwards, 2003).

Synchronization of carbohydrate maxima with the zone of high ^{14}C uptake at 15 to 20 cm bsf is possibly suggestive of chemoautotrophy by mixotrophs. Large fractions of heterotrophic bacteria inhabited this lower non-dateable stratigraphic transition within the Tertiary sediments as these sediments are too old to be amenable to carbon or thorium dating. Higher adaptability and resilience of bacteria are associated with relatively

oligotrophic sediments (Harder & Dijkhuizen, 1982; Goltekar *et al.*, 2006) like the organically depleted core TVBC 08. Similar unexplained high heterotrophic populations have been reported in some earlier findings in vent sites with low organic carbon (Karl, 1995).

Although the nitrifiers, aerobic sulphur oxidizers and heterotrophs exist in large numbers and contribute partly to ATP and ^{14}C uptake, they do not have a statistically significant relationship with the pore-water nitrogen species or the C/N ratio in TVBC 08. This is contrary to the diagenetic TVBC 26 where these retrievable bacteria show a statistically significant relationship with other biochemical and pore-water parameters. The results indicate the predominance and activity of a distinct functional group capable of exhibiting chemolithotrophy through multiple metabolic pathways. These microbes flourish in the remnant inorganic substrates derived from explosive hydrovolcanism that geochemists believe to have occurred about 200 years ago (Nath *et al.*, 2008).

In CIOB sediments, a decrease in organic matter tends to elevate microbial carbon uptake in the bacterial communities. The northern core TVBC 26 is predominantly heterotrophic with chemosynthetic signatures at the tan-green mottled zones. The bacterial activity is only partially dependent on the surface productivity at core TVBC 26. The depth of reactive layers and tan-green mottled zones coincides with high chemosynthetic activity and lower palaeo-surface productivity. The autotrophy prevailing in the tan-green transition is analogous to the organic matter fossilization and hydrocarbon formation in organic rich sedimentary settings (Ma *et al.*, 2006; Campbell, 2006).

The southern TVBC 08 is predominantly autotrophic with heterotrophic microbial signatures in the deeper layers. Here chemoautotrophy is totally independent of surface productivity. The heterotrophy in the deeper parts of southern core TVBC 08 is possibly akin to the formation of new degradable organic compounds in hydrothermal settings. This system is possibly analogous to settings like the Loihi Seamount. Further study of this location may provide interesting insights into tracing pre-biotic origins and explorations for lunar, martian or jovian planetary systems (Goodman *et al.*, 2004).

The role of thiotrophs in deep-sea sediments is prominent in both diagenetic and hydrothermally altered sediments. Processes like thiotrophic nitrate reduction may be more influential in the northern TOC and sulphide-rich sediments. The data highlights the necessity of renewed investigations involving pore-water NH_4^+ , HS^- , Mn and Fe in oxic conditions. Thiotrophs in hydrothermally altered sediments or diffuse flow systems might be influencing sulphide-oxidation and iron metabolism. The presence of large numbers of iron-oxidizers, manganese-oxidizers and thiotrophs at the mottled zones of TVBC 26 and in hydrothermally altered core TVBC 08 indicate their close relationship to rock alteration and mineralization processes. Like spatial variations, temporal variations are also obvious in the deep-sea abyssal environment.

5.6 Temporal Distribution

5.6.1 Inter-annual variations conceal seasonal variations in microbial and biochemical parameters in Central Indian Basin

In depth understanding of the microbial interactions with sediment biochemistry would be prospective for sustainable harnessing of mineral resources with minimal effect

on the system. Hence, to examine if the deep-ocean basins responded to annual and seasonal changes, observations were carried out in the Central Indian Basin, including the Indian Ocean Nodule field (IONF). The parameters analysed for this study were total bacterial counts, bacterial retrievability, Adenosine Triphosphate (ATP) and Labile Organic Matter (LOM). Variations in the basin were examined between April, 2003 (EVDC-I) and April, 2005 (EVDC-II) for inter-annual changes and between April, 2005 (EVDC-II, Austral Winter) and December, 2007 (EVDC III, Austral Summer) for seasonal influence. Statistically significant differences in microbial ($p < 0.01$) and biochemical parameters ($p < 0.01$) were observed between EVDC-I and EVDC-II, suggesting inter annual temporal variations. Between EVDC-II and EVDC-III there was distinct variability in microbial ($p < 0.01$) and biochemical parameters ($p > 0.01$), which could be attributed to seasonal effect. Thus, variations with greater significance were noticed in higher number of parameters (4/6 parameters, $n=35$), annually, than seasonally (3/6 parameters, $n=100$). Consequently, the deep-sea bed apparently exhibits both seasonal and annual changes with annual variations sometimes surpassing the seasonal ones in the temporal and spatial context examined. Inter-annual variations in bacterial activity are generally more pronounced in the deep-sea environments (Eardly *et al.*, 2001). Eardly *et al.*, 2001 identified no seasonal variation in bacterial activity but pronounced inter-annual variability. In the CIOB although seasonal variations were observed, inter-annual variations surpassed the seasonal ones.

Sedimentation of organic material from the euphotic zone is the main energy input into the abyssal benthic food-web (Rowe *et al.*, 1991; Pfannkuche, 1992; Deming and Yager, 1992). The utilization of the organic input into the abyss by benthic organisms

depends on the age and the composition of the detritus (Lochte, 1992). The main contribution to degradation of organic material in deep-sea sediments comes from micro-organisms, which represent up to 90% of the benthic biomass (Tietjen, 1992; Boetius 1995).

Very low amounts of available food material and other physico-chemical extremities have made the deep-sea environments unusually diverse in terms of species and versatile with respect to physiological activity (Vlatcheslav, 2005).

Earlier studies on this region had been restricted to a few locations and a simulated experiment had been conducted in CIOB to understand the ecological responses to artificial disturbance (Nair *et al.*, 2000; Raghukumar *et al.*, 2001; Loka Bharathi and Nair 2005).

The abyssal environment of the CIOB shows both inter-annual and seasonal changes. The inter-annual variations in the basin surpasses the seasonal variations as significant differences were noticed in higher number of parameters (4/6 parameters, n=35), annually between EVDC I and EVDC II, than seasonally between EVDC II and EVDC III (3/6 parameters, n=100).

The TC and the heterotrophs kept progressively and significantly increasing from EVDC I to EVDC III. The ATP on the other hand decreased drastically by one to two orders during the same time. In general it is interesting to note that both the ammonium oxidizers and nitrite oxidizers were not influenced by seasonal variations in the given time frame significantly. However, nitrite oxidizers showed significant annual variations with EVDC I showing the lowest number. Labile organic matter showed no annual variation but significant seasonal variations, with the lowest values during EVDC III or

austral summer. It appears that the increase in TC is due to the increase in heterotrophs, which consume the labile organic matter. The seasonal variation for TC was significantly higher for EVDC III at $p < 0.001$

Interrelationships between the parameters during EVDC I, were limited to NI and NII alone (36%, $p > 0.001$) between the two groups. The relationship increased during EVDC II with variants controlling each other up to 92% ($p > 0.001$). Heterotrophs related to nitrifiers (21-32%, $p > 0.001$). During EVDC III strong positive relations between all microbial parameters showed their interdependence. The LOM shows very weak positive correlation with microbial parameters during EVDC I, which changed from weak negative relations during EVDC II to very strong negative relations during EVDC III. Thus apparently there is a progressive shift from a net LOM producing community to an LOM consuming community from EVDC I to III. This is also highlighted by the increasing dominance of heterotrophs during the said time-span. The relationship between the two nitrifier groups increases from EVDC I to II. During EVDC III, the ammonium oxidizers correlate equally to the nitrite oxidizers and heterotrophs at 59%, $p < 0.001$. It appears that the ammonium oxidizers are a ubiquitous standing population not significantly affected by inter-annual and seasonal changes in the CIOB. However, the distribution of the nitrite oxidizers shows a gradual succession within the given temporal and seasonal time-frame. The coupling of the nitrite oxidizers with the ammonium oxidizers reduces from EVDC I to EVDC III. During EVDC III these nitrite oxidizers appear to be more related to the heterotrophs. The change from the ammonium oxidizers to nitrite oxidizers is an annual variation and appears more significantly drastic rather

than the gradual take over by the heterotrophs. The increased dominance of heterotrophs and their consumption of LOM is therefore a gradual seasonally influenced aspect.

Interestingly the present data-set show lack of correlation between the nitrifying populations and ATP for all the sampling seasons, while the heterotrophs showed very strong correlation with the energy currency during EVDC III. This indicates that heterotrophy dominated autotrophy during the austral summer.

The present study appears to validate the hypothesis of the experimental study of Ram *et al.*, 2001 with a nitrifying bacterium exhibiting both the phases of nitrification. The authors suggested a common population diverging into two groups as performing carbon fixation and nitrification by the same group could prove energetically expensive. The concept of Ram *et al.*, 2001 is helpful in elucidating the ecological succession in the present context. The ammonium oxidizers appear to be a primary population which initially performed the multiple functions. With inter-annual and seasonal variation these organisms showed a diverging succession to fragment the nitrite oxidizers and the heterotrophs.

The more detritally influenced Northern CIOB shows greater seasonal fluctuations than the hydrothermally influenced south especially with respect to ATP and labile organic matter. The potential autotrophic populations like ammonium oxidizers are omnipresent and unaffected by annual and seasonal change suggesting abiogenic source of ammonia. Consequently, the nitrite oxidizers are also not influenced by seasons.

The total bacterial counts and heterotrophs are seasonally influenced and are greatest during the austral summer. The heterotrophs however show a progressive

increase from EVDC I to III especially in the Southern pelagic red clay dominated stations.

EVDC I is strange though, in the fact that the ATP is measurable at $\mu\text{g g}^{-1}$ as compared to the usual ng g^{-1} dry sediment concentrations of the CIOB. The heterogeneity in the LOM marked by large deviations is unusual during this sampling. The values and trends surpass all records of microbial and biochemical studies in the CIOB over the last one decade. After carefully ruling out variations due any technical lacunae, we are convinced that EVDC I had been influenced by major phenomenal natural disturbance, which at the moment we are not able to accurately associate. However, the CIOB has been experiencing severe geo-catastrophic events in the recent past. The 15 July 2003 large earthquake (M_w 7.6) at Mid-Indian Ocean at Carlsberg Ridge (Antolik *et al.*, 2003), tectonic activation Rodrigues Triple junction, and the $>M$ 9 earthquake of 26 December 2004 that generated the devastating tsunami occurred in proximity of four plates – two oceanic (Indian, Australian) and two continental (Burma and Sunda) plates. It has been suggested that the Indian Ocean geodynamics is undergoing irreversible changes of major consequence continuing M 4–7 aftershocks (more than 9700) (Mukhopadhyay and De, 2005). The extreme proximity of these events to the EVDC I sampling in April 2003 and EVDC II sampling during March-May 2005 appear to be a predominant if not the sole cause for the shift of dimensions in microbial environment and activity.

These sequences of geo-tectonic disturbances have triggered the evidently discernable ecological succession in the microbial community of CIOB. Further studies are underway to suitably substantiate this hypothesis.

The ATP and LOM indicate that the biomass and the organic matter nature in northern CIOB are more detrital and seasonally influenced. Temporally, autotrophic potential decreases from EVDC I to EVDC III, while spatially the southern hydrothermally influenced stations are more autotrophic. The progressive increase in heterotrophic population, which is more pronounced in south, possibly indicating an ecological succession after catastrophic events like benthic storms or earthquakes. Annual variation in CIOB from April 2003 to April 2005 is significantly more intense than seasonal variation between April 2005 (austral winter) to December 2007 (austral summer). Geologists and geophysicists nationally and globally are in constant effort to equate several unsolved queries about sudden reactivation of the Indian Ocean lithosphere. The present data set suggests that microbial biogeochemistry and ecology needs better understanding about the possible shifts in microbial biomes, their true extent and implications on the “irreversibly” (Mukhopadhyay and De, 2005) changing lithosphere at the CIOB.

5.7 Bacterial activity in relation to cell morphology sediment-biochemistry geotechnical properties and sediment texture

This study focuses on the distribution of two main morphological forms, cocci and rod morphotypes, in the total direct counts of bacteria vis-à-vis the textural and geotechnical properties. Geometrical constraints, mechanical interactions and consolidation of deep sediment sequences may restrict bacterial movement and activity (Fredrickson *et al.*, 1997; Rebata-Landa & Santamarina, 2006), limit nutrient transport (Wellsbury *et al.*, 2002) as well as diminish space availability (Zhang *et al.*, 1998). The

effects of all these properties on the sediment biochemistry and bacterial abundance have been examined here.

Enzymatic properties of bacterial isolates showed that the rods were capable of degrading relatively more recalcitrant compounds in the deeper layers. Competition for labile organic substrates by coccoidal forms in the surface layers could have restricted the rods to the deeper regions. Geotechnical properties had opposite influence on the distribution of coccoidal and rod forms of bacteria. Rods were affected negatively by water content/porosity and positively by wet bulk density suggesting their preference for deeper niches with more compacted sediments.

The bacterial distribution and activity along the depth of the sediment could be due to the influence of preferential paths in transport through the sediment profile (Abu-Ashour *et al.*, 1994), limited input of fresh organic carbon (Suess *et al.*, 1980; Danovaro *et al.*, 1999; Dixon & Turley, 2002) and/or use of recalcitrant old buried organic matter by deep bacteria (Zhang *et al.*, 1998; Parkes *et al.*, 2000; Wellsbury *et al.*, 2002). However, bacteria adapt to changes in their immediate surrounding environments by undergoing morphological differentiations due to differences in the organic nutrients (Young, 2006) and their concentrations. Some microbes respond by increasing the size of individual cells when nutrient availability is more, yet others do not change their size. Under starvation or nutrient depletion the cells shrink in size and yet others form long filaments. Besides, it is the quantity and quality of LOM and not TOM that is responsible for density of organisms (Danovaro *et al.*, 1993).

Culturable representative bacterial isolates checked for enzyme expression indicated that the rod shaped morphotypes were capable of degrading gelatin and DNA

unlike the coccoidal forms that preferred starch and *p*-nitrophenyl phosphate. This property suggested that the rods, although less in number, were capable of degrading relatively more recalcitrant compounds in the deep-sea sediments thus substantiating their abundance in the deeper layers where the denser and recalcitrant substrates tend to accumulate.

Natural processes that can disturb deep-sea sediments are bioturbation, sedimentation and physical mixing with horizontally advected material (Turnewitsch *et al.*, 2000) and re-suspension by near bottom currents (Lampitt, 1985). Artificial disturbances are brought about by deep-sea mining activities. Simulated experiments have been conducted in the Pacific and Indian oceans to evaluate the effect of natural and artificial disturbance in the deep sea (Thiel & Forschungsverbund, 2001; Sharma *et al.*, 2001). The immediate impact observed on sediment characteristics has been highlighted by a number of workers (Sharma *et al.*, 2001; Valsangkar, 2001; Ingole *et al.*, 2001). Long-term changes have shown mixed effects of sediment disturbance (Raghukumar *et al.*, 2006). Interestingly, in the present study we have been able to project the possible effects from a new perspective against a backdrop of interactions between parameters hitherto not examined.

5.8 Bacterial role on geological time scale: Early diagenesis and bacteria

The study has also examined the possible role of bacteria on geological time scale (Das *et al.*, 2010a). Early phases of diagenesis are controlled by several abiotic and biotic factors, an important component being bacteria. Multiple phases of nitrification and oxic respiration are observed corroborating to previous results (Ram *et al.*, 2001, Nath and

Mudholkar, 1989). Sub-oxic mottles have been discussed in literature as aspects of paleoproductivity, preservation, and current bacterial activity. The results suggest that present bacterial activity in this otherwise geologically "old" sediment sequences are significant. An interesting functional synergy between the ammonia oxidizers and *Thiobacillus denitrificans* like-organisms is seen in their ability to utilize C₁ compounds like formaldehyde.

5.9 Activity of bacteria in sediments

5.9.1 Heterotrophic activity

5.9.1.1. Hydrolytic enzyme activity

In CIOB the isolates from the siliceous and carbonaceous oozes hydrolysed DNase and lipase, while the pelagic red clays were more versatile because of paucity of organic matter (Table 4.4). Bacteria are known to digest various organic compounds with specific extracellular hydrolases (Chrost 1991). Only monomers and small oligomers can be incorporated by bacterial cells and participate in their physiological pathways. Therefore extracellular enzymatic hydrolysis is the key process in the degradation of organic material (Billen 1982, Meyer-Reil, 1991). Since the production of most of the extracellular hydrolases are substrate inducible (Priest, 1984) the potential hydrolytic activity of specific enzymes may reflect the availability of their respective organic substrates.

5.9.1.2. *Carbon substrate utilization*

Metabolic profiling of BIOLOG ECO plates showed that the deep sea sediments utilized relatively low numbers of substrates. Consequently, it is suggested that the deep sea bacteria are either obligate chemolithoautotrophic or these substrates are alien to the deep-sea microbial community (Table 4.5). This was more so with the calcareous ooze and pelagic red clay. Concomitant with the study of carbon substrate utilization it would be pertinent to understand the patterns of phosphorus uptake and release. Alkaline phosphatase activity was thus examined.

5.9.1.3. *Alkaline Phosphatase activity*

In order to test the hypothesis that pore water phosphate in Central Indian Ocean Basin (CIOB) sediments is controlled intrinsically by bacterial enzymes, pore water phosphate and alkaline phosphatase (ALP) activity were measured. Sediment cores along north-south and top-bottom gradients were chosen for the study (Figs 4.40, 4.41A, 4.41B and 4.42). The basin-scale patterns of ALP activity showed ubiquitous distribution of the enzyme activity in CIOB sediment cores. Latitudinal gradients in activity with decreasing activity from north to south was discernible with maximum enzyme activity generally at the surface in the north, and deeper layers in the south. Definite longitudinal or down-core gradients in activity were not evident. Both phosphate and phosphatase relate negatively with total count of bacteria (TC) suggesting that they apparently partition their energy either for enzymatic activity or multiplication. Moreover, enzymes are known to be expressed during the lag phase (Pirt, 1975). It is therefore inferred that sediment ALP could play a significant role of supplying inorganic phosphate and organic

carbon to CIOB sediments and that direct bacterial participation could complement the process. The contribution of the hydrothermal component in the pore-water and microbial geochemistry has been hitherto under-examined and the present work discusses these interactions for the first time in deep sea sediments of CIOB.

Phosphorus is an essential nutrient for all living forms in the form of ions like PO_4^{3-} and HPO_4^{2-} . Most importantly, it is a part of genetic elements like DNA, RNA and energy storage molecules like ATP and ADP. ALP enzymes are significant components of most marine bacteria and are responsible for the solubilization of bound phosphate in marine environments. It is therefore inferred that sediment ALP could play a significant role of supplying inorganic phosphate and organic carbon to CIOB sediments and that direct bacterial participation could complement the process.

Both hydrothermal and volcanic processes are known to influence the P- cycle by scavenging the dissolved phosphate and precipitating it as particulate phosphate (Feely *et al.*, 1990; Martin and Russel, 2007).

The enzyme activity and pore-water phosphate have a positive relation suggesting that ALP activity could be responsible for releasing the bound phosphate in CIOB sediments. It is possible that the release of the dissolved phosphate is not localized but gets diffused spatially and precipitated elsewhere. Significant difference in the enzyme activity was not evident, but the concentration of the enzyme was usually higher at the greater depths, in the southern sector. The above result is in contrast to the observations made by Taga and Kobori, (1978), Poremba, (1994); Boetius, (1995); and Hoppe, (1999) who reported a decrease in enzyme activity with increasing depth.

Phosphatase relates negatively to ATP suggesting that the variation in ATP is responsible for the variation in phosphate. With the increase in live biomass, phosphate concentrations tend to decrease because soluble phosphate is taken up by live cells. This parameter is also controlled negatively by LOM which suggests that ATP denoting living cells tend to decrease the LOM concentration. Also pore-water phosphate shows positive relation with the proteins which indirectly suggests that enzymes which contribute to the proteins in the sediments facilitate the release of bound phosphate. This property of ALP may be very useful to deep sea ecosystem which is generally depleted in organic matter (Carlsson and Graneli, 1993). ALP activity detected in the sediments would include both free and organism-associated enzymes. Some free enzymes might be secreted by phosphatase producing organisms and others might be liberated from non-viable and lysed cells (Kobori and Taga 1979). When the inorganic phosphate concentration is insufficient to support the growth of organisms, ALP are produced in response to obtain a supply of this essential nutrient (Takano *et al.*, 2005).

It has been observed that in the more oligotrophic realms, bacteria show lower motility, accumulate lipids, and are under lower grazing pressure. In contrast, copiotrophic realms show the opposite pattern. Oligotrophs may have evolved to minimize the number of energy intensive transporters and instead rely on a relatively smaller number of broad specificity and high affinity ATP-binding cassette (ABC) transporters. Specific cluster of orthologous groups (COG) are more in the copiotrophic bacteria (Lauro *et al.*, 2009). These observations explain the behaviour of the relatively more oligotrophic bacteria in the southern CIOB and relatively more copiotrophic bacteria in the TOC- richer northern CIOB.

In CIOB sediments therefore, inorganic phosphate is possibly made available to biota, by variable rates of ALP activity, depending on factors like lability of organic matter, hydrothermal influence on pore-water geochemistry and also sediment geochemistry. ALP activity thus could serve a dual ecological function of supplying the pools of both P and organic C simultaneously and sustaining deep sea ecosystem of CIOB with these nutrients.

Heterotrophic activities are followed by autotrophic activities in the next few passages.

5.9.2 Autotrophic activity

5.9.2.1. Formaldehyde tolerance

Formaldehyde is common fixative used for fixing microbes before counting. Formaldehyde is generally used as a preservative for bacteria at $\geq 2\%$ concentration. However, it is also known to be an intermediate in many metabolic reactions. Therefore bacteria have been known to tolerate the compound at low concentrations. Many microbes are known to oxidize (dissimilate) or utilize (assimilate) this compound. These formaldehyde utilizing bacteria are essentially methylotrophs that utilize formaldehyde both by dissimilation and assimilation. Under dissimilatory processes two possibilities are known for the oxidation of formaldehyde to CO_2 in methylotrophic bacteria. One of these is a linear pathway and involves the sequential action of enzymes formaldehyde dehydrogenase and formate dehydrogenase. The second is a cyclic pathway that involves the condensation of the C_1 compounds with a five carbon acceptor molecule, followed by

the oxidation of the resulting six-carbon compound. This cyclic pathway essentially involves the RuMP cycle (Antony, 1982).

The assimilation of formaldehyde involves cycles in which condensation reaction between a C₁ compound and a multicarbon compound occurs, followed by the regeneration of the acceptor molecule and production of a C₃ compound (Antony, 1982). Assimilation of formaldehyde involves RuMP, Serine or RuBP pathways. Methane from abiotic and biotic sources may come in contact with oxygen to form C₁ compounds like formaldehyde.

Environmental studies carried out on these bacteria (Hanson, 1980; Rudd and Taylor, 1980) showed that they exist widespread in nature wherever oxygen and one-carbon compounds coexist. Methylophs are obligate aerobes but a few methanol utilizers are capable of denitrification and may exist in anoxic denitrification zones. In both freshwater and marine aquatic environments methane oxidation activity and population of methanotrophs are stratified in a narrow band at the oxic-anoxic interface where concentrations of methane and oxygen is highest (Hanson, 1980; Rudd and Taylor, 1980; Ward *et al.*, 1989).

The deep-sea sediments of the CIOB harbour an interesting niche of formaldehyde utilizing bacteria (Fig 4.33). These facultative C₁ utilizing bacteria fix carbon by the Calvin-Benson-Bassham cycle. They may play a major role in the formation of mottled zones and thus in sub-oxic diagenesis as hypothesized by earlier studies (Nath and Mudholkar, 1989; Konig *et al.*, 1997). Alternatively, this strange niche distinction may be an effect of hydrothermal fluid-alterations (D'Hondt *et al.*, 2002, 2004) and its effects on infiltrated organic matter otherwise known as hydrothermal

diagenesis. Hydrothermal fluids are a source of methane and other organic gases that are derived from mantle processes. CIOB sediments are generally poor in organic content (~0.3%) and lie ca. 1000m below the calcite compensation depth (Gupta and Jauhari, 1994). Lateral diffusion of hydrothermally derived fluids (D'Hondt *et al.*, 2002, 2004; Ma *et al.*, 2006) might play an important role in the abundance, functional diversity of these bacteria over space and time. The behaviour of these microbes in regimes that are depleted in organic matter and carbonate content, under oxic and sub-oxic conditions would be helpful in understanding processes like diagenesis and/or hydrocarbon formation in more reduced and organically enriched environments.

In this study, a detail of a surprising encounter with bacterial community that does not get arrested but rather stimulated by formaldehyde is highlighted. Their distributory pattern on a basin scale is examined along with laboratory experiments that measure carbon fixation, RuBisCO activity and formaldehyde utilization by representative isolates and the implications discussed.

Chemoautotrophic utilization of formaldehyde with the involvement of RuBisCO enzyme activity is widespread in CIOB sediments. In CIOB, primary production is limited to chemolithotrophy, where energy is derived from redox reactions involving inorganic substrates. With a wide array of potential electron donors (e.g. H₂, CH₄, NH₄⁺, H₂S, Fe²⁺ and other reduced metals) and acceptors (e.g. O₂, NO₃⁻, SO₄⁻², CO₂, Fe³⁺ and other oxidants) often present (Vick *et al.*, 2010) in cold and perpetual darkness, a number of metabolic zones may overlap and co-occur (Wang *et al.*, 2008 ; Canfield and Thamdrup, 2009). Formaldehyde is an intermediate between methanogenesis and methylotrophy via shunts like the tetrahydromethopterin (H₄MPT). Formaldehyde

reduction rather than $\text{CH}_3\text{-S-CoM}$ ($\text{CH}_3\text{-S-coenzyme M}$) reduction to CH_4 with H_2 occurs depending on co-factor 420. The reduction of methylene H_4MPT reduction to methyl- H_4MPT requires F_{420} as electron carrier. The disproportionation of formaldehyde to CO_2 and CH_4 rather than formaldehyde reduction with H_2 to CH_4 or methanogenesis from acetyl-CoA was found to be dependent on methanofuran (Fischer and Thauer, 1989). To this end, distribution and chemosynthetic potential of formaldehyde utilizing bacteria in CIOB sediments were examined together with experimental evidence from cultured bacterial isolates.

The sediments showed presence of motile bacteria, in 2% formaldehyde fixed samples stained with 0.01% acridine orange under epifluorescence microscope. The motile formaldehyde utilizing bacteria generally occurred 15 cm below sea floor. These populations were seen to exist at the transition of sediment colour types commonly referred to as the sub-oxic or tan-green mottled zone (Nath and Mudholkar, 1989; Konig *et al* 1997). These colour transition layers are analogous to oxic-anoxic transitions of interfaces and are probably dominated by both electron donors and acceptors, thus harbouring these extremely tolerant mixotrophic bacteria capable of multiple metabolic activity. In the northern latitudes of 10-12°S, they occur at the transition of 10YR4/2 and 10YR5/4. In the central latitudes of 12-14°S, they occur at a wider variety of colour transitions between 10YR4/2, 5Y5/2, 5YR3/4 and 10YR5/4. At the southern latitudes, they become rarer and occur at the deepest layers of 5YR3/4.

In the present study the formaldehyde utilizers exist at the tan-green mottled zones where oxygen and low amounts of sulphide and ammonium co-exist (Das *et al.*, 2010a). The tan-green transition layer is a feature that has been formed either by the

microbial diagenesis or is an effect of rock alteration feature probably induced by fluid flow from the fracture zones, in this case the trace of the Rodrigues Triple Junction (Kamesh Raju and Ramprasad, 1989; Nath *et al.*, 2008). It is difficult to suggest whether these microbial activities are a product of diagenesis, paleo-productivity and preservation of the low amount of organic matter, or fluid flow and alterations, or a complex combined effect of all of these processes.

Earlier studies using fluorescent antibodies to enumerate particular species of methanotrophs show that these populations are diverse and that they vary from habitat to habitat (Abramochkina *et al.*, 1987; Galchenko *et al.*, 1988). In general, dissolved oxygen concentration does not appear to be a limiting factor (Kuivila *et al.*, 1988). However, in some specific cases, it appears that methylotrophic populations can become nitrogen limited and therefore may be restricted to the zone of dissolved oxygen tension that is sufficiently low to allow microaerophilic nitrogen fixation to occur (Rudd and Taylor, 1980). The tan-green mottles are often nitrogen limited with high C/N ratio of about 15 (Das *et al.*, 2010a).

Thus it is suggested that these facultative C_1 degrading, carbon fixing bacteria could play a major role in the mottled transition zones and thus sub-oxic diagenesis as hypothesized by earlier studies (Nath and Mudholkar, 1989; Canfield and Thamdrup, 2009). The abundance and activity of these bacteria could also elucidate questions as to why large amount of methane and similar compound evolving out of the earth's mantle suddenly disappear at the upper oceanic lithosphere. Alternatively, this strange niche distinction may be an effect of hydrothermal fluid-alterations.

During diffuse hydrothermal alteration a temperature range of 0° to 25°C can commonly occur in the seabed (Chevaldonne *et al.*, 1991; Childress, *et al.*, 1991). Heat flux data for CIOB is not presently available. Varying temperatures influence the rates of carbon fixation, RuBisCO and formaldehyde utilization. This is suggestive of a great exploratory potential towards *in situ* hydrothermal alterations and diverse modes of chemosynthetic functioning in this basin. The presence of a large amount organic-matter, carbonates and ambient reducing conditions often make it difficult to decipher the microbial processes that mask each other in many environmental samples. Being able to understand the processes in the remote abyssal basins would help us to define them in continental shelves and the coastal systems.

The formaldehyde utilizing bacteria of CIOB show many features that can be attributed to methylotrophy. Methylotrophy and mixotrophy might be important processes in these oligotrophic abyssal sediments, where limited amount of photosynthetically-derived organic matter is available.

It is increasingly being observed that sea-floor circulation of hydrothermally derived fluids have affected large parts of the ocean basin (D'Hondt *et al.*, 2004). While very high temperature would prevail at classical vent locales, diffuse flow would ensure that temperature gradients of 2°-25°C are more widespread. The present results suggest that the same bacterium may behave differently along a temperature gradient allowing an array of rates within the given temperature range. This leaves a massive scope of quantifying the relative role of organic matter diagenesis and hydrothermal alterations at different temperatures. Most importantly the carbon sequestration can be most efficiently experimented in these deep abyssal basins.

5.9.2.2. *Extent of autotrophy and chemosynthetic hotspots in CIOB*

It is primarily hypothesized that chemosynthetic potential increases with depleting organic matter in oligotrophic environments. Special emphasis is given to hydrothermally altered and volcanic environments. In general, carbon fixation by sediments below the calcite compensation depth is higher with decrease in organic matter content. The northern siliceous oozes are lower in their carbon uptake than the pelagic red clays. Calcareous oozes fix at least an order more of carbon than the pelagic clays. A part of these results have been presented at the 4th International Chemosynthesis-Based Ecosystems, Okinawa, Japan, (Das *et al.*, 2009). Though the rates of carbon fixation are low, these values may be of quantitative importance on crustal and global scales.

Chemosynthesis may be exhibited by generalists like facultative autotrophs or mixotrophs and specialists like strictly autotrophic bacteria. Strict autotrophs could be any of the following: 1. nitrifiers (e.g., *Nitrococcus*, *Nitrosomonas*), 2. sulphide oxidizers (e.g. photosynthetic *Chromatium* and chemosynthetic *Thiobacillus thiooxidans*), 3. metal oxidizers (e.g. *Thiobacillus ferrooxidans*), and 4. methane oxidizers (e.g. *Methylomonas*). Facultative autotrophs like *Pseudomonas* and *Alcaligenes* may also exhibit chemoautotrophy or mixotrophy (Karl, 1995, Loka Bharathi 1989, Loka Bharathi *et al* 1994). Both generalists and specialists could be involved in the chemosynthetic processes. While specialists could be high in their activity and restricted to unique niches like black smokers, generalists could be more widespread with lower ability to fix CO₂. Many bacteria possess the RuBisCO enzyme for carbon fixation using the Calvin Benson

Cycle. Yet others like photosynthetic bacteria use the rTCA cycle. The methanotrophs are known to use the Serine and RuMP Pathways (Karl, 1995).

Comparison of carbon fixation rates of CIOB sediments with those recorded in other chemosynthetic settings worldwide show that CIOB values are 1–2 orders of magnitude smaller than for bacterial mats, anoxic fjords, waters near hydrothermal vents, and also solar salterns, and up to 3 orders of magnitude smaller than for other active vents like the Rose Garden. However, they are comparable to waters of white smokers of 21°N East Pacific Rise. Carbon fixation rates in calcareous oozes are comparable to those of bacterial mats and solar salterns (Table 2, Das *et al.*, 2010b). The elevation of chemosynthetic potential in the CIOB pelagic clays can be explained by depletion of organic matter, both TOC and LOM and possible increase in inorganic substrates due to hydrothermal alterations (Nath *et al.* 2008; Das *et al.*, 2010b).

5.9.2.3. *RuBisCO enzyme activity in isolates and whole sediments*

The enzyme D-ribulose-1, 5-bisphosphate carboxylase/oxygenase (RuBisCO, EC 4.1.1.39) enables bacteria to fix carbon dioxide. RuBisCO is the most abundant enzymatic protein on Earth, found in higher plants, algae, cyanobacteria and other photosynthetic organisms. There are two types of RuBisCO: L8S8 type (type I or form I) found in most organisms as hexadecamer and consists of eight large (L) and eight small (S) subunits, and L2 type (type II or form II) found in some photosynthetic purple bacteria such as *R. rubrum* and consists of homodimer of L subunit only. RuBisCO behaves as a bifunctional enzyme catalyzing carboxylation as well as oxygenation. Its bifunctionality stems from its lack of specificity between CO₂ and O₂ as substrates. The

two gases compete as alternative substrate leading to either carboxylation of D-ribulose-1,5-bisphosphate (RuBP) to produce 3-phosphoglycerate (3-PGA) or oxygenation to produce 2-phosphoglycolate. The recombinant higher plant RuBisCO has been proven refractory to heterologous expression in active form. However, recombinant RuBisCO from different species of cyanobacteria as well as from archaea has been expressed and purified in active form. Its enzymatic activity of carbon dioxide fixation makes it one of the very important enzymes (Chakrabarti *et al.*, 2002 and references therein).

RuBisCO activity was found ubiquitous in the CIOB sediments (Figs 4.38A and B). All the three representative samples namely siliceous ooze 26, pelagic red clay 36 and calcareous ooze 37 showed distinct presence of the enzyme activity. Down-core variations were however different for the three different samples.

The siliceous ooze showed a decline in RuBisCO activity with depth (Fig. 4.38A). It is interesting to note that at these depths of core 26, the CO₂ fixation was higher and it formed a niche for the formaldehyde bacteria. These contradictory results indicate that RuBisCO is possibly not the only enzyme that fixes carbon here. The presence of Ribulose monophosphate (RuMP) pathway or Serine pathways or any other carbon fixation pathway might be involved in rendering higher carbon fixation.

Core 36 showed lower activity than core 26 but increased at greater depths (Fig. 4.38A). Core 37 with its highest enzyme activity showed an increase with depth both in whole samples and fractionated samples (Fig. 4.38B). In carbonates, the activity ranged from 10.94 to 8555.44 nmol min⁻¹mg protein⁻¹. It appeared that the presence of calcareous oozes masked the high enzyme activity of the clay fraction when measured in

whole sediment (Fig. 4.38B). The values matched with those recorded in bacterial mats (Karl, 1995).

Five deep-sea cultures representing different functional groups, used in formaldehyde utilization experiment were also tested for RuBisCO. The enzyme activity was detected in all of these cultures. Thus it is possible that ammonium oxidation, nitrite oxidation, formaldehyde utilization and sulphur oxidation are coupled to RuBisCO activity in these sediments and their indigenous bacteria (Table 4.7; Fig 4.39).

Activity of bacteria is next followed by diversity both for individual cultures and sediments.

5.10 Diversity of Bacteria in Central Indian Ocean Basin

5.10.1 Biochemical identification

Although culturable bacteria form a very small fraction of 0.1% of the total diversity, they are often functionally important groups that dominate biogeochemical processes. A few examples of such ecological functions are given here (Table 4.2). The presence of *Cytophaga* group reflects the presence of macroaggregates. The dominance of *Moraxella* indicates presence of aged particulate matter. The heterotrophs like *Pseudomonas-Alcaligenes* group break larger particles of organic matter to smaller ones (LokaBharathi and Nair, 2005). *Pseudoalteromonas* sp. is a psychrotolerant bacterium isolated from deep-sea sediment which is known to produce exopolysaccharide (EPS). This EPS could enhance the stability of the cold-adapted protease secreted by the same bacteria through preventing their autolysis. The EPS could bind many metal ions, including Fe^{2+} , Zn^{2+} , Cu^{2+} , Co^{2+} . It was also a very good flocculating agent and could

conglomerate colloidal and suspended particles. The EPS secreted might help these bacteria enrich the proteinaceous particles. It is probable that the trace metals in the deep-sea environment, stabilize the secreted cold-adapted proteases and avoid its diffusion (Qin *et al.*, 2007). These bacteria may thus have various roles in the growth and quality of polymetallic nodules in the CIOB.

5.10.2. 16S rDNA phylogenetic affinities of CIOB cultures

Culture CIB 25A (Fig 4.34A) is a γ -proteobacter belonging to the genus *Pseudoalteromonas*. Other related species like *Pseudoalteromonas* sp. SM9913 are psychrotolerant bacterium isolated from deep-sea sediment. The structural characterization and ecological roles of the exopolysaccharide (EPS) secreted by these strains could serve as enhancers for the survival of deep-sea bacteria in a fluctuating environment (Qin *et al.*, 2007).

Culture BIN 2 (Fig 4.34B) is a Firmicute showing affinity to *Bacillus*. Manganese (II) oxidation mediated by heterotrophic *Bacillus* species in hydrothermal plumes was reported from the Guaymas Basin hydrothermal field (Dick *et al.*, 2006). Spores of *Bacillus*-like organisms can rest dormant for long time periods and they are resistant to damage through desiccation and radiation. *Bacillus*-like organisms have been isolated from deep subsurface sediments and from inclusions inside materials like amber, salt crystals or glacial ice, where the spores must have been included since the time of deposition. The age of the inclusions in the salt crystals and amber was estimated in the range of several million years, the age of those in glacial ice in the range of 5 to 750,000 years. *Bacillus*-like strains that are physiologically capable of growing under these

conditions in the brine, i.e. extremely high salinity combined with anoxia and a sulfide concentration of several millimol per liter (Sass *et al.* , 2008).

Culture BIN 3 (Fig 4.34C) showed affinity to *Pseudomonas* which have similar ecological role like biofilm formation with that of *Pseudoalteromonas*.

Culture BIN 4 (Fig 4.34D) showed affinity to *Alcanivorax*. *Alcanivorax* belongs to γ -proteobacteria. *Alcanivorax*, *Marinobacter*, *Thalassolituus*, *Cycloclasticus*, *Oleispira* and few others belong to the obligate hydrocarbonoclastic bacteria (OHCB). Hydrocarbons and their derivatives, not only include solid, liquid and gaseous fossil carbon deposits, but also compounds of biological origin, such as lipids and fatty acids from plants, animals and microbes. The products of their conversion in anoxic zones, are ubiquitous in the biosphere, though highly heterogeneous in type and concentration, and in time and space. Given the high carbon content available for biomass production, and the high energy content of such highly reduced compounds, it is hardly surprising that many microbes have evolved or acquired the ability to utilize hydrocarbons as sources of carbon and energy. More than 250 *Alcanivorax*-affiliated bacteria have been isolated or detected as 16S rRNA gene sequences in all types of marine environment: surface water, shallow and deep-sea water bodies, sediments, hydrothermal vents and mud volcanoes, ridge flank crustal fluids and gray whale carcass. Interestingly, although *Alcanivorax*-related 16S rRNA gene sequences have been retrieved from microbial communities inhabiting cold polar areas, the organism itself has so far only been isolated from more temperate latitudes. Despite these qualifications about experimental approaches, it is clear that oil hydrocarbon degradation in marine systems is carried out by microorganisms belonging to a relatively small group of genera, and that there are certain important

differences in the compositions of oil-degrading communities at high and low latitudes that need to be considered when developing potential mitigation strategies to combat oil pollution in marine systems (Yakimov *et al.*, 2007).

5.10.3. Diversity of bacteria by 454 pyrosequencing technique

The α - proteobacter mostly include the phototrophic non-sulfur bacteria. The aerobic anoxygenic phototrophic genus *Erythrobacter* is very different from the lot as it does not have an anaerobic phototrophic growth. The genus grows heterotrophically under aerobic conditions. However *Erythrobacter* is different from other heterotrophs as it has a light driven electron transport system and uses light as an auxiliary energy sources. It requires oxygen for synthesis of bacteriochlorophyll *a*. It has a complete set of Calvin Benson Bassham cycle enzymes and is known to exist in diverse marine environments from oceanic waters to hydrothermal locales. This amazing genus is associated to the Mn(II) oxidation in basaltic glass, and low temperature hydrothermal alterations (Tebo *et al.*, 2005). Recently, several heterotrophic Mn(II) oxidizers associated with the rinds of deep sea basaltic glass recovered from the Loihi Seamount, an active submarine volcano off the Island of Hawaii, have been described (Templeton *et al.*, 2005). Based upon 16S rRNA analysis, *Pseudoaltermonas* species were the most common isolates of the γ -proteobacteria. Numerous α -proteobacteria in the *Rhodobacter* group were also isolated (Templeton *et al.*, 2005) and were considered to potentially play an important role in the cycling of organic sulfur compounds. The role of these bacteria in the dissolution of volcanic glasses and the oxidation of rock-derived Mn(II) remains to be shown. Nevertheless, the study indicates the presence and abundance of

phylogenetically diverse Mn(II)-oxidizing bacteria in oligotrophic deep sea environments. The results suggest significant role of the genus *Erythrobacter* in the biogeochemistry of organically poor, Fe- and Mn-oxide rich deep-sea pelagic red clay at the depth of >5000m below sea surface.

Bacteria belonging to the candidate division OP11, OP3 and one unassigned phylum were detected. Though low in abundance (0.026%), sequences belonging to the Phylum Thermomicrobia were also detected. The important groups were the Firmicutes, Gemmatimonadetes, Nitrospira, Planctomycetes, Bacteroidetes, Chloroflexi and Deferribacteres (Loka Bharathi *et al.*, 2009; Gonsalves *et al.*, 2009). The ϵ - proteobacter which forms one of the dominant class in many chemosynthetic environments were not detected in this system.

Species richness indices (Table 4.3) reveal polarization of the bacterial community as implied by the dominance of *Erythrobacteriaceae* suggesting the prevalence of a simple community. However, it has been shown earlier by massively parallel tag sequencing strategy, that bacterial communities of deep water masses of the North Atlantic and diffuse flow hydrothermal vents are one to two orders of magnitude more complex than previously reported for any microbial environment. In the present study, rarefaction analysis (Fig. 4) showed that a large part of the rare biosphere in TVBC 08 still remains untapped although the dominant genus is *Erythrobacter* (Fig 4.35). Sogin *et al.*, 2006 have shown that relatively small number of different populations dominated all samples, but thousands of low-abundance populations accounted for most of the observed phylogenetic diversity. This “rare biosphere” is very ancient and may represent a nearly inexhaustible source of genomic innovation. Members of the rare

biosphere are highly divergent from each other and, at different times in earth's history, may have had a profound impact on shaping planetary processes (Sogin *et al.*, 2006). Tracing and analysis of these rare genera would substantiate processes that have led to the formation of present biomes. Conventional sequencing of 16S rRNA genes has revealed much about the diversity of bacteria in the oceans and other environments (Fuhrman and Hagström, 2008), but new technology, such as 454 pyrosequencing (Margulies *et al.*, 2005), potentially could yield even more insights into the structure of microbial communities. So far, this approach has been applied to a few bacterial communities from soils, hydrothermal vents, the deep North Atlantic Ocean and the English Channel (Sogin *et al.*, 2006, Huber *et al.*, 2007 Roesch *et al.*, 2007, Gilbert *et al.*, 2009), to archaeal communities (Galand *et al.*, 2009) and to bacterial communities in the Arctic Ocean (Kirchman *et al.*, 2010). The present study suggests the plausible role of *Erythrobacter* in organically depleted but volcanically active site in chemosynthesis.

5.11. Parameter-wise cluster pattern of microbial and biochemical parameters

Various factors like topography, carbon deposition, nitrogen depletion, pore-water concentration, porosity and permeability, fluid flow and currents determine the distribution of microorganisms. Some parameter like TOC and C/N may themselves be governed by microbial activity. By cluster analysis of various parameters measured, the distribution patterns and the factors that govern such patterns are projected more clearly (Figs 4.7 A and B).

The TOC and C/N distribution patterns are most likely affected by topography, flow of current and fluid flow within the sediment column (D'Hondt *et al.*, 2002, 2004;

Miester *et al.*, 2007). While TOC is affected by topography and current flow (Fig. 3.1 note the seamounts along the fracture zones), C/N is additionally affected by possible fluid flow or rock alterations (Fig. 4.7 A and B). Neighbouring cores 26 and 25 may be affected by similar intensity of these factors, while distant cores like 19 and 36 cluster together possibly by similarity in features like volcanic alterations (Nath *et al.*, 2008).

The distribution of ATP is dependent on pore-water phosphate concentration and volcanic alterations (Fig 4.14). While the former seems to affect stations like 26, the latter clusters distant cores like 19 and 36 together. Total counts and frequency of dividing cells may be affected by TOC content, porosity, permeability, shear strength and rock alterations. Geochemically contrasting distant cores like 26 and 08 cluster together possibly due to similar porosity ranges. A concentric pattern of naturally viable cells is noted with their origin at station 19 at the central part of the basin. It appears that this deep part of the basin is a source of some natural disturbance which spreads around in waves determining the distribution of viable cells (Fig 4.18).

Cluster analysis and down-core profiles however showed different clustering patterns and profiles for different sediment types (Fig 4.23). In the case of the heterotrophs on ZMA the siliceous oozes were separated from the rest of the cores at 65% dissimilarity. For ammonium oxidizers (NI), siliceous station 26 and 25 were separated from the other cores at 70%. In case of nitrite oxidizers (NII), calcareous ooze 37 clustered with the siliceous oozes 26 and 25 at 70% cut off. Siliceous core 25 and pelagic red clay 36 clustered at 55% in case of TDLO. Although all the cores showed the presence of these groups of retrievable bacteria their abundance and distribution patterns varied both latitudinally and down the core making the niches of each core unique in

themselves. The culturable bacteria like heterotrophs on ZMA are affected by TOC content and show a north- south cluster pattern. The two nitrifier groups are dependent on TOC and C/N ratio. Cores 26 and 25 cluster together while distant cores 20, 34 and 36 group together due to similar amounts of available nitrogen or similar activity in the nitrification-denitrification couples. Aerobic TDLO flourish wherever oxidizable sulphur is available. This sulphur may be biogenic or abiogenic. It is apparent that the sulphur in CIOB is more abiogenic and is related to rock alteration processes rather than from biogenic materials. For this reason very distant siliceous ooze 25 clusters with pelagic clay 36, and 26 clusters with 34.

The Fe oxidizers of core 36 were separated from the other cores at 80% dissimilarity (Fig 4.25). In the case of Mn-oxidizers cores 36 and 08 were separated from the cores at 60% dissimilarity. The distribution of Fe-oxidizers and Mn-oxidizers are similar. This is as per the accepted concept that Fe and Mn are co-active in natural systems. The cluster pattern shows that these two groups of bacteria co-occur with each other and are not much affected by topography, TOC or C/N ratios. Thus fluid alterations may be examined further to understand the distribution patterns of these metal oxidizing autotrophs.

Phosphates solubilizers of cores 35 and 36 separated from the other cores at 75% dissimilarity (Fig 4.27). The silicate solubilizers of core 34 separated from the other cores at 80% dissimilarity. A second split comprising of cores 36 and 38 separated out at 60% dissimilarity. The distribution pattern of phosphate solubilizers is dependent on ATP and pore-water phosphate in the north. Origin of phosphate in the south may be more volcanic and the phosphate solubilizers in the south could be related to this

volcanically derived phosphate along with alkaline phosphatase activity. The distribution pattern of phosphate and silicate solubilizers showed similarity suggesting that the source of the phosphate and silicate available to bacteria could be the same in greater part of the basin. Differences in the distribution patterns are however noted in the seamount cores. These suggestions regarding the distribution pattern of the culturable bacteria in relation to environmental parameters need further confirmation. However, it is emphasized here that culturable bacteria do throw light on biogeochemical activity of environments. The distributory patterns are consistent over large stretches of the ocean floor (D'Hondt *et al.* 2002 and 2004). The influence of hydrothermally derived fluids on pore-water chemistry and the indigenous bacterial community need to be further probed.

The carbon fixation activity pattern shows that hydrovolcanically altered station 8 stands separate from the rest of the basin (Fig 4.36B). Two more major clusters occur parallel in a north south alignment. The pattern reveals that carbon fixation by microbes in the basin is affected by topography, carbon accumulation and preservation, nitrogen depletion but not as much by porosity and shear- strength.

With the availability of more data on heat flux, magnetic anomaly, acoustic anomaly and application of neural networking it would be possible to improve the understanding of the microbial interactions in this basin.

5.12 Interactions between bacteria and environmental parameters

In the northern part of CIOB, TOC and LOM significantly correlated to each other ($r = 0.75$; $p > 0.05$) highlighting the interdependence of organic flux to sea floor and lability of organic matter enhanced by bacteria. TOC related to pore-water pH,

nitrite oxidizers, carbon uptake rates ($r = 0.75, -0.65, 0.69$ respectively, $p > 0.01$) and to ammonium oxidizers ($r = 0.72$; $p > 0.05$) signifying its stimulatory role on the microbial population while promoting diagenetic reactions. LOM determined total bacterial counts, FDC, DVC-a and heterotrophs recoverable on 50% ZMA ($r = 0.66, 0.66, 0.68$ respectively; $p > 0.05$). These relations are suggestive of aerobic heterotrophic degradation of organic matter. Pore-water NO_2^- related with NO_3^- ($r = -0.98$; $p > 0.001$), TOC ($r = -0.65$; $p > 0.05$) and ammonium oxidizers ($r = -0.94$; $p > 0.001$) indicating coupling of heterotrophic degradative process with denitrification /metal reduction during early diagenetic reactions. This in turn could be coupled to nitrification or other oxidative processes for enhancing autotrophic fixation. This process again could feed the diagenetic reactions thus completing cycles which could be self-sustaining. The ^{14}C uptake ($r = 0.66$; $p > 0.05$) is positively correlated with nitrite oxidizers.

In the southern part of CIOB, lower surface productivity (Matondkar *et al.*, 2005), lower sedimentation rates and negligible continental influx are attributed to the low TOC, recalcitrant LOM and the lack of a relationship between the two parameters. The total bacterial counts are dominated by a viable anaerobic population ($r = 0.78$; $p > 0.01$) that is negatively correlated with TOC, LOM and C/N ratio.

The ^{14}C uptake related positively only to nitrite oxidizers ($r = 0.66$; $p > 0.05$) in the north suggesting that chemosynthesis is highly driven by this intermediate compound in this region. On the contrary, in the southern core, the absence of such a relationship suggests that the chemosynthetic activity is not limited by availability of reduced substrates. Further, this relationship is not restricted to any specific group.

a. *Siliceous ooze-Core 26*

The close positive relation of the nitrifiers and denitrifiers indicates nitrification-denitrification couple. LOM related negatively to Fe oxidizers implying that the Fe-oxidizers could be chemosynthetic and do not require the LOM for survival. Phosphate and silicate solubilizers relate negatively to the nitrate reducers implying their affinity to oxidative or synthetic processes.

b. *Siliceous ooze -Core 25*

Core 25 is a hotspot of carbon fixation in the north. However this fixation is indicated to be anapleurotic and involves heterotrophs rather than autotrophs. This is indicated by the negative correlation of Fe-, Mn-oxidizers, NII and TDLO with carbon uptake. Unlike core 26, in this siliceous core, phosphate solubilizers have close affinity to facultative or reductive processes.

c. *Siliceous-Pelagic transition-Core 34*

In core 34, the heterotrophs correlated to carbon uptake and negatively to LOM. In these LOM-poor locations the heterotrophs might be constrained towards carbon fixation as the only mode to acquiring their carbon requirement.

d. *Pelagic red clay- Core 08*

This core is primarily autotrophic with TC and Mn-oxidizers relating positively to carbon uptake. But a negative relation of Fe-oxidizers to carbon uptake is intriguing as generally bacterial oxidation of metal is closely associated to carbon uptake.

e. *Pelagic red clay 36*

Like core 08, core 36 is also a primarily autotrophic with carbon uptake relating positively to Mn-oxidizers and negatively to LOM. Denitrifiers related positively to Fe-

oxidizers and phosphate solubilizers indicating co-precipitation of Fe with phosphorus and possible coupling with the nitrification-denitrification couple.

f. Calcareous ooze 37

Core 37 is an autotrophic core with carbon uptake strongly related to Fe-oxidizers. However, it also supports heterotrophic growth as the LOM in these oozes may be sufficient to support heterotrophs and other functional groups. The phosphate and silicate solubilizers show close positive relation to heterotrophs and LOM indicating their association to degradative processes in this core.

5.13 Core-wise principal component analysis (PCA) of distribution patterns

The sediment cores of CIOB form unique niches in themselves even if they belong to the same sediment type. Large variations and heterogeneity exist among neighbouring cores. It is therefore difficult to choose representative sediment types microbiologically. Here the PCA plots of two or three cores each are presented from siliceous, siliceous-pelagic transition and pelagic red clays and one calcareous core. Cores 26, 25 and 20 belong to the siliceous oozes in the north. Cores 34 and 35 belong to the siliceous-pelagic transitions in the centre. Cores 8, 36 and 38 belong to the pelagic red clays in the south. Core 37 is a calcareous ooze in the south at the summit of a seamount. The analyses throw light on the extent of complexity of interrelations in each of the cores (Fig 4.46 A, B, C and D).

The PCA plots show that the contribution of the first component is highest up to 75.6% in the centre and declines to 53.7% in the north and to 53.9% in the south. In core 20 and the central stations 35 and 36, Mn-oxidizers and Fe-oxidizers do not contribute to

the variation along the first component indicating that they are non-limiting factors. In volcanically altered sea-mount stations Fe and Mn cause co-variance in the first component. Similar is the case for siliceous ooze 25. It is to be noted that 25 is a chemosynthetic hotspot like 8 and 38 in south. Therefore, such similarities in distribution and activity patterns are expected.

Microbial carbon fixation contributes to variation along the first component in the relatively more heterotrophic cores 26, 25, 20, and the autotrophic 34 and 08. However, it is noted that LOM contributes to variation along the first component in cores 25, 20, 36, 38 and 37.

Core 34 in the siliceous-pelagic transition is the simplest system with 100% of its variation explained by four components. Core 36 is the most complex system with only 89.7% of its variation explained by 5 components. Complexity of microbial ecosystems is least in the centre and increases northward and southward. This pattern synchronizes with the similar gradation in ^{14}C uptake and is quite contrary to the general paradigm that overlapping niches cause higher ecological richness. The siliceous-pelagic transition zone in the centre of the CIOB harboured ecologically simpler systems than the siliceous or pelagic cores. This stenohabitat is more inhibitory than simulatory as compared to northern siliceous and southern pelagic red clays. Further studies could contribute to understand more about the endemic microflora of this transition region.

Interestingly, the autotrophic uptake in the northern siliceous oozes is not related to Mn oxidation but more to the nitrifiers. The carbon fixation in core 26 is nitrogen based and linked to nitrifiers, while at core 25, it is linked to the aerobic TDLO or sulphur oxidizers. The silicate and the phosphate solubilizers in the north are dependent

on the LOM suggesting that it is derived from the siliceous oozes that are probably solubilized by silicate solubilizing bacteria. ATP is also closely related to the above parameters indicating its biogenic origin.

In contrast, in the southern stations, the phosphate and silicate solubilizers are delinked from LOM either because the regions are oligotrophic or the silicate and phosphate are more abiogenic in origin. Phosphate solubilizers and ATP related very closely to each other in the southern cores, possibly suggesting that these bacteria could be solubilizing the particulate phosphorus from volcanogenic sources.

The principle component analyses indicate a large variation in microbiology and biochemistry of cores even within similar sediment types. Though the cores with similar geochemical origin show similarities in microbiological and biochemical parameters, factors like fracture zones, fluid flow, depth of the stations might bring about differences. For example, quality of organic matter might influence the carbon fixation rates both within and between the sediment types. These aspects of ecological interactions have not been dealt by other previous researchers. It is therefore suggested that these perspectives of deep-sea systems could be simulated further using these interrelations as the starting point.

5.14 Numerical Simulations

5.14.1 Quantification of the influence of non-steady state diagenetic condition on microbial community by numerical simulation

The numerical simulation (Fig. 4.48A, Das *et al.*, 2010a), suggests the prevalence of bacterial nitrate reduction nitrite-oxidation coupling at the reactive layers.

Consequently, a mottled zone forms at deeper layers and reduced metal species oxidize near the sediment-water interface. Sigmoid profiles of NO_3^- concentration at the reactive layers are suggestive of formation and subsequent utilization of the ion at this shallow depth. The deposition of a 4cm thick organic carbon-rich layer and upward migration of reduced metal species like Mn^{2+} leads to the coupling of nitrate reduction to nitrite oxidation. These coupled processes may reach a rate of $\pm 1000 \mu\text{M m}^{-3} \text{ yr}^{-1}$. Consequently this leads to rapid formation and removal of NO_3^- and a new nitrite oxidizing-nitrate reducing interface may be formed. This interface may potentially migrate upwards from 3 to 9cmbsf to the surface thus allowing manganese nodule precipitation in the form of MnO_2 at the surface. The precipitation of these manganese nodules could be analogous to dolomite precipitation above sulphate-methane interfaces (Rao *et al.*, 2003, Meister *et al.*, 2007, 2009). High chemosynthetic activity has been noted in these reactive layers similar to that in sulphate methane interfaces and dolomite deposits observed at Blake Ridge (Rodriguez *et al.*, 2000) and ODP site 1229 in the Eastern Equatorial Pacific (Meister *et al.*, 2007). The relative compactness of porous siliceous ooze sediments at these depths (Fig.3A; Das *et al.*, 2010a) reduces permeability, partially restricting horizontal transfer and utilization of NO_3^- in these clay-rich sediments. This results in the formation of horizontal mottled layers.

5.14.2 Quantification of hydrothermal alterations on pore-water and microbial community by numerical simulation

The numerical simulation (Fig.4.48B; Das *et al.*, 2010a), suggests the prevalence of a nitrite oxidation-nitrate reduction coupling at the Pleistocene-Tertiary stratigraphic

interface due to lateral dispersion and phase separation of solute during cooling of upwelled hydrothermal fluid. Consequently, there is an enhancement of bacterial abundance and activity at the stratigraphic transition zone (Figs 5 to 7; Das *et al.*, 2010a) due to the availability of inorganic substrates made utilizable by processes such as phase separation of solutes. Sigmoid profiles of NO_3^- concentration at the stratigraphic transition are suggestive of formation and subsequent utilization of the ions at this transition zone. The 6 cm transition zone in core TVBC 08 and upward migration of reduced chemical species from hydrothermally altered fluids leads to the coupling of nitrate reduction to nitrite oxidation. Consequently, this leads to rapid formation and removal of NO_3^- . A new nitrite oxidizing-nitrate reducing transition gets formed. The pore-water NO_2^- profile would run parallel to that of NO_3^- and would not be analogous to those derived from organic matter diagenesis (eg. Core TVBC 26) when there is continuous supply. Hence, the NO_3^- profile is altered by the presence of hydrothermally derived reduced substrates.

An initial vertical focused-jet of hydrothermally altered fluid evolves into a lateral diffusion at the Pleistocene-Tertiary stratigraphic transition and allows for hydrothermal precipitation of Fe, Ti, P etc. as reported earlier by Nath *et al.* (2008). A negative rock alteration index (RAI) denoting precipitation (Zhao *et al.*, 2009) may be expected at 3 to 7 cm bsf sandwiched between positive ones denoting dissolution. Although neutral chloride type hydrothermal activity is indicated by previous studies (Nath *et al.*, 2008), more comprehensive data on thermal and Cl^- anomalies would be helpful for simulating improved models.

Variation in porosity (Fig. 3B; Das *et al.*, 2010a) at the stratigraphic transition zone is sharp. The effect of advection and interactions between fluid flow, heat transfer, mass transport and chemical reactions need to be considered in a comprehensive manner using coupled transport models or finite element models (Zhao *et al.*, 2009; Ma *et al.*, 2006; Yang *et al.*, 2004) taking into account the complex stratigraphic features.

5.15 Bacterial participation affects quantity and quality of nodules

Polymetallic/ferro-manganese nodules (Mn-nodules) reach sizes of up to 10 cm in diameter and are abundantly found on the seabed. To date, the origin of Mn-nodules remains unclear, and both abiogenic and biogenic origins have been proposed (Wang *et al.*, 2008).

In the present study, besides sediments, nodules have also been examined for bacterial abundance and activity. Some possible relations between early diagenesis in sediment profiles and nodules are highlighted. This section aims to derive the optimal conditions for the best nodule formation through geomicrobial proxies. Contrary to the generally accepted paradigm, it is hypothesized that the quality, quantity and size of the nodules could be influenced more by the bacterial action in relatively higher organic loading in the north as compared to the southern region of CIOB. The present observations are indicative of the role that the relatively reducing sediments in the north could play in the formation and abundance of nodules of higher quantity and quality. It is speculated that less intense reducing rates and therefore slower oxidation could have promoted smaller nodule formation in the pelagic red clay realm.

The microbial role in the formation of nodules is quite well-appreciated through a number of studies made in the Clarion-Clipperton nodule field in the Pacific Ocean and the Indian Ocean nodule field in the Central Indian Ocean Basin. However, the exact microbial processes of nodule formation are still not well-defined. From the geological point of view both these basins have some similarities. Both are bound by fracture zones, and have an overall oxic setting. However, the formation of nodules might have a sub-oxic origin where microbial redox reactions are involved. Reduced metal oxidation, sulphide oxidation and possibly even methane oxidation are involved.

Selective enrichment of carbon and depletion of nitrogen are noted in the nodules. Volatilization of nitrogen, microbial consortia and diffuse hydrothermal flow could be a reason for this selective nitrogen depletion. The protein to carbohydrate and carbohydrate to LOM ratios (Fig.4.43) indicate relatively fresher organic matter in the surface nodule and its associated sediment than the buried one. In contrast to the sediments of CIOB, the nodules are enriched in lipids. Low-maturity hydrocarbons were detected in the nodules and oozes of the Pacific Ocean. According to the geological settings of the sampling area and its organic geochemical characteristics, it was considered that the hydrothermal activities on the ocean floor facilitated the decomposition of organic matter in the sediment, which led to the generation and migration of hydrocarbon into manganese nodules and ooze. This discovery was important for understanding the mechanisms of hydrocarbon generation in the ocean floor and for expanding the potential of oil and gas exploration in the ocean (Wenxuan *et al.*, 2002).

Like biochemical parameters, microbial parameters also brought out some interesting findings. Presence of autofluorescent bacteria would indicate the possible

presence of methylotrophic methanogens in the manganese nodules. Earlier, using fluorescence microscope, abundant microbe “bodies” and clear microbial fluorescent microstructure were determined in the ferromanganese nodules collected from the East Pacific deep sea floor. The microbial fluorescent structure showed a close relation to the formation of the ferromanganese nodules (Wenxuan *et al.*, 2002).

Presence of naturally viable frequency of dividing cells and the aerobic and anaerobic viable cells up to the inner-most layers of the nodules indicate the role of live bacterial activity in the nodule formation process. Earlier studies with the Pacific nodules showed organized bacterial assemblies which could have participated in the formation S-layers in metal deposition. Endolithic microorganisms existed and were arranged in a highly organized manner on plane mineral surfaces within the nodules. These microorganisms were adorned on their surfaces with S-layers, which were indicative for bacteria. Moreover, the data suggested that these S-layers are the crystallization seeds for the mineralization process. The authors concluded that the mineral material of the Mn-nodule had a biogenic origin (Wang *et al.*, 2008).

The microbial community of the nodules could fix carbon and utilize carbon substrates (Fig 4.45 and Table 4.9). The buried nodule fixed higher amount of carbon than the surface nodule. This indicated that the bacteria were chemotrophic and mixotrophic and took part in metal oxidation, organic matter utilization and carbon fixation.

5.16 Conclusion and Future scope

In a brief conclusion it can be said that hydrothermal activity and associated rock alteration processes may be more relevant than organic matter delivery in CIOB. Microbes could be involved in diagenetic and hydrothermal alterations on varying timescales. The biogeochemical analyses of CIOB sediments suggests that the minor components like the rod morphotypes amongst bacteria and sand component in sediment texture of CIOB, wield a large influence on the variability of other parameters. In CIOB sediments, inorganic phosphate is possibly made available to biota, by variable rates of alkaline phosphatase (ALP) activity. ALP activity thus could serve a dual ecological function of supplying the pools of both P and organic C simultaneously and sustaining deep sea ecosystem of CIOB with these nutrients. Oxidative and reductive processes operate in close tandem one feeding the other during diagenesis. These cycles could be complete and self-sustaining. Extent of chemosynthesis although low in rates is of quantifiable importance. The presence of C-1 metabolism and excess ATP in some stations probably due to pyrophosphate formation indicates the presence of primordial reactions. The present study suggests the plausible role of the Aerobic Anoxygenic Phototrophic bacterium *Erythrobacter* in organically depleted and hydrothermally altered site in promoting chemosynthesis.

As a part of future research, more robust numerical simulations explaining thermodynamics of the biogeochemical reactions in CIOB would be possible with the availability of data on heat flux and fluid flow. Kinetic models could also add to the understanding. It would also trigger interesting research on the deep-biosphere in CIOB. The present study on carbon fixation potential could stimulate the pursuit of

chemosynthesis for sequestering CO₂ in the deep sea floor. A detailed conclusion, future scope and implications are presented in the next chapter.

“There’s more to life than increasing its speed.”

-The Mahatma

Chapter VI

Summary, Conclusion and Future Scope

Distribution, Diversity and Activity of Bacteria from the Central Indian Ocean Basin

The present thesis entitled “*Distribution, Diversity, and Activity of Bacteria from the Central Indian Ocean Basin*” (CIOB), aims to study the above aspects of sediment bacteriology in the context of geochemical and sedimentological background of this ocean basin. The study deals with bacteria and their interaction with deep-sea sediments and nodules. The interactions cover three austral seasons with samples collected from area enclosed within 10°-16°S and 73°30'-77°30'E. Chemosynthetic potential has been measured in these sediments to understand the chemoautotrophic contribution to carbon fixation. Though several enzymes have been shown to participate in chemosynthetic activity, the present study is restricted to the enzyme RuBisCO. The activity of this enzyme is detected for the first time in this part of the ocean basin. Other activities examined include those that drive chemosynthetic processes like nitrification and metal oxidation. Phosphate and silicate solubilization give insights into the community's contribution to the release of these essential nutrients into the surrounding environments. Some of the salient findings are as follows:

1. Sediments TOC varied from non-detectable levels to <1%. Generally the northern latitude showed a higher TOC content than south. Most of the samples were from 1000 m below the Calcite Compensation Depth (CCD) and the TIC varied from negligible to 0.1%. The calcareous sea-mount summit was the only exception with 6-10% of TIC.

2. Labile organic matter (LOM) and its components protein, carbohydrate and lipids showed latitudinal and temporal variation. The abyssal sediments of Central Indian Basin, ca. 5000 m depth, were organically-poor with labile organic matter content varying from ≤ 0.5 to ≤ 1.0 mg g⁻¹ sediment weight. The gradation in lability was in the order North > South > Central region. The central part of CIOB at the transition between siliceous and pelagic red clays appears to be containing the most recalcitrant C in the basin.
3. Adenosine triphosphate (ATP) varied from 10⁰⁻⁴ ng g⁻¹ dry sediment. ATP showed latitudinal, inter-annual and inter-seasonal variation within this wide range.
4. Total bacterial abundance in Central Indian Basin sediments ranged from 10⁶-10⁹ cells g⁻¹ and exhibited latitudinal, depth-wise, seasonal and annual variation. Total bacterial abundance in nodules ranged from 10⁷-10⁸ cells g⁻¹.
5. Direct viable counts (DVC) generally varied from 10⁵-10⁷ cells g⁻¹ dry sediment and formed about 1-10% of total counts. DVC-a (viability under aerobic condition) was marginally \geq DVC-an (viability under anaerobic condition) in the north and an order higher than DVC –an in the south. In the calcareous ooze the DVC-an was marginally \geq DVC-a.
6. The aerobic culturability varied from non-detectable to >10⁴ colony forming units (CFU) g⁻¹ dry sediment. The functional groups isolated were heterotrophs, ammonium oxidizers, nitrite oxidizers, aerobic sulphur oxidizers, phosphate solubilizers, silicate solubilizers, Fe- oxidizers and Mn-oxidizers. Among anaerobes autotrophic denitrifiers and heterotrophic nitrate reducers varied from non-detectable to $\geq 10^3$ CFU g⁻¹ dry sediment.

7. Culturability improved by two orders from 10^2 - 10^4 cfu g^{-1} on 50% ZMA as compared to 100%. The maximum culturability was obtained on 25% ZMA concentration.
8. Biochemical identification of isolates revealed taxonomic affinities to *Pseudomonas I-IV*, *Alteromonas*, *Pseudoalteromonas*, *Moraxella*, *Aeromonas*, *Flavobacterium*, *Alcaligenes*, *Cytophaga*, and *Xanthomonas*.
9. 16S rRNA identifications of isolates revealed taxonomic affinities to *Pseudomonas*, *Alkanivorax*, *Bacillus* and bacteria of unknown genera.
10. Pyrosequencing using 454 technology showed that the Aerobic Anoxygenic Phototrophic (AAP) bacteria of the Genus *Erythrobacter* dominated the sediment of pelagic red clay TVBC 08. Total number of sequences recovered in the analysis amounted to 15,223 representing 14 different phyla. The first 4 dominant phyla were Proteobacteria: 97.86 %, Actinobacteria: 0.75 %, Unassigned phylum: 0.45 %, Firmicutes: 0.28 %.
11. The present study suggests the plausible role of the Aerobic Anoxygenic Phototrophic bacterium *Erythrobacter* in organically depleted and hydrothermally altered site in promoting chemosynthesis.
12. Autotrophic carbon uptake in sediments varied from 10 to 10,000 $nmol\ C\ g^{-1}day^{-1}$. Surprisingly, austral summer (Dec-Jan, ABP-26) generally showed an order higher uptake of carbon than the austral winters. Pelagic and calcareous cores in southern location showed least response to seasonal variation. North-south gradient recorded more prominent variations than East-West. Along $75.5^{\circ}E$, the autotrophic carbon uptake varied from 15.30 to 696.39 $nmol\ g^{-1}\ dry\ wt\ day^{-1}$. At

the seamount situated at 16°S the uptake was highest for the calcareous ooze BC 37 with 5399.53 nmol g⁻¹ dry wt day⁻¹.

13. RuBisCO enzyme activity was measured in cell-free extracts from sediments. The activity varied from 10-1,00,000 nmol C fixed min⁻¹ mg protein⁻¹. RuBisCO enzyme activity was found to be ubiquitous and was detected in all types of sediments namely siliceous ooze, pelagic red clay, and calcareous ooze sediments.
14. Extent of chemosynthesis although low in rates is of quantifiable importance. The presence of C-1 metabolism, excess ATP in some stations probably due to pyrophosphate formation indicates the presence of primordial reactions.
15. Content and quality of organic matter and flow of hydrothermal heat, fluid and solutes are the most important factors controlling autotrophic activity in deep-sea sediments.
16. Hydrothermal activity and associated rock alteration processes may be more relevant than organic matter delivery in CIOB. Microbes could be involved in diagenetic and hydrothermal alterations on varying timescales.
17. The biogeochemical analyses of CIOB sediments suggests that the minor components like the rod morphotypes amongst bacteria and sand component in sediment texture of Central Indian Basin, wield a large influence on the variability of other parameters.
18. Oxidative and reductive processes operate in close tandem one feeding the other during diagenesis. These cycles could be complete and self-sustaining.

19. It is observed that the more chemoautotrophic cores utilized fewer numbers of substrates on the BIOLOG ECO plates suggesting that these sediments perhaps harboured obligate chemoautotrophs.
20. Contrary to the generally accepted paradigm, the quality, quantity and size of the nodules could be influenced more by the bacterial action in relatively higher organic loading in the north as compared to the southern region of CIOB. The present observations are indicative of the role that the relatively reducing sediments in the north could play in the formation and abundance of nodules of higher quantity and quality.

Future scope

1. More robust numerical simulations explaining thermodynamics of the biogeochemical reactions in CIOB would be possible with the availability of data on heat flux and fluid flow.
2. It would also trigger interesting research on the deep-biosphere in CIOB.
3. The present study on carbon fixation potential could stimulate the pursuit of chemosynthesis for sequestering CO₂ in the deep sea floor.

Implications and applications

1. In the long run, the knowledge on bacterial distribution and activity could be used for better management of deep-sea ecosystems for marine mining of resources.

2. Understanding deep-sea bacterial diversity, and harnessing marine microbes for biotechnological applications could be some of the important outcomes of the present work.

References

- Abramochinka F.N., Bezrukova L.V., Koshelev A.V., Galchenko V.F., Ivanov, M.V. (1987). Microbial oxidation of methane in a body of fresh water. *Microbiologiya* 56: 375-382.
- Abu-Ashour, J., Joy, D. M., Lee, H., Whiteley, H. R., and Zelin S. (1994). Transport of microorganisms through soil. *Water Air Soil Pollut.*, 75(1-2); 141-158.
- Aldrich, A.P. and van der Berg, C. M. G. (1998). Determination of Fe and its redox speciation in seawater using catalytic cathodic stripping voltametry. *Electroanal.* 10(6): 369-373.
- Aller, J. Y. (1997). Benthic community response to temporal and spatial gradients in physical disturbance within a deep-sea western boundary region *Deep-Sea Res I*, 44(1); 39-69.
- Alt, J.C., (1995). Subseafloor processes in mid-ocean ridge hydrothermal systems. In: *Humphris, S.E., Zierenberg, R.A., Mullineaux, L.S., Thomson, R.E. (Eds.), Seafloor Hydrothermal Systems: Physical, Chemical, Biological and Geological Interactions*. American Geophysical Union, Washington, DC, pp. 85-114.
- Amend, J.P., Teske, A. (2005). Expanding frontiers in deep subsurface microbiology. *Palaeogeog. Palaeoclimat. Palaeoecol.* 219; 131-155.
- Ammerman, J.W., Fuhrman, J.A. Hagström, Å. and Azam, F. (1984). Bacterioplankton growth in seawater. I. Growth kinetics and cellular characteristics in seawater cultures. *Mar. Ecol. Prog. Ser.* 18; 31-39.
- Anderson, J.R., Davies, I.P., (1973). Investigations on the extraction of adenosine triphosphate from soils. *Bulletins from the Ecological Research Committee (Stockholm)* 17; 272-273.
- Antolik, M., Abercrombie, RE, Pan, J, Ekstöm, G. (2006). Rupture characteristics of the 2003 Mw 7.6 mid-Indian Ocean earthquake: Implications for seismic properties of young oceanic lithosphere. *J. Geophys. Res.* 111, B04302, doi:10.1029/2005JB003785.
- Antony C (1982). *The biochemistry of methylotrophs*. Academic Press London.
- Arnebrant, K., SchnuÈrer, J., (1990). Changes in ATP content during and after chloroform fumigation. *Soil Biol and Biochem* 22; 875-877.

- Ausmus, B.S., (1973). The use of ATP assay in terrestrial decomposition studies. *Bulletins from the Ecological Research Committee (Stockholm)*. 17; 223-234.
- Bach, W. and Edwards, K. (2003). Iron and sulphide oxidation within the basaltic ocean crust: Implications for chemolithoautotrophic microbial biomass production. *Geochim Cosmochim Acta*, 67(20); 3871–3887.
- Bahl BS, Bahl A (1995). A text book of organic chemistry. S.Chand and Co., New Delhi 14th revised edition p 345.
- Baldwin, D. S. (1998). Reactive “organic” phosphorus revisited. *Water Res.* 32; 2265–2270.
- Banakar, V.K., Gupta, S.M. and Padmavathi, V.K. (1991). Abyssal sediment erosion in the Central Indian Basin: Evidence from radiochemical and radiolarian studies. *Mar.Geol.*, 96; 167-173.
- Banerjee, R., Mukhopadhyay, R., (1991). Nature and Distribution of Manganese Nodules from Three Sediment Domains of the Central Indian Basin, Indian Ocean. *Geo-Mar. Lett.*11; 39-43.
- Beardsley,C. Perntaler, J., Wosniok,W., and Amann, R (2003). Are readily culturable bacteria in Coastal North Sea waters suppressed by selective grazing mortality? *Appl Environ Microbiol.* 69(52); 624–2630.
- Bebout G. E., and Fogel M. L. (1992). Nitrogen-isotope compositions of metasedimentary rocks in the Catalina Schist, California: Implications for metamorphic devolatilization history. *Geochim. Cosmochim. Acta*, 56, 2839–2849.
- Bender, M. L., Fanning K . A., Froelich P . N., Heath G . R. and Maynard V. (1977). Interstitial nitrate profiles and oxidation of sedimentary organic matter in the eastern equatorial Atlantic. *Science* 198; 605-609.
- Bender, M.L. (1971). Does upward diffusion supply the excess manganese in pelagic sediments? *J. Geophys. Res.* 76; 4212-4215.
- Berner, R.A. (1981). Authigenic mineral formation resulting from organic matter decomposition in modern sediments, *Oceanologica Acta*, 1; 99-105.
- Bhadra, B., Raghukumar,C., Pindi, P.K. and Shivaji, S.(2008). *Brevibacterium oceani* sp. nov., isolated from deep-sea sediment of Chagos trench, Indian Ocean. *Int J of System and Evolution Microbiol*, 58; 57-60.

- Biddle, J.F., Lipp, J.S., Lever, M.A., Lloyd, K.G., Sørensen, K.B., Anderson, R., Fredricks, H.F., Elvert, M., Kelly, T.J., Schrag, D.P., Sogin, M.L., Brechley, J.E., Teske, A., House, C.H., and Hinrichs, K.-U. (2006). Heterotrophic Archaea dominate sedimentary subsurface ecosystems off Peru. *Proc Natl Acad Sci* 103(10); 3846-3851.
- Billen, G. (1982). Modelling the process of organic matter degradation and nutrient recycling in sedimentary systems. In: *Sediment microbiology* Eds. D.B. Nedwell and C.M. Brown. Academic Press London 15-52.
- Bischoff J. L. and Ku T. L. (1970). Pore fluids of recent marine sediments-I. Oxidizing sediments of 20°N, Continental Rise to Mid-Atlantic Ridge. *J. Sediment. Petrol.* 40; 960-972.
- Bjerrum, C. J., and D. E. Canfield. (2002). Ocean productivity before about 1.9 Gyr ago limited by phosphorus adsorption onto iron oxides. *Nature* 417; 159–162.
- Bligh, E.G. and Dyer, W.J. (1959). A rapid method of total lipid extraction and purification. *Can. J. Biochem. Physiol.*, 37; 911-917.
- Blöchl, E., et al., (1997). *Pyrolobus fumarii*, gen. and sp. nov., represents a novel group of archaea, extending the upper temperature limit for life to 113 °C. *Extremophiles* 1; 14–21.
- Boetius, A. (1995) Microbial hydrolytic enzyme activities in deep-sea sediments. *Helgoländer Meeresunters.* 49; 177-187.
- Boetius, A. Ferdelman, T., and Lochte K. (2000). Bacterial activity in sediments of the deep Arabian Sea in relation to vertical Flux *Deep-Sea Res II* 47; 2835-2875.
- Boetius, A., Scheibe, S., Tselepidis, A., Thiel, H., 1996. Microbial biomass and activities in deep-sea sediments of the Eastern Mediterranean: trenches are benthic hotspots. *Deep-Sea Research I* 43; 299–307.
- Boivin-Jahns, V., Ruimy, R. Bianchi, A. Dumas, S., and Christen, R. (1996). Bacterial diversity in a deep-subsurface clay environment, *Appl. Environ. Microbiol.*, 62(9); 3405–3412.
- Borole, D. V., (1993). Late Pleistocene sedimentation: A case of the Central Indian Ocean Basin. *Deep-Sea Res. A*, 40 (4); 761-775.

- Brocks, J.J., Logan, G.A., Buick, R., Summons, R.E., (1999). Archean molecular fossils and the early rise of eukaryotes. *Science* 285; 1033– 1036.
- Buckley, D.E. and Cranston, R. E. (1988). Early diagenesis in deep sea turbidites: The imprint of palaeo-oxidation zones *Geochim. Cosmochim. Acta.*, 52; 2925-2939.
- Buridge D. J. and Gieskes J. M. (1983). A pore water/solid phase diagenetic model for manganese in marine sediments. *Amer. J. Sci.* 283; 29-47.
- Button, D. K., Robertson, B. R. Lepp, P. W. and Schmidt. T. M. (1998). A small, dilute-cytoplasm, high-affinity, novel bacterium isolated by extinction culture and having kinetic constants compatible with growth at ambient concentrations of dissolved nutrients in seawater. *Appl. Environ. Microbiol.* 64; 4467–4476.
- Button, D. K., Schut, F., Quang, P., Martin, R. and Robertson, B. R. (1993). Viability and isolation of marine bacteria by dilution culture: theory, procedures, and initial results. *Appl. Environ. Microbiol.* 59; 881–891.
- Calvert, S.E. and Price, N.B. (1972). Diffusion and reaction profiles of dissolved manganese in the pore waters of marine sediments. *Earth Planet. Sci. Lett.* 16; 245-249.
- Campbell, K. A. (2006). Hydrocarbon seep and hydrothermal vent paleoenvironments and paleontology: Past developments and future research directions. *Palaeogeogr. Palaeoclimatol. Palaeoecol.*, 232, 362 – 407, doi:10.1016/j.palaeo.2005.06.018.
- Canfield DE, Thamdrup B (2009). Towards a consistent classification scheme for geochemical environments, or, why we wish the term ‘suboxic’ would go away. *Geobiology* 7, 385–392.
- Canfield, D. E. (1991). Sulfate reduction in deep sea sediments, *Am. J. Sci.*, 291; 177–188.
- Carlson, C. A., and H. W. Ducklow (1996). Growth of bacterioplankton and consumption of dissolved organic carbon in the Sargasso Sea. *Aquat. Microb. Ecol.* 10; 69–85.
- Carlsson, P., Graneli E. (1993). Availability of humic bound nitrogen for coastal phytoplankton. *Estuar. Coast. Shelf Sci.* 36; 433-477.
- Carpenter, J.H. (1965). The Chesapeake Bay Institute technique for the Winklers dissolve oxygen method. *Limnol Oceanogr* 10; 141-143.

- Casamayor E.O., Garcia-Cantizano J., Mas J., Pedros-Alio, C. (2001). Microbial primary production in marine oxic-anoxic interfaces: main role of dark fixation in the Ebro River salt wedge estuary. *Mar Ecol Prog Ser* 215; 49–56.
- Casamayor EO, Garcia-Cantizano J, Pedros Alio C (2008). Carbon dioxide fixation in the dark by photosynthetic bacteria in sulphide rich stratified lakes with oxic-anoxic interfaces *Limnol Oceanogr* 53(4);1193–1203.
- Cauwet, G. (1978). Organic chemistry of seawater particulates: Concepts and developments. *Oceanologica Acta*, 1; 99-105.
- Chakrabarti, S., Bhattacharya, S., Bhattacharya, S.K. (2003). Immobilization of D-Ribulose-1,5-bisphosphate Carboxylase/Oxygenase A Step Toward Carbon Dioxide Fixation Bioprocess *Biotechnol and Bioengineer* 81(6); 706-711.
- Chandramohan, D., Loka Bharathi, P.A., Nair S. and Matondkar, S.G.P. (1987). Bacteriology of Ferromanganese nodules from the Indian Ocean *Geomicrobiology J.* 5(1); 17-31.
- Chapman, A.G. and Atkinson, D. E. (1977). Adenine nucleotide concentrations and turnover rates. Their correlation with biological activity in bacteria and yeast. *Adv. Microb. Physiol.* 15; 253-306.
- Chevaldonne, P, Desbruyeres, D, Le Haitre, M (1991). Time-series of temperature from three deep-sea hydrothermal vent sites. *Deep Sea Research A* 38; 1417-1430.
- Childress, JJ, Fisher, CR, Favuzzi, JA, Kochevar, RE, Sanders, NK, Alayse, AM (1991) Sulphide-driven autotrophic balance in the bacterial symbiont-containing hydrothermal vent tubeworm *Riftia pachyptila*. *Biological Bulletin* 180; 135-153.
- Chrost, R.J. (1991). Environmental control of the synthesis and activity of aquatic microbial ectoenzymes. *In: Microbial enzymes in the aquatic environment. Ed by R.J.Chrost. Springer, New York* 29-59.
- Claypool, G.E. and Kvenvolden, K.A. (1983). Methane and other hydrocarbon gases in marine sediment. *Ann. Rev. Earth and Planet. Sci.* 11; 299-327 .
- Colley, S. and Thomson, J. (1985). Recurrent uranium relocations in distal turbidites emplaced in pelagic conditions. *Geochim. Cosmochim. Acta* 49; 2339-2348.

- Colley, S., Thomson, J., Wilson, T. R. S. and Higgs, N. C. (1984). Post depositional migration of elements during diagenesis in brown clay and turbidite sequences in the North East Atlantic. *Geochim. Cosmochim. Acta* 48; 1223- 1235.
- Colombini, M.P. and Fuocco, R. (1983). Determination of manganese at ng /ml levels in natural water by differential pulse polarography. *Talanta*, 30(12); 901-905.
- Colwell, F.S., (2001). Constraints on the distribution of microorganisms in subsurface environments. In: *Fredrickson, J.K., Fletcher, M. (Eds.), Subsurface microbiology and biogeochemistry*. Wiley-Liss, New York, pp. 71– 95.
- Conklin, A.R., MacGregor, A.N., (1972). Soil adenosine triphosphate: extraction, recovery and half-life. *Bull. of Evt. Contam. Toxicol.* 72; 296-300.
- Connon, S.A. and Giovannoni, S.J (2002). High-Throughput Methods for Culturing Microorganisms in Very-Low-Nutrient Media Yield Diverse New Marine Isolates *Appl Environ Microbiol* 68(8); 3878–3885.
- Contin, M., Todd, A. Brookes, P.C. (2001). The ATP concentration in the soil microbial biomass *Soil Biol. and Biochem.* 33;701-704.
- Contin, M., Jenkinson, D.S., Brookes, P.C. (2002). Measurement of ATP in soil: correcting for incomplete recovery *Soil Biol. and Biochem.* 34; 1381–1383.
- Copley, J. (2005). Springtime in the abyss. *New Scientist Environment. New Scientist* 187 (2525); 44-49.
- Corre, E., Reysenbach, A-L., Prieur, D. (2001). ϵ -Proteobacterial diversity from a deep-sea hydrothermal vent on the Mid-Atlantic Ridge. *FEMS Microbiol Lett* 205; 329-335.
- Curtis, T. P., Sloan, W.T. (2004). Prokaryotic diversity and its limits: microbial community structure in nature and implications for microbial ecology *Current Opin in Microbiol.* 7;221–226.
- D'Hondt, S., Jørgensen, B.B., Miller, D.J., Batzke, A., Blake, R., Cragg, B.A., Cypionka H., Dickens G.R., Ferdelman T., Hinrichs K-U, Holm N.G., Mitterer, R., Spivack, A., Wang, G., Bekins, B., Engelen, B., Ford, K., Gettemy, G., Rutherford, S.D., Sass, H., Skilbeck, C.G., Aiello, I.W., Gue`rin, G, House, C.H., Inagaki, F., Meister, P., Naehr, T., Niitsuma, S., Parkes, R.J., Schippers, A., Smith, D.C., Teske,

- A., Wiegel, J., Padilla, C.N., Acosta, J.L.S. (2004) Distributions of microbial activities in deep seafloor sediments. *Science* 306; 2216-2221.
- D'Hondt, S., Rutherford, S., Spivack, A.J. (2002). Metabolic activity of subsurface life in deep-sea sediments. *Science* 295; 2067–2070.
- D'Hondt, S., *et al.*, (2003). Controls on microbial communities in deeply buried sediments, Eastern Equatorial Pacific and Peru Margin. Proceedings of the ocean drilling program. Initial report, vol. 201. Ocean Drilling Program, College Station, TX.
- Damare, S., Raghukumar, C., Raghukumar, S., (2006). Fungi in deep-sea sediments of the Central Indian Basin. *Deep-Sea Res. I.* 53; 14-27.
- Danovaro, R., Fabiano, M., Della Croce, N. (1993). Labile organic matter and microbial biomass in deep sea sediments (Eastern Mediterranean sea). *Deep-sea Res* 40; 953-965.
- Danovaro, R. Della Croce, N., Dell'Anno, A., Pusceddu, A. (2003). A depocenter of organic matter at 7800m depth in the SE Pacific Ocean. *Deep-Sea Research I* 50 1411–1420.
- Danovaro, R., Dell'Anno, A., Corinaldesi, C., Magagnini, M., Noble, R., Christian Tamburini, C. and Weinbauer, M. (2008). Major viral impact on the functioning of benthic deep-sea ecosystems. *Nature* 454(28); 1084-1088.
- Danovaro, R., Fabiano, M., Della Croce, N., (1993). Labile organic matter and microbial biomasses in deep-sea sediments (Eastern Mediterranean Sea). *Deep-Sea Research I* 40, 953-965.
- Das, A., Fernandes, C.E.G., Naik, S.S. Nagender Nath, B., Suresh, I., Mascarenhas-Pereira, M.B.L., Gupta, S.M., Khadge, N.H., Prakash Babu, C., Borole, D.V., Sujith, P.P., Valsangkar, A. B., Shashikant Mourya, B., Biche, S.U., Sharma, R. and LokaBharathi P. A. (2010a). Bacterial response to contrasting sediment geochemistry in Central Indian Basin. *Sedimentology* doi: 10.1111/j.1365-3091.2010.01183.x (2010).
- Das, A., Sujith, P.P., Mourya, B.S., Biche, S.U. and LokaBharathi, P.A. (2010b) Chemosynthetic activity prevails in deep-sea sediments of Central Indian Basin. *Extremophiles* DOI 10.1007/s00792-010-0346-z.

- Das, P., Iyer, S.D., and Kodagali, V.N. (2007). Morphological characteristics and emplacement mechanism of the seamounts in the Central Indian Ocean Basin. *Tectonophysics*, 443; 1–18.
- Das, P., Iyer, S.D., Kodagali, V.N. and Krishna, K.S. (2005). A new insight into the distribution and origin of seamounts in the Central Indian Ocean Basin. *Mar. Geod.*, 28; 259-269.
- de Souza, S.N., Sardesai S.D., Ramsh Babu V., Murty, V.S.N., Gupta G.V.M. (2001). Chemical characteristics of Central Indian Basin waters during southern summer. *Deep-Sea Res II* 48; 3343-3352.
- Delescluse, M., and Chamot-Rooke, N. (2008). Serpentinization pulse in the actively deforming Central Indian Basin. *Earth Planet Sci Lett.*, 276 (1-2); 140-151.
- Delistraty, D.A. and Hershner, C. (1983). Determination of adenine nucleotide levels in *Zostera marina* (eelgrass). *J. Appl. Biochem.*, 5; 404–405.
- Dell'Anno, A. and Danovaro, R. (2005). Extracellular DNA plays a key role in deep-sea ecosystem functioning. *Science* 309; 2179.
- DeLong, E.F., Franks, G. D., Yayanos, A.A. (1997). Evolutionary Relationships of Cultivated Psychrophilic and Barophilic Deep-Sea Bacteria. *Appl. Environ. Microbiol.* 63(5); 2105–2108.
- DeMaere, M.Z., Ting,L., Ertan,H., Johnson,J., Ferriera,S., Lapidus,A., Iain Anderson,I., Kyrpides,N., Munk, A.C., Detterg,C., Han,C.S., Brown,M.V., Robb, F.T., Kjelleberga S., and Ricardo Cavicchioli, R. (2009). The genomic basis of trophic strategy in marine bacteria. *Proc Natl Acad Sc* 106(37) 15527–15533.
- Deming, J. W., and J. A. Baross. (2000). Survival, dormancy, and nonculturable cells in extreme deep-sea environments, p. 147–197. In R. R. Colwell and D. J. Grimes (ed.), *Nonculturable microorganisms in the environment*. ASM Press, Washington, D.C.
- Deming, J. W., Yager, P. L., (1992). Natural bacterial assemblages in deep-sea sediments: towards aglobal view. In: *Deep-sea food chains and the global carbon cycle*. Ed. by G. T. Rowe & V. Pariente. Kluwer, Dordrecht, 11-28.

- Deming, J.W., and Baross, J.A., (1993a). The early diagenesis of organic matter: bacterial activity. In: Engel, M.H., Macko, S. (Eds.), *Organic geochemistry: principles and applications*. Plenum Press, New York, pp. 119-144.
- Deming, J.W., and Baross, J.A., (1993b). Deep-sea smokers: windows to a subsurface biosphere. *Geochim. Cosmochim. Acta* 57; 3219– 3230.
- Deming, J.W., Somers, L.K., Straube, W.L., Swartz, D.G., and MacDonell, M.T. (1988). Isolation of an obligately barophilic bacterium and description of a new genus, *Colwellia* gen. nov. *System. Appl. Microbiol.* 10; 152-160.
- Dick, G.J., Lee Y.E. & Tebo B.M. (2006). Manganese(II)-oxidizing *Bacillus* spores in Guaymas Basin hydrothermal sediments and plumes. *Appl Environ Microbiol* 72: 3184–3190.
- Dixon, J.L., Turley, C.M., (2002). Measuring bacterial production in deep-sea sediments using ³H-thymidine incorporation: ecological significance. *Microbial Ecology* 42; 549- 561.
- Dyment, J. (1993). Evolution of the Indian Ocean Triple Junction between 65 and 49 Ma (anomalies 28 to 21). *J. Geophys. Res.*, 98; 13863-13878.
- Eardly, D.F., Carton, M.W., Gallagher, J.M. and Patching J.W. (2001). Bacterial abundance and activity in deep-sea sediments from the eastern North Atlantic *Progr Oceanogr* 50; 245–259.
- Edwards, K. J., Rogers, D. R., Wirsén, C. O and McCollom, T. M. (2003). Isolation and Characterization of Novel Psychrophilic, Neutrophilic, Fe-Oxidizing, Chemolithoautotrophic α - and γ -*Proteobacteria* from the deep Sea. *Appl. Environ Microbiol.*, 69(5); 2906–2913.
- Edwards, K.J., Bach, W., Thomas M., McCollom, T.M., and Rogers, D.R. (2004). Neutrophilic Iron-Oxidizing Bacteria in the Ocean: Their Habitats, Diversity, and Roles in Mineral Deposition, Rock Alteration, and Biomass Production in the Deep-Sea. *Geomicrobiology Journal*, 21; 393–404,
- Ehrlich, H.L. (1998). Geomicrobiology: its significance for geology. *Earth-Sci. Rev.* 45; 45–60.

- Eilers, H., Pernthaler, J. and Amann R. (2000a). Succession of pelagic marine bacteria during enrichment: a close look on cultivation-induced shifts. *Appl. Environ. Microbiol.* 66; 4634–4640.
- Eilers, H., Pernthaler, J. Glöckner F. O., and Amann R. (2000b). Culturability and in situ abundance of pelagic bacteria from the North Sea. *Appl. Environ. Microbiol.* 66; 3044–3051.
- Emerson, S., and Hedges, J.I. (1988). Processes controlling the organic carbon content of open ocean sediments. *Paleoceanography* 3; 621-634.
- Emerson, S., Janhke, R., Bender, M., Froelich, P., Klinkhammer, G., Bowser, C. and Setlock, G. (1980). Early diagenesis in sediments from the eastern equatorial Pacific: I. Pore water nutrient and carbonate results. *Earth Planet. Sci. Lett.* 49, 57-80.
- Fabiano, M., Pusceddu, A., Dell'Anno, A., Armeni, M., Vanucci, S., Lampitt, R.S., Wolff, G.A., Danovaro, R., (2001). Fluxes of phytopigments and labile organic matter to the deep ocean in the NE Atlantic Ocean. *Progr Oceanogr* 50; 89–104.
- Fairbanks, B.C., Woods, L.E., Bryant, R.J., Elliot, E.T., Cole, C.V., Coleman, D.C., (1984). Limitations of ATP estimates of microbial biomass. *Soil Biol Biochem* 16, 549-558.
- Farjalla, V. F., F. A. Esteves, R. L. Bozelli, and F. Roland. (2002). Nutrient limitation of bacterial production in clear water Amazonian ecosystems. *Hydrobiologia* 489; 197–205.
- Farrimond P., Eglinton G., Brassell S.C. and Jenkyns H.C. (1989). Toarcian anoxic event in Europe an organic geochemical study. *Mar. Petrol. Geol.*, 6, 136-147.
- Feely, R.A., Massoth, G.J., Baker, E.T., Cowen, J.P., Lamb, M.F., Kroglund, K.A. (1990). The effect of hydrothermal processes on midwater phosphorus distributions in the northeast Pacific. *Earth Planet Sci Lett* 96; 305-318.
- Felsenstein, J. (1993). PHYLIP (Phylogeny Inference Package), v. 3.5. University of Washington, Seattle.
- Fenchel, T. (2002). Microbial behavior in a heterogeneous world. *Science* 296; 1068–1071.

- Fenney, B. P., Lyle, M. W., and Heath, G. R. (1989). Sedimentation at MANOP site H (eastern equatorial Pacific) over the past 400,000 years: Climatically induced redox variations and their effects on transition metal cycling; *Paleoceanography* 3(2); 165-189.
- Fichez, R. (1991). Composition and fate of organic matter in submarine cave sediments: implications for the biogeochemical cycle of organic carbon. *Oceanol. Acta.*, 14; 369–377.
- Fischer, R., and Thauer, R.K. (1989). Methyltetrahydromethanopterin as an intermediate in methanogenesis from acetate by *Methanosarcina barkeri*. *Arch of Microbiol* 131; 459-465.
- Fredrickson, J. K., Balkwill, D. L., Zachara, J. M., Li, S. M., Brockman, W. F. J. and Simmons M. A. (1991). Physiological diversity and distributions of heterotrophic bacteria in deep cretaceous sediments of the Atlantic Coastal Plain, *Appl. Environ. Microbiol.*, 57(2); 402–411.
- Fredrickson, J. K., McKinley, J.P., Bjornstad, B.N., Long, P.E., Ringelberg, D.B., White, D.C., Krumholz, L.R., Suflita, J.M., Colwell, F.S., Lehman, R.M., Phelps, T.J. and Onstott, T.C. (1997). Pore-size constraints on the activity and survival of subsurface bacteria in a late Cretaceous shale-sandstone sequence, northwestern New Mexico. *Geomicrobiol. J.* 14(3); 183–202.
- Fredrickson, J.K., Onstott, T.C., (2001). Biogeochemical and geological significance of subsurface microbiology. In: *Fredrickson, J.K., Fletcher, M. (Eds.), Subsurface Microbiology and Biogeochemistry*. Wiley-Liss, New York, pp. 3– 37.
- Froelich, P. N., Klinkhammer, G. P., Bender, M. L., Luedtke, G. R., Heath, G. R., Cullen, D., Dauphin, P., Hammond, D., Hartman, B. and Maynard, V. (1979) Early oxidation of organic matter in pelagic sediments of the eastern equatorial Atlantic: Sub-oxic diagenesis. *Geochim. Cosmochim. Acta* 43; 1075-1090.
- Froelich, P.N., Authur, M.A., Burnett, W.C., Deakin, M., Hensley, V., Jahnke R., Kaul, L., Kim K.-H., Roe, K., Soutar, A. and Vathakanon C. (1988). Early diagenesis of organic matter in Peru continental margin sediments: Phosphorite precipitation. *Mar Geol.* 80; 309-343.

- Fry, J.C., Parkes, R.J., Cragg, B.A., Weightman, A.J. and Webster, G. (2008). Prokaryotic biodiversity and activity in the deep seafloor biosphere *FEMS Microbiol Ecol* 66; 181–196.
- Fuhrman, J.A., and Hagström, Å. (2008). Bacterial and archaeal community structure and its patterns. In *Microbial Ecology of the Oceans*, 2nd Ed. Kirchman, D.L. (ed.). New York, USA: Wiley-Blackwell, pp. 45–90.
- Galand, P.E., Casamayor, E.O., Kirchman, D.L., Potvin, M., and Lovejoy, C. (2009). Unique archaeal assemblages in the Arctic Ocean unveiled by massively parallel tag sequencing *ISME J* 3; 860–869.
- Galchenko VF, Abramochkina FN, Berzrukova LN, Sorolova EN, Ivanov MV (1988) Species composition of aerobic methanotrophic microflora in the Black Sea. *Microbiology* 57; 248-253.
- García-Cantizano, J., Casamayor, E.O., Gasol, J.M., Guerrero, R., Pedros-Alio, C. (2005) Partitioning of CO₂ incorporation among guilds of microorganisms in lakes with oxic-anoxic interfaces and estimation of *in situ* specific growth rates. *Microb Ecol* 50:230–241.
- Garven, G. and Freeze, R. A. (1984). Theoretical analysis of the role of groundwater flow in the genesis of stratabound ore deposits: Mathematical and numerical model, *Am J of Sci*, 284; 1085-1124.
- Gauthier, G., Guthier M., Christen R. (1995) "Phylogenetic analysis of the genera *Alteromonas*, *Shewanella*, and *Moritella* using genes coding for small-subunit rRNA sequences and division of the genus *Alteromonas* into two genera, *Alteromonas* (emended) and *Pseudoalteromonas* gen. nov., and proposal of twelve new species combinations.", *Int J Syst Bacteriol*, 45(4);755-61.
- Ghosh, A.K. and Mukhopadhyay, R. (1999). Exploration. In: *Mineral wealth of the Ocean*. Oxford and IBH Publishing Co. Pvt. Ltd. pp. 176-203.
- Ghosh, A.K. and Mukhopadhyay, R. (1999a). Manganese nodules. In: *Mineral wealth of the Ocean*. Oxford and IBH Publishing Co. Pvt. Ltd. pp. 87-120.
- Gieskes, J.M., Simoneit, B. R.T., Goodfellow, W.D., Baker, P.A. and Mahn, C. (2002) Hydrothermal geochemistry of sediments and porewaters in Escanaba Trough—ODP Leg 169. *Appl Geochem.*, 17; 1435–1456.

- Gilbert, J.A., Field, D., Swift, P., Newbold, L., Oliver, A., Smyth, T., *et al.* (2009). Seasonal succession of microbial communities in the Western English Channel using 16S rRNA-tag pyrosequencing of the V6 region. *Environ Microbiol* 11; 3132–3139.
- Glasby, G. P. (2006). Manganese: Predominant role of nodules and crusts, In: *Marine Geochemistry*, edited by H. D. Schulz and M. Zabel, pp. 371–428, Springer, Berlin.
- Glazer, B.T., Luther III, G.W., Konovalov, S. K., Friederich, G.E., Trouwborst, R.E. and Romanov, A.S. (2006). Spatial and temporal variability of the Black Sea suboxic zone. *Deep-Sea Res II*, 53, 1756–1768.
- Glud, R.N., Ramsing N.B., Gundersen J.K., Klimant, I. (1996). Planaroptrodes: a new tool for fine scale measurements of two-dimensional O₂ distribution in benthic communities. *Mar Ecol Prog Ser* 140; 217–226.
- Goffredi, S.K., Johnson, S.B. and Vrijenhoek, R.C. (2007). "Genetic Diversity and Potential Function of Microbial Symbionts Associated with Newly Discovered Species of *Osedax* Polychaete Worms". *Appl Environ Microbiol* 73 (7); 2314–2323. doi:10.1128/AEM.01986-06. PMID 17277220
- Gold, T. (1992). The deep, hot biosphere. *Proc. Natl. Acad. Sci. U. S.A.* 89; 6045–6049.
- Gold, T. (1999). The deep hot biosphere. Springer-Verlag, New York (235 pp.).
- Gold, T., and Soter, S. (1982). Abiogenic methane and the origin of petroleum. *Energy Explor. Exploit.*, 1; 89– 104.
- Goloway, F., and Bender, M. (1982). Diagenetic models of interstitial nitrate profiles in deep sea suboxic sediments. *Limnol. Oceanogr.* 27; 624-638.
- Goltekar, R.C., Krishnan, K.P., DeSouza, M.J.B.D., Paropkari, A.L. and Loka Bharathi, P.A. (2006). Effect of carbon source concentration and culture duration on retrievability of bacteria from certain estuarine, coastal and offshore areas around peninsular India. *Curr. Sci.*, 90(1); 103-106.
- Gonsalves, M-J., Fernandes C.E.G., Fernandes, S.O. Sujith P.P., Das, A. Naik, S., Loka Bharathi P.A. (2009). Perspectives of microbial diversity in varied marine ecosystems in the Indian Ocean region. International Census of Marine Microbes 454 Users Spring Meeting, April 6-9th, 2009, Woods Hole, Massachusetts, USA (Poster).

- González, J.M., Whitman, W.B., Hodson R.E and Moran, M.A. (1996). Identifying Numerically Abundant Culturable Bacteria from Complex Communities: an Example from a Lignin Enrichment Culture *Appl Environ Microbiol* 62(12); 4433-4440.
- Goodman, J. C., Collins, G. C., Marshall, J. and Pierrehumbert, R. T. (2004). Hydrothermal plume dynamics on Europa: Implications for chaos formation, *J. Geophys. Res.*, 109, E03008, doi:10.1029/2003JE002073
- Gottschal, J.C., Harder, W., and Prins, R.A. (1991). Principles of enrichment, isolation, cultivation and preservation. In: *The Prokaryotes 11nd Edition A Handbook on the biology of Bacteria: Ecophysiology, Isolation, Identification, Applications*. Eds Balows, A., Trüper, H.G., Dworkin, M., Harder, W., Schleifer, K.-H. Vol. I pp.149-196.
- Grasshoff, K., Ehrhardt, M., and Kremling, K. (1983). *Methods of seawater analysis* (2nd ed.). Verlag Chemie, 419 pp.
- Greaves M.P., Wheatley R. E., Shepherd, H. and Knoght, A.H. (1973). Relationship between microbial populations and adenosine triphosphate in a basin peat. *Soil Biol. Biochem.* 5; 685-687.
- Green, P.N. (1991). The genus methylobacterium. In: *The prokaryotes: A handbook on biology of Bacteria: Ecophysiology, Isolation, Identification, Application*. Eds Balows, A., Trüper, H.G., Dworkin, M., Harder, W., Schleifer, K.-H., Vol III, 2nd Edition Springer-Verlag.
- Gugliandolo, C. and Maugeri, T.L. (1998). Temporal Variations in Heterotrophic Mesophilic Bacteria from a Marine Shallow Hydrothermal Vent off the Island of Vulcano (Eolian Islands, Italy). *Microb Ecol.*, 36; 13-22.
- Gupta S.M. and Jauhari P. (1994). Radiolarian abundance and geochemistry of the surface-sediments from the Central Indian Basin: Inferences to the Antarctic bottom water current. *Curr. Sc.* 66(9); 659-663.
- Gupta, S.M. (2000). Biostratigraphic analysis of the top layer of sediment cores from the reference and test sites of the INDEX area *Mar. Georesour. Geotechnol.*: 18(3); 2000; 259-262.

- Habicht, K.S., Gade, M., Thamdrup, B., Berg, P., Canfield, D.E. (2002). Calibration of sulfate levels in the Archean ocean. *Science*, 298: 2372–2374.
- Hallam, S.J., Girguis, P.R., Preston, C.M., Richardson, P.M., DeLong, E.F. (2003). Identification of methyl coenzyme M reductase A (*mcrA*) genes associated with methane-oxidizing archaea. *Appl Environ Microbiol* 69; 5483–5491.
- Hallam, S.J., Putnam, N., Preston, C.M., Detter, J.C., Rokhsar, D., Richardson, P.M., DeLong, E.F. (2004). Reverse methanogenesis: testing the hypothesis with environmental genomics. *Science* 305; 1457–1462.
- Hanson, R.S. (1980). Ecology and diversity of methylotrophic bacteria. *Adv in Appl Microbiol* 26, 3-39.
- Harder, W. and Dijkhuizen, L. (1982). Strategies of mixed substrate utilization in microorganisms. *Philos. Trans. R. Soc. London. B.*, 297; 459-480.
- Hartmann, M. (1979). Evidence for early diagenetic mobilization of trace metals from discolorations of pelagic sediments. *Chem. Geol.* 26; 277-293.
- Hayes, J. M. (2001). Fractionation of carbon and hydrogen isotopes in biosynthetic processes. *Rev. Min. Geochem.* 43; 225–278.
- Hesselmann, R.P.X, Von Rummell, R., Resnick, S.M., Hany R., Zehnder A.J.B. (2000). Anaerobic metabolism of Bacteria performing enhanced biological phosphate removal. *Wat. Res.* 34(14); 3487-3494.
- Hobbie, J.E., Daley, R.J. and Jasper, S. (1977). Use of Nucleopore filters for counting bacteria by fluorescent microscopy *Appl Environ. Microbiol.*, 3; 1225-1228.
- Holm, N.G., Charlou, J.L., (2001). Initial indications of abiotic formation of hydrocarbons in the rainbow ultramafic hydrothermal system. *Earth Planet. Sci. Lett.* 191; 1 – 8.
- Holm-Hansen, O. and Booth, C. R. (1966). The measurement of adenosine triphosphate in the ocean and its ecological significance. *Limnol. Oceanogr.*, 11; 510-519.
- Hoppe, H. G., Ullrich, S. (1999). Profiles of ectoenzymes in the Indian Ocean: phenomena of Phosphatase activity in the mesopelagic zone. *Aquat. Microb. Ecol.* 19; 129-138.
- House, C. H., Schopf, J. W. and Stetter, K. O. (2003). Carbon isotopic fractionations by archaeans and other thermophilic prokaryotes. *Org. Geochem.* 34; 345–356.

<http://www.ncbi.nlm.nih.gov/pubmed>

- Huber, J.A., Mark Welch, D.B., Morrison, H.G., Huse, S.M., Neal, P.R., Butterfield, D.A., Sogin, M.L. (2007). Microbial Population Structures in the Deep Marine Biosphere. *Science* 318; 97-100.
- Hugler, M., Huber, H., Stetter, K. O. and Fuchs, G. (2003). Autotrophic CO₂ fixation pathways in archaea (Crenarchaeota). *Arch. Microbiol.* 179; 160–173.
- Ikner L.A., Toomey, R.S., Nolan, G., Neilson, J.W., Pryor, B.M. and Maier, R.M. (2007). Culturable Microbial Diversity and the Impact of Tourism in Kartchner Caverns, Arizona. *Microb Ecol* 53; 30–42.
- Inagaki, F., Nunoura, T., Nakagawa, S., Teske, A., Lever, M., Lauer, A., *et al.* (2006). In search of the deep biosphere: biogeographical distribution and diversity of microbes in deep marine sediments associated with methane hydrates on the Pacific Ocean Margin. *Proc Natl Acad Sci USA* **103**: 2815–2820.
- Inagaki, F., Suzuki, M., Takai K., Oida, H., Sakamoto, T., Aoki, K., Neilson, K.H. and Horikoshi, K. (2003). Microbial communities associated with geological horizons in coastal subseafloor sediments from the Sea of Okhotsk. *Appl Environ Microbiol* 69; 7224–7235.
- Ingole, B.S., Ansari, Z.A., Rathod, V., Rodrigues, N., (2001). Response of deep-sea macrobenthos to a small-scale environmental disturbance. *Deep-Sea Research II* 48; 3401–3410.
- Ingole, B.S., Pavitran, S., Goltekar, R. and Gonsalves, S. (2005). Faunal diversity and abundance. *In: Benthic environmental variability in the Central Indian Ocean Basin-I*. Project report submitted to Department of Ocean Development, Govt. of India.
- Iyer, S.D., Mascarenhas-Pereira, M.B.L. and Nath B.N. (2007). Native aluminium (spherules and particles) in the Central Indian Basin sediments: Implications on the occurrence of hydrothermal events. *Mar. Geol.*, 240, 177-184.
- Iyer, S.D., Shyam Prasad, M., Gupta, S.M. and Charan, S.N. (1997). Evidence of recent hydrothermal activity in the Central Indian Basin. *Deep-Sea Res.*, 44; 1167-1184.

- Jahnke, R., Emerson, S. and Murray, J. W. (1982). A model of oxygen reduction, denitrification and organic matter mineralization in marine sediments. *Limnol. Oceanogr.* 27; 610-623.
- Jahnke, R.A. and Jahnke, D.B. (2004). Calcium carbonate dissolution in deep sea sediments: Reconciling microelectrode, porewater and benthic flux chamber results. *Geochim Cosmochim Acta*, 68(1), 47–59.
- Jahnke, R.A.. (1996). The global ocean flux of particulate organic carbon: areal distribution and magnitude. *Global Biogeochemical Cycles* 10, 71–88.
- Jahnke, R.A., Jahnke, D.B., (2000). Rates of C, N, P and Si recycling and denitrification at the US Mid-Atlantic continental slope depocenter. *Deep-Sea Res I* 47, 1405–1428.
- Jahnke, R.A., Reimers, C.E., Craven, D.B., (1990). Intensification of recycling of organic matter at the sea floor near ocean margins. *Nature* 348, 50–54.
- Jannasch, H.J., Eimjellen, K. Wirsen, C.O. and Farmanfarmaian (1971). Microbial degradation of organic matter in the deep-sea. *Science* 171, 672-675.
- Jannasch, H. W. (1979). Microbial turnover of organic matter in the deep-sea. *Bioscience*. 29; 228-232.
- Jannasch, H.W. and Wirsen C.O. (1973). Deep-sea micro-organisms: In situ response to nutrient enrichment. *Science*. 180; 641-643.
- Jannasch, H. W., and G. E. Jones. (1959). Bacterial populations in seawater as determined by different methods of enumeration. *Limnol. Oceanogr.* 4;128–139.
- Jannasch, H.W. (1989). Chemosynthetically sustained ecosystems in the deep sea. In: Schlegel HG, Bowien B (eds) Autotrophic bacteria. Springer, Berlin Heidelberg New York, pp 147–166.
- Jannasch, H.W., and Taylor, C.D. (1984). Deep-sea microbiology. *Annu. Rev. Microbiol.* 38; 487-514.
- Jarvis, I. and Higgs N. (1987). Trace-element mobility during early diagenesis in distal turbidites: Late Quaternary of the Madeira Abyssal Plain, N. Atlantic. In: *Geology and Geochemistry of Abyssal Plains* (eds. P. P. E. Weaver and J. Thomson). DD. 179-213. Geol. Soc. Spec. Pub]. 3 I.

- Jasper, J.P. and Gagosian, R.B. (1990). The sources and deposition of organic matter in the Late Quaternary Pygmy Basin, Gulf of Mexico. *Geochim Cosmochim Acta* 54 ; 117-132 .
- Jauhari, P. and Pattan, J.N., (1999). In : *Marine Mineral Deposits*, (Ed D. S. Cronan). pp 171-195.
- Jenkinson, D.S. (1988). Determination of microbial biomass nitrogen and carbon in soil. In: *Wilson, J.T. (Ed). Advances in Nitrogen Cycling in Agricultural Ecosystems. Commonwealth Agricultural Bureau International, Wallingford*, pp. 368-386.
- Jenkinson, D.S., and Ladd, J.N. (1981). Microbial biomass in soil: measurement and turnover. In: *Paul, E.A., Ladd, J.N. (Eds.). Soil Biochemistry, vol.5. Marcel Dekker, New York*, pp. 415-471.
- Jenkinson, D.S., and Powlson, D.S., (1976). The effects of biocidal treatments on metabolism in soil. V. A method for measuring soil biomass. *Soil Biol. Biochem.* 8; 208-213.
- Jenkinson, S. and Oades, J. M. (1979). A method for measuring adenosine triphosphate in soil. *Soil Biol. Biochem.* 11; 193-199.
- Jensen, P.R., Gontang, E., Mafnas, C., Mincer T.J. and Fenical, W. (2005). Culturable marine actinomycete diversity from tropical Pacific Ocean sediments. *Environ Microbiol* 7(7); 1039–1048.
- Jørgensen, R.G., Brookes, P.C., Jenkinson, D.S., (1989). Some relationships between microbial ATP and soil microbial biomass, measured by the fumigation-extraction procedure and soil organic matter. *Mitteilungen der Deutschen Bodenkundlichen Gesellschaft* 59, 585-588.
- Jørgensen, B.B. and Boetius, A. (2007). Feast and famine – microbial life in the deep sea bed. *Nat Rev Microbiol* 5; 770–781.
- Jørgensen, B.B., Kuenen, J.G. and Cohen, Y. (1979). Microbial transformation of sulfur compounds in a stratified lake (Solar Lake, Sinai). *Limnol Oceanogr* 24:799–822.
- Jørgensen, B.B., Fossing, H., Wirsén, C.O. and Jannasch, H.W. (1991). Sulfide oxidation in the anoxic Black Sea chemocline. *Deep-sea Res.* 38(suppl.2): 1083-1103.
- Joux, F. and Lebaron, P. (1997). Ecological implications of an improved Direct Viable Count Method for Aquatic Bacteria. *Appl. Environ. Microbiol.*, 63(9); 3643-3647.

- Jürgens, K., Gasol, J.M. and Vaqué, D.(2000). Bacteria–flagellate coupling in microcosm experiments in the Central Atlantic Ocean *J of Expt Mar Biol Ecol.* 245; 127–147.
- Juniper, S.K., Brinkhurst, R.O. (1986). Water-column dark CO₂ fixation and bacterial-mat growth in intermittently anoxic Saanich Inlet, British Columbia. *Mar Ecol Prog Ser* 33:41–50.
- Kaczmarek W., Kaszubiak, H., and Pedziwilk, Z. (1976). The ATP content in soil microorganisms. *Ekologia Polska* 24; 399-406.
- Kamesh Raju, K.A., Ramprasad, T. (1989). Magnetic lineations in the Central Indian Basin for the period A24-A21: a study in relation to the Indian Ocean Triple Junction trace. *Earth Planetary Science Letters* 95(3-4), 395-402.
- Karl, D. M. (1978). Determination of GTP, GDP and GMP in cell and tissue extracts. *In Methods in Enzymology Vol. 57, Bioluminescence and Chemiluminescence* (S. P. Colowick and N. O. Kaplan, Eds) pp. 85-94. Academic Press, London.
- Karl, D. M. (1980). Cellular nucleotide measurements and applications in microbial ecology. *Microbiol Rev* 44; 739-796.
- Karl, D. M. and La Rock, P. A. (1975). Adenosine triphosphate measurements in soil and marine sediments. *J. Fish. Res. Bd Can.* 32; 599-607.
- Karl, D.M. (1995). Ecology of free-living, hydrothermal vent microbial communities. *In: The microbiology of deep-sea hydrothermal vents (ed Karl, D.M.). CRC press.* pp 35-124.
- Karl, D.M., McMurtry, G.M., Malohoff, A., Garcia, M.O. (1988). Loihi seamount, Hawaii: A mid-plate volcano with a distinctive hydrothermal system. *Nature* 335; 532–535.
- Kashefi, K., Lovley, D.R., (2003). Extending the upper temperature limit for life. *Science* 301; 934.
- Kato, C. (1999). Barophiles (piezophiles). *In: Horikoshi K, Tsujii K (eds) Extremophiles in deep-sea environments.* Springer-Verlag, Tokyo, pp 91–111.
- Kato, C., Inoue, A., and Horikoshi, K. (1996a). Isolating and characterizing deep-sea marine microorganisms. *Trends Biotechnol.* 14; 6-12.

- Kato, C., Li, L., Nakamura, Y., Nogi, Y., Tamaoka, J., and Horikoshi, K. (1998). Extremely barophilic bacteria isolated from the Mariana Trench, Challenger Deep, at a depth of 11,000 meters. *Appl. Environ. Microbiol.* 64; 1510-1513.
- Kato, C., Masui, N., and Horikoshi, K. (1996b). Properties of obligately barophilic bacteria isolated from a sample of deep-sea sediment from the Izu-Bonin Trench. *J. Mar. Biotechnol.* 4; 96-99.
- Khadge, N. H., (2002). Geotechnical properties of siliceous sediments from the Central Indian Basin. *Curr. Sci.*, 82 (3); 338-343.
- Kieft, T. L., Murphy, E.M., Haldeman, D.L., Amy, P.S., Bjornstad, B.N., McDonald, E.V., Ringelberg, D.B., White, D.C., Stair, J., Griffiths, R.P., Gsell, T.C., Holben, W.E. and Boone, D.R. (1998). Microbial transport, survival, and succession in a sequence of buried sediments. *Microbial Ecol.* 36(3); 336–348.
- Kirchman, D. L., Cottrell, M. T. and Lovejoy, C. (2010). The structure of bacterial communities in the western Arctic Ocean as revealed by pyrosequencing of 16S rRNA genes. *Environ Microbiol* doi:10.1111/j.1462-2920.2010.02154.x
- Kobori, H., Taga, N. (1979). Occurance and distribution of Phosphatase in neritic and oceanic sediments. *Deep Sea Res* 26; 799-808.
- Kochert, G. (1978). Carbohydrate determined by the phenol-sulfuric acid method. In: *Handbook of physiological methods: Physiological and biochemical methods*. (Eds JA Hellebust and J J Craigie). Cambridge University Press, Cambridge. pp. 95-97.
- Kogure, K., Simidu, U. and Taga, N. (1984). An improved direct viable count method for aquatic bacteria. *Arch. Hydrobiol.*, 102; 117-122.
- Kogure, K., U. Simidu, and N. Taga. (1979). A tentative direct microscopic method for counting living marine bacteria. *Can. J. Microbiol.* 25; 415–420.
- Konig, I., Drodts, M., Suess, E. and Trautwein, A.X. (1997). Iron reduction through the tan-green color transition in deep-sea sediments. *Geochim. Cosmochim. Acta.* 61 (8), 1679-1683.
- Koroleff, F. (1969). Direct determination of ammonia in natural waters as indophenol blue. *ICES paper C.M./C* , p. 9.

- Kotelnikova, S., Pedersen, K. (1998). Distribution and activity of methanogens and homoacetogens in deep granitic aquifers at Äspö Hard Rock Laboratory, Sweden. *FEMS Microbiol. Immunol.* 26; 121–134.
- Kuivila, K.M., Murray, J.W., Devol, A.H., Lidsstrom, M.E., and Reimers, C.E. (1988). Methane cycling in the sediments of Lake Washington. *Limnol Oceanogr* 33; 571-581.
- Lahajnar, N., Rixen, T., Gaye-Haake, B., Schäfer, P. and Ittekkot, V. (2005). Dissolved organic carbon (DOC) fluxes of deep-sea sediments from the Arabian Sea and NE Atlantic. *Deep-Sea Res II* 52; 1947–1964.
- Lallier-Verge's E., Bertrand P., and Desprairies. A. (1993). Organic matter composition and sulfate reduction intensity in Oman Margin sediments. *Mar. Geol.* 112; 57-69.
- Lampitt, R.S., (1985). Evidence for the seasonal deposition of detritus to the deep-sea floor and its subsequent resuspension. *Deep-Sea Research* 32, 885-897.
- Lampitt, R.S., Antia, A.N., (1997). Particle flux in deep seas: regional characteristics and temporal variability. *Deep-Sea Research I* 4, 1377–1403.
- Lauro, F.M., McDougald, D. Thomas, T., Williams, T.J. Egan, S. Rice, S., DeMaere, M., Ting, L., Ertan, H., Johnson, J., Ferreira, S., Lapidus, A., Anderson, I., Kyrpides, N., Munk, C.A., Detter, C., Han, S. C., Brown, M.V., Robb, F.T., Kjelleberg, S. and Cavicchioli (2009) The genomic basis of trophic strategy in marine bacteria *Proc Natl Acad Sc.* 106 (37) 15527–15533.
- Lee, C.C., Harris, R.F., Williams, J.D.H., Armstrong, D.E. and Syers, J.K. (1971). Adenosine triphosphate in lake sediments: I. Determination. *Soil Sci Soc Am Proc* 35; 82-86.
- Leefeldt, R.H., and Matin, A. (1980). Growth and physiology of *Thiobacillus novellas* under nutrient limited mixotrophic conditions. *J Bacteriol* 142; 645-650.
- Leigh, J.A., Rinehart Jr., K.L., and Wolfe, R.S. (1985) Methanofuran (carbon dioxide reduction factor). a formyl carrier in methane production from carbon dioxide in *Methanobacterium*. *Biochemistry* 24, 995-999.
- Li T.-Y., Bischoff J. and Mathieu G. (1969). The migration of manganese in the Arctic Basin sediment cores. *Earth Planet. Sci. Lett.* 7; 265-270.

- Li Y.-H. and Gregory S. (1974). Diffusion of ions in sea water and in deep-sea sediments. *Geochim. Cosmochim. Acta* 38; 703-714.
- Li, W. K. W., and Dickie, P. M. (1985). Growth of bacteria in seawater filtered through 0.2 µm nucleopore membranes: implications for dilution experiments. *Mar. Ecol. Prog. Ser.* 26; 245–252.
- Licciano, M., Terlizzi, A., Giangrande, A., Cavallo, R.A. and Stabili, L. (2007). Filter-feeder macroinvertebrates as key players in culturable bacteria biodiversity control: A case of study with *Sabella spallanzanii* (Polychaeta: Sabellidae). *Mar Environ Res.* 64;504–513.
- Lin, Q., Brookes, P.C. (1996). Comparison of methods to measure microbial biomass in unamended, rye grass-amended and fumigated soils. *Soil Biol. Biochem.* 28; 933-939.
- Liu, C-L, Hart, N., Peck and Jr, H.D. (1982). Inorganic pyrophosphate: energy source for sulfate-reducing bacteria of the genus *Desulfotomaculum*. *Science*, 217, 363-364.
- Lochte, K., (1992). Bacterial standing stock and consumption of organic carbon in the benthic boundary layer of the abyssal North Atlantic. In: Deep-sea food chains and the global carbon cycle. Ed. by G. T. Rowe & V. Pariente. Kluwer, Dordrecht, 1-10.
- Lochte, K., Boetius, A. and Petry, C. (1999). Microbial food webs under severe nutrient limitations: Life in the deep sea in Aquatic Microbial Food Webs: Structure and Function, Microbial Biosystems: New Frontiers, *Proceedings of the 8th International Symposium on Microbial Ecology*.
- Loka Bharathi, and Nair, S. (2005). Rise of the Dormant: Simulated Disturbance improves culturable abundance, diversity and function of deep-sea bacteria of Central Indian Basin. *Marine Geores and Geotechnol.* 23; 419-428.
- Loka Bharathi, P.A. and Nair, S. (2005). Rise of the Dormant: Simulated Disturbance Improves Culturable Abundance, Diversity, and Functions of Deep-Sea Bacteria of Central Indian Ocean Basin. *Mar. Geores. Geotechnol.*, 23; 419-428.
- Loka Bharathi, P.A. (1989). The occurrence of denitrifying colourless sulphur-oxidizing bacteria in marine waters and sediments as shown by the agar shake technique. *FEMS Microbiol Ecol.* 62, 335-342.

- Loka Bharathi, P.A. and Chandramohan, D. (1990). Sulfate-reducing bacteria from the Arabian Sea- their distribution in relation to thio-sulfate oxidizing and heterotrophic bacteria. *Bull Mar Sc.*, 47 (3); 622-630.
- Loka Bharathi, P.A., Gonsalves M-J., Fernandes C.E.G., Fernandes, S.O.Christabelle E.G. Fernandes, Sujith P.P., Das, A. and Naik, S. (2009). The Indian Ocean Cooperative 454 Run Project International Census of Marine Microbes 454 User Spring Meeting, April 6-9th, 2009 Marine Biological Laboratory Woods Hole, MA USA (Proceedings).
- Loka Bharathi, P.A. Ortiz-conde, B.A., Nair, S., Chandramohan, D. and Colwell, R.R. (1994). 5S rRNA sequences and fatty acid profiles of colourless sulfur-oxidising bacteria Ocean technology: Perspectives. eds. by: Sushilkumar; Agadi, V.V.; Das, V.K.; Desai, B.N.(Symp. on Ocean Technology; National Institute of Oceanography, Goa; India; 27-29 Aug 1992). Publ. and Inf. Dir.; New Delhi; India.
- Loka Bharathi, P.A., De Souza, M.J.B.D., Nair, S. and Chandramohan, D. (1999). Abundance, Viability and Culturability of Antarctic Bacteria. *Fifteenth Indian Expedition to Antarctica, Scientific Report. Dept. of Ocean Development*, Technical Publication No. 13; 79-92.
- Loka Bharathi, P.A., Pradeep Ram, A.S., Nair, S., Nath, B.N. and Chandramohan, D. (2004). Distribution of baroduric, psychrotrophic and culturable nitrifying and denitrifying bacteria in the Central Indian Basin. *Proc. Natl. Seminar on New Frontiers in Mar. Biosci. Res.*, 319-330.
- Lowry, O.H., Rosebrough, N.J., Farr, A.L. and Randall, R.J. (1951). Protein measurement with the Folin-Phenol reagents. *J. Biol. Chem.*, 193; 265-275.
- Lundin A. and Thore A. (1975). Comparison of methods for extraction of bacterial adenine nucleotides determined by firefly assay. *Appl. Microbiol.* 30; 713-721.
- Luther III, G.W., Sundby Bjørn, Lewis L. Brent, Brendel P.J., and Silverberg, N. (1997). Interactions of manganese with the nitrogen cycle: Alternative pathways to dinitrogen. *Geochim Cosmochim Acta* 61(19); 4043-4052.
- Lyle, M. (1983). The brown-green color transition in marine sediments: a marker of the Fe (III)-Fe(II) redox boundary. *Limnol. Oceanogr.* 28(5); 1026-1033.

- Lynn, D.C and Bonatti, .E. (1965). Mobility of manganese in diagenesis of deep-sea sediments. *Mar. Geol.* 3; 457-474.
- Lyons, T.W., Kah, L.C. and Gellatly, A.M., (2004). The Proterozoic sulphur isotope record of evolving atmospheric oxygen. *In: Eriksson, P.G.E.A. (Ed.), The Precambrian Earth: Tempos and Events: Developments in Precambrian Geology.* Elsevier, pp. 421–439.
- Ma, F., Al-Aasm, I. and Yang, J. (2006). Numerical modeling of hydrothermal fluid flow coupled with mass transport: An example from the Devonian Wabamun Group, northeast British Columbia, Canada. *J. Geochem. Explor.* 89, 247–250.
- MacLeod, N.H., Chappelle, E.W. and Crawford, A.M (1969). ATP assay of terrestrial soils : a test of an exobiological experiment. *Nature Lond.* 223; 267-268.
- Maniatis, T., Fritsch, E.F. and J. Shambrook. (1982). Molecular cloning. A laboratory manual, II edition, Cold Spring Laboratory Press, New York.
- Margulies, M., Egholm, M., Altman, W.E., Attiya, S., Bader, J.S., Bemben, L.A., *et al.* (2005). Genome sequencing in microfabricated high-density picolitre reactors *Nature* 437; 376–380
- Martens, R. (2001). Estimation of ATP in soil: extraction methods and calculation of extraction efficiency. *Soil Biol. Biochem.* 33; 973-982.
- Martin, W. and Russel, M.J. (2007). On the origin of biochemistry at an alkaline hydrothermal vent. *Phil Trans R Soc Lond B Biol Sc.* 362(1486); 1887-925.
- Maruyama, A. Mita, N. and Higashihara, T. (1993). Particulate Materials and Microbial Assemblages around the Izena Black Smoking Vent in the Okinawa Trough. *J. Oceanogr.* 49; 353 - 367.
- Mascarenhas-Pereira, M.B.L., Nath, B.N., Borole, D.V. and Gupta, S.M. (2006). Nature, source and composition of volcanic ash in sediments from a fracture zone trace of Rodriguez Triple Junction in the Central Indian Basin. *Mar Geol.*, 229(1); 79-90.
- Matondkar, S.G.P., Nair, K.K.C. and Ansari, Z.A. (2005). Biological characteristics of Central Indian Basin Water during the Southern Summer. *Mar. Geores. Geotechnol.*, 23(4); 299-314.

- Maurice, P.A., Vierkorn, M.A., Hersman, L.E., Fulghum, J.E. and Ferryman, A. (2001). Enhancement of Kaolinite Dissolution by an Aerobic *Pseudomonas mendocina* Bacterium *Geomicrobiol. J.* 18; 21–35.
- McCollom, T.M., Ritter, G., and Simoneit, B.R.T. (1999). Lipid synthesis under hydrothermal conditions by Fischer–Tropsch-type reactions. *Orig. Life Evol. Biosph.* 29; 153– 166.
- Meister, P., Bernasconi, S.M., Aiello, I.W., Vasconcelos, C. and McKenzie, J. A. (2009). Depth and controls of Ca-rhodochrosite precipitation in bioturbated sediments of the Eastern Equatorial Pacific, ODP Leg 201, Site 1226 and DSDP Leg 68, Site 503 *Sedimentology* doi: 10.1111/j1365-3091.2008.01046.x.
- Meister, P., McKenzie, J.A., Vasconcelos, C., Frank, M. and Gutjahr, M. (2007). Dolomite formation in the dynamic deep biosphere: results from the Peru margin (ODP Leg 201). *Sedimentology*, 54; 1007–1032.
- Meyer-Reil, L.A.(1991). Ecological aspects of enzymatic activities in marine sediments. In: *Microbial enzymes in the aquatic environment*. Ed by R.J.Chrost. Springer, New York. 84-95.
- Meyers, P.A. (1994). Preservation of elemental and isotopic source identification of sedimentary organic matter. *Chem. Geol.* 144; 289-302.
- Michard, G. (1971). Theoretical model for manganese distribution in calcareous sediment cores. *J. Geophys. Res.* 76; 2179-2181.
- Mino T., van Loosdrecht M. C. M., and Heijnen J. J. (1998). Microbiology and biochemistry of the enhanced biological phosphate removal process. *Water Res.* 32(11); 3193-3207.
- Morgan C. (2005). Results and standards from previous sea-bed mining environmental studies. In: *International Sea-bed authority handbook* 88-96.
- Mudholkar, A. V., Pattan, J. N., and Parthiban, G., (1993). Geochemistry of deep-sea sediment cores from the Central Indian Ocean Basin. *Ind. J. Mar. Sc.*, 22 (4); 241-246.
- Müller J. J. and Suess, E. (1979). Productivity, sedimentation rate and sedimentary organic matter in the oceans-I. Organic carbon preservation. *Deep Sea Res.* 26A, 1347-1362.

- Mukhopadhyay, R., and De, S. (2005) Dealing with 26/12. *Curr. Sc.* 88(11), 1713.
- Mukhopadhyay, R., Iyer, S.D. and Ghosh, A.K. (2002). The Indian Ocean Nodule Field: Petrotectonic Evolution and Ferromanganese Nodules. *Earth Sc. Rev.*, 60; 67-130.
- Naganuma, T., Otsuki, A. and Seki, H. (1989). Abundance and growth rate of bacterioplankton community in hydrothermal vent plumes of the North Fiji Basin. *Deep-sea Res.*, 36; 1379-1390.
- Nair, S., Mohandass, C., Loka Bharathi, P.A., Sheelu, G. and Raghukumar, C., (2000) Microscale response of sediment variables to benthic disturbance in the Central Indian Ocean Basin. *Mar. Geores. Geotechnol.*, 18, 273-283.
- Nash, T.. (1953). The Colorimetric Estimation of Formaldehyde by Means of the Hantzsch Reaction *Biochemical J.* 55; 416-421.
- Nath, B. N., Borole, D. V. Aldahan, A. Patil, S. K, Mascarenhas-Pereira M. B. L., Possnert, Ericsson, G., T., Ramaswamy, V. and Gupta, S. M., (2008). ^{210}Pb , ^{230}Th , and ^{10}Be in Central Indian Basin seamount sediments: Signatures of degassing and hydrothermal alteration of recent origin, *Geophys. Res. Lett.*, 35; L09603.
- Nath, B. N., Rao, V. P. and Becker, K. P. (1989). Geochemical evidence of terrigenous signature influence in deep-sea sediments up to 8°S in the Central Indian Basin. *Mar. Geol.*, 87; 301- 313.
- Nath, B.N. and Mudholkar, A.V. (1989) Early diagenetic processes affecting nutrients in the porewaters of Central Indian Ocean cores. *Mar. Geol.*, 86; 57-66.
- Nath, B.N., Bau, M., Rao, B.R. and Rao, Ch.M. (1997). Trace and rare earth elemental variation in Arabian Sea sediments through a transect across the oxygen minimum zone. *Geochim. Cosmochim. Acta*: 61(12); 2375-2388.
- Nath, B.N., Mascarenhas-Pereira, M.B.L., Kurien, S., Selvaraj, K., Naman, D., Desai, N., D'souza, V. and Naik, T. (2005). Porewater nutrients and sediment chemistry. In: *Benthic environmental variability in the Central Indian Ocean Basin-I*. Project report submitted to Department of Ocean Development, Govt. of India.
- Nath, B.N., Roelandts, I., Sudhakar, M. and Plüger, W.I. (1992). Rare earth element patterns of the Central Indian Basin sediments related to their lithology. *Geophys. Res. Lett.*, 19(12); 1197-1200.

- Nelson, D.C and Fisher, C.R. (1995). Chemoautotrophic and methanotrophic endosymbiotic bacteria at deep-sea vents. *In: The microbiology of deep-sea hydrothermal vents(Ed) Karl D.M.* CRC Press, Boca Raton, FL, pp 125-167.
- Oades J. M. and Jenkinson. S. (1979). Adenosine triphosphate content of the soil microbial biomass. *Soil Biol. Biochem.* 11; 201-204.
- Oliver J. D. (1982). Taxonomic scheme for the identification of marine bacteria. *Deep-Sea Res.* 29, 795-798.
- Pachmayr, F. (1960). Vorkommen und Bestimmung Von Schwefelverbindungen in Mineralwasser. Diss, Univ. Munchen, 48pp.
- Pai, S.C., Gong, G.C., Liu, K.K. (1993). Determination of dissolved oxygen in seawater by direct spectrophotometry of total iodine. *Mar Chem* 41; 343–351.
- Parkes, R. J., B. A. Cragg, S. J. Bale, J. M. Getliff, K. Goodman, P. A. Rochelle, J. C. Fry, A. J. Weightman, and Harvey, S. M. (1994). Deep bacterial biosphere in Pacific Ocean sediments. *Nature.* 371(6496); 410–413.
- Parkes, R. J., Cragg, B. A. and Wellsbury P. (2000). Recent studies on bacterial populations and processes in subseafloor sediments: A review, *Hydrogeol. J.* 8(1); 11–28.
- Parkes, R.J., Webster, G., Cragg, B. A., Weightman, A.J., Newberry, C.J., Ferdelman, T.G., Kallmeyer, J., Bo Jørgensen, B., Ivano W. Aiello, I.W. and Fry, J.C. (2005). Deep sub-seafloor prokaryotes stimulated at interfaces over geological time. *Nature* 436, 390-394.
- Parkinson, D. and Paul, E.A. (1982). Microbial biomass. *In: Methods of soil Analysis, Part 2 Chemical and Microbiological Properties (A.L. Page, R.H Miller and D.R.Keeney, Eds), pp.* 821-830. American Society of Agronomy Inc. Madison.
- Patience, R.L., Clayton, C.J., Kearsley, A.T., Rowland, S.J., Bishop, A.N., Rees, A.W.G., Bibby, K.G., and Hopper, A.C., (1990). An integrated biochemical, geochemical, and sedimentological study of organic diagenesis in sediments from Leg 112. *In* Suess, E., von Huene, R., et al., *Proc. ODP, Sci. Results*, 112: College Station, TX (Ocean Drilling Program), 135–153. [doi:10.2973/odp.proc.sr.112.191.1990](https://doi.org/10.2973/odp.proc.sr.112.191.1990)
- Pattan, J. N., Masuzawa, T., Borole, D. V., Parthiban, G., Jauhari, P., and Yamamoto, M., (2005). Biological productivity, terrigenous influence and noncrustal elements

- supply to the Central Indian Ocean Basin: Paleoceanography during the past *ca* 1 Ma. *J. Earth Syst. Sci.*, 114(1); 63-74.
- Pattan, J.N. and Jauhari, P. (2001). Major, Trace, and Rare Earth Elements in the Sediments of the Central Indian Ocean Basin: Their Source and Distribution. *Mar. Geores. Geotechnol.*, 19; 85-106.
- Paul E.A and Clark F.E (1989). *Soil Microbiol and Biochem.* Academic Press New York.
- Paul E.A. and Johnson R.L. (1977). Microscopic counting and adenosine 5'-triphosphate measurement in determining microbial growth in soils. *Appl. Environ. Microbiol.* 34; 263-269.
- Pedersen, K. (1997). Microbial life in deep granitic rock. *FEMS Microbiol. Rev.*, 20; 399– 414.
- Pedersen, K. (2000a). Exploration of deep intraterrestrial microbial life: current perspectives. *FEMS Microbiol. Lett.* 185; 9 –16.
- Pedersen, K., (2000b). The hydrogen driven intra-terrestrial biosphere and its influence on the hydrochemical conditions in crystalline bedrock aquifers. In: *Stober, I., Bucher, K. (Eds.), Hydrogeology of crystalline rocks.* Kluwer Academic Publishers, pp. 249– 259.
- Pedersen, K., (2001). Diversity and activity of microorganisms in deep igneous rock aquifers of the fennoscandian shield. In: *Fredrickson, J.K., Fletcher, M. (Eds.), Subsurface Microgeobiology and Biogeochemistry.* Wiley-Liss, New York, pp. 97– 139.
- Pederssen T. F. and Price N. B. (1982). The geochemistry of manganese carbonate in Panama basin sediments. *Geochim. Cosmochim. Acta* 46; 59-68.
- Perner, M., Kuever, J., Seifert, R., Pape, T., Koschinsky, A., Schmidt, K., Strauss, H. and Imhoff, J.F. (2007). The influence of ultramafic rocks on microbial communities at the Logatchev hydrothermal field, located 15 degrees N on the Mid-Atlantic Ridge *FEMS Microbiol Ecol.* 61(1):97-109.
- Pfannkuche, O., (1992). Organic carbon flux through the benthic community in the temperate abyssal northeast Atlantic. In: *Deep-sea food chains and the global carbon cycle.* Ed. by G. T. Rowe & V. Pariente. Kluwer, Dordrecht, 183-197.

- Pfannkuche, O., (1993). Benthic response to the sedimentation of particulate organic matter at BIOTRANS station, 47°N, 20°W. *Deep-Sea Res I* 40, 135–149.
- Phelps, T. J., Pfiffner, S. M. Sargent, K. A. and White D. C. (1994). Factors influencing the abundance and metabolic capacities of microorganisms in eastern coastal-plain sediments, *Microbial Ecol.*, 28(3); 351–364.
- Pinchuk, G.E., Ammons, C., Culley, D.E., Li, S-M. W, McLean, J.S., Romine, M.F., Kenneth H. Nealson, K.H., Fredrickson, J.K., and Beliaev, A.S., (2008). Utilization of DNA as a Sole Source of Phosphorus, Carbon, and Energy by *Shewanella* spp.: Ecological and Physiological Implications for Dissimilatory Metal Reduction *Appl Evt Microbiol.*, 74(4); 1198–1208.
- Pirt, S.J. (1975). Principles of microbe and cell cultivation, 1st Edition, Blackwell Scientific Publication, UK, p115-117.
- Poremba, K. (1994). Hydrolytic enzymatic activity in deep-sea sediments. *FEMS Microbiol Ecol* 16, 213-222.
- Poulton, S.W. and Canfield, D.E. (2006). Co-diagenesis of iron and phosphorus in hydrothermal sediments from the southern East Pacific Rise: Implications for the evaluation of paleoseawater phosphate concentrations *Geochim. Cosmochim. Acta.* 70; 5883–5898.
- Prahl, F.G., Ertel, J.R., Sparrow, M.A., and Eversmeyer, B. *et al.*, (1994). Terrestrial organic carbon contributions to sediments on the Washington margin. *Geochim Cosmochim Acta* 58; 3055-3048.
- Premuzic, E.T., Benkovitz, C.M., Gaffney, J.S., and Walsh, J.J. (1982). The nature and distribution of organic matter in the surface sediments of world oceans and seas. *Org Geochem* 4; 63-77.
- Presley B. J., Brooks R. R. and Kaplan I. R. (1967). Manganese and related elements in the interstitial water of marine sediments. *Science* 158; 906-909.
- Priest, F.G. (1984) Extracellular enzymes. *Aspects microbiol.*, 9; 1-79.
- Qin, G., Zhu, L., Chen, X., Wang, P.G. and Zhang, Y. (2007). Structural characterization and ecological roles of a novel exopolysaccharide from the deep-sea psychrotolerant bacterium *Pseudoalteromonas* sp. SM9913 *Microbiology*, 153; 1566–1572.

- Raghukumar, C., Nath, B.N., Sharma, R., Loka Bharathi, P.A., Dalal, S.G., (2006). Long-term changes in microbial and biochemical parameters in the Central Indian Basin *Deep-Sea Res I* 53; 1695-1717.
- Raghukumar, C., Nath, B.N., Sharma, R., LokaBharathi, P.A., Dalal, S.G. ,(2006). Long-term changes in microbial and biochemical parameters in the Central Indian Basin. *Deep-Sea Res. I*, 53(10); 1695-1717.
- Raghukumar, C., Sheelu, G., Loka Bharathi, P.A., Nair, S, Mohandass, C. (2001a). Bacterial standing stock, meiofauna and sediment-nutrient characteristics: indicators of benthic disturbance in Central Indian Basin. *Deep-Sea Res. II*, 48: 3381-3399.
- Raghukumar, C., Sheelu, G., Loka Bharathi, P.A., Nair, S., Mohandass, C., (2001b). Microbial biomass and organic nutrients in the deep-sea sediments of the Central Indian Ocean Basin. *Mar. Geores. Geotech.* 19; 1-16.
- Ram, A.S.P., Loka Bharathi, P.A., Nair, S. and Chandramohan, D. (2001). A deep-sea bacterium with unique nitrifying property. *Curr Sc.*, 80(9); 1222-1224.
- Ramesh Babu, V., Suryanarayana, A.,and Murty V.S.N.(2001). Thermohaline circulation in the Central Indian Basin during austral summer and winter periods of 1997. *Deep-Sea Res II* 48, 3327-3342.
- Rao, V.P., Kessarkar, P.M., Krumbein, W.E., Krajewski, K.P. and Schneiders, R.J. (2003). Microbial dolomite crusts from the carbonate platform of western India. *Sedimentology* 50; 819-830.
- Rao, V.P.C. and Nath, B.N. (1988). Nature, distribution and origin of clay minerals in grain size fractions of sediments from Manganese Nodule Field, Central Indian Ocean Basin. *Ind. J. Mar. Sc.*, 17; 202-207.
- Rappe, M. S., S. A. Connon, K. L. Vergin, and S. J. Giovannoni. (2002). Cultivation of the ubiquitous SAR11 marine bacterioplankton clade. *Nature*; 418:630–633.
- Rebata-Landa V. and Carlos, S.J.(2006). Mechanical limits to microbial activity in deep sediments. *Geochem Geophysys Geosys.* 7(11), Q11006, doi:10.1029/2006GC001355
- Rodriguez, N.M., Paull, C.K. and Borowski, W.S. (2000). Zonation of authigenic carbonates within gas hydrate-bearing sedimentary sections on the Blake Ridge:

- offshore southeastern North America. In: Proc. ODP, Sci. Results (Eds C.K. Paull, R. Matsumoto, P.J. Wallace and W.P. Dillon), 164, 301–312. Ocean Drilling Program, College Station, TX.
- Roesch, L.F.W., Fulthorpe, R.R., Riva, A., Casella, G., Hadwin, A.K.M., Kent, A.D., *et al* (2007). Pyrosequencing enumerates and contrasts soil microbial diversity *ISME J* 1, 283–290.
- Roesch, L.F.W., Fulthorpe, R.R., Riva, A., Casella, G., Hadwin, A.K.M., Kent, A.D., *et al* (2007). Pyrosequencing enumerates and contrasts soil microbial diversity *ISME J* 1; 283–290.
- Romanova, A. C., Vedenina, I. N., Kornizkaya, V. M., Doman, N. G. (1971). The purification of ribulose diphosphate carboxylase of hydrogen bacteria *Hydrogenomonas*. *Biochemika* 36; 408-414.
- Ronaghi M, Karamohamed S, Pettersson B, Uhlén M, Nyrén P. (1996). Real-time DNA sequencing using detection of pyrophosphate release *Anal Biochem* 242(1); 84-9.
- Ronaghi M. (2001). Pyrosequencing Sheds Light on DNA Sequencing *Genome Research* 11; 3–11.
- Ross, D.J., Tate, K.R., Cairns, A., Pansier, E.A., (1980). Microbial biomass estimations in soils from tussock grasslands by three biochemical procedures. *Soil Biol. Biochem.* 12; 375-383.
- Rowe, G. T., Sibuet, M., Deming, J., Khripounoff, A., Tietjen, J., Macko, S. & Theroux, R.. (1991). "Total" sediment biomass and preliminary estimates of organic residence time in deep-sea benthos . *Mar. Ecol. Prog. Ser.* 79, 99-114.
- Rowe, G.T., Pariente, V., (1992). Deep sea food chains and the global carbon cycle. Kluwer Academic Publisher, Dordrecht, Netherlands, p. 400.
- Rudd, J.W., Taylor, C.D. (1980). Methane cycling in aquatic environments. *Adv Aquat Microbiol*, 2; 77-150.
- Sakiyam, T., and Ohwada, K., (1998). Effect of hydrostatic pressure on the growth of deep-sea bacterial communities. *Proc. NIPR Symp. Polar Biol.* 11; 1-7.
- Sardessai, S., and de Sousa, S.N. (2001). Dissolved organic carbon in the INDEX area of Central Indian Basin *Deep-Sea Res II* 48; 3353-3361.
- Sass, A.M., McKew, B.A., Sass, H., Fichte, J., Timmis, K.N., McGenity, T. J.(2008)

- Diversity of *Bacillus*-like organisms isolated from deep-sea hypersaline anoxic sediments. *Saline Systems* 2008, 4:8 doi:10.1186/1746-1448-4-8.
- Sawlan, J. L. and Murray, J. W. (1983). Trace metal remobilization in the interstitial waters of red clay and hemipelagic marine sediments. *Earth Planet. Sci. Lett.* 64; 213-230.
- Sayles, F. L. (1981). The composition and diagenesis of interstitial solutions-B. Fluxes and diagenesis at the water-sediment interface in the high latitude North and South Atlantic. *Geochim. Cosmochim. Acta* 48; 1935-1948.
- Schippers, A., Neretin, L.N., Kallmeyer, J., Ferdelman, T.G., Cragg, B.A., Parkes, R.J., and Jørgensen, B.B (2005). Prokaryotic cells of the deep sub-seafloor biosphere identified as living bacteria *Nature* 433; 861-864.
- Schouten, S., Strous, M., Kuypers, M.M.M., Irene, W., Rijpstra, C., Baas, M., Schubert, C.J., Jetten, M.S.M. and Jaap S. Sinninghe Damsté (2004). Stable Carbon Isotopic Fractionations Associated with Inorganic Carbon Fixation by Anaerobic Ammonium-Oxidizing Bacteria. *Appl Environ Microbiol*, 70(6); 3785–3788.
- Schulz, H.D. and Zabel, M. (eds) (2000). Marine geochemistry. Springer, Berlin Heidelberg New York.
- Schulz, H.D. (2000). Quantification of Early Diagenesis: Dissolved constituents in Marine porewater. In: *Marine Geochemistry* (Eds. H.D. Schulz and M. Zabel) Springer Verlag, Berlin-Heidelberg, pp. 87-122.
- Schwarz, J. R. and Colwell, R. R. (1975). Heterotrophic Activity of Deep-Sea Sediment Bacteria *Appl. Microbiol.* 30(4); 639-649.
- Sharma, R., (2005). Benthic environmental variability in the Central Indian Basin. Phase I of Environmental Variability Data Collection program. Report submitted to the Department of Ocean Development, New Delhi, India by National Institute of Oceanography, Goa, India, 21-44.
- Sharma, R., Nath, B.N., (2000). Selection of test and reference areas for the Indian deep-sea environment (INDEX). *Deep-Sea Res., Part 1, Oceanogr. Res. Pap.* 18(3); 177-187.

- Sharma, R., Nath, B.N., Parthiban G., Jai Sankar, S., (2001). Sediment redistribution during simulated benthic disturbance and its implications on deep seabed mining. *Deep-Sea Res II* 48; 3363–3380.
- Shock, E.L., (1990). Geochemical constraints on the origin of organic compounds in hydrothermal systems. *Orig. Life Evol. Biosph.*, 20; 331–367.
- Shock, E.L., Schulte, M.D., (1998). Organic synthesis during fluid mixing in hydrothermal systems. *J. Geophys. Res.* 103; 28513–28527.
- Sibuet, M. (2005). Data standards utilized in the environmental studies of l' Institut francais de recherche pour l' exploration de la mer (IFREMER) and l' association francaise pour la exploration et la recherches des nodules (AFERNOD) .In: International Sea-bed authority handbook. 222-233.
- Sieburth, J.McN., Johnson, P.W., Macario, A.J.L., de Macario, E.C. (1993). C1 bacteria in the water column bacteria of Chesapeake Bay, USA. II. The dominant O₂ and H₂S-tolerant methylotrophic methanogens, coenriched with their oxidative and sulphate reducing bacterial consorts, are all new immunotypes and probably include new taxa. *Mar. Ecol Prog Ser.* 95;81-89
- Sivan, O., Schrag, D. P. and R.W. Murray (2007). Rates of methanogenesis and methanotrophy in deep-sea sediments *Geobiology* DOI: 10.1111/j.1472-4669.2007.00098.x 1-11.
- Sizaret, S., Branquet, Y., Gloaguen, E., Chauvet, A., Barbanson, L., Arbaret, L., and Chen, Y. (2009). Estimating the local paleo-fluid flow velocity: New textural method and application to metasomatism *Earth Planet Sci Lett* 280 71–82.
- Smetacek, V. (1999). Bacteria and silica cycling *Nature* 397; 475-476.
- Smirnov, A., Hausner, D., Laffers, R., Strongin, D.R., Schoonen, M.A.A.(2008). Abiotic ammonium formation in the presence of Ni-Fe metals and alloys and its implications for the Hadean nitrogen cycle. *Geochem T* , 9; 5-24.
- Soetaert, K., Herman, P.M.J. and Middelburg, J.J. (1996). A model of early diagenetic processes from the shelf to abyssal depths. *Geochim. Cosmochim Acta* 60(6), 1019-1040.

- Sogin, M.L., Morrison H.G., Huber, J.A., Welch, D.M., Huse, S.M., Neal, P.R. Arrieta, M.J. and Herndl, G.J. (2006). Microbial diversity in the deep sea and the underexplored “rare biosphere” *Proc Natl Acad Sci* 103 (32), 12115–12120.
- Sparling, G.P. (1981). Microcalorimetry and other methods to assess biomass and activity in soil. *Soil Biol. Biochem.* 13; 93-98.
- Staley, J. T., and Konopka, A. (1985). Measurements of in situ activities of nonphotosynthetic microorganisms in aquatic and terrestrial habitats. *Annu. Rev. Microbiol.* 39:321–346.
- Steeffel, C. I. and Lasaga, A. C. (1994). A coupled model for transport of multiple chemical species and kinetic precipitation/dissolution reactions with application to reactive flow in single phase hydrothermal systems, *Amer J of Sci*, 294; 529-592.
- Stein, C.A., Weissel, J.K., (1990). Constraints on the Central Indian Basin thermal structure from heat flow, seismicity and bathymetry. *Tectonophysics*, 176; 315-332.
- Stevens, T. (1997). Lithoautotrophy in the subsurface. *FEMS Microbiol. Rev.*, 20; 327-337.
- Stevens, T.O., McKinley, J.P., (1995). Lithoautotrophic microbial ecosystems in deep basalt aquifers. *Science* 270; 450– 454.
- Stewart, F.J., Newton, I.L.G. and Cavanaugh, C.M. (2005). Chemosynthetic endosymbioses: adaptations to oxic–anoxic interfaces. *Trends Microbiol* 13(9), 439-448.
- Strous, M., Heijnen, J. J., Kuenen, J. G., and Jetten, M. S. M.. (1998). The sequencing batch reactor as a powerful tool for the study of slowly growing anaerobic ammonium-oxidizing microorganisms. *Appl. Microbiol. Biotechnol.* 50; 589–596.
- Stumm, W., Morgan, J.J., (1996). Aquatic chemistry: chemical equilibria and rates in natural waters. John Wiley & Sons, New York (1022 pp).
- tyriaková, I., Tyriak, I. Nandakumar M.P. and Mattiasson B. (2003). Bacterial destruction of mica during bioleaching of kaolin and quartz sands by *Bacillus cereus*. *World J. Microbiol. Biotechnol.* 19; 583–590.
- Sudhakar, M. (1989). Ore grade manganese nodules from the Central Indian Basin: An evaluation. *Mar. Mining.*, 8; 201-214.

- Suess, E. (1979). Mineral phases formed in anoxic sediments by microbial decomposition of organic matter. *Geochim. Cosmochim. Acta* 43; 339-352.
- Suess, E., Muller, P.J., Powell, H.S., Reimers, C.E. (1980). A closer look at nitrification in pelagic sediments. *Geochem. J.* 14, 129-137.
- Summons, R.E., Jahnke, L.L., Hope, J.M., Logan, G.A., (1999). 2-Methylhopanoids as biomarkers for cyanobacterial oxygenic photosynthesis. *Nature* 400; 554–556.
- Taga, N., Kobori H. (1978). Phosphatase activity in eutrophic Tokyo Bay. *Mar Biol.* 49, 2109-2123.
- Takano, Y., Kobayashi, K., Yamanaka, T., Marumo, K. and Urabe T. (2004). Amino acids in the 308°C deep-sea hydrothermal system of the Suiyo Seamount, Izu-Bonin Arc, Pacific Ocean. *Earth Planetary Sc. Letts.*, 219, 147-153.
- Tate, K. R. and D. S. Jenkinson (1982). Adenosine triphosphate measurement in soil-An improved method. *Soil Biol. Biochem.* Vol. 14, pp. 331 - 335.
- Tebo, B.M., Johnson, H.A., McCarthy, J.K., and Templeton A.S. (2005). Geomicrobiology of manganese(II) oxidation *Trends in Microbiol* 13(9); 421-428.
- Templeton, A. S., H. Staudigel, and B. M. Tebo. 2005. Diverse Mn(II)-oxidizing bacteria isolated from submarine basalts at Loihi Seamount. *Geomicrobiol. J* 22;127–139.
- Teske, A.P., (2006). Microbial Communities of Deep Marine Subsurface Sediments: Molecular and Cultivation Surveys *Geomicrobiology Journal*, 23; 357–368.
- Thiel, H., Forschungsverbund, T.-U., (2001). Evaluation of the environmental consequences of polymetallic nodule mining based on the results of the TUSCH Research Association. *Deep-Sea Res II* 48; 3433–3452.
- Thistle, D., Yingst, J.Y. and Fauchald K. (1985). A Deep-Sea Benthic Community exposed to strong near-bottom currents on the Scotian Rise (Western Atlantic) *Mar. Geol.* 66; 91—112.
- Thomson, J., Carpenter, M. S. N., Colley, S., Wilson, T. R. S., Elderfield, H. and Kennedy, H. (1984b). Metal accumulation rates in Northwest Atlantic pelagic sediments. *Geochim. Cosmochim. Acta* 48; 1935-1948.
- Thomson J., Wilson, T. R. S., Culkin, F. and Hydes, D. J. (1984a). Non-steady state diagenetic record in eastern equatorial Atlantic sediments. *Earth Planet. Sci. Lett.* 71; 23-30.

- Tietjen, J. H., 1992. Abundance and biomass of metazoan meiobenthos in the deep-sea. In: Deep-sea food chains and the global carbon cycle. Ed. by G. T. Rowe & V. Pariente. Kluwer, Dordrecht, 45-62.
- Treves, D. S., Xia, B., Zhou, J. and Tiedje, J. M. (2003). A two species test of the hypothesis that spatial isolation influences microbial diversity in soil, *Microbial Ecol.*, 45(1); 20–28.
- Turnewitsch, R., Witte, U., and Graf, G. (2000). Bioturbation in the abyssal Arabian Sea: influence of fauna and food supply *Deep-Sea Res II* 47; 2877-2911.
- Tuttle, J.H. and Jannasch, H.W. (1977). Thiosulfate stimulation of microbial dark assimilation of carbon dioxide in shallow marine waters. *Microb. Ecol.*, 4; 9–25.
- Valsangkar, A. B., (2004). Clay as indicator of sediment plume movement in deep-sea environment. *Curr. Sci.* 87 (12), 1747-1751.
- Valsangkar, A.B., (2001). Implications of post-disturbance studies on the grain size of the sediments from the Central Indian Basin. *Curr Sci* 81, 1365-1373.
- Van Aken H.M., Ridderinkhof H., and P.M. de Ruijter W.P.M. (2004). North Atlantic Deep-Water in the south western Indian Ocean *Deep-Sea Res I*, 51, 755–776.
- Van Cappellen. P. and Wang, Y. (1996). Cycling of iron and manganese in surface sediments: A General Theory for the coupled transport and reaction of carbon, oxygen, nitrogen, sulphur, iron and manganese. *Am J Sci* 296; 197-243.
- Van der Meer, M. J. T., S. Schouten, B. E. Van Dongen, W. I. C. Rijpstra, G. Fuchs, J. S. Sinninghe Damste', J. W. De Leeuw, and D. M. Ward. (2001). Biosynthetic controls on the ¹³C contents of organic components in the photoautotrophic bacterium *Chloroflexus aurantiacus*. *J. Biol. Chem.* 276; 10971–10976.
- Van der Meer, M. J. T., S. Schouten, G. Fuchs, and J. S. Sinninghe Damste' (2001). Stable carbon isotope fractionations of the hyperthermophilic crenarchaeon *Metallosphaera sedula*. *FEMS Microbiol. Lett.* 196; 67–70.
- Van Es, F.B. and Meyer-Reil, L.-A. (1982). Biomass and metabolic activity of heterotrophic marine bacteria. In: *Advances in microbial ecology* (ed. Marshal, K.C.). Plenum Press, New York, 6; 111-170.

- Vetriani, C., Jannasch, H.W., Macgregor, B.J., Stahl, D.A., Resysenbach, A.L., (1999). Population structure and phylogenetic characterization of marine benthic archaea in deep-sea sediments. *Appl Environ Microbiol* 65; 4375–4384.
- Vick, T.J., Dodsworth, J.A., Costa, K.C., Shock, E.L., Hedlund, B.P. (2010). Microbiology and geochemistry of Little Hot Creek, a hot spring environment in the Long Valley Caldera *Geobiology* 8; 140–154.
- Vlatcheslav, M.P. (2005). Data standards utilized in the environmental studies of Yuzhmorgeologiya (Russian Federation). In: International Sea-bed authority handbook 264-277.
- Von Damm, K. (1995). Controls on the chemistry and temporal variability of seafloor hydrothermal fluids. In: *Humphris, S.E., Zierenberg, R.A., Mullineaux, L.S., Thomson, R.E. (Eds.), Seafloor Hydrothermal Systems: Physical, Chemical, Biological and Geological Interactions*. American Geophysical Union, Washington, D.C, pp. 222– 247.
- Wang, P., Wang, F., Xu, M., Xiao, X. (2004). Molecular phylogeny of methylotrophs in a deep-sea sediment from a tropical west Pacific Warm Pool. *FEMS Microbiol Ecol* 47;77–84.
- Wang, G., Spivack, A. J., Rutherford, S., Manor, U. and D’Hondt, S. (2008). Quantification of co-occurring reaction rates in deep subseafloor sediments. *Geochim et Cosmochim Acta* 72; 3479–3488.
- Wang, P., Xiao, X., Wang, F. (2005). Phylogenetic analysis of Archaea in the deep-sea sediments of west Pacific Warm Pool. *Extremophiles* 9; 209–217.
- Ward BB, Kilpatrick KA, Wopat AE, Minnich EC, Lidstrom ME (1989) Methane oxidation in Saanich Inlet during summer stratification. *Continental Shelf Research* 9, 65-75.
- Ward, B.B, Kilpatrick, K.A., Renger, E.H. and Eppley, R.W. (1989). Biological nitrogen cycling in the nitracline. *Limnol. Oceanogr.* 34(3); 493-513.
- Warren, B.A. and Johnson, G.C. (2002). The overflows across the Ninetyeast Ridge. *Deep-Sea Res II* 49; 1423–1439.
- Warren, B.A., (1982). The deep water of the Central Indian Basin. *J of Mar Res* 40 (Suppl.), 823–860.

- Weidicke-Horneback M. (2005). Results and standards from previous sea-bed mining environmental studies. In: International Sea-bed authority handbook 88-96.
- Wellsbury, P., Mather, I. and Parkes R. J. (2002). Geomicrobiology of deep, low organic carbon sediments in the Woodlark Basin, Pacific Ocean, *FEMS Microbiol. Ecol.* 42(1); 59–70.
- Wenxuan, H., Huaiyang, Z., Lianxing, G., Wenlan, Z., Xiancai, L., Qi, F., Jianming, P., Haisheng, Z. (2000). New evidence of microbe origin for ferromanganese nodules from the East Pacific deep sea floor. *Science in China (Series D)* 43(2) 187-192.
- Wenxuan, H., Zhijun, J., Suping, Y., Xiancai, L., Zhilin, C., Linye, Z., Xuejun, Z., and Huaiyang, Z., (2000). Discovery of low-mature hydrocarbon in manganese nodules and ooze from the Central Pacific deep sea floor. *Chinese Sci. Bull.* 47 (11); 939-944.
- Wheat, C.G., Feely, R.A. and Mottl, M.J. (1996). Phosphate removal by oceanic hydrothermal processes: An update of the phosphorus budget in the oceans. *Geochim. Cosmochim. Acta.* 60(19); 3593-3608.
- Whitman, W.B., Coleman, D.C., Wiebe, W.J. (1998). Prokaryotes: the unseen majority. *Proc Natl Acad Sci USA* 95; 6578–6583.
- Wilson T. R. S., Thomson J., Colley S., Hydes D. J., Higgs, N. C. and Sørensen J. (1985). Early organic diagenesis: The significance of progressive subsurface oxidation fronts in pelagic sediments. *Geochim. Cosmochim. Acta* 49; 811-822.
- Wilson T. R. S., Thomson J., Hydes D. J., Colley S., Culkin, F. and Sørensen, J. (1986). Oxidation fronts in pelagic sediments: Diagenetic formation of metal-rich layers. *Science* 232; 972-975.
- Wirsen, C.O., Tuttle, J.H. and Jannasch, H.W. (1986) Activities of sulfur-oxidizing bacteria at the 21°N East Pacific Rise Vent site. *Mar. Biol.*, 92; 449-456.
- Xu, M., Wang, P., Wang, F. and Xiao, X. (2005). Microbial diversity at a deep-sea station of the Pacific nodule province. *Biodiv. Conserv.* 14; 3363–3380.
- Yakimov, M.M., Timmis, K.N., Golyshin, P.N. (2007) Obligate oil-degrading marine bacteria *Curr Opin Biotechnol*, 18 (3), pp. 257-266.
- Yam, E.M. and Tang, K.W. (2007). Effects of starvation on aggregate colonization and motility of marine bacteria *Aquat Microb Ecol* 48; 207–215.

- Yamagata, Y., Watanabe, H., Saitoh, M. and Namba, T. (1991) Volcanic production of polyphosphates and its relevance to prebiotic evolution. *Nature*, 352; 516-519.
- Yang, J., Bull, S. and Large, R. (2004). Numerical investigation of salinity in controlling ore-forming fluid transport in sedimentary basins: example of the HYC deposit, Northern Australia. *Mineral Deposit* 39; 622–631.
- Yayanos, A. A. (1986). Evolutional and ecological implications of the properties of deep-sea barophilic bacteria. *Proc. Natl. Acad. Sci.* 83; 9542-9546.
- Yayanos, A.A., Dietz, A. S., and Boxtel, R. V. (1979). Isolation of a deep-sea barophilic bacterium and some of its growth characteristics. *Science*. 205; 808-810.
- Yeh, G. T. and Tripathi, V. S. (1991). A model for simulating transport of reactive multispecies components: Model development and demonstration, *Water Resources Research*, 27; 3075-3094.
- Yingst, J.Y. and Aller, R.C., (1982). Biological activity and associated sedimentary structures in HEBBLE-area deposits, western North Atlantic. *Mar. Geol.*, 48; M7--M15.
- Young, K.D., 2006. The selective value of bacterial shape. *Microbiol and Molecul Biol Rev* 70; 660-703.
- Zhang, C. L., Palumbo, A. V., Phelps, T. J, Beauchamp, J. J., Brockman, F. J., Murray, C. J., Parsons, B. S., and Swift D. J. P. (1998). Grain size and depth constraints on microbial variability in coastal plain subsurface sediments, *Geomicrobiol. J.* 15(3); 171–185.
- Zhang, C. L., Y. Qi, A.-L. Reysenbach, D. Gotz, A. Peacock, D. C. White, J. Horita, D. R. Cole, J. Fong, L. Pratt, J. Fang, and Y. Huang. (2002). Carbon isotopic fractionation associated with thermophilic bacteria *Thermotoga maritime* and *Persephonella marina*. *Environ. Microbiol.* 4; 58–64.
- Zhao, C., Hobbs, B. E. and Ord, A. (2008a). Investigating dynamic mechanisms of geological phenomena using methodology of computational geosciences: an example of equal-distant mineralization in a fault, *Science in China Series D: Earth Sciences*, 51; 947-954.

- Zhao, C., Hobbs, B.E. and Ord, A. (2009). Theoretical and Numerical Investigation into Roles of Geofluid Flow in Ore Forming Systems: Integrated Mass Conservation and Generic Model Approach. *J. Geochem. Explor.* doi:10.1016/j.gexplo.2009.11.005.
- Zhou, J. Z., Xia, B. C. Huang, H. Palumbo, A. V. and Tiedje J. M. (2004). Microbial diversity and heterogeneity in sandy subsurface soils. *Appl. Environ. Microbiol.*, 70(3); 1723–1734.
- Zhou, J. Z., Xia, B. C., Treves, D. S., Wu, L. Y., Marsh, T. L., O'Neill, R. V., Palumbo, A. V. and Tiedje, J. M. (2002). Spatial and resource factors influencing high microbial diversity in soil. *Appl. Environ. Microbiol.*, 68(1); 326–334.

"I didn't do anything. Nature makes penicillin, I just found it"

-Alexander Fleming

Appendices

Appendix I

List of tables

- Table 4.1 . Percentage of averaged formaldehyde utilizing bacteria (FUB) in averaged total bacterial counts at different cores in CIB.
- Table 4.2 Generic diversity by biochemical characterisation of bacteria from representative stations in CIOB.
- Table 4.3 Similarity-based OTUs and species richness estimates
- Table 4.4 Hydrolytic enzyme activity in bacterial isolates.
- Table 4.5 Carbon substrate utilization by sediments
- Table 4.6 Carbon substrate utilization by cultures
- Table 4.7 Details of bacterial isolates used for detecting chemosynthetic potential and carbon substrate utilization.
- Table 4.8 Carbon fixation, RuBisCO activity and HCHO utilization at 5°C on 288 hrs of incubation. Concentration of formaldehyde used for the experiment is 2000ppm.
- Table 4.9. Carbon substrate utilization by nodules and associated sediments

Appendix II

List of Figures

- Fig. 4.1 Seabed topography derived from water depth data at sampled stations. Plot indicates good replication of station positions. Variation noted at 76.5°E and 12°S are due to rough sea-state and ship-drift.
- Fig. 4.2 Down-core variation of rock colour along North-South transect along 75°30'.
- Fig. 4.3 Down core variation of temperature, pH and Eh checked on-board.
- Fig. 4.4. pH-Eh correlation in stations IVBC 20A and IVBC 18C.
- Fig.4.5 Change of pH and Eh of sample on-board with increasing temperature and time.
- Fig. 4.6 Pore water oxygen, manganese, iron, ammonium and sulphide in core IVBC 20A.
- Fig. 4.7A Cluster analysis of CIB stations based on TOC content. Inset shows station locations in the basin. Cluster shows stations under influence of trace of Rodrigues triple junction on Indian Plate (RTJ-IO) grouping together. Organic depocentres in valleys like 38 in the south cluster with organic rich northern sediments.
- Fig. 4.7B Cluster analysis of CIB stations based on C/N-ratios. Like TOC stations under the influence of RTJ-IO.
- Fig. 4.8 Down-core variation of TOC and C/N ratio along North-South transect along 75°30'.

- Fig. 4.9 Seasonal variation in LOM (mg g^{-1} dry sediment) in sediment cores Central Indian Ocean Basin. Numbers on x-axis denote core numbers.
- Fig. 4.10 Cluster analysis of CIB stations based on LOM content. Inset shows station locations
- Fig. 4.11 Down-core variation of LOM along North-South transect along $75^{\circ}30'$.
- Fig. 4.12 Down-core profiles of LOM of relatively nodule rich and nodule poor cores.
- Fig. 4.13 Down-core profiles of ATP in relatively nodule rich and nodule poor cores
- Fig. 4.14 Cluster analysis of CIB stations based on ATP content. Inset shows station locations.
- Fig. 4.15 Seasonal Variation in ATP at CIB stations
- Fig. 4.16 Down-core variation of ATP along North-South transect along $75^{\circ}30'$
- Fig. 4.17A Cluster analysis of CIB stations based on total counts of bacteria. Similar TC counts in geographically distant cores may be due to similar porosity.
- Fig. 4.17B Cluster analysis of CIB stations based on frequency of dividing cells (FDC). Similar TC counts in geographically distant cores may be due to similar porosity. Similarity in geochemical properties may also be responsible for FDC distribution patterns.
- Fig. 4.18 Down-core variation of TC and FDC along N-S transect along $75^{\circ}30'$ showing concentric pattern emanating from the centre of the basin at 13°S .

- Fig. 4.19. Seasonal variation in total bacterial counts showing general increase especially towards south.
- Fig. 4.20 Total counts of relatively nodule-rich and nodule-poor cores. Down-core seasonal profile of TC showing marginally higher abundance at nodule rich than nodule poor cores.
- Fig. 4.21 Direct viable counts- DVC-a (aerobes) and DVC-an (anaerobes)
- Fig. 4.22 Retrievable count from cores IVBC 20A and IVBC 18C. Note that the scale of IVBC 18C is different.
- Fig. 4.23 Cluster analyses of CIB stations based on ZMA, NI, NII and aerobic TDLO. The north-south clustering is featured only by the heterotrophs.
- Fig. 4.24A. Heterotrophs (ZMA), ammonium oxidizers (NI), nitrite oxidizers (NII) and aerobic sulphur oxidizers (Aerobic TDLO) in cores SVBC 26 and SVBC 25.
- Fig. 4.24 B. Heterotrophs (ZMA), ammonium oxidizers (NI), nitrite oxidizers (NII) and aerobic sulphur oxidizers (Aerobic TDLO) in cores SVBC 20 and SVBC 35.
- Fig. 4.24 C. Heterotrophs (ZMA), ammonium oxidizers (NI), nitrite oxidizers (NII) and aerobic sulphur oxidizers (Aerobic TDLO) in cores SVBC 36 and SVBC 37.
- Fig. 4.25. Cluster of CIB stations based on distribution of Fe and Mn oxidizing bacteria. Inset shows station locations.
- Fig. 4.26 Fe- and Mn- oxidizer profiles for representative stations in CIB
- Fig. 4.27 Cluster of CIB stations based on distribution of phosphate solubilizers and silicate solubilizers. Inset shows station locations.

- Fig. 4.28 . Phosphate and silicate solubilizer profiles for representative stations in CIB.
- Fig. 4.29 Culturability of bacteria on varying strengths of Zobell Marine Agar
- Fig.4.30A Increase in culturable counts in core 18C by serial dilution of sediment slurry.
- Fig. 4.30B Increase in culturable counts in core 20A by serial dilution of sediment slurry.
- Fig. 4.31 Cluster analysis of CIB stations based on distribution of denitrifiers and nitrate reducing bacteria.
- Fig. 4.32 Denitrifier and Nitrate reducing bacterial profiles for representative stations in CIB.
- Fig. 4.33 Distribution of formaldehyde utilizing bacteria (FUB) occur at interfaces of changing rock colour.
- Fig. 4.34 A Phylogenetic affiliation of culture CIB 25A
- Fig. 4.34B Phylogenetic affiliation of culture CIB BIN2
- Fig. 4.34C Phylogenetic affinity of isolate CIB BIN3
- Fig. 4.34D Phylogenetic affinity of isolate CIB BIN4
- Fig. 4.35 Rarefaction analysis of bacterial diversity at station TVBC-08
- Fig. 4. 36A Carbon fixation by CIB sediments during austral winter sampling (ABP-04)
- Fig. 4.36 .B Cluster analysis of CIB stations based on microbial carbon uptake during austral winter sampling (ABP-04).
- Fig.. 4.36.C Microbial carbon fixation along cores of 75.5°E during austral winter sampling (ABP-04).

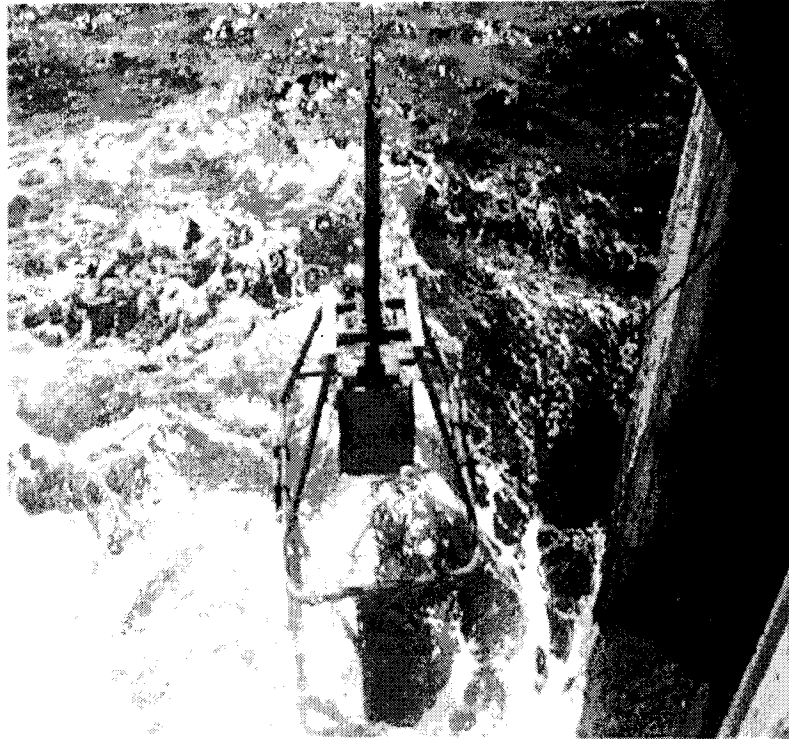
- Fig. 4.36.D Microbial carbon fixation along cores of 13°S during austral winter sampling (ABP-04).
- Fig. 4.36 .E Down-core variation of microbial carbon uptake ($\text{nmol g}^{-1} \text{ day}^{-1}$) showing mid-depth hot-spots along 75.5°E during austral winter sampling (ABP-04).
- Fig. 4.36 .F Microbial carbon uptake along the slope of seamount with volcanic alterations at 16°S
- Fig. 4.36 .G Seasonal variation in microbial carbon uptake during TVBC and SVBC samplings.
- Fig. 4.36 .H Variation in microbial carbon uptake in different fractions of calcareous core 37
- Fig. 4.37 Carbon fixation in presence of reduced nitrogen species
A. Aerobic condition B. Microaerophilic condition
- Fig. 4.38A. RuBisCO activity in siliceous core SVBC 26 and pelagic red clay SVBC 36.
- Fig. 4.38B. RuBisCO activity in whole and fractions of calcareous ooze SVBC 37.
- Fig. 4.39 RuBisCO activity in cultures at 25°C and 5°C.
- Fig. 4.40 Cluster analysis of CIB stations based on pore-water phosphate.
(Data courtesy to Dr. B.N.Nath and M.B.L. Mascarenhas Pereira NIO, Goa)
- Fig. 4.41A Alkaline phosphatase activity in CIB sediments.
- Fig. 4.41B Alkaline phosphatase activity in CIB sediments under 1atm and 500atm pressure.
- Fig. 4.42 Spatial distribution of a. pore water phosphate and b. alkaline phosphatase activity.

- Fig. 4.42 Spatial distribution of a. pore water phosphate and b. alkaline phosphatase activity.
- Fig. 4.43 TOC, biochemical and ATP contents in nodules and associated sediments
- Fig. 4.44 Bacterial counts in nodules and associated sediments
- Fig.4.45 Microbial uptake of carbon in nodules and associated sediments
- Fig. 4.46 A. PCA plots and eigenvectors for microbial and biochemical parameters for siliceous ooze
- Fig. 4.46 B. PCA plots and eigenvectors for microbial and biochemical parameters for siliceous-pelagic transition.
- Fig. 4.46 C. PCA plots and eigenvectors for microbial and biochemical parameters for pelagic red clay.
- Fig. 4.46D. PCA plots and eigenvectors for microbial and biochemical parameters for calcareous ooze.
- Fig. 4.47A. Interrelation between microbial and biochemical parameters in the surface nodule SN 147 interrelations
- Fig. 4.47B. Interrelation between microbial and biochemical parameters in the buried nodule BN 142 interrelations
- Fig. 4.48 A. Quantification of the influence of non-steady state diagenetic condition on microbial community by numerical simulation.
- Fig. 4.48B Quantification of hydrothermal alterations on pore water and microbial community by numerical simulation.

Appendix III

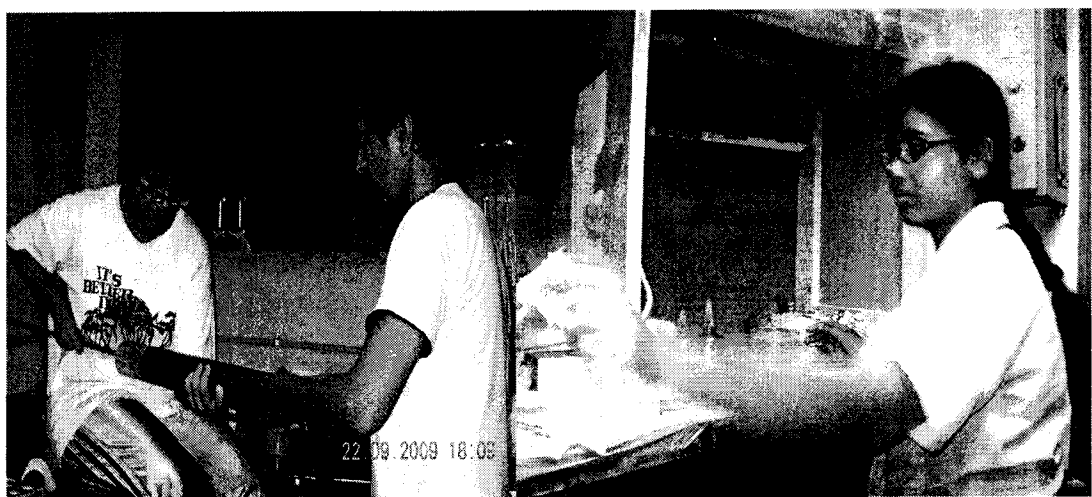
Photographs

1. Box-coring operation

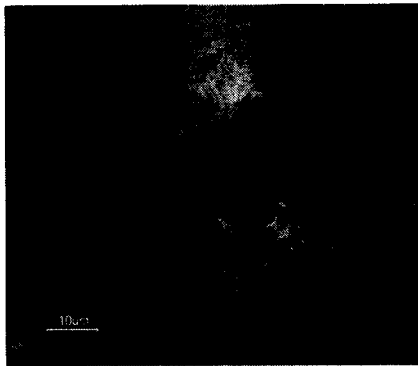


Courtesy: PMN EIA collections, NIO, Goa

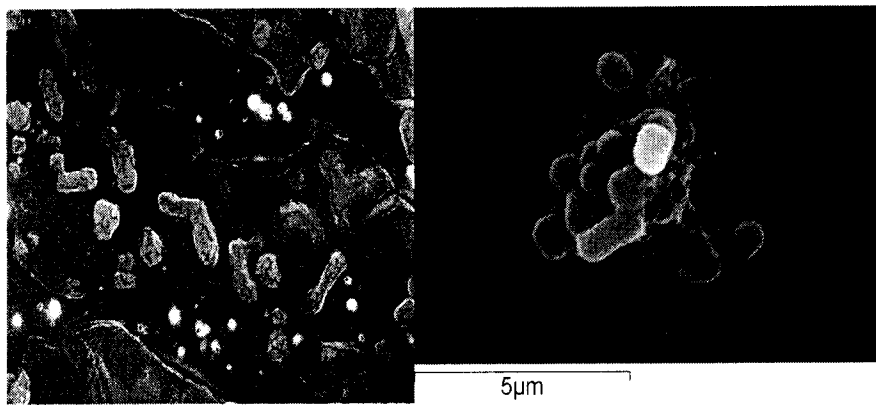
2. On-board sample processing



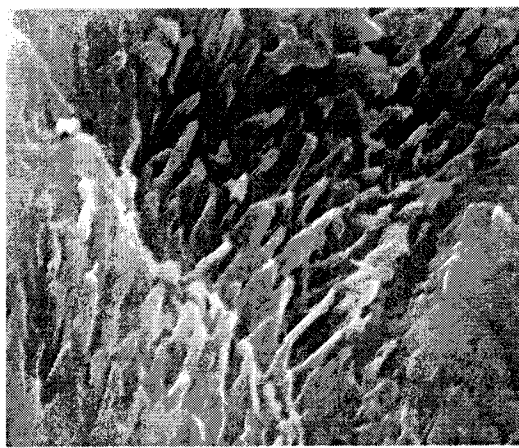
3. Total counts of bacteria



4. Matrix-bound bacteria in sediments and formaldehyde utilizing bacteria



5. *Thiobacillus*-like microbial mat in volcanically altered TVBC -08



Appendix IV

List of abbreviations

CIOB	Central Indian Ocean Basin
IONF	Indian Ocean Nodule Formation
CCD	Calcite compensation depth
TIC	Total inorganic carbon
TOC	Total organic carbon
TOM	Total organic matter
C/N	Carbon/ Nitrogen
LOC	Labile organic carbon
LOM	Labile organic matter
TC	Total counts
FDC/NVC	Frequency of dividing cells/ Naturally viable cells
DVC-a	Direct viable counts -aerobic
DVC-an	Direct viable counts -anaerobic
ATP	Adenosine triphosphate
PRIMER	Plymouth routines in multivariate ecological research
RTJ-IO	Rodrigues Triple Junction-Indian Ocean
BC	Box-core
TVBC	Temporal variability box-core
SVBC	Seasonal variability box-core
IVBC	Intermediate variability box-core
EVDC	Environmental variability data collection
ZMA	ZoBell Marine Agar

NI	Nitrifiers I
NII	Nitrifiers II
Ndl	Non-detectable levels
TDLO	<i>Thiobacillus Denitrificans</i> like organisms
NRB	Nitrate reducing bacteria
RuBisCO	Ribulose bis-phosphate carboxylase/ oxygenase

List of media used for culturable bacteria

The Aerobes

1. ZoBell Marine Broth and Agar (Himedia) as per manufacturer's instructions.

The broth concentrations 12.5, 20, 50 and 100% were amended with 1.5% agar agar.

2. Ammonium oxidizers (NI)

KH_2PO_4 0.25g

$\text{MgSO}_4 \cdot 7\text{H}_2\text{O}$ 1.5g

$\text{FeSO}_4 \cdot 7\text{H}_2\text{O}$ 0.1g

MnSO_4 0.1g

Na_2MoO_4 0.05g

Pure agar 15g

Aged sea water 1 litre

pH 7.5-8

$(\text{NH}_4)_2\text{SO}_4$ 1.32g/50ml of distilled water

10ml l^{-1} of $(\text{NH}_4)_2\text{SO}_4$ solution to be autoclaved separately and added just before pouring.

3. Nitrite oxidizers (NII)

KH_2PO_4 0.25g

$\text{MgSO}_4 \cdot 7\text{H}_2\text{O}$ 1.5g

$\text{FeSO}_4 \cdot 7\text{H}_2\text{O}$ 0.1g

MnSO_4 0.03g

Na_2MoO_4 0.05g

Pure agar 15g

Aged sea water 1 litre

pH 7.5-8

NaNO_2 0.165g/50ml of distilled water

10ml l^{-1} of NaNO_2 solution to be autoclaved separately and added just before pouring.

4. Aerobic sulfur oxidizers (aerobic *Thiobacillus denitrificans*-like organisms)

Na ₂ S ₂ O ₃ 5H ₂ O	5g
K ₂ HPO ₄	0.2g
MgCl ₂ 6H ₂ O	0.1g
CaCl ₂ 6H ₂ O	0.01g
FeCl ₃ 6H ₂ O	0.01g
Phenol red	0.01g
Agar	10g
Sea water	1litre
NaHCO ₃	1g/10ml of distilled water

10ml l⁻¹ of NaHCO₃ solution to be autoclaved separately and added just before pouring.

5. Fe- oxidizers (Himedia, Mumbai, India)

Two parts A and B of the medium were prepared separately.

Part A

(NH ₄) ₂ SO ₄	3.0 g,
KCl	0.10g,
K ₂ HPO ₄	0.5g,
MgSO ₄	0.5g,
Ca(NO ₃)	0.01g was dissolved in 700 ml of seawater containing 1ml of 10N H ₂ SO ₄ .

Part B

FeSO₄ 44.22g was dissolved in 300ml of distilled water and mixed to Part A.

Final salinity 35ppt

Final pH was adjusted to 6.8± 0.2 in order to maintain a mild acidic to near neutral condition.

6. Mn- oxidizers

Two parts A and B of the medium were prepared separately.

Part A

NaHCO ₃	0.1g,
--------------------	-------

(NH₄)₂SO₄ 0.1 g,
K₂HPO₄ 0.5g,
MgSO₄ 0.5g, was dissolved in 900 ml of seawater.

Part B

MnCl₂ 12.5g was dissolved in 100ml of distilled water and mixed to Part A.

Final salinity 35ppt

Final pH was adjusted to 7.8± 0.2 in order to maintain a near neutral condition.

7. Modified mineral medium for formaldehyde utilizers (MMF)

K ₂ HPO ₄	0.12g
KH ₂ PO ₄	0.062g
CaCl ₂ 6H ₂ O	0.05g
MgSO ₄ 7H ₂ O	0.2g
FeCl ₃ 6H ₂ O	1.0mg
(NH ₄) ₂ SO ₄	0.5mg
CuSO ₄ 5H ₂ O	0.5mg
MnSO ₄ 5H ₂ O	10µg
Na ₂ MoO ₄ 2H ₂ O	10 µg
H ₃ PO ₄	10 µg
ZnSO ₄ 7H ₂ O	70 µg
CoCl ₂ 6H ₂ O	5 µg
HCHO	0.2%
Seawater	1litre
pH	8

8. Silicate solubilizers

(NH ₄) ₂ SO ₄	0.5g
K ₂ HPO ₄	0.8g
KCl	0.1g
MgSO ₄ 7H ₂ O	0.3g
Yeast extract	2.5g
Agar	20g
Bentonite clay	40g l ⁻¹
Trace element soln	1ml
Seawater	1litre
pH	7.8

9. Phosphate solubilizers

(NH ₄) ₂ SO ₄	0.5g
K ₂ HPO ₄	0.8g
KH ₂ PO ₄	0.2g
KCl	0.1g
MgSO ₄ 7H ₂ O	0.3g
Yeast extract	2.5g
Trace element soln	1ml
Agar	20g
Ca ₃ (PO ₄) ₂	2.5g
Sea water	1litre

The Anaerobes

1. Denitrifiers (anaerobic Thiobacillus denitrificans-like organisms)

Medium composition per litre of aged sea water:

Na ₂ S ₂ O ₃ .5H ₂ O	5g
K ₂ HPO ₄	0.2g
MgCl ₂ .6H ₂ O	0.1g
CaCl ₂ .6H ₂ O	0.01g
FeCl ₃ .6H ₂ O	0.01g
Phenol red indicator	0.01g
Pure agar (Difco)	10g

NaHCO ₃	1g
pH	8-8.3.

KNO₃ at 1g l⁻¹ was added as terminal electron acceptor.

Sodium bicarbonate solution was filter sterilized and added to medium just before pouring.

2. Nitrate Reducers

Medium composition per litre of aged sea water:

KNO₃ -0.101g

Nutrient agar 3.5 g l⁻¹

The original 14 g l⁻¹ of nutrient agar was modified to 25% strength of nutrient broth amended with pure agar to give a final agar concentration of 0.8%.

pH 7.5-8.

Appendix VI

List of important chemicals and buffers

1. Eh reference solutions

Reference solution A: (192mV)

Potassium ferrocyanide ($K_4Fe(CN)_6$)	0.1M
Potassium ferricyanide ($K_3Fe(CN)_6$)	0.05M

Reference solution B: (258mV)

Potassium ferrocyanide ($K_4Fe(CN)_6$)	0.01M
Potassium ferricyanide ($K_3Fe(CN)_6$)	0.05M
Potassium fluoride $KF_2 \cdot H_2O$	0.36M

2. Dissolved oxygen fixative and other reagents

- i. Winkler A- Dissolve manganese (II) chloride ($MnCl_2 \cdot 5H_2O$) (40g) in distilled water (100ml).
- ii. Winkler B- Dissolve separately potassium iodide (KI) (10g) and sodium hydroxide (NaOH) (36g) in minimum amount of distilled water. Mix two solutions in a 100 ml volumetric flask and make up to the volume with distilled water.
- iii. Hydrochloric acid (50%)- Carefully add the concentrated HCl (50ml) to distilled water (50ml).
- iv. Sodium thiosulphate solution (approximately 0.01N): Dissolve $Na_2S_2O_3 \cdot 5H_2O$ (2.49g) in distilled water and make up to 1 litre with distilled water.
- v. Starch indicator solution: Dispense 1g of starch powder in 100ml of distilled water and quickly heat the suspension to boiling. This solution should not be kept longer than a week.
- vi. Standard iodate solution (0.01): Weigh accurately KIO_3 A.R. (0.35g) and dissolve in 1 litre of distilled water.

3. Ammonium estimation reagents

- i. NaOH (0.8 mol^{-1}) -Dissolve 8g NaOH in 250cc distilled water
- ii. Phenol reagent -Dissolve 20g phenol in 75cc ethanol. Add 50 cc of distilled water. Then dissolve 150mg sodium nitroprusside in 25 cc of water. This is stable for months. Add the Na nitroprusside solution to phenol.
- iii. Trione solution: Dissolve 0.5g trione in 100cc of NaOH. This is stable for 3 weeks.
- iv. Tri sodium citrate solution: Dissolve 120g of trisodium citrate in 50 cc of distilled water. Add 5cc of NaOH solution. This reagent is stable indefinitely.

Preparation of stock

To 53.5 mg of ammonium chloride in volumetric flasks add 100ml of de-ionised water. This is stock 1. Take 1ml from stock 1 and add to another volumetric flask and make up the volume to 100ml with de-ionised water. This is stock 2.

From stock 2 take 1ml and make up to 100ml to give $1 \mu\text{M}$

take 2ml and make up to 100ml to give $2 \mu\text{M}$

take 5ml and make up to 100ml to give $5 \mu\text{M}$

Work flow:

A 10ml working volume of sample was taken in graduated stoppered tube. To this 0.4ml of phenol reagent was added followed by 0.2ml of trisodium citrate and 0.4ml of trione solution. Mixed well and incubated for 6hrs or microwaved for 60 seconds. Taken the absorbance at 630nm in a glass cuvette. In case of ELISA reader an absorbance of 650nm was used.

4. Sulphide estimation reagents

- i. Zinc acetate (2%)- Prepare by adding 2g of the 100ml of boiled and cooled distilled water. The solution is acidified with 1ml of 2M acetic acid/ L of Zn acetate and store at 4°C .
- ii. N,N-Dimethyl-p-phenylene diamine sulphate (0.2%): Prepare by adding 0.2g of salt in 100ml of 20% sulphuric acid and store in dark.

iii. Ammonium Ferric sulphate (10%)- Prepare by adding 10g of the chemical salt in 100ml of 2% concentrated sulphuric acid. Dissolve the salt by using magnetic stirrer overnight.

Standard stock solution (Sodium Sulphide hydrate, Flakes):

Primary stock ($1000\mu\text{g ml}^{-1}$) Prepare the primary stock of salt by suspending 100mg in a small volume of boiled and cooled distilled water and make up to 100ml

Secondary stock ($100\mu\text{g ml}^{-1}$) Prepare from the primary stock by taking 10ml and making up the volume 100ml with the same boiled and cooled distilled water in a separate volumetric flask. This is the working stock.

Work Flow:

Taken 10ml Zn acetate in 50 ml volumetric flask and 0.01ml of the 2° stock.

Repeated the same step for all other concentrations by pipetting the respective volumes of 2° stock.

Added 5ml of DMPD and 0.25ml of FAS and immediately stopper the flask and swirl once.

Incubated in the dark for 10mins to develop colour.

Taken the absorbance at 670nm in a glass cuvette. In case of ELISA reader an absorbance of 650nm was used.

5. Total Fe

- i. MilliQ water (resistance 18.2M ohm)
- ii. 0.01M NN (1-nitroso-2-naphthol)solution in methanol
- iii. 1M HEPPS (N-2- hydroxyethylpiperazine-N'-3-propanesulphonic acid) buffer (pH 8.0) made up with MilliQ and cleaned by equilibration with $50\mu\text{M MnO}_2$ and filtration using acid washed membrane filter (whatman cellulose nitrate 0.2μ pore size). A 0.4M bromate solution (potassium bromate, AnalaR was prepared and cleaned in the same way.
- iv. For determination of Fe (III) a 2mM Bp (2,2-bipyridyl) solution was prepared in 0.01M HCl. Standard solutions of Fe (III) chloride were made up in 0.01M HCl. A Fe(II) standard (10^{-6} M) was prepared in 0.01M HCl using ammonium ferrous sulphate

hexahydrate ($\text{FeH}_8\text{N}_2 \text{ O}_8\text{S}_2 \times 6\text{H}_2\text{O}$). Hydroxyl-ammonium hydrochloride ($\text{NH}_2\text{OH}\cdot\text{HCl}$) (0.1mM) was added to dilute Fe(II) solutions for stabilization. Hydrochloric acid, ammonia and methanol were purified by subboiling distillation using a quartz cold finger distillation unit. 0.4 μm filtered seawater from Central Indian Ocean.

6. Total Mn

- i. Citrate solution – A 1M citric acid solution, adjusted to pH 9 with concentrated sodium hydroxide solution
- ii. Ascorbate solution- A 1M ascorbic solution adjusted to pH 9 with concentrated sodium hydroxide solution.
- iii. Ammonium buffer solution- A 6M ammonia / 3M ammonium chloride buffer solution (pH 9.8).
- iv. Borate buffer solution- A 0.5M borax/0.34M sodium hydroxide buffer (pH 9.5)
- v. Synthetic sea-water – NaCl (30g), $\text{MgSO}_4 \cdot 7\text{H}_2\text{O}$ (3.5g) and $\text{CaCl}_2 \cdot 6\text{H}_2\text{O}$ (2.2g) were dissolved in 1 litre of pure water. The concentration of nitrate ions was 1ppm, except where otherwise specified.
- vi. Nitrate solution 0.01M.

7. Labile organic matter

Proteins

Reagents

Reagent A (2% Na_2CO_3 in 0.1N NaOH)

Na_2CO_3	2g
0.1N NaOH	100ml

Reagent B (0.5% CuSO_4 in 1% sodium potassium tartarate solution)

a. CuSO_4	0.5g
DW	50ml

b. Na-K-tartarate	1g
DW	50ml
Mix a and b together to get Reagent C	
Reagent A	50ml
Reagent B (prepare fresh)	1 ml
Folin's reagent(1:1 dilution)	
Folin ciocalteau phenol reagent	5ml
DW	5ml
1N NaOH	
NaOH	4g
DW	100ml
DW	

A known amount of sediment sample was weighed in triplicate and 2ml of 1N NaOH was added to these tubes. After mixing the tubes were placed in boiling water bath for 5min at 100°C. The tubes were cooled and centrifuged at 5000 rpm for 5min for clear supernatant. 0.5ml of the supernatant was mixed with 0.5ml DW, and 5ml Reagent C was added to it. The tubes were mixed and kept in dark for 10min. After 10min, 0.5ml Folin Ciocalteau reagent (1:1 dilution) was added to the tubes. The tubes were mixed and again kept in the dark for 20min. The OD was measured at 750nm using a spectrophotometer (Jasco). The standard curves were prepared using bovine serum albumin as standard. The stock solution of 1mg/ml was made with the known concentration of BSA.

Carbohydrates

Estimation of carbohydrates was done by using phenol-sulphuric acid methods, (Kochert, 1978) the test was based on the formation of yellow color, and where concentrated sulphuric acid was added to the sample mixed with phenol solution. Carbohydrates were dehydrated by the sulphuric-acid to form furfural and variety of other degradation products.

Reagents

5% TCA solution

Trichloroacetic acid	5g
DW	100ml

5% phenol solution

Phenol crystals	5g
DW	100ml

H₂SO₄ (95.5%, specific gravity 1.82)

DW

A known amount of sediment sample was weighed in triplicate and 1.5ml of 5% of TCA solution was added to the tubes. The tubes for heated for 3h in boiling water bath at 80-90°C and cooled. The tubes were centrifuge at 5000rpm for 5min and supernatant was collected. 0.5ml of the clear supernatant was mixed with 0.5ml of distilled water to form 1ml of treated sample solution (TSS). 1ml of TSS was added to 1ml of 5% phenol reagent and mixed. 5ml of conc. H₂SO₄ was added and kept in dark for 30min. The OD was measured at 480nm using a spectrophotometer (Jasco). The standard curves were prepared using glucose as standard.

Lipids

Estimation of Total Lipids

The test is based on the oxidation of acid dichromate, which is followed by a decrease in the dichromate color. The extraction of reaction mixture has an inverse relationship based on the decrease of dichromate color.

Reagents

0.5% dichromate in conc. H₂SO₄

K ₂ Cr ₂ O ₄	0.75g
DW	10ml
H ₂ SO ₄ (95.5%, specific gravity 1.82)	500ml

Organic solvent	
CHCl ₃	200ml
CH ₃ OH	400ml
DW	160ml
Analytical grade chloroform CHCl ₃	
DW	

A known amount of sediment sample was weighed in triplicate. 8ml of organic solvent was added to these tubes and mixed. The tubes were homogenized at 9000rpm for 1min and centrifuge at 5000rpm for 5min. The supernatant was added to a separating funnel followed by 2ml of CHCl₃ and 2ml DW. The funnels were shaken thoroughly, allowed to stand for some time. After clear separation of the two layers, the lower layer was collected in an evaporating flask. The flasks were evaporated to dryness using rotary vacuum evaporator. To the dried lipid sample, 2ml 0.15% acid dichromate was added and the flasks were heated in boiling water bath for 15 mins. The flasks were cooled thoroughly. 4.5ml DW was added to the flasks, mixed and kept aside to cool. The OD was measured at 440nm using a spectrophotometer (Jasco). The standard curves were prepared using stearic acid as standard.

8. Adenosine Triphosphate

Luciferine-Luciferase (Sigma Chemicals). Hydrated with 5ml of 0.22 μ m filtered double autoclaved distilled water.

Tris buffer

Tris (hydroxymethyl) amino methane 0.75g

DW 200ml

pH 7.7-7.8

pH was adjusted with 20% HCL

Firefly extract preparation

Luciferin-luciferase enzyme (Sigma, FLE 50) 50mg

Autoclaved DW 5ml

Age the enzyme at 4(\pm 2) $^{\circ}$ C for 3h

9. Bacterial counts

Acridine orange solution	0.01%
Acridine orange	0.1 g
Formaldehyde (5%)	100 ml
Filter through 0.22 µm polycarbonate paper	
Store in amber colored bottle at 4(±2)°C	

Yeast extract solution	0.001%
DW	30 ml
Yeast extract	0.3 g

The yeast extract is dissolved in DW.

The solution is autoclaved, filter sterilized and stored in vials at 4(±2)°C.

Antibiotic cocktail of nalidixic, piromedic and pipemedic acid

0.0016%

DW	30 ml
Nalixidic acid	0.024 g
Piromedic acid	0.012 g
Pipemedic acid	0.012g
Saturated NaOH solution	150 µL

The antibiotics are dissolved in saturated NaOH solution and DW

The solution is filter sterilized and stored in vials at 4(±2)°C

Na₂S 9H₂O	0.125%
DW	100 ml
Na ₂ S.9H ₂ O	5 g

The compound is mixed in autoclaved DW, filter sterilized and used immediately.

Buffered Formaldehyde	2%
Formaldehyde (38%)	
Hexamine	
Saturate formalin with hexamine.	

Filter sterilize and store at room temperature

Additions for incubation and fixing for direct total counts

	TC	DVC a	DVC an
	μL	μL	μL
Sample	5000	5000	5000
Yeast extract	-	50	50
Antibiotic cocktail	-	50	50
Sulfide solution	-	-	20
Buffered formalin (0 hr)	250	-	-
Buffered formalin (after 7hrs)	-	250	250

Biochemical characterization

Cultural Characteristics

The following characteristics were noted:

Size, Shape, Color, Margin, Elevation, Opacity

Morphological and biochemical tests

Gram staining

- a) Crystal violet
 - Crystal violet 2 g
 - Ethyl alcohol (95%) 20 ml
- a) Gram's iodine
 - Iodine 1 g
 - Potassium iodide 2 g
 - Distilled water 300 ml
- c) Ethyl alcohol 70%
- d) Safranin

Smear of the isolates was prepared on slides, air-dried and heat fixed.

The slides were treated with crystal violet (1min) followed by Gram's iodine (1min).

Slides were then washed with decolorizing solution (ethyl alcohol) till the blue color disappears and counter stained with safranin for 30s.

Slides were washed with water, dried and observed under oil- immersion .
Gram positive bacteria are stained purple while gram negative bacteria are stained pink

Motility

Motility was observed using hanging drop method.

Oxidase test

The enzyme oxidase is a part of the electron transfer system used by some organisms that use molecular oxygen as a terminal electron acceptor. Oxidase interacts with the membrane bound cytochromes and delivers cytochromes to oxygen. As a result H_2O_2 or H_2O is generated. Strict anaerobes do not use oxygen and hence do not possess the oxidase enzyme. Most gram positive bacteria are oxidase negative as well as the members of the family Enterobacteriaceae. Oxidase positive bacteria possess cytochrome oxidase or indophenol oxidase (an iron containing haemoprotein). These both catalyze the transport of electrons from donor compounds (NADH) to electron acceptors (usually oxygen). The test reagent, N, N, N', N'-tetra-methyl-p-phenylenediamine dihydrochloride acts as an artificial electron acceptor for the enzyme oxidase. The oxidised reagent forms the coloured compound indophenol blue. The cytochrome system is usually only present in aerobic organisms which are capable of utilizing oxygen as the final hydrogen receptor. The end product of this metabolism is either water or hydrogen peroxide (broken down by catalase).

Oxidase reagent

DW	100 ml
N, N, N', N'-tetra-methyl-p-phenylenediamine dihydrochloride	1 g

A drop of oxidase reagent was placed on Whatman filter paper no.1

Isolates were picked using sterile toothpicks and smeared on treated filter paper to check for the presence of cytochrome oxidase in the isolates.

The observations were inferred from the following table

Observation	Report
1. Deep violet color developed immediately after smearing	Oxidase positive
2. Deep violet color developed after 30 sec positiveness	delayed
3. No color change.	Oxidase negative

Catalase test

The catalase test is used to detect the presence of catalase enzymes by the decomposition of hydrogen peroxide to release oxygen and water. Hydrogen peroxide is formed by some bacteria as an oxidative end product of the aerobic breakdown of sugars and if allowed to accumulate, is highly toxic. Catalase either decomposes hydrogen peroxide or oxidizes secondary substrates.

Hydrogen peroxide (3%)

Scrape the growth from a slant or plate with a non-metallic instrument.

Suspend it in 3 % hydrogen peroxide on a slide.

Examine for effervescence, presence of effervescence denotes catalase positive and absence denotes negative reaction.

Hugh and Leifson's medium (OF test)

Oxidative organisms can only metabolize glucose or other carbohydrates under aerobic conditions ie oxygen is the ultimate hydrogen acceptor. Other organisms ferment glucose and the hydrogen acceptor is then another substance eg sulphur. This fermentative process is independent of oxygen and cultures of organisms may be aerobic or anaerobic. The end product of metabolizing a carbohydrate is acid. Oxidizing organisms produce an acid reaction towards the top of the tube. Fermenting organisms produce an acid reaction throughout the medium. Organisms that cannot break down the carbohydrate aerobically or anaerobically, produce an alkaline reaction in the tube. Hugh and Leifson's medium can also be used for recording gas production and motility.

OF medium

1	Dextrose	1 g
2	Peptone	0.2 g
3	KH ₂ PO ₄	0.03 g
4	Agar	1.5 g
5	Bromothymol blue	0.002 g
6	50% SW	100 ml

* Dextrose was filter sterilized and added to the medium later

The tubes containing the OF medium was stab inoculated with the cultures and incubated at room temperature for 48 hrs.

The observations were inferred from the following table

Observation	Report
1. Bottom to top yellow/ Bottom yellow	Fermentative (with or without gas)
2. Yellow only on top	Oxidative
3. Blue color	Alkaline
Growth, no color	Growth only
No Growth	Inert

Metabolic diversity of bacterial isolates

Screening for Amylase

Amylolytic medium

Nutrient Agar	28 g
Starch	2 g
50% SW	1000 ml
pH	7.5-7.8

Culture was spot inoculated on the medium and incubated for 24 –48 hrs at room temperature. On addition of iodine to the plate, the whole plate turns dark blue except for yellow/colourless halos around the colonies indicating amylase production.

Screening for Protease

a) Proteolytic medium

Nutrient Agar	28 g
Caesin	2 g
50% Sea water	1000 ml
pH	7.5-7.8

b) HgCl₂ solution

HgCl ₂	15 g
HCl	20 ml
DW	100 ml

Culture was spot inoculated on the proteolytic medium and incubated for 24 – 48 hrs at room temperature.

After the colonies have grown, overlay the plate with HgCl₂ solution
Observe for the clearance zone around the colony.

Screening for Lipase

Lipolytic medium

Peptone	10 g
NaCl	5 g
CaCl ₂	0.1 g
*Tween	10 ml
Agar	15 g
50% SW	1000 ml
pH	7.0-7.4

* Tween was autoclaved separately and added to the medium just before pouring

Culture was spot inoculated on the medium and incubated for 24 –48 hrs at room temperature. Observe for precipitate around the colony.

Screening for Phosphatase

Phosphatase medium

Nutrient Agar	28.0 g
50% SW	120 ml

After autoclaving and just before pouring the substrate, filter sterilized p-nitrophenyl phosphatase (sigma) was added to the medium so as to obtain a final concentration of 0.02%. Culture was spot inoculated on the medium and incubated for 24 –48 hrs at room temperature. Presence of a greenish yellow color around the colony is indicative of phosphatase production.

Screening for DNase

DNase test medium

DNase test agar	5.04 g
Toluidine blue	0.012 g
50% SW	120 ml
pH	7.5-7.8

Culture was spot inoculated on the medium and incubated for 24 –48 hrs at room temperature. Presence of a clearance zone indicated DNase production

10. Ribulose bis-phosphate carboxylase/oxygenase (RuBisCO) enzyme

Chemical required

Tris-hydroxymethyl aminomethane

HCl, 2M

EDTA, disodium salt

DL-Dithiothreol (DTT)

Glutathione reduced form (GSH)

MgCl₂ · 6H₂O

NaHCO₃

NaH¹⁴CO₃ 60mCi mmol⁻¹

D-ribulose-1, 5 bisphosphate (RuBP) tetrasodium salt

Trichloroacetic acid TCA 24% w/v

Homogenisation buffer: In double dist water

i. 100mM Tris-HCl pH 8

ii. 1mM EDTA

iii. 1mM DTT

3.022g Tris in 200ml water and adjust pH 8 with 2M HCl

93.0mg EDTA+38.6mg DTT in Tris buffer

Make up the solution to 250ml with water. Store at 2-4°C

Substrate co-factors:

- a. 10ml stocks of :
- i. 1M Tris HCl buffer pH 8
 - ii. 1mM EDTA
 - iii. 80mM MgCl₂.6H₂O
 - iv. 50mM GSH
 - v. 200 mM NaH¹⁴CO₃ (0.4μCi mol⁻¹)

Soln A- 1.214g of Tris in 6ml H₂O, pH 8 with 2M HCl, make up to 10ml

Soln B- 168mg NaHCO₃ in 8ml of H₂O. Add 80μCi NaH¹⁴ CO₃ and make up to 10ml

Soln C- 3.72mg EDTA, 162.7mg MgCl₂.6H₂O, 154mg GSH. Individually dissolve each of these components in 10ml H₂O.

b. 5ml of 10mM RuBP, 19.9mg RuBP in 5ml H₂O.

These prepared solutions are kept in serum bottles with rubber stopper in cold or crushed ice.

11. Preparation of Schiff's reagent:

1. Dissolve 5g of basic fuchsin in 900ml of boiling distilled water
2. Cool to approximately 50°C and slowly add 100ml of 1N HCl
3. Cool to approximately 25°C and dissolve 10g of K₂S₂O₅
4. Shake for 3 minutes and incubate in the dark at room temperature for 24 hours
5. Add 5 grams of fine activated charcoal and shake for 3 minutes
6. Filter solution (should be clear)
7. Store at 4°C in a foil covered bottle

Appendix VII

Molecular probes

The following sequence adaptors and primers were used (<http://vamps.mbl.edu/resources>).

Roche amplicon sequencing adaptors:

A-adaptor 5'-GCCTCCCTCGCGCCATCAG-3'

B-adaptor 5'-GCCTTGCCAGCCCGCTCAG-3'

For bacterial V6 sequencing a mixture of the following 5 forward and 4 reverse primers were used.

Forward Primers (967F)

CNACGCGAAGAACCTTANC

CAACGCGAAAAACCTTACC

CAACGCGCAGAACCTTACC

ATACGCGARGAACCTTACC

CTAACCGANGAACCTYACC

Reverse Primers (1046R)

CGACAGCCATGCANACCT

CGACAACCATGCANACCT

CGACGGCCATGCANACCT

CGACGACCATGCANACCT

Thus, to amplify the V6 hypervariable region of the bacterial 16S rRNA (*Escherichia coli* positions 967-1046) (Sogin *et al.*, 2006) and sequence it in the forward direction (relative to the 5'-3' orientation of the gene) using the Roche A

primer, the forward primer consisted of the A-adaptor, 5-base key and sequence designed to bind to the 967F region of the SSU.

5'-GCCTCCCTCGCGCCATCAGgatctCNACGCGAAGAACCTTANC-3'

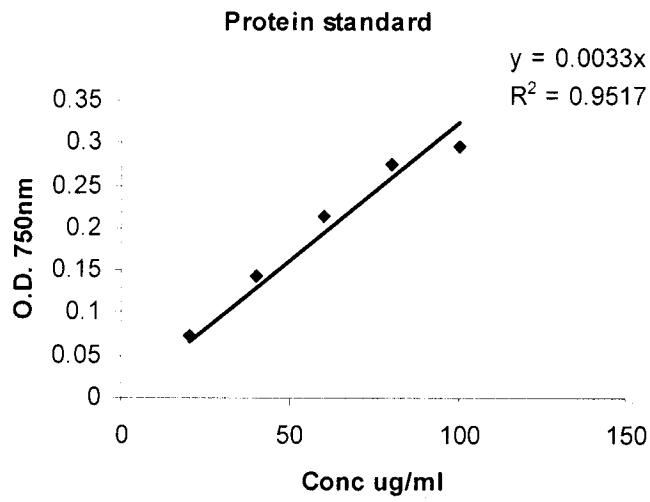
The reverse primer would consist of the B-adaptor and a sequence designed to bind to 1046R:

5'-GCCTCCCTCGCGCCATCAG CGACAGCCATGCANACCT -3'

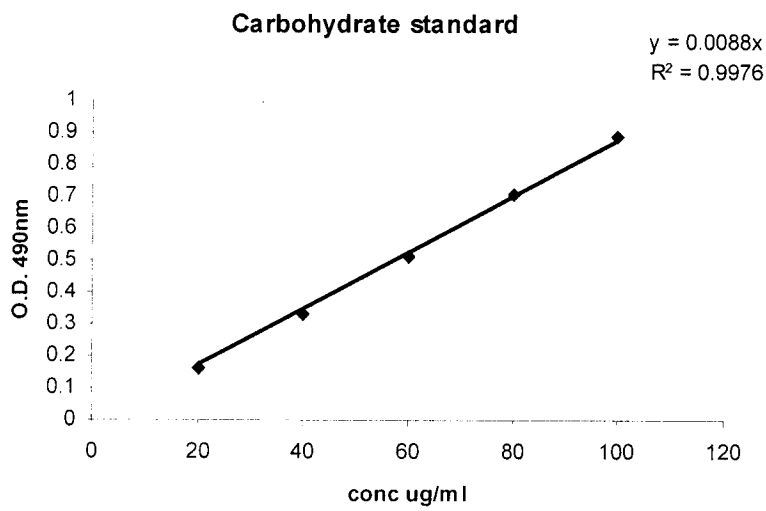
Appendix VIII

Standard curves

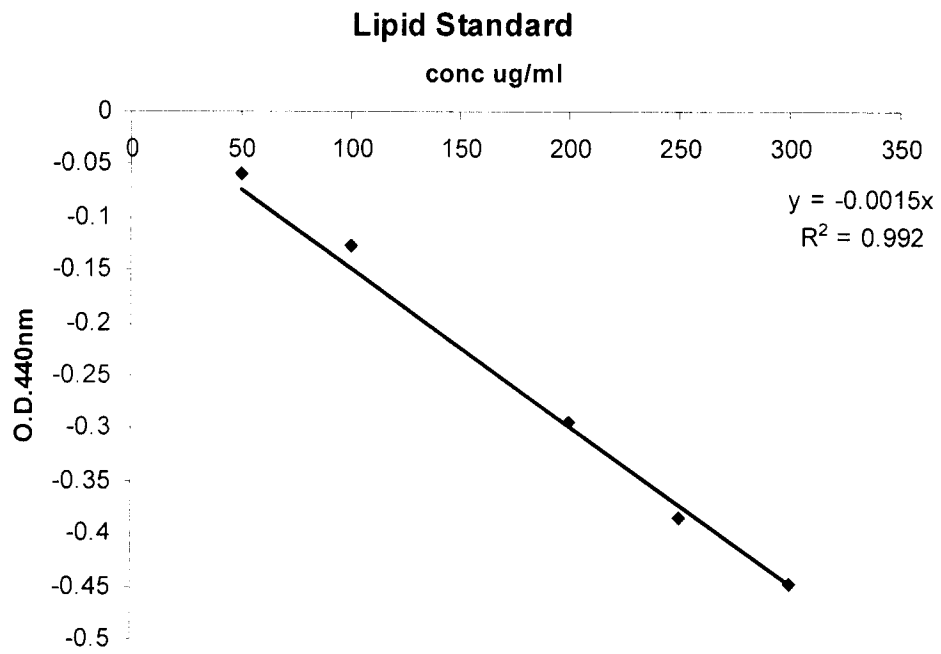
Proteins-Bovin serum albumin



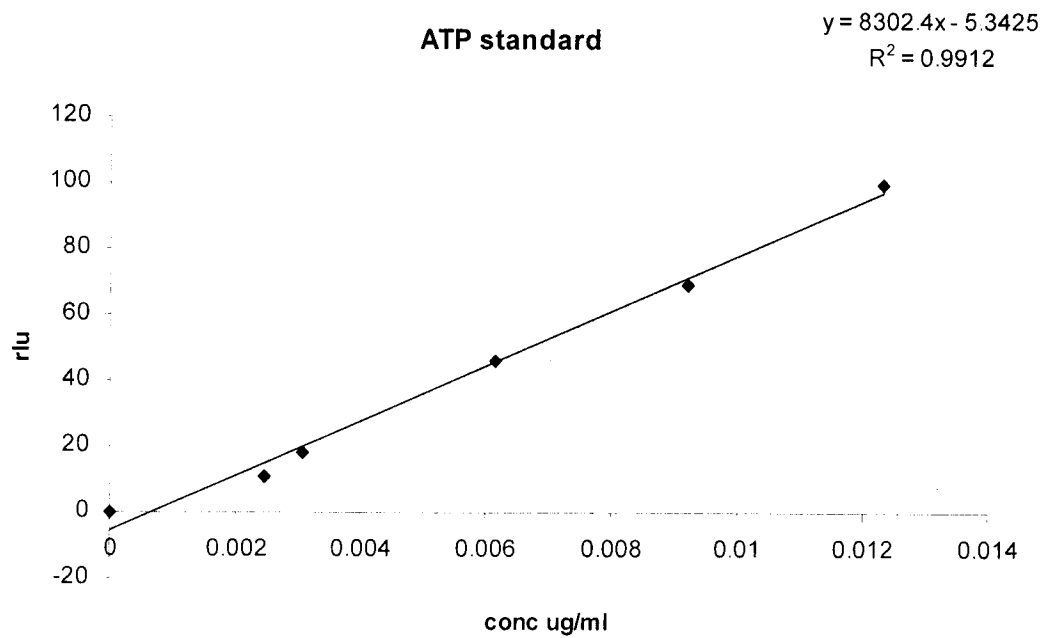
Carbohydrates- Glucose



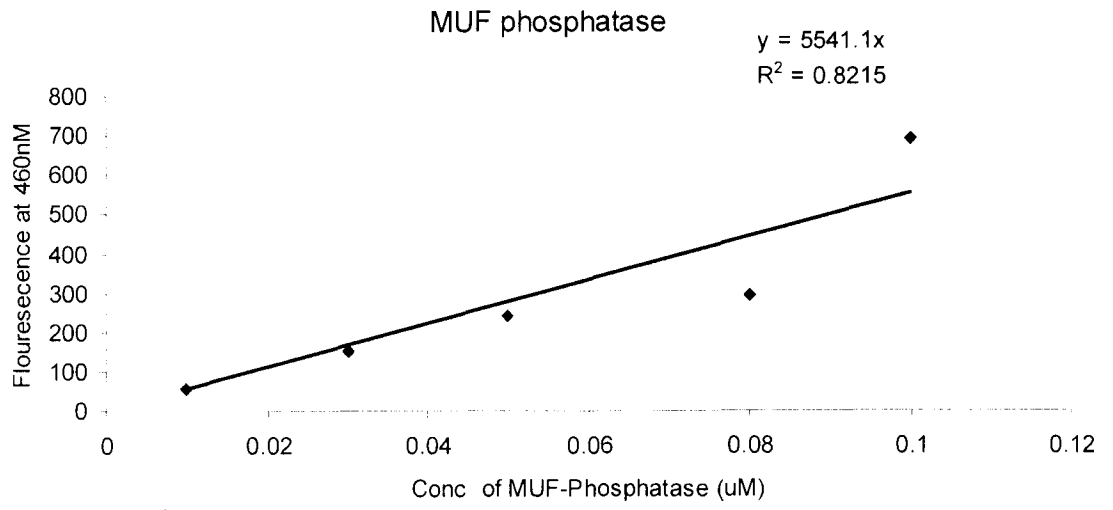
Lipids- stearic acid



ATP – Na ATP salt



MUF-Phosphatase



Appendix IX

MATLAB code

```
%%%%%%%%%%%%%%%%%%%%%%%%%%%%%%%%%%%%%%%%%%%%%%%%%%%%%%%%%%%%%%%%%%%%%%%%%%
%      File  CIB.m Supplementary material
%      Reference model  Meister et al., (2007)
%      Coded on 2/2009  for the submission Das et al., 2010
"Bacterial response to contrasting sediment geochemistry in Central
Indian Basin"
%      I. Suresh (National Institute of Oceanography)
%      isuresh@nio.org
%      Type: Explicit Finite Difference Model
%      Purpose: Geomicrobial simulations including time factor
%      MATLAB 7.4.0
%%%%%%%%%%%%%%%%%%%%%%%%%%%%%%%%%%%%%%%%%%%%%%%%%%%%%%%%%%%%%%%%%%%%%%%%%
clear;
clc;
close all;

% Input data
dx=; % step size in x
conv2sec=365*24*60*60;
dt=*conv2sec; % step size in t
x=:dx:; % Range of x
t=:dt:*conv2sec; % Range of t

Ds=; % Diffusion coefficient
F=; % Tortuosity factor
%%%%%%%%%%%%%%%%%%%%%%%%%%%%%%%%%%%%%%%%%%%%%%%%%%%%%%%%%%%%%%%%%%%%%%%%%
k=Ds/F;
M = length(x);
N = length(t);
fac = k*dt/dx^2;
c = zeros(N,M);
init(1:M)=zeros(1,M);
c(1,:)=init;
c(1,1)=; % Initial condition
grid

% Define s(x)
s=zeros(N,M);
for j=1:N
    for i=1:M
        if t(j)>10000*conv2sec && t(j)<11400*conv2sec
            if x(i)> && x(i)< % x(i) is boundary condition for
length
                s(j,i)=r/conv2sec/1000; % r is a microbial rate
            end
        end
    end
end
end

for n = 1:N-1
    c(n+1, 2:M-1) = fac*(c(n, 3:M) + c(n, 1:M-2)) + (1 - 2*fac)*c(n,
2:M-1)+dt*s(n,2:M-1);
end
```

```

% Boundary condition of concentration
c(n+1, 1) = ;
c(n+1, M) = ;

end
% Checking for stability
fac
1-2*fac

Figure(1)
surf(x,t,c)

Figure(2)
surf(s)

Figure(3)
plot(c(T,:),x,'b')
hold
plot(c(T1,:),x,'r')
plot(c(T2,:),x,'m')
plot(c(T3,:),x,'k')
plot(c(T4,:),x,'--k')
plot(c(T5,:),x,'*k')
set(gca,'YDir','reverse');

% T,T1,T2,T3,T4,T5 (Concentration-depth plots at various time steps)

```

Appendix X

List of publications

I. Full length papers -(8)

1. **Anindita Das**, Christabelle E. G. Fernandes, Sonali S. Naik, B. Nagender Nath I. Suresh, M.B.L. Mascarenhas-Periera, S.M. Gupta, N.H. Khadge, C. Prakash Babu, D.V. Borole, Sujith, P.P. A.B. Valsangkar, Babu Shashikant Mourya, Sushanta U. Biche and Loka Bharathi, P. A. (2010a). Bacterial responses to contrasting sediment geochemistry in Central Indian Basin. *Sedimentology* doi: 10.1111/j.1365-3091.2010.01183.x_ 2010 IF 2.11
2. **Anindita Das**, P. P. Sujith, Babu Shashikant Mourya, Sushanta U. Biche and P.A. Loka Bharathi (2010b). Chemosynthetic activity prevails in deep-sea sediments of Central Indian Basin. *Extremophiles* doi: 10.1007/s00792-010-0346z IF 2.0
3. P. P. Sujith, **Anindita Das**, Babu Shashikant Mourya, and P.A. Loka Bharathi (2011). Immobilization of manganese, cobalt and nickel by deep-sea-sediment-microbial communities *Chemistry and Ecology*.(2011) (Accepted) IF 0.6.
4. M.-J. Gonsalves, **Anindita Das** and P.A. Loka Bharathi (2009) Marine organisms and their adaptations. *Enviroscan-A CES Newsletter* 12(1) 4-7.
5. **Anindita Das**, M.-J. Gonsalves and P.A. Loka Bharathi (2008) Role of microbes in marine environment. *Enviroscan -A CES Newsletter* 1(2)7-9.
6. Christabelle E. G. Fernandes, **Anindita Das**, Sonali Naik , Rahul Sharma, Loka Bharathi, P.A. (2007) Intermediate effect of simulated sand mining on the variation of bacterial parameters in coastal waters of Kalbadevi Bay, Ratnagiri. National Seminar on Exploration, Exploitation, Enrichment and Environment of coastal placer minerals. Eds Loveson, V.J., Sen, P.K., and A.Sinha . Central Mechanical Engineering Research Institute Durgapur India 25-27March , Macmillan India, New Delhi India 270-277.
7. Christabelle E. G. Fernandes, **Anindita Das**, Daphne G. Faria and P. A. Loka Bharathi, (2005). Microbiology and Biochemistry of placer rich beach sediment: Short term response to small scale simulated mining. National Seminar on Development planning of Coastal placer minerals (Placer-2005), 26-27, October 2005 organized by Manonmanium Sundaranar University, Tirunelveli, Tamil Nadu and Central Marine Research Institute, Dhanbad, India .248-255.
8. **Anindita Das**, Christabelle E. G. Fernandes, Sonali S. Naik, B. Nagender Nath and Loka Bharathi, P. A. (2005). Bacterial responses to contrasting geochemistry in the sediments of Central Indian Ocean Basin. National Seminar on Polymetallic Nodules, 29-30, September, 2005 organized by Regional Research laboratory, Bhubaneswar, Orissa, India 1-8.

II. Symposium Abstracts- (10)

1. Christabelle E.G. Fernandes, Sheryl O. Fernandes, Maria-Judith Gonsalves, **Anindita Das**, Sujith, P.P. and P.A. LokaBharathi. Benthic bacterial diversity: Iron-ore dominated mangroves versus ilmenite-rich beach sediments. A Decade of Discovery - Census of Marine Life 2010. 4-6th October 2010. London. U K

2. Sheryl O. Fernandes, Maria-Judith Gonsalves, Christabelle E. G. Fernandes, Sujith P.P., **Anindita Das**, Sonali Naik, P.A. Lokabharathi. Insights on Bacterial diversity in varied marine ecosystems in the Indian Ocean region with special reference to Mangroves. International Conference on Aquatic Microbiology (Status, Challenges and opportunities (AMSCO)2nd-4th September, 2010 CAS in Marine Biology Annamalai University Tamil Nadu, India.
3. **Anindita Das**, Sujith P.P., Sheryl O. Fernandes, Runa Antony and P.A. Loka Bharathi Chemosynthetic activity in Deep-Sea Environments of Indian Ocean 4th International symposium on Chemosynthesis-Based ecosystems, 29th June -3rd July, 2009 Okinawa, Japan (Poster).
4. Maria-Judith Gonsalves, Christabelle E.G. Fernandes, Sheryl O. Fernandes, Sujith P.P., **Anindita Das**, Sonali Naik, P.A. Loka Bharathi. Perspectives of microbial diversity in varied marine ecosystems in the Indian Ocean region. International Census of Marine Microbes 454 Users Spring Meeting, April 6-9th, 2009, Woods Hole, Massachusetts, USA (Poster).
5. P.A. Loka Bharathi, Maria Judith Gonsalves, Christabelle E.G. Fernandes, Sheryl O. Fernandes, **Anindita Das**, Sonali S. Naik and Sujith PP. The Indian Ocean Cooperative 454 Run Project International Census of Marine Microbes 454 User Spring Meeting, April 6-9th, 2009 Marine Biological Laboratory Woods Hole, MA USA (Proceedings).
6. **Anindita Das**, Sonali S. Naik, Neelam Sharma, Mohamed Riyas Theyyambattil, Christabelle E. G. Fernandes and P. A. Loka Bharathi, (2006). Abundance, diversity and activity of culturable bacteria in central Indian Ocean Basin. 7th Asia Pacific Marine Biotechnology Conference (7th APMBC - India '06), 2-5, November 2006 organized by National Institute of Oceanography, Goa, India.
7. Christabelle E. G. Fernandes, **Anindita Das**, Sonali S. Naik, Rahul Sharma and P. A. Loka Bharathi, (2007). Immediate effect of simulated sand mining on the variation of bacterial parameters in coastal waters of Kalbadevi bay, Ratnagiri. National Seminar on Exploration, Exploitation, Enrichment and Environment of Coastal Placer Minerals (PLACER 2007), 25-26, March 2007 organized by Central Mechanical engineering Research Institute, Durgapur and Central Mining Research Institute, Dhanbad at CMERI Campus, Durgapur, India.
8. Christabelle E. G. Fernandes, Nisha Pillai, Sonali S. Naik, **Anindita Das** and P. A. Loka Bharathi, (2006). Placer deposits reduce diversity and function: Examples from culturable bacteria of Kalbadevi beach, Ratnagiri. 7th Asia Pacific Marine Biotechnology Conference (7th APMBC - India '06), 2-5, November 2006 organized by National Institute of Oceanography, Goa, India (Presenting author).
9. Sonali S. Naik, Manisha Fushe, **Anindita Das**, Christabelle E. G. Fernandes, and P. A. Loka Bharathi, (2006). Evolution of culturable diversity of deep sea sediments: Effect of simulated disturbance. 7th Asia Pacific Marine Biotechnology Conference (7th APMBC - India '06), 2-5, November 2006 organized by National Institute of Oceanography, Goa, India (Presenting author).
10. **Anindita Das**, P.A. Loka Bharathi, G. Sheelu, Shanta Nair, and D. Chandramohan (2004). Generic distribution and activity of culturable bacteria in a tropical estuary: premonsoon scenerio. Proceedings of the Conference on Microbiology in the Tropical Seas, National Institute of Oceanography, Goa, India (Presenting author).

III Technical Reports and presentations (8):

1. Annual report for the year 2005-2006 of task group for Environmental studies for placer minerals. CSIR Network Project.
2. Annual report for the year 2006-2007 of task group for Environmental studies for placer minerals. CSIR Network Project.
3. Annual report for the year 2007-2008 of task group for Environmental studies for placer minerals. CSIR Network Project.
4. Restoration and recolonisation of benthic environment in the Central Indian Basin. Fourth Monitoring Report. Microbial and Biogeochemical parameters. December 2005. Submitted to Dept. Of Ocean Development. Govt of India.
5. Benthic environmental variability in the Central Indian Basin -II. Bacterial and biochemical variability. October 2006. Submitted to Dept. Of Ocean Development. Govt of India.
6. Benthic environmental variability in the Central Indian Basin -III. Microbiology and Biochemistry of sediments. January (2008). Submitted to Ministry of Earth Sciences, Govt of India.
7. Environmental Variability of Biochemistry and Microbiology in nodule area of CIB. Polymetallic Nodules- Environmental Impact Assessment (PMN-EIA). National Institute of Oceanography, Dona Paula, Goa. 9-10th February, 2009.
8. Benthic Environmental Variability in the Central Indian Basin-IV. Microbiology and Biochemistry. September 2010. Submitted to Ministry of Earth Sciences, Govt of India pp 49-56.

IV. Papers under review -(6)

1. Sonali Shyam Naik, N. H. Khadge, A. B. Valsangkar, **Anindita Das**, Christabelle E. G. Fernandes, and P.A. Loka Bharathi (2009). Relationship of sediment-biochemistry, bacterial morphology and activity to geotechnical properties and sediment texture in Central Indian Basin. *Manuscript under review J Asian Earth Science*.
2. **Anindita Das**, Sujith, P.P., Sheryl O. Fernandes, Runa Antony, Loka Bharathi P.A. Extent of chemosynthetic activity in environments of Indian Ocean GCA
3. **Anindita Das**, Christabelle E.G. Fernandes, Sonali S. Naik, Rahul Sharma and P. A. Loka Bharathi Interrelationships between microbial and biochemical parameters in deep-sea sediments and effect of storage at normal tropical conditions. *Manuscript ready to be communicated*.
4. Christabelle, E.G. Fernandes, **Anindita Das**, Nath, B.N., LokaBharathi, P.A. Mixed Response In Bacterial And Biochemical Variables To Simulated Sand Mining In Placer-Rich-Beach-Sediments, Ratnagiri, West Coast Of India. *Manuscript sent back to author for major revision and resubmission MarGeores and Geotechnol*.
5. T. Remya, **Anindita Das** and P.A. LokaBharathi Phylogeny and phylogeography in microbes associated with vent and seep ecosystems and their contribution to primary production. *Manuscript ready to be communicated*.

6. Christabelle, E.G. Fernandes, Ashish Malik, Jineesh, V.K., Sheryl O. Fernandes, **Anindita Das**, Sunita Pandey, Geeta Kanolkar, Sujith, P.P., Samita Helekar, Maria Judith Gonsalves, P.A. Loka Bharathi. Estuarine influence on coastal waters: Comparison of proximate systems off Goa and Ratnagiri, Westcoast of India. *Manuscript submitted to Estuarine, Coastal Shelf Science.*

7. **Das, Anindita** and P.A. LokaBharathi et al., Inter-annual variations conceal seasonal variations in microbial and biochemical parameters in Central Indian Basin. *Manuscript under preparation*

Bacterial response to contrasting sediment geochemistry in the Central Indian Basin

ANINDITA DAS, CHRISTABELLE E. G. FERNANDES, SONALI S. NAIK, B. NAGENDER NATH, I. SURESH, M. B. L. MASCARENHAS-PEREIRA, S. M. GUPTA, N. H. KHADGE, C. PRAKASH BABU, D. V. BOROLE, P. P. SUJITH, ANIL B. VALSANGKAR, BABU SHASHIKANTMOURYA, SUSHANTA U. BICHE, RAHUL SHARMA and P. A. LOKA BHARATHI
National Institute of Oceanography, (Council of Scientific and Industrial Research) Dona Paula, Goa 403004, India (E-mail: loka@nio.org)

Associate Editor – Daniel Ariztegui

ABSTRACT

In order to investigate whether geochemical, physiographic and lithological differences in two end-member sedimentary settings could evoke varied microbe–sediment interactions, two 25 cm long sediment cores from contrasting regions in the Central Indian Basin have been examined. Site TVBC 26 in the northern siliceous realm (10°S, 75.5°E) is organic-C rich with $0.3 \pm 0.09\%$ total organic carbon. Site TVBC 08 in the southern pelagic red clay realm (16°S, 75.5°E), located on the flank of a seamount in a mid-plate volcanic area with hydrothermal alterations of recent origin, is organic-C poor ($0.1 \pm 0.07\%$). Significantly higher bacterial viability under anaerobic conditions, generally lower microbial carbon uptake and higher numbers of aerobic sulphur oxidizers at the mottled zones, characterize core TVBC 26. In the carbon-poor environment of core TVBC 08, a doubling of the ^{14}C uptake, a 250 times increase in the number of autotrophic nitrifiers, a four-fold lowering in the number of aerobic sulphur oxidizers and a higher order of denitrifiers exists when compared with core TVBC 26; this suggests the prevalence of a potentially autotrophic microbial community in core TVBC 08 in response to hydrothermal activity. Microbial activity at the northern TVBC 26 is predominantly heterotrophic with enhanced chemosynthetic activity restricted to tan-green mottled zones. The southern TVBC 08 is autotrophic with increased heterotrophic activity in the deepest layers. Notably, the bacterial activity is generally dependent on the surface productivity in TVBC 26, the carbon-rich core, and mostly independent in TVBC 08, the carbon-poor, hydrothermally influenced core. The northern sediment is more organic sink-controlled and the southern sediment is more hydrothermal source-controlled. Hydrothermal activity and associated rock alteration processes may be more relevant than organic matter delivery in these deep-sea sediments. Thus, this study highlights the relative importance of hydrothermal activity versus organic delivery in evoking different microbial responses in the Central Indian Basin sediments.

Keywords Autotrophy, bacteria, Central Indian Basin, diagenesis, hydrothermal, non-steady state, numerical simulation, sediment, transition zone.

INTRODUCTION

The deep-sea floor is predominantly a microbial habitat with a relatively low input (0.01% to 1%) of photosynthetically produced organic matter

(Suess *et al.*, 1980). The average temperature and pressure generally remain *ca* 2°C and 500 bars, respectively, in these sediments. However, the more subtle differences in organic matter, pore water and sediment geochemistry dictate

variations among the local communities of micro-organisms in terms of numbers and activity. The role played by the number of micro-organisms in terms of total counts and relative abundance is gaining importance. Recent microbiological studies on the Namibian Shelf (GeoB cores) and Eastern Equatorial Pacific [Ocean Drilling Program (ODP) Leg 201] show that culturable bacteria are constant in abundance over large stretches of the ocean. Cultured bacteria vary consistently from one sub-sea floor environment to another and have been shown to contribute significantly to important biogeochemical processes (D'Hondt *et al.*, 2004).

The abundance and activity of culturable bacteria are linked directly to mineralization processes (Schulz & Schulz, 2005) adapted to very low metabolic rates (Teske, 2004). These mineralization processes are dependent on organic matter diagenesis and hydrothermal fluid interactions (Ma *et al.*, 2006). Hydrothermal fluids from magmatic hotspots, faults and fractures are spread over large stretches of the ocean basin (D'Hondt *et al.*, 2002, 2004). These fluid interferences link the nutrient and the rock cycle providing a wide array of electron donors and acceptors for microbial proliferation and activity, including chemosynthesis. Co-occurrence of multiple metabolic pathways (Wang *et al.*, 2008) or overlap of multiple metabolic zones (Canfield & Thamdrup, 2009) emphasizes the extensive chemosynthetic potential of bacteria.

The aim of this study is to investigate how geochemical, physiographic and lithological differences in two end-member sedimentary settings evoke different microbe–sediment interactions. To address this objective, two geochemically and sedimentologically contrasting cores of the Central Indian Basin (CIB; Fig. 1A and B) were examined for distinctions between microbial communities and the extent of chemoautotrophy. Modern microbial and biochemical processes, along with the pore water geochemistry and porosity, have been integrated with stratigraphic data in order to understand and quantify the factors determining the extent of chemosynthetic potential in these two end-member sedimentary settings in the CIB.

GEOLOGICAL SETTING OF THE CENTRAL INDIAN BASIN

The CIB, with an area of 5.7×10^6 km² (Ghosh & Mukhopadhyay, 1999), has five sediment types,

namely: terrigenous mud, siliceous ooze with and without nodules, pelagic red clays and carbonaceous ooze (Fig. 1A; Nath *et al.*, 1989; Rao & Nath, 1988). The basin is bordered by the Indian Ocean Ridge system and marked by prominent fracture zones (FZ) and seamounts hosting normal to Mid Ocean Ridge Basalts (Fig. 1B; Kamesh Raju & Ramprasad, 1989; Mukhopadhyay *et al.*, 2002; Das *et al.*, 2007).

The oxygen and nutrient-rich Antarctic Bottom Water Current (AABW) entering the CIB from 5°S (Gupta & Jauhari, 1994) maintained oxic conditions during the past *ca* 1100 kyr (Pattan *et al.*, 2005). Terrigenous influx decreases from north to south (Rao & Nath, 1988; Nath *et al.*, 1989). Higher surface productivity, and therefore higher detrital rain from overlying surface waters (Matondkar *et al.*, 2005), make the organic matter supply to the siliceous ooze higher than that to the red clays (Gupta & Jauhari, 1994). Other factors influencing distribution of organic carbon are sedimentation rates, bottom water oxygenation, water depth, topography, bioturbation, recalcitrance and age (Lyle, 1983; Nath *et al.*, 1997; Lochte *et al.*, 2000). The two stations studied here are located along transect 75°5'E, in close proximity to the Trace of Rodriguez Triple Junction.

Geological features of northern siliceous oozes

The sea floor spreading rate at this location is fast at 90 mm kyr⁻¹ (Mukhopadhyay *et al.*, 2002). Temperature and dissolved oxygen of bottom water is 0.9 to 1.03°C and 4.2 to 4.3 ml l⁻¹, respectively (Warren, 1982; Nath *et al.*, 1992). Surface C/N ratios of this total organic carbon (TOC)-rich core range from 3 to 6 (Gupta & Jauhari, 1994; Pattan *et al.*, 2005). Illite is the dominant clay type with a SiO₂/Al₂O₃ ratio of 6:7 and biogenic silica varies from 10 to 35%. Early diagenetic processes are attributed to the formation of rough nodules when the Mn/Fe ratio > 1, with higher Mn, Cu, Ni and todorokite mineralogy (Rao & Nath, 1988; Nath *et al.*, 1989).

Geological features of southern pelagic red clay

The sea floor spreading rate is slow at 26 mm kyr⁻¹ (Mukhopadhyay *et al.*, 2002). Temperature and dissolved oxygen of bottom waters are >1.03°C and 4.1 to 4.2 ml l⁻¹, respectively (Warren, 1982; Nath *et al.*, 1992). The surface C/N ratio of this TOC-poor core ranges from 3 to 6 (Gupta & Jauhari, 1994). The dominant clay type is montmorillonite

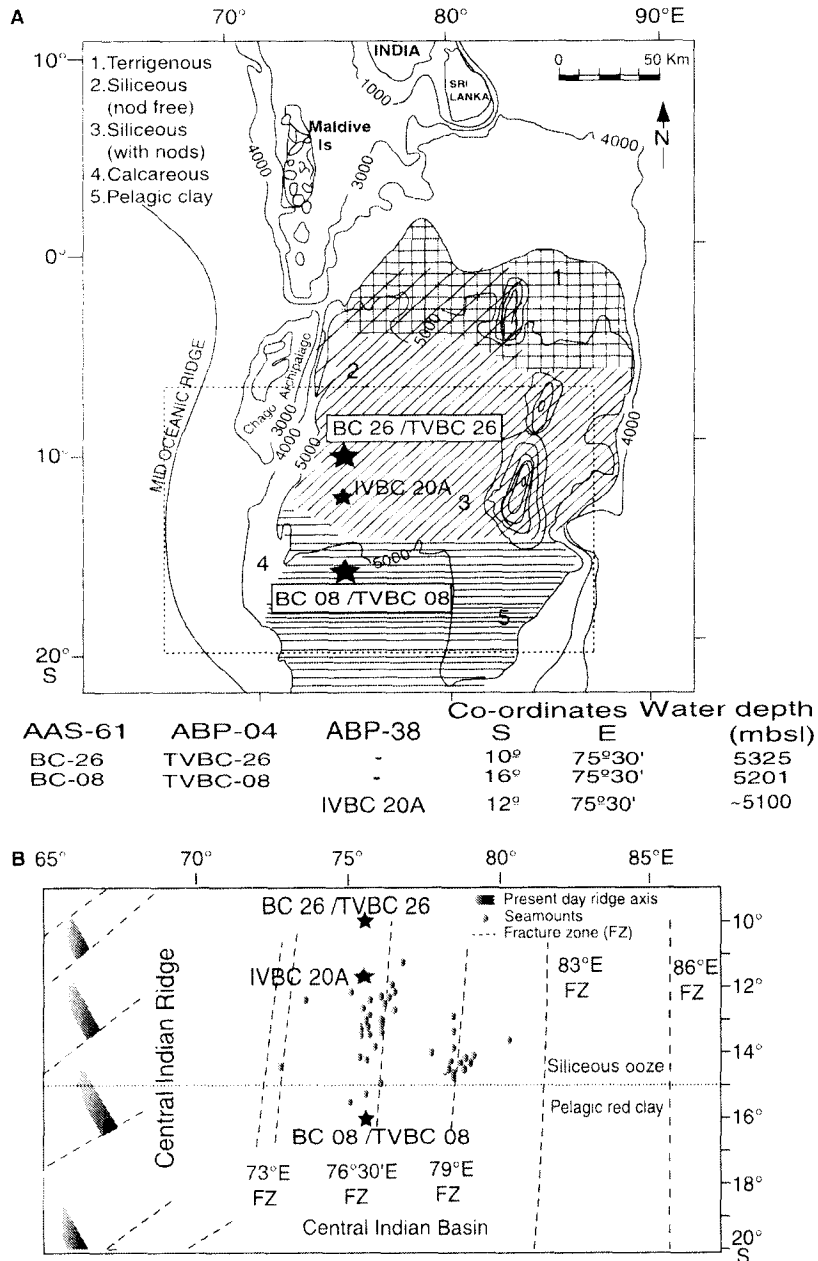


Fig. 1. Area map modified from Mascarenhas-Pereira *et al.* (2006). (A) Station locations with bathymetric and sediment types marked '1' to '5'. (B) Station locations according to topographic features.

with a $\text{SiO}_2/\text{Al}_2\text{O}_3$ ratio of 4.5 and biogenic silica amounting to 5 to 10%. The Mn/Fe ratio is < 1 suggesting hydrogenetic metal precipitation (Rao & Nath, 1988; Nath *et al.*, 1989). The nature of the glass shards (Mascarenhas-Pereira *et al.*, 2006), native aluminium content (Iyer *et al.*, 2007) and signatures of degassing (Nath *et al.*, 2008) suggest hydrothermal alteration of recent origin in some locations. Late Tertiary sediments probably are exposed in this area due to explosive volcanism (Mascarenhas-Pereira *et al.*, 2006).

GEOMICROBIOLOGY OF THE CENTRAL INDIAN BASIN

Northern siliceous ooze

The northern siliceous setting is rich in TOC with a concentration *ca* 0.3%. Early diagenetic processes and extensive nitrification in this region influence the origin, type and quality of manganese nodules (Nath & Mudholkar, 1989) and sediment biogeochemistry as a whole. The

microbial community might co-express both chemolithotrophy and organotrophy; this would enable efficient recycling of the limited photosynthetically derived organic matter (Stevens, 1997; Ehrlich, 1998). Cultured bacterial representatives showing both phases of nitrification have been isolated from this region (Ram *et al.*, 2001). Microbial processes like manganese oxidation (Ehrlich, 1998 & references therein) and manganese cycling in tan-green mottled zones (Meister *et al.*, 2009) possibly co-occur (Wang *et al.*, 2008) along with the coupling of nitrification–denitrification (Luther *et al.*, 1997). Similarly, sulphide oxidation and iron reduction could co-occur. Here, the mixotrophic combination of chemolithotrophy and organotrophy might be due to simultaneous dependence on the supply of organic matter and possible rock alteration features. The setting might be analogous to that of the hydrocarbon deposits except for the scale and extent (Canfield, 1991; Campbell, 2006; Ma *et al.*, 2006).

Southern pelagic red clay

The southern pelagic red clay setting is TOC-poor with a concentration of <0.1%. It bears the signature of recent hydrothermal alteration due to tectonic reactivation of fracture zones (Mascarenhas-Pereira *et al.*, 2006; Iyer *et al.*, 2007; Nath *et al.*, 2008). Microbiologically, the southern part of the CIB is largely unexplored. It is therefore hypothesized that chemolithotrophy, though widespread, would be more pronounced in the oligotrophic southern CIB than in the detritally dominated northern region. Proximity to tectonic features such as the Trace of Rodrigues Triple Junction (Kamesh Raju & Ramprasad, 1989) may indicate sulphide oxidation with iron reduction (Bach & Edwards, 2003). Thirotrophic nitrate reduction may also be an important contributing process especially in diffuse flow regimes (Childress *et al.*, 1991) with temperatures varying between 2 and 25°C (Chevaldonne *et al.*, 1991). The chemoautotrophy might be totally independent of organic matter rain and this system could be analogous to settings like the Loihi Seamount (Edwards *et al.*, 2004).

MATERIALS AND METHODS

Sampling area and method

The samples for the present study were collected and processed during cruises on-board *R/V Akademik Alexandr Siderenko* (AAS), and *R/V Akademik Boris Petrov* (ABP) as a part of the PMN-EIA (Polymetallic Nodules-Environmental Impact Assessment) programme in the CIB. Two end-member settings, represented by stations TVBC 26 and TVBC 08, were examined in detail for microbial and biochemical parameters during ABP-04 (March to May 2005). Station TVBC 26 (10°S, 75.5°E) lies in the siliceous ooze realm of the northern CIB. Station TVBC 08 (16°S, 75.5°E) is a seamount flank in the volcanic realm of pelagic red clays in the southern CIB. Both stations are situated below the calcite compensation depth, which is ca 4500 m below the sea surface (Fig. 1A). Pore water chemistry, porosity, lithology and biostratigraphy were also studied for these two cores during ABP-04. Supporting data on radiometric dating were available from the same locations (BC-26 and BC-08) during an earlier cruise AAS-61 (March to April 2003). Additional pore water data for O₂, Mn, Fe, NH₄⁺ and HS⁻ were acquired from core IVBC 20A, adjacent to core TVBC 26, during Cruise ABP-38 (September to October 2009).

The samples were collected with the help of the United States Naval Electronics Laboratory (USNEL) – using a type box core with dimensions 50 cm × 50 cm × 50 cm. Sub-cores were collected using acrylic cores with a 6.3 cm inner diameter. The sediment cores were sectioned at 2 cm intervals up to 10 cm and at 5 cm intervals thereafter unless mentioned otherwise. The sediments were collected in sterile plastic bags for further processing. Both the cores were analysed up to 25 cm bsf (below sea floor). Hard bottom sediments hindered the collection of deeper cores at TVBC 08. Microbial samples were processed onboard at 4°C and 1 atm pressure immediately after sediment collection.

The samples were collected with the help of the United States Naval Electronics Laboratory (USNEL) – using a type box core with dimensions 50 cm × 50 cm × 50 cm. Sub-cores were collected using acrylic cores with a 6.3 cm inner diameter. The sediment cores were sectioned at 2 cm intervals up to 10 cm and at 5 cm intervals thereafter unless mentioned otherwise. The sediments were collected in sterile plastic bags for further processing. Both the cores were analysed up to 25 cm bsf (below sea floor). Hard bottom sediments hindered the collection of deeper cores at TVBC 08. Microbial samples were processed onboard at 4°C and 1 atm pressure immediately after sediment collection.

Lithology, stratigraphy and age

Rock colour was analysed on-board in accordance with the *Rock color chart* of the Geological Society of America, Boulder, Colorado (Courtesy: Cruise report of ABP-04, NIO, Goa, India). The percentage of sand, silt and clay components was determined from desalted samples according to Folk (1968). A lithologue was constructed according to Zervas *et al.* (2009) using the SEDLOG version 2.1.4 software program to show sand, silt and clay content. Neogene radiolarian (NR) biostratigraphy was studied according to Gupta (1991a) and Johnson *et al.* (1989). Radiometric dating using ²³⁰Th_{exc} was analysed according to Krishnaswami & Sarin

(1976). Details of this analysis are presented in Mascarenhas-Pereira *et al.* (2006) and Nath *et al.* (2008).

Pore water geochemistry and geotechnical properties

Shipboard analysis of modern pore water pH, NO_2^- , NO_3^- , PO_4^{3-} and SiO_3^{2-} was performed using the standard methods described in Grasshoff *et al.* (1983). Pore water O_2 , NH_4^+ and HS^- were determined according to Pai *et al.* (1993), Grasshoff *et al.* (1983) and Pachmayr (1960), respectively. The determination of Fe and Mn in pore water was performed by sampled direct current (Aldrich & van der Berg, 1998) and differential pulse polarographic (Colombini & Fuocco, 1983) methods using a Metrohm voltammeter (Metrohm Limited, Herisau, Switzerland). Porosity, wet bulk density, water content and specific gravity were measured using the standard method described in ASTM (1995).

Total organic carbon and C/N ratio

Total carbon and nitrogen were measured using an NCS 2500 Elemental Analyser (Thermo Quest Italia Spa, Milan, Italy; Patience *et al.*, 1990) using an L-Cistina (Thermo Quest Italia SpA) as a standard. Total carbon was counter-checked with a UIC CM 5014 coulometer and found to be similar in range. Total inorganic carbon was analysed by a UIC CM 5014 coulometer (UIC inc., Joliet, IL, USA) using CaCO_3 (Merck KGAA, Darmstadt, Germany) as a standard. The accuracy of measurements was verified by the analysis of a standard reference material (USGS-MAG-1). The TOC was determined by subtracting total inorganic carbon from total carbon. The C/N was calculated as the ratio between TOC and total nitrogen.

Labile organic matter

Total protein concentrations within sediments were estimated by the Folin Ciocalteu method of Lowry using bovine serum albumin as a standard (Lowry *et al.*, 1951). Total carbohydrate concentrations within sediments were estimated using the phenol-sulphuric acid method of Kochert (1978) with glucose as a standard. Total lipids of sediments were estimated using stearic acid as a standard (Bligh & Dyer, 1959). The sum of total proteins, carbohydrates and lipids was expressed as labile organic matter (LOM). The nature and

origin of the organic matter was estimated by the protein/carbohydrate ratio (Cauwet, 1978; Fichez, 1991).

Adenosine triphosphate

Adenosine triphosphate (ATP) was estimated to determine the total biomass of living organisms in deep-sea sediments by luciferin-luciferase reaction (Holm-Hansen & Booth, 1966), using ATP disodium salt as a standard (Sigma Chemicals, St Louis, MO, USA). Photons produced were counted on a Perkin Elmer, Wallac 1409 DSA, Liquid Scintillation Counter (Perkin Elmer Wallac, Waltham, MA, USA) as counts per minute and converted to ATP equivalents (Delistraty & Hershner, 1983).

Bacterial counts

Total counts of bacteria

Total bacterial cells were counted according to Hobbie *et al.* (1977). About 1 g of sediment was diluted with 9 ml of sterile sea water; 3 ml of this slurry was fixed with buffered formalin at an end concentration of 2% and stored at 4°C until analysis. At the on-shore laboratory, the aliquot was sonicated at 15 Hz for 15 sec. The supernatant (1 ml) was stained with 75 µl of 0.01% acridine orange (3 min, in dark) and filtered onto 0.22 µm black polycarbonate filter paper (Millipore, Middlesex County, MA, USA). This procedure minimized masking by sedimentary particles. About 10 to 15 microscopic fields were counted to include a total of 300 to 600 cell counts per sample using a Nikon 80i epifluorescence microscope (Nikon, Tokyo, Japan). The counts were normalized per gram of dry sediment.

Frequency of dividing cells

The frequency of dividing cells (FDC) was enumerated among the total counts (Naganuma *et al.*, 1989) and represented as the natural viable population. In the filtered and stained samples of total bacterial counts, dividing bacteria cells were counted as elaborated above. Bacteria showing an invagination, but not a clear intervening zone between cells were considered as one dividing cell (Hagstrom *et al.*, 1979).

Direct viable counts

Direct viable counts (cell numbers) (DVC) were determined according to Kogure *et al.* (1984). Aerobic viable counts (DVC-a) and anaerobic viable counts (DVC-an) were enumerated sepa-

ately. Three millilitres of sediment slurry was prepared as above by diluting 1 g of sediment with 9 ml of sterile sea water into two sets. The first set was amended with 0.001% final concentration of yeast extract and 0.0016% final concentration of an antibiotic cocktail solution containing piromedic, pipemedic and nalidixic acid in the ratio 1:1:1 and incubated statically in the dark at 4°C for 30 h. In the second set, used to determine viability under anaerobic conditions, in addition to yeast extract and antibiotic cocktail, 12 µl of Na₂S 9H₂O was added as a reductant at a final concentration of 0.125% before incubation (Loka Bharathi *et al.*, 1999). At the end of the incubation, the aliquots were fixed with 2% buffered formalin and stored at 4°C until analysis.

The cocktail composition was suitably modified from Joux & Lebaron (1997) by using three of five antibiotics. Antibiotics were dissolved in 0.05 M NaOH [nalidixic, piromidic and pipemidic acids (Sigma)]. All antibiotic solutions were filter sterilized through 0.2 µm pore-size membrane filters (Millipore, USA) before use.

The addition of yeast extract in low concentrations permits cell growth and replication of nucleic acid but the antibiotic cocktail prevents cell division for the period of incubation. The elongated and enlarged dividing cells were counted as DVC-a or DVC-an using a similar procedure to that employed for total counts (Kogure *et al.*, 1984).

Heterotrophic counts

Colony forming units (cfu) on varying concentrations of ZoBell Marine Agar (ZMA) were assessed using three different concentrations of ZoBell Marine broth 2216 (Himedia, Mumbai, India) in 1.5% agar (Difco Lawrence, KS, USA) namely, 100%, 50% and 12.5%. The 100% concentrated broth was prepared according to the manufacturers' instructions, whereas 50% and 12.5% were diluted to half and one-eighth strengths, respectively, with a final pH of 7.6 ± 0.2 (ZoBell, 1941). The plates were incubated at 2 to 5°C. Heterotrophic colonies appeared within four to 10 days.

Potential autotrophs

Nitrifying bacteria were enumerated on modified Winogradsky's media for ammonia oxidizers and nitrite oxidizers by substituting the medium with (NH₄)₂SO₄ at 2 mM (final concentration) or NaNO₂ at 0.5 mM (final concentration) as an energy source (Ram *et al.*, 2001). The medium for aerobic sulphur oxidizing bacteria was similar

to that of denitrifiers, as described below, except for the addition of KNO₃. Inoculation for all oxidizers was carried out by standard plating techniques.

Nitrate reducers were enumerated on modified Leiske's medium (Loka Bharathi, 1989; Loka Bharathi & Chandramohan, 1990; Loka Bharathi *et al.*, 2004). The bacteria cultured on this medium reduce nitrate at the expense of thiosulphate. For simplicity, this group is identified as denitrifiers in the rest of the manuscript as these are known to be functionally similar to *Thiobacillus denitrificans*. Medium composition per litre of aged sea water: Na₂S₂O₃ 5H₂O – 5 g, K₂HPO₄ – 0.2 g, MgCl₂ 6H₂O – 0.1 g, CaCl₂ 6H₂O – 0.01 g, FeCl₃ 6H₂O – 0.01 g, phenol red indicator – 0.01 g, pure agar (Difco) – 10 g, NaHCO₃ – 1 g, pH 8 to 8.3. KNO₃ at 1 g l⁻¹ was added as a terminal electron acceptor. Sodium bicarbonate solution was filter sterilized and added to the medium just before inoculation. A second group of nitrate-reducing bacteria (NRB) that reduce nitrate at the expense of organic matter were enumerated. For simplicity, this group is identified as NRB. The medium composition per litre of aged sea water is: 0.101 g KNO₃ and nutrient agar at a pH of 7.5 to 8. The original 14 g l⁻¹ of nutrient agar was modified to 25% strength of nutrient broth amended with pure agar to give a final agar concentration of 0.8%. Reducers were inoculated in agar-shake tubes as described in Loka Bharathi (1989).

Fe-oxidizers were cultivated on iron oxidizers medium (Himedia, Mumbai, India). Two parts (A and B) of the medium were prepared separately. Part A consisting of (NH₄)₂SO₄ – 3.0 g, KCl – 0.10 g, K₂HPO₄ – 0.5 g, MgSO₄ – 0.5 g, Ca(NO₃)₂ – 0.01 g was dissolved in 700 ml of sea water containing 1 ml of 10 N H₂SO₄. Part B containing 44.22 g of FeSO₄ was dissolved in 300 ml of distilled water and mixed to Part A. The final salinity was adjusted to 35 ppt and the final pH was adjusted to 6.8 ± 0.2 in order to maintain a mild acidic to near neutral condition (Rodina, 1972).

Mn-oxidizers were cultivated on modified Beijerinck's medium (Rodina, 1972; Havert, 1992). Two parts (A and B) of the medium were prepared separately. Part A consisting of NaHCO₃ – 0.1 g, (NH₄)₂SO₄ – 0.1 g, K₂HPO₄ – 0.5 g, MgSO₄ – 0.5 g was dissolved in 900 ml of sea water. Part B containing 12.5 g of MnCl₂ was dissolved in 100 ml of distilled water and mixed to Part A. The final salinity was adjusted to 35 ppt and the final pH was adjusted to 7.8 ± 0.2 in order to maintain a near neutral condition.

Microbial uptake of carbon in sediments

Microbial uptake of carbon in sediments was measured using $\text{NaH}^{14}\text{CO}_3$ uptake [$5 \mu\text{Ci ml}^{-1}$ activity, Board of Radiation and Isotope Technology (BRIT), Navi Mumbai, India] adopting methods described earlier (Tuttle & Jannasch, 1977; Nelson *et al.*, 1989). Briefly, *ca* 1 g of sediment was suspended in 9 ml sterile sea water and this sediment slurry was incubated with $0.08 \mu\text{Ci ml}^{-1}$ final concentration of $\text{NaH}^{14}\text{CO}_3$ at 4°C with 24 h incubation in the dark. Unincorporated labelled carbon was carefully washed with sterile sea water. The filtered slurry was acidified to remove unbound ^{14}C and trace inorganic carbon. The filter with the trapped sediment was dried further at 35°C and then suspended in a scintillation vial containing cocktail. The sample was counted after 12 to 24 h in a Liquid Scintillation counter (Model Perkin Elmer, Wallac 1409 DSA). Suitable controls for unlabelled and heat-killed sediments, wash water and labelled carbon were included. The incorporation of carbon was read as disintegrations per minute (integrated for 5 min) and was expressed as $\text{nmol C g}^{-1} \text{day}^{-1}$.

Calculations of organic carbon flux from surface primary productivity

The organic carbon flux to the sea floor was derived (Schenau *et al.*, 2000) from previously reported productivity values based on values of ^{14}C incorporation by primary productivity (Matondkar *et al.*, 2005). The net primary productivity was derived from the difference between light and dark bottle incubations in this study. The calculations below consider only this net primary productivity. Potential carbon flux to the sea floor $J_{\text{C}\rightarrow 0}$ was calculated using the relationship:

$$J_{\text{C}\rightarrow 0} = 2\text{PP}^{0.5} \times (\text{PP}/100) \times (1/z + 0.025) \quad (1)$$

where PP is the integrated column productivity rate in $\text{g C m}^{-2} \text{year}^{-1}$ and z is the water depth expressed in hundreds of metres (i.e. 5000 m depth is expressed as 50×100 , where $z = 50$; Schenau *et al.*, 2000).

The accumulation rate of sediment at the sea floor was calculated as a product of sedimentation rate and dry bulk density as:

$$\text{Sediment accumulation rate, } S_{\text{acc}} = S\rho(1 - \phi) \quad (2)$$

where S is the linear sedimentation rate (0.834

and $0.041 \text{ cm kyr}^{-1}$ in TVBC 26 and TVBC 08, respectively), ρ is the wet bulk density in g cm^{-3} and ϕ is the porosity.

The accumulation rate of carbon at the sea floor was calculated as a product of sediment accumulation rate and C_{org} (%) as:

$$C_{\text{org}} \times S_{\text{acc}} \quad (3)$$

The preservation factor was calculated as the ratio of the rate of carbon accumulation to primary production rate (Wenbo *et al.*, 2008). Palaeoproductivity (PaP) was calculated from TOC:

$$\text{PaP} = 5.31[C(\rho - 1.026\phi/100)]^{0.71} S^{0.07} Z^{0.45} \quad (4)$$

Palaeoproductivity is a function of carbon flux near the sea floor and is related to both productivity and water depth (Stein, 1991), and expressed as $\text{g C m}^{-2} \text{kyr}^{-1}$. Palaeoproductivity profiles are compared with those of autotrophic microbial carbon fixation profiles to understand time-dependent variations in the extent of chemoautotrophy.

Data analysis and statistical significance

In the case of epifluorescence counts, 10 to 15 microscopic fields cumulating in not less than 500 cells were considered for deriving standard deviations. Plate counts, ATP, $\text{NaH}^{14}\text{CO}_3$ uptake and LOM were analysed in triplicate. All parameters were normalized per gram of sediment dry weight unless mentioned otherwise. Parameters were plotted as averaged profiles with error bars representing the range of individual samples. Two-factor analysis of variance without replication was used for confirming significance in variations. Correlation between the TOC contents, microbial, biochemical parameters and pore water data were analysed for Spearman's rank correlation using STATISTICA version 6 (StatSoft Inc., Tulsa, OK, USA).

Quantification of the influence of non-steady-state diagenetic condition on microbial community by numerical simulation

A non-steady-state diagenetic model was considered to explain the formation of the tan-green mottled zone showing chemoautotrophy in core TVBC 26. A transient diffusion model (Meister *et al.*, 2007), including a sink term, was used to

simulate NO_3^- pore water profiles as shown in Eq. 5:

$$\partial c/\partial t = k(\partial^2 c/\partial x^2) + s(x) \quad (5)$$

where $c(x,t)$ is the concentration of NO_3^- (μM), t is time (years) and x is the depth below sea floor (cm bsf):

$$\kappa = \phi\tau^{-2}D_s \quad \text{and} \quad \tau^2 = \phi F \quad (6)$$

where D_s is the diffusion coefficient for NO_3^- ($\text{m}^2 \text{sec}^{-1}$), ϕ is the porosity (dimensionless) and F is the formation factor (dimensionless). Nitrite oxidation rate $s(x)$ and the nitrate reduction rate $s'(x)$ is:

$$\begin{aligned} s(x) &= 0 \mu\text{mol m}^{-3} \text{ year}^{-1}, \text{ if } t < 10000 \text{ year} \\ s(x) &= 1000 \mu\text{mol m}^{-3} \text{ year}^{-1}, \\ &\text{if } 10000 \text{ year} < t < 11200 \text{ year and} \\ &3 < x < 7 \text{ cm bsf} \\ s'(x) &= -1000 \mu\text{mol m}^{-3} \text{ year}^{-1}, \\ &\text{if } 10000 \text{ year} < t < 11200 \text{ year and} \\ &5 < x < 9 \text{ cm bsf} \end{aligned}$$

Thus, $s(x)$ represents nitrification and is substituted by $s'(x)$ in case of denitrification. The following initial conditions and boundary conditions were used:

$$\begin{aligned} c &= 26.13 \mu\text{M} \quad \text{for } x > 0 \\ c &= 8.87 \mu\text{M} \quad \text{for } x = 0 \\ c(0, t) &= 8.87 \mu\text{M} \\ c(L, t) &= 26.13 \mu\text{M} \end{aligned}$$

where L is the length of the model domain.

The explicit finite difference method was used to solve Eq. 5. A time step of 10 years and a grid size of 1 cm were chosen. The tortuosity factor was calculated from porosity and formation factor (Schulz, 2000). A diffusion coefficient for NO_3^- of $9.03\text{E-}10 \text{ m}^2 \text{sec}^{-1}$, at 0°C was considered (Schulz, 2000). Both $s(x)$ and $s'(x) = 0$ for the first 10 000 years of the computation, which is the time required for an organic matter pulse to reach the present tan-green mottled zone at 13 to 25 cm bsf without being diagenetically altered. After setting these conditions, nitrite oxidation and nitrate reduction are switched on separately in the depth interval $3 < x < 7$ cm and $5 < x < 9$ cm bsf, respectively, to simulate the effect of strong nitrite oxidation followed by nitrate reduction in an organic carbon-rich sediment layer. A nitrite

oxidation rate of $1000 \mu\text{M m}^{-3} \text{ year}^{-1}$ was assumed in a horizon from 3 to 7 cm bsf (Ward *et al.*, 1989). In the horizon from 5 to 9 cm bsf a maximum nitrate reduction rate of $-1000 \mu\text{M m}^{-3} \text{ year}^{-1}$ was assumed.

Quantification of hydrothermal alterations on pore water and microbial community by numerical simulation

A modified transient diffusion model (Meister *et al.*, 2007) including a source term was considered to explain the influence of hydrothermal activity on the pore water profile. This model, in turn, was used to explain the enhanced chemoautotrophic microbial activity at the Pleistocene–Tertiary stratigraphic transition zone of core TVBC 08. Pore water NO_3^- profiles were simulated as shown in Eq. 7:

$$\partial c/\partial t = \kappa'(\partial^2 c/\partial x^2) + sr(x) \quad (7)$$

where $c(x,t)$ is the concentration of NO_3^- (μM), t is time (years), and x is the depth below sea floor (cm bsf):

$$\kappa' = \phi\tau'^{-2}D_s \quad \text{and} \quad \tau'^2 = \phi F' \quad (8)$$

where D_s is the diffusion coefficient for NO_3^- ($\text{m}^2 \text{sec}^{-1}$), ϕ is the porosity (dimensionless) and F is the formation factor (dimensionless). Nitrite oxidation rate $sr(x)$ and the nitrate reduction rate $sr'(x)$ is:

$$\begin{aligned} sr(x) &= 0 \mu\text{mol m}^{-3} \text{ year}^{-1}, \text{ if } t < 1000 \text{ year} \\ sr(x) &= 1000 \mu\text{mol m}^{-3} \text{ year}^{-1}, \\ &\text{if } 1000 \text{ year} < t < 1170 \text{ year and} \\ &3 < x < 7 \text{ cm bsf} \\ sr'(x) &= -1000 \mu\text{mol m}^{-3} \text{ year}^{-1}, \\ &\text{if } 1000 \text{ year} < t < 1170 \text{ year and} \\ &5 < x < 9 \text{ cm bsf} \end{aligned}$$

Thus, $sr(x)$ represents nitrification and is substituted by $sr'(x)$ in the case of denitrification. The following initial conditions and boundary conditions were used:

$$\begin{aligned} c &= 9.71 \mu\text{M} \quad \text{for } x > 0 \\ c &= 4.85 \mu\text{M} \quad \text{for } x = 0 \\ c(0, t) &= 4.85 \mu\text{M} \\ c(L, t) &= 9.71 \mu\text{M} \end{aligned}$$

where L is the length of the model domain.

The explicit finite difference method was used to solve Eq. 7. A time step of one year and a grid size of 1 cm were chosen. The tortuosity factor was calculated from porosity and formation factor (Schulz, 2000). A diffusion coefficient for NO_3^- of $9.03\text{E-}10 \text{ m}^2 \text{ sec}^{-1}$, at 0°C was considered (Schulz, 2000). Both $sr(x)$ and $sr'(x) = 0$ for the first 1000 years of the computation, when upwelling of hydrothermally derived NO_3^- occurs as a focused jet to the present Pleistocene–Tertiary stratigraphic transition zone at 3 to 12 cm bsf without being dispersed laterally. After setting these conditions, nitrite oxidation and nitrate reduction are switched on separately in the depth interval $3 < x < 7 \text{ cm}$ and $5 < x < 9 \text{ cm}$ bsf, respectively. The effect of strong nitrite oxidation followed by nitrate reduction in the stratigraphic transition zone is simulated due to lateral dispersion and phase separation of solutes carried upward by the hydrothermal fluid and resultant microbial activity. A nitrite oxidation rate of $1000 \mu\text{M m}^{-3} \text{ year}^{-1}$ was assumed in a horizon from 3 to 7 cm bsf (Ward *et al.*, 1989). In the horizon from 5 to 9 cm bsf a maximum nitrate reduction rate of $-1000 \mu\text{M m}^{-3} \text{ year}^{-1}$ was assumed. The model source code in MATLAB 7.0.4 (The Mathworks, Natick, MA, USA) used for this work is available as a '.doc-file' and provided as an electronic supplement to this study.

RESULTS

Northern core TVBC 26

Lithology, stratigraphy and age

The siliceous core TVBC 26 shows tan-green mottled transitions, a distinct feature in northern CIB sediments. Here the moderate yellowish brown (10YR 4/2) sediments from 13 to 25 cm bsf showed intense mottling with light olive grey (5Y 5/2) and dark yellowish brown (10YR 4/2) continuous intercalations. The surface of both cores BC 26 and reoccupied station TVBC 26 were covered with Mn nodules, indicating that the surface was preserved during sample retrieval (Borole, 1993). The sediment of core TVBC 26 is composed of 0.37% to 4.17% sand, 25.37% to 49.45% silt and 49.2% to 74.10% clay. Sand content $\leq 4\%$ and is not resolvable in the lithology (Fig. 2).

Neogene radiolarian biostratigraphy of the core TVBC 26 suggested that the first appearance of index species *Collospheara invaginata* is 24 cm bsf, representing an approximate date of *ca*

180 ka (Johnson *et al.*, 1989). *Collospheara tuberosa* and *Collospheara orthoconus* are present from 16 to 3 cm core depth. Most importantly, *Stylatractus universus* is conspicuously absent suggesting that the base of the core was younger than *ca* 300 ka (Fig. 2). The biostratigraphic sedimentation rate of *ca* 1.1 mm kyr^{-1} was consistent with previous findings (Banakar *et al.*, 1991 and Borole, 1993). However, radiometric dating from the same location (BC 26, AAS-61) using $^{230}\text{Th}_{\text{exc}}$ showed a much higher sedimentation rate of 8.34 mm kyr^{-1} (Fig. 2).

Pore water geochemistry and geotechnical properties

The pore water of TVBC 26 was nearly neutral, with pH averaging 7.30 ± 0.07 (Fig. 3A). NO_2^- concentrations up to $0.14 \mu\text{M}$ were detected only in the top 0 to 2 cm. The NO_3^- concentration averaged at $21.83 \pm 5.97 \mu\text{M}$, PO_4^{3-} at $1.79 \pm 0.20 \mu\text{M}$ and SiO_3^{2-} at $478 \pm 74 \mu\text{M}$ (Fig. 3A). Porosity at the tan-green mottled zone shows a decrease indicating relative compaction. Pore water O_2 , Mn, Fe, NH_4^+ and HS^- concentrations were obtained from a neighbouring siliceous core IVBC 20A (Fig. 3B). Like TVBC 26, this core also showed mottled structures at 12 to 19 cm bsf. The oxygen concentrations varied from 180 to $370 \mu\text{M l}^{-1}$ with peaks at 10 and 20 cm bsf indicating consumption of oxygen at the reactive layers above 10 cm and mottles above 20 cm. Ammonium concentrations varied from non-detectable to $0.14 \mu\text{M l}^{-1}$ of pore water with peaks generally corresponding to oxygen depletion. Sulphide concentrations varied from 0.03 to $0.18 \mu\text{M l}^{-1}$ with peak concentration at 7 cm bsf. Mn concentrations varied from 0.14 to 9.95 mg l^{-1} with peaks above 7 and 19 cm bsf. Fe concentrations varied from 0.39 to 9.94 mg l^{-1} with the highest peak at 17 cm bsf (Fig. 3B).

Total organic carbon, total inorganic carbon and C/N ratio

The northern siliceous sediment TVBC 26 was twice as rich in TOC when compared with the pelagic red clays from the southern TVBC 08 (Fig. 2). The averaged down-core TOC profile of siliceous TVBC 26 was 0.15% to 0.45%. The TIC varied from non detectable to $< 0.1 \text{ ppm}$. Total inorganic carbon was detected only at 2 to 4 cm and 20 to 25 cm bsf. A TOC peak at 2 to 4 cm bsf was followed by a TIC peak at 4 to 6 cm bsf in the reactive Layer 1. Total inorganic carbon showed a tendency to increase at the sub-oxic mottled-zone. TVBC 26 showed a C/N ratio ranging from

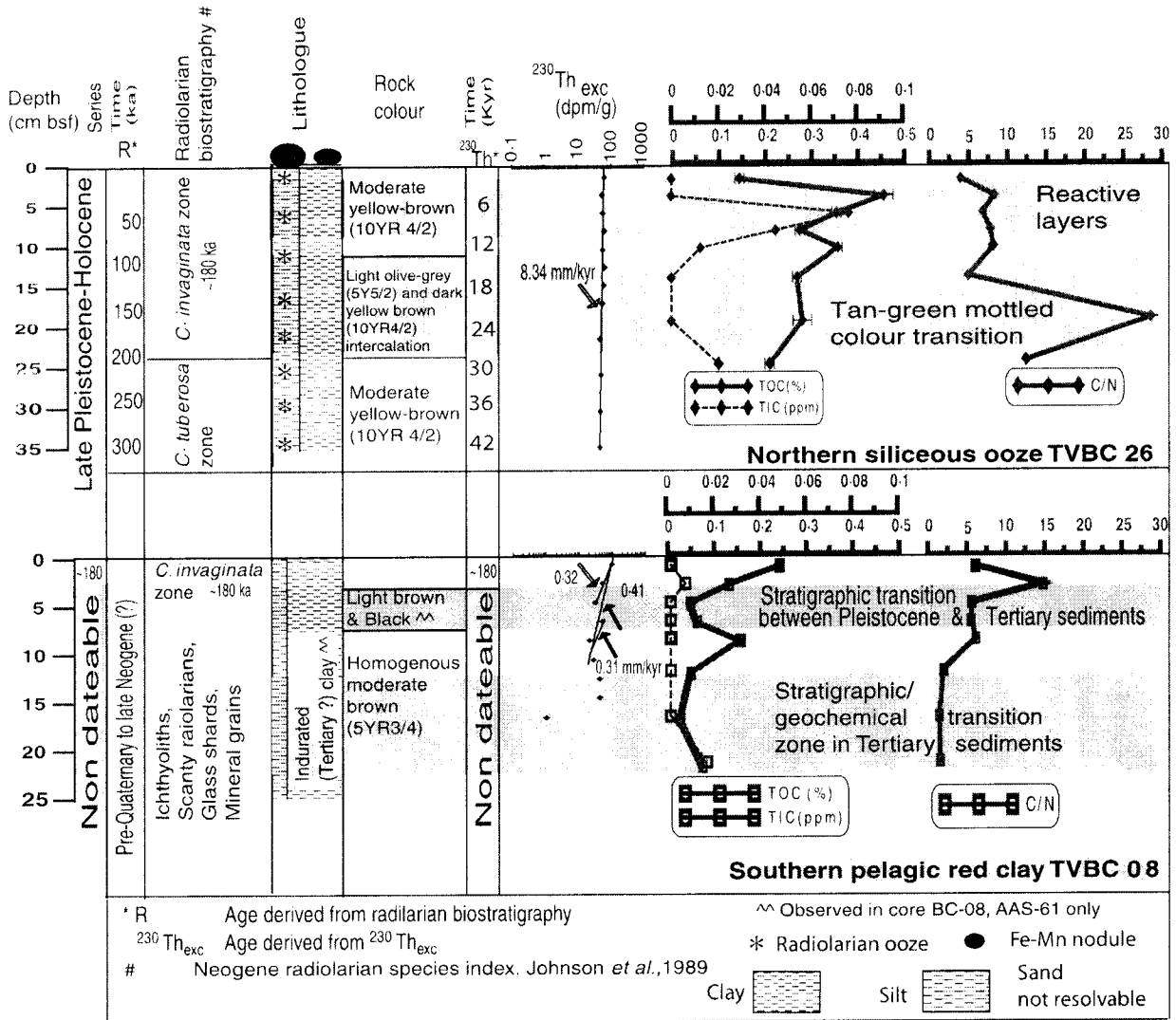


Fig. 2. Age, biostratigraphy, lithology, elemental carbon and nitrogen profiles of TVBC 26 and TVBC 08 (data points on the y-axis suggest values below detection limit).

4 to 8.3. At the sub-oxic mottle (15 to 25 cm bsf) ratio was 28.6 (Fig. 2).

Labile organic matter

Though quantities of carbohydrates and lipids were almost similar, proteins were four times higher in TVBC 26 than its southern counterpart. Protein/carbohydrate ratios were > 1 at TVBC 26 indicating fresher LOM content. Significant variations in down-core profiles of all parameters were noted at the reactive layer of TVBC 26 (Fig. 4). In the tan-green mottled zone of TVBC 26, the carbohydrates show relatively better preservation and coincided with a higher C/N ratio (Fig. 2), increasing ATP (Fig. 5), higher aerobic sulphur oxidizers (Fig. 6A) and higher carbon

uptake (Fig. 7), indicating a chemo-autotrophic pocket in a predominantly heterotrophic setting.

Adenosine triphosphate

In TVBC 26 the values ranged from 50 to 105 ng g^{-1} dry wt with the highest value at 20 to 25 cm bsf (Fig. 5).

Bacterial counts

Total bacterial counts and frequency of dividing cells. The total bacterial counts in core TVBC 26 varied from $3.6\text{E} + 08$ to $7.2\text{E} + 08$ cells g^{-1} . The down-core profile was almost homogenous. In core TVBC 26, 14% of the total bacteria were naturally viable. The FDC was two and a half

times higher in the surface layer of 0 to 10 cm at TVBC 26 than in the subsequent sub-surface layer (Fig. 5).

Direct viable counts (DVC-a and DVC-an). DVC-an was three times higher at the TOC-rich TVBC 26 than at TVBC 08 ($P > 0.05$) (Fig. 5). Prominent variations in TC, FDC, DVC-a and DVC-an are seen at or near the reactive Layer 1. DVC-an shows an increase in the sub-oxic mottled zone of TVBC 26.

Heterotrophic counts. Triplicate plate counts on ZMA showed that the retrievability from organic-rich TVBC 26 was strangely lower than TVBC 08 with a few exceptions. A conspicuous depletion of heterotrophs on 12.5% ZMA was noted at the tan-green mottled colour transition zone (Fig. 6A).

Potential autotrophs. The ammonium and nitrite oxidizer population generally was lower in TVBC 26 than the southern counterpart. The aerobic sulphur oxidizers, however, followed a different pattern with the average values at TVBC 26 being nearly four times the value in TVBC 08 (Fig. 6A and B). The deep sea bacterial isolates from the CIB were able to grow almost equally well at 28 and 5°C. Nitrifiers and aerobic sulphur oxidizers appeared within 10 to 35 days. Culturable denitrifiers and nitrate reducers generally took longer to grow than aerobe. The incubation period was often as long as three to 12 months, or more, at $5 \pm 2^\circ\text{C}$.

Denitrifiers showed a peak culturability at 4 to 6 cm bsf (in between reactive Layers 1 and 2) with 10^3 cfu g⁻¹ dry sediment in the northern TOC-rich core. A second peak with 10 cfu g⁻¹ dry sediment was seen at the commencement of the mottled zone. The NRB that are dependent on organic matter showed two peaks at 2 to 4 cm and 6 to 8 cm bsf with 670 and 20 cfu g⁻¹, respectively. An increase in NRB counts was noted at the tan-green mottled zone, perhaps representing the remnant of an older reaction front (Fig. 6A).

Fe-oxidizers varied from $1.11\text{E} + 02$ to $1.12\text{E} + 03$ cfu g⁻¹ in the northern core TVBC 26. Mn-oxidizers varied from $2.22\text{E} + 02$ to $1.06\text{E} + 03$ cfu g⁻¹ in core TVBC 26. The peaks of Mn-oxidizers lie in the reactive layers and tan-green mottled zone (Fig. 6A). The pore water Mn profile of a similar neighbouring core, IVBC 20A (Fig. 3B), corroborates with that of Mn-oxidizers of core TVBC 26.

Microbial uptake of carbon in sediments

Measurement of autotrophic microbial carbon fixation by whole sediment slurries showed

maximum uptake at 4 to 6 cm and 20 to 25 cm bsf in core TVBC 26. The heat-killed controls showed markedly lower values than the actual experimental uptake (Fig. 7).

Organic carbon flux, palaeoproductivity and modern microbial autotrophic uptake

The rate of column productivity recorded over the siliceous oozes was $103 \text{ mg C m}^{-2} \text{ day}^{-1}$ corresponding to 18.91 to $37.74 \text{ g C m}^{-2} \text{ year}^{-1}$ (Matondkar *et al.*, 2005). About 0.4 to 0.6% of carbon from surface production reaches the sea floor as organic carbon flux over the northern siliceous ooze of TVBC 26. The organic C flux was between 0.07 to $0.205 \text{ g C m}^{-2} \text{ year}^{-1}$. The corresponding carbon accumulation rates were $0.028 \text{ g C m}^{-2} \text{ year}^{-1}$. Preservation factors for these sediments were extremely low with 1.04×10^{-6} for siliceous TVBC 26. Palaeoproductivity calculated from organic carbon content in the sediment cores ranged from 0.097 to $0.157 \text{ g C m}^{-2} \text{ kyr}^{-1}$ in the siliceous oozes. This palaeoproductivity profile was compared with autotrophic carbon uptake in the present Quaternary times. The modern microbial autotrophic uptake profile showed a similar trend to the palaeoproductivity profile except at 3 to 5 cm and 20 to 25 cm bsf where the trend was opposite. This trend was observed at the reactive layer (age 6 kyr) and the tan-green mottled transition (age 24 kyr) (Fig. 8). Here, the low surface productivity layer was superimposed on a layer with high chemosynthetic activity.

Inter-relationship between bacterial and geochemical parameters in northern core TVBC 26

The TOC and LOM significantly correlated to each other ($P > 0.05$) highlighting the interdependence of organic flux to sea floor and lability of organic matter enhanced by bacteria. Total organic carbon related to pore water pH, nitrite oxidizers, carbon uptake rates ($P > 0.01$) and to ammonium oxidizers ($P > 0.05$) signifying its stimulatory role on the microbial population while promoting diagenetic reactions. Labile organic matter determined total bacterial counts, FDC, DVC-a and heterotrophs recoverable on 50% ZMA ($P > 0.05$). These relations are suggestive of aerobic heterotrophic degradation of organic matter. Pore water NO_2^- showed a negative relationship with NO_3^- ($P > 0.01$), SiO_3^{2-} ($P > 0.001$), TOC ($P > 0.05$) and ammonium oxidizers ($P > 0.001$) indicating coupling of a heterotrophic degradative process with nitrification during early diagenetic reactions. The ^{14}C uptake ($P > 0.05$) is correlated positively with nitrite

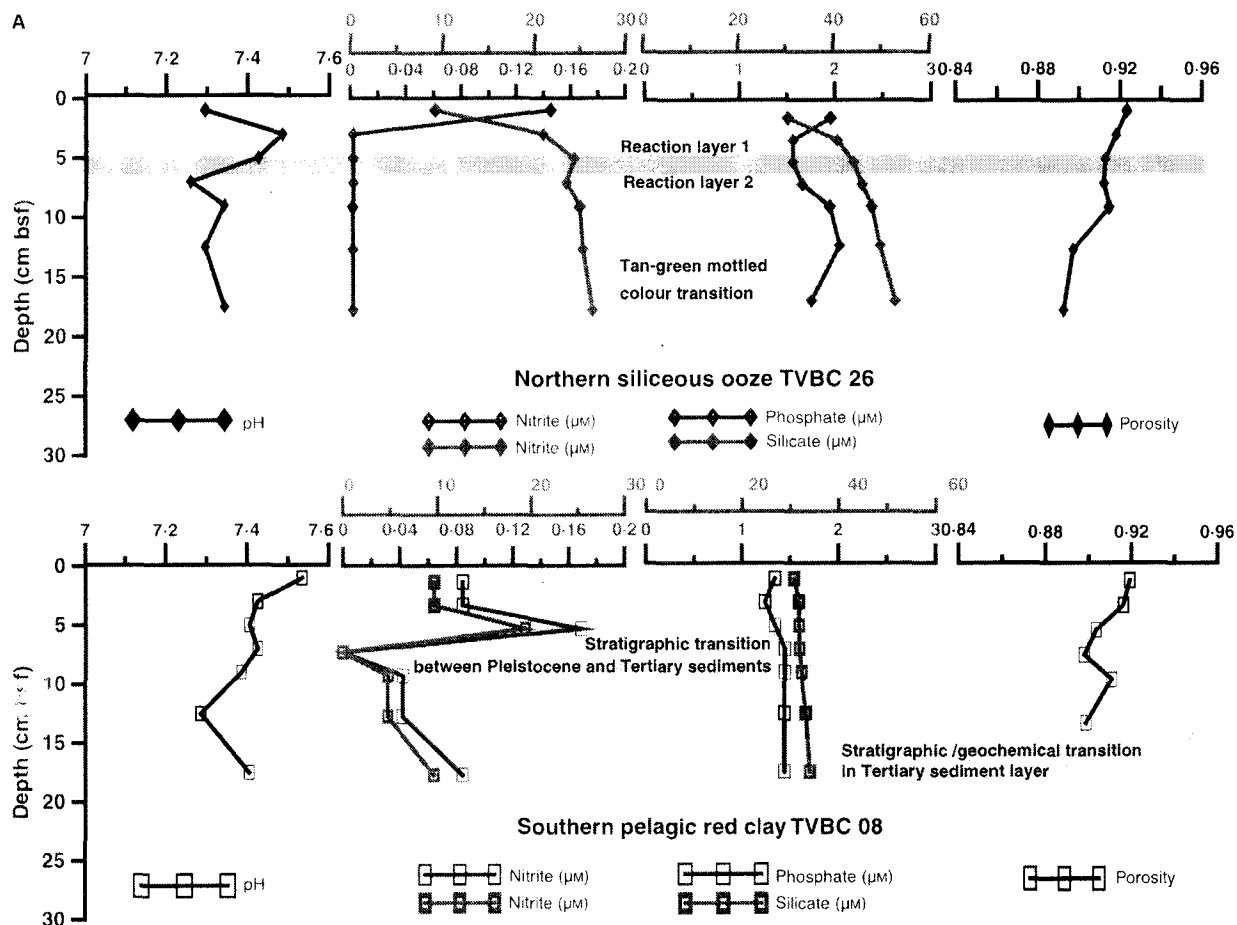


Fig. 3. (A) Pore water profiles of NO_2^- , NO_3^- , PO_4^{3-} , SiO_3^{2-} (data points on y-axis suggest values below detection limit), pH and porosity. (B) Pore water O_2 , Mn, Fe, NH_4^+ and HS^- of core IVBC 20A in the vicinity of TVBC 26 (data points on the y-axis suggest values below detection limit).

oxidizers. The strong correlation at $P > 0.001$ existed between aerobic sulphur oxidizers and DVC-an suggesting their affinity with facultative anaerobic heterotrophy.

Quantification of the influence of non-steady-state diagenetic condition on microbial community by numerical simulation

The NO_3^- concentration profile measured by shipboard analysis was simulated using a transient diffusion numeric model (Fig. 9A). At the sea floor interface, the observed NO_3^- concentration of $8.87 \mu\text{M}$ was used as a starting condition. It is also assumed that NO_3^- in sediment pore water is 0. The model calculated the concentration as a function of time and depth. Considering the residence time of NO_3^- and the sedimentation rate of an organic matter pulse, a 10 000 year time scale is required for NO_3^- to reach 17.5 cm bsf. Assuming a surface layer with a nitrite oxidation

rate of $1000 \mu\text{M m}^{-3} \text{ year}^{-1}$ in the section 3 to 7 cm bsf, the model also shows that the reactant, NO_2^- , will be consumed within a time period of 1000 years in this zone. Conversely, at 5 to 9 cm bsf the reactant NO_3^- would be reduced at a reduction rate of $-1000 \mu\text{M m}^{-3} \text{ year}^{-1}$. The reactant NO_3^- will be consumed within 1000 years. The profile returns to its original shape within another 1000 years soon after the consumption of NO_2^- in the upper 3 to 7 cm layer and the simultaneous reduction of NO_3^- in the lower 5 to 9 cm ceases. In both halves of the reaction couple a steady nitrification profile is finally achieved and they reproduce the pore water NO_3^- profile measured in the core TVBC 26 (Fig. 9A), showing net nitrification. The effect of advection in this single core system is neglected; this is because the variations in TOC (Fig. 2) are more important than the variation in porosity (Fig. 3).

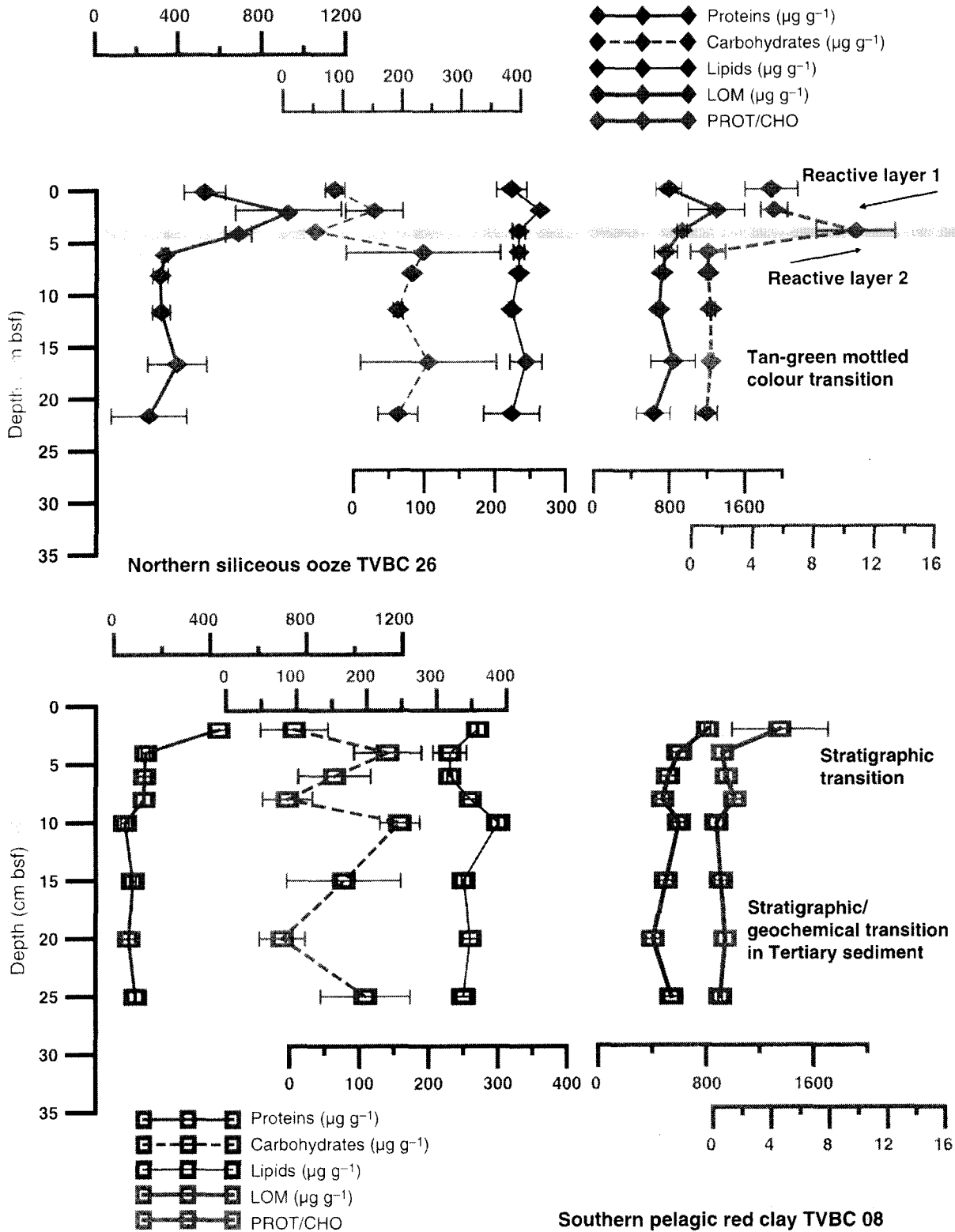


Fig. 4. Biochemical parameters per gram dry sediment (error bars represent sample ranges at individual depths).

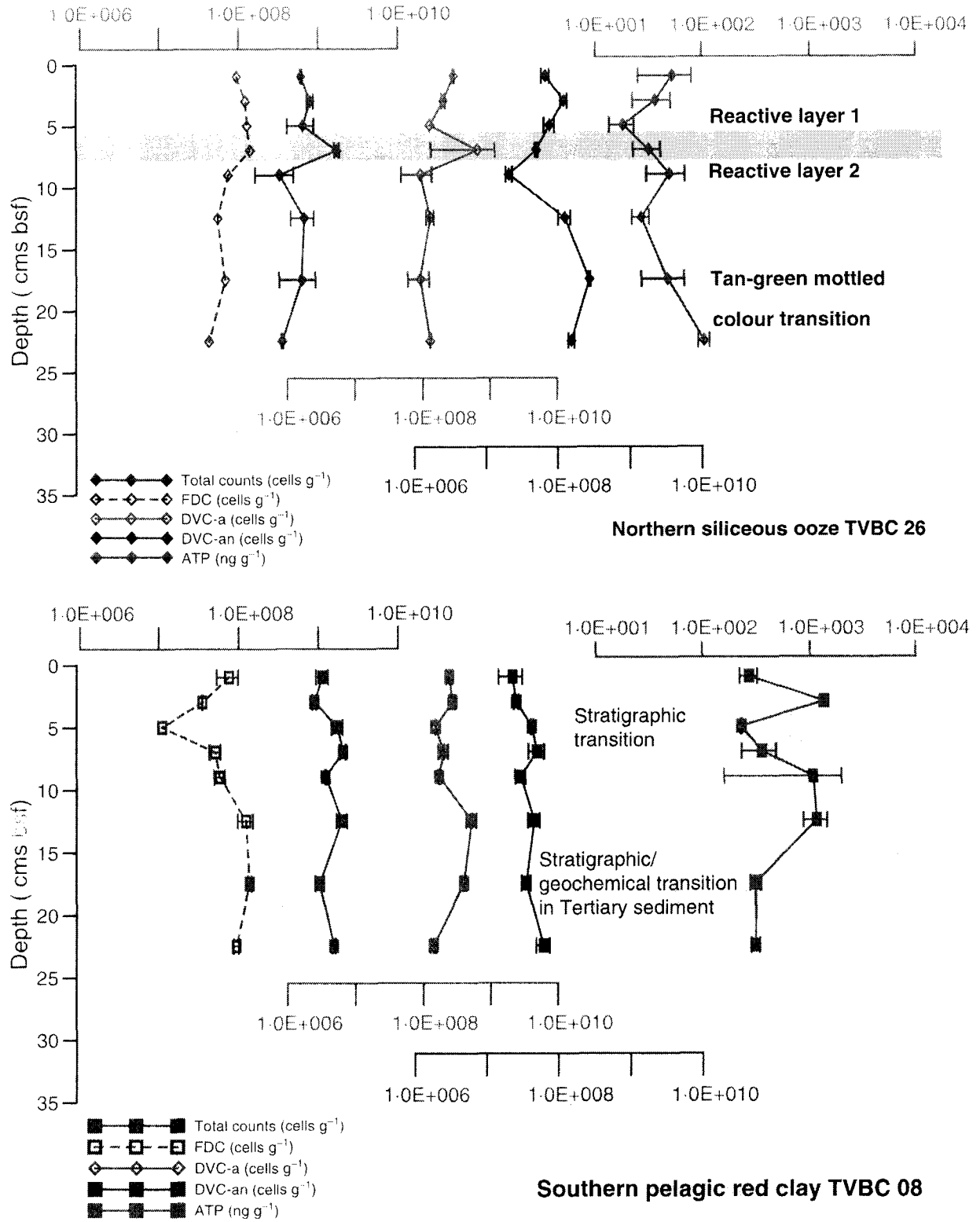
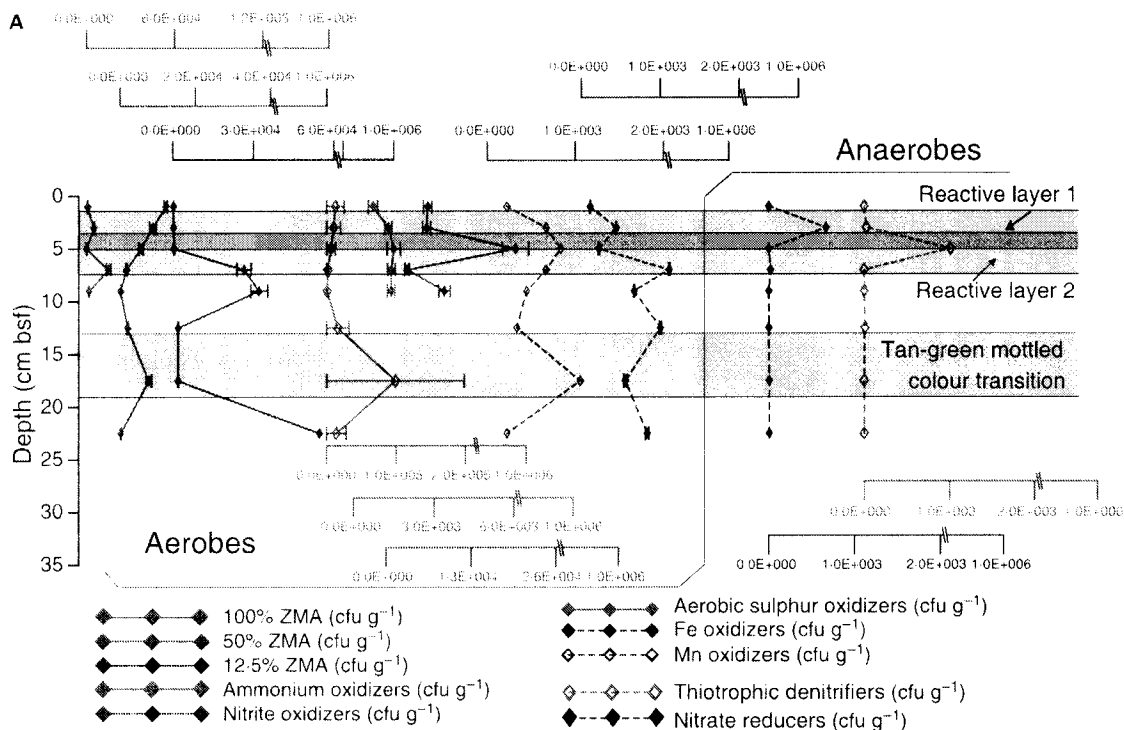
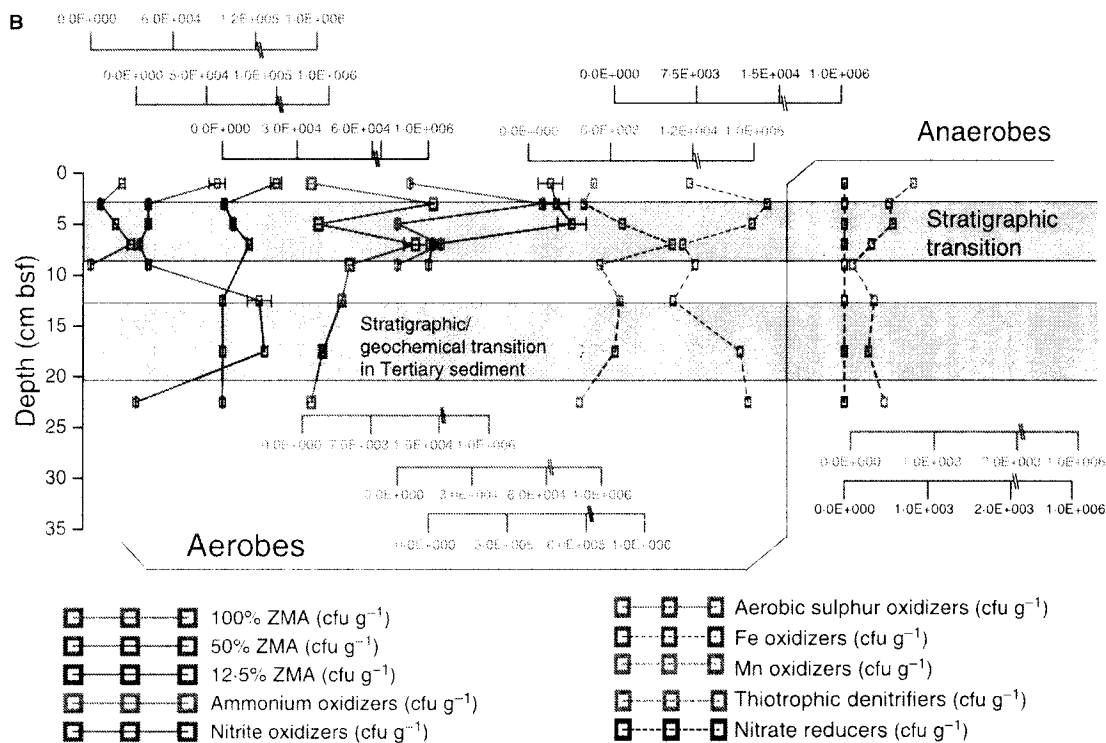


Fig. 5. Bacterial counts and ATP content per gram dry sediment (error bars represent range for samples at individual depths).



Northern siliceous ooze TVBC 26



Southern pelagic red clay TVBC 08

Fig. 6. (A) Culturable bacteria per gram dry sediment in core TVBC 26. (B) Culturable bacteria per gram dry sediment in core TVBC 08 (data points on the y-axis suggest very low culturability; the narrow range of less than $\pm 0.01\%$ variation for individual samples does not appear on this scale).

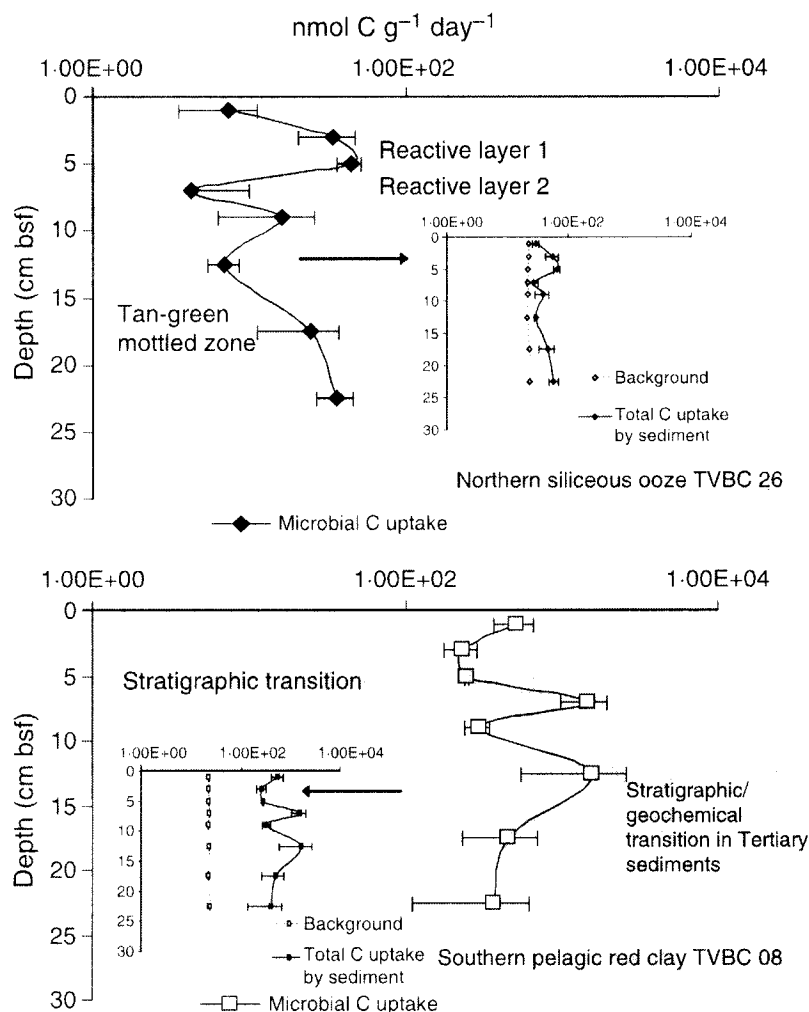


Fig. 7. Microbial carbon uptake by sediments of TVBC 26 and TVBC 08 expressed in $\text{nmol C g}^{-1} \text{ dry sediment day}^{-1}$. Insets show background values representing heat-killed controls and experimental C uptake.

both in the upper stratigraphic transition and in the deeper 15 to 20 cm bsf layer (Fig. 2). C/N ratio averages *ca* 5 except for a high peak of 14 at the upper limit of the stratigraphic transition zone (2 to 4 cm bsf) indicating preferential nitrogen loss. At greater depths (15 to 25 cm bsf) C/N ratios < 1 were observed indicating relative nitrogen enrichment (Fig. 2). The Tertiary–Pleistocene stratigraphic transition in TVBC 08 coincided with that of geochemical and geotechnical boundaries at 2 to 8 cm bsf with abrupt changes in the C/N ratio, pore water NO_2^- and NO_3^- (Fig. 3A).

Labile organic matter

Labile organic matter values at TVBC 08 were only *ca* 50% of TVBC 26. Protein/carbohydrate ratios were < 1 at TVBC 08, except at 0 to 2 cm and 6 to 8 cm bsf indicating greater recalcitrance (Cauwet, 1978). Significant variations in

down-core profiles of all parameters were noted at the stratigraphic transitions of TVBC 08 (Fig. 4). At the deeper layer at 15 to 20 cm bsf, the carbohydrate oxidation coincided with a lower ATP (Fig. 5), higher heterotrophic counts (Fig. 6B) and carbon uptake (Fig. 7), indicating chemo-heterotrophic sections in a predominantly autotrophic core.

Adenosine triphosphate

Adenosine triphosphate values were an order higher in TVBC 08 than in northern TVBC 26 with values ranging from 232 to 1069 ng g^{-1} (Fig. 5).

Bacterial counts

Total bacterial counts and frequency of dividing cells. The total bacterial counts in core TVBC 08 ranged from $8.9\text{E} + 08$ to $2.0\text{E} + 09$ cells g^{-1} .

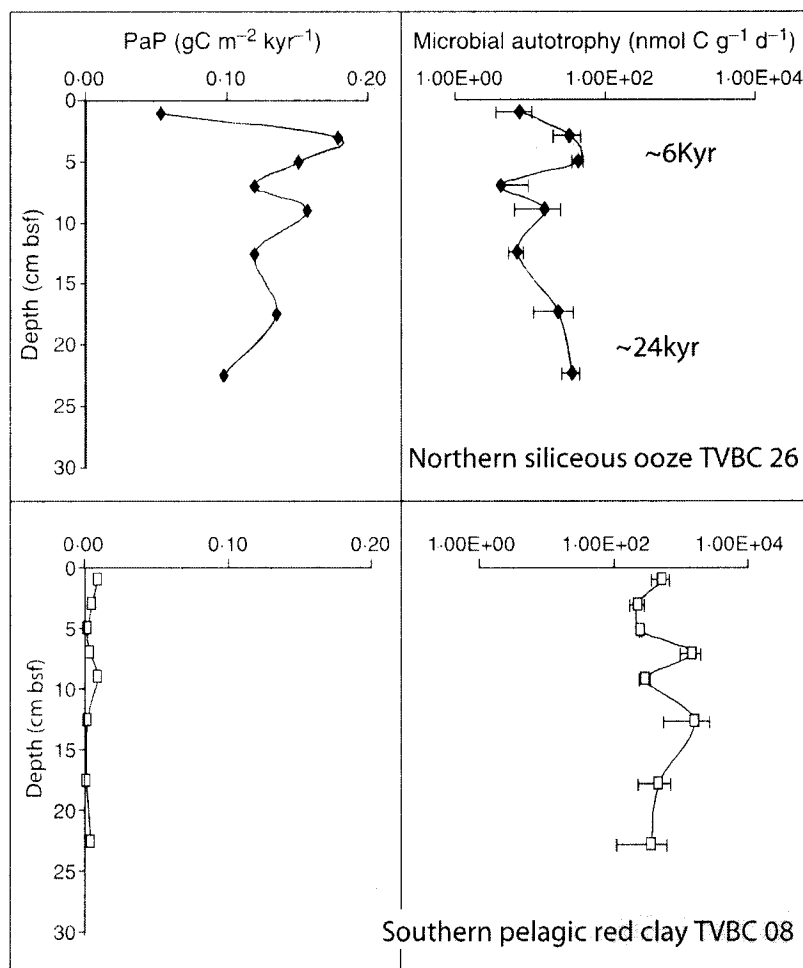


Fig. 8. Comparative profiles of palaeoproductivity and modern autotrophic carbon uptake with respect to geochemical boundaries in the radiometrically determined late Pleistocene to Holocene time scale.

Down-core profiles were almost homogenous (Fig. 5). In core TVBC 08, 5% of the total bacteria were naturally viable. The FDC at station TVBC 08 was two times higher in sub-surface depths of 10 to 25 cm than at the surface (Fig. 5).

Direct viable counts (DVC-a and DVC-an). DVC-a were nearly two times higher at the southern TVBC 08 than at TVBC 26 but the difference was not statistically significant. Prominent variations in TC, FDC, DVC-a and DVC-an were noted at the upper stratigraphic transition and at the deeper 15 to 20 cm bsf layer of TVBC 08 (Fig. 5).

Heterotrophic counts. Triplicate plate counts on ZMA showed that the retrievability from TVBC 08 was generally higher than that from TVBC 26 with a few exceptions. It was more than 15 times higher than TVBC 26 at 100% ZMA, seven times higher at 50% ZMA and almost

1.2 times higher at 12.5% ZMA. A conspicuous peak of $>10^4$ cells g^{-1} of heterotrophs on 50% ZMA was observed at the stratigraphic transition within the Tertiary sediments (Fig. 6A and B).

Potential autotrophs. Total nitrifiers estimated on mineral agar amended with ammonium salt were 250 times higher in TVBC 08. The difference was less in nitrite-amended medium. The retrievability of nitrite oxidizers in TVBC 08 was twice that of TVBC 26 (Fig. 6A and B). Denitrifiers were present uniformly in the southern core TVBC 08 ranging from 250 to 750 $cfu g^{-1}$, with an order of magnitude less at 8 to 10 cm bsf. The NRB were notably absent in the TOC-poor south in contrast to the northern core (Fig. 6A and B).

In core, TVBC 08, both the Fe-oxidizers and Mn-oxidizers were one order higher than in core TVBC 26. Here, Fe-oxidizers varied from $5.33E+03$ to $1.39E+04$ $cfu g^{-1}$. Mn-oxidizers

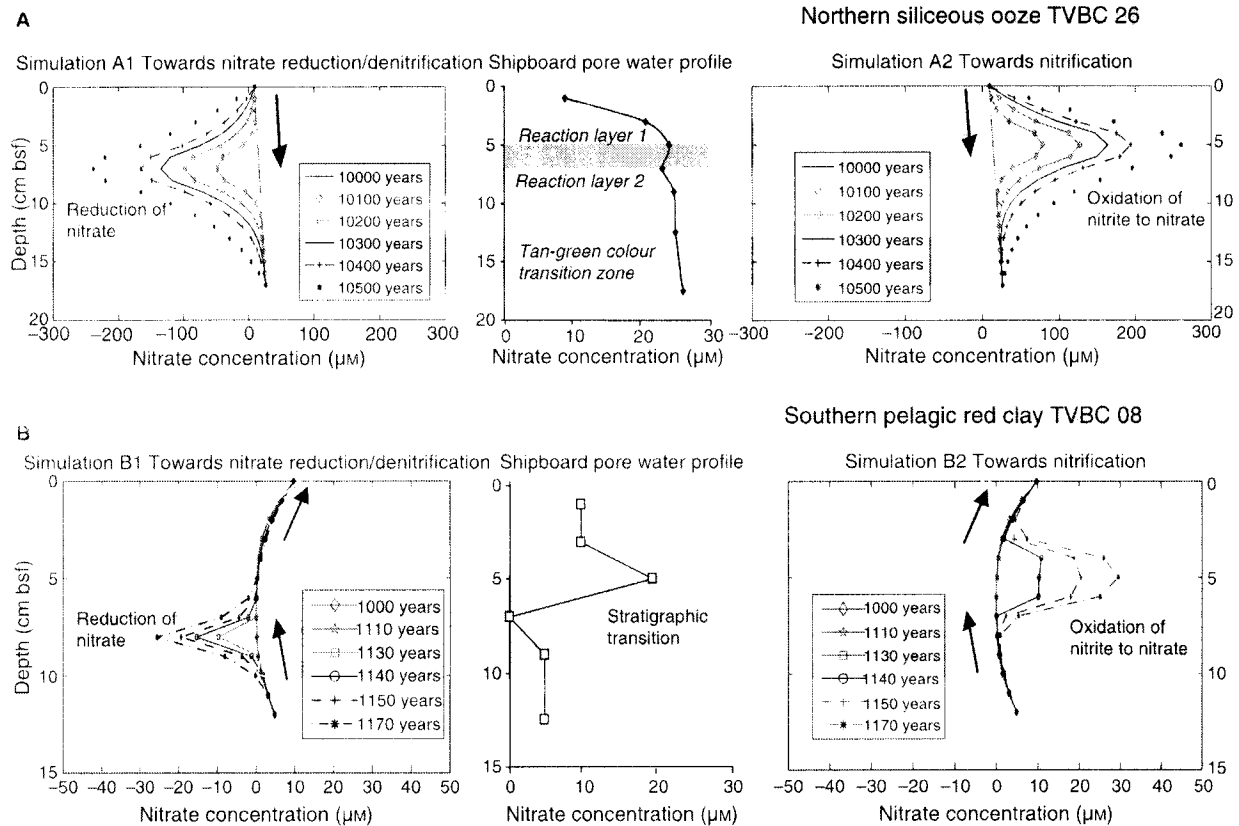


Fig. 9. Numerical simulations (A) Core TVBC 26. Simulation of non-steady state of NO_3^- concentrations in pore water due to diffusion, production and consumption, showing the prevalence of a nitrification–denitrification coupling at 3 to 9 cm bsf. (B) Core TVBC 08. Simulation of hydrothermal alteration of pore water NO_3^- concentrations initiated by production, upward diffusion, dispersion due to phase change and consumption by microbes showing the existence of nitrification–denitrification couple at 3 to 9 cm bsf.

varied from 3.72×10^3 to 1.05×10^4 cfu g^{-1} dry sediment. A distinct increase in the abundance of these groups is noted at the stratigraphic transition zones (Fig. 6B).

Microbial uptake of carbon in sediments

Measurement of autotrophic microbial carbon fixation by whole sediment slurries showed marked differences, with nearly 30 times more uptake at TVBC 08 than at TVBC 26. Occasionally, at certain depths of TVBC 08, the carbon uptake was 300 times or more than that of TVBC 26. Core TVBC 08 showed two mid-depth maxima at 6 to 8 cm and 10 to 15 cm, respectively (Fig. 7).

Organic carbon flux, palaeoproductivity and modern microbial autotrophic uptake

Pelagic red clays showed a lower productivity of 30 to 50 $\text{mg C m}^{-2} \text{ day}^{-1}$ corresponding to 10.95 to 18 $\text{g C m}^{-2} \text{ year}^{-1}$ (Matondkar *et al.*, 2005). Less than 0.3% of carbon produced from surface production rains over reaches the red clays.

Organic C flux was $0.03 \text{ g C m}^{-2} \text{ year}^{-1}$ and carbon accumulation rates were $0.00046 \text{ g C m}^{-2} \text{ kyr}^{-1}$. The preservation factor was 3.07×10^{-8} for pelagic red clay at TVBC 08. Palaeoproductivity ranged from 0.0016 to 0.0097 $\text{g C m}^{-2} \text{ year}^{-1}$ in the pelagic red clays (Fig. 8). Palaeoproductivity and modern microbial autotrophic uptake were independent of each other.

Inter-relationship between bacterial and geochemical parameters

Lower surface productivity (Matondkar *et al.*, 2005), lower sedimentation rates and negligible continental influx are attributed to the low TOC, recalcitrant LOM and the lack of a relationship between the two parameters in the southern TVBC 08 (Figs 2 and 4). The total bacterial counts are dominated by a viable anaerobic population ($P > 0.01$) that is correlated negatively with TOC, LOM and C/N ratio. The ^{14}C uptake correlated positively with total bacterial counts and ($P > 0.05$).

The ^{13}C uptake related positively only to nitrite oxidizers ($P > 0.05$) in the north suggesting that chemosynthesis is highly dependent on the reducing agents that are limited in availability. On the contrary, in the southern core the absence of such a relationship suggests that the chemosynthetic activity is not limited either by availability of reduced substrates. Further, this relationship is not restricted to any specific group.

Quantification of hydrothermal alterations on pore water and microbial community by numerical simulation

The NO_3^- concentration profile measured by shipboard analysis was simulated using a transient diffusion numeric model (Fig. 9B). At 12.5 cm bsf, i.e. below the stratigraphic transition, the observed NO_3^- concentration of $4.85 \mu\text{M}$ was used as a starting condition. It was also assumed that NO_3^- in sediment pore water is 0. The model calculated the concentration as a function of time and height of core using the core bottom as height zero. The precise time and duration of the explosion is unknown. However, the alteration features indicate a 200 year time span between the explosion and the present time (Nath *et al.*, 2008). Thus an assumption of a 1000 year focused jet-flow was made to simulate the model. For the first 1000 years of explosive volcanism, NO_3^- had diffused upwards as a focused jet after which it started dispersing laterally. Assuming a surface layer with a nitrite oxidation rate of $1000 \mu\text{M m}^{-3} \text{ year}^{-1}$ at 9 to 5 cm bsf, the model also shows that the reactant, NO_2^- , will be dispersed and consumed by microbes within a time period of 100 to 200 years in this zone. Conversely, at 7 to 3 cm bsf, the reactant, NO_3^- will be dispersed and consumed within 100 to 200 years with a nitrate reduction rate of $-1000 \mu\text{M m}^{-3} \text{ year}^{-1}$. The profile returns to its original shape within another 100 to 200 years soon after the utilization of NO_2^- in the lower 9 to 5 cm layer and the simultaneous reduction of NO_3^- in the upper 7 to 3 cm ceases. Due to the continuous abiotic supply of NO_2^- and NO_3^- , in both halves of the reaction, a non-steady nitrification–denitrification coupled profile is sustained and they reproduce the pore water NO_3^- profile measured in the core TVBC 08 (Fig. 9B).

DISCUSSION

Although it was argued that the culturable fraction could wield greater influence on the

environment, such inferences remained controversial for two decades, as only 0.001% to 0.01% of the total bacterial count is amenable to cultivation techniques (Van Es & Meyer-Reil, 1982). Prokaryotic processes are now known to be operating on geological time scales and culturable prokaryotes are reported to be stimulated at interfaces (Parkes *et al.*, 2005). The present work reiterates the prevalence of such enhanced bacterial culturability in the CIB that was earlier shown in the Eastern Equatorial Pacific (Parkes *et al.*, 2005; Meister *et al.*, 2007; Wang *et al.*, 2008). This study also demonstrates the occurrence of chemoautotrophic activity coinciding with geochemical and stratigraphic transition zones in both diagenetic and hydrothermally altered sedimentary settings.

Northern core TVBC 26

Influence of organic carbon on microbial carbon uptake

The comparison of a modern microbial autotrophic uptake profile with the palaeoproductivity profile shows a similar trend suggesting heterotrophy dependent on surface-based production. The microbial degradation and recycling of organic matter is evident in reactive layers 1 and 2 representing two halves of any redox cycle in metabolic zones (Fig. 2; see Schulz, 2000 for detailed definitions). Interestingly, the occurrence of this process is evident at the tan-green colour transition zone (Konig *et al.*, 1997) and appears to have operated at a *ca* 10 000 year time span on the Late Pleistocene to Holocene scale (age derived from ^{230}Th decay). Surprisingly, the biostratigraphic change at 180 ka BP also coincides with the tan-green mottled zone; however, its relationship with elemental carbon and nitrogen, if any, is not clear (Fig. 2). Although, a clear dependence on surface derived organic matter is shown by the heterotrophic microbes of TVBC 26, the enhanced chemoautotrophic features at the reactive layers and tan-green transition show that this process is also operational.

Bacteria response to pore water geochemistry in the tan-green mottled zone

The tan-green mottled zones are colour transitions associated with the iron redox boundary. These layers, often referred to as 'sub-oxic' mottles, had been correlated with dissolved NO_3^- , Mn and Fe (Lyle, 1983; Konig *et al.*, 1997). The tan-green mottled zones are found generally below reactive layers 1 and 2 which, in turn, are

prominent below the sediment–water interface (Fig. 2). Formations of these mottles in the Pacific Ocean sediments were attributed to high palaeo-productivity, differential sedimentation rates and fluctuations in oceanic redox conditions caused by changes in bottom water oxygen content (Lyle, 1983). Formation of metal enrichment zones in the upper part of the deep-sea sediment column (Colley *et al.*, 1984; Colley & Thomas, 1985) with the active involvement of microbes (Froelich *et al.*, 1979) are also believed to be the cause of these formations.

Non-steady-state diagenetic processes due to downward diffusing oxidants, such as O_2 and NO_3^- , result in the depletion of initially deposited organic carbon. Both oxidized and reduced forms of nitrogen are produced in the active oxidation zones (Buckley & Cranston, 1988). More recently, the temporal shift of geochemical interfaces from shallower temporary reactive to deeper layers results in mottle formation in predominantly detrital settings (Meister *et al.*, 2007, 2009).

Tan-green transitions in the sediment columns from the northern CIB were reported to influence pore water and sedimentary organic carbon profiles. Extensive nitrification coupled with oxic respiration and the possible involvement of bacteria was suggested previously (Nath & Mudholkar, 1989). However, the relevant direct microbial evidence is now presented in this study. Microbiologically, the zone is characterized by an increasing trend of ^{14}C uptake and higher values for the C/N ratio, ATP, DVC-an and denitrifiers (Figs 2, 5, 6 and 7A). Higher C/N ratios in sub-oxic depths of sediments with TOC < 1% has been associated with bacterial oxidation of metals (Farrimond *et al.*, 1989) and reworking of residual organic matter.

Earlier studies on bacteria from these tan-green mottles at 20 to 25 cm bsf highlighted their capability of showing different phases of nitrification (Ram *et al.*, 2001). Nitrate reduction coupled to oxidation of organic matter, followed by fixing of CO_2 , is suggestive of recycling and conservation of available organic matter. The depleted NO_2^- concentration (Fig. 3A) and its negative correlation to NO_3^- indicate a coupled bacterial nitrification–denitrification process if explained traditionally. However, formation of dinitrogen and loss of nitrogen under the influence of reactive Mn (Luther *et al.*, 1997) can be attributed to elevated C/N ratios at these depths. Bacterial chemo-denitrification is known to exist in oxygen containing sediments (Luther *et al.*,

1997). Non-steady Mn diagenesis resulting in the enrichment of Mn below these sub-oxic or tan-green transition depths has been suggested earlier in these sediments (Pattan & Jauhari, 2001).

Organic carbon in the reactive layers (Fig. 2) stimulates oxygen consumption by active micro-aerophilic or facultative anaerobic bacteria (for example, nitrifiers, nitrate reducers, aerobic sulphur oxidizers and heterotrophs) during oxic respiration. This oxic process is followed by nitrate reduction within the total 6 cm thick overlapping reactive layers 1 and 2. Also, in these layers, manganese reduction possibly synchronizes with sulphide oxidation. Consequently, the resultant upward diffusion of dissolved metals could feed the nodule accretion process at the sediment water interface (see IVBC 20A pore water profiles in Fig. 3B).

Pore water oxygen concentrations are within ranges previously reported for the deep-sea (Jahnke & Jahnke, 2004). Warren & Johnson (2002) reported *ca* 4 to 4.5 ml l^{-1} (175 to 197 μM) in waters of the northern CIB at *ca* 4600 m below the surface, along 90°E longitude. The convex profile of NO_3^- (Fig. 3A) is indicative of predominantly oxic conditions with net nitrification (Soetaert *et al.*, 1996). A distinct early diagenetic reactive layer is seen at 3 to 9 cm bsf in station TVBC 26. The PO_4^{3-} concentrations are depleted at the diagenetic reactive layer (Schulz, 2000) and within the tan-green mottled zone, and are possibly related to the nitrification–denitrification coupled zones where nitrification is more prominent. The SiO_3^{2-} concentration shows a typical downward increasing trend in TVBC 26 indicating a diffusive flux from the sediment water interface (Nath & Mudholkar, 1989).

The presence of iron-bacteria and manganese-bacteria in higher numbers, along with the thiotrophs, suggests the possible occurrence of sulphide-oxidation along with iron and manganese oxido-reduction in this diagenetic setting, especially at the mottled zone. These associations are common in hydrothermally altered sediments or diffuse flow systems (Bach & Edwards, 2003). Although bacterially mediated Mn^{2+} oxidation by O_2 or NO_3^- may be restricted near oxic zones, processes like thiotrophic nitrate reduction in deep-sea settings are gaining importance. These processes over time lead to the formation of tan-green mottled zones dominated by facultative heterotrophs, manganese-oxidizers and aerobic sulphur oxidizers (Fig. 6A). These bacteria conserve the organic matter chemolithotrophically

by recycling (Stevens, 1997) and re-fixing CO₂ formed during breakdown of organic matter.

The occurrence of sulphide in some of these oligotrophic sediments highlights the greater importance of hydrothermal influence and requires renewed investigations. Although, the co-existence of sulphide and oxygen in 'sub-oxic' or 'oxic-anoxic' transitions are well-known (Glazer *et al.*, 2006), the trends suggest that an inverse distribution of oxygen versus sulphide in pore waters may not always be true. Co-existence of detectable amounts of sulphide, ammonium and oxygen (Fig. 3B), and the presence of manganese oxidizers and thiotrophic bacteria, indicate the possibility of co-occurrence (Wang *et al.*, 2008) or overlap of multiple metabolic zones (Canfield & Thamdrup, 2009). The present results reiterate the importance of sulphide and a possibly underestimated hydrothermal influence in the formation process of ferro-manganese nodules (cf. Glasby, 2006).

Alternatively, rock alteration and volcanic degassing could be a significant process in station TVBC 26 due to its proximity to the Trace of Rodrigues Triple Junction. Under such conditions, autotrophy at the mottled zones could be associated with fluid percolation through these sediment strata (Sizaret *et al.*, 2009). Even then, station TVBC 26 would not be an independent chemoautotrophic system as a major fraction of the organic flux is derived from the highly productive South Equatorial Boundary Current-driven surface waters. Core TVBC 26 would be analogous to hydrocarbon rich layers mutually influenced by organic matter rain and hydrothermal fluid flow. However, the scale and extent of the processes could be highly reduced.

Quantification of the influence of non-steady-state diagenetic condition on microbial community by numerical simulation

The numerical simulation (Fig. 9A) suggests the prevalence of bacterial nitrate reduction–nitrite oxidation coupling at the reactive layers. Consequently, a mottled zone forms at deeper layers and reduced metal species oxidize near the sediment–water interface. Sigmoid profiles of NO₃[−] concentration at the reactive layers are suggestive of formation and subsequent utilization of the ion at this shallow depth. The deposition of a 4 cm thick organic carbon-rich layer and upward migration of reduced metal species like Mn²⁺ leads to the coupling of nitrate reduction to nitrite oxidation. These coupled processes may reach a rate of ± 1000 μm m^{−3} year^{−1}; consequently, this leads to

rapid formation and removal of NO₃[−] and a new nitrite oxidizing–nitrate reducing interface may be formed. This interface may potentially migrate upwards from 3 to 9 cm bsf to the surface, thus allowing manganese nodule precipitation in the form of MnO₂ at the surface. The precipitation of these manganese nodules could be analogous to dolomite precipitation above sulphate–methane interfaces (Rao *et al.*, 2003; Meister *et al.*, 2007, 2009). High chemosynthetic activity has been noted in these reactive layers similar to that in sulphate–methane interfaces and dolomite deposits observed at Blake Ridge (Rodriguez *et al.*, 2000) and ODP site 1229 in the Eastern Equatorial Pacific (Meister *et al.*, 2007). The relative compactness of porous siliceous ooze sediments at these depths (Fig. 3A) reduces permeability, partially restricting horizontal transfer and utilization of NO₃[−], in these clay-rich sediments; this results in the formation of horizontal mottled layers (Figs 2 and 3).

Southern core TVBC 08

Influence of organic carbon on microbial carbon uptake

The microbial autotrophic uptake profile of core TVBC 08 shows no relationship to the palaeoproductivity profile suggesting greater chemoautotrophy and independence from surface based production (Fig. 8). The depletion of organic content and the additional influence of hydrothermally derived pore-fluids appear to have triggered a greater microbial carbon uptake. A net autotrophic bacterial community with higher nitrifiers and nutritionally flexible heterotrophs inhabit the southern TOC-poor sediments of TVBC 08. These observations are further supported by a positive correlation ($P > 0.05$) between ¹⁴C uptake and total bacterial counts. The greater number of FDC at the TOC-depleted lower depths suggests the utilization of inorganic substrates in hydrothermally altered fluids promoting greater autotrophic activity.

Influence of hydrothermal alterations on pore water and bacterial activity

Mid-plate volcanic and hydrothermally altered area, TVBC 08 (Mascarenhas-Pereira *et al.*, 2006; Iyer *et al.*, 2007; Nath *et al.*, 2008) hosts a predominantly chemoautotrophic microbial population. The possibility of nitrogen species emanating out of the circulating hydrothermal fluids (Gieskes *et al.*, 2002) and advecting upwards before spreading laterally at 4 to 8 cm bsf (Fig. 3A)

due to diffusive transport at the stratigraphic interface (Gieskes *et al.*, 2002) is explored in the present work.

Fluid phase separation during hydrothermal alterations is known to produce higher and lower phases of solutes. Although the higher phases rapidly migrate by advection towards the surface, presumably along cracks and faults, the lower ones get transported laterally along more porous zones in the sediments; here they may get utilized by bacteria. A recent study by Nath *et al.* (2008) interpreted the influence of neutral chloride type hydrothermal fluids to be predominant in these altered sediments. Intense hydrothermal alteration features were reflected in: (i) the depleted sedimentary organic carbon (also observed in the present study, see Fig. 2); (ii) dissolution features of radiolarian skeletons; (iii) the presence of altered minerals such as smectite and zeolites; and (iv) distinctly different magnetic properties in the altered sediments. An excess of ^{210}Pb over its parent was recorded in the lower semi-indurated sediments. Bioturbation and slumping of older sediments from the shallower portions of the seamount were ruled out for the $^{210}\text{Pb}_{\text{ex}}$ as the sediments lacked benthic biota, organic matter and detectable carbonate content (Nath *et al.*, 2008).

The PO_4^{3-} in TVBC 08 is lower than TVBC 26. However, the presence of a PO_4^{3-} concentration $> 1 \mu\text{M}$ in organically depleted environments with distinct enrichment in Fe in an oxidized state,

compared to the pelagic clays occurring in the CIB (Nath *et al.*, 2008) indicates possible hydrothermal origin and co-precipitation with the metal oxides (Yamagata *et al.*, 1991; Karl, 1995). The SiO_3^{2-} concentrations show little variation and a lower diffusional gradient in TVBC 08.

Adenosine triphosphate values (Fig. 5) are similar to the range reported from Guaymas Basin (Table 1). Although extensively reported from waters and bacterial mats of vent fields, reports on ^{14}C incorporation rates of whole sediments are still scanty. It is noted that ^{14}C incorporation rates (Fig. 7) of CIB sediments when normalized to bacterial numbers are similar to some water samples of Juan de Fuca and white smokers of the 21°N East Pacific Rise (Table 2).

The contribution of LOM and faunal numbers to higher measurements of ATP at TVBC 08 is minimal. Negligible numbers of macrofauna and meiofauna (Ingole *et al.*, 2005) suggest that there could be little contribution by these organisms. Moreover, ATP does not relate to any of the other parameters measured, suggesting that the higher ATP in the south could be due more to hydrothermally produced analogues rather than being organically derived (Liu *et al.*, 1982; Yamagata *et al.*, 1991). The high ATP in TVBC 08 (Fig. 5, Table 1) could therefore be due to the inclusion of large amounts of pyrophosphate or polyphosphates formed during rapid cooling in hydrothermal systems (Yamagata *et al.*, 1991). The presence of Fe in an oxidized state (Nath *et al.*,

Table 1. Comparison of ATP values of other established vent fields to Central Indian Basin stations.

Location	Type	Range of ATP (ng g^{-1})	Reference
21°N EPR	Particulate matter, black smoker	71–125	Karl <i>et al.</i> (1989)
Guaymas Basin	Sediments	68–1005	Haberstroh & Karl (1989)
	Control deep-sediments	100–200	Haberstroh & Karl (1989)
TVBC-26, 10°S, 75°30'E	Sediments (northern, TOC-rich)	18–106	Present work
TVBC-08, 16°S, 75°30'E	Sediments (southern, TOC-poor)	232–1354	Present work

Table 2. Comparison of ^{14}C incorporation values of Central Indian Basin stations to other established vent fields.

Location	Type	^{14}C incorporation*	Condition	Reference
21°N, EPR	Water, White smoker	12.7	1 atm, 3 °C, 24 h, dark	Wirsén <i>et al.</i> (1986)
Juan de Fuca	Water	201.7	1 atm, dark	Chase <i>et al.</i> (1985)
Guaymas Basin	Bacterial mats	444 000	1 atm, dark, 28 °C	Nelson <i>et al.</i> (1989)
Guaymas Basin	Bacterial mats	12 000	1 atm, dark, 8 °C	Nelson <i>et al.</i> (1989)
TVBC-26	Sediments	5–45	1 atm, dark, 5 °C	Present work
TVBC-08	Sediments	230–1600	1 atm, dark, 5 °C	Present work

* ^{14}C incorporation units are $\text{nmol l}^{-1} \text{day}^{-1} \text{CO}_2$ for water samples and $\text{nmol g}^{-1} \text{dry wt day}^{-1}$ for sediments and bacterial mats. The rates are normalized to bacterial numbers for comparison.

2008) and the anomalous bulk phosphate (Nath *et al.*, 2005) suggests scavenging of hydrothermal phosphorus by iron, leading to the formation of bio-available pyrophosphate and its subsequent utilization as an alternate pathway for channeling geothermal-based energy in the biosphere (Liu *et al.*, 1982).

The hydrothermal origin of ammonium or other reduced nitrogenous species from deeper layers is indicated by the pore water profiles of NO_2^- and NO_4^- . Higher total nitrogen values and a C/N ratio < 1 at 20 to 25 cm bsf both indicate excess of nitrogen. The high C/N ratio and depletion of NO_2^- and NO_3^- is probably caused by the preferential loss of N during metamorphic volatilization (Bebout & Fogel, 1992) at the upper stratigraphic transition between Pleistocene and Tertiary sediments (Fig. 2). Where there is minimal contribution of organic matter, this excess can only be derived from hydrothermal fluids. Similar findings have been reported from Suiyo Seamount at Izu-Bonin backarc system (Takano *et al.*, 2004) and the shallow vent systems of Vulcano Islands (Gugliandolo & Maugeri, 1998). Rapid conversion of dissolved NO_3^- and NO_2^- to NH_4^+ rather than to N_2 , particularly in the presence of Fe and Ni as seen in ODP Leg 201 pore water data (Smirnov *et al.*, 2008), could explain the abrupt fluctuations of nitrogen. Different transport routes for higher and lower phases of hydrothermally altered fluids while cooling can produce distinct changes both in bacterial number and activity. These alterations occur (Figs 5 to 7) at sediment layers with varying porosity and pH (Figs 2 and 3; Gieskes *et al.*, 2002).

The high peak of the C/N ratio with low TOC (Fig. 2) and LOM in the upper 2 to 4 cm bsf (Fig. 4) corresponds to the highest ATP, ammonia oxidizers and aerobic sulphur oxidizers (Figs 5 and 6). This layer is sandwiched between carbon uptake maxima (Fig. 7) suggesting the chemolithotrophic utilization of inorganic substrates made available during phase separation of solutes.

Venting activities can produce ammonia where nitrifying bacteria can thrive (Karl, 1995). The higher number of autotrophic nitrifiers and the significant correlation between ammonium oxidizers and aerobic sulphur oxidizers suggests a more hydrothermal origin for the ammonium feeding the nitrite oxidizers (Wirsen *et al.*, 1986; Karl, 1995). The presence of large numbers of thiotrophs, iron-oxidizers and manganese-oxidizers indicates that hydrothermal alterations or

diffuse flow might influence the sulphide-oxidation and iron metabolism in this core (Bach & Edwards, 2003).

Synchronization of carbohydrate maxima with the zone of high ^{14}C uptake at 15 to 20 cm bsf possibly is suggestive of chemoautotrophy by mixotrophs. Large fractions of heterotrophic bacteria inhabited this lower non-dateable stratigraphic transition within the Tertiary sediments. Higher adaptability and resilience of bacteria are associated with relatively oligotrophic sediments (Harder & Dijkhuizen, 1982; Goltekar *et al.*, 2006) like the organically depleted core TVBC 08. Similar unexplained high heterotrophic populations have been reported in some earlier findings in vent sites with low organic carbon (Karl, 1995).

Although the nitrifiers, aerobic sulphur oxidizers and heterotrophs exist in large numbers and contribute partly to ATP and ^{14}C uptake, they do not have a statistically significant relationship with the pore water nitrogen species or the C/N ratio in TVBC 08. This observation is contrary to the diagenetic TVBC 26 where these retrievable bacteria show a statistically significant relationship with other biochemical and pore water parameters. The results indicate the predominance and activity of a distinct functional group capable of exhibiting chemolithotrophy through multiple metabolic pathways. These microbes flourish in the remnant inorganic substrates derived from explosive hydrovolcanism that geochemists believe to have occurred *ca* 200 years ago (Nath *et al.*, 2008). Examining the whole community at the molecular level would complement the present studies and throw more light on both their taxonomy and function.

Quantification of hydrothermal alterations on pore water and microbial community by numerical simulation

The numerical simulation (Fig. 9B) suggests the prevalence of a nitrite oxidation–nitrate reduction coupling at the Pleistocene–Tertiary stratigraphic interface due to lateral dispersion and phase separation of solute during cooling of upwelled hydrothermal fluid. Consequently, there is an enhancement of bacterial abundance and activity at the stratigraphic transition zone (Figs 5 to 7) due to the availability of inorganic substrates made utilizable by processes such as phase separation of solutes. Sigmoid profiles of NO_3^- concentration at the stratigraphic transition are suggestive of formation and subsequent utilization of the ions at this transition zone. The 6 cm

transition zone in core TVBC 08 and upward migration of reduced chemical species from hydrothermally altered fluids leads to the coupling of nitrate reduction to nitrite oxidation; consequently, this leads to rapid formation and removal of NO_3^- . A new nitrite oxidizing–nitrate reducing transition gets formed. The pore water NO_2^- profile would run parallel to that of NO_3^- and would not be analogous to those derived from organic matter diagenesis (for example, Core TVBC 26) when there is continuous supply. Hence, the NO_3^- profile is altered by the presence of hydrothermally derived reduced substrates.

An initial vertical focused-jet of hydrothermally altered fluid evolves into a lateral diffusion at the Pleistocene–Tertiary stratigraphic transition and allows for hydrothermal precipitation of Fe, Ti, P, etc., as reported earlier by Nath *et al.* (2008). A negative rock alteration index denoting precipitation (Zhao *et al.*, 2009) may be expected at 3 to 7 cm bsf sandwiched between positive ones denoting dissolution. Although neutral chloride type hydrothermal activity is indicated by previous studies (Nath *et al.*, 2008), more comprehensive data on thermal and Cl^- anomalies would be helpful for simulating improved models.

Variation in porosity (Fig. 3B) at the stratigraphic transition zone is sharp. The effect of convection and interactions between fluid flow, heat transfer, mass transport and chemical reactions needs to be considered in a comprehensive manner using coupled transport models or finite element models (Yang *et al.*, 2004; Ma *et al.*, 2006; Zhao *et al.*, 2009) taking into account the complex stratigraphic features.

CONCLUSION

The distinctions between types of microbial autotrophic activity at different geological end-member settings are identifiable and quantifiable by multi-disciplinary approaches. Content and quality of organic matter and flow of hydrothermal heat, fluid and solutes are the most important factors controlling autotrophic activity in deep-sea sediments. The present study explores the domain of chemoautotrophy in the deep-abyssal basins of the Central Indian Basin with a combination of low organic content and diffuse low temperature hydrothermal alterations.

In Central Indian Basin sediments, a decrease in organic matter tends to elevate microbial carbon uptake in the bacterial communities.

The northern core TVBC 26 is predominantly heterotrophic with chemosynthetic signatures at the tan-green mottled zones. The bacterial activity is only partially dependent on the surface productivity at core TVBC 26. The depth of reactive layers and tan-green mottled zones coincides with high chemosynthetic activity and low palaeosurface productivity. The autotrophy prevailing in the tan-green transition is analogous to the organic matter fossilization and hydrocarbon formation in organic rich sedimentary settings (Campbell, 2006; Ma *et al.*, 2006; Mazumdar *et al.*, 2009).

The southern core TVBC 08 is predominantly autotrophic with heterotrophic microbial signatures in the deeper layers. Here chemoautotrophy is totally independent of surface productivity. The heterotrophy in the deeper parts of southern core TVBC 08 is possibly akin to the formation of new degradable organic compounds in hydrothermal settings. This system is possibly analogous to settings like the Loihi Seamount. Further study of this location may provide interesting insights into tracing pre-biotic origins and explorations for lunar, martian or jovian planetary systems (Goodman *et al.*, 2004).

The role of thiotrophs in deep-sea sediments is prominent in both diagenetic and hydrothermally altered sediments. Processes like thiotrophic nitrate reduction may be more influential in the northern total organic carbon and sulphide-rich sediments. The data highlights the necessity for renewed investigations involving pore water NH_4^+ , HS^- , Mn and Fe in oxic conditions. Thiotrophs in hydrothermally altered sediments or diffuse flow systems might be influencing sulphide-oxidation and iron metabolism. The presence of large numbers of iron-oxidizers, manganese-oxidizers and thiotrophs at the mottled zones of TVBC 26 and in hydrothermally altered core TVBC 08 indicate their close relationship to rock alteration and mineralization processes.

These findings could stimulate the pursuit of chemosynthesis for sequestering CO_2 in the deep sea floor. The present study also adds a theoretical dimension for expanding the potential for hydrocarbon exploration in the ocean as discussed earlier in the Pacific nodule province by Wenxuan *et al.* (2002). In these stretches of metal-rich oligotrophic abyssal sediments, hydrothermal activities may predominate, at least over a 100 to 1000 year time scale and require further quantification. However, hydrothermal activity and associated rock alteration processes may be

more relevant than organic matter delivery in these deep-sea sediments.

ACKNOWLEDGEMENTS

The authors are grateful to S. R. Shetye, Director, National Institute of Oceanography for his encouragement. V. Subramaniam and M.-J. B. D. De Souza helped with the microbial ^{14}C uptake analyses. J. N. Pattan, K. P. Krishnan and Siby Kurian are acknowledged for their help during the course of the work. V. Nanjundaiah (IISc, India), Dieter Wolf-Gladrow (AWI, Germany), D. Shankar, A. Mazumdar and N.T. Manoj introduced AD to the field of numerical simulations and codes, conceptual biogeochemical and biological modelling. Facilitation on-board by the shipboard scientific party and crew of *Akademik Alexandr Sidorenko* (Cruise 61, 2003), *Akademik Boris Petrov* (Cruise 4, 2005) and *Akademik Boris Petrov* (Cruise 38, 2009) is acknowledged. Special thanks are due to Patrick Meister (ETH-Zürich/Bremen University) and other anonymous reviewer(s) for their critical guidance leading to the significant improvement in the manuscript. This work was financially supported by the Ministry of Earth Sciences, Government of India. AD, CEGF and SPP acknowledge the Council of Scientific and Industrial Research (CSIR), New Delhi, for funding their research work. This study is NIO Contribution No. 4786.

REFERENCES

- Aldrich, A.P. and van der Berg, C.M.G. (1998) Determination of Fe and its redox speciation in seawater using catalytic cathodic stripping voltametry. *Electroanalysis*, **10**, 369–373.
- ASTM (1995). *Annual Book of ASTM Standards*. 04.08. Soil and Rocks (I) D420-D4914. ASTM, Philadelphia, PA, 981 pp.
- Bach, W. and Edwards, K. (2003) Iron and sulphide oxidation within the basaltic ocean crust: implications for chemolithoautotrophic microbial biomass production. *Geochim. Cosmochim. Acta*, **67**, 3871–3887.
- Banakar, V.K., Gupta, S.M. and Padmavathi, V.K. (1991) Abyssal sediment erosion in the Central Indian Basin: evidence from radiochemical and radiolarian studies. *Mar. Geol.*, **96**, 167–173.
- Bebout, G.E. and Fogel, M.L. (1992) Nitrogen-isotope compositions of metasedimentary rocks in the Catalina Schist, California: implications for metamorphic devolatilization history. *Geochim. Cosmochim. Acta*, **56**, 2839–2849.
- Bhargava, E.G. and Dyer, W.J. (1959) A rapid method of total lipid extraction and purification. *Can. J. Biochem. Physiol.*, **37**, 911–917.
- Borole, D.V. (1993) Late Pleistocene sedimentation: a case study of the Central Indian Ocean Basin. *Deep-Sea Res.*, **40**, 761–775.
- Buckley, D.E. and Cranston, R.E. (1988) Early diagenesis in deep sea turbidites: the imprint of palaeo-oxidation zones. *Geochim. Cosmochim. Acta*, **52**, 2925–2939.
- Campbell, K.A. (2006) Hydrocarbon seep and hydrothermal vent paleoenvironments and paleontology: past developments and future research directions. *Palaeogeogr. Palaeoclimatol. Palaeoecol.*, **232**, 362–407; doi: 10.1016/j.palaeo.2005.06.018.
- Canfield, D.E. (1991) Sulfate reduction in deep sea sediments. *Am. J. Sci.*, **291**, 177–188.
- Canfield, D.E. and Thamdrup, B. (2009) Towards a consistent classification scheme for geochemical environments, or, why we wish the term 'suboxic' would go away. *Geobiology*, **7**, 385–392.
- Cauwet, G. (1978) Organic chemistry of seawater particulates: concepts and developments. *Oceanol. Acta*, **1**, 99–105.
- Chase, R.L., Delaney, J.R., Karsten, J.L., Johnson, H.P., Juniper, S.K., Lupton, J.E., Scott, S.D., Tunncliffe, V., Hammond, S.R. and McDuff, R.E. (1985) Hydrothermal vents on an axis seamount of the Juan de Fuca ridge. *Nature*, **313**, 212–214.
- Chevaldonne, P., Desbruyeres, D. and Le Haitre, M. (1991) Time-series of temperature from three deep-sea hydrothermal vent sites. *Deep-Sea Res. A*, **38**, 1417–1430.
- Childress, J.J., Fisher, C.R., Favuzzi, J.A., Kochevar, R.E., Sanders, N.K. and Alayse, A.M. (1991) Sulphide-driven autotrophic balance in the bacterial symbiont-containing hydrothermal vent tubeworm *Riftia pachyptila*. *Biol. Bull.*, **180**, 135–153.
- Colley, S. and Thomas, J. (1985) Recurrent uranium relocations in distal turbidites emplaced in pelagic conditions. *Geochim. Cosmochim. Acta*, **49**, 2339–2348.
- Colley, S., Thomson, J., Wilson, T.R.S. and Higgs, N.C. (1984) Post depositional migration of elements during diagenesis in brown clay and turbidite sequences in the North East Atlantic. *Geochim. Cosmochim. Acta*, **48**, 1223–1235.
- Colombini, M.P. and Fuocco, R. (1983) Determination of manganese at ng/ml levels in natural water by differential pulse polarography. *Talanta*, **30**, 901–905.
- Das, P., Iyer, S.D. and Kodagali, V.N. (2007) Morphological characteristics and emplacement mechanism of the seamounts in the Central Indian Ocean Basin. *Tectonophysics*, **443**, 1–18.
- Delistraty, D.A. and Hershner, C. (1983) Determination of adenine nucleotide levels in *Zostera marina* (eelgrass). *J. Appl. Biochem.*, **5**, 404–405.
- D'Hondt, S., Rutherford, S. and Spivack, A.J. (2002) Metabolic activity of sub-surface life in deep-sea. *Science*, **295**, 2067–2070.
- D'Hondt, S., Jørgensen, B.B., Miller, D.J., Batzke, A., Blake, R., Cragg, B.A., Cypionka, H., Dickens, G.R., Ferdeman, T., Kai-Uwe Hinrichs, K.-U., Holm, N.G., Mitterer, R., Spivack, A., Wang, G., Bekins, B., Engelen, B., Ford, K., Gettemy, G., Rutherford, S.D., Sass, H., Skilbeck, C.G., Aiello, I.W., Gue'rin, G., Christopher, H., House, C.H., Inagaki, F., Meister, P., Naehr, T., Niituma, S., Parkes, R.J., Schippers, A., Smith, D.C., Teske, A., Wiegand, J., Padilla, C.N. and Juana Luz Solis Acosta, J.L.S. (2004) Distributions of microbial activities in deep seafloor sediments. *Science*, **306**, 2216–2221.
- Edwards, K.J., Bach, W. and McCollom, T.M. (2004) Neutrophilic iron-oxidizing bacteria in the ocean: their habitats,

- diversity, and roles in mineral deposition, rock alteration, and biomass production in the deep-sea. *Geomicrobiol. J.*, **21**, 393–404.
- Ulrich, H.L. (1998) Geomicrobiology: its significance for geology. *Earth-Sci. Rev.*, **45**, 45–60.
- Farrimond, P., Eglinton, G., Brassell, S.C. and Jenkyns, H.C. (1989) Toarcian anoxic event in Europe: an organic geochemical study. *Mar. Petrol. Geol.*, **6**, 136–147.
- Fichez, R. (1991) Composition and fate of organic matter in submarine cave sediments: implications for the biogeochemical cycle of organic carbon. *Oceanol. Acta*, **14**, 369–377.
- Folk, R.L. 1968. *Petrology of Sedimentary Rocks*. University of Texas, Austin, TX, 170 pp.
- Froelich, P.N., Klinkhammer, G.P., Bender, M.L., Luedtke, G.R., Heath, G.R., Cullen, D., Dauphin, P., Hammond, D., Hartman, B. and Maynard, V. (1979) Early oxidation of organic matter in pelagic sediments of the eastern equatorial Atlantic: sub-oxic diagenesis. *Geochim. Cosmochim. Acta*, **43**, 1075–1090.
- Ghosh, A.K. and Mukhopadhyay, R. (1999) Exploration. In: *Mineral Wealth of the Ocean*. pp. 176–203. Oxford and IBH Publishing Co. Pvt. Ltd, New Delhi.
- Gieskes, J.M., Simoneit, B.R.T., Goodfellow, W.D., Baker, P.A. and Mahn, C. (2002) Hydrothermal geochemistry of sediments and porewaters in Escanaba Trough – ODP Leg 169. *Appl. Geochem.*, **17**, 1435–1456.
- Glasby, G.P. (2006) Manganese: predominant role of nodules and crusts. In: *Marine Geochemistry* (Eds H.D. Schulz and M. Zabel), pp. 371–428. Springer, Berlin.
- Glazer, B.T., Luther III, G.W., Kononov, S.K., Friederich, G.E., Trouwborst, R.E. and Romanov, A.S. (2006) Spatial and temporal variability of the Black Sea suboxic zone. *Deep-Sea Res. II*, **53**, 1756–1768.
- Goltekar, R.C., Krishnan, K.P., DeSouza, M.J.B.D., Paropkari, A.L. and Loka Bharathi, P.A. (2006) Effect of carbon source concentration and culture duration on retrievability of bacteria from certain estuarine, coastal and offshore areas around peninsular India. *Curr. Sci.*, **90**, 103–106.
- Goodman, J.C., Collins, G.C., Marshall, J. and Pierrehumbert, R.T. (2004) Hydrothermal plume dynamics on Europa: implications for chaos formation. *J. Geophys. Res.*, **109**, E03008; doi: 10.1029/2003JE002073.
- Grasshoff, K., Ehrhardt, M. and Kremling, K. (1983) *Methods of Seawater Analysis*. 2nd edn. Verlag Chemie, Weinheim, Deerfield Beach, FL, 419 pp.
- Gugliandolo, C. and Maugeri, T.L. (1998) Temporal variations in heterotrophic mesophilic bacteria from a marine shallow hydrothermal vent off the Island of Vulcano (Eolian Islands, Italy). *Microb. Ecol.*, **36**, 13–22.
- Gupta, S.M. (1991a) Radiolarian zonation and volcanic ash-layers in two sediment cores from the Central Indian Basin. *J. Paleontol. Soc. India*, **33**, 59–71.
- Gupta, S.M. (1991b) New ichthyofossils from ferromanganese crusts and nodules from the Central Indian Ocean Basin. *Micropaleontology*, **37**, 125–147.
- Gupta, S.M. and Jauhari, P. (1994) Radiolarian abundance and geochemistry of the surface sediments from the Central Indian Basin. *Curr. Sci.*, **66**, 659–663.
- Haberstroh, P.R. and Karl, D.M. (1989) Dissolved free amino acids in hydrothermal vent habitats of the Guaymas Basin. *Geochim. Cosmochim. Acta*, **53**, 2937–2945.
- Hagstrom, A., Larsson, U., Horstedt, P. and Normark, S. (1979) Frequency of dividing cells, a new approach to the determination of bacterial growth rates in aquatic environments. *Appl. Environ. Microbiol.*, **37**, 805–812.
- Harder, W. and Dijkhuizen, L. (1982) Strategies of mixed substrate utilization in microorganisms. *Philos. Trans. Roy. Soc. London B*, **297**, 459–480.
- Havert, H.H. (1992) Genus *Siderocapsa* (and other iron or manganese-oxidizing eubacteria). In: *The Prokaryotes – A Handbook on the Biology of Bacteria, Ecophysiology, Isolation, Identification and Applications* (Eds A. Balows, H.C. Trüper, M. Dworkin, W. Harder and K.-H. Schleifer), Vol. IV, pp. 4102–4113. Springer-Verlag, New York, Inc.
- Hobbie, J.E., Daley, R.J. and Jasper, S. (1977) Use of Nucleopore filters for counting bacteria by fluorescent microscopy. *Appl. Environ. Microbiol.*, **3**, 1225–1228.
- Holm-Hansen, O. and Booth, C.R. (1966) The measurement of adenosine triphosphate in the ocean and its ecological significance. *Limnol. Oceanogr.*, **11**, 510–519.
- Ingole, B.S., Pavitran, S., Goltekar, R. and Gonsalves, S. (2005) Faunal diversity and abundance. In: *Benthic Environmental Variability in the Central Indian Ocean Basin-I*. pp. 83–103. Project report submitted to Department of Ocean Development, Government of India, New Delhi.
- Iyer, S.D., Mascarenhas-Pereira, M.B.L. and Nath, B.N. (2007) Native aluminium (spherules and particles) in the Central Indian Basin sediments: implications on the occurrence of hydrothermal events. *Mar. Geol.*, **240**, 177–184.
- Jahnke, R.A. and Jahnke, D.B. (2004) Calcium carbonate dissolution in deep sea sediments: reconciling microelectrode, porewater and benthic flux chamber results. *Geochim. Cosmochim. Acta*, **68**, 47–59.
- Johnson, D.A., Schneider, D.A., Nigrini, C.A., Caulet, J.P. and Kent, D.V. (1989) Pliocene–Pleistocene radiolarian events and magnetostratigraphic calibrations for the Tropical Indian Ocean. *Mar. Micropaleontol.*, **14**, 33–66.
- Joux, F. and Lebaron, P. (1997) Ecological implications of an improved direct viable count method for aquatic bacteria. *Appl. Environ. Microbiol.*, **63**, 3643–3647.
- Kamesh Raju, K.A. and Ramprasad, T. (1989) Magnetic lineations in the Central Indian Basin for the period A24–A21: a study in relation to the Indian Ocean Triple Junction trace. *Earth Planet. Sci. Lett.*, **95**, 3–4.
- Karl, D.M. (1995) Ecology of free-living, hydrothermal vent microbial communities. In: *The Microbiology of Deep-Sea Hydrothermal Vents* (Ed. D.M. Karl), pp. 35–124. CRC press, Boca Raton, FL.
- Karl, D.M., Brittain, A.M. and Tilbrook, B.D. (1989) Hydrothermal and microbial processes at Loihi seamount, a mid plate hot-spot volcano. *Deep-Sea Res.*, **36**, 1655–1673.
- Kochert, G. (1978) Carbohydrate determined by the phenol-sulfuric acid method. In: *Handbook of Physiological Methods: Physiological and Biochemical Methods* (Eds J.A. Hellebust and J.J. Craigie), pp. 95–97. Cambridge University Press, Cambridge.
- Kogure, K., Simidu, U. and Taga, N. (1984) An improved direct viable count method for aquatic bacteria. *Arch. Hydrobiol.*, **102**, 117–122.
- König, I., Drodt, M., Suess, E. and Trautwein, A.X. (1997) Iron reduction through the tan-green color transition in deep-sea sediments. *Geochim. Cosmochim. Acta*, **61**, 1679–1683.
- Krishnaswami, S. and Sarin, M.M. (1976) The simultaneous determination of Th, Pu, Ra isotopes, ²¹⁰Pb, ⁵⁵Fe, ³²Si and ¹⁴C in marine suspended phases. *Anal. Chim. Acta*, **83**, 143–156.
- Liu, C.-L., Hart, N. and Peck Jr, H.D. (1982) Inorganic pyrophosphate: energy source for sulfate-reducing bacteria of the genus *Desulfotomaculum*. *Science*, **217**, 363–364.

- Lochte, K., Boetius, A. and Petry, C. (2000) Microbial food webs under severe nutrient limitations: life in the deep sea. In: *Microbial Biosystems: New Frontiers. Proceedings of the 8th International Symposium on Microbial Ecology* (Eds C.R. Bell, M. Brylinsky and P. Johnson-Green), pp. 95–102. Atlantic Canada Society for Microbial Ecology, Halifax, Canada.
- Loka Bharathi, P.A. (1989) The occurrence of denitrifying colourless sulphur-oxidizing bacteria in marine waters and sediments as shown by the agar shake technique. *FEMS Microbiol. Ecol.*, **62**, 335–342.
- Loka Bharathi, P.A. and Chandramohan, D. (1990) Sulfate-reducing bacteria from the Arabian Sea – their distribution in relation to thio-sulfate oxidizing and heterotrophic bacteria. *Bull. Mar. Sci.*, **47**, 622–630.
- Loka Bharathi, P.A., De Souza, M.J.B.D., Nair, S. and Chandramohan, D. (1999) Abundance, viability and culturability of antarctic bacteria. *Fifteenth Indian Expedition to Antarctica. Scientific Report*, Department of Ocean Development, New Delhi, Technical Publication No. 13, pp. 79–92.
- Loka Bharathi, P.A., Pradeep Ram, A.S., Nair, S., Nath, B.N. and Chandramohan, D. (2004) Distribution of baroduric, psychrotrophic and culturable nitrifying and denitrifying bacteria in the Central Indian Basin. In: *Proc. Natl. Seminar on New Frontiers in Mar. Biosci. Res.*, (Eds S.A.H. Abidi, M. Ravindran, R. Venkatesan and M. Vijaykumar), 319–330. Allied Publishers Pvt Ltd., Chennai.
- Lowry, O.H., Rosebrough, N.J., Farr, A.L. and Randall, R.J. (1951) Protein measurement with the Folin-Phenol reagents. *J. Biol. Chem.*, **193**, 265–275.
- Luther III, G.W., Bjørn, S., Brent, L.L., Brendel, P.J. and Silverberg, N. (1997) Interactions of manganese with the nitrogen cycle: alternative pathways to dinitrogen. *Geochim. Cosmochim. Acta.*, **61**, 4043–4052.
- Lyle, M. (1983) The brown-green colour transition in marine sediments: a marker of Fe(III)-Fe(II) redox boundary. *Limnol. Oceanogr.*, **28**, 1026–1033.
- Ma, F., Al-Aasm, I. and Yang, J. (2006) Numerical modeling of hydrothermal fluid flow coupled with mass transport: an example from the Devonian Wabamun Group, northeast British Columbia, Canada. *J. Geochem. Explor.*, **89**, 247–250.
- Mascarenhas-Pereira, M.B.L., Nath, B.N., Borole, D.V. and Gupta, S.M. (2006) Nature, source and composition of volcanic ash in sediments from a fracture zone trace of Rodriguez Triple Junction in the Central Indian Basin. *Mar. Geol.*, **229**, 79–90.
- Matondkar, S.G.P., Nair, K.K.C. and Ansari, Z.A. (2005) Biological characteristics of Central Indian Basin water during the Southern Summer. *Mar. Georesour. Geotechnol.*, **23**, 299–314.
- Mazumdar, A., Dewangan, P., João, H.M., Peketi, A., Khosla, V.R., Kocherla, M., Badesab, F.K., Joshi, R.K., Roxanne, P., Ramamurty, P.B., Karisiddaiah, S.M., Patil, D.J., Dayal, A.M., Ramprasad, T., Hawkesworth, C.J. and Avanzinelli, R. (2009) Evidence of paleo-cold seep activity from the Bay of Bengal, offshore India. *Geochim. Geophys. Geosyst.*, **10**, 1–15.
- Meister, P., McKenzie, J.A., Vasconcelos, C., Frank, M. and Gutjahr, M. (2007) Dolomite formation in the dynamic deep biosphere: results from the Peru margin (ODP Leg 201). *Sedimentology*, **54**, 1007–1032.
- Meister, P., Bernasconi, S.M., Aiello, I.W., Vasconcelos, C. and McKenzie, J.A. (2009) Depth and controls of Ca-rhodochrosite precipitation in bioturbated sediments of the Eastern Equatorial Pacific. ODP Leg 201, Site 1226 and DSDP Leg 68, Site 503. *Sedimentology*, **56**, 1552–1568; doi: 10.1111/j.1365-3091.2008.01046.x.
- Mukhopadhyay, R., Iyer, S.D. and Ghosh, A.K. (2002) The Indian Ocean nodule field: tectonic evolution and ferromanganese nodules. *Earth-Sci. Rev.*, **60**, 67–130.
- Naganuma, T., Otsuki, A. and Seki, H. (1989) Abundance and growth rate of bacterioplankton community in hydrothermal vent plumes of the North Fiji Basin. *Deep-Sea Res.*, **36**, 1379–1390.
- Nath, B.N. and Mudholkar, A.V. (1989) Early diagenetic processes affecting nutrients in the porewaters of Central Indian Ocean cores. *Mar. Geol.*, **86**, 57–66.
- Nath, B.N., Rao, V.P. and Becker, K.P. (1989) Geochemical evidence of terrigenous influence in deep-sea sediments up to 8°S in the Central Indian Basin. *Mar. Geol.*, **87**, 301–313.
- Nath, B.N., Roelandts, I., Sudhakar, M. and Plüger, W.I. (1992) Rare earth element patterns of the Central Indian Basin sediments related to their lithology. *Geophys. Res. Lett.*, **19**, 1197–1200.
- Nath, B.N., Bau, M., Rao, B.R. and Rao, Ch.M. (1997) Trace and rare earth elemental variation in Arabian Sea sediments through a transect across the oxygen minimum zone. *Geochim. Cosmochim. Acta.*, **61**, 2375–2388.
- Nath, B.N., Mascarenhas-Pereira, M.B.L., Kurien, S., Selvaraj, K., Naman, D., Desai, N., D'souza, V. and Naik, T. (2005) Porewater nutrients and sediment chemistry. In: *Benthic Environmental Variability in the Central Indian Ocean Basin-I*, pp. 45–64. Project report submitted to Department of Ocean Development, Govt. of India, New Delhi.
- Nath, B.N., Borole, D.V., Aldahan, A., Patil, S.K., Mascarenhas-Pereira, M.B.L., Possnert, G., Ericsson, T., Ramaswamy, V. and Gupta, S.M. (2008) ²¹⁰Pb, ²³⁰Th, and ¹⁰Be in Central Indian Basin seamount sediments: signatures of degassing and hydrothermal alteration of recent origin. *Geophys. Res. Lett.*, **35**, L09603.
- Nelson, D.C., Wirsén, C.O. and Jannasch, H.W. (1989) Characterization of large, autotrophic Beggiatoa spp. abundant at hydrothermal vents of the Guaymas basin. *Appl. Environ. Microbiol.*, **55**, 2909–2917.
- Pachmayr, F. (1960) *Vorkommen und Bestimmung Von Schwefelverbindungen in Mineralwasser*. Dissertation, University of Munchen, Munich, Germany, 48 pp.
- Pai, S.C., Gong, G.C. and Liu, K.K. (1993) Determination of dissolved oxygen in seawater by direct spectrophotometry of total iodine. *Mar. Chem.*, **41**, 343–351.
- Parkes, R.J., Webster, G., Cragg, B.A., Weightman, A.J., Newberry, C.J., Ferdelman, T.G., Kallmeyer, J., Bo Jørgensen, B., Ivano W. Aiello, I.W. and Fry, J.C. (2005) Deep subsurface prokaryotes stimulated at interfaces over geological time. *Nature*, **436**, 390–394.
- Patience, R.L., Clayton, C.J., Kearsley, A.T., Rowland, S.J., Bishop, A.N., Rees, A.W.G., Bibby, K.G. and Hopper, A.C. (1990). An integrated biochemical, geochemical, and sedimentological study of organic diagenesis in sediments from Leg 112. In: *Proceedings of the Ocean Drilling Program, Scientific Results*, (Eds E. Suess, R. von Huene), Vol. 112, pp. 135–153. *Proc. ODP, Sci. Results*, College Station, TX (Ocean Drilling Program); doi: 10.2973/odp.proc.sr.112.191.1990.
- Pattan, J.N. and Jauhari, P. (2001) Major, trace, and rare earth elements in the sediments of the central Indian Ocean basin: their source and distribution. *Mar. Georesour. Geotechnol.*, **19**, 85–106.

- Pattan, J.N., Masuzawa, T., Borole, D.V., Parthiban, G., Jauhari, P. and Yamamoto, M. (2005) Biological productivity, terrigenous influence and noncrustal elements supply to the Central Indian Ocean Basin: Paleooceanography during the past ca 1 Ma. *J. Earth Syst. Sci.*, **114**, 63–74.
- Ram, A.S.P., Loka Bharathi, P.A., Nair, S. and Chandramohan, D. (2001) A deep-sea bacterium with unique nitrifying property. *Curr. Sci.*, **80**, 1222–1224.
- Rao, V.P. and Nath, B.N. (1988) Nature, distribution and origin of clay minerals in grain size fractions of sediments from Manganese Nodule Field, Central Indian Ocean Basin. *Ind. J. Mar. Sci.*, **17**, 202–207.
- Rao, V.P., Kessarkar, P.M., Krumbein, W.E., Krajewski, K.P. and Schneiders, R.J. (2003) Microbial dolomite crusts from the carbonate platform of western India. *Sedimentology*, **50**, 819–830.
- Rodina, A.G. (1972) Methods of culturing iron bacteria. In: *Methods in Aquatic Microbiology* (Eds R.R. Colwell and M.S. Zambruskii), pp. 358–367. University Park Press, Baltimore, CA.
- Rodriguez, N.M., Paull, C.K. and Borowski, W.S. (2000) Zonation of authigenic carbonates within gas hydrate-bearing sedimentary sections on the Blake Ridge: offshore southeastern North America. In: *Proceedings of the Ocean Drilling Program, Scientific Results* (Eds C.K. Paull, R. Matsumoto, P.J. Wallace and W.P. Dillon), Vol. 164, pp. 301–312. Ocean Drilling Program, College Station, TX.
- Schenau, S.J., Slomp, C.P. and De Lange, G.-J. (2000) Phosphogenesis and active phosphorite formations in sediments from Arabian Sea oxygen minimum zone. *Mar. Geol.*, **169**, 1–20.
- Schulz, H.D. (2000) Quantification of Early Diagenesis: dissolved constituents in Marine porewater. In: *Marine Geochemistry* (Eds H.D. Schulz and M. Zabel), pp. 87–122. Springer Verlag, Berlin-Heidelberg.
- Schulz, H.N. and Schulz, H.D. (2005) Large sulfur bacteria and the formation of phosphorite. *Science*, **307**, 416–418.
- Sizaret, S., Branquet, Y., Gloaguen, E., Chauvet, A., Barbançon, L., Arbaret, L. and Chen, Y. (2009) Estimating the local paleo-fluid flow velocity: new textural method and application to metasomatism. *Earth Planet. Sci. Lett.*, **280**, 71–82.
- Smirnov, A., Hausner, D., Laffers, R., Strongin, D.R. and Schoonen, M.A.A. (2008) Abiotic ammonium formation in the presence of Ni-Fe metals and alloys and its implications for the Hadean nitrogen cycle. *Geochem T.*, **9**, 5–24.
- Soetaert, K., Herman, P.M.J. and Middelburg, J.J. (1996) A model of early diagenetic processes from the shelf to abyssal depths. *Geochim. Cosmochim. Acta*, **60**, 1019–1040.
- Stein, R. (1991) Accumulation of organic carbon in marine sediment. *Lect. Notes Earth Sci.*, **34**, 1–217.
- Stevens, T. (1997) Lithoautotrophy in the subsurface. *FEMS Microbiol. Rev.*, **20**, 327–337.
- Suess, E., Muller, P.J., Powell, H.S. and Reimers, C.E. (1980) A closer look at nitrification in pelagic sediments. *Geochem. J.*, **14**, 129–137.
- Takano, Y., Kobayashi, K., Yamanaka, T., Marumo, K. and Urabe, T. (2004) Amino acids in the 308°C deep-sea hydrothermal system of the Suiyo Seamount, Izu-Bonin Arc, Pacific Ocean. *Earth Planet. Sci. Lett.*, **219**, 147–153.
- Teske, A.P. (2004) The deep subsurface biosphere is alive and well. *Trends Microbiol.*, **13**, 402–404.
- Tuttle, J.H. and Jannasch, H.W. (1977) Thiosulfate stimulation of microbial dark assimilation of carbon dioxide in shallow marine waters. *Microb. Ecol.*, **4**, 9–25.
- Van Es, F.B. and Meyer-Reil, L.-A. (1982) Biomass and metabolic activity of heterotrophic marine bacteria. In: *Advances in Microbial Ecology* (Ed. K.C. Marshal), pp. 111–170. Plenum Press, New York, 6.
- Wang, G., Spivack, A.J., Rutherford, S., Manor, U. and D'Hondt, S. (2008) Quantification of co-occurring reaction rates in deep seafloor sediments. *Geochim. Cosmochim. Acta*, **72**, 3479–3488.
- Ward, B.B., Kilpatrick, K.A., Renger, E.H. and Eppley, R.W. (1989) Biological nitrogen cycling in the nitracline. *Limnol. Oceanogr.*, **34**, 493–513.
- Warren, B.A. (1982) The deep water of the Central Indian Basin. *J. Mar. Res.*, **40**(Suppl.), 823–860.
- Warren, B.A. and Johnson, G.C. (2002) The overflows across the Ninetyeast Ridge. *Deep-Sea Res. II*, **49**, 1423–1439.
- Wenbo, S., Yongbiao, W., Cramer, B.D., Munnecke, A., Zhiming, I. and Lipu, F. (2008) Preliminary estimation of Paleoproductivity via TOC and habitat types: which method is more reliable? – A case study on the Ordovician–Silurian Transitional Black Shales of the Upper Yangtze Platform, South China. *J. China Univ. Geosci.*, **19**, 534–548.
- Wenxuan, H., Zhijun, J., Suping, Y., Xiancai, L., Zhilin, C., Linye, Z., Xuejun, Z. and Huaiyang, Z. (2002) Discovery of low-mature hydrocarbon in manganese nodules and ooze from the Central Pacific deep sea floor. *Chinese Sci. Bull.*, **47**, 939–944.
- Wirsen, C.O., Tuttle, J.H. and Jannasch, H.W. (1986) Activities of sulfur-oxidizing bacteria at the 21°N East Pacific Rise Vent site. *Mar. Biol.*, **92**, 449–456.
- Yamagata, Y., Watanabe, H., Saitoh, M. and Namba, T. (1991) Volcanic production of polyphosphates and its relevance to prebiotic evolution. *Nature*, **352**, 516–519.
- Yang, J., Bull, S. and Large, R. (2004) Numerical investigation of salinity in controlling ore-forming fluid transport in sedimentary basins: example of the HYC deposit, Northern Australia. *Mineral. Deposita*, **39**, 622–631.
- Zervas, D., Nichols, G.J., Hall, R., Smyth, H.R., Charlotta, L. and Murtagh, F. (2009) SedLog: a shareware program for drawing graphic logs and log data manipulation. *Comput. Geosci.*, **35**, 2151–2159.
- Zhao, C., Hobbs, B.E. and Ord, A. (2009) Theoretical and numerical investigation into roles of geofluid flow in ore forming systems: integrated mass conservation and generic model approach. *J. Geochem. Explor.*, **106**, 251–260.
- ZoBell, C.E. (1941) The cultural requirements of heterotrophic aerobes. *J. Mar. Res.*, **4**, 42–75.

Manuscript received 8 October 2008; revision accepted 6 July 2010

Supporting Information

Additional Supporting Information may be found in the online version of this article:

Material S1. Explicit finite difference model.

Please note: Wiley-Blackwell are not responsible for the content or functionality of any supporting materials supplied by the authors. Any queries (other than missing material) should be directed to the corresponding author for the article.

Chemosynthetic activity prevails in deep-sea sediments of the Central Indian Basin

Anindita Das · P. P. Sujith · Babu Shashikant Mourya · Sushanta U. Biche · P. A. LokaBharathi

Received: 29 June 2010 / Accepted: 1 December 2010
© Springer 2010

Abstract It is hypothesized that in the deep-sea, under psychrophilic, barophilic and oligotrophic conditions, microbial community of Central Indian Basin (CIB) sediments could be chemosynthetic. In the dark, at near ambient temperature, $4 \pm 2^\circ\text{C}$, 500 atm pressure, pelagic red clay could fix carbon at rates ranging from 100 to 500 nmol C g^{-1} dry wt day^{-1} . These clays accumulate in the deepest and the most remote areas of the ocean and contain <30% biogenic material. These clays with volcanic signatures fixed 230–9,401 nmol C g^{-1} dry wt day^{-1} while siliceous radiolarian oozes of the basin fixed only 5–45 nmol C g^{-1} dry wt day^{-1} . These rates are comparable to those of white smoker waters and are 1–4 orders of magnitude less than those of bacterial mats and active vents recorded at other localities worldwide. The experimental ratios of carbon fixation to metal oxidation in the sediments were 0–1 order of magnitude higher than the corresponding average theoretical ratio of 0.0215 (0.0218, 0.0222, 0.0207 and 0.0211 for Fe, Mn, Co and Ni, respectively) in the siliceous ooze. In case of pelagic red clay it was 0–2 orders higher than theoretical ratio. Thus, chemosynthetic activity could be more widespread, albeit at low rates, than previously considered for abyssal basins. These environments may be dependent partially or even wholly on in situ microbial primary production for their carbon requirements rather than on photosynthetically derived detritus from surface waters.

Keywords Chemosynthesis · Metal oxidation · Bacteria · Bioenergetics · Central Indian Basin

Introduction

Chemosynthetic bacteria are primary producers that use chemical energy to produce biomass. Chemolithoautotrophic bacteria oxidize reduced inorganic compounds to obtain both energy and reducing power for fixing inorganic carbon. Access to both oxygenated seawater and reduced compounds is important for chemosynthetic communities. The term *chemosynthesis* is generally used to describe chemolithoautotrophic processes at hydrothermal vents and seeps (Jannasch 1989). Chemoautotrophy to some extent is also possible without dissolved oxygen by using nitrate as electron acceptor to oxidize sulphide. Thiotrophic nitrate reduction may also be an important contributing process especially in diffuse flow regimes (Childress et al. 1991) with temperatures varying between 2 and 25°C (Chevaldonne et al., 1991). It is being increasingly appreciated that this activity is more widespread than commonly thought, as synthesis of organic carbon by primary producers is one of the essential functions in any ecosystem. A huge expanse of the dark deep sea waters and sediments has the potential for primary production through chemosynthesis. Autotrophic bacterial processes, other than those of cyanobacteria, have been shown to be significant in oxic–anoxic interfaces (e.g. Casamayor et al. 2001 and references therein). In the case of primary production, dark incorporation is either subtracted from carbon incorporation in light bottles or ignored (Casamayor et al. 2008 and references therein). The importance of dark carbon fixation has been shown for oxic–anoxic interfaces, anoxic waters in lakes (Culver and Brunskill 1969; Jørgensen et al. 1979;

Communicated by T. Matsunaga.

A. Das · P. P. Sujith · B. Shashikant Mourya · S. U. Biche · P. A. LokaBharathi (✉)
Biological Oceanography, National Institute of Oceanography,
Dona Paula, Goa 403004, India
e-mail: loka@nio.org

Published online: 24 December 2010

 Springer

García-Cantizano et al. 2005 and references therein) and seas (Tuttle and Jannasch 1977; Juniper and Brinkhurst 1986; Jørgensen et al. 1991). It is therefore hypothesized that the perpetually dark, deep abyssal basins with scanty amounts of organic detritus would therefore be constrained to fix carbon to various extents depending upon the accessibility of reduced inorganic substrates.

Reduced compounds may become available in an environment either via the degradation of organic matter or from magmatic/geothermal sources. Ambient oxygen, nitrate and sulphate in seawater might be consumed to varying extents depending on the amount of organic matter available for early or late diagenesis (Schulz and Zabel 2000). These processes have long been associated with the degradation of organic matter settling from surface waters. Although well known to co-occur with nitrification, metal oxidation and even oxalic respiration, the process of fixation of carbon dioxide is disproportionately biased towards the iron, sulphur and methane cycles.

The present work therefore focuses on the chemosynthetic potential of the microbial community of abyssal ocean sedimentary basin harbouring polymetallic nodules in the CIB. Microbial autotrophic carbon fixation at the expense of reduced inorganic substrates (reduced metals Ni, Co, Mn, Fe) is evaluated in deep-sea sediments. The approach is based on the bioenergetic concepts developed by McCarty (1965, 1975), according to which microbial redox reactions can be formulated by combining three half-reactions: the

electron donor reaction, the electron acceptor reaction and the cell (biomass) synthesis reaction.

Theoretical ratios of carbon fixation to metal oxidation are compared with experimental values (Hatzikioseyian and Tsezos 2006). It is hypothesized that chemosynthetic activity could be more widespread than commonly thought and that deep ocean oligotrophic sediments could have retained their chemosynthetic potential. Additionally, the ratio of carbon fixation to metal oxidation could vary among different sediments, possibly depending on their geological and geochemical origins and the type of bacterial communities.

Geological setting

The CIB has five sediment types, namely terrigenous mud, siliceous radiolarian ooze with and without nodules, pelagic red clays and calcareous foraminiferal ooze (Fig. 1a; Rao and Nath 1988; Nath and Mudholkar 1989). The basin is bordered by the Indian Ocean Ridge system and marked by prominent fracture zones and seamounts hosting normal Mid-Ocean Ridge Basalts (Fig. 1b; Kamesh Raju and Ramprasad 1989; Mukhopadhyay et al. 2002). The oxygen- and nutrient-rich Antarctic Bottom Water Current entering the CIB from 5°S (Gupta and Jauhari 1994) maintains oxic conditions. The pH is near-neutral with sub-oxic pockets in sediments (Nath and Mudholkar 1989). The siliceous oozes

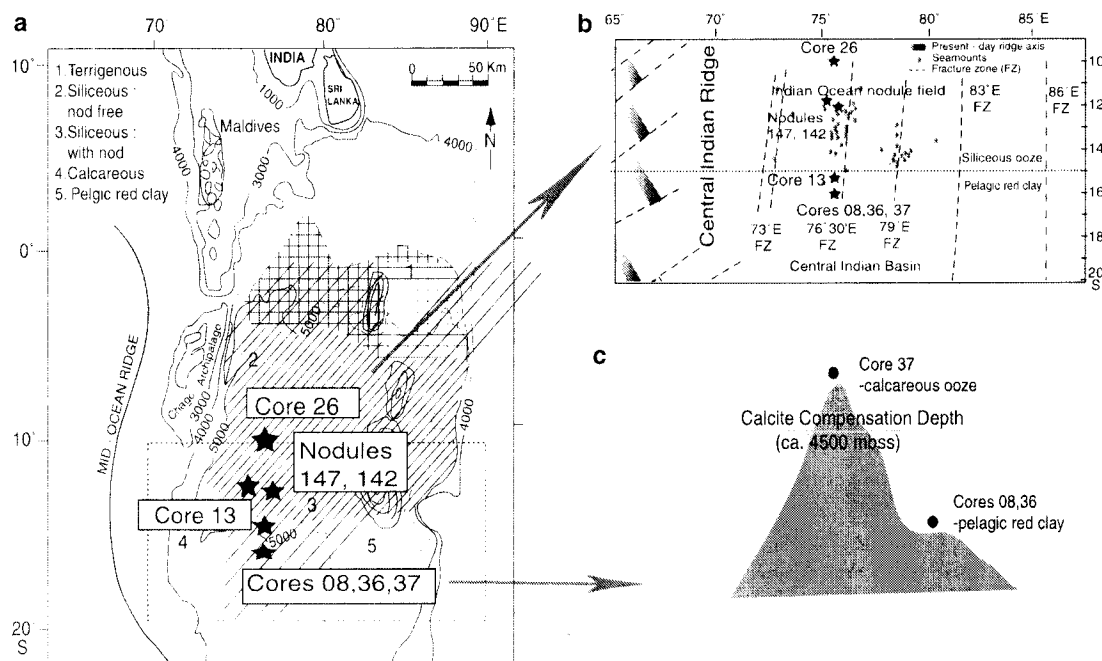


Fig. 1 Site location. **a** Central Indian Basin and its sediment types. **b** Station locations vis-à-vis geological features (adapted from Mascarenhas-Pereira et al. 2006). **c** Schematic representation of station on seamount in the pelagic clay realm

harbour most of the polymetallic nodules both at the sediment–water interface and buried under the sediment (Sudhakar 1989). Hydrothermal alterations are seen in some pelagic clays (Mascarenhas-Pereira et al. 2006; Nath et al. 2008). The calcareous oozes are available on the ridge flanks and the seamount tops that rise above the calcite compensation depth ~4,500 m below the sea surface.

Materials and methods

Sampling and processing

Samples of siliceous ooze, pelagic red clay with hydro-volcanic signatures, calcareous ooze and polymetallic nodules were collected and processed during the 4th, 17th and 26th expeditions on-board the RV *Akademik Boris Petrov* (ABP-04, 17, 26 during 2005, 2006 and 2007; Fig. 1) in the CIB. Samplings were done by means of USNEL-type box cores of dimensions 50 × 50 × 50 cm. Nodules along with their associated sediments were collected using van Veen grab. Station locations and details of experiments conducted with each set of samples are presented in Table 1. The in situ temperature of CIB was generally reported to be around 2°C (Warren 1982). Hence, all the experiments were conducted at near ambient temperature of 4 ± 2°C. Preliminary analyses were conducted

with one of the cores (13) at 4 ± 2°C, 1 atm and 4 ± 2°C, 500 atm. As there was no difference in the results obtained with both the sets, experiments were conducted at 4 ± 2°C, 1 atm. Besides in the deep-sea, the change in bacterial activity is measurably affected by change in temperature rather than pressure (Jannasch 1989). Metal oxidation and carbon fixation experiments on sediments of cores 26 and 36 were carried out on aliquots from 0 to 30 cm bsf, at 2-cm interval up to 10 and 5-cm interval thereafter.

Autotrophic ¹⁴C uptake by sediments and nodules

Microbial uptake of carbon was measured using NaH¹⁴CO₃ uptake [5 µCi/ml activity, Board of Radiation and Isotope Technology (BRIT), Navi Mumbai, India] adopting methods described earlier (Tuttle and Jannasch 1977; Nelson et al. 1989). Briefly, about 1 g of sediment/nodule was suspended in 9 ml sterile seawater and incubated with 0.08 µCi ml⁻¹ final concentration of NaH¹⁴CO₃ for 24 h in the dark. Unincorporated labelled carbon was carefully washed with sterile seawater. The filtered slurry was acidified to remove unbound ¹⁴C and trace inorganic carbon. The filter with the trapped sediment was further dried at 35°C and then suspended in vial containing scintillation cocktail. The samples were counted after 12–24 h in a Liquid Scintillation counter (Model Perkin Elmer, Wallac

Table 1 Comparison of carbon fixation rates of the Central Indian Basin from the present work and other chemosynthetic sites extracted from Karl (1995) and Mandernack and Tebo (1999)

Environment	Location	Type	¹⁴ C incorporation ^a	Conditions	Reference
Hydrothermal vents	21°N, EPR ^b	Water, white smoker	13	1 atm, dark, 3°C, 24 h	Wirsen et al. (1986)
	Juan de Fuca	Water	202	1 atm, dark	Chase et al. (1985)
	Guaymas Basin	Bacterial mats	12,000	1 atm, dark, 8°C	Nelson et al. (1989)
	Mid-Atlantic Ridge				
	“TAG” site	Water	54–183	In situ	Wirsen et al. (1993)
Anoxic basins	Galapagos, Rose Garden	Water	1,500–5,000	In situ	Mandernack and Tebo (1999)
	Black Sea	Water	2–833	In situ	Sorokin (1972)
	Framvaren Fjord	Water	5,800–11,200	In situ	Mandernack and Tebo (1999)
Oxic basins	Solar Lake, Sinai	Water	12,000–22,000	In situ	Jørgensen et al. (1979)
	Central Indian Basin	Siliceous ooze ^c	5–45	1 atm, dark, 5°C	Present work
		Red clay with Volcanic signature ^d	230–9,401	1 atm, dark, 5°C	
		Red clay with va ^{c, h}	100–500	1 atm, dark, 5°C	
		Red clay with va ^{c, h}	100–500	500 atm, dark, 5°C	
Calcareous ooze ^f		1,000–15,000	1 atm, dark, 5°C		
Manganese nodules ^g	58–448	1 atm, dark, 5°C			

^a ¹⁴C incorporation units are nmol l⁻¹ day⁻¹ CO₂ for water samples and nmol g⁻¹ dry wt day⁻¹ for sediments and bacterial mats. Rates are normalized to bacterial numbers; ^b East Pacific Rise; ^c Box-core 26; ^d Box-cores 08 and 36; ^e Box-core 13; ^f Box-core 37; ^g BN-142, SN-147; ^h Volcanic ash

1409 DSA). Suitable controls for unlabelled and heat killed sediments, wash water and labelled carbon were included. The incorporation of carbon was read as disintegrations per minute (integrated for 5 min) and was expressed as $\text{nmol C g}^{-1} \text{ day}^{-1}$. Siliceous ooze of core 26 and pelagic red clay of core 36 were examined for carbon fixation rates under oxic and sub-oxic conditions at $4 \pm 2^\circ\text{C}$, 1 atm, pH 7. Hyperbaric incubations were done in pressurized vessels at $4 \pm 2^\circ\text{C}$, 500 atm (Tsurumi-Seiki, Japan; Kato et al. 1995).

Oxygen consumption

Oxygen in the aqueous phase of the experimental tubes was measured according to Pai et al. (1993). The difference in oxygen concentration from the final day of incubation to the first day was calculated as oxygen consumption and expressed in $\mu\text{M g}^{-1} \text{ day}^{-1}$.

Metal analysis and oxidation rates in sediments

Siliceous ooze and pelagic red clays were examined for metal oxidation rates under oxic and sub-oxic conditions using a $100 \mu\text{M}$ metal spike, at $4 \pm 2^\circ\text{C}$, 1 atm. About $1.5 \pm 0.5 \text{ g}$ of sediment was inoculated into 15 ml screw-capped tubes containing $100 \mu\text{M}$ concentrations of metal chlorides or sulphates prepared in sterile seawater. The incubation was carried out under oxic and sub-oxic conditions. The oxic incubation was assured by directly inoculating wet sediment in half-filled tubes and sub-oxic in completely filled tubes. Azide-treated (10 mM) sediment controls were prepared as above to correct for metal adsorption. Sterile controls without any inocula to account for abiotic precipitation were also included. Samples (1 ml) at zero hour were centrifuged (8,000 rpm for 10 min at 4°C) and the supernatant was acidified with 1 N HCl and stored at 4°C until analysis for assessing the metal concentration at 0 h. Further analysis was carried out at the shore laboratory.

After 45-day incubation, the above centrifugation step was repeated. An aliquot of 1 ml supernatant from each tube was used for estimating the residual metal concentration by spectrophotometric method using Multiskan Thermo Spectrum. The Mn concentration in the sample was determined with 1-(2-pyridylazo)-2-naphthol method at 560 nm (Chin et al. 1992). The determination of Ni with dimethylglyoxime at 460 nm and Co with nitroso-R-salt at 500 nm was done according to the scheme of Chester and Magness (1968). Fe was performed by sampled direct current (Aldrich and van der Berg 1998) using a Metrohm (Switzerland) voltammeter. Mean and standard deviations were calculated for microbially and non-microbially promoted metal immobilization and were corrected for

chemical precipitation in different experimental setups. The sediment slurry from each tube was rinsed and poured onto a pre-weighed filter positioned in a filtration setup at the end of analysis. The filter with sediment was dried at 105°C and reweighed until constant. The filter weight was subtracted from the sediment weight to derive the actual dry weight of sediment. The residual metal concentration in the experimental tubes for the whole slurry was determined by spectrophotometric method and the concentrations were corrected for corresponding controls. The values were later normalized per gram of sediment to derive the actual metal content in the sediment (cf. Flemming and Delafontaine (2000), for explanations on content and concentration).

Ratio of carbon fixation to metal oxidation

Cell synthesis half-reactions and bioenergetic concepts developed by McCarty were applied to calculate theoretical stoichiometric ratios of carbon fixation to metal oxidation by Hatzikioseyan and Tsezos (2006). These theoretical ratios available for 1 atm, 40°C were compared to the present experimental values. In this study, calculations were done on the basis of net microbial oxidation of four metals Fe, Mn, Ni and Co contributing to microbial carbon fixation. Only the metals showing oxidation are considered for the calculation of ratio of carbon fixation to metal oxidation.

Biomass yield on Fe, Mn, Co and Ni

Yield was calculated as increase in cell biomass per gram of metal oxidized and expressed as $\mu\text{gC g}^{-1}$. The total counts of bacteria of two consecutive samplings were used for the yield calculations.

Total organic carbon (TOC) and C/N ratio

Total carbon and nitrogen was measured by NCS 2500 Elemental Analyser (Patience et al. 1990) using L-Cistina (Therma Quest Italia SpA) as standard. Total carbon was counter-checked with UIC CM 5014 coulometer and found similar in range. Total inorganic carbon was analysed by UIC CM 5014 coulometer using CaCO_3 (Merck, Germany) as standard. The accuracy of measurements was verified by analysis of a standard reference material (USGS-MAG-1). Total organic carbon was determined by subtracting total inorganic carbon from total carbon. The C/N was calculated as the ratio between total organic carbon and total nitrogen.

Labile organic matter (LOM)

Total proteins in sediments were estimated by Lowry's Folin Ciocalteu method using bovine serum albumin as

standard (Lowry et al. 1951). Total carbohydrates in sediments were estimated by phenol–sulphuric acid method using glucose as standard (Kochert 1978). Total lipids in sediments were estimated by Bligh and Dyer method using stearic acid as standard (Bligh and Dyer 1959). The sum of total proteins, carbohydrates and lipids was expressed as LOM (Danovaro et al. 1993).

Total counts of bacteria

Total bacterial cells were counted according to Hobbie et al. (1977). About 1 g of sediment was diluted with 9 ml of sterile seawater; 3 ml of this slurry was fixed with buffered formalin at an end concentration of 2% and stored at 5°C until analysis. At the on-shore laboratory the aliquot was sonicated at 15 Hz for 15 s. The supernatant (1 ml) was stained with 75 µl of 0.01% acridine orange (3 min, in dark) and filtered on 0.22 µm black polycarbonate filter paper (Millipore, USA). This procedure minimized masking by sedimentary particles. About 10–15 microscopic fields were counted to include a total of 300–600 cells per sample using Nikon 80i epifluorescence microscope. The counts were normalized per gram dry sediment.

Results

Carbon fixation

In the study area, the highest carbon uptake rates were recorded for southern calcareous oozes, and the lowest for siliceous oozes in the north of CIB (Table 1). Polymetallic nodules show carbon uptake rates intermediate between those of siliceous oozes and pelagic red clays with volcanic alterations. Carbon fixation in sediments below the Calcite Compensation Depth, (siliceous ooze and pelagic red clay) generally increases with the

decrease in TOC and LOM (Tables 1, 2). Values vary from 100 to 500 nmol g⁻¹ dry wt day⁻¹ without showing any statistically significant difference between the results at 4 ± 2°C, 1 atm and 4 ± 2°C, 500 atm. The difference could not be discerned in the time frame used for the experiment (Table 1).

C/N ratios, TOC, TIC, LOM and bacterial counts

In the CIB sediments, elemental C/N ratios varied from 0.7 to infinitely large values due to very low levels of total nitrogen. TOC varied from <0.05 to 1.54%, TIC varied from non-detectable in most of the deep-sea sediment to 10% in calcareous oozes. LOM varied from 0.025 to 0.14%. Bacterial densities ranged from 10⁶ to 10⁹ cells g⁻¹ dry sediment (Table 2).

pH and Eh

The initial pH was 7.8 ± 0.2 in the experimental tubes. At the end of incubation the pH varied from 6.58 to 6.91 in the oxic tubes and 5.54 to 6.6 in the sub-oxic tubes of BC 26. The pH varied from 6.97 to 7 in oxic tubes and from 6.8 to 7.06 in the sub-oxic tubes of core BC 36 (Fig. 2).

The Eh is a measure of oxidizing and reducing conditions. At the initial stage BC 26 is slightly more reducing than BC 36. However, at the end of the incubation the situation reverses.

The initial Eh in the experimental tubes ranged from +75.81 to +79.96 mV in the incubations for BC 26. At the end incubation, the Eh ranged from –66 to –144 in the oxic tubes and from –87.4 to –128.7 in the sub-oxic tubes of BC 26.

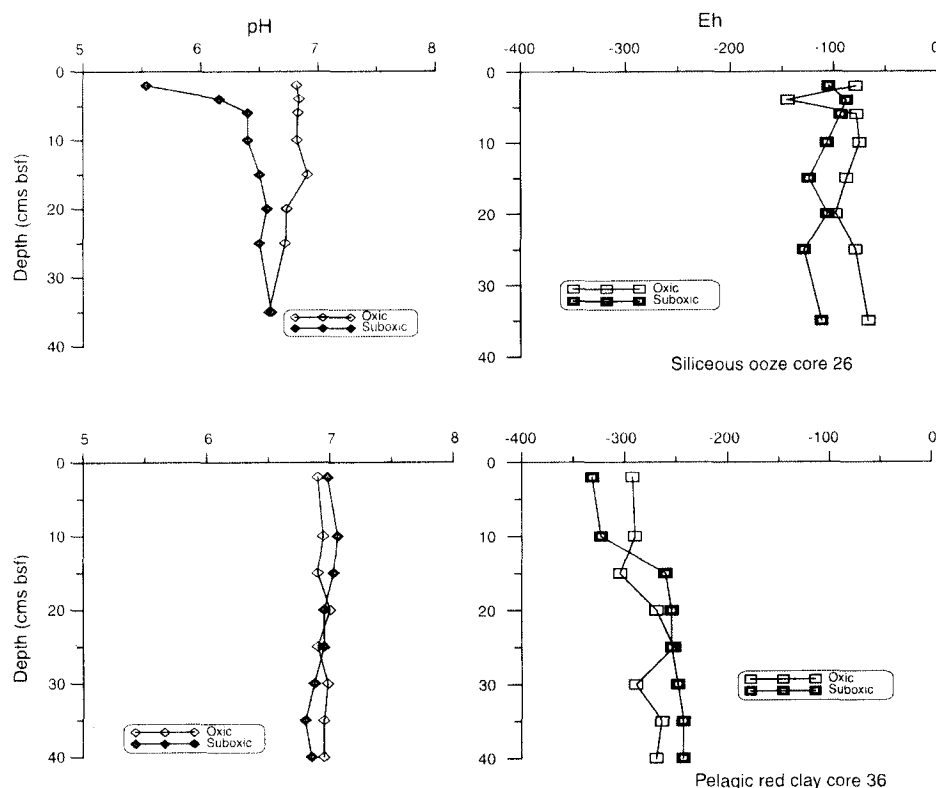
The initial Eh in the experimental tubes ranged from +77.32 to +80.2 mV for BC 36. In the oxic tubes of BC 36 the Eh varied from –252.2 to –304.4 while in sub-oxic tubes the Eh varied from –243 to 331.8 (Fig. 2).

Table 2 Total organic and inorganic carbon contents (TOC, TIC), elemental carbon/nitrogen ratios, bacterial counts and labile organic matter contents (LOM) of sediments in the Central Indian Basin

Sample type	Water depth (mbss)	TOC (%)	TIC (%)	C/N	Bacterial counts (cells g ⁻¹)	LOM (mg g ⁻¹)
Siliceous ooze 26	5,325	0.25 ± 0.09	nd–trace	8 ± 5	10 ⁷ –10 ⁸	0.035–0.135
Red clay 08	5,210	0–0.70	nd	0.7–∞	10 ⁶ –10 ⁹	0.045–0.550
Red clay 36	4,894	0.05–0.40	nd	2–31	10 ⁶ –10 ⁸	0.035–0.080
Calcareous ooze 37	3,992	1.02 ± 0.52	9–10	60–1,525	10 ⁶ –10 ⁹	0.025–0.085
Polymetallic surface nodule						
SN-147 (at sediment–water interface)	~ 5,100	0.16 ± 0.14	nd	10–600	10 ⁸	0.040–0.140
Polymetallic buried nodule						
SN-142 (buried under sediment)	~ 5,100	0.09 ± 0.00	nd	479–∞	10 ⁸	0.04–0.07

mbss metres below sea surface, ∞ infinitely large C/N ratio due to nitrogen below detection level, nd not detected

Fig. 2 pH and Eh profiles at the end of the incubation experiment



Oxygen consumption

Oxygen consumption in the oxic tubes of BC 26 varied from non-detectable to $5.43 \mu\text{M g}^{-1} \text{day}^{-1}$. In the sub-oxic tubes of BC 26, the consumption varied from non-detectable to $15.63 \mu\text{M g}^{-1} \text{day}^{-1}$. A mid depth maximum was noted in the sub-oxic condition in core BC 26. In BC 36 oxic tubes, the oxygen consumption was below detection level. In BC 36 sub-oxic tubes the consumption varied from non-detectable to $0.64 \mu\text{M g}^{-1} \text{day}^{-1}$ (Fig. 3).

Carbon fixation

The carbon fixation in the southern pelagic clay with volcanic signatures is 1–3 orders higher than the northern siliceous ooze (Table 1; Fig. 4). Carbon fixation in core 26 varies from 6.96×10^{-7} to $4.59 \times 10^{-6} \text{ g CO}_2 \text{ g}^{-1} \text{ dry sediment}$ ($15.82\text{--}104.22 \text{ nmol g}^{-1} \text{day}^{-1}$). In core 36 it varies from 1.97×10^{-5} to $4.14 \times 10^{-4} \text{ g CO}_2 \text{ g}^{-1} \text{ dry sediment}$ ($447.92\text{--}9400.62 \text{ nmol g}^{-1} \text{day}^{-1}$).

Ratio of carbon fixation to metal oxidation

The change in level of metal in the aqueous phase has been measured to infer either oxidation or reduction. The fall in level of metal could be due to removal of the metal from aqueous phase for precipitation/oxidation/immobilization

in the biotic tubes. Likewise, the rise in level of the metal in aqueous phase could be due to release of metal for dissolution/reduction/mobilization in these tubes.

The highest metal oxidation/precipitation/immobilization is shown by reduced Fe both in oxic and in sub-oxic tubes of core 26. This is denoted by lowest Fe concentration in the aqueous phase. The highest metal dissolution/reduction/mobilization is shown by Mn in the sub-oxic tubes of core 26 at the deeper layers of the sediment column (Fig. 5a, b). In case of core 36 the highest metal oxidation is shown by reduced Mn under both oxic and sub-oxic conditions (Fig. 5c, d). Oxidation to some extent is also shown by Co in core 36 under oxic condition (Fig. 5c). Ni shows only dissolution and no oxidation in both the cores under both oxic and sub-oxic conditions. Dissolution of metals is prominent in the TOC-richer core 26, while oxidation is greater in the TOC-poor core 36.

The experimental ratio of carbon fixed to metal oxidised in CIB sediments varied from 0.0216 ± 0.0116 in the siliceous core 26 and $0.1292 \pm 0.1457 \text{ g C fixed g}^{-1}$ in the pelagic red clay with volcanic signatures at $4 \pm 2^\circ\text{C}$ under oxic condition. Uncertainty in down-core variation was ± 0.227 in core 26 and ± 0.2857 in core 36 under oxic condition. Under sub-oxic condition the experimental ratio of carbon fixed to metal oxidised was 0.0521 ± 0.0532 in the siliceous core 26 and $0.6392 \pm 0.7776 \text{ g C fixed g}^{-1}$ in the pelagic red clay 36 (Fig. 6). Uncertainty in down-core

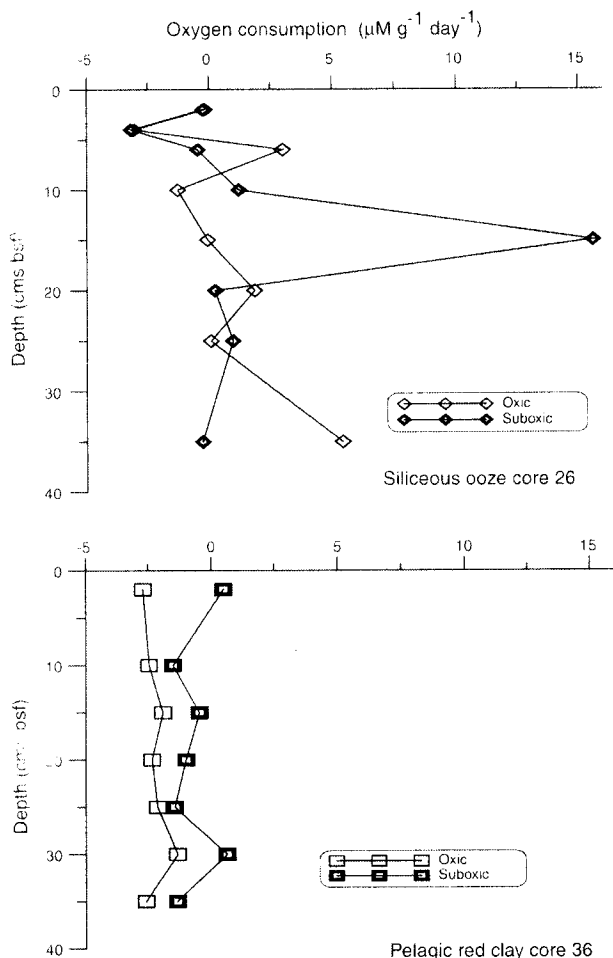


Fig. 3 Bacterial oxygen consumption rates in cores 26 and 36

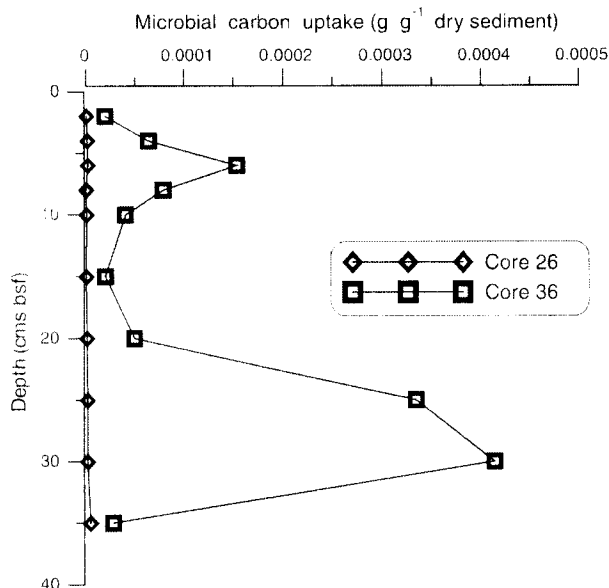


Fig. 4 Carbon fixation by sediments in cores 26 and 36

variation was ± 0.1044 in core 26 and ± 1.5241 in core 36 under sub-oxic condition.

Biomass yield on Fe, Mn, Ni and Co

In the organically richer core 26, the biomass yield was entirely contributed by Fe oxidation. Yield varied from 10 to $100 \mu\text{C g}^{-1}$ metal oxidized under oxic condition. Under sub-oxic condition yield varied from 10 to $1,000 \mu\text{C g}^{-1}$ metal oxidized. In core 36 the biomass yield was contributed by Fe and Mn both in oxic and in sub-oxic condition and by cobalt under oxic condition. Ni did not show any significant contribution both under oxic and sub-oxic conditions (Fig. 7).

Discussion

Both generalists and specialists could be involved in the chemosynthetic processes. While specialists could be high in their activity and restricted to unique niches like black smokers, generalists could be more widespread with lower ability to fix CO_2 . Many bacteria possess the RuBisCO enzyme for carbon fixation using the Calvin Benson Cycle. Yet others like green sulphur bacteria use the rTCA cycle. The methanotrophs are known to use the Serine and RuMP Pathways (Karl 1995).

Chemosynthesis may be exhibited by generalists like facultative autotrophs or mixotrophs and specialists like strictly autotrophic bacteria. Strict autotrophs could be any of the following: 1. nitrifiers (e.g. *Nitrococcus*, *Nitrosomonas*), 2. sulphide oxidizers (e.g. photosynthetic *Chromatium* and chemosynthetic *Thiobacillus thiooxidans*), 3. metal oxidizers (e.g. *Thiobacillus ferroxidans*) and 4. methane oxidizers (e.g. *Methylomonas*). Facultative autotrophs like *Pseudomonas* and *Alcaligenes* may also exhibit chemoautotrophy or mixotrophy (Karl 1995; LokaBharathi 1989; LokaBharathi et al. 1994). Methanotrophs could be mixotrophic or a combination of both autotroph and heterotroph. However, in deep-sea oligotrophic systems where organic matter is lean these bacteria may be constrained towards autotrophy.

General bacteria can thus switch to chemosynthetic behaviour and not necessarily be specialists of the Hydrothermal Vents. This process can be triggered under various situations. In oligotrophic environments, chemosynthesis sustains microbial life at the expense of diverse electron donors available at redox fronts of fractures, seamounts, nodules and crusts (Bach and Edwards 2003; Edwards et al. 2004; Wenxuan et al. 2000).

The chemosynthetic CO_2 fixed/metal oxidised ratio in siliceous ooze under both oxic and sub-oxic experimental conditions (Fig. 6) is 0–2 orders of magnitude higher than

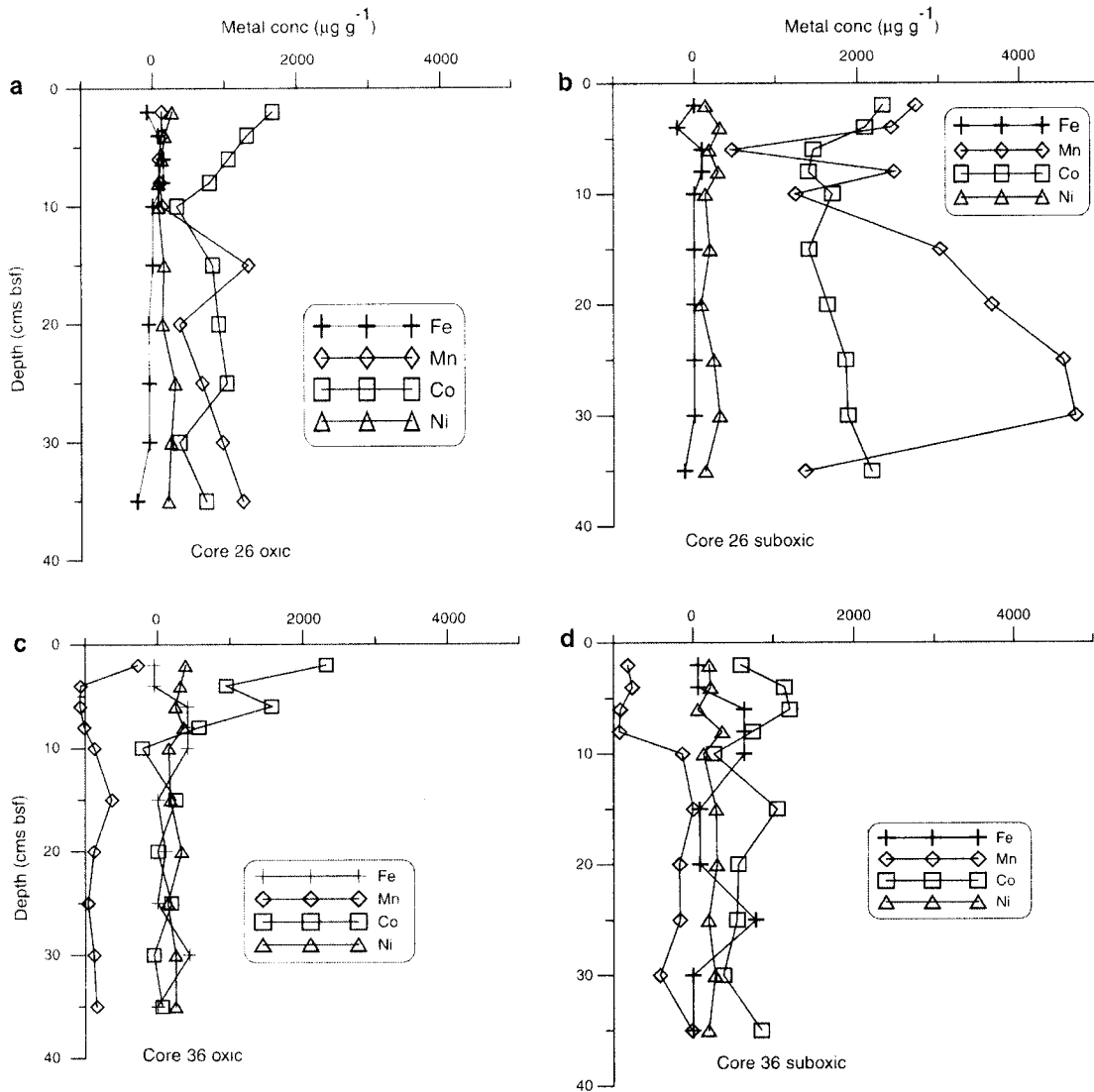


Fig. 5 Metal concentration in aqueous phase of the slurry set ups. Higher metal concentrations indicate dissolution or reduction while lower concentration indicates oxidation or precipitation

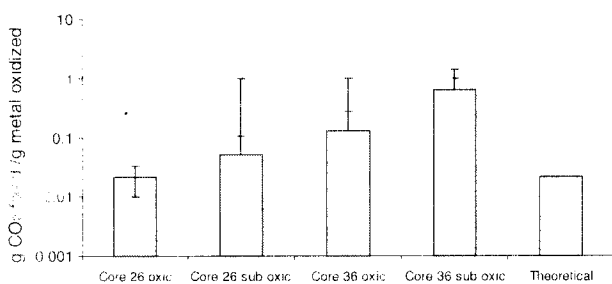


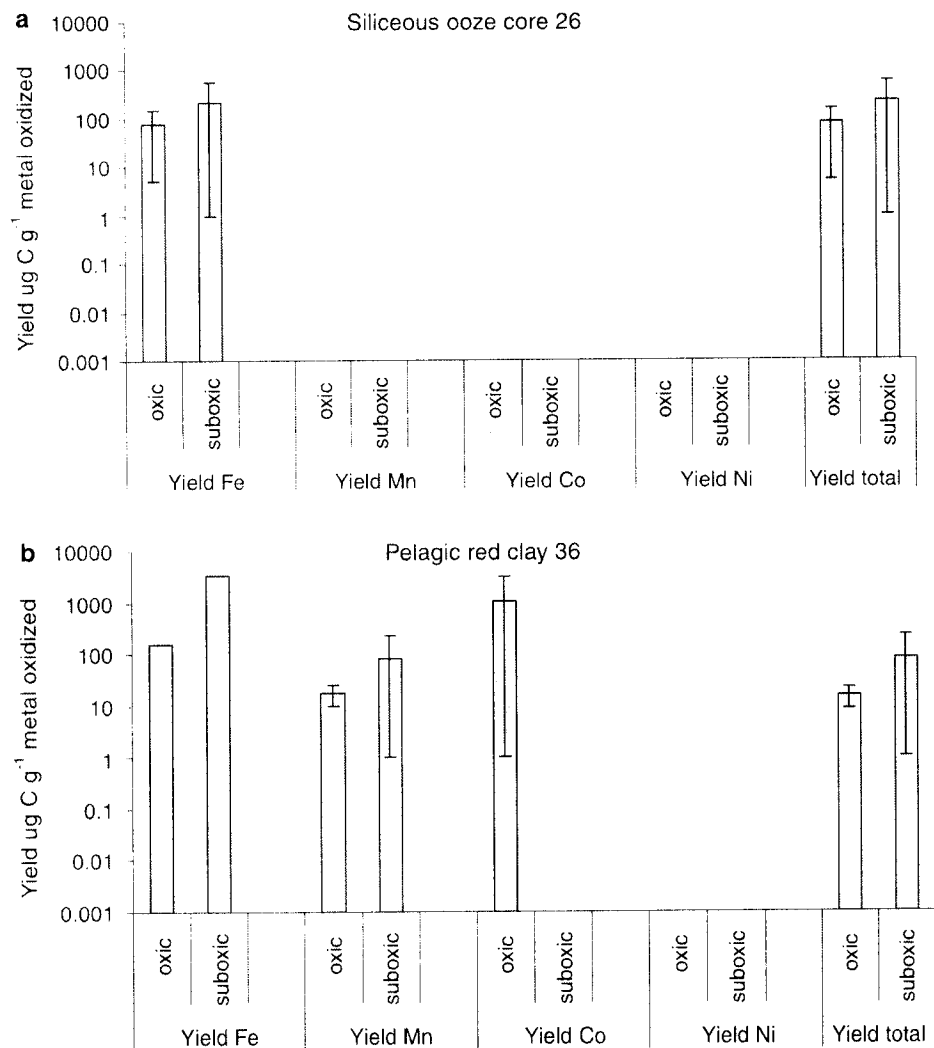
Fig. 6 Experimental ratios of carbon fixed to metal oxidized compared to theoretical value

the corresponding theoretical stoichiometric ratios calculated at 40°C at pH 1.5 by Hatzikioseyan and Tsezou (2006). Interestingly, the experimental ratios obtained in

the present study are much higher than theoretical values given by these authors. This difference could be attributed to better chemosynthetic ability that is promoted under deep-sea environmental conditions like higher dissolution of CO₂ at lower temperatures. Although the pH is different from that of seawater, these values are used due to paucity of theoretical values in literature.

In the north, the profile shows increased carbon fixation in the deeper layers. This is attributed to the downward diffusion of metals by bacterial reduction to sub-surface (15–25 cm bsf). In the south, the carbon fixation shows two peaks one at 0–10 cm bsf and the other at the deeper 25–35 cm bsf. This could perhaps be attributed to a small amount of reduced metal released from the organic rain from the euphotic layers above and a greater availability of

Fig. 7 Average potential yield in terms of carbon fixed by different metals. Calculations assume that single metal fixes the whole amount of carbon fixed. **a** Core 26; **b** Core 36



reduced metal from abiogenic sources below which move upward by diffusion from the deep-biosphere.

Comparison of carbon fixation rates of CIB sediments with those recorded in other chemosynthetic settings worldwide shows that CIB values are 1–2 orders of magnitude smaller than for bacterial mats, anoxic fjords, waters near hydrothermal vents and also solar salterns, and up to 3 orders of magnitude smaller than for other active vents like the Rose Garden. However, they are comparable to waters of white smokers of 21°N East Pacific Rise. Carbon fixation rates of calcareous oozes are comparable to those of bacterial mats and solar salterns (Table 1). The elevation of chemosynthetic potential in the CIB pelagic clays can be explained by depletion of organic matter, both TOC and total sulfur and possible increase in inorganic substrates due to hydrothermal alterations (Nath et al. 2008; Das et al. 2010).

The present results suggest that even at cold temperature, microbial metal oxidation and the resultant elevated microbial immobilization of metals could be responsible

for the high metal contents in bulk sediments reported by Pattan and Jauhari (2001). Such conditions could be accompanied by microbial CO₂ fixation. Metal toxicity could probably play a role in explaining some of these patterns. It is suggested that higher CO₂ fixation in the presence of Co could be partly attributed to Co toxicity. Carbon fixation at the cost of metal oxidation could be both for obligate fixation of carbon or to mitigate/modulate the toxic effect of some metals. This is achieved by oxidizing/precipitating the excess metal. Our recent study on Co immobilization supports the above mechanism to counteract metal toxicity in Mn oxidizing bacteria (Antony et al. 2010). Microbes from similar environments have been shown to precipitate metal salts in different forms under the natural oligotrophic condition (Sujith et al. 2010).

In warm seeps high carbon fixation is accompanied by high biomass (Karl 1995). Carbon fixation is also known in cold seeps from continental shelves and margins. For example, Louisiana Shelf of Gulf of Mexico (Dattagupta

et al. 2006, 2007), California Bay (Levin and Michener 2002) and Nambian shelf (Schulz and Schulz 2005). Eastern boundary upwelling regions like west coast of India are also known for preservation of organic matter produced by photosynthetic primary production (Rao et al. 2003; Paropkari et al. 1992). Anoxic sapropels and hypersaline realms (Sorokin 1972; Jørgensen et al., 1979) are all situated on the continental shelves and margins. While sediment organic matter might reflect the surface photosynthetic primary productivity, preservation of this organic matter could promote chemosynthesis for modulating excess pools of electron donors and acceptors. Chemosynthesis can occur either under organically depleted or replete conditions. Under organically depleted conditions with high amount of electron donors like in hydrothermal vents and deep-sea volcanic environments, microbes are facilitated towards chemosynthetic mode of growth. They fix the carbon dioxide in the sea water or those emanating from vents by oxidizing electron donors like reduced metals in the plumes. Under organic rich conditions like cold seeps, chemosynthesis could be a bacterial response to counter toxicity from excess electron donors like H_2S/NH_3 .

Chemosynthesis is also observed on active vents of 21°N East Pacific Rise (Wirsen et al. 1986), Juan de Fuca (Chase et al. 1985) and Mid-Atlantic Ridge (Wirsen et al. 1993). These sites are all above the Calcite Compensation Depth (CCD) implying that high particulate inorganic carbon is available.

The chemosynthesis in warm vents is mainly driven by the rich supply of electron donors which could compensate for the poor dissolution of electron acceptor like CO_2 . In contrast, the process in cold seeps could be supported by an excess availability of both electron donors and acceptors.

Chemosynthetic carbon fixation is carried out by a number of pathways: Calvin Benson Bassham cycle, reductive acetyl-CoA pathway, 3-hydroxypropionate (3-HP) bicycle, 3-hydroxypropionate/4-hydroxybutyrate (3-HP/4-HB), dicarboxylate/4-hydroxybutyrate (DC/4-HB) cycles and the reductive tricarboxylic acid (rTCA) cycle (Karl 1995). For replenishment of the TCA or Krebs cycle, the intermediates are regenerated by anaplerotic reactions. These reactions are generally achieved through the insertion of either one carbon fragment in the form of CO_2 or two carbon fragments in the form of acetyl CoA into the appropriate metabolic pathway. There are number of microorganisms that make an appreciable fixation of CO_2 by this pathway. In the present study, though it is not clear which pathway is predominantly used, it is probable that a substantial amount of CO_2 can be fixed through this means. *Acetobacter denitrificans* uses the anaplerotic pathways mainly via the malic enzyme to fix 10–15% of protein carbon from CO_2 (Tang et al. 2009). It is probable that

some bacterial communities use this mode of CO_2 fixation when the ambient concentration of utilizable substrate is low.

In the CIB it is possible that multiple carbon fixation pathways might occur. One of the cores in the southern CIB where the community is dominated by *Erythrobacteria*, multiple carbon fixation pathways including the anaplerotic rTCA cycle could be prevalent (Das and LokaBharathi, under review).

It is suggested that chemosynthesis in oligotrophic deep-sea environments of the present study could be facilitated by higher availability of dissolved CO_2 due to higher pressures prevailing below CCD. Besides, there could be a moderate supply of electron donors in the form of dissolved metals. In most natural environments there could be overlaps of the above factors in varying degrees.

CO_2 is not limiting in the deep-sea environment, however, due to severe depletion of organic carbon, the microbes are constrained/facilitated to fix CO_2 at the expense of oxidation of reduced metals. The deep-sea environment can have a plethora of electron donors like ammonia and sulphide besides reduced metals, as in hydrothermal vents. However, the concentrations could be considerably lower. The CIB is a source of both oxidized and reduced metals. The oxidized metals are mostly in the form of polymetallic nodules while reduced metals occur in the pore-water of sediments.

Studies on chemosynthesis from the abyssal depths like CIB can thus provide a valuable baseline or a clear background of microbial chemosynthesis. Here, organic matter is low, but dissolved inorganic carbon and metal content could be high. Diffuse hydrothermal fluid-flow and alterations predominate and persuade microbes towards chemosynthetic mode of metabolism.

The present results show that the values for carbon fixation vary from 5 to 1,000 $nmol\ g^{-1}day^{-1}$. Biomass yield of 10–1,000 $\mu g\ C\ g^{-1}$ metal oxidized has been measured. Under cold oxic near neutral conditions, with high concentration of metals and very low organic matter, the yield is low with very high conversion of reduced metal to oxidised form. In contrast, warm and anoxic conditions with high sulphide concentrations and higher organic matter promote increase in biomass (Karl 1995; Hatzikiosyan and Tsezos 2006). It is speculated that there are number of rates operating between these two extremes. It can therefore be suggested that chemosynthesis is widespread in this environment with the southern locations contributing more than the north. These environments may be more dependent partially or even wholly on in situ microbial primary production for their carbon requirements, rather than on photosynthetically derived detritus from surface waters (Ehrlich 1998). Either way the processes contribute to immobilization of metals.

Microbial immobilization of metals can be either catalytic or non-catalytic; it proceeds through four different mechanisms namely biosorption, bioaccumulation, redox reaction and complex formation. Immobilization may be through cellular sequestration and accumulation, or through extra-cellular precipitation (Sujith et al., under review).

The contribution of chemoautotrophic activity in deep-sea sediments is a few orders less than that of active hydrothermal vents in terms of carbon fixation per unit area per unit time. However, the vast extent of oligotrophic abyssal basins would make its contribution far from negligible. The framework of the present study assumes that microbial oxidation of four metals Fe, Mn, Ni and Co contributes to the microbial carbon fixation under psychrophilic and piezophilic conditions. The present experiments throw light on how differences in organic matter concentrations, temperature and relative variations in metal concentrations in geochemically contrasting sediments could induce chemosynthetic activity to varying degrees. The contribution of other major processes like nitrification, iron and sulphide oxidation could give a more holistic picture.

Like photosynthesis of the euphotic world, chemosynthesis of the aphotic zone could have its own implications. Surprisingly, in the present study, the difference in these rates between normal atmosphere and 500 bars are not significantly different. It is well known that the dissolution of CO₂ is much higher at elevated pressures. In this study, excess CO₂ was not supplied to the pressurized microcosm. Perhaps, varying the amount of dissolved carbon dioxide in the pressurized microcosm would change the results marginally. However, it is often seen that although the amount of carbon dioxide dissolved is significantly different under hyperbaric conditions, the change in microbial rate of carbon fixation is measurably affected by change in temperature rather than pressure (Jannasch 1989). Hence, our experiments conducted at 4°C, 1 atm and 4°C, 500 atm did not show much difference.

It is therefore hypothesised that in the deep sea sediments of CIB, higher ratio of CO₂ fixed/metal oxidized could be either due to mixotrophy or higher efficiency of this process under hyperbaric condition in the cold. Chemosynthesis is an obligate and ancient microbial process. Many microbes seem to retain this ability. They tend to express this activity either under extremely eutrophic or oligotrophic conditions for different reasons. This process helps them to counteract either excess electron donor/acceptor or help survive under nutrient starved conditions. The present study on microbial carbon fixation and metal oxidation might find useful application in deep-sea metal mining and carbon dioxide sequestration.

Acknowledgments The authors acknowledge the Director, NIO for encouragement and constant support. Thanks are extended to the project leaders of "Environmental studies for nodule mining in Central Indian Basin (PMN-EIA)" and PMN-Survey, and the onboard teams of the ABP-04, 17 and 26 cruises for facilities and samples. The Ministry of Earth Sciences (MoES), New Delhi, India is acknowledged for financial support, and the CNS and Particle Flux laboratories, Geological Oceanography, NIO for analytical support. AD thanks SC Dalal for valuable suggestions. AD and SPP acknowledge the CSIR, New Delhi for research grants. An abridged version of these results was presented as poster in the 4th International Symposium Chemosynthesis-based Ecosystems, 2009, Okinawa, Japan, with financial aid from Chemosynthetic Ecosystem Science (ChEss). The manuscript is NIO contribution no. 4885.

References

- Aldrich AP, van der Berg CMG (1998) Determination of Fe and its redox speciation in seawater using catalytic cathodic stripping voltametry. *Electroanal* 10(6):369–373
- Antony R, Sujith PP, Fernandes SO, Verma P, Khedekar VD, LokaBharathi PA (2010) Cobalt immobilization by manganese oxidizing bacteria from the Indian Ridge System. *Curr Microbiol*. doi:10.1007/s00284-010-9784-1
- Bach W, Edwards K (2003) Iron and sulphide oxidation within the basaltic ocean crust: implications for chemolithoautotrophic microbial biomass production. *Geochim Cosmochim Acta* 67(20):3871–3887
- Bligh EG, Dyer WJ (1959) A rapid method of total lipid extraction and purification. *Can J Biochem Physiol* 37:911–917
- Casamayor EO, Garcia-Cantizano J, Mas J, Pedros-Alio C (2001) Microbial primary production in marine oxic–anoxic interfaces: main role of dark fixation in the Ebro River salt wedge estuary. *Mar Ecol Prog Ser* 215:49–56
- Casamayor EO, Garcia-Cantizano J, Pedros-Alio C (2008) Carbon dioxide fixation in the dark by photosynthetic bacteria in sulphide rich stratified lakes with oxic–anoxic interfaces. *Limnol Oceanogr* 53(4):1193–1203
- Chase RL, Delaney JR, Karsten JL, Johnson HP, Juniper SK, Lupton JE, Scott SD, Tunnicliffe V, Hammond SR, McDuff RE (1985) Hydrothermal vents on an axis seamount of the Juan de Fuca ridge. *Nature* 313:212–214
- Chester R, Hughes MJ (1968) Scheme for the spectrophotometric determination of Cu, Pb, Ni, V and Co in marine sediments: applied earth science. *Trans Inst Miner Metall* 77:37–41
- Chevaldonne P, Desbruyeres D, Le Haitre M (1991) Time-series of temperature from three deep-sea hydrothermal vent sites. *Deep Sea Res A* 38:1417–1430
- Childress JJ, Fisher CR, Favuzzi JA, Kochevar RE, Sanders NK, Alayse AM (1991) Sulphide-driven autotrophic balance in the bacterial symbiont-containing hydrothermal vent tubeworm *Riftia pachyptila*. *Biol Bull* 180:135–153
- Chin CS, Johnson KS, Coale KH (1992) Spectrophotometric determination of dissolved manganese in natural waters with 1-(2-pyridylazo)-2-naphthol: application to analysis *in situ* in hydrothermal plumes. *Mar Chem* 37:65–82
- Culver DA, Brunskill GJ (1969) Fayetteville Green Lake, New York. V. Studies of primary production and zooplankton in a meromictic marl lake. *Limnol Oceanogr* 14:862–873
- Danovaro R, Fabiano M, Della Croce N (1993) Labile organic matter and microbial biomass in deep sea sediments (Eastern Mediterranean sea). *Deep-sea Res* 40:953–965
- Das A, Fernandes CEG, Naik SS, Nagender Nath B, Suresh I, Mascarenhas-Pereira MBL, Gupta SM, Khadge NH, Prakash

- Babu C, Borole DV, Sūjith PP, Valsangkar AB, Mourya BS, Biche SU, Sharma R, LokaBharathi PA (2010) Bacterial response to contrasting sediment geochemistry in Central Indian Basin. *Sedimentology*. doi:10.1111/j.1365-3091.2010.01183.x
- Dattagupta S, Miles LL, Barnabei MS, Fisher CR (2006) The hydrocarbon seep tubeworm *Lamellibrachia luymesii* primarily eliminates sulfate and hydrogen ions across its roots to conserve energy and ensure sulfide supply. *J Exp Biol* 209:3795–3805
- Dattagupta S, Telesnicki G, Luley K, Predmore B, McGinley M, Fisher CR (2007) Submersible operated peepers for collecting porewater from deep-sea sediments. *Limnol Oceanogr: Methods* 5:263–268
- Edwards KJ, Bach W, McCollom TM (2004) Neutrophilic iron-oxidizing bacteria in the Ocean: their habitats, diversity, and roles in mineral deposition, rock alteration, and biomass production in the deep-sea. *Geomicrobiol J* 21:393–404
- Ehrlich HL (1998) Geomicrobiology: its significance for geology. *Earth-Sci Rev* 45:45–60
- Flemming BW, Delafontaine MT (2000) Mass physical properties of muddy intertidal sediments: some applications misapplications and non-applications. *Cont Shelf Res* 20:1179–1197
- García-Cantizano J, Casamayor EO, Gasol JM, Guerrero R, Pedros-Alio C (2005) Partitioning of CO₂ incorporation among guilds of microorganisms in lakes with oxic-anoxic interfaces and estimation of in situ specific growth rates. *Microb Ecol* 50:230–241
- Gupta SM, Jauhari P (1994) Radiolarian abundance and geochemistry of the surface sediments from the central Indian Basin. *Curr Sci* 66(9):659–663
- Hatzikioseyan A, Tsezos M (2006) Modelling of microbial metabolism stoichiometry: application in bioleaching processes. *Hydrometallurgy* 83:29–34
- Hobbie JE, Daley RJ, Jasper S (1977) Use of nucleopore filters for counting bacteria by fluorescent microscopy. *Appl Environ Microbiol* 3:1225–1228
- Jannasch HW (1989) Chemosynthetically sustained ecosystems in the deep sea. In: Schlegel HG, Bowien B (eds) *Autotrophic bacteria*. Springer, Berlin, Heidelberg, New York, pp 147–166
- Jørgensen BB, Kuenen JG, Cohen Y (1979) Microbial transformation of sulfur compounds in a stratified lake (Solar Lake, Sinai). *Limnol Oceanogr* 24:799–822
- Jørgensen BB, Fossing H, Wirsén CO, Jannasch HW (1991) Sulfide oxidation in the anoxic Black Sea chemocline. *Deep-sea Res* 38(suppl.2):1083–1103
- Juniper SK, Brinkhurst RO (1986) Water-column dark CO₂ fixation and bacterial-mat growth in intermittently anoxic Saanich Inlet, British Columbia. *Mar Ecol Prog Ser* 33:41–50
- Kamesh Raju KA, Ramprasad T (1989) Magnetic lineations in the Central Indian Basin for the period A24–A21: a study in relation to the Indian Ocean Triple Junction trace. *Earth Planet Sci Lett* 95(3/4):395–402
- Karl DM (1995) Ecology of free-living, hydrothermal vent microbial communities. In: Karl DM (ed) *The microbiology of deep-sea hydrothermal vents*. CRC Press, Boca Raton, FL, pp 35–124
- Kato C, Sato T, Horikoshi K (1995) Isolation and properties of barophilic and barotolerant bacteria from deep-sea mud samples. *Biodivers Conserv* 4:1–9
- Kochert G (1978) Carbohydrate determined by the phenol-sulfuric acid method. In: Hellebust JA, Craigie JJ (eds) *Handbook of physiological methods: physiological and biochemical methods*. Cambridge University Press, Cambridge, pp 95–97
- Levin LA, Michener RH (2002) Isotopic evidence for chemosynthesis-based nutrition of macrobenthos: The lightness of being at Pacific methane seeps. *Limnol Oceanogr* 47(5):1336–1345
- LokaBharathi PA (1989) The occurrence of denitrifying colourless sulphur-oxidizing bacteria in marine waters and sediments as shown by the agar shake technique. *FEMS Microbiol Ecol* 62:335–342
- LokaBharathi PA, Ortiz-conde BA, Nair S, Chandramohan D, Colwell RR (1994) FiveS rRNA sequences and fatty acid profiles of colourless sulfur-oxidising bacteria Ocean technology: perspectives. In: Sushilkumar, Agadi VV, Das VK, Desai BN (eds) *Symposium on ocean technology*. National Institute of Oceanography, Goa, India, 27–29 August 1992. Publ and Inf Dir, New Delhi, India
- Lowry OH, Rosebrough NJ, Farr AL, Randall RJ (1951) Protein measurement with the Folin-Phenol reagents. *J Biol Chem* 193:265–275
- Mandernack KW, Tebo BM (1999) In situ sulfide removal and CO₂ fixation rates at deep-sea hydrothermal vents and the oxic-anoxic interface in Framvaren Fjord, Norway. *Mar Chem* 66:201–213
- Mascarenhas-Pereira MBL, Nath BN, Borole DV, Gupta SM (2006) Nature, source and composition of volcanic ash in sediments from a fracture zone trace of Rodriguez Triple Junction in the Central Indian Basin. *Mar Geol* 229(1):79–90
- McCarty PL (1965) Thermodynamics of biological synthesis and growth. In: Baers J (ed) *Advances in water pollution research*. Proceedings of 2nd international conference on water pollution research. Pergamon Press, Oxford, pp 169–199
- McCarty PL (1975) Stoichiometry of biological reactions. *Prog Water Technol* 7:157–172
- Mukhopadhyay R, Iyer SD, Ghosh AK (2002) The Indian Ocean Nodule Field: petro-tectonic evolution and ferromanganese nodules. *Earth Sci Rev* 60:67–130
- Nath BN, Mudholkar AV (1989) Early diagenetic processes affecting nutrients in the pore waters of Central Indian Ocean cores. *Mar Geol* 86:57–66
- Nath BN, Borole DV, Aldahan A, Patil SK, Mascarenhas-Pereira MBL, Possnert G, Ericsson T, Ramaswamy V, Gupta SM (2008) ²¹⁰Pb, ²³⁰Th, and ¹⁰Be in Central Indian Basin seamount sediments: signatures of degassing and hydrothermal alteration of recent origin. *Geophys Res Lett* 35:L09603. doi: 10.1029/2008GL033849
- Nelson DC, Wirsén CO, Jannasch HW (1989) Characterisation of large, autotrophic *Beggiatoa* species abundant at the hydrothermal vents of the Guaymas Basin. *Appl Environ Microbiol* 55:2909–2917
- Pai SC, Gong GC, Liu KK (1993) Determination of dissolved oxygen in seawater by direct spectrophotometry of total iodine. *Mar Chem* 41:343–351
- Paropkari AL, Prakash Babu C, Mascarenhas A (1992) A critical game of depositional parameters controlling the variability of organic carbon in Arabian Sea sediments. *Mar Geol* 107:213–226
- Patience RL, Clayton CJ, Kearsley AT, Rowland SJ, Bishop AN, Rees AWG, Bibby KG, Hopper AC (1990) An integrated biochemical, geochemical, and sedimentological study of organic diagenesis in sediments from Leg 112. In: Suess E, von Huene R, et al (eds) *Proceedings of ODP, Science Results, vol 112*, College Station, TX (Ocean Drilling Program), pp 135–153. doi:10.2973/odp.proc.sr.112.191.1990
- Pattan JN, Jauhari P (2001) Major, trace, and rare earth elements in the sediments of the Central Indian Ocean Basin: their source and distribution. *Mar Georesour Geotechnol* 19:85–106
- Rao VP, Nath BN (1988) Nature, distribution and origin of clay minerals in grain size fractions of sediments from Manganese Nodule Field, Central Indian Ocean Basin. *Ind J Mar Sci* 17:202–207
- Rao VP, Kessarkar PM, Krumbein WE, Krajewski KP, Schneiders RJ (2003) Microbial dolomite crusts from the carbonate platform of western India. *Sedimentology* 50:819–830

- Schulz HN, Schulz HD (2005) Large sulfur bacteria and the formation of phosphorite. *Science* 307:416–418
- Schulz HD, Zabel M (eds) (2000) *Marine geochemistry*. Springer, Berlin, Heidelberg, New York
- Sorokin YI (1972) The bacterial population and the processes of hydrogen sulphide oxidation in the Black Sea. *J Cons Int Explor Mer* 34:423–454
- Sudhakar M (1989) Ore grade manganese nodules from the Central Indian Basin: an evaluation. *Mar Mining* 8:201–214
- Sujith PP, Khedekar VD, Girish AP, LokaBharathi PA (2010) Immobilization of Nickel by bacterial isolates from Indian Ridge System and chemical nature of the accumulated metal. *Geomicrobiol J* 27:424–434
- Tang K-H, Feng X, Tang YJ, Blankenship RE (2009) Carbohydrate metabolism and carbon fixation in *Roseobacter denitrificans* OCh114. *PLoS ONE* 4(10):e7233. doi:10.1371/journal.pone.0007233
- Tuttle JH, Jannasch HW (1977) Thiosulfate stimulation of microbial dark assimilation of carbon dioxide in shallow marine waters. *Microb Ecol* 4:9–25
- Warren BA (1982) The deep water of the Central Indian Basin. *J Mar Res* 40(Suppl.):823–860
- Wenxuan H, Zhijun J, Suping Y, Xiancai L, Zhilin C, Linye Z, Xuejun Z, Huaiyang Z (2000) Discovery of low-mature hydrocarbon in manganese nodules and ooze from the Central Pacific deep sea floor. *Chinese Sci Bull* 47(11):939–944
- Wirsen CO, Tuttle JH, Jannasch HW (1986) Activities of sulfur-oxidizing bacteria at the 21°N East Pacific Rise vent site. *Mar Biol* 92:449–456
- Wirsen CO, Jannasch HW, Molyneux SJ (1993) Chemosynthetic microbial activity at mid-Atlantic Ridge hydrothermal vent sites. *J Geophys Res* 98:9693–9703